JSC-04217
Revision D

NATIONAL AERONAUTICS AND SPACE ADMINISTRATION

PROJECT/SPACE SHUTTLE

# SPACE SHUTTLE GUIDANCE, NAVIGATION, AND CONTROL DESIGN EQUATIONS

VOLUME III

GUIDANCE

SYSTEMS ANALYSIS BRANCH
GUIDANCE AND CONTROL DIVISION
MANNED SPACECRAFT CENTER
HOUSTON, TEXAS
MARCH 15, 1973

DOCUMENT DISTRIBUTION LIST

AC/Technical Assistant
AP/Public Affairs Office
AT/P. Fitzgerald
J. Loftus
BC4/S. Armstrong
CA/Director of Flight Crew Operations
CA/Asst. Director for Space Shuttle
CB/K. Bobko
C. Duke
J. Engle
C. Fullerton
T. Mattingly
D. Peterson
R. Parker
J. Swigert
J. Young
CD12/J. Bigham
CE/Chief, Crew Training & Simulation Division
CE3/A. Nolting
O. Olasky
CF/D. Lang
CG4/M. Contella
P. Kramer
EA/Director of Engineering and Development
EA3/Asst. Director for Electronic Systems
EB/Chief, Information Systems Division
EB5/Asst. Chief for Spacecraft Data Systems
EE/Chief, Telemetry & Communications Systems Division
EE/J. Sheppard
W. Zrubek
EE6/J. Griffin
J. Lamoreaux
EE8/R. Moorehead
EG/Chief, Guidance and Control Division
EG/Asst. Chief, Guidance and Control Division
EG2/Systems Analysis Branch (25)
EG3/J. VanArtsdalen
J. Lawrence
EG4/E. Chevers
J. T. Edge
EG4/G. Rice
H. Shelton
J. Vernon
A. Turley
EG5/T. Barry
M. Jones
C. Manry
W. Swingle
EG6/D. Gilbert
R. Reid
H. Smith
EG7/C. Wasson
EG8/P. Kurten
R. Wilson
EG13/R. Kennedy
J. Klinar
EJ/W. Bradford
R. Burghduff
J. Brown
G. Holloway
R. Lewis
C. McCullough
R. Swint
ER/H. Davis
ER4/F. Casey
ES/D. Wade
ES2/P. Glynn
C. Modlin
EX/J. Hondros
B. Jackson
B. Redd
EX2/F. Garcia
D. Howes
C. Teixeira
P. Thomas
EX3/I. Fossler
EX4/R. Barton
J. Gamble
EW/W. Petynia
FA/Office of Director for Flt Operations
FA/R. Ernull
FA3/R. Rose
FA12/L. Dunseith
FC/Chief, Flight Control Division
FC4/H. Loden
D. Thorson
FC5/J. Bostick
J. Ferguson
W. Middleton
FC5/C. Parker
FD7/C. Hackler
A. Hambleton
T. Keeton
FM/Chief, Mission Planning & Analysis Div.
FM/T. Gibson
C. Huss
S. Mann
F. Suler
FM2/C. Graves
FM3/C. Hyle
FM4/M. Jenkins
P. Pixley
FM5/R. Savely
FM7/A. Bordano
A. Long
R. Nobles
T. Murtagh
FM9/E. Fridge
E. McHenry
W. Sullivan
FS/Chief, Flight Support Division
FS/J. Satterfield
L. Hamilton
FS6/J. Garman
G. Sabionaki
J. Williams
FS7/J. Watkins
KA/Manager, Skylab Program
LA/Manager, Space Shuttle Program
LA2/H. Dotts
LA3/H. Gartrell
LC/B. Gay
LF/B. Evans
V. Neshyba
LP/J. Heberlig
MA/Aaron Cohen
O. Morris
ME/S. Andrich
R. Bradley
P. Deans
J. Defife
C. Frasier
R. Kubicki
M. Silveira
MO/D. Cheatham
W. Koons
NA2/Planning & Assessment Office

SA/Flight Safety Office
ZR1/C. Essmeier

XRZT/Capt. D. G. Keach
USAF Unit Postal Office
Los Angeles, CA 90045

NASA Hqs/MD/-P/Deputy Associate
Administrator/OMSF
NASA Hqs/USS-1-Library (2)
NASA Hqs/MHE/R. Murad
NASA Hqs/MTG/R. Livingston

NASA Centers Technical Libraries:
Ames Research Center/Moffett Field, CA (2)
Flight Research Center/ Edwards, CA
Goddard Space Flight Center,KSC, FL (2)
John F. Kennedy Space Center (2)
Lewis Research Center/Cleveland, O (2)
Langley Research Center/Langley, VA (2)
Marshall Space Flight Center, Huntsville,
AL (2)

Ames Research Center/Moffett Field, CA
FSM/B. Creer
FSN/H. Lessing
Flight Research Center/Edwards, CA/
CA/R/Shu Gee
John F. Kennedy Space Center/IS-CAS-12/Chief,
Mail & Reports Management Sec/KSC, FL
John F. Kennedy Space Center/KSC, FL/FP-A/R. Smith
John F. Kennedy Space Center/KSC, FL/LS-ENG-6/
Thomas Walton
Marshall Space Flight Center/Huntsville, AL/
S&E-ASTR-SGA/H. Brown
R. Ryan
S. Winder
G. Gillino
SP-EM/C. Griswold
S&E-ASTR-SD/H. Mink
S&E-CSE-1/L. Thionnet
PD-RV-V/H. Hight
S&E-ASTR-SD/H. Scofield

Honeywell, Inc./13350 US Hwy 19, St. Petersburg,
FL 33733/
(818-3) Pete Smith (2)
N. Berlagé
R. Omoth

Intermetrics, Inc.
701 Concord, Cambridge, MA 02138
J. Miller
F. Martin
W. Widnall

MIT/DL/EG/JSC, Houston, TX
E. Olsson (10)
T. Lawton

MIT/DL/Cambridge,MA 02142
73 DL7-211/G. Levine (5)
63 DL7-150/N. Sears (5)
60 DL7-215H/D. Fraser
73 DL7-210/B. Kriegsman
63 DL7-159/R. McKern

NR/Downey, CA
AE55/G. Anderson
C. Chadwick
C. Conrad
D. Engels
R. Epple
FC04/W. Fouts
AA60/G. Fraser
AE55/S. Githens
J. Jansen
D. Levine
EB09/G. Lindewall
GE24/J. Ling
AE55/K. McQuade
AA60/G. Minott
AC60/R. Newman
SF-34/G. Peller
AC84/S. Rubenstein
AA60/W. Schleich

JSC-04217
Revision D

NASA SPACE SHUTTLE PROGRAM WORKING PAPER

# SPACE SHUTTLE GUIDANCE, NAVIGATION AND CONTROL DESIGN EQUATIONS

## VOLUME III

Revised
March 15, 1973


NATIONAL AERONAUTICS AND SPACE ADMINISTRATION
MANNED SPACECRAFT CENTER
HOUSTON, TEXAS

Prepared by
Systems Analysis Branch
Guidance and Control Division

K. J. Cox

K. J. Cox, Chief
Systems Analysis Branch


Authorized for Distribution William C. Bradford
for Maxime A. Faget
Director of Engineering and Development

VOLUME III

TABLE OF CONTENTS


| | | |
|---|---|---|
| 1. | Introduction | 3-1 |
| 2. | Multi-Stage Boost Control | S53-1 |
| 3. | Rendezvous Targeting | S37-1 |
| 4. | Rendezvous Terminal Phase Automatic Braking Sequence and Targeting | S41-1 |
| 5. | Station-Keeping Guidance | S46-1 |
| 6. | Deborbit Targeting | S28-1 |
| 7. | Powered Flight Guidance | S25-1 |
| 8. | Entry Guidance | S44-1, S59-1 |
| 9. | Approach Guidance | S58-1 , S60-1 |
| 10. | Final Approach Guidance | S29-1 |
| 11. | Conic State Extrapolation | S6-1 |
| 12. | Required Velocity Determination, Conic | S24-1 |
| 13. | Required Velocity Determination Precision | S27-1 |
| 14. | Boost Abort Guidance | S51-1 |
| 15. | Sequence | 3-9 |


The other Volumes of this document are:

| | |
|---|---|
| Vol I | STATUS |
| Vol II | NAVIGATION |
| Vol IV | CONTROL |

## Introduction

Guidance activity generally relates to the perturbation of spacecraft trajectory or state by the application of translational control effectors. The Space-Shuttle mission includes three relatively distinct guidance phases: Atomospheric Boost (characterized by an adaptive guidance law), Extra-Atmospheric Activities and Re-Entry Activities (where aerodynamic surfaces are the principal effectors). Guidance tasks include pre-maneuver targeting and powered flight guidance (where powered flight is defined to include the application of aerodynamic forces as well as thruster forces). Figure 3.1 is a flow chart which follows guidance activities throughout the mission from the Pre-launch phase through touchdown. Table 3.1 lists the main guidance programs and subroutines used in each phase of a typical rendezvous mission. A brief description of each such program and routine follows. Detailed software design requirements are presented in Vol. III.

1. Atmospheric Boost Guidance

This program, when completed, will (at a minimum) provide a programmed pitch over and attitude hold until sometime after max-q. It may also include some minimal closed-loop guidance to limit dispersion in the presence of wind and gust disturbances. This program (not yet submitted) will fulfill functional requirement 2G1*.

2. Multi-Stage Boost Guidance

These powered ascent guidance equations provide inertial steering commands during boost to insertion. The equations accommodate to engine throttle capability and to discontinous boost, i.e., PSR shutdown and jettison with controlled thrust from the MPS. These equations fulfill requirement 2G2.

3. Rendezvous Targeting

This Targeting Routine has the capability of constructing inflight the rendezvous maneuver sequence which satisfies the requirements of the particular mission. The routine can handle sequences with any given number of maneuvers, each of which can have a variety of constraints. These equations fulfill requirements 3G2.

4. Rendezvous Braking

This Targeting Routine has the capability to bring the vehicle into the station-keeping zone by automatic line-of-sight corrections and braking corrections. These equations fulfill requirements 3G3.

*Functional Requirement Module (See App. I).

5. Station Keeping Guidance

This targeting Routine is for use during the station-keeping phase and is designed to maintain the orbiter in a small zone which may be arbitrarily located with respect to the target vehicle. The orbiter is maintained in the zone by the periodic application of small velocity corrections computed so as to minimize the average expenditure of propellant per orbit. These equations satisfy requirements [illegible].

6. Deorbit Targeting

This targeting Routine is for the computation of an optional phasing maneuver to place the vehicle in a phasing orbit prior to landing, and an in-plane minimum fuel deorbit maneuver satisfying entry-interface and landing-site constraints. The program is designed to allow the crew to determine [illegible] deorbit opportunities and to select one desired. The program satisfies requirement 3G6.

7. Powered Flight Guidance

These Guidance Routines are for use in computing steering and engine cutoff commands during either a maneuver with a specified velocity change, or a Lambert aim point maneuver, or a deorbit maneuver. The concepts of a current position offset and [illegible] state-vector navigation are used for the Lambert and deorbit [illegible]. Cross product steering is used for all maneuvers. These equations satisfy the requirements 3G1.

8. Entry and Transition Guidance

This routine will provide guidance commands from entry interface through the heat control phase, through transition, to 40,000 feet altitude. The requirements for this phase are 4G1.

9. Approach (Terminal Area) Guidance

This routine provides steering commands which guide the S/S from an altitude of 40,000 ft to a point on the final approach (glide) path at an altitude of approximately [illegible] ft. These requirements are listed as 4G2.

10. Final Approach Guidance

This routine provides steering commands which maintain the shuttle on the two-flare approach path through touchdown. These equations satisfy requirements 4G3.

11. Conic State Extrapolation Subroutines

These subroutines are for conic state vector extrapolation as a function of time (Kepler) or as a function of angle (Theta), and are required both for guidance targeting and for navigation.

12. Precision State and Filter Weighting Matrix Extrapolation

This subroutine has an Encke integration scheme which includes the capability for precision extrapolation of a vehicle state vector and the associated submatrix of the Navigation filter weighting matrix in the earth's $J_2$ gravity field. Additional perturbing accelerations due to higher order gravity terms, lunar and solar gravity, and atmospheric forces have not been included since the requirements for them have not been established. This subroutine is presented in Navigation Volume II.

13. Conic Required Velocity

This subroutine is for the solution to the multi-revolution Lambert required velocity determination problem.

14. Precision Required Velocity

This subroutine is for use by a targeting routine to compute the parameters needed by the Powered Flight Guidance Routines to perform a Lambert aim point or de-orbit maneuver.

15. Abort Guidance Targeting

This program, available only in preliminary form, provides guidance targeting for the transition from booster failure to acquisition of the nominal entry trajectory with virtually empty OMS fuel tanks. This program fulfills some of the requirements of 2G3.

The Multi-Stage Boost Guidance presentation is by R. F. Jaggers of the Boeing Co. There are other designs under consideration, but none differ significantly from the Linear Tangent Guidance which is the basis of Jagger's presentation.

The On-Orbit guidance submittals are the work of C. S. Draper Laboratory. Rendezvous Targeting is documented by W. H. Templeman, Rendezvous Braking by P. M. Kachmar, Station Keeping Guidance by Gustafson and Kreigsman, Deorbit Targeting by Brand and Brennan, Powered Flight Guidance by Brand, Brown, Higgins and Pu, the Precision Required Velocity routine by T. J. Brand and the Conic State routine, the Precision State routine and the Conic Required Velocity routine by W. M. Robertson. An alternative Rendezvous design has been published by D. J. Jezewski of the NASA/MSC Mission Planning and Analysis Division. It is anticipated that the Linear Tangent Guidance, in a modified form, will replace the Powered Flight Guidance design documented herein.

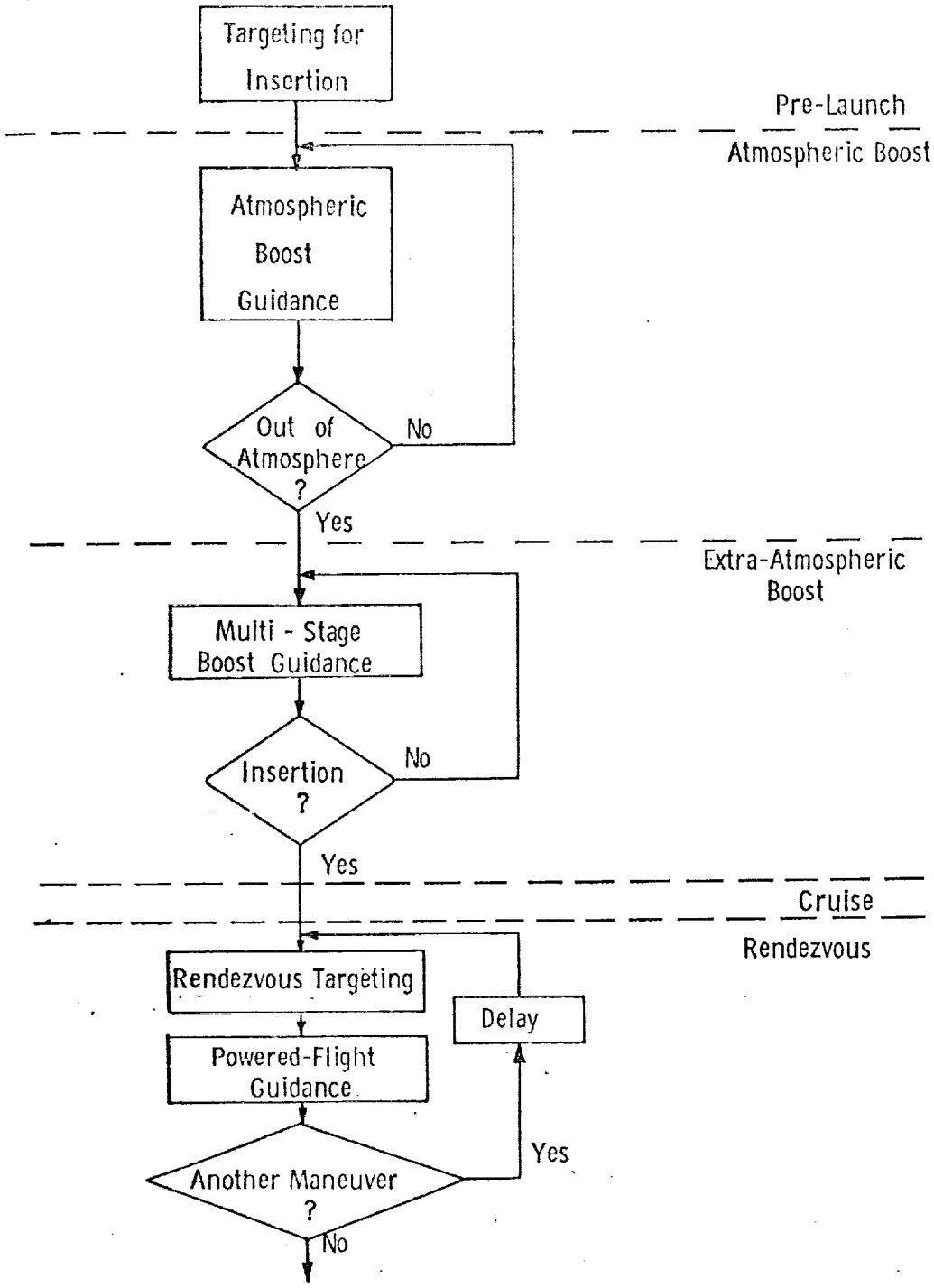


Figure 3.1 Guidance

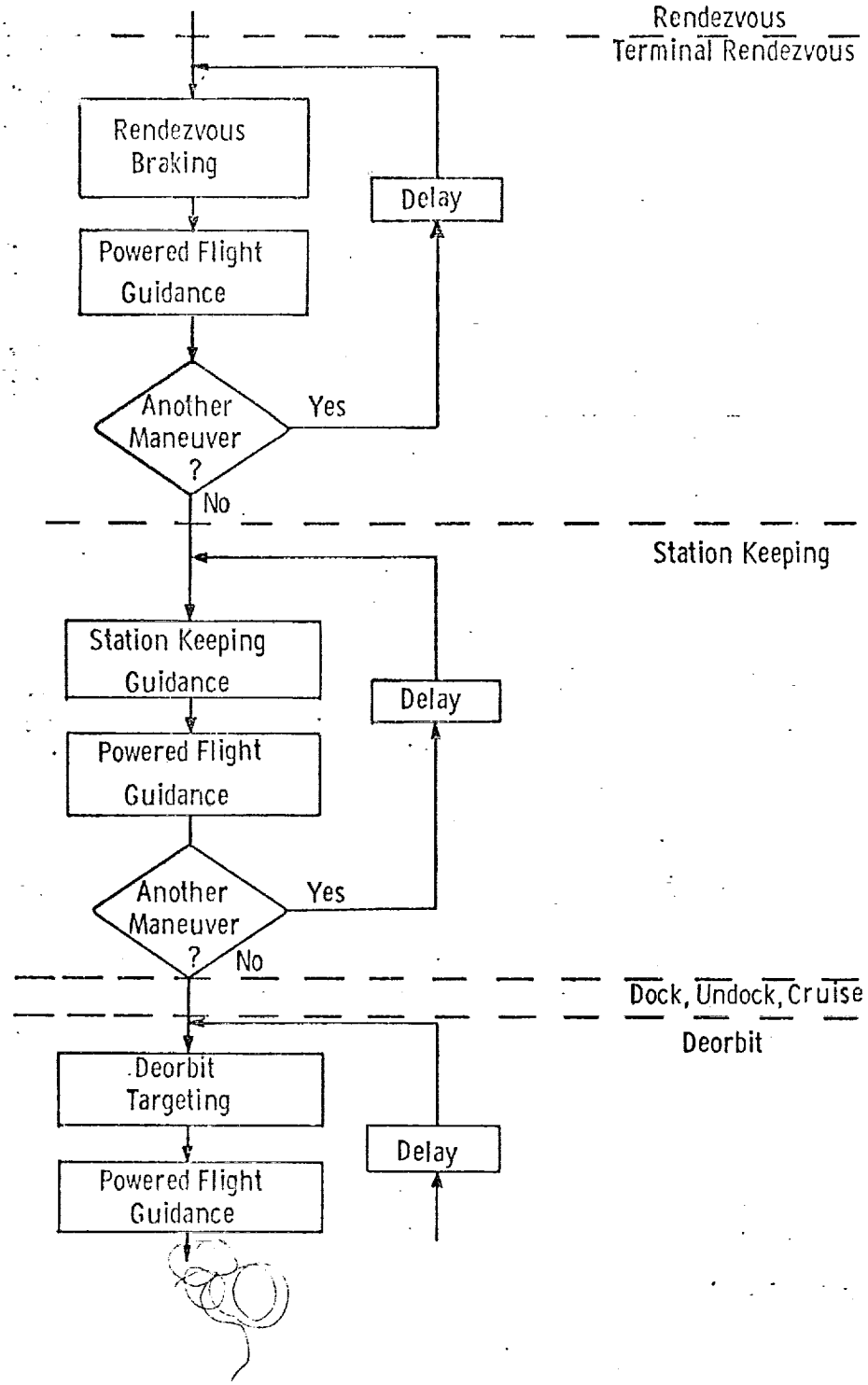
Rendezvous
Terminal Rendezvous
Rendezvous Braking
Delay
Powered Flight Guidance
Another Maneuver ?
Yes
No
Station Keeping
Station Keeping Guidance
Delay
Powered Flight Guidance
Another Maneuver ?
Yes
No
Dock, Undock, Cruise
Deorbit
Deorbit Targeting
Delay
Powered Flight Guidance

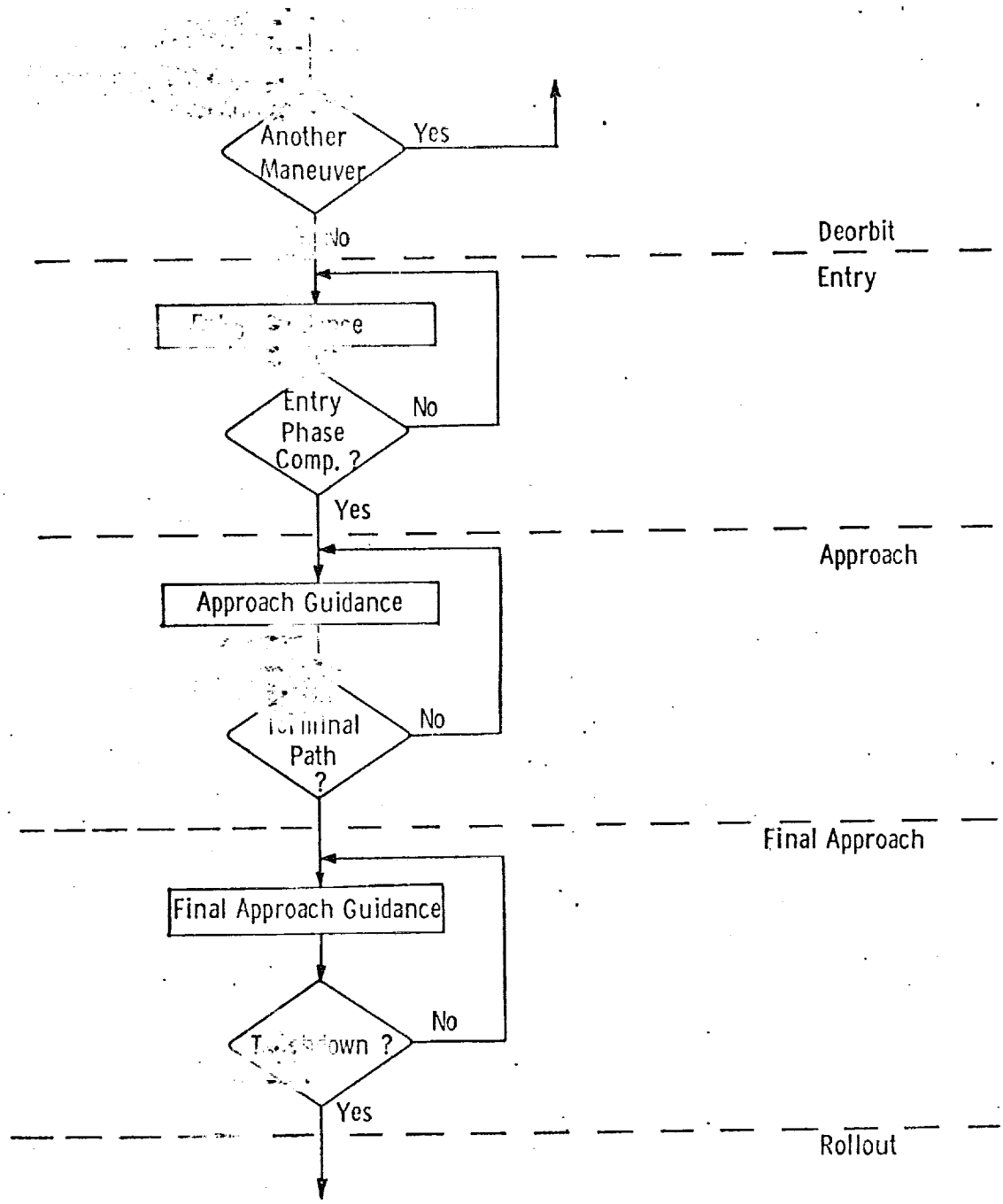
Another Maneuver
Yes
No
Deorbit
Entry
Entry Phase Comp. ?
No
Yes
Approach
Approach Guidance
Path
No
Final Approach
Final Approach Guidance
No
Yes
Rollout

| MISSION PHASE | MAIN PROGRAM | SUBROUTINES | | | | |
|---|---|---|---|---|---|---|
| | | KEPLER C-ST | THETA C-ST | PRECISION STATE | CONIC REQ. VEL. | PREC. REQ. VEL. |
| BOOST | ATM. BOOST GUIDANCE<br>MULTI-STAGE BOOST GUID. | | | | | |
| RENDEZVOUS | * RENDEZVOUS TARG.<br>* POW. FLIGHT GUID. | ✓<br>✓ | ✓ | ✓<br>✓ | ✓<br>✓ | ✓ |
| TERMINAL RENDEZVOUS | * RDZ BRAKING<br>* POW. FLIGHT GUID. | ✓<br>✓ | | ✓<br>✓ | ✓<br>✓ | ✓ |
| STATION KEEPING | * S-K GUIDANCE<br>* POW. FLIGHT GUID. | <br>✓ | | <br>✓ | <br>✓ | |
| DEORBIT | * DEORBIT TARGETING<br>* POW. FLIGHT GUID. | ✓<br>✓ | ✓ | ✓<br>✓ | ✓<br>✓ | ✓ |
| ENTRY LANDING | ENTRY GUIDANCE<br>APPROACH GUIDANCE<br>FINAL APPR. GUID. | | | | | |

*TARGETING AND POWERED FLIGHT GUIDANCE USED SEQUENTIALLY FOR EACH MANEUVER

TABLE 3.1 SHUTTLE GUIDANCE

The Entry through Landing guidance submittals are produced by Kriegsman (CSDL) and Harpold (MPAD) for Entry, NASA/MSC Crew Procedures Division (documented by Tao) and Elias (CSDL) for Approach, and D. Dyer of GCD for Final Approach. Other Entry Guidance designs include Fast Time Integration by Sunkel (G&CD). The Harpold design and the Kriegsman design for Entry Guidance are both included in this volume because both have outstanding features and it is conjectured that the final design will represent a combination of the best features of each. Likewise both the Crew Procedures and the Elias designs are presented in expectation that the final design will include features of each. An alternate Terminal Area Approach design by T. Moore (GCD) is more complicated, but is a strong contender for implementation because it includes capability for low-altitude redesignation.

The preliminary Boost Abort Targeting submittal is by G. McSwain of G&C Div., NASA/MSC.

Except for Boost Abort Targeting all Guidance submittals are complete, according to the requirements of Appendix I.

## Introduction

The purpose of the powered ascent guidance equations is to provide inertial steering commands during the boost to orbit maneuver. Throttle setting can also be provided if this is a requirement of boost guidance, however, this feature is not incorporated in the equations presented here.

The linear tangent guidance law presented here was developed to meet at least the following requirements: multi-stage capability, ability to handle flight perturbations and maintain orbital insertion accuracy, abort to alternate conditions, engine out capability, and throttle for constant acceleration.

## Computational Flow of Multi-Stage Guidance Equations

Guidance input and output parameters are listed and defined below. Essentially, guidance input is the present state vector and orbital parameters defining the desired terminal state vector, and the output is steering commands and time-to-go.

### Guidance Presettings (PREFLIGHT INPUT)

| | |
|---|---|
| $R_D$ | Magnitude of desired terminal radius vector |
| $V_D$ | Magnitude of desired terminal velocity vector |
| $\gamma_D$ | Desired terminal flight path angle |
| $G_{21}$ | X component of unit vector normal to desired orbit plane* |
| $G_{23}$ | Z component of unit vector normal to desired orbit plane* |
| $V_{ex_i}$ | Effective exhaust velocity of stage i |
| $\tau_i$ | Initial m to m ratio of stage i |
| $T_{Bi}$ | Nominal burn time of stage i |
| $T_{Ci}$ | Coast time between stage i and stage i + 1 |
| $a_{Li}$ | Acceleration limit of stage i |
| n | Number of guided stages |

### Navigational Quantities (INFLIGHT MEASURED INPUT)

| | |
|---|---|
| $\bar{a}_p$ | Inertial platform measured acceleration vector |
| $\bar{V}_p$ | Inertial platform velocity vector |
| $\bar{R}_p$ | Inertial platform radius vector |
| $\bar{g}_p$ | Inertial platform gravity vector (Calculated function of $\bar{R}_p$) |

---

* Optional inputs are $i_D$, desired inclination, and $\theta_D$, desired longitude of descending node.

Guidance Output

| | |
|---|---|
| $\theta_c$ | Commanded inertial pitch angle |
| $\psi_c$ | Commanded inertial yaw angle |
| $T_{GO}$ | Time-to-go till orbital insertion |
| f | Throttle setting if applicable (to be determined) |

Guidance Precalculations

(Coordinate transformation from platform system to desired orbit system)

Input $G_{21}$ and $G_{23}$, X and Z components of unit vector normal to desired orbit plane. Compute unit vector in desired orbit plane normal to launch vertical, and unit vector defined by intersection of desired orbit plan and the plane containing launch vertical and vector normal to desired orbit.

$$G_{22} = (1 - G_{21}^2 - G_{23}^2)^{1/2}$$

$$G_{11} = (G_{22}^2 + G_{23}^2)^{1/2}$$

$$G_{31} = 0$$

$$G_{32} = -G_{23}/G_{11}$$

$$G_{33} = G_{22}/G_{11}$$

$$G_{12} = -G_{21}G_{33}$$

$$G_{13} = G_{21}G_{32}$$

NOTE: For due East launch and no plane change, $[G] = \begin{bmatrix} 1 & 0 & 0 \\ 0 & 1 & 0 \\ 0 & 0 & 1 \end{bmatrix}$

ENTER GUIDANCE PRE-TURN ON

Inp[illegible] $\theta_D$

$$\begin{bmatrix} G_{21} \\ G_{22} \\ G_{23} \end{bmatrix} = \begin{bmatrix} \cos\psi_L & \sin A_L & -\sin\psi_L \cos A_L \\ 0 & \cos A_L & \sin A_L \\ \sin\psi_L & -\cos\psi_L \sin A_L & \cos\psi_L \cos A_L \end{bmatrix}^T \begin{bmatrix} \sin i_D \sin\theta_D \\ -\sin i_D \cos\theta_D \\ -\cos i_D \end{bmatrix}$$

$G_{11} = (G_{22}^2 + G_{23}^2)^{1/2}$

$G_{31} = 0$

$G_{32} = -G_{23}/G_{11}$

$G_{21} = G_{22}/G_{11}$

$G_{12} = -G_{21}G_{33}$

$G_{33} = G_{21}G_{32}$

DESIRED ORBIT COORDINATE SYSTEM, G MATRIX

$i = 1$
$T_{GO} = 0$

$T_{Li} = T_{Bi}$
$U_{Yi} = G_{2i}$
$T_{GO} = T_{GO} + T_{Bi} + T_{Ci}$

$i = n$

NO → $i = i+1$

YES → $k = 1$

EXIT TO GUIDANCE

$A_L$ = Launch Azimuth

$\psi_L$ = Geodetic Launch Latitude

$i_D$ = Desired orbit inclination

$\theta_D$ = Desired Longitude of descending node (measured from launch meridian)

ENTER GUIDANCE (MAJOR CYCLE LOOP)

$$\bar{R}_4 = [G]\ \bar{R}_p$$

$$\phi_o = \tan^{-1}(Z_4/X_4)$$

INITIAL RANGE ANGLE

$$\hat{U}_Z = \text{Unit}\ (\bar{R}_p \times \hat{U}_y)$$

$$\hat{U}_X = \hat{U}_y \times \hat{U}_Z$$

$$[E] = \begin{bmatrix} U_{X1} & U_{X2} & U_{X3} \\ U_{Y1} & U_{Y2} & U_{Y3} \\ U_{Z1} & U_{Z2} & U_{Z3} \end{bmatrix}$$

LOCAL GUIDANCE COORDINATE SYSTEM

$$\bar{R}_G = [E]\ \bar{R}_p$$

$$\bar{V}_G = [E]\ \bar{V}_p$$

RADIUS AND VELOCITY IN LOCAL GUIDANCE FRAME

$$a = \text{ABS}\ (\bar{a}_p)$$

MEASURED ACCELERATION MAGNITUDE

$$R = \text{ABS}\ (\bar{R}_p)$$

$$g_r = -(\bar{g}_p \cdot \bar{R}_p)/R$$

$$g_{AV} = .5\ g_r \left[1 + \left(\frac{R}{R_D}\right)^2\right]$$

AVERAGE RADIAL GRAVITY MAGNITUDE

1

k = NO. OF PRESENT BURNING STAGE

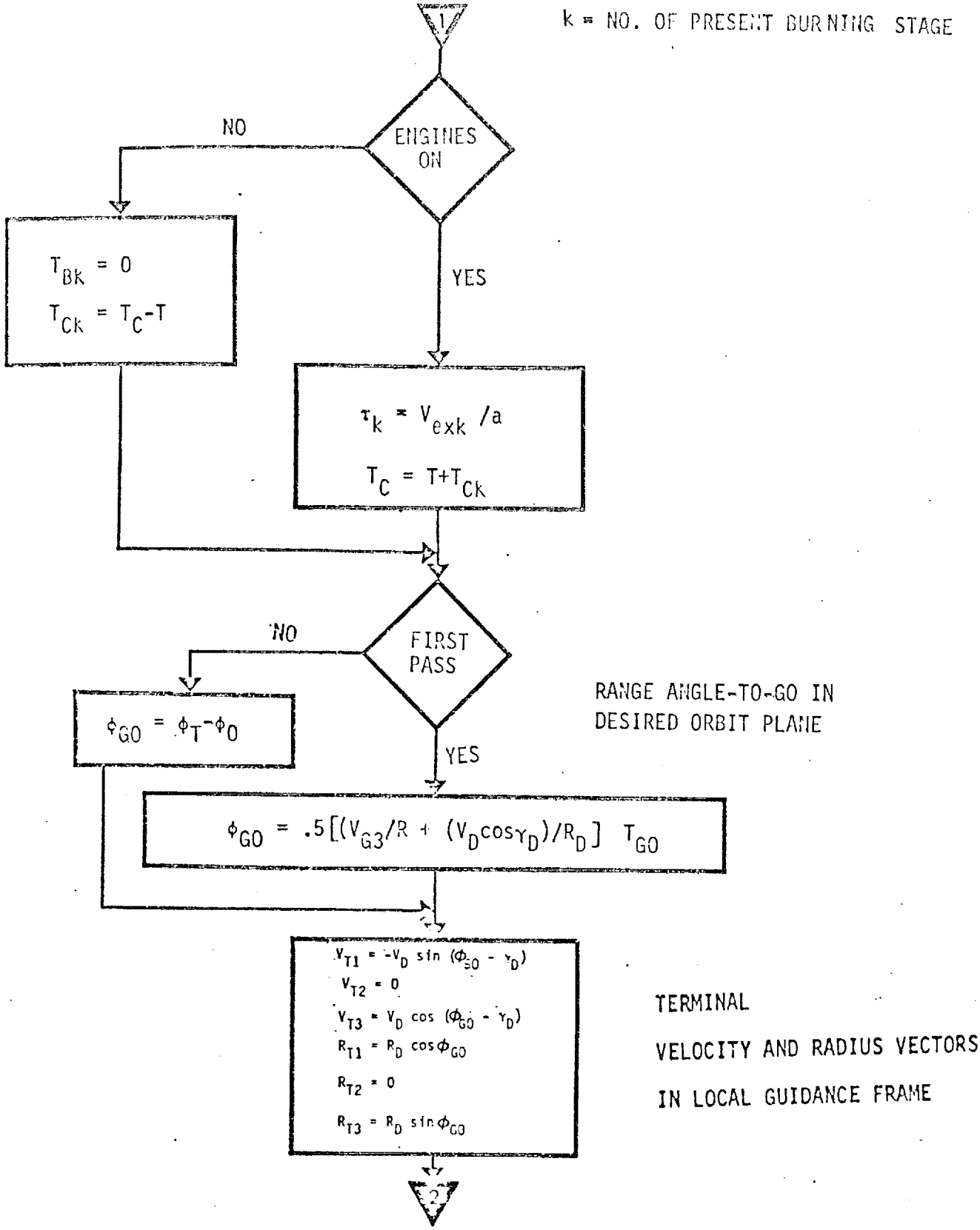


RANGE ANGLE-TO-GO IN DESIRED ORBIT PLANE

TERMINAL VELOCITY AND RADIUS VECTORS IN LOCAL GUIDANCE FRAME

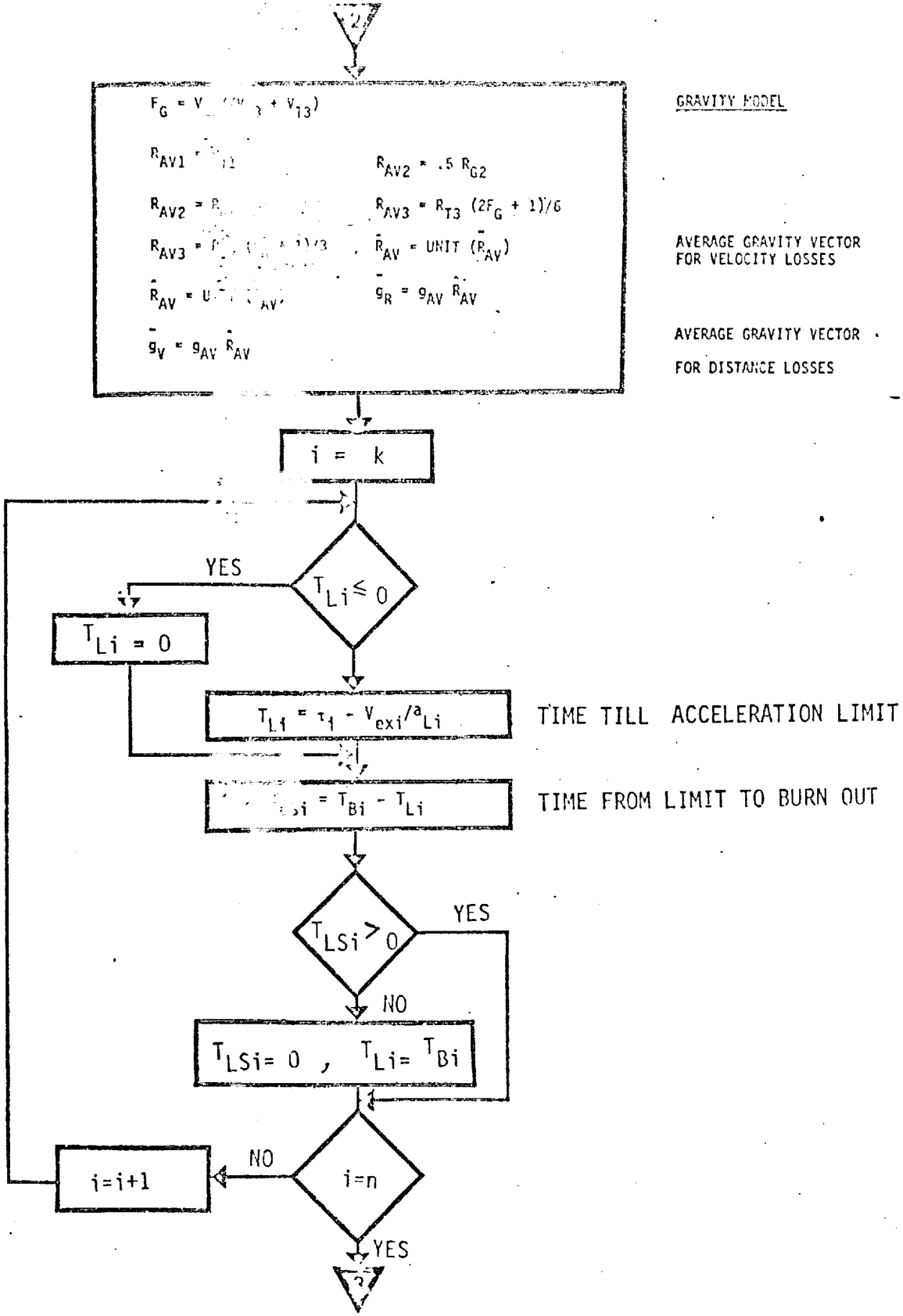
GRAVITY MODEL
$F_G = V$ [illegible] $+ V_{T3})$
$R_{AV1}$ [illegible]
$R_{AV2} = .5\ R_{G2}$
$R_{AV2} = R$ [illegible]
$R_{AV3} = R_{T3}\ (2F_G + 1)/6$
$R_{AV3} = R$ [illegible] $+ 1)/3$
$\bar{R}_{AV} = \text{UNIT}\ (\bar{R}_{AV})$
AVERAGE GRAVITY VECTOR FOR VELOCITY LOSSES
$\bar{R}_{AV} = U$ [illegible] $_{AV}$
$\bar{g}_R = g_{AV}\ \bar{R}_{AV}$
$\bar{g}_V = g_{AV}\ \bar{R}_{AV}$
AVERAGE GRAVITY VECTOR FOR DISTANCE LOSSES
$i = k$
$T_{Li} \leq 0$
YES
$T_{Li} = 0$
$T_{Li} = \tau_1 - V_{exi}/a_{Li}$
TIME TILL ACCELERATION LIMIT
[illegible] $_{Si} = T_{Bi} - T_{Li}$
TIME FROM LIMIT TO BURN OUT
$T_{LSi} > 0$
YES
NO
$T_{LSi} = 0\ ,\ T_{Li} = T_{Bi}$
$i = n$
NO
$i = i+1$
YES

## TIME-TO-GO CALCULATION

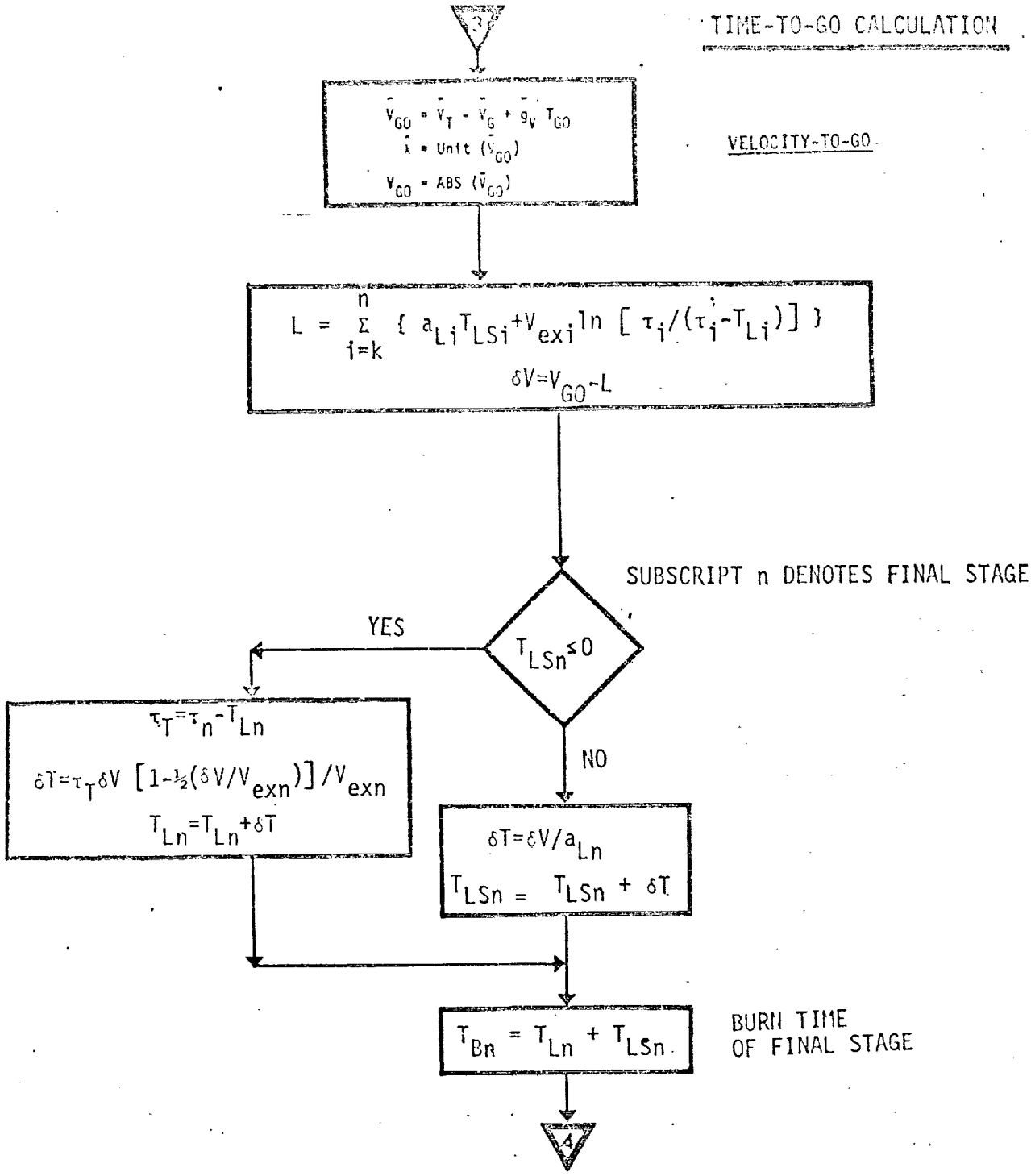

## TIMES USED FOR MULTI-STAGE INTEGRALS

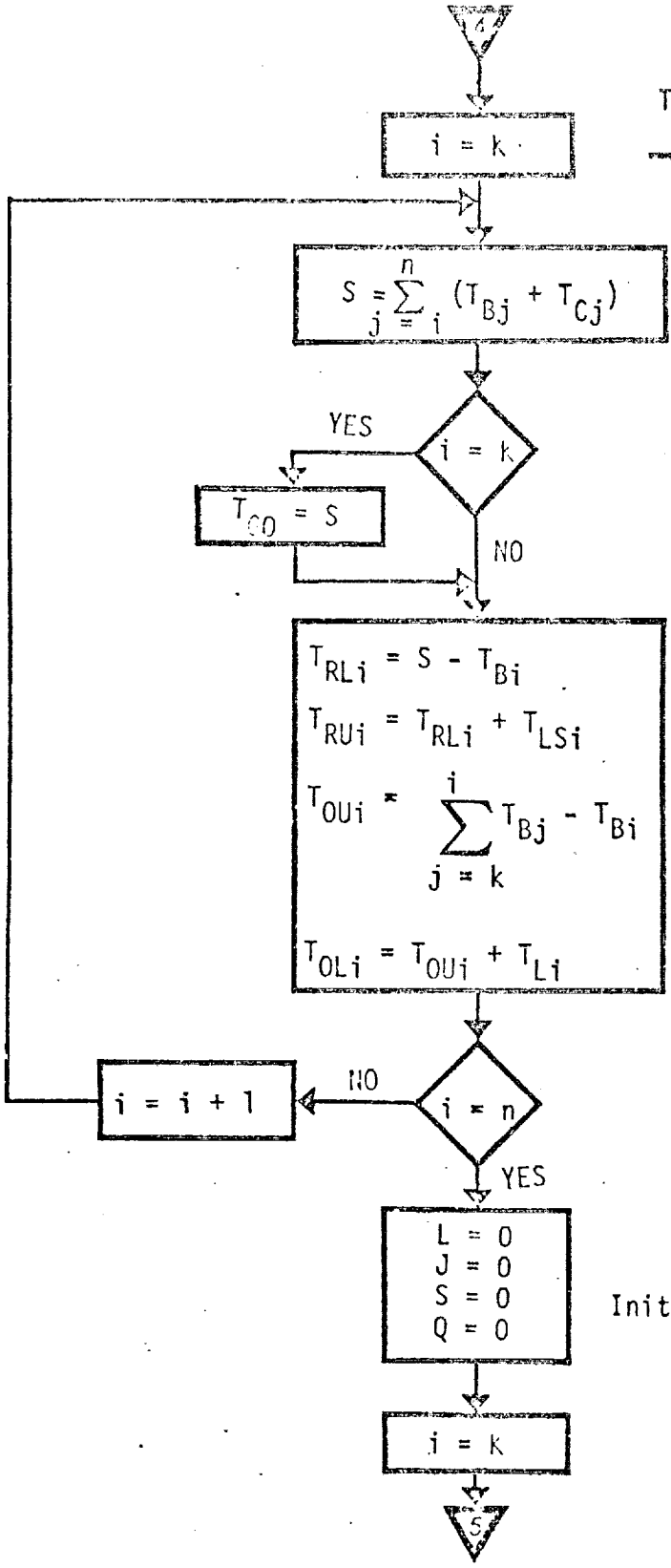


k = No. of present burning stage

n = No. of final stage

Time remaining after constant acceleration burn

Time remaining after constant thrust burn

Initial Time of constant thrust burn

Initial Time of constant acceleration burn

Initialize Summation Loop

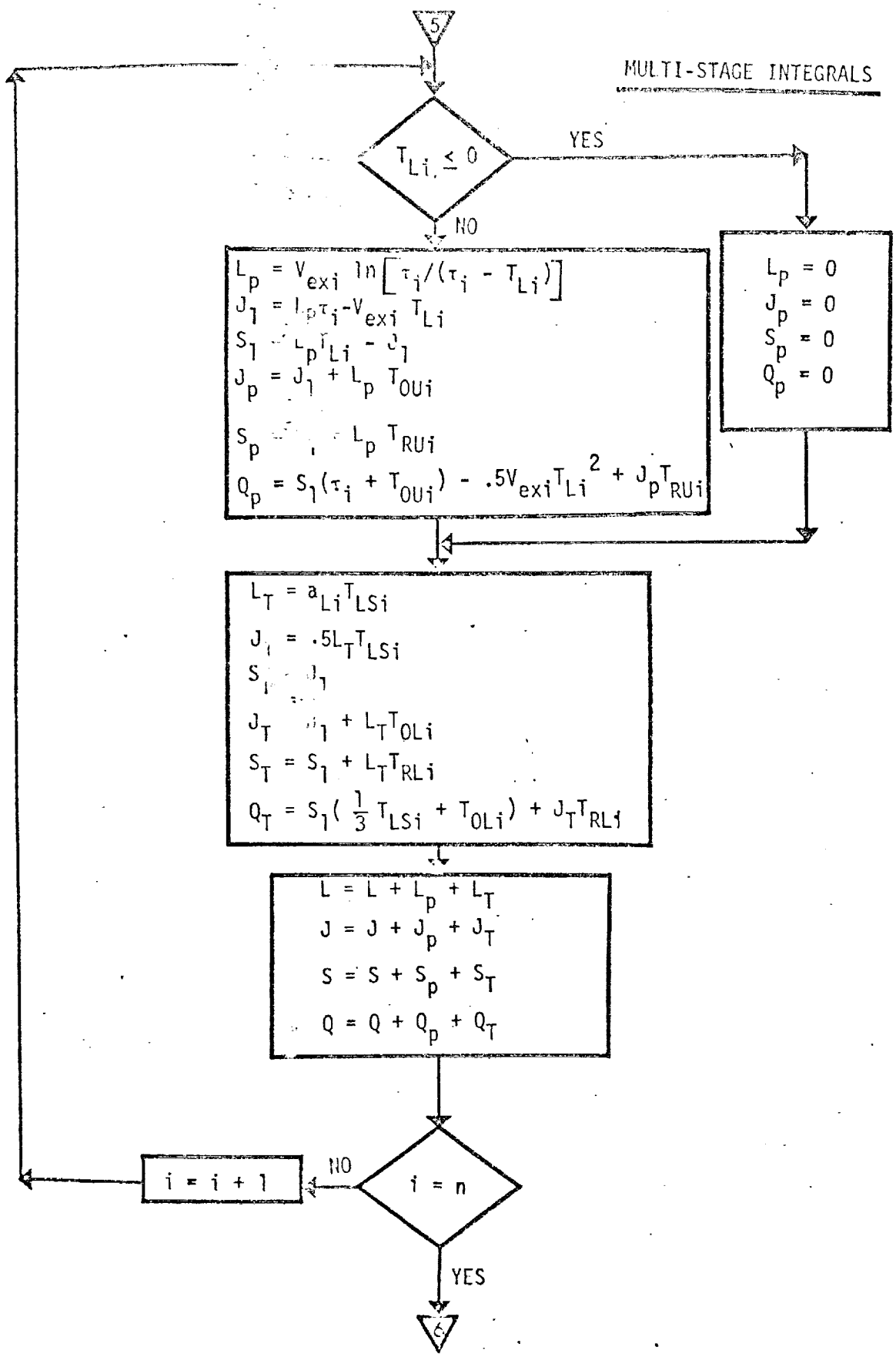
5
MULTI-STAGE INTEGRALS
$T_{Li} \leq 0$
YES
NO
$L_p = V_{exi} \ln[\tau_i/(\tau_i - T_{Li})]$
$J_1 = L_p\tau_i - V_{exi} T_{Li}$
$S_1 = L_p T_{Li} - J_1$
$J_p = J_1 + L_p T_{OUi}$
$S_p = S_1 + L_p T_{RUi}$
$Q_p = S_1(\tau_i + T_{OUi}) - .5V_{exi}T_{Li}^2 + J_pT_{RUi}$
$L_p = 0$
$J_p = 0$
$S_p = 0$
$Q_p = 0$
$L_T = a_{Li}T_{LSi}$
$J_1 = .5L_TT_{LSi}$
$S_1 = J_1$
$J_T = J_1 + L_TT_{OLi}$
$S_T = S_1 + L_TT_{RLi}$
$Q_T = S_1(\frac{1}{3}T_{LSi} + T_{OLi}) + J_TT_{RLi}$
$L = L + L_p + L_T$
$J = J + J_p + J_T$
$S = S + S_p + S_T$
$Q = Q + Q_p + Q_T$
$i = n$
NO
$i = i + 1$
YES
6

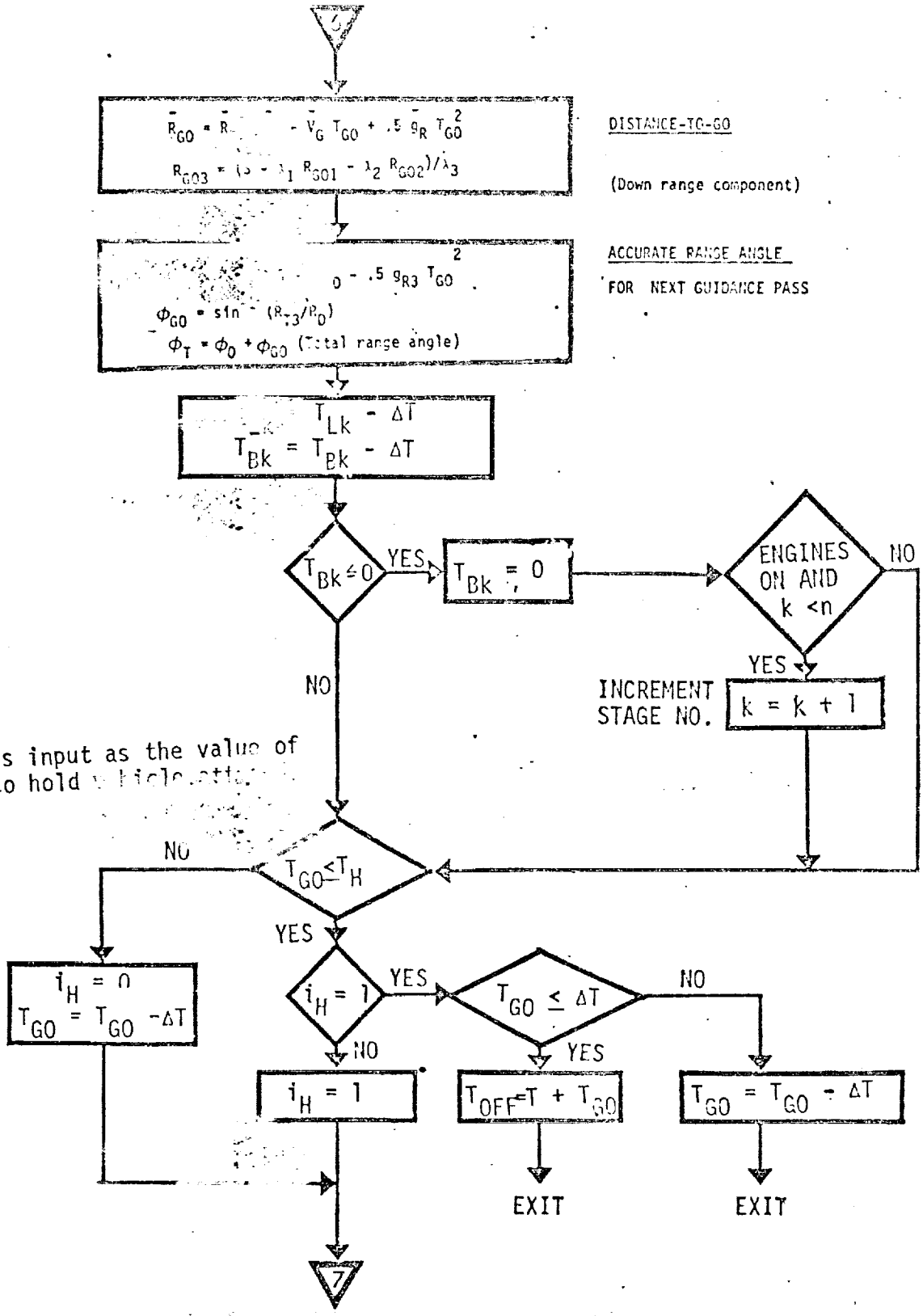
6
$\bar{R}_{GO} = \bar{R}$ [illegible] $- \bar{V}_G T_{GO} + .5\, \bar{g}_R T_{GO}^2$
$R_{GO3} = (\bar{\lambda}_3 - \lambda_1 R_{GO1} - \lambda_2 R_{GO2})/\lambda_3$
DISTANCE-TO-GO
(Down range component)
[illegible] $_0 - .5\, g_{R3} T_{GO}^2$
$\Phi_{GO} = \sin^{-1} (R_{T3}/R_0)$
$\Phi_T = \Phi_0 + \Phi_{GO}$ (Total range angle)
ACCURATE RANGE ANGLE
FOR NEXT GUIDANCE PASS
$T_{Lk} = \Delta T$
$T_{Bk} = T_{Bk} - \Delta T$
$T_{Bk} \leq 0$
YES
$T_{Bk} = 0$
ENGINES ON AND $k < n$
NO
YES
INCREMENT STAGE NO.
$k = k + 1$
NO
$T_H$ is input as the value of
$T_H$ to hold vehicle attitude
$T_{GO} \leq T_H$
NO
YES
$i_H = 0$
$T_{GO} = T_{GO} - \Delta T$
$i_H = 1$
YES
$T_{GO} \leq \Delta T$
NO
NO
YES
$i_H = 1$
$T_{OFF} = T + T_{GO}$
$T_{GO} = T_{GO} - \Delta T$
EXIT
EXIT
7

7

$$K = J/L$$

$$D = Q - SK$$

$$\dot{\bar{\lambda}} = (\bar{R}_{GO} - \hat{\lambda}S)/D$$

STEERING VECTOR RATE

$$\hat{\lambda}_p = [E]^T \hat{\lambda}$$

$$\dot{\bar{\lambda}}_p = [E]^T \dot{\bar{\lambda}}_p$$

$$T_0 = T$$

TRANSFORM COMPONENTS OF STEERING VECTOR FROM LOCAL GUIDANCE FRAME TO PLATFORM FRAME

EXIT MAJOR CYCLE LOOP

---

ENTER MINOR CYCLE LOOP

$$\Delta t = T - T_0$$

$$\bar{\lambda} = \hat{\lambda}_p + \dot{\bar{\lambda}}_p (\Delta t - K)$$

INERTIAL STERRING ANGLE COMMANDS

$$\theta_c = \tan^{-1} (\lambda_1/\lambda_3) - \pi/2 \quad \text{(PITCH)}$$

$$\psi_c = \tan^{-1} \left[ \lambda_2/(\lambda_1^2 + \lambda_3^2)^{1/2} \right] \text{(YAW)}$$

EXIT

# 1. INTRODUCTION

The rendezvous of the Orbiter (primary vehicle) with a target vehicle (e.g. the Space Station) is accomplished by maneuvering the Orbiter into a trajectory that intercepts the target vehicle orbit at a time that results in the rendezvous of the two vehicles. The function of rendezvous targeting is to determine the targeting parameters for the powered flight guidance for each of the maneuvers made by the Orbiter during the rendezvous sequence.

In order to construct the multimaneuver rendezvous trajectory, sufficient constaints must be imposed to determine the desired trajectory. Constraints associated with the Orbiter mission will involve such considerations as fuel, lighting, navigation, communication, time, and altitude. The function of premission analysis is to convert these—which are generally qualitative constraints-into a set of secondary quantitative constraints that can be used by the onboard targeting program. By judicious selection of the secondary constraints, it should be possible to determine off-nominal trajectories that come close to satisfying the primary constraints.

The proposed onboard rendezvous targeting program consists primarily of a main program and a generalized multiple-option maneuver subroutine. The driving program automatically and sequentially calls the maneuver subroutine to construct the rendezvous configuration from a series of maneuver segments. The main program is capable of handling rendezvous sequences involving any given number of maneuvers. Enough different types of maneuver constraints are incorporated into the subroutine to provide the flexibility required to select the best set of secondary constraints during premission planning. In addition, the astronaut has a large, well defined list of maneuver options if he chooses to modify the selected nominal rendezvous scheme.

As the new approach represents, in essence, just one targeting program, there is considerable savings in computer-storage requirements compared to former approaches in which each maneuver used in the rendezvous scheme had a separate targeting program. The programming and verification processes of this unified approach will also result in implementation efficiencies.

## 1.1 Number of Independent Constraints Involved in a Rendezvous Sequence

During the Gemini and Apollo flights and in the design of the Skylab rendezvous scheme various numbers of maneuvers were utilized in the rendezvous sequence. The range went from two (Apollo 14 and 15) to six (Skylab).

The number of independent constraints (i.e., the number of explicitly satisfied constraints) in each rendezvous sequence must equal the number of degrees of freedom implicitly contained in the sequence. To establish this number, a rendezvous configuration can be constructed by imposing arbitrary constraints until the configuration is uniquely defined. For example, a four maneuver coplanar sequence is shown in Figure 1, followed by [illegible] terminal point. Using the constraints $v_i$ (velocity magnitude), $r_i$ a[illegible] easy to establish that the total number involved is 12, assuming the time of the first maneuver has been established. Removing one maneuver will reduce the number of degrees of freedom by three. Hence, the number of independent constraints necessary to uniquely determine the maneuver sequences are

| Number of maneuvers in sequence | Number of independent constraints required |
|---|---|
| 1 | 3 |
| 2 | 6 |
| 3 | 9 |
| 4 | 12 |
| etc | |

If the above rendezvous are not coplanar, one additional constraint has to be added to each sequence to allow for the out-of-plane component.

In some cases the number of [illegible]y constraints may be insufficient to uniquely determine a rendezvous trajectory for the desired number of maneuvers. One way of overcoming this deficiency in constraints is by introducing sufficient variables to complete the determination of the rendezvous trajectory and then determining values for these variables by minimizing the fuel used.

In order to take advantage of updated state vectors due to navigation or ground updates, the rendezvous targeting program is called prior to each maneuver to compute the upcoming maneuver. In general, each maneuver computation will involve a multimaneuver sequence as the nature of the targeting constraints do not allow the maneuvers to be independently computed. The relationship between the rendezvous sequence involving n m[illegible]vers and the maneuver sequences is shown below.

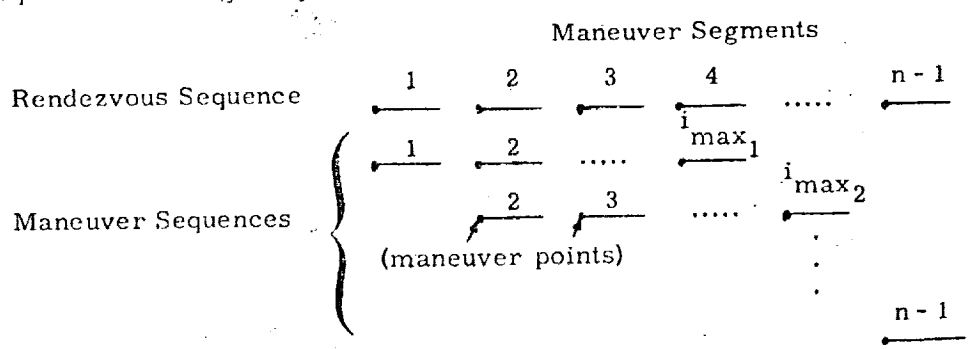

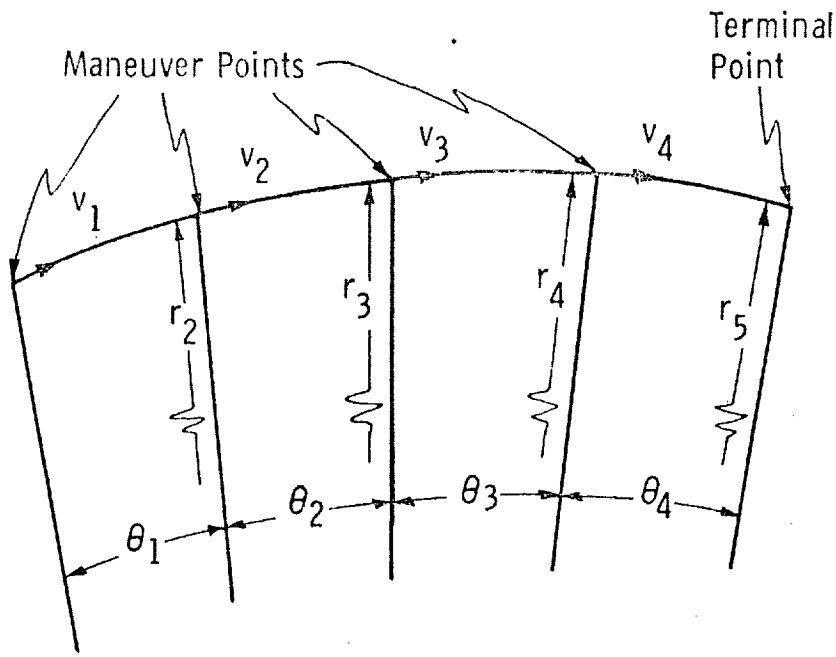


Figure 1. A Possible Set of Constraints Involved in a Four Maneuver Rendezvous Sequence

Each maneuver s[illegible] is composed of a number of maneuver segments and is basically indepe[illegible] from the other maneuver sequences. These sequences must have the same n[illegible] independent constraints as tabulated above.

## 1.2 The Con[illegible]action of a Maneuver Segment

Each n-1[illegible] ezvous sequence can be divided into n-1 maneuver segments. Each se[illegible]s, basically, the addition of a maneuver to the primary vehicle's velocity v[illegible] and an update of both vehicle's state vectors to the next maneuver point.

A maneuver segment is herein generated in one of three ways:

**Forward generation** — A maneuver $\Delta \underline{v}$ is computed and added to the velocity vector in a specified direction. The state vector of the primary vehicle is then updated through a specified amount to arrive at the next maneuver position.

**Target generation** — The target vehicle is updated through a specified amount and then offset to establish a target vector. An option is available at this point to compute a coelliptic velocity vector and update through $\Delta t$ to establish a new target vector as shown below.

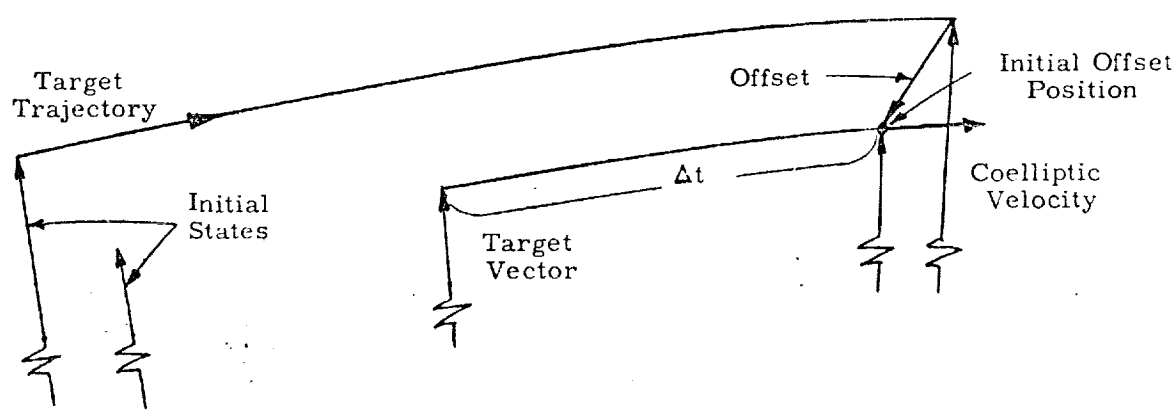


The maneuver is then computed by uniquely specifying the nature of the traverse between the primary vehicle's position and the target vector.

Integrated generation — In this case, the maneuver segment is computed as an integral part of a maneuver sequence involving more than one maneuver segment. The nature of the constraints are such that the maneuver sequence cannot be subdivided into uniquely defined maneuver segments. The maneuver segment will usually have one degree of freedom, which will generally be assumed to be the magnitude of the maneuver.

Each of the above methods is defined by specifying trajectory constraints by setting certain switches and parameter values. Specifying a trajectory constraint is equivalent to specifying one or more independent constraints. On the other hand, specifying an independent constraint can also be equivalent to specifying one or more trajectory variables. (See Ref. 9) A trajectory constraint common to all three of the above methods is the state vector update switch $s_{update}$. The options associated with this switch are:

$$s_{update} = \begin{cases} 1 & \text{Update from time } t \text{ to time } t_F \\ 2 & \text{Update through time interval } \Delta t \\ 3 & \text{Update through } n \text{ revolutions} \\ 4 & \text{Update through } \theta \text{ radians} \\ 5 & \text{Update to be colinear with a specified position vector} \end{cases}$$

In the next three sections, the trajectory constraints associated with each of the above methods will be listed.

### 1.2.1 Maneuver Options in Forward Generation of Maneuver Segment

The forward generation of a maneuver segment is accomplished in one of two ways. Either the maneuver magnitude is uniquely determined in terms of the state vector at the maneuver time or the maneuver is determined by an iterative search to satisfy a terminal constraint.

The maneuver magnitude $\Delta v$ is either calculated or assumed depending on the maneuver switch $s_{man}$, and it is applied in a direction controlled by the direction switch $s_{direct}$. The options associated with the maneuver switch are:

$$s_{man} = \begin{cases} 1 & \Delta v \text{ is assumed specified} \\ 2 & \Delta v \text{ is computed based on a post maneuver velocity vector being "coelliptic" with the state vector of the target vehicle} \\ 3 & \Delta v \text{ is computed from the conic circular velocity constraint} \\ 4 & \Delta v \text{ is computed based on a Hohmann type transfer resulting in a } \Delta h \text{ change in altitude} \end{cases}$$

The options associated with the maneuver direction switch are:

$$s_{direct} = \begin{cases} -1 & \text{Apply } \Delta v \text{ is horizontal direction in plane of primary vehicle} \\ 1 & \text{Apply } \Delta v \text{ in horizontal direction parallel to orbital plane of the target vehicle} \\ -2 & \text{Apply } \Delta v \text{ along velocity vector in plane of primary vehicle} \\ 2 & \text{Apply } \Delta v \text{ along velocity vector parallel to orbital plane of the target vehicle} \end{cases}$$

The selection of the update switch $s_{update_P}$ determines the update of the primary vehicle's trajectory following the maneuver to the position of the next maneuver. A terminal constraint can be imposed at this point by setting the terminal switch $s_{term}$:

$$s_{term} = \begin{cases} 1 & \text{Terminal constraint is a height constraint} \\ -1 & \text{Terminal constraint is a phasing constraint} \end{cases}$$

Following the computation of the height/phasing error, the maneuver magnitude is varied in an iterative search to satisfy the height/phasing constraint.

### 1.2.2 Maneuver Options in Target Generation of Maneuver Segment

The target generation of a maneuver segment starts with the selection of the update switch for the target vehicle. If this switch equals four, $\theta$ will be augmented by the central angle between the primary and target vehicles before being used. The position of the target vehicle is then offset through either $(e_L, \Delta h)$ or $(\Delta\theta, \Delta h)$, depending on whether $s_{tar}$ is negative or positive, to obtain a target vector. The "TPI offsets" $(e_L, \Delta h)$ are discussed in Section 5 (see Figure 2 for definition of $e_L$). If $|s_{tar}|$ equals two, a coelliptic velocity vector is computed based on the target vector, and a new target vector is defined by updating the coelliptic state vector through $\Delta t$. The options associated with $s_{tar}$ are:

$$s_{tar} = \begin{cases} -2 & \text{Offset target } (e_L, \Delta h). \text{ Compute coelliptic velocity and update through (negative) } \Delta t. \\ -1 & \text{Offset target } (e_L, \Delta h) \\ 0 & \text{No target offset} \\ 1 & \text{Offset target } (\Delta\theta, \Delta h) \\ 2 & \text{Offset target } (\Delta\theta, \Delta h). \text{ Compute coelliptic velocity and update through (negative) } \Delta t \end{cases}$$

The nature of the traverse between the primary vehicle's initial state vector and the target vector is controlled by the maneuver switch $s_{man}$:

$$s_{man} = \begin{cases} 5 & \text{Lambert - the trajectory is time constrained} \\ 6 & \text{Horizontal - the maneuver is constrained to be in the horizontal direction} \\ 7 & \text{Tangential - the maneuver is constrained to be in the direction of the velocity vector} \\ 8 & \text{Apogee/Perigee - the trajectory has an apogee/perigee occurring at the target point.} \end{cases}$$

There is a minimum $\Delta v$ option associated with the above maneuvers which is controlled with the optimization switch $s_{opt}$:

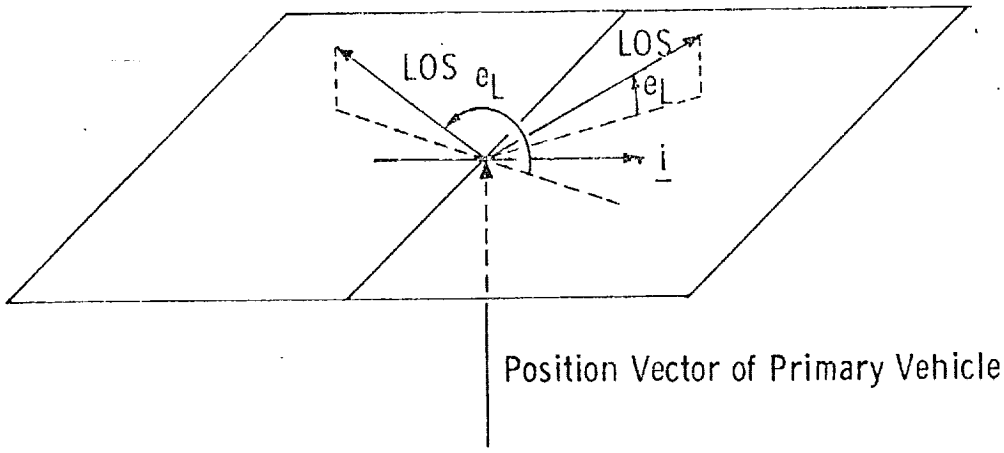


$\underline{i}$ = Unit horizontal in forward direction for primary vehicle

LOS = Line of Sight

1. If the LOS projection on $\underline{i}$ is positive:
   a. When the LOS is above the horizontal plane, $0 < e_L < \pi/2$
   b. When the LOS is below the horizontal plane, $3\pi/2 < e_L < 2\pi$
2. If the LOS projection on $\underline{i}$ is negative:
   a. When the LOS is above the horizontal plane, $\pi/2 < e_L < \pi$
   b. When the LOS is below the horizontal plane, $\pi < e_L < 3\pi/2$

Figure 2. Definition of the Elevation Angle $e_L$

$$s_{opt} = \begin{cases} -2 & \text{Minimize the sum of the magnitude of the first and the next maneuver (based on a coelliptic parting velocity) by varying } \Delta t\text{, the time of update of the target vehicle.} \\ -1 & \text{Minimize the magnitude of the first maneuver by varying } \Delta t\text{, the time of update of the target vehicle.} \\ 1 & \text{Minimize the magnitude of the first maneuver by varying } \Delta t\text{, the time between the next maneuver and the initial offset position. (See sketch on page 1-4 )} \\ 2 & \text{Minimize the sum of the magnitudes of the first and the next maneuver (based on a coelliptic parting velocity) by varying } \Delta t\text{, the time between the next maneuver and the initial offset position (see sketch on page 1-4 ).} \end{cases}$$

This minimization is accomplished by driving the slope ($\Delta v$ / independent variable) to zero using a Newton Raphson iteration scheme.

### 1.2.3 Maneuver Options - Integrated Generation of Maneuver Segment

The integrated generation of a maneuver segment involves an iterative solution to determine a maneuver sequence which cannot be sequentially solved for its maneuver segment components. The maneuver is computed by guessing its magnitude, assigning a direction and plane through selection of the direction switch $s_{direct}$, updating the primary vehicle's state vector after selecting switch $s_{update_p}$ and then calling additional maneuver segments until reaching the point at which the terminal constraint is to be attained. The maneuver is then iteratively determined by satisfying the terminal constraint. The number of additional maneuver segments and the nature of the terminal constraint are controlled by the terminal constraint switch $s_{term}$

$$s_{term} = \begin{cases} -2, -3, \ldots & \text{The terminal constraint is a phasing constraint and it occurs at the } |s_{term}| \text{ maneuver point from the start of the maneuver segment.} \\ 2, 3.. \ldots < 10 & \text{The terminal constraint is a height constraint and it occurs at the } s_{term} \text{ maneuver point from the start of the maneuver segment.} \\ (10 < s_{term} < 100) & \text{Both a height and phasing constraint occur at the same maneuver point. The first digit } n_1 \text{ of } s_{term} \text{ represents a phasing constraint that occurs at the } n_1 \text{ maneuver point from the start of the phasing maneuver segment. The last digit } n_2 \text{ of } s_{term} \text{ represents a height constraint that occurs at the } n_2 \text{ maneuver point from the start of the height maneuver segment.} \end{cases}$$

### 1.2.4 Summary of the Maneuver Segment Constraints

The maneuver and trajectory constraints that can be imposed on a maneuver segment can be divided into the following catagories (see Figure 3).

Primary vehicle update constraints

Target vehicle update constraints

Initial velocity constraints

Offset constraints

Terminal constraints

Traverse constraints

Table 1 contains a detailed listing of the constraints. The three independent constraints (four in the case of noncoplanar traverses) which govern a maneuver segment cannot be chosen arbitrarily from this list for two reasons:

(1) There is not a one-to-one correspondence between the trajectory constraints and the independent constraints.

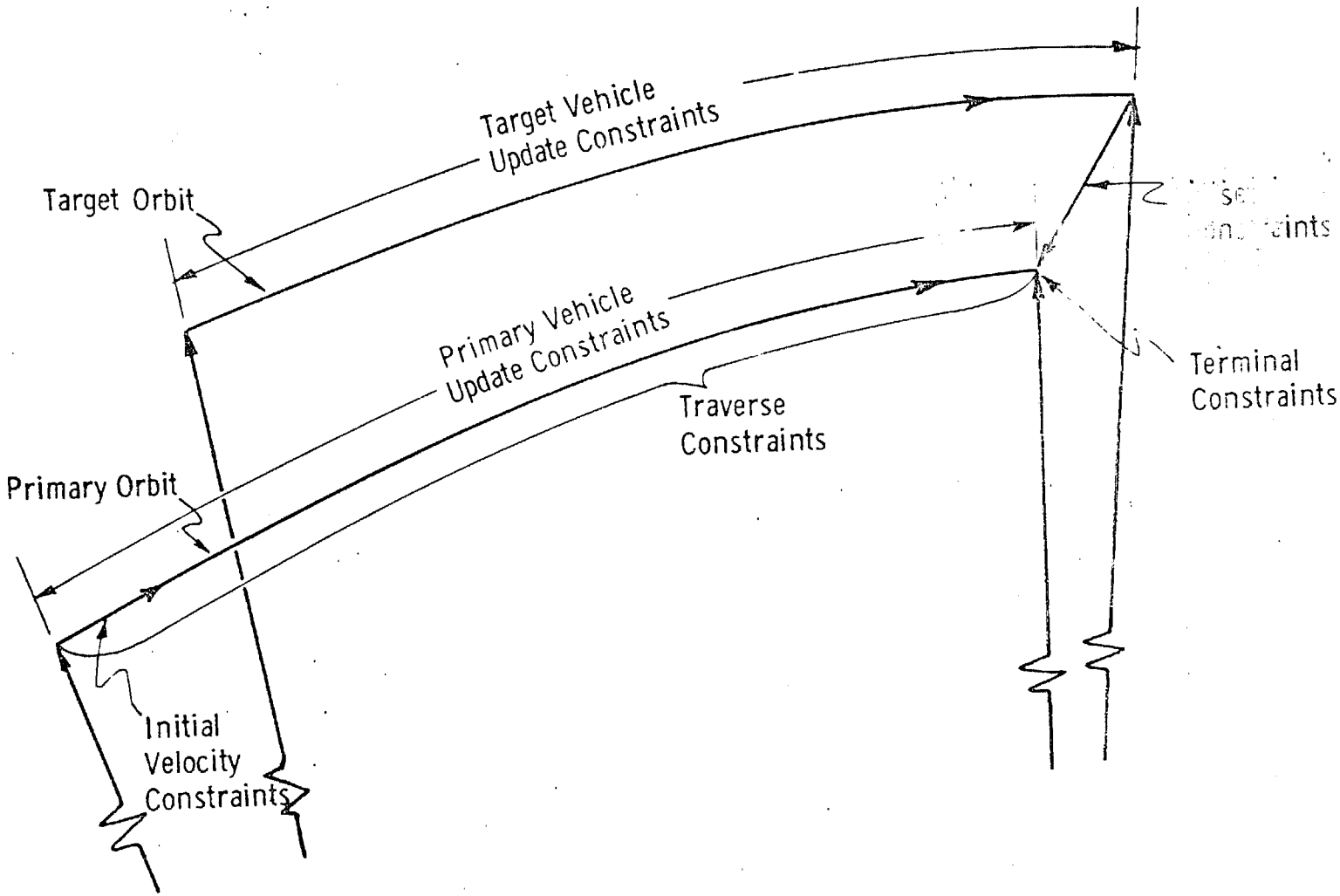


Figure 3. Constraint Catagories on a Maneuver Segment

(2) Selecting some constraints negates the need for some others (e.g. selecting a Lambert constraint negates the need for a maneuver direction constraint).

In the case of a straight forward rendezvous profile, a basic understanding of the nature of the constraints should allow the constructor of the rendezvous sequence to choose a set of trajectory constraints which determine the required number of independent constraints. For a complex rendezvous profile, such as Skylab a more formal approach such as presented in Reference 11 should be used. One of the justifications for presenting the three methods of generating a maneuver segment was to aid the constructor of the rendezvous sequence in choosing compatible sets of constraints.

TABLE 1

DETAILED LISTING OF CONSTRAINTS

(Sheet 1 of 2)

Primary and Target Vehicle Update Constraints

- Delta time
- Initial and final time
- Central angle
- Number of revolutions
- Terminal position vector

Initial Velocity Constraints

- Plane
  - Parallel to target orbit
  - Parallel to primary orbit
- Direction
  - Horizontal
  - Along velocity vector
- Magnitude
  - Circular
  - Coelliptic
  - Altitude change
  - Specified

Offset Constraints

- Angle
- Altitude
- Elevation angle

Terminal Constraints

- Height
- Phase

TABLE 1

DETAILED LISTING OF CONSTRAINTS

(Sheet 2 of 2)

Traverse Constraints

- Minimum Fuel
  - One maneuver optimization
  - Two maneuver optimization
- Apogee/Perigee designation
- Horizontal maneuver
- Tangential maneuver
- Lambert (time)

## NOMENCLATURE

| | |
|---|---|
| [illegible] | [illegible] axis of a conic |
| $a_i$ | Alarm code i |
| $a_1$ | Failure in fuel optimization loop |
| $a_2$ | Failure in height loop |
| $a_3$ | [illegible] phasing loop |
| $a_4$ | Fa[illegible] in obtaining Lambert solution in General Maneuver Routine |
| $a_5$ | Failure to find perigee/apogee in Search Routine |
| $a_6$ | Incompatible altitudes and elevation angle |
| $a_7$ | Failure to find time corresponding to elevation [illegible] Search Routine |
| $a_8$ | [illegible] to find desired position vector in Desired Position Routine |
| $a_9$ | Failure to update through $\theta$ in Update Routine |
| c | Iteration counter |
| $c_h$ | Height iteration counter |
| $c_p$ | Phase iteration counter |
| $c_1, c_2, c_3$ | [illegible] diate variables |
| $\Delta h$ | Delta altitude |
| $\Delta r_{proj}$ | Delta projected position |

| | |
|---|---|
| $\Delta t$ | Delta time |
| $\Delta t_{max}$ | Maximum time step allowed in Search Routine iteration |
| $\Delta \underline{v}$ | Maneuver velocity |
| $\Delta \underline{v}_{LOS}$ | Maneuver in line-of-sight coordinates |
| $\Delta \underline{v}_{LV}$ | Maneuver in local vertical coordinates |
| $\Delta v_h$ | $\Delta v$ used during height maneuver |
| $\Delta v_p$ | $\Delta v$ used during phasing maneuver |
| $\Delta v_T$ | Delta velocity used in fuel minimization loop |
| $\Delta x$ | Delta independent variable |
| $\Delta \theta$ | Delta central angle |
| $e$ | Error |
| $e_c$ | Eccentricity |
| $e_h$ | Height error |
| $e_p$ | Phasing error |
| $e_L$ | Elevation angle (defined in Figure 2) |
| $\underline{i}$ | Unit vector |
| $\underline{i}_N$ | Unit normal to the plane used in powered flight guidance |
| $i$ | Number of the maneuver |
| $i_{max}$ | Number of the last maneuver in the maneuver sequence |
| $m$ | Estimated vehicle mass |
| $M$ | Rotational matrix |
| $\underline{n}$ | Vector normal to the orbital plane |
| $n_r$ | Number of revolutions |

| | |
|---|---|
| $p$ | Partial used in Newton Raphson iteration |
| $r$ | Distance ratio |
| $\underline{r}$ | Position vector |
| $\underline{r}_D$ | Desired position vector |
| $\underline{r}_{1c}$ | Target vector used in powered flight guidance |
| $s$ | Switch used in Desired Position Routine |
| $s_{astro}$ | Astronaut overwrite switch |
| $s_{coplan}$ | Coplanar switch |
| $s_{direct}$ | Maneuver direction switch |
| $s_{eng}$ | Engine select switch |
| $s_{exit}$ | Program exit switch |
| $s_{fail}$ | Failure switch |
| $s_{man}$ | Maneuver switch |
| $s_{opt}$ | Maneuver optimizing switch |
| $s_{outp}$ | Out-of-plane switch |
| $s_{pert}$ | Perturbation switch |
| $s_{phase}$ | Phase match switch |
| $s_{proj}$ | Projection switch |
| $s_{rdes}$ | Desired position switch |
| $s_{soln}$ | Solution switch |
| $s_{search}$ | Search switch |
| $s_{tar}$ | Target offset switch |
| $s_{term}$ | Terminal constraint switch |
| $s_{update}$ | Update switch |

| | |
|---|---|
| $t$ | Time |
| $t_F$ | Final time |
| $\underline{v}$ | Velocity vector |
| $v_v$ | Vertical component of velocity |
| $v_c$ | Circular velocity |
| $x$ | Independent variable in Iteration Routine |
| $y_P$, $\dot{y}_P$, $\dot{y}_T$ | Out-of-plane parameters (see Figure 6a) |
| $\alpha$ | Radial component of velocity divided by $v_C$ |
| $\beta$ | Horizontal component of velocity divided by $v_C$ |
| $\epsilon_1$ | Tolerance on time in fuel optimizing loop |
| $\epsilon_2$ | Tolerance on height in height loop |
| $\epsilon_3$ | Tolerance on central angle in phasing loop |
| $\epsilon_4$ | Tolerance on central angle in Search Routine |
| $\epsilon_5$ | Tolerance on elevation angle in Search Routine |
| $\epsilon_6$ | Altitude increment in Search Routine |
| $\epsilon_7$ | Tolerance on central angle in Desired Position Routine |
| $\epsilon_8$ | Tolerance on central angle in Update Routine |
| $\gamma$ | Flight path angle |
| $\mu$ | Gravitational constant |
| $\theta$ | Central angle |
| $\theta_p$ | Perigee angle |

Subscripts

| | |
|---|---|
| F | Final |
| i | Number of the maneuver |
| I | Initial |
| LOS | Line-of-sight |
| LV | Local vertical |
| N | New |
| 0 | Old |
| P | Primary |
| S | Stored |
| T | Target |
| TA | Target for primary vehicle |

## 2. FUNCTIONAL FLOW DIAGRAMS

The rendezvous targeting program consists of two major parts—a generalized maneuver subroutine which basically computes a maneuver and updates the state vectors of both vehicles to the time of the next maneuver and a main program which sequentially calls the subroutine to assemble a rendezvous sequence. These programs call a number of subroutines which are briefly described below and in detail in Section 5.

| | | |
|---|---|---|
| Search | - | To update the state vectors to either a specified apsidal crossing, a time, or an elevation angle. |
| Phase Match | - | To phase match the target vehicle's state vector to the primary vehicle's position vector. |
| Desired Position | - | To compute an offset target vector or a desired position to be used in a phasing constraint. |
| Update | - | To update a state vector through a specified interval. |
| Coelliptic Maneuver | - | To compute a coelliptic velocity vector. |
| Iteration | - | To determine a new estimate of the independent variable in a Newton Raphson iteration scheme. |

The functional flow diagram for the main program is shown in Figure 4. The main function of this program is to sequentially call the General Maneuver Routine to compute each maneuver segment for maneuvers numbered from $i$ to $i_{max}$. There are three major options that can be exercised prior to the calculation of the first maneuver segment:

(1) A search for the time of the first maneuver. This time can be specified by:

(a) An elevation angle, which is to be attained at the maneuver time.

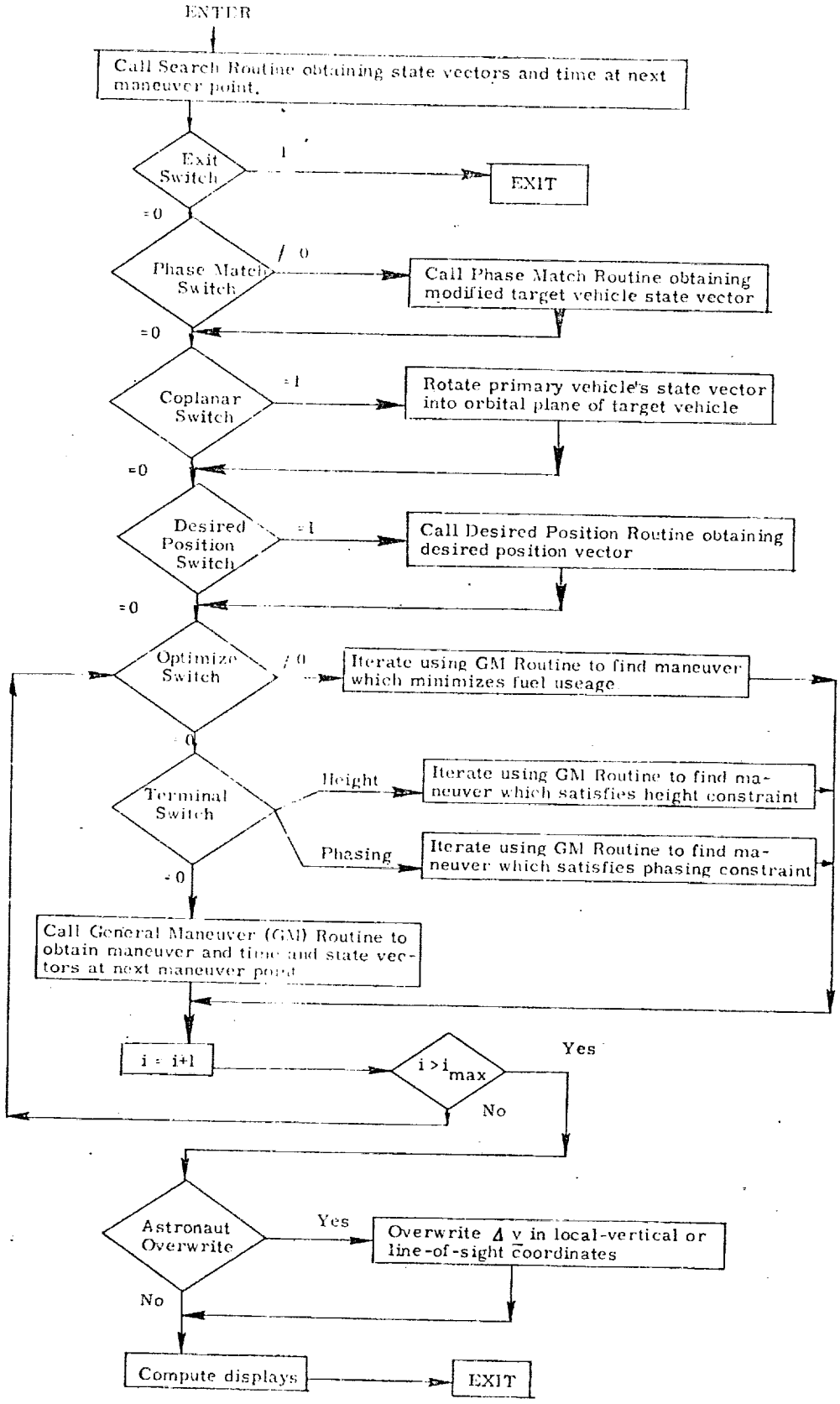


Figure 4. Main Program - Function Flow Diagram

(b) Whether the next maneuver should occur at the next apsidal crossing, the next perigee crossing or the nth apsidal crossing.

(2) A phase matching of the state vector.

(3) A rotation of the primary vehicle's state vector into the plane of the target vehicle.

There are three separate iterative loops built around the call to the general maneuver routine. One loop serves to minimize the fuel used during a maneuver segment with the options determined by the optimizing switch.

The other two iterative loops involve maneuver segments which contain constraints that do not allow the explicit calculation of the maneuver. These constraints are height and phasing constraints imposed at the end of a maneuver segment and controlled with the terminal switch. The iterative loop will involve several maneuver segments if sufficient constraints are not imposed to solve each segment uniquely.

The functional flow diagram for the general maneuver routine is shown in Figure 5. This routine generates the departure velocity at the initial point in one of two ways:

(1) As an explicit function of the initial state vectors.

(2) By defining a target vector and then computing an intercept trajectory based on a specified constraint (as indicated by the setting of $s_{man}$). The target vector is determined by offsetting the updated position vector of the target vehicle. Depending on the setting of the switch $s_{tar}$, a coelliptic velocity vector is computed at the offset point and the coelliptic state vector is updated through $\Delta t$ to obtain a target vector.

Following an update of both vehicle's state vectors to the time of the next maneuver, the $\Delta v$ used or the terminal height/phase errors are calculated as required.

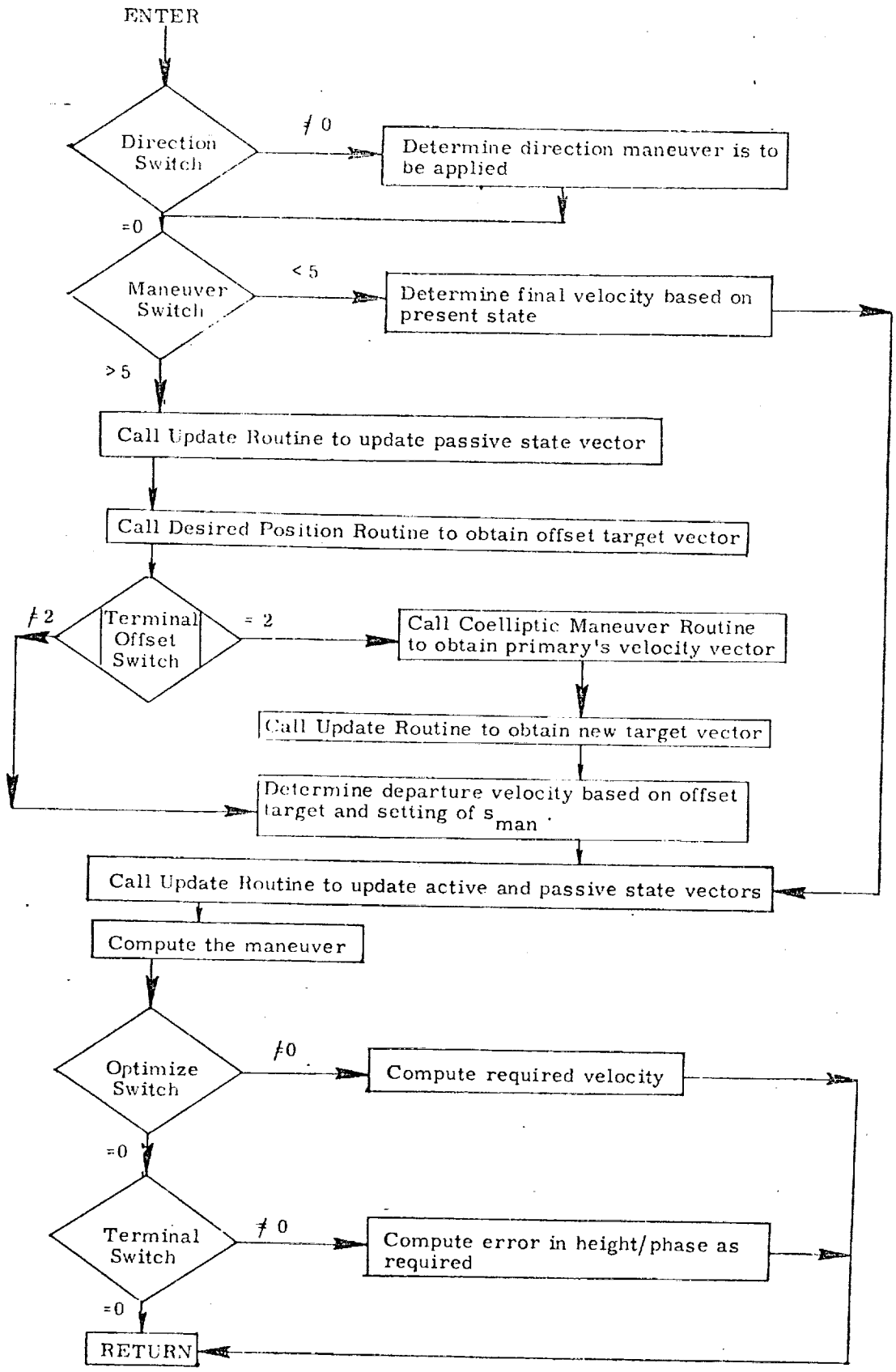


Figure 5. General Maneuver Routine - Functional Flow Diagram

## 3. INPUT AND OUTPUT VARIABLES

The inputs to the orbiter rendezvous targeting program can be divided into five catagories.

### Pre-Maneuver Switches

Upon selecting a maneuver from the rendezvous sequence, these switches (specified for each maneuver) serve in determining the state vectors at the maneuver point, the out-of-plane parameters and the calculation of a desired position vector. These inputs can also be used in determining the time of a specified apsidal crossing or the time at which a specified elevation angle is to be attained.

Coplanar switch

$$s_{coplan} = \begin{cases} 0 & \text{Bypass} \\ 1 & \text{Rotate primary state vector into plane of target vehicle's orbit} \end{cases}$$

Exit switch

$$s_{exit} = \begin{cases} 0 & \text{Bypass} \\ 1 & \text{Exit from routine} \end{cases}$$

Out-of-plane switch

$$s_{outp} = \begin{cases} 0 & \text{Bypass} \\ 1 & \text{Compute out-of-plane parameters} \\ 2 & \text{Compute out-of-plane parameters and modify maneuver by } -\dot{y}_P \end{cases}$$

Perturbation switch

$$s_{pert} = \begin{cases} 0 & \text{Do conic state vector updates} \\ 1 & \text{Include oblateness based on } J_2 \\ \ldots & \text{Other perturbations as required} \end{cases}$$

Phase match switch

$$s_{phase} = \begin{cases} 0 & \text{Bypass} \\ 1 & \text{Phase match state vectors (target leading primary)} \\ 2 & \text{Phase match state vectors based on target leading primary by more than } 360^{\circ} \\ -1 & \text{Phase match state vectors (primary leading target)} \\ -2 & \text{Phase match state vectors based on primary leading target by more than } 360^{\circ} \end{cases}$$

Desired position switch

$$s_{rdes} = \begin{cases} 0 & \text{Bypass} \\ -1 & \text{Compute desired position vector based on } (e_L, \Delta h) \\ 1 & \text{Compute desired position vector based on } (\Delta\theta, \Delta h) \end{cases}$$

Search switch

$$s_{search} = \begin{cases} -4 & \text{Compute elevation angle} \\ -3 & \text{Search for elevation angle} \\ -2 & \text{Update to time } t_i \\ -1 & \text{Search for next perigee crossing} \\ 0 & \text{Bypass} \\ n & \text{Search for the nth apsidal crossing } (n>0) \end{cases}$$

Maneuver Switches

These switches (specified for each maneuver) set the constraints employed in determining the maneuver segments.

Direction switch

$$s_{direct} = \begin{cases} -2 & \Delta v \text{ in direction of primary's velocity vector, parallel to primary's orbital plane} \\ -1 & \Delta v \text{ in horizontal direction, parallel to primary's orbital plane} \\ 0 & \text{Bypass} \\ 1 & \Delta v \text{ in horizontal direction, parallel to target's orbital plane} \\ 2 & \Delta v \text{ in direction of primary's velocity vector, parallel to target's orbital plane} \end{cases}$$

Maneuver switch

$$s_{man} = \begin{cases} 1 & \Delta v \text{ is specified} \\ 2 & \Delta v \text{ is based on coelliptic velocity} \\ 3 & \Delta v \text{ is based on circular velocity} \\ 4 & \Delta v \text{ is based on altitude change} \\ 5 & \text{Lambert maneuver to offset target vector} \\ 6 & \text{Horizontal maneuver to offset target vector} \\ 7 & \text{Tangential maneuver to offset target vector} \\ 8 & \text{Perigee/apogee insertion at offset target vector} \end{cases}$$

Maneuver optimizing switch

$$s_{opt} = \begin{cases} 0 & \text{Bypass} \\ 1 & \text{Minimize } \Delta v_i \\ 2 & \text{Minimize } \Delta v_i + \Delta v_{i+1} \end{cases}$$

Revolution solution switch

$$s_{soln} = \begin{cases} -1 & \text{Solution with smallest initial flight path angle (measured from local vertical)} \\ 1 & \text{Solution with largest initial flight path angle} \end{cases}$$

$$s_{tar} = \begin{cases} -2 & \text{Offset target } (e_L, \Delta h). \text{ Compute coelliptic velocity and update through (negative) } \Delta t \\ -1 & \text{Offset target } (e_L, \Delta h) \\ 0 & \text{No target offset} \\ 1 & \text{Offset target } (\Delta\theta, \Delta h) \\ 2 & \text{Offset target } (\Delta\theta, \Delta h). \text{ Compute coelliptic velocity and update through (negative) } \Delta t \end{cases}$$

Terminal constraint switch

$$s_{term} = \begin{cases} n & (< 0) \text{ Compute phasing error and back up } (n+1) \text{ maneuvers for start of phase loop} \\ 0 & \text{Bypass} \\ n & (0 < n < 10) \text{ Compute height error and back up } n - 1 \text{ maneuvers for start of height loop} \\ n & (10 < n < 100) \text{ Phase and height loop terminate on same maneuver. For phase loop back up } x - 1 \text{ (where x is first digit of n) maneuvers for start of phase loop. For height loop back up } y - 1 \text{ (where y is last digit of n) maneuvers for start of height loop} \end{cases}$$

Update switch

$$s_{update} = \begin{cases} 0 & \text{Bypass} \\ 1 & \text{Update through } t_F - t \\ 2 & \text{Update through } \Delta t \\ 3 & \text{Update through } n_r \\ 4 & \text{Update through } \theta \\ 5 & \text{Update to be colinear with } \underline{r}_D \end{cases}$$

Parameter Values

The parameter values (specified for each maneuver) are values for the constrained parameters.

| | |
|---|---|
| $\Delta h$ | Delta altitude |
| $\Delta h_F$ | Delta altitude, final |
| $\Delta \theta$ | Delta central angle |
| $\Delta t$ | Delta time |
| $\Delta v$ | Maneuver magnitude |
| $n_r$ | Number of revolutions |
| $t_F$ | Final time |
| $e_L$ | Elevation angle |

Post-Maneuver Switch

This switch determines the options available following the calculation of the maneuver.

Astronaut overwrite switch

$$s_{astro} = \begin{cases} 0 & \text{Bypass} \\ 1 & \text{Overwrite maneuver in local vertical coordinates} \\ 2 & \text{Overwrite maneuver in line-of-sight coordinates} \end{cases}$$

Maneuver Call Variables

The maneuver call variables have to be specified for each call to the maneuver sequence.

| | |
|---|---|
| $\underline{r}_P, \underline{v}_P$ | State vector of the primary vehicle |
| $\underline{r}_T, \underline{v}_T$ | State vector of the target vehicle |
| $i$ | Maneuver number |
| $t$ | Current time |
| $t_i$ | Time of the $i^{th}$ maneuver |
| $s_{eng}$ | Engine select switch |
| $m$ | Estimated vehicle mass |

Depending on the rendezvous sequence, there may also be some switches that have to be modified as a function of the maneuver number.

Excluding the maneuver call variables, all the input variables can be set prior to the flight.

The output parameters for the initial maneuver in the sequence are more complete than for the succeeding maneuvers.

Output Parameters for the Initial Maneuver

| | |
|---|---|
| $\Delta v_i$ | Maneuver magnitude |
| $\Delta \underline{v}_{LOS\,i}$ | Maneuver in line of sight coordinates |
| $\Delta \underline{v}_{LV\,i}$ | Maneuver in local vertical coordinates |
| $\underline{r}_{1c}$ | Target vector used in Powered Flight Guidance Routine (See Ref. 5) |
| $\underline{i}_N$ | Unit normal to plane used in same routine |

Other parameters such as delta altitude, phasing angle, elevation angle and perigee altitude can be computed as required.

Output Parameters for the Other Maneuvers in the Sequence

| | |
|---|---|
| $t$ | Time of the maneuver |
| $\Delta v$ | Maneuver magnitude |

Illustration of Inputs

Table 2 contains a set of inputs for the Orbiter targeting program based on the five maneuver Skylab rendezvous configuration. The following switches and parameters are not used as inputs to the Orbiter program:

$$s_{astro},\ s_{exit},\ s_{opt},\ s_{outp},\ s_{soln},\ \Delta\theta,$$

The inputs in Table 2 are set prior to the mission so they will not have to be inserted by the astronaut. The astronaut will have to modify the following quantities upon resetting the maneuver number as well as inserting the time of the next maneuver.

$i = 2$: $s_{term_2} = 0$, $s_{term_4} = 32$

$i = 3$: $s_{man_3} = 5$, $\Delta t_3 = -\Delta t_{NSR-TPI}$

$i = 4$: $s_{term_4} = 0$

TABLE 2

INPUT VARIABLES FOR SKYLAB RENDEZVOUS CONFIGURATION

| Input Variable | Maneuver 1 (NC1) | 2 (NC2) | 3 (NCC) | 4 (NSR) | 5 (TPI) |
|---|---|---|---|---|---|
| $s_{coplan}$ | 1 | 1 | 0 | 1 | 0 |
| $s_{direct}$ | 1 | 1 | 1 | 0 | 0 |
| $s_{man}$ | 1 | 1 | 1 | 2 | 5 |
| $s_{pert}$ | 1 | 1 | 1 | 0 | 1 |
| $s_{phase}$ | 1 | 1 | 0 | 0 | 0 |
| $s_{rdes}$ | -1 | -1 | 0 | 0 | 0 |
| $s_{search}$ | -2 | -2 | -2 | -2 | -3 |
| $s_{tar}$ | | | -2 | | 0 |
| $s_{term}$ | 0 | 1 | 0 | 42 | 0 |
| $s_{update_P}$ | 3 | 3 | 2 | 1 | 2 |
| $s_{update_T}$ | | | 1 | | 4 |
| $e_L$ | $e_L$ | $e_L$ | $e_L$ | | |
| $i_{max}$ | 4 | 4 | 3 | 4 | 5 |
| $n_r$ | $n_{rNC1-NC2}$ | $n_{rNC2-NCC}$ | | | |
| $t_F$ | $t_{TPI}$ | $t_{TPI}$ | $t_{TPI}$ | $t_{TPI}$ | |
| $\theta$ | | | | | $\theta_{TPF-TPI}$ |
| $\Delta t$ | | | $\Delta t_{NSR-NCC}$ | | |
| $\Delta h$ | | $\Delta h_{NCC}$ | $\Delta h_{TPI}$ | $\Delta h_{TPI}$ | |
| $\Delta h_F$ | $\Delta h_{TPI}$ | $\Delta h_{TPI}$ | | | |
| $\Delta v$ | $\Delta v_{NC1}$ | $\Delta v_{NC2}$ | $\Delta v_{NCC}$ | | |

## 4. DESCRIPTION OF EQUATIONS

The only equations contained in this document which are not trivial are those involved in computing the traverse between two specified position vectors. The required equations can be derived from the equation of the conic expressed in the form

$$r = r_F / r_I = \beta_I^2 / \left[ 1 + e_c \cos(\theta + \theta_P) \right]$$

where

$$e_c = \left[ \alpha_I^2 \beta_I^2 + (\beta_I^2 - 1)^2 \right]^{1/2}$$

$$\theta_p = \cos^{-1} \left[ (\beta_I^2 - 1)/e_c \right] \quad \text{(perigee angle)}$$

$$v_c = (\mu / r_I)^{1/2}$$

$\alpha_I$ and $\beta_I$ are the normalized (with respect to $v_c$) radial and horizontal components of velocity.

The above equation can be expressed

$$p_s/r_I = \beta_I^2 = c_2/(\alpha_I \sin\theta/\beta_I - c_1) \tag{1}$$

where

$$c_1 = \cos\theta - 1/r$$

$$c_2 = 1 - \cos\theta$$

$$p_s = \text{semilatus rectum}$$

For a maneuver that is constrained to be in a horizontal direction, Eq. (1) can be solved for $\beta_I$ as a function of the specified $\alpha_I$.

$$\beta_I = \left[ \alpha_I \sin\theta \pm (\alpha_I^2 \sin^2\theta - 4 c_1 c_2)^{1/2} \right] / 2 c_1$$

As there has to be both a positive and negative $\beta_I$ solution to this equation (one trajectory in each rotational direction), the sign choice is resolved in favor of plus $\beta_I$.

For a maneuver that is applied along the velocity vector, the flight path angle $\gamma_1$ is to be held fixed. Using Eq. (1)

$$\tan \gamma_I = \alpha_I/\beta_I = (c_1 \beta_I^2 + c_2)/\beta_I^2 \sin \theta$$

Therefore,

$$\beta_I = [\, c_2/(\sin \theta \tan \gamma_I - c_1)]^{1/2}$$

By interchanging the I and F subscripts, Eq. (1) can be expressed

$$p_s = r_F\, c_2/(\alpha_F \sin \theta/\beta_F - \cos \theta + r_F/r_I)$$

Combining with Eq. (1) using the apogee/perigee constraint $\alpha_F/\beta_F = 0$ results in

$$\tan \gamma_0 = \alpha_I/\beta_I = (1 - 1/r)/\tan(\theta/2)$$

Inserting into Eq. (1) gives the required horizontal component of velocity for apogee/perigee designation maneuvers.

$$\beta_I = [\, r\, c_2/(r - \cos \theta)\,]^{1/2}$$

The derivation of the equation

$$\theta = \cos^{-1} [\, r_P \cos (e_L')/r_T] - e_L'$$

where

$$e_L' = \begin{cases} e_L \text{ if } e_L \leq \pi \\ e_L - \pi \text{ if } e_L > \pi \end{cases}$$

for computing the desired central angle $\theta$ between two positions $(r_P, r_T)$ which satisfies the TPI constraints $(e_L, \Delta h)$ is discussed in Ref. 12. This equation is used in the Desired Position Routine.

## 5. DETAILED FLOW DIAGRAMS

Figures 6 and 7 contain the detailed flow diagrams of the main Orbiter rendezvous targeting program and the general maneuver routine, respectively. The following six routines are called by these two programs.

### Iteration Routine

This routine contains a Newton Raphson iterative driver based on numerically computed partials. The routine computes a new estimate of the dependent variable x and returns the old values of the error e and x. If the iteration counter c exceeds 15, a convergence switch $s_{conv}$ is set equal to one.

### Coelliptic Maneuver Routine

This routine computes a coelliptic velocity vector $\underline{v}_N$ based on a target vehicle's state vector and a delta altitude.

### Phase Match

This routine phase matches the target state vector to the primary state vector. The controlling switch ($s_{phase}$) equals two if the leading vehicle leads the other vehicle by more than one revolution: otherwise the switch equals one. If the primary vehicle leads to target vehicle, the switch is negative.

### Desired Position Routine

This routine updates a specified state vector to the time $t_F$ and then offsets the updated state vector through either ($\Delta\theta$, $\Delta h$) or ($e_L$, $\Delta h$), depending on the setting of the switch s, to obtain $\underline{r}_D$. The routine contains an iterative search to solve the ($e_L$, $\Delta h$) offset problem, where $e_L$ is defined in Figure 2 and $\Delta h$ (positive when the target orbit is above the primary) is defined as shown below. (This represents the TPI geometry used in Apollo and Skylab.)

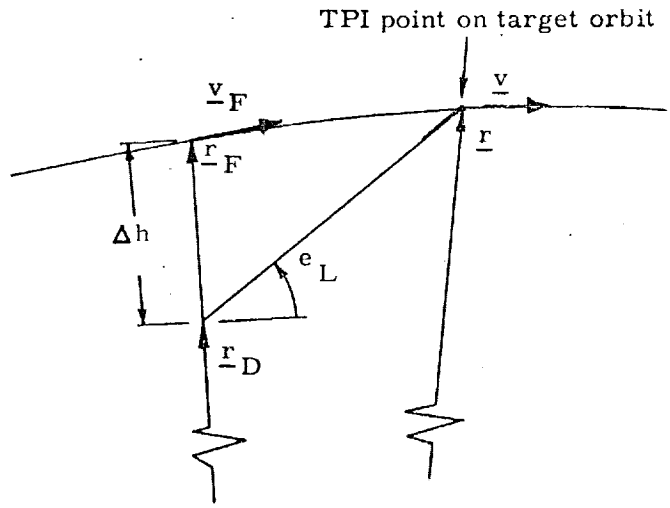

Update Routine

This ro[illegible] updates a state vector based on the update switch $s_{update}$

$s_{update}$
- = 1 Updates through the time $t_F - t$
- [illegible] Updates through the time $\Delta t$
- [illegible] Updates through $n_r$ revolutions
- = 4 Updates through the angle $\theta$
- = 5 Updates to where the orbit intersects the line defined by $\underline{r}_D$

Search Routine

This rou[illegible] [illegible]s the following computations depending on the setting of the search swi[illegible] $s_{search}$

$s_{search}$
- = n (> 0) Finds the time of the $n^{th}$ apsidal crossing and updates the state vector to that time
- = -1 Finds the time of the next perigee crossing and updates the state vector to that time
- = -2 Updates the state vector through the time $t_F - t$ and computes the elevation angle
- = -3 Finds the time associated with a specified elevation angle and updates the state vector to that time

The detailed flow charts for these routines are shown in Figures 8 to 13. The iterative algorithm used to determine the time associated with the elevation angle is described in Ref. 8.

Each input and output variable in the routine and subroutine call statements can be followed by a symbol in brackets. This symbol identifies the notation for the corresponding variable in the desired description and flow diagrams of the called routine. When identical notation is used, the bracketed symbol is omitted.

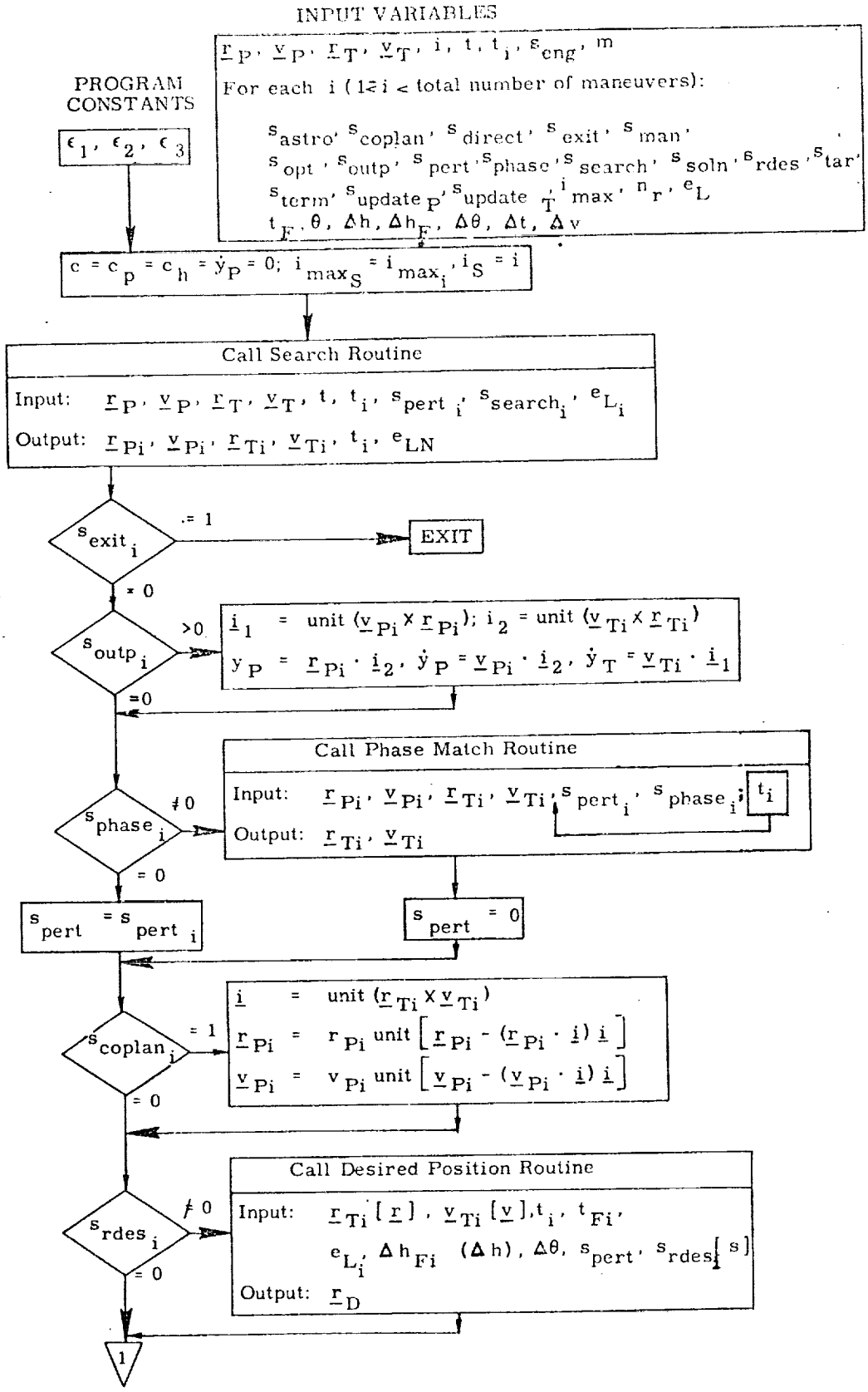


Figure 6a. Main Program - Detailed Flow Diagram

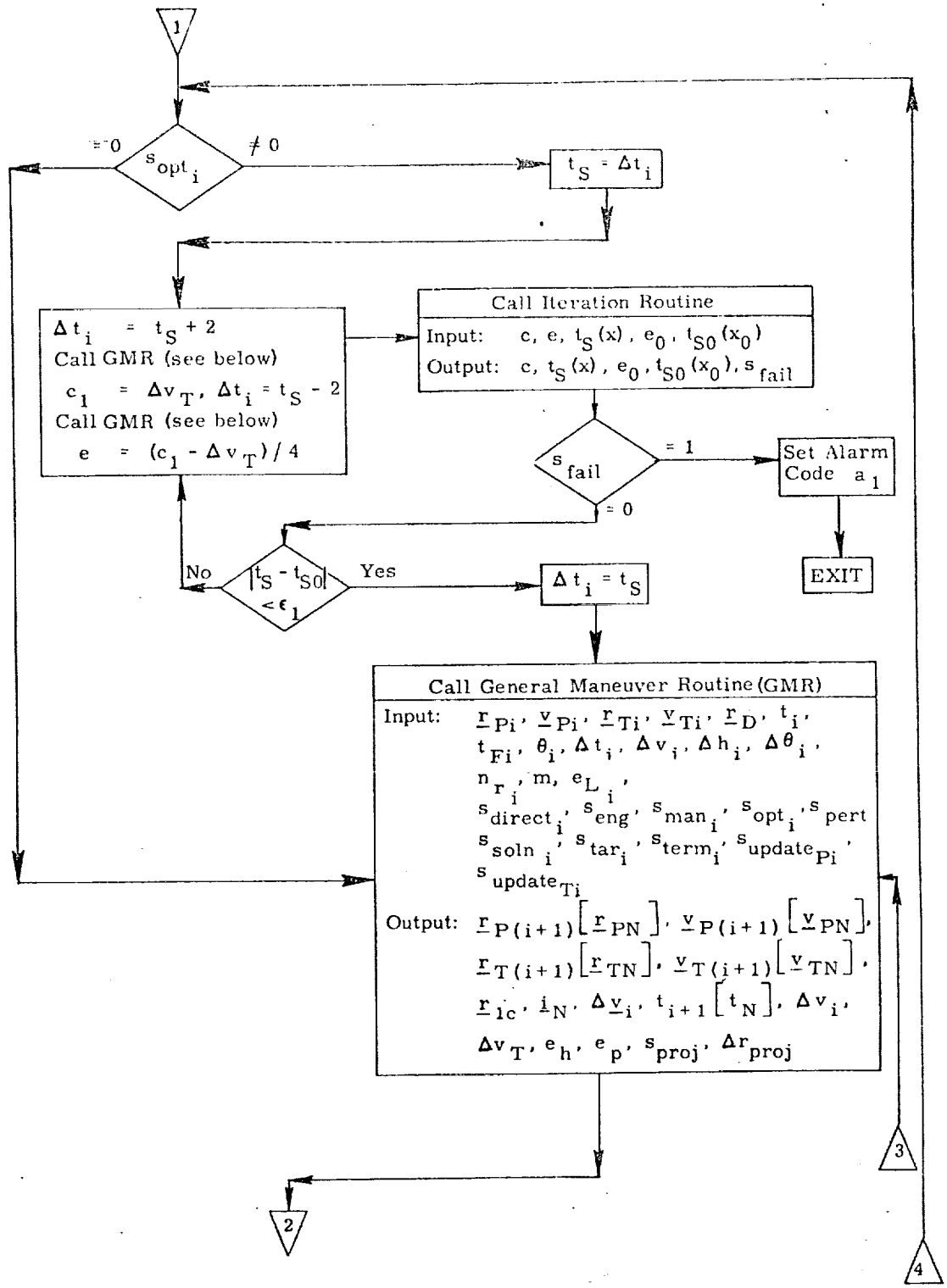


Figure 6b. Main Program - Detailed Flow Diagram

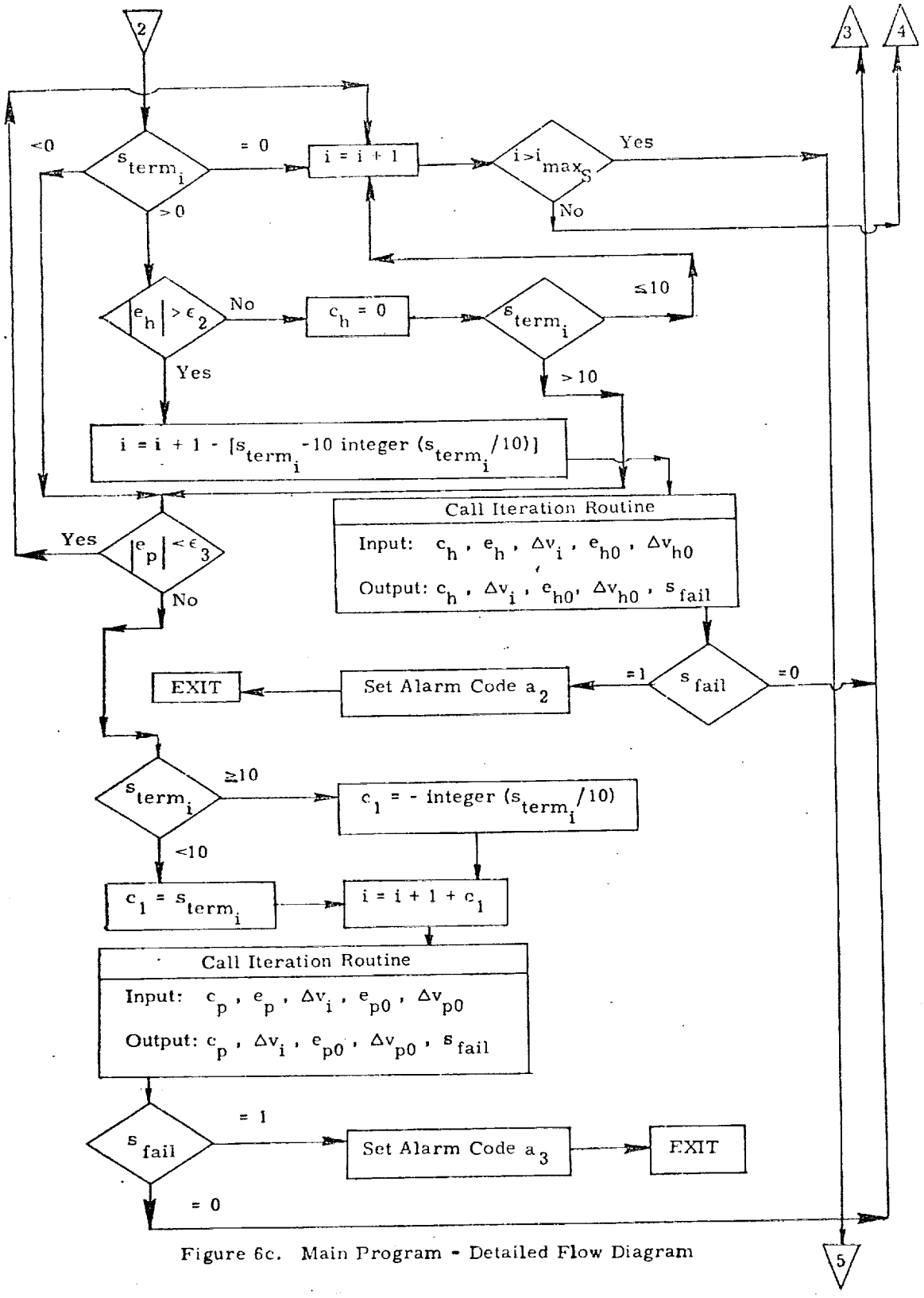


Figure 6c. Main Program - Detailed Flow Diagram

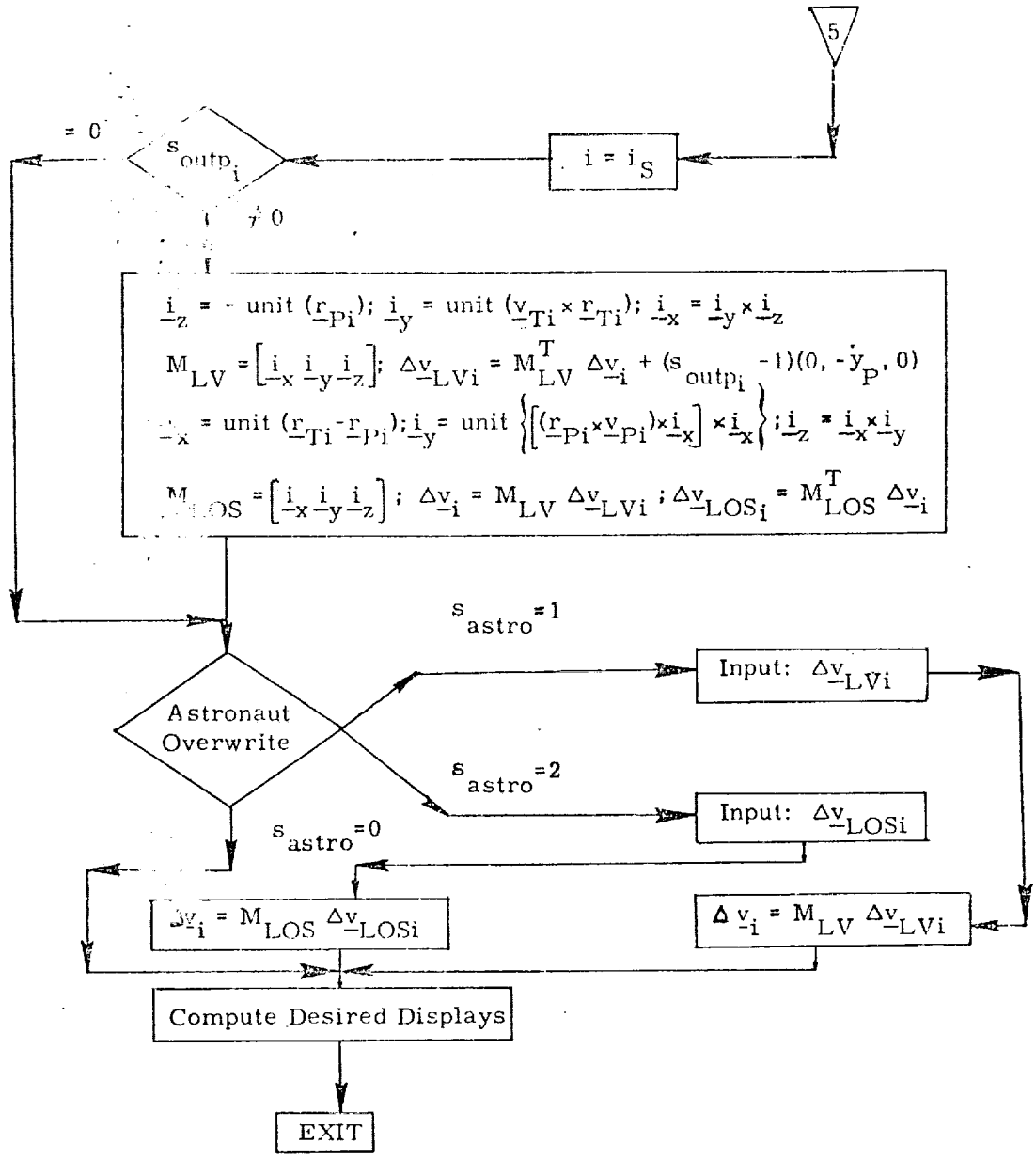


Figure 6d. Main Program - Detailed Flow Diagram

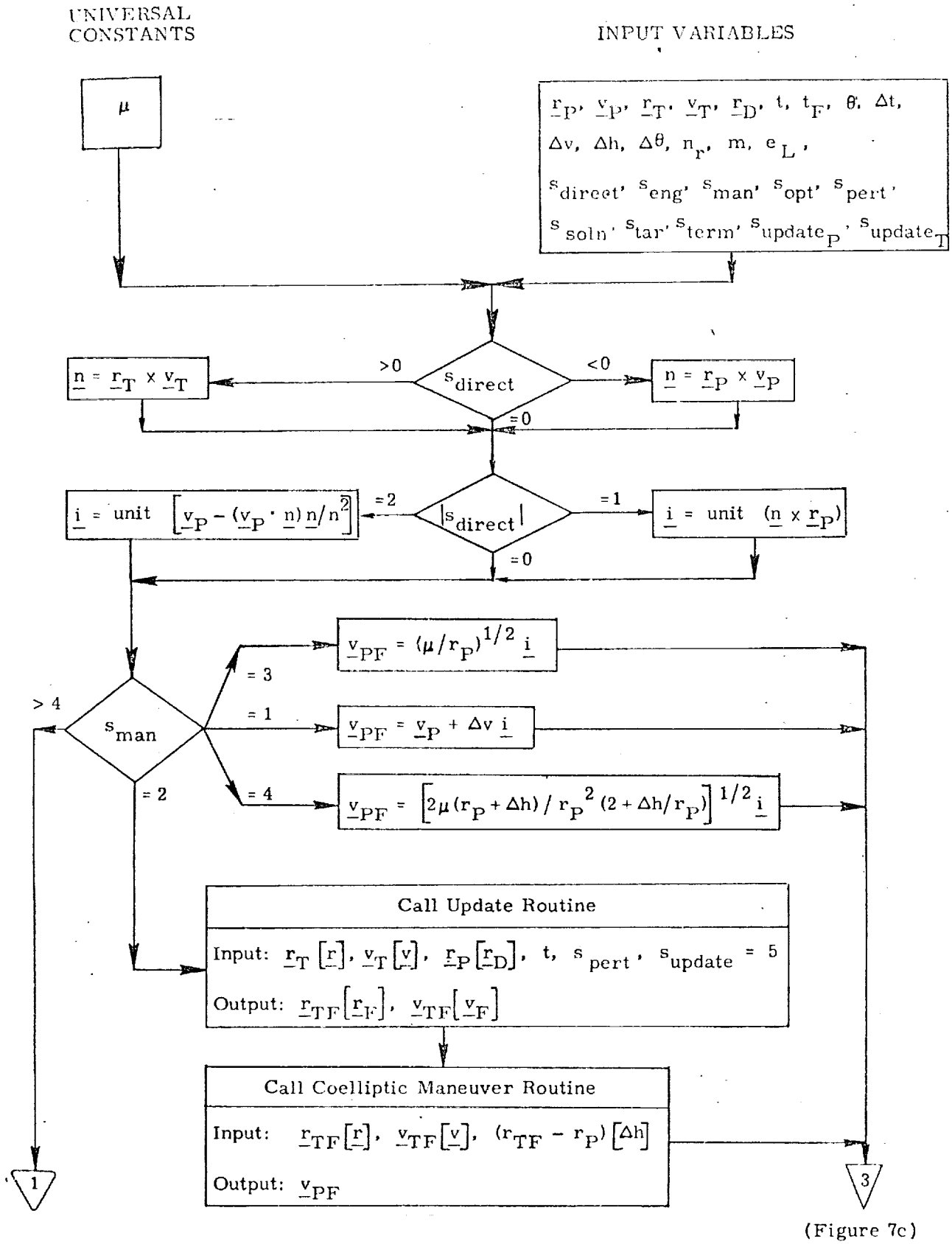


Figure 7a. General Maneuver Routine - Detailed Flow Diagram

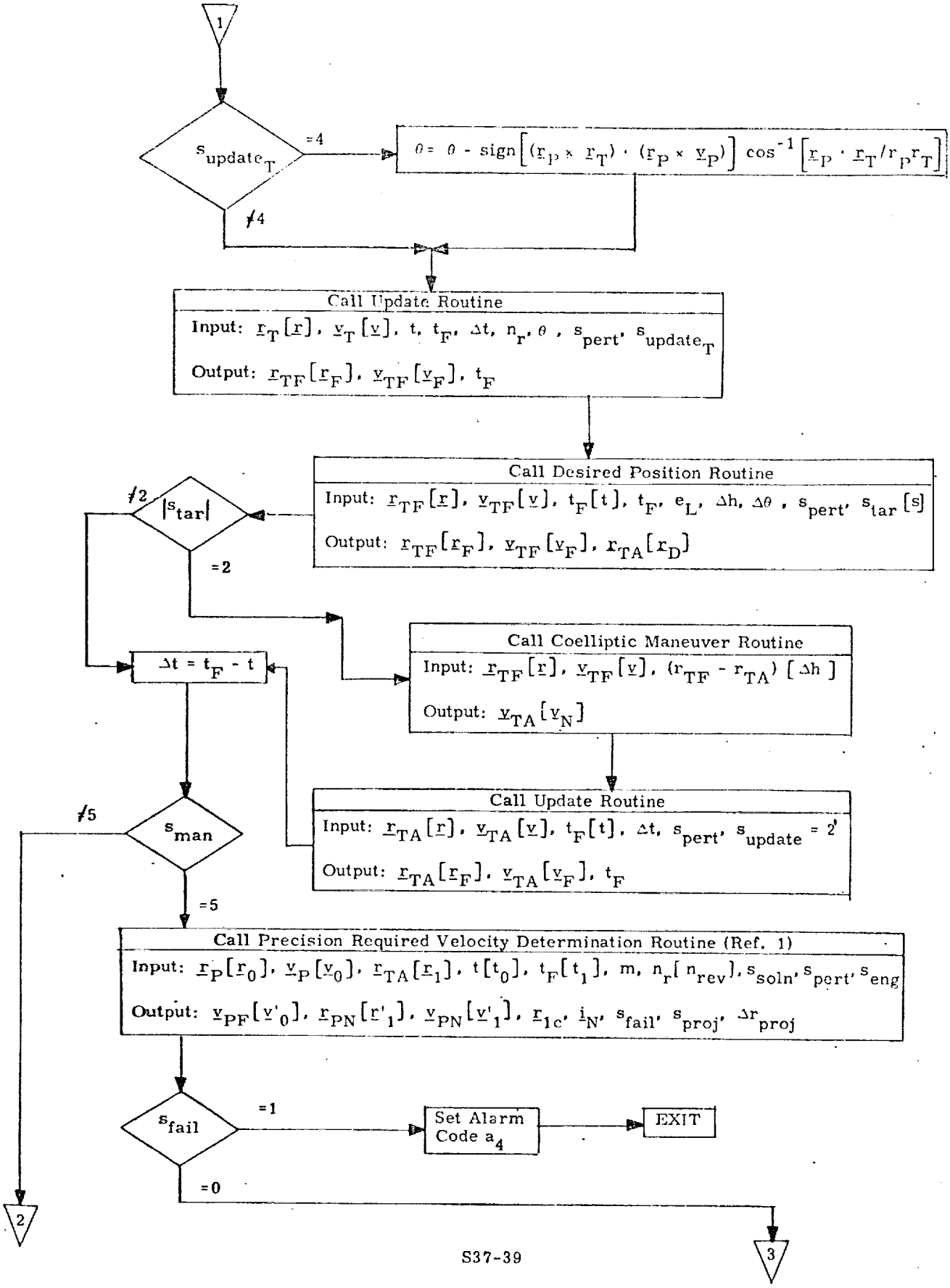


Figure 7b. General Maneuver Routine - Detailed Flow Diagram

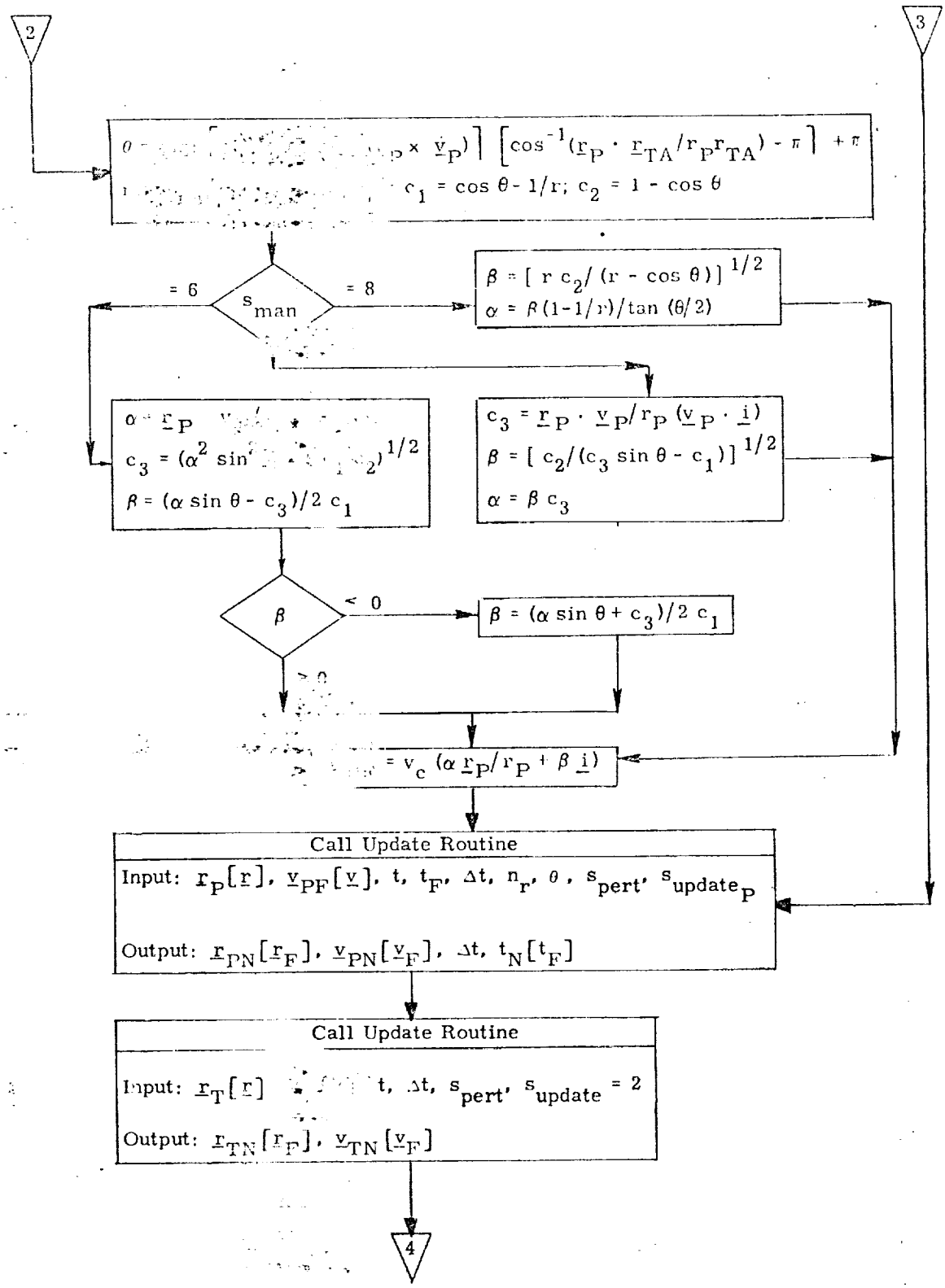


Figure 7c. C[illegible] Maneuver Routine - Detailed Flow Diagram

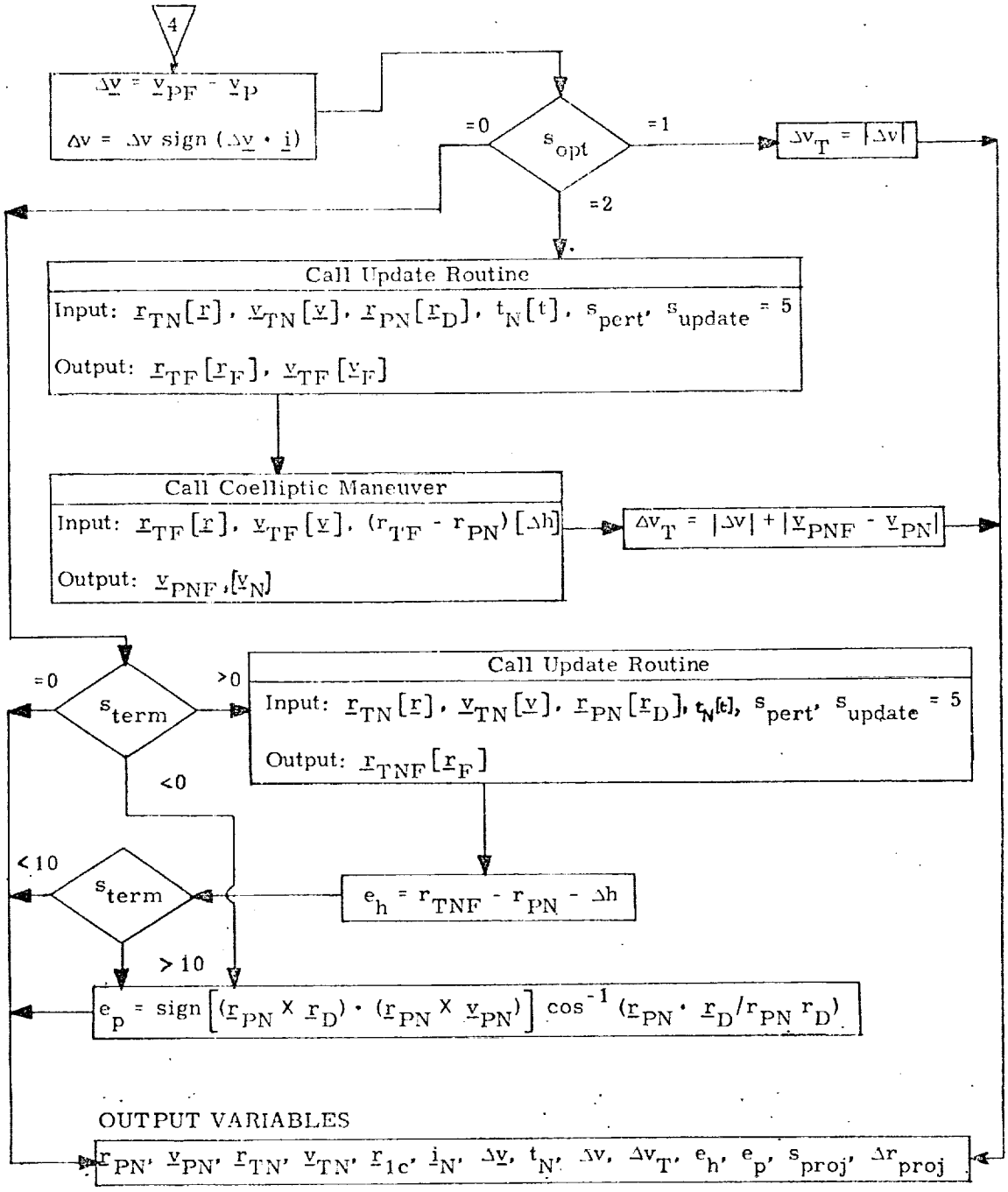


Figure 7d. General Maneuver Routine - Detailed Flow Diagram

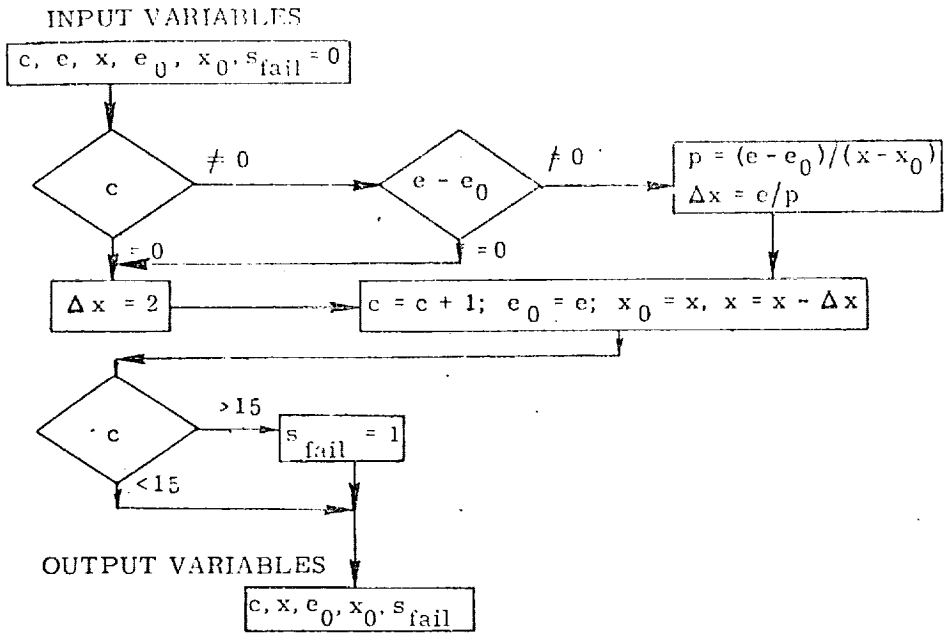


Figure 8. Iteration Routine - Detailed Flow Diagram

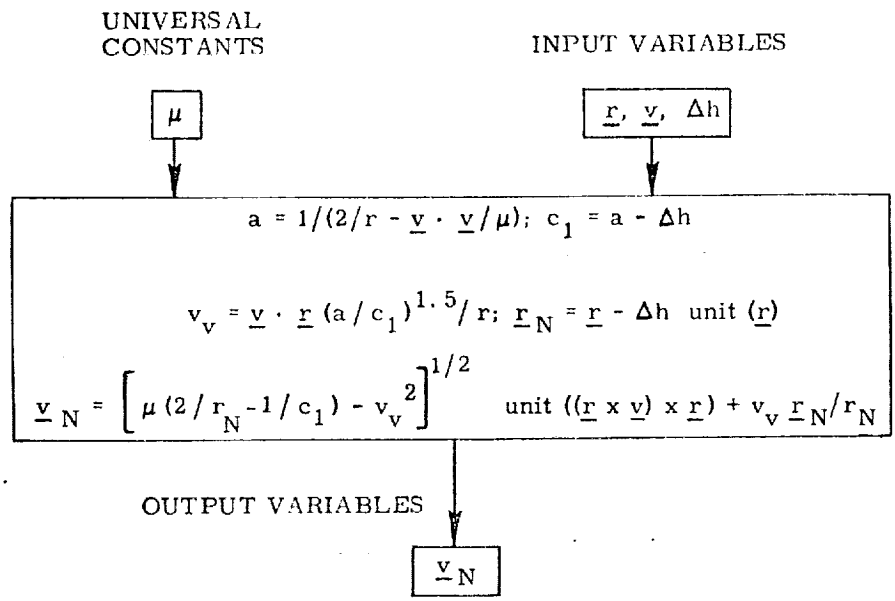


Figure 9. Coelliptic Maneuver Routine - Detailed Flow Diagram

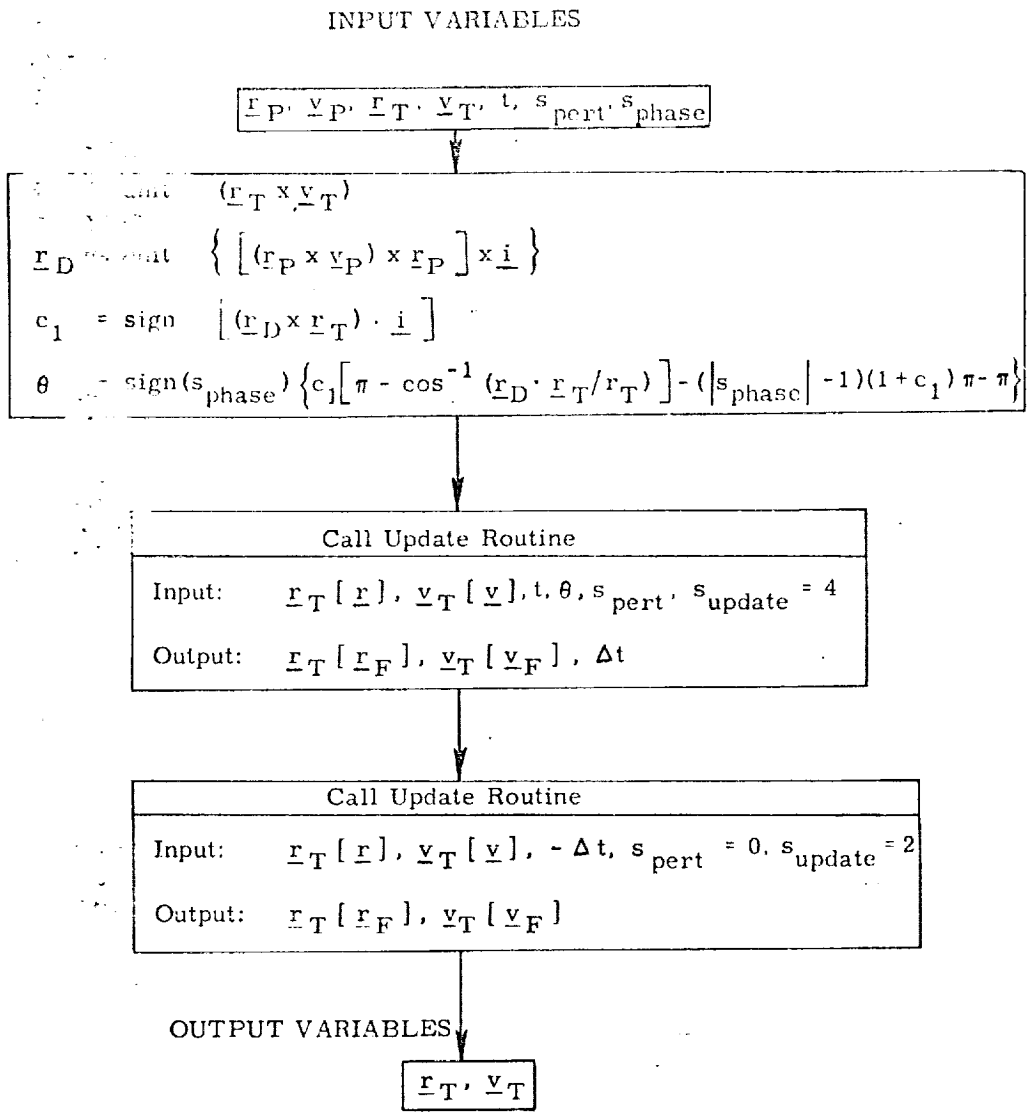


Figure 10. Phase Match Routine - Detailed Flow Diagram

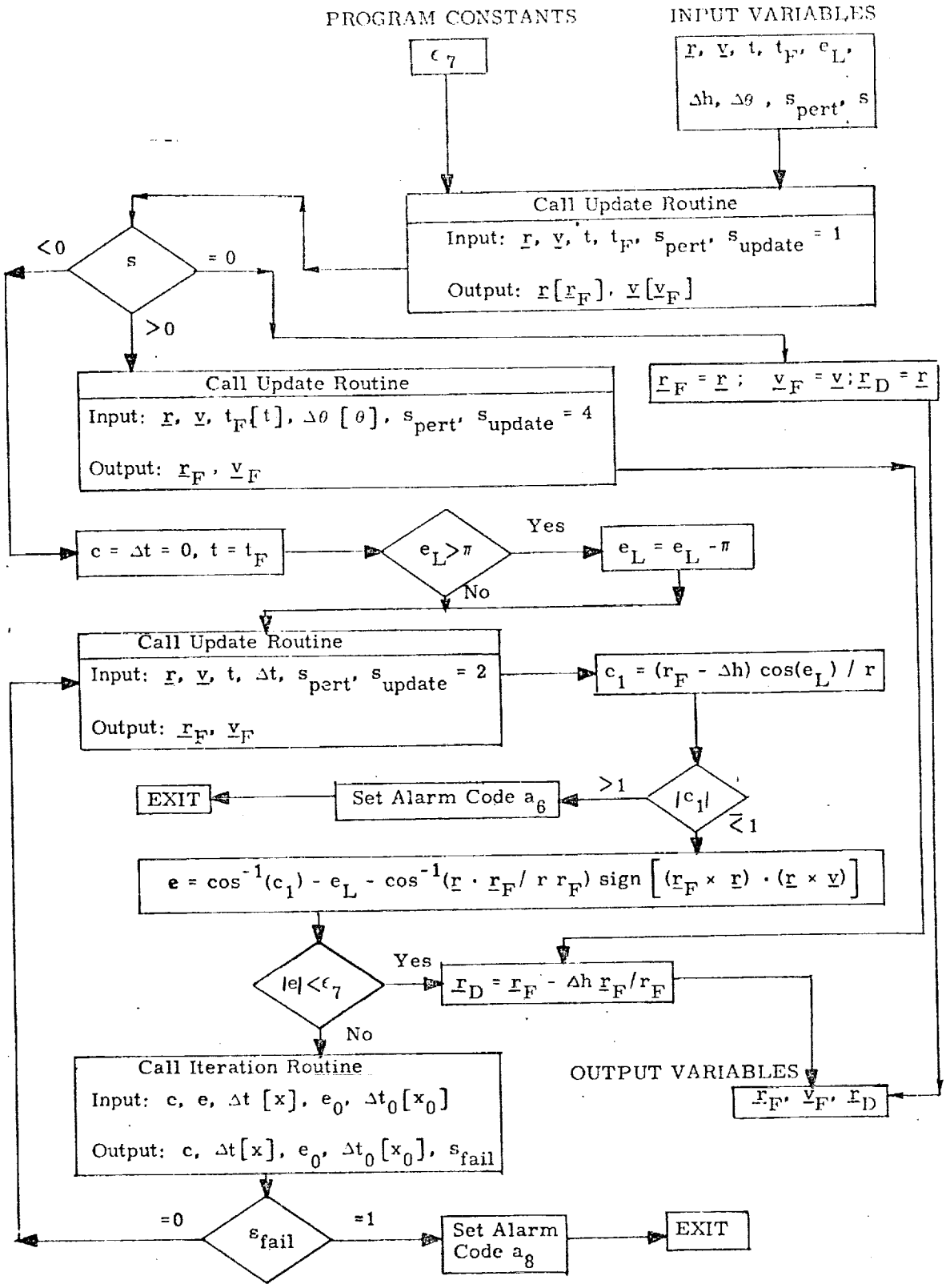


Figure 11. Desired Position Routine - Detailed Flow Diagram

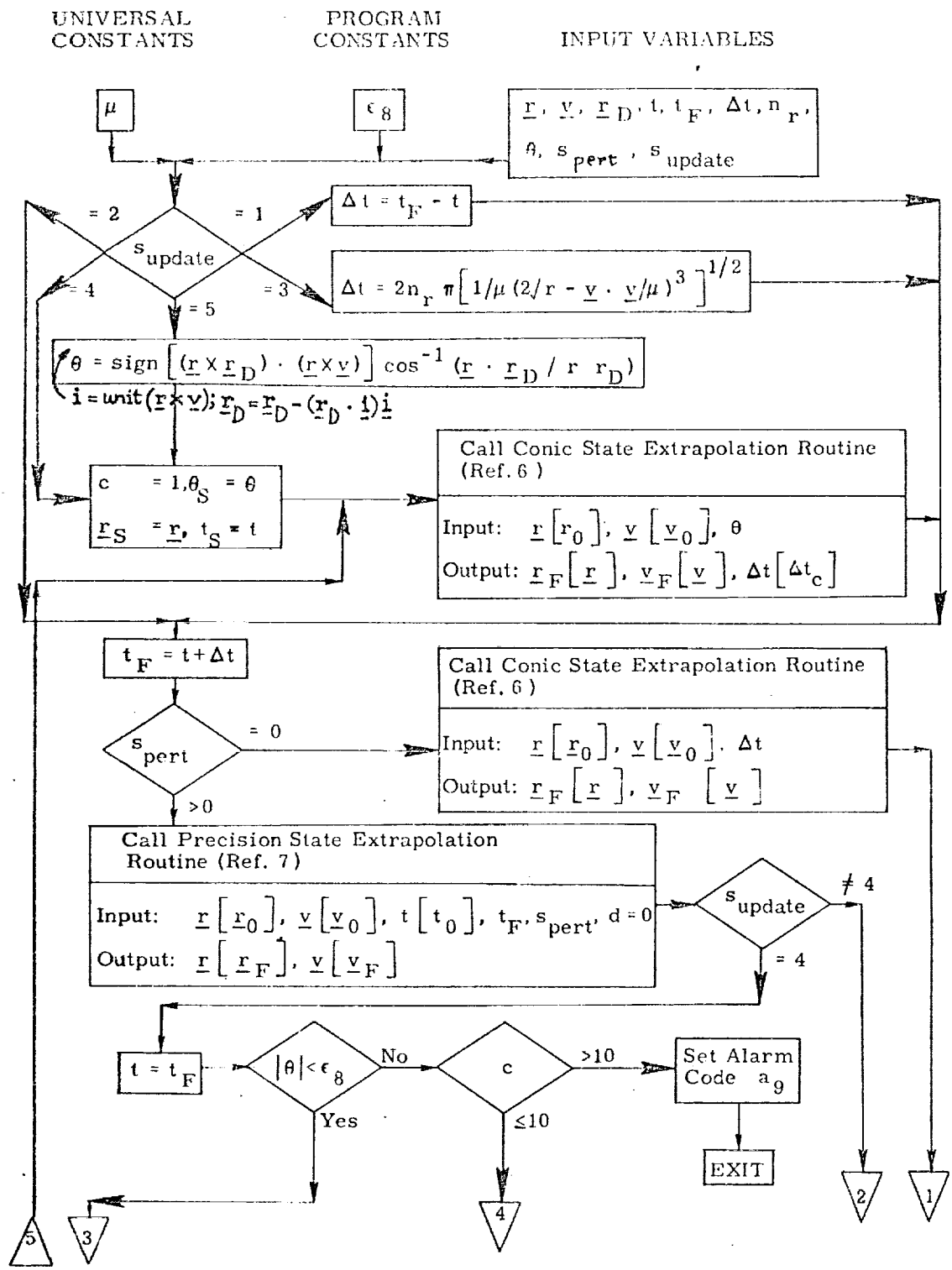


Figure 12a. Update Routine - Detailed Flow Diagram

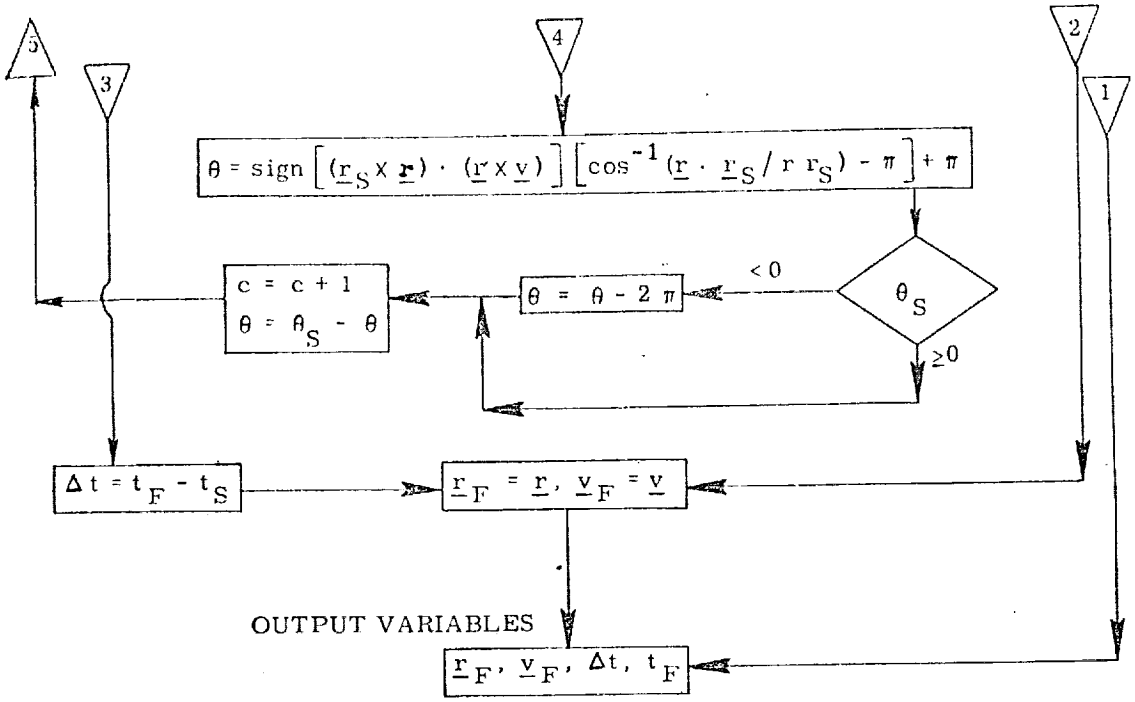


Figure 12b. Update Routine - Detailed Flow Diagram

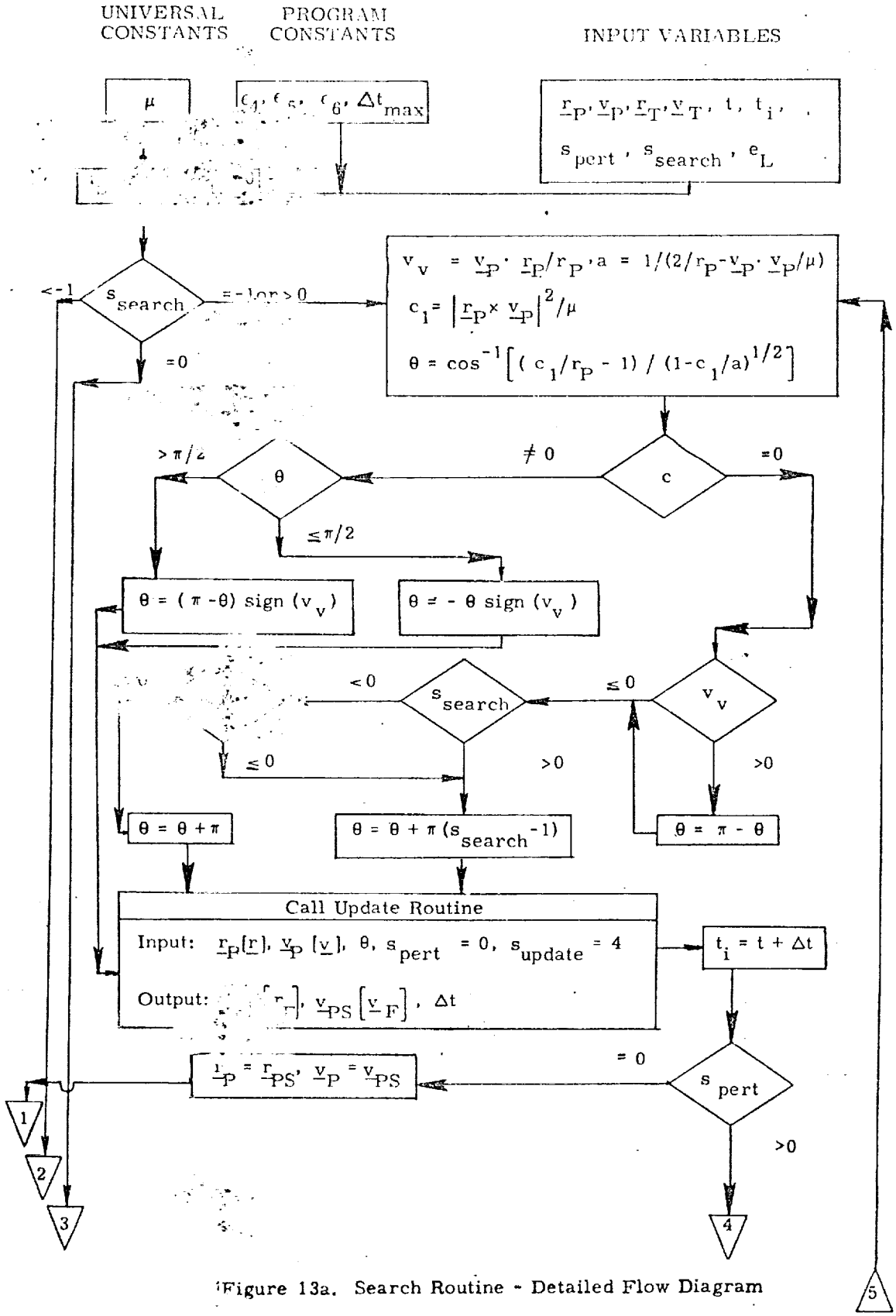


Figure 13a. Search Routine - Detailed Flow Diagram

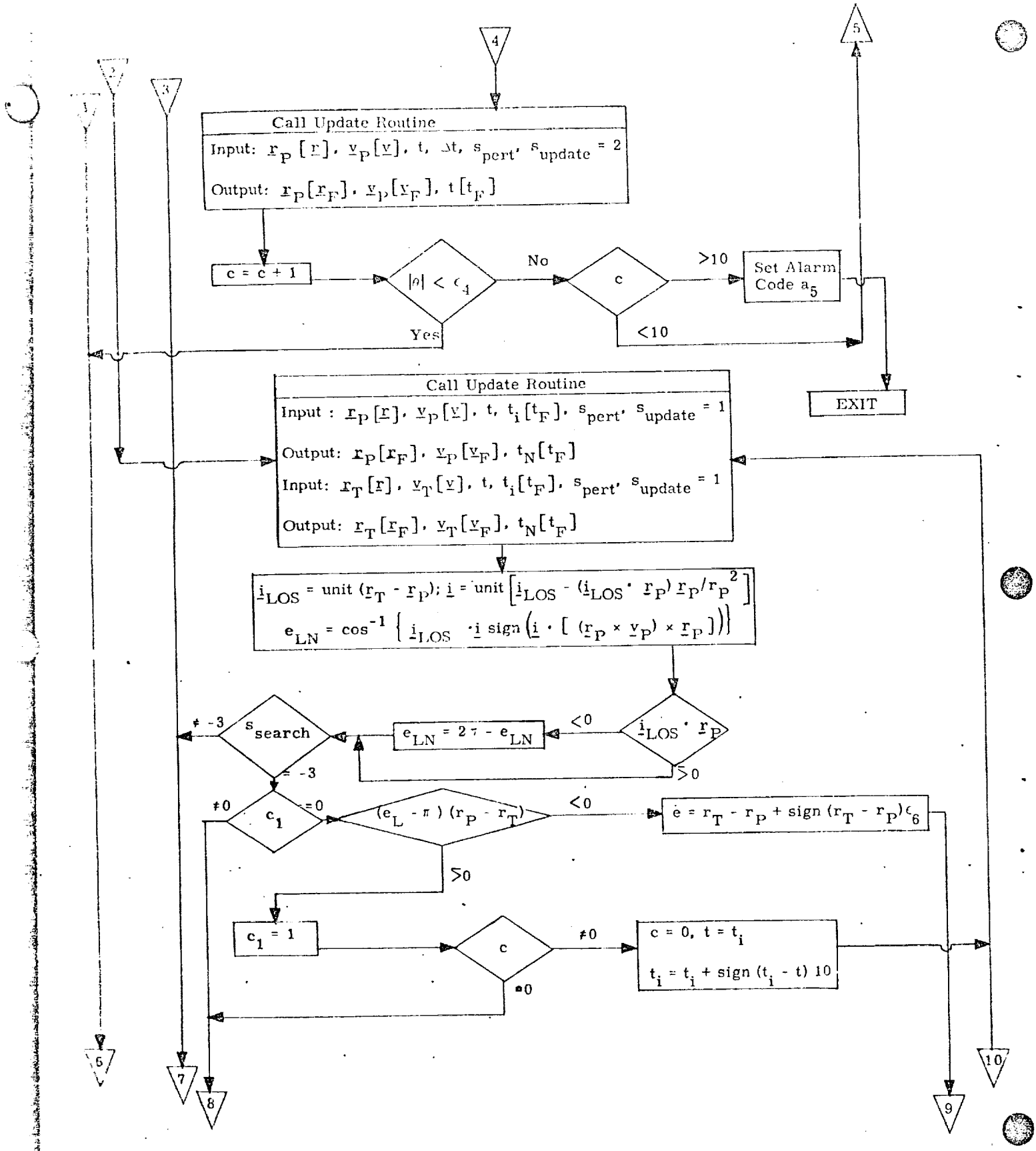


Figure 13b. Search Routine - Detailed Flow Diagram

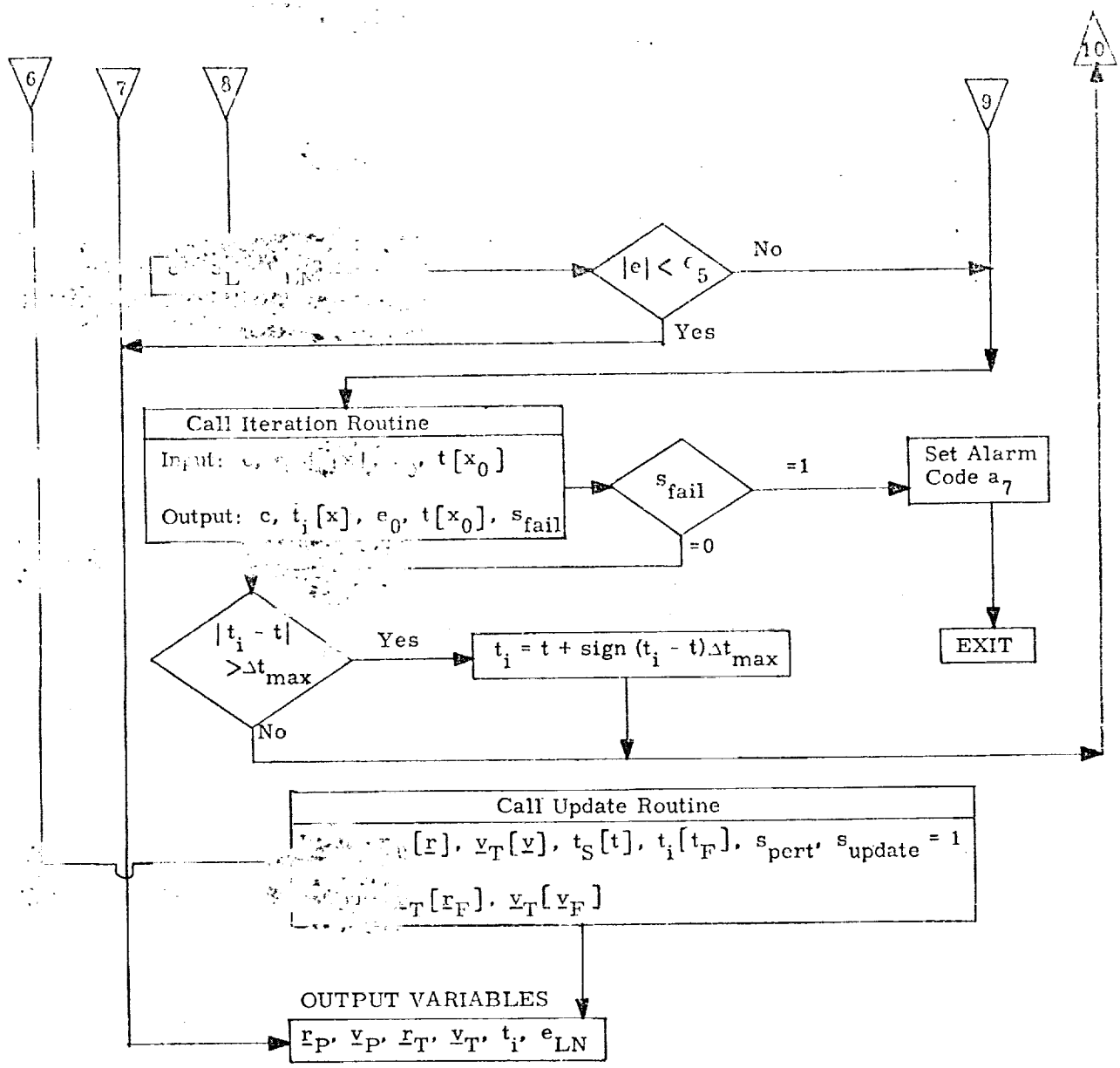


Figure 13c. Search Routine - Detailed Flow Diagram

## 1. INTRODUCTION

The purpose of the Rendezvous Terminal Phase Braking Program is to provide the means of automatically bringing the primary vehicle (Orbiter) within desired station-keeping boundaries relative to the target vehicle (or satellite). To accomplish this task, the program of necessity contains navigation, targeting and guidance functions.

The program is initiated subsequent to the last midcourse maneuver of the rendezvous targeting sequence. Line-of-sight corrections, braking corrections, and filtering of rendezvous measurement sensor data to improve vehicle and target state estimates are performed in a sequential manner. At program initiation, the relative range is on the order of three to five miles.

When the primary vehicle has achieved a position (and velocity) relative to the target which places it within the desired station-keeping boundaries so that the station-keeping function can be initiated and maintained, the program is terminated.

## NOMENCLATURE

| | |
|---|---|
| $b$ | Number of biases to be estimated in Unified Navigation Filter program |
| $c_i$ | Measurement code identifying $i^{th}$ measurement at $t_m$ |
| $f_i$ | Thrust of the engine selected for the maneuver; used in the Powered Flight Guidance Routines |
| $i_{prev}$ | Previous range gate passed; subscript used in braking (range) gate loop |
| $\underline{i}_\rho$ | Unit vector in direction of relative position vector, $\underline{\rho}$ |
| $\underline{i}_s$ | Unit vector which defines center of station-keeping boundary, relative to target vehicle |
| $k_1$ | Constant used to determine the range at which each range gate search starts when approaching that particular range gate |
| $k_2$ | Constant used to determine how often the line-of-sight targeting loop is entered; integer number of terminal phase program cycles |
| $k_3$ | Constant value of range rate added to the minimum range rate at a given range to insure primary vehicle intercept of target vehicle |
| $k_4$ | Constant used to determine how often the range-rate correction targeting loop is entered |
| $m$ | Current estimated primary vehicle mass |
| $M_{R-B}$ | Transformation matrix from reference coordinate frame to body axes coordinate frame |

| | |
|---|---|
| $M_{R-LOS}$ | Transformation matrix from reference coordinate frame (in which vehicle states are expressed) to LOS coordinate frame axes |
| $M_{R-M}$ | Transformation matrix from reference coordinate frame to measurement coordinate frame |
| $M_{R-SM}$ | Transformation matrix from reference coordinate frame to stable member coordinate frame |
| $M_{NB-B}$ | Transformation matrix from navigation base frame to body axes |
| $M_{NB-M}$ | Transformation from navigation base to measurement coordinate frame |
| $M_{SM-NB}$ | Transformation matrix from stable member coordinate frame to navigation base |
| $n$ | Number of discrete braking gates in the range/range rate correction schedule |
| $q_i$ | $i^{th}$ measured relative parameter at $t_m$ |
| $q_{PN}$ | Process noise acceleration |
| $\underline{r}_L$ | Local vertical relative position vector (target vehicle local vertical) |
| $\underline{r}_P$ | Primary vehicle position vector |
| $\underline{r}_T$ | Target vehicle position vector |
| $\underline{r}(t_A)$ | Aimpoint vector used in Lambert targeting calculations |
| $s_B$ | Switch which controls braking gate targeting cycle |
| $s_{eng}$ | Engine select switch |
| $s_{freq}$ | Switch which controls measurement processing (navigation) cycle |

| | |
|---|---|
| $s_{GM}$ | Switch which indicates guidance mode to be used in Powered Flight Guidance Routine; "2"- two axis thrusting; "3"- modified Delta-v mode; "4" - modified Lambert mode |
| $s_{init}$ | Signifies first entry into Unified Navigation Filter program |
| $s_{LAM}$ | Switch used to select type of targeting scheme used in the Terminal Phase Braking Sequencing Program |
| $s_{LOS}$ | Switch which controls line-of-sight targeting cycle |
| $s_{search}$ | Indicates target search routine is needed in the Unified Navigation Filter program |
| $s_{mk}$ | Switch which controls navigation cycle |
| $s_{\Delta v}$ | Switch which indicates if a velocity correction is to be made or not |
| $s_{\Delta v\,LOS}$ | Switch which indicates LOS correction is to be made |
| $t_c$ | Current time |
| $t_{ig}$ | Maneuver ignition time |
| $t_m$ | Measurement time |
| $t_s$ | Time associated with primary and target vehicle state vectors |
| $t_\gamma$ | Time of bias estimate |
| $\underline{v}_L$ | Relative velocity vector in target vehicle local vertical frame |

| | |
|---|---|
| $\underline{v}_P$ | Primary vehicle velocity vector |
| $\underline{v}_T$ | Target vehicle velocity vector |
| $W_I$ | Initial filter weighting matrix |
| $\overline{\alpha_i^2}$ | Measurement variance used in filter to process $i^{th}$ measurement data |
| $\beta$ | Elevation angle of line-of-sight in measurement frame |
| $\delta t_B$ | Delta time to ignition for a range-rate correction maneuver |
| $\delta t_{LOS}$ | Delta time to ignition for a line-of-sight correction |
| $\delta t_m$ | Time between successive measurements within the measurement loop |
| $\Delta t_m$ | Basic sequencing cycle time |
| $\Delta \underline{v}_B$ | Velocity change expressed in the body coordinate frame |
| $\Delta v_{LIM}$ | Magnitude of velocity change below which no maneuver will be applied |
| $\Delta \underline{v}_{LOS}$ | Velocity change expressed in line-of-sight coordinate frame |
| $\gamma$ | Value of station-keeping boundary cone angle |
| $\gamma_b$ | Current estimate of bias |
| $\mu$ | Gravitational constant of the earth |
| $\underline{\nu}$ | Relative velocity vector |

| | |
|---|---|
| $v_u$ | Upper bound on station-keeping velocity |
| $v_\ell$ | Lower bound on station-keeping velocity |
| $\underline{\omega}_{LIM}$ | Angular velocity lower limit below which no line-of-sight rotation is made; value to which line-of-sight angular velocity is driven if a line-of-sight rotation is made |
| $\underline{\omega}_{LOS}$ | Angular velocity vector of the line-of-sight between the primary and target vehicle |
| $\omega_{LOS}$ | Magnitude of $\underline{\omega}_{LOS}$ |
| $\rho$ | Magnitude of relative position vector, $\underline{\rho}$ |
| $\dot{\rho}$ | Range rate between the primary and target vehicles |
| $\underline{\rho}$ | Relative position vector |
| $\rho_{Bi}$ | Range of the $i^{th}$ braking gate |
| $\rho_\ell$ | Lower bound on station-keeping position |
| $\dot{\rho}_{max\ i}$ | Range rate desired at $i^{th}$ braking gate and maximum between braking gates i and i + 1 |
| $\dot{\rho}_{min\ i}$ | Minimum range rate desired between braking gates i and i + 1 |
| $\underline{\rho}_{off(LV)}$ | Offset aimpoint relative to target point expressed in target local vertical frame |
| $\rho_u$ | Upper bound on station-keeping position |
| $\theta$ | Azimuth angle of line-of-sight in measurement frame |
| $[\ \ ]_m$ | Vector expressed in measurement coordinate frame |
| $(\ \ )'$ | Prime indicates previous values of a variable, e.g. prior measurement parameters, prior measurement time, etc. |

## 2. FUNCTIONAL FLOW DIAGRAM

The functional flow diagram for the Rendezvous Terminal Phase Braking Program is shown in Figure 1. The program is initiated after the last rendezvous midcourse correction maneuver of the rendezvous targeting sequence. The relative range between the primary and target vehicle at this point is on the order of three to five miles and closing.

The program sequencing begins with the updating of the estimated primary and target vehicle relative state parameters with the appropriate sensor data.

These relative parameters are then used in the Terminal Phase Targeting Program where the necessary calculations are performed to see if a line-of-sight and/or a braking correction is required to maintain the desired characteristics of the rendezvous trajectory. The line-of-sight corrections (if performed) maintain the intercept by nulling out line-of-sight rates which exceed a desired rate. At selected ranges between the primary and target vehicles, braking corrections are performed to reduce the closing rate to that specified in the terminal range/range rate profile, if the closing rate exceeds the desired value. During the program sequencing a continuous check is made to insure that the closing rate is sufficiently high so that the primary vehicle will intercept the target.

If either a line-of-sight correction and/or range-rate correction is necessary, the velocity correction is applied using the appropriate guidance mode.

The program sequencing is then repeated. The program is terminated when the desired relative position and velocity conditions are achieved so that the station-keeping mode can be initiated and maintained.

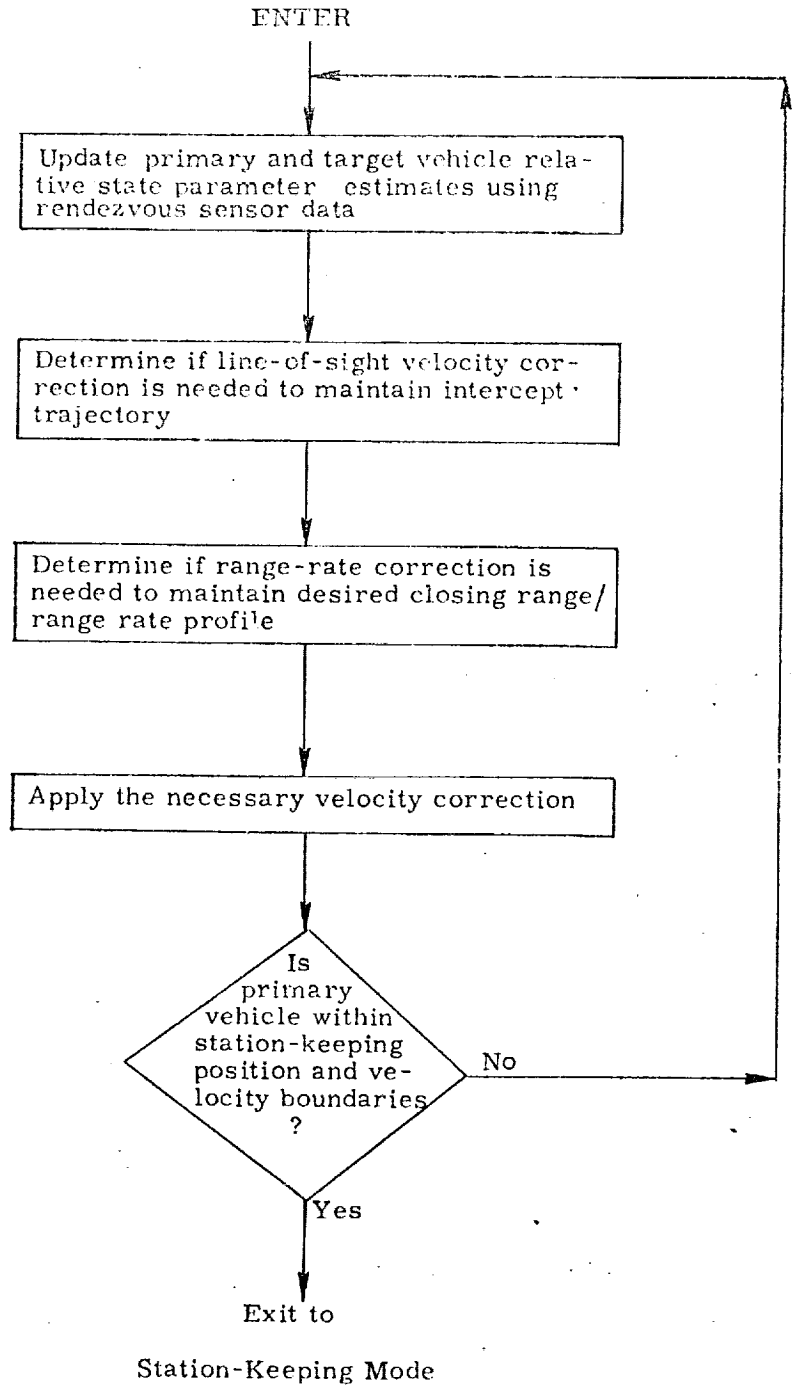


Figure 1. Rendezvous Terminal Phase Braking Program, Functional Flow Diagram

## 3. INPUT AND OUTPUT VARIABLES

The Terminal Phase Braking Program consists of three basic functions - navigation, targeting and guidance. The following is a description of the input and output variables for the basic sequencing program, the navigation program and the targeting program. The Powered Flight Guidance Program is described in Ref. 3.

### 3.1 Terminal Phase Braking Sequencing Program

#### Input Variables

| | |
|---|---|
| $\underline{r}_P(t_s)$, $\underline{v}_P(t_s)$ | Estimated primary vehicle state vector at time $t_s$ |
| $\underline{r}_T(t_s)$, $\underline{v}_T(t_s)$ | Estimated target vehicle state vector at time $t_s$ |
| $n$ | Number of discrete range gate corrections |
| $\rho_{B0}, \ldots \rho_{Bn}$ | Range values of the $n$ braking gates |
| $\dot{\rho}_{B0}, \ldots \dot{\rho}_{Bn}$ | Range rates desired at the $n$ braking gates |
| $s_{freq}$ | Switch which controls navigation cycle |
| $s_{LAM}$ | Switch used to select type of targeting scheme used in the Terminal Phase Braking Program |

#### Output Variables

| | |
|---|---|
| $\underline{r}_P$, $\underline{v}_P$ | Primary vehicle state vector for use in station-keeping phase |
| $\underline{r}_T$, $\underline{v}_T$ | Target vehicle state vector for use in station-keeping phase |
| $t_s$ | Time tag of above state vectors (can be different for active and passive vehicles) |

## 3.2 Terminal Phase Targeting Routine

### Input Variables

| | |
|---|---|
| $\underline{r}_P, \underline{v}_P$ | Primary vehicle state vector |
| $\underline{r}_T, \underline{v}_T$ | Target vehicle state vector |
| $\rho$ | Relative range between primary and target vehicle |
| $\dot{\rho}$ | Range rate between primary and target vehicle |
| $\underline{i}_\rho$ | Unit vector in direction of relative range vector |
| $\underline{\omega}_{LOS}$ | Angular velocity vector of the line-of-sight between the primary and target vehicles |
| $\omega_{LOS}$ | Magnitude of $\underline{\omega}_{LOS}$ |
| $M_{R-B}$ | Matrix transformation between the reference coordinate frame and body coordinates |
| $M_{R-LOS}$ | Matrix transformation between the reference coordinate frame and the line-of-sight coordinate frame |
| $s_{LAM}$ | Switch used to select type of targeting scheme |
| $t_c$ | Current time |

### Output Variables

| | |
|---|---|
| $\underline{i}_N$ | Unit normal to the trajectory plane (in the direction of the angular momentum at ignition ) |
| $\underline{r}_{1c}$ | Offset target position |

| | |
|---|---|
| $t_{ig}$ | Time of upcoming maneuver |
| $\Delta \underline{v}_B$ | Velocity change of upcoming maneuver in body coordinates |
| $\Delta \underline{v}_{LOS}$ | Velocity change of upcoming maneuver in line-of-sight coordinates |
| $\Delta \underline{v}_{LV}$ | Velocity correction in local vertical coordinates |
| $s_{eng}$ | Engine select switch |
| $s_{\Delta v}$ | Switch which indicates if velocity correction is to be performed during this sequencing of the Terminal Phase Braking Program |
| $s_{proj}$ | Switch set when the target vector must be projected into the plane defined by $\underline{i}_N$ |
| $s_{GM}$ | Switch which indicates guidance mode to be used in the Powered Flight Guidance Sequencing Program |

## 4. DESCRIPTION OF OPERATIONS

### 4.1 Terminal Phase Braking Sequencing Program

The Terminal Phase Braking Sequencing Program (Figure 4), which is the main sequencing program for the terminal phase, is initiated after the last midcourse correction in the rendezvous targeting sequence.

The range/range rate terminal braking schedule used in the program is determined prior to the initiation of the program and consists of discrete range gates and their associated desired range rates. A minimum range rate is also specified throughout the terminal phase to insure primary vehicle intercept of the target vehicle. An example of such a braking schedule is shown in Figure 2.

The sequencing begins with the processing of rendezvous sensor data to obtain estimates of range, range rate, line-of-sight rates, etc. These estimates are derived from processing the sensor data in the Relative State Updating Routine (which is also used throughout the rendezvous sequence, Ref. 2)

These relative parameter estimates are then used in the Terminal Phase Targeting Routine to determine if a maneuver (either a braking maneuver, line-of-sight correction or a combination of both) is to be performed. The associated maneuver time and guidance parameters are also computed.

If a maneuver is to be performed, the Powered Flight Guidance Sequencing Program (similar to the Servicer Routine in Apollo) is entered with the appropriate inputs to accomplish the maneuver.

This basic sequencing is repeated until the primary vehicle is within desired station-keeping boundaries relative to the target vehicle (Figure 3).

### 4.2 Terminal Phase Targeting Routine

The Terminal Phase Targeting Routine (Figure 6) computes the necessary maneuvers to maintain the primary vehicle on an intercept with the target vehicle while keeping the range/range rate profile within the desired boundaries.

Two modes of operation are available. The first mode is referred to as automatic line-of-sight control braking and the second automatic Lambert braking.

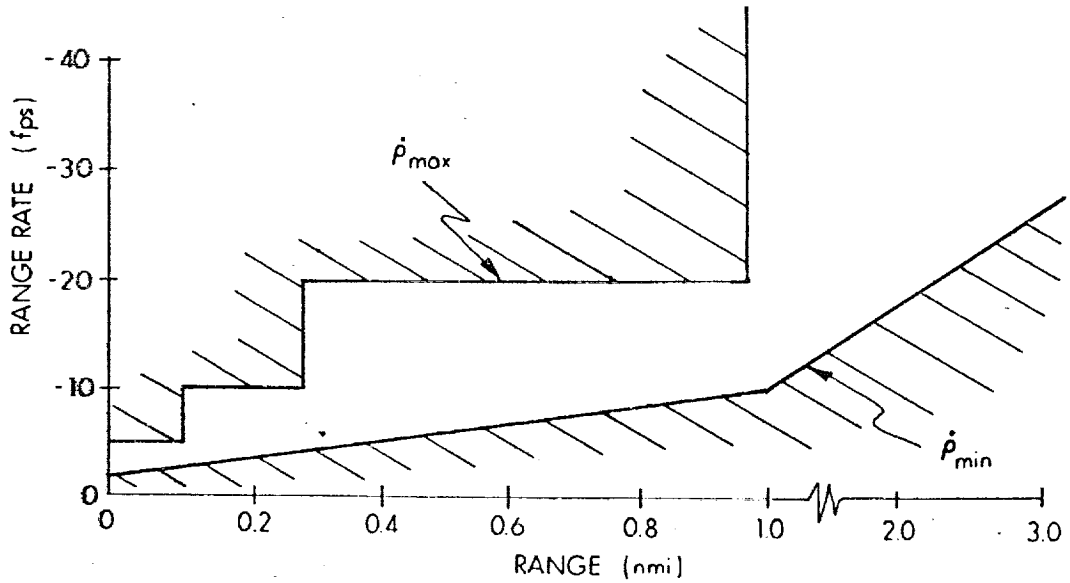


NOTE: Change of scale on range axis.

Figure 2. Typical Range/Range Rate Schedule

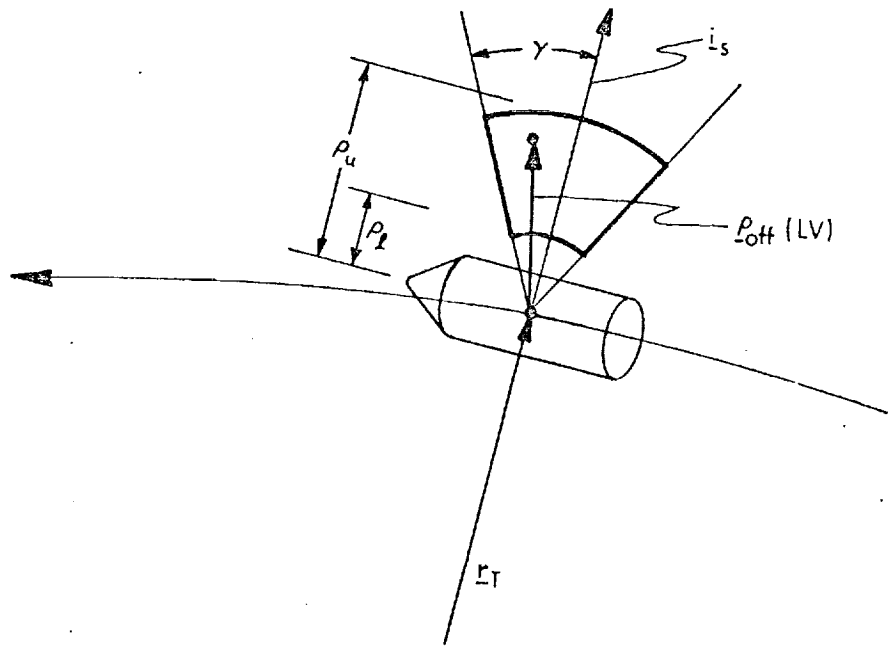


$\gamma$ - Cone angle of station-keeping zone

$\rho_u$, $\rho_\ell$ - Upper and lower values of station-keeping boundaries

$\underline{\rho}_{off}$(LV) - Relative offset vector in target vehicle local vertical, used to target Lambert braking corrections; primary vehicle will intercept this point in the station-keeping zone

Figure 3. Station-Keeping Boundaries–Station-Keeping Above

When $s_{LAM}$ is set to zero, the automatic line-of-sight control braking mode is used. If the line-of-sight rate as determined from processing the sensor data is above a set limit (typically 0.1 mr/sec), the line-of-sight correction necessary to drive the line-of-sight rate to some level is computed and the appropriate ignition time, engine selection and guidance mode switches are set. Since these line-of-sight corrections are made frequently, the maneuver magnitudes are small (several feet/second or less) and hence the small RCS thrusters are used to effect the maneuver. The maneuver is accomplished by using two-axis thrusting normal to the line-of-sight.

The line-of-sight correction check is typically made every two cycles of the main program. (Line-of-sight cycling is determined by $k_2$)

The range/range rate checks, to insure that the desired terminal profile is being followed, are made after the line-of-sight checks. If the range rate at certain pre-selected ranges exceeds the desired range rate a braking maneuver is performed to reduce the closing rate. Continuous checks are made to insure that the closing rate is above the minimum value to maintain intercept. If it is not, then the closing rate is increased.

The ignition time which is set $\delta t_B$ seconds from the present time allows the necessary burn preparations to be made before ignition since these corrections typically involve significant maneuver sizes.

The second mode of operation, the automatic Lambert braking, targets for an intercept point (either the target vehicle or a point offset from the target vehicle indicated by $\underline{\rho}_{off}$, Figure 3) at each pre-selected braking gate. Line of sight rate is implicitly corrected to maintain the intercept trajectory when using this mode of operation.

When the range between the vehicles reaches $(1 + k_1)$ times the pre-selected range gate, the time of arrival at the range gate is computed. The calculation assumes the present range-rate remains constant until the range gate is reached. The primary and target vehicle state vectors are then advanced to this ignition time.

The time of arrival at the intercept point is redefined by the equation

$$t_{go} = \frac{\text{(Range at ignition)}}{\text{(Desired range rate at this range gate)}}$$

This $t_{go}$ is then used to calculate a new target vector for use in the Lambert routine to determine the necessary velocity correction.

By redefining the intercept point in this manner, the Lambert solution forces a reduction in range rate to the desired range rate, insuring intercept in a length of time equivalent to the time it would take to travel the present range at the constant desired range rate. The line-of-sight rate is automatically corrected in the Lambert solution to assure intercept.

The new target vector, time-of-arrival, ignition time and guidance mode switches are then used in the Powered Flight Guidance Routines (Ref. 3) to effect the maneuver.

Between braking gates, line of sight corrections are made when necessary (as in the first mode of operation) to insure arrival at subsequent braking gates and to insure intercept, based on the latest navigated state estimates. (These additional line of sight corrections are not normally needed until the last braking gates has been passed since the Lambert targeted corrections at each gate are adequate to maintain rendezvous intercept.)

## 5. DETAILED FLOW DIAGRAMS

This section contains detailed flow diagrams of the Terminal Phase Braking Sequencing Program, and the Terminal Phase Targeting Routine.

Each input and output variable in the routine and subroutine call statments can be followed by a symbol in brackets. This symbol identifies the notation for the corresponding variable in the detailed description and flow diagrams of the called routine. When identical notation is used, the bracketed symbol is omitted.

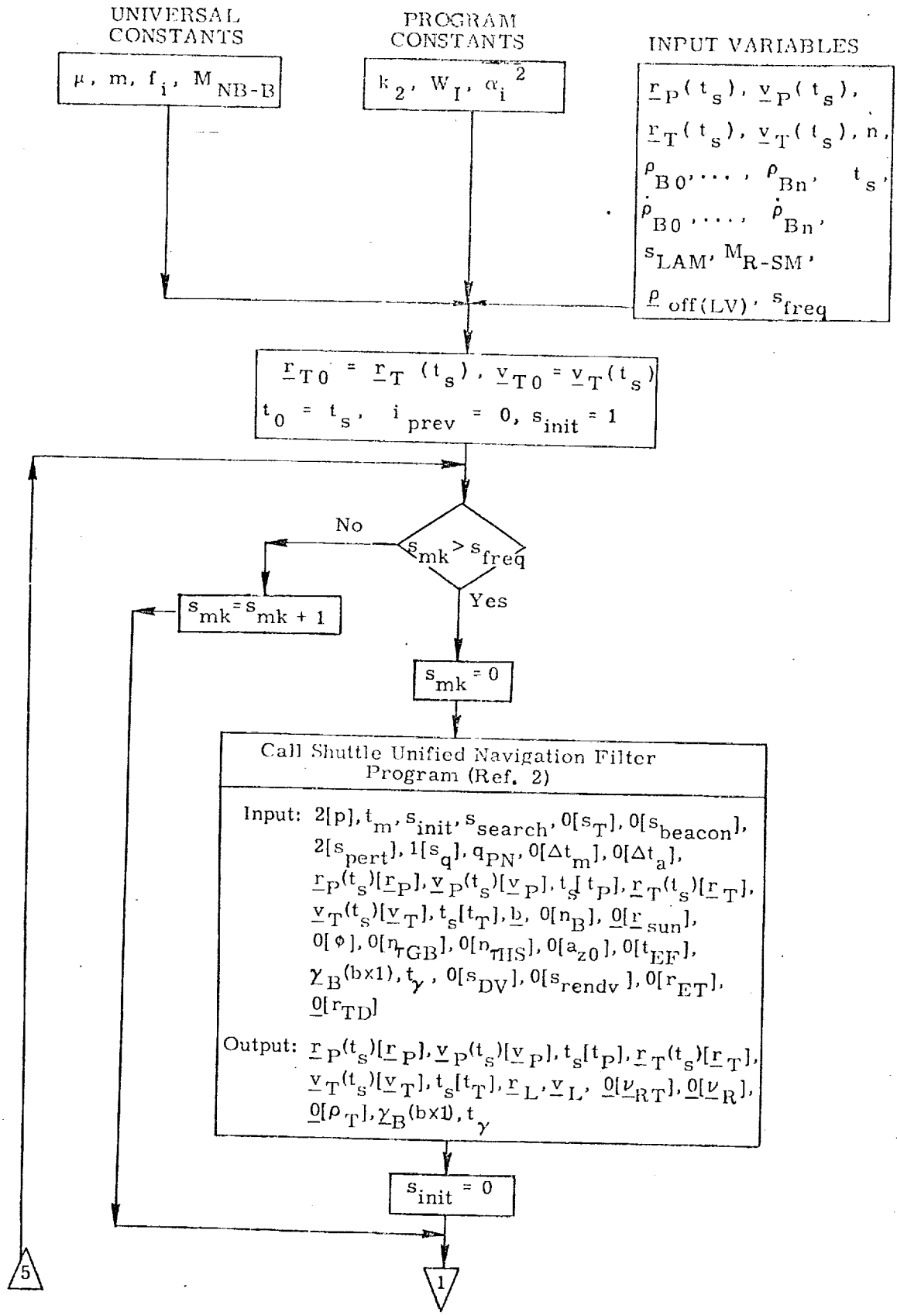


Figure 4a. Terminal Phase Braking Sequencing Program, Detailed Flow Diagram

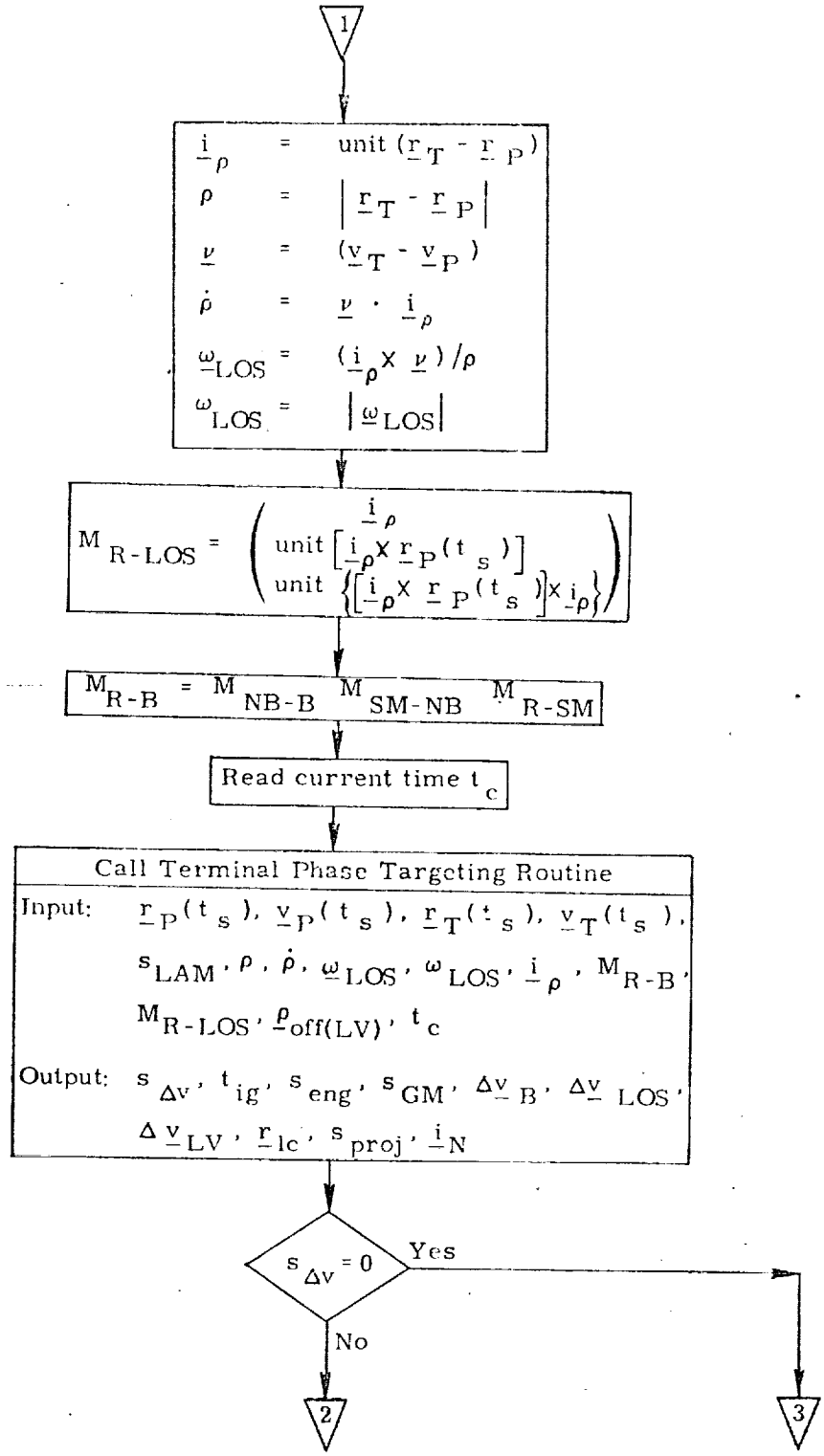


Figure 4b. Terminal Phase Braking Sequencing Program, Detailed Flow Diagram

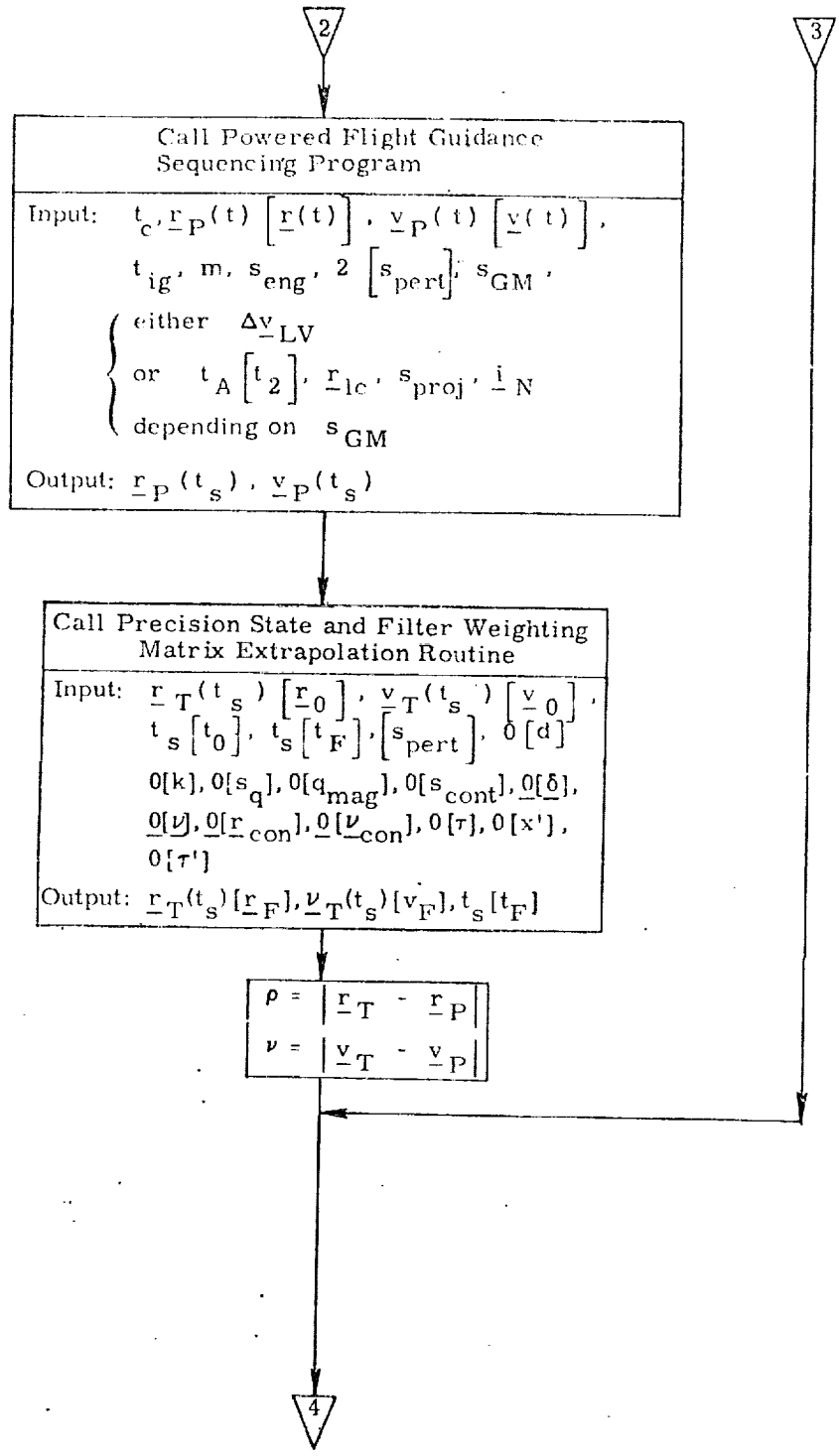


Figure 4c. Terminal Phase Braking Sequencing Program, Detailed Flow Diagram

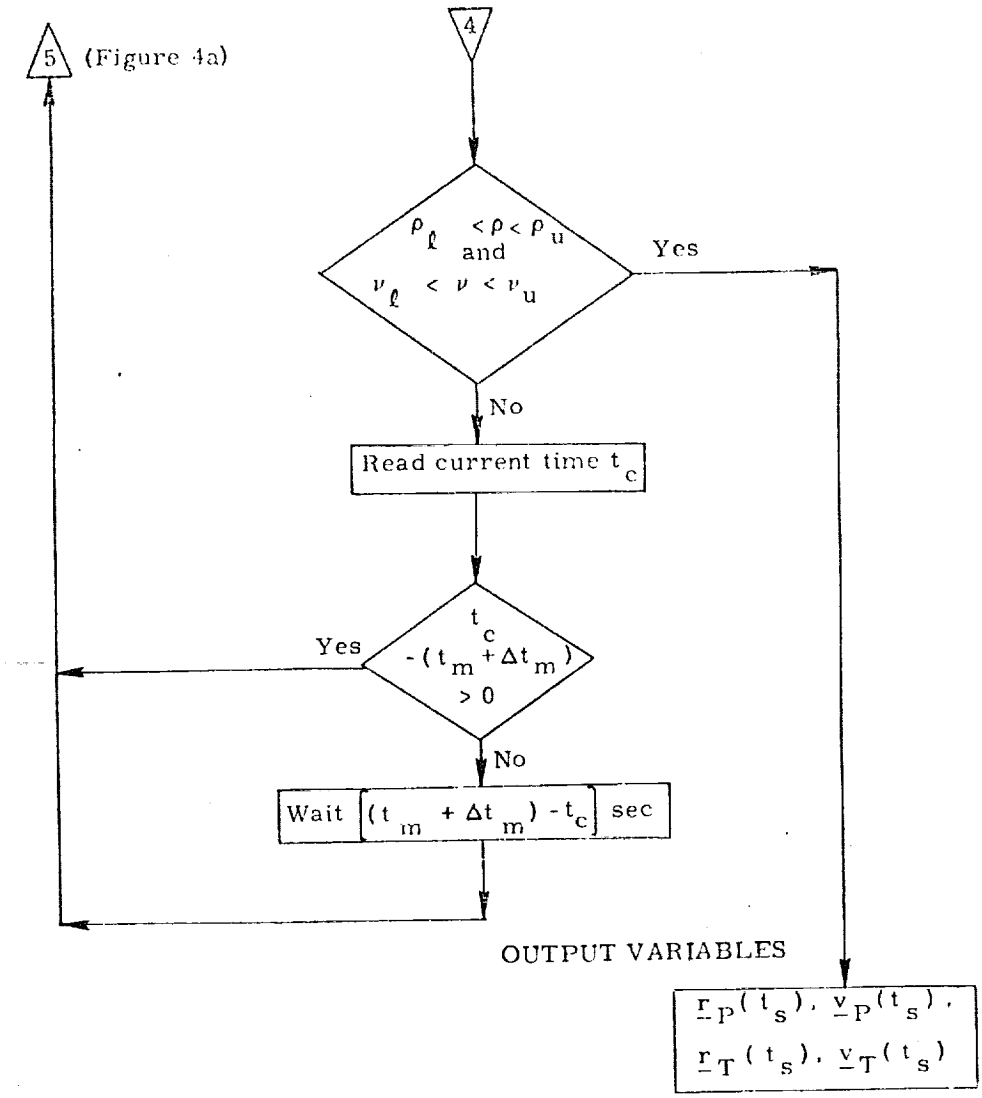


Figure 4d. Terminal Phase Braking Sequencing Program, Detailed Flow Diagram

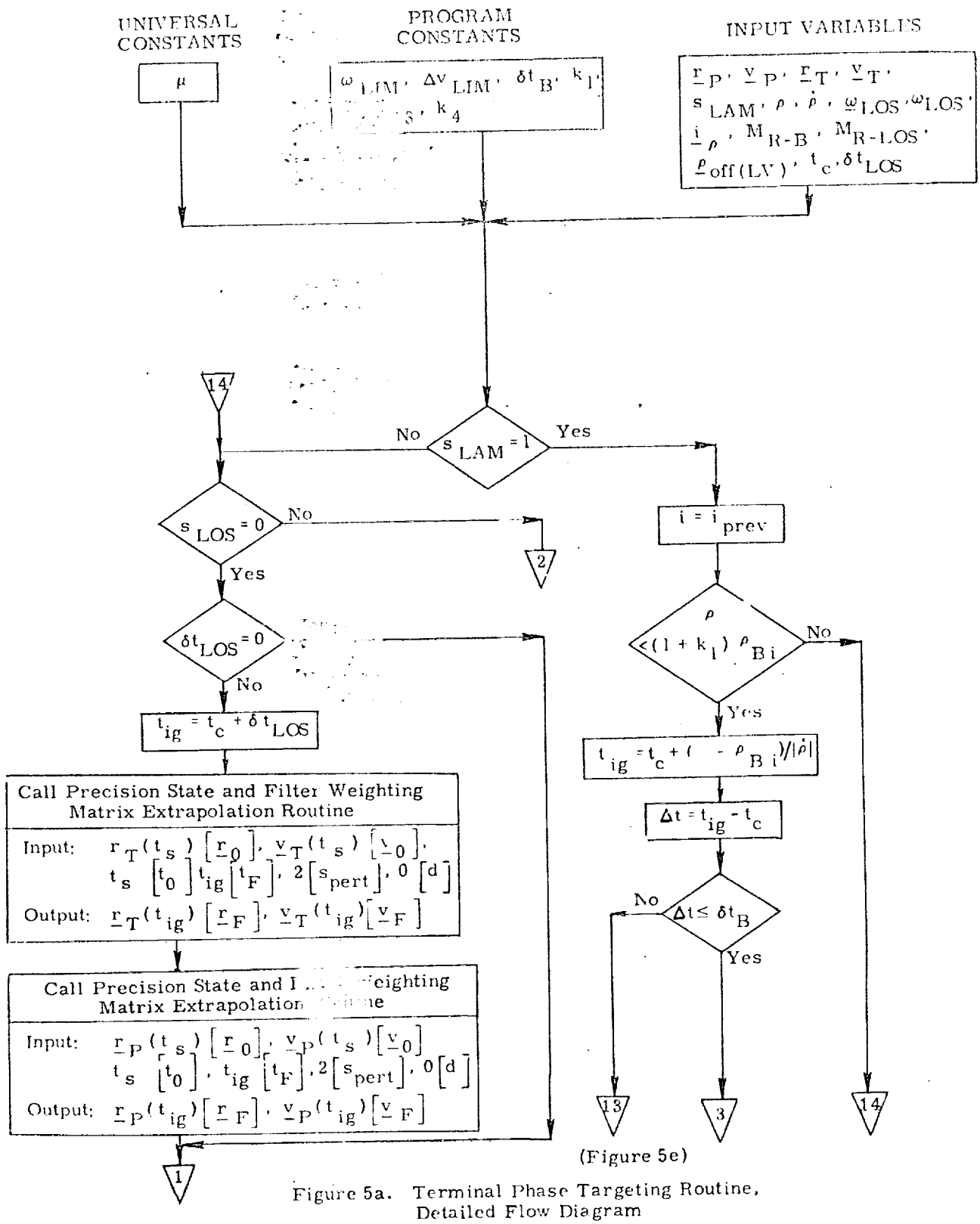


(Figure 5e)

Figure 5a. Terminal Phase Targeting Routine, Detailed Flow Diagram

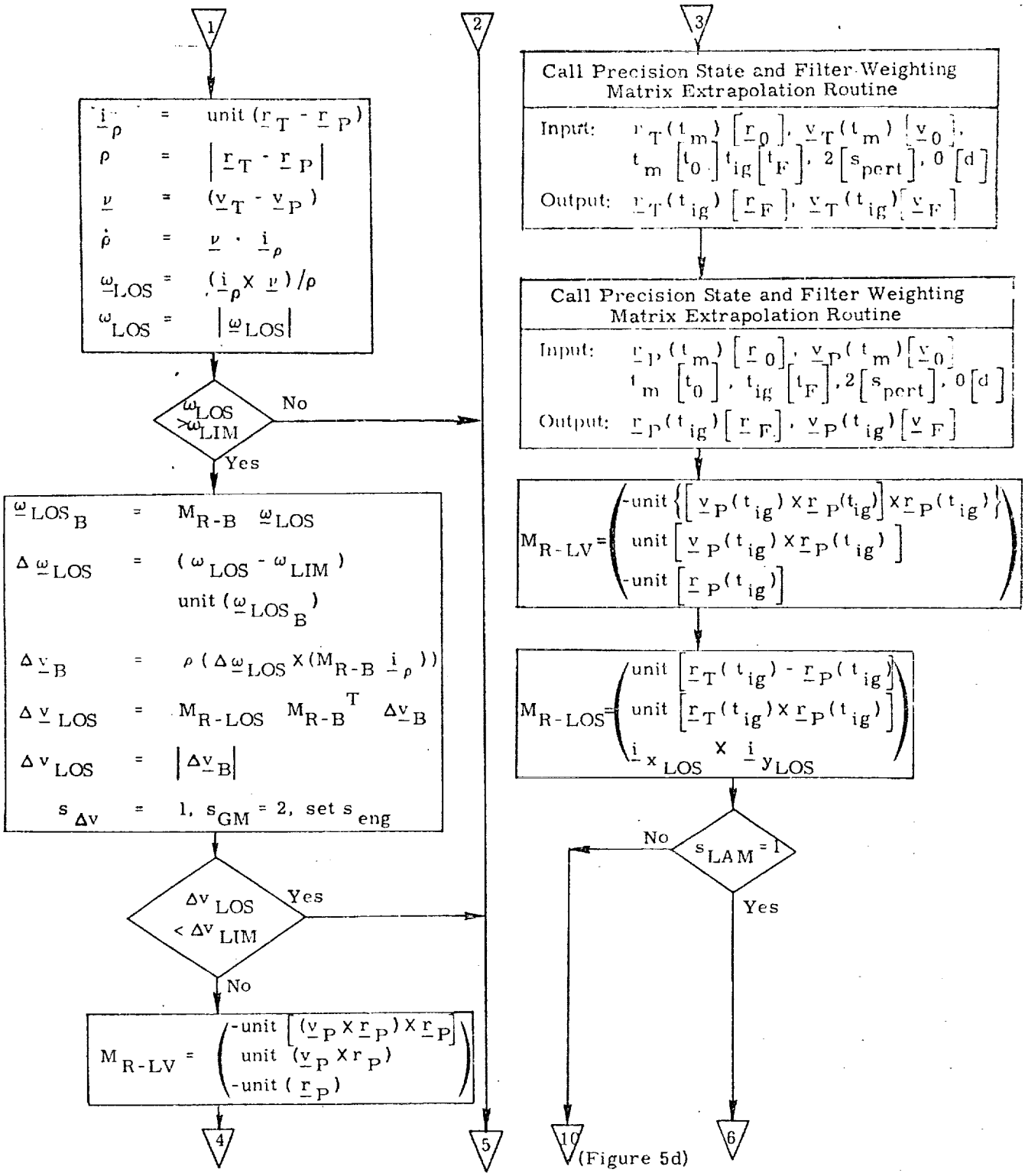


Figure 5b. Terminal Phase Targeting Routine, Detailed Flow Diagram

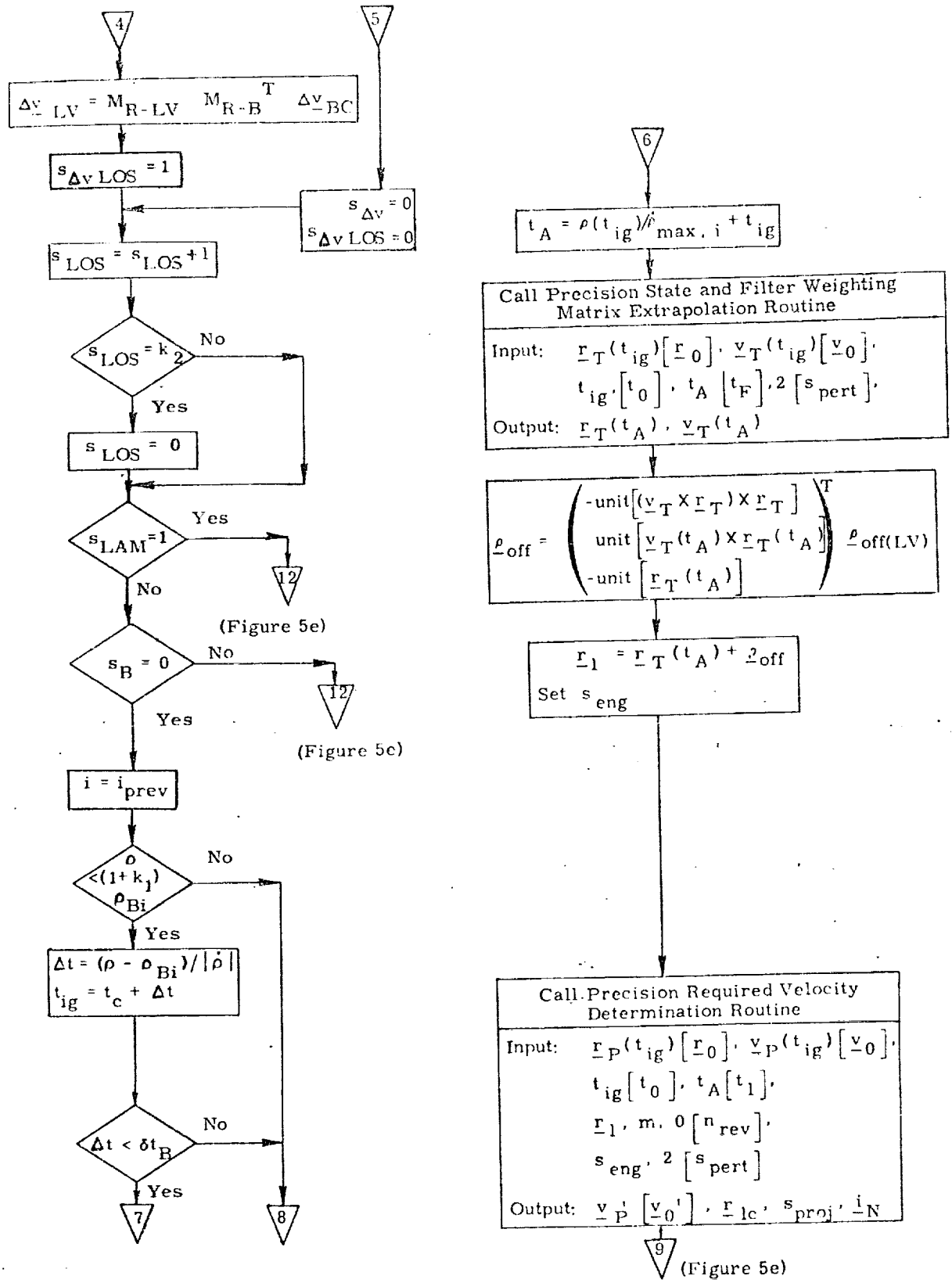


Figure 5c. Terminal Phase Targeting Routine, Detailed Flow Diagram

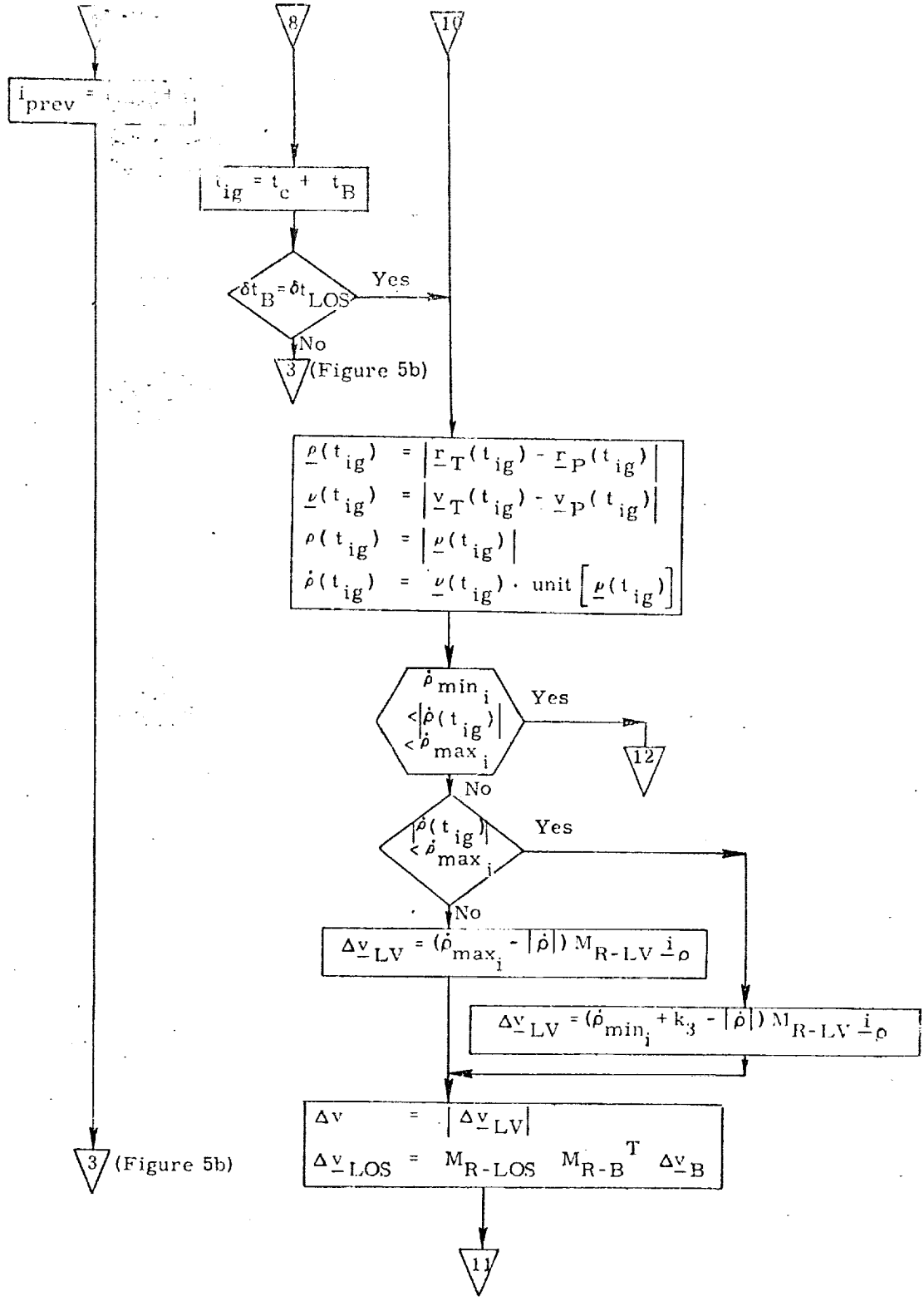


Figure 5d. Terminal Phase Targeting Routine, Detailed Flow Diagram

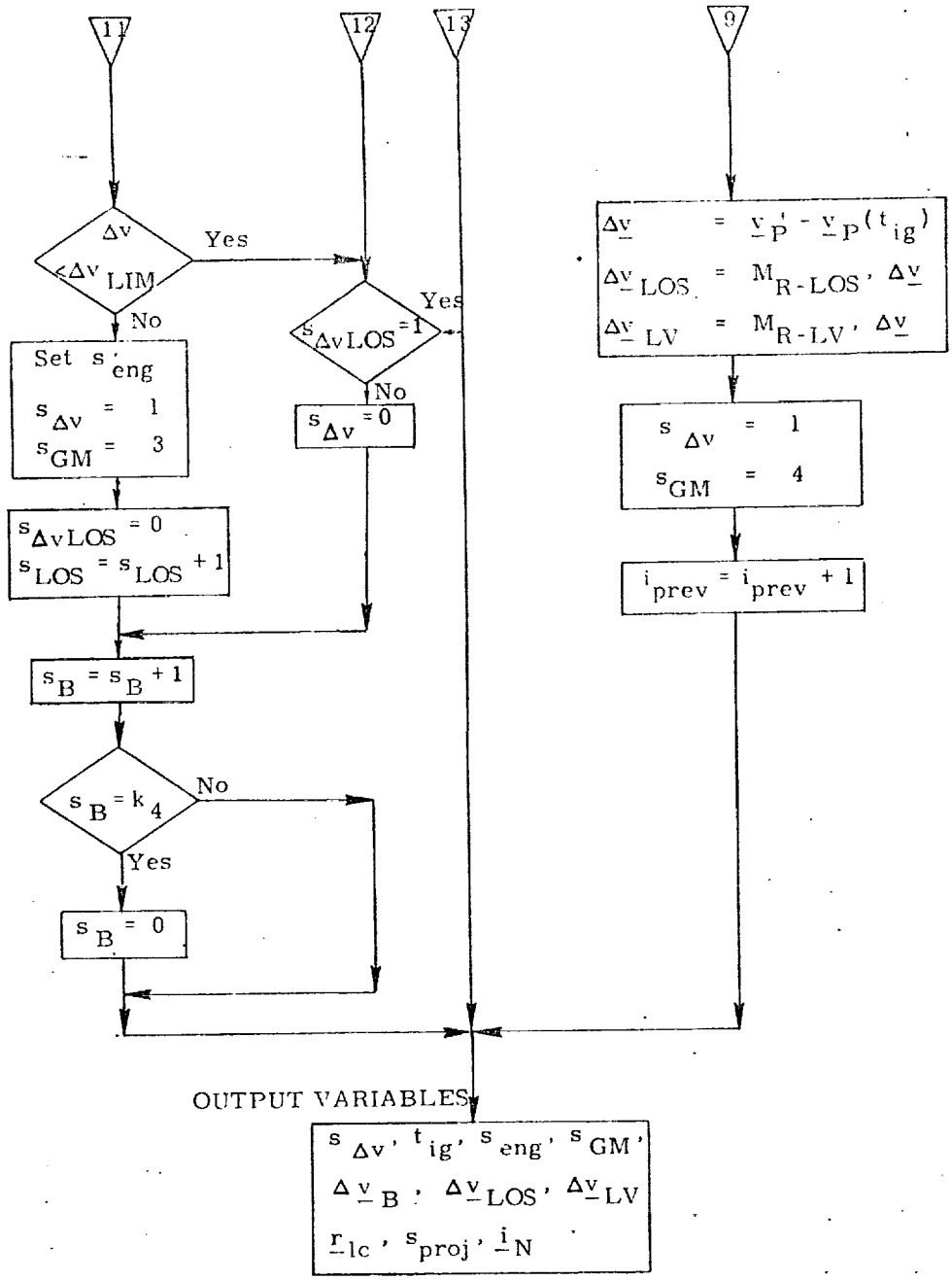


Figure 5e. Terminal Phase Targeting Routine, Detailed Flow Diagram

## 6. SUPPLEMENTARY INFORMATION

The Rendezvous Terminal Phase Braking Targeting and Sequencing Programs utilize an inertial state vector formulation of both the target and primary vehicle. This formulation is the same as that employed throughout the rendezvous phase and therefore the navigation filter used to process the relative measurements is the same in both phases.(see Ref. 1).

The Targeting Program contains two options; (1) "Lambert" maneuvers at the discrete braking gates with line of sight corrections performed as needed and (2) corrections down the line of sight at the discrete braking gates with line of sight corrections as needed.

Powered flight guidance studies have shown that for reduced thrust capability in the terminal phase powered flight guidance is required. Thus, in this situation, option 1 above would be preferred.

Final studies are presently being done to answer the following questions.

1. What is the relative range between the target and primary vehicle below which it is necessary to switch to a relative state formulation of the problem as is done in the station-keeping phase?
2. What modification of the Powered Flight Guidance Routine (if any) is necessary to improve performance in the reduced thrust situation and provide the best performance in the nominal thrust case ?
3. What modification is necessary to a standard (nominal) range, range rate braking schedule for reduced thrust cases to provide adequate time between range gates for thrusting and navigation functions ?

## REFERENCES


1. Muller, E. S., "Shuttle Unified Navigation Filter", Space Shuttle GN&C Equation Document, No. 21, MIT/DL.

2. Brand, T. J., et al, "Powered Flight Guidance", Space Shuttle GN&C Equation Document, No. 11, (Rev. 2), MIT/DL.

3. Robertson, W. M., "Precision State and Filter Weighting Matrix Extrapolation", Space Shuttle GN&C Equation Document, No. 4 (Rev. 2), MIT/DL.

## 1. INTRODUCTION

The purpose of the station-keeping guidance system is to automatically keep one orbiting vehicle within a prescribed zone fixed with respect to another orbiting vehicle. The active vehicle, i.e. the one performing the station-keeping maneuvers, is referred to as the shuttle. The other passive orbiting vehicle is denoted as the workshop. The passive vehicle is assumed to be in a low-eccentricity near-earth orbit.

The primary navigation sensor considered is a gimballed tracking radar located on board the shuttle. It provides data on relative range and range rate between the two vehicles. Also measured are the shaft and trunnion axes gimbal angles. An inertial measurement unit (IMU) is assumed to be provided on board the orbiter. The IMU is used at all times to provide an attitude reference for the vehicle. The IMU accelerometers are used periodically to monitor the velocity-correction burns applied to the shuttle during the station-keeping mode.

The guidance system presented here is capable of station-keeping the shuttle in any arbitrary position with respect to the workshop. This objective is accomplished by periodically applying velocity-correction pulses to the shuttle. These velocity corrections are computed by the guidance routine with the objective of minimizing the average expenditure of propellant (by the shuttle) per orbit.

## 2. FUNCTIONAL FLOW DIAGRAM

A functional flow diagram for the station-keeping guidance routine is shown in Figure 1. The overall structure of the routine is simple and straight-forward. There are two basic subroutines: one is used for computing the normal velocity corrections ($s_{mode} = 1$) and the small midcourse corrections ($s_{mode} = 2$); the other is used for computing boundary-avoidance velocity corrections. The guidance-routine call times and mode selection are accomplished by the Station-Keeping Executive Routine (Ref. 7).

Both subroutines use relative position and velocity (shuttle w.r.t. workshop) from the Station-Keeping Navigation Routine (Ref. 6) as a basis for computing the required velocity corrections. Local-vertical coordinates are used in the normal and midcourse-correction modes, workshop fixed coordinates are used in the boundary-avoidance mode. In-plane and out-of-plane velocity corrections are computed separately in the normal and midcourse correction modes.

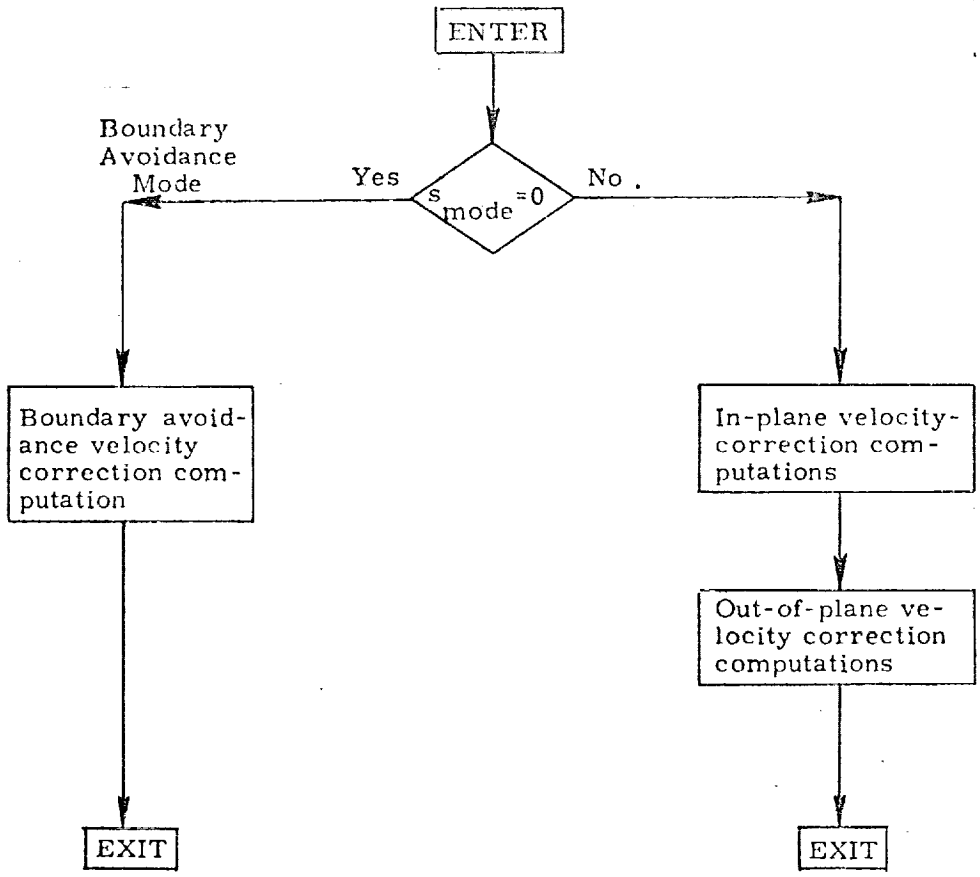


Figure 1. Station-Keeping Guidance Routine, Functional Flow Diagram

## NOMENCLATURE

### Notational Conventions

- Upper-case letters represent matrices
- Lower-case and Greek letters reserved for scalars and vectors
- Vector quantities are underlined, e.g. $\underline{x}$
- Vectors are assumed to be column vectors unless explicitly noted

### Symbols

| | |
|---|---|
| A | Dummy 2 x 2 matrix used in velocity-correction computations |
| a | Elements of A |
| B | Dummy 2 x 2 matrix used in velocity-correction computations |
| b | Elements of B |
| C | Dummy 2 x 2 matrix used in velocity-correction computations |
| c | Elements of C |
| d | Dummy variable used in velocity-correction computations |
| $h_{\ell c}$ | Height of desired station-keeping limit cycle |
| $\underline{i}_{RL}$ | Unit vector along $\underline{r}$ (local-vertical coordinates) |

| | |
|---|---|
| $\underline{i}_{RW}$ | Unit vector along $\underline{r}$ (workshop-fixed coordinates) |
| $\underline{i}_{NW}$ | Unit vector normal to station-keeping cone boundary (workshop-fixed coordinates) |
| $\underline{i}_{XWL'}$ $\underline{i}_{YWL'}$ $\underline{i}_{ZWL}$ | Workshop-fixed frame unit vectors (local-vertical coordinates) |
| k | Midcourse-correction fractions |
| $M_{L-W}$ | Transformation matrix from local-vertical to workshop-fixed coordinates |
| $M_{L-P}$ | Transformation matrix from local-vertical to stable-member coordinates |
| q, $\dot{q}$ | Dummy test variables used in boundary avoidance calculations |
| $\underline{r}$ | Shuttle position w.r.t. workshop (stable-member coordinates) |
| $\underline{r}_L$ | Shuttle position w.r.t. workshop (local-vertical coordinates) |
| $\underline{r}_W$ | Shuttle position w.r.t. workshop (workshop coordinates) |
| $r_{XZ}$ | Magnitude of component of $\underline{r}$ in workshop frame X-Z plane |
| $r_{MIN}$ | Lower limit on $r_W$ along workshop Y-axis for which boundary-avoidance velocity corrections may be required |
| $\underline{r}_{DL}$ | Desired target position for orbiter w.r.t. workshop at terminal time $t_F$ |

| | |
|---|---|
| $s_{OPG}$ | Switch used to select out-of-plane guidance mode |
| $s_{VCORR}$ | Switch set at unity if velocity correction is required |
| $s_{mode}$ | Switch to select current mode of operation of routine |
| $s_{nut_F}$ | Switch set at unity when new $t_F$ is required |
| $t$ | Current time |
| $t_F$ | Terminal time for current guidance limit cycle |
| $\underline{v}_L$ | Shuttle velocity w.r.t. workshop (local-vertical coordinates) |
| $v_{DN}$ | Velocity-correction level used for boundary avoidance |
| $y_{min}$ | Lowest part on desired limit cycle w.r.t. workshop (along vertical axis) |
| $z_{MAX}$ | Maximum desired out-of-plane distance for orbiter |
| $z_{MIN}$ | Minimum desired out-of-plane distance for orbiter |
| $z_0$ | Dummy variable |
| $\underline{\omega}_W$ | Workshop angular velocity (stable-member coordinates) |
| $\theta$ | Dummy variable equal to $\omega_W (t_F - t)$ |
| $\tau$ | Dummy time interval $(t_n - t_{n-1})$ |
| $\delta v_{min}$ | Lower limit on computed velocity-correction magnitude |
| $\delta \underline{v}_L$ | Required velocity correction (local-vertical coordinates) |
| $\theta_Z$ | Station-keeping cone half angle |

| | |
|---|---|
| $\delta v_{XL}$, $\delta v_{YL}$, $\delta v_{ZL}$ | Components of $\delta \underline{v}_L$ |

Special Notation

| | |
|---|---|
| $(\ )'$ | A-priori estimated value prior to measurement incorporation |
| $(\overline{\ })$ | Ensemble average of ( ) |
| $\lvert(\ )\rvert$ | Magnitude of ( ) |
| $(\ )^T$ | Transpose of ( ) |
| unit ( __ ) | Unit vector for ( ___ ) |

## 4. DESCRIPTIO[illegible]ATIONS

### 4.1 General Infor[illegible]n

The station-k[illegible]idance routine is capable of maintaining an active vehicle (shuttle) in a small zone which may be arbitrarily located with respect to a passive orbiting vehicle (workshop). The passive vehicle is assumed to be in a low-eccentricity orbit around the earth. The station-keeping is accomplished by the periodic application [illegible] small velocity-correction pulses. The size and location of the station-keeping zone are specified as program constants and input variables (e.g. $h_{\ell c}$, $y_{min}$, [illegible] x, $z_{min}$, $\underline{r}_{DL}$).

The guidance [illegible]ine has three primary modes: (1) normal station-keeping, (2) midcourse correction, and (3) boundary avoidance. In the normal mode the velocity corrections required to hold the shuttle in the specified zone w.r.t. the workshop are computed. In typical situations these corrections are relatively small (e.g. 2-5 ft/sec or less). The magnitude and frequency of these corrections is dependent on the size and location of the station-keeping zone. The midcourse-correction mode uses essentially the same relations as the normal mode. The basic idea here is tha[illegible] applying small velocity corrections in between the normal velocity-correction [illegible] the total velocity-correction propellant expenditure may be reduced. In the b[illegible]ary-avoidance mode, special tests are made to see if the shuttle is outside of the station-keeping zone and heading away from it. Appropriate velocity-correction pulses are applied to the orbiter to return it to the desired zone.

The times at which each mode of the station-keeping guidance routine is called are determined by the Station-Keeping Executive Routine (Ref. 7).

Three coordinate systems are used in the station-keeping guidance routine: (1) stable-member, (2) local-vertical, and (3) workshop-fixed coordinates. All three systems are orthogonal right-handed systems. The relationships between these frames are shown in Figure 2. The stable-member system is fixed w.r.t. the inertial measure[illegible]nt unit (IMU). The local-vertical system rotates with the workshop, as shown in Figure 2, with its X-axis along the local vertical and its Z-axis along the workshop-orbit angular-momentum vector. The normal-mode and midcourse-correction computations in the guidance routine are done primarily in this local-vertical frame. The workshop-fixed frame is fixed w.r.t. the desired station-keeping zone. The boundary-avoidance mode computations in the guidance routine are performed in this frame.

### 4.2 Normal Guidance Mode

The analytical development of the basic guidance concept has been extensively documented in Refs. 1 and 3 for AAP missions, and in Ref. 2 for SSV missions.

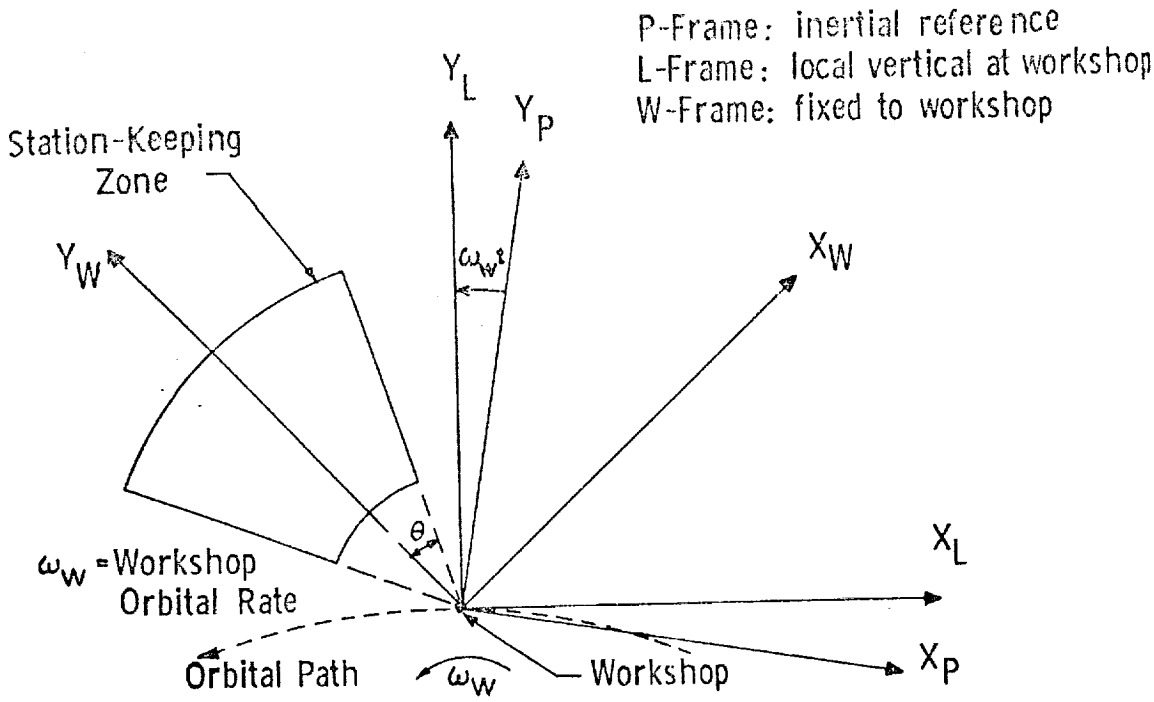


Figure 2. Station-keeping System Relative Geometry

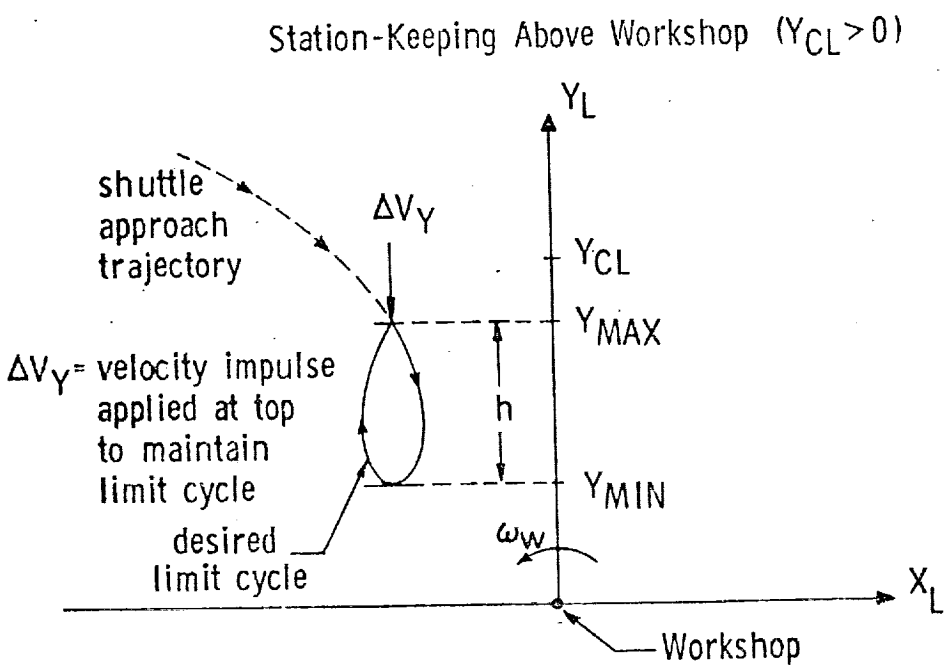


Figure 3. Geometry for Guidance Limit Cycles

Extensive pe[illegible]nce data is given in these references. It is most convenient to consider the in-plane and out-of-plane guidance equations separately. This approach will be f[illegible]ed here.

The in-pl[illegible]problem will be considered first. The basic idea is to put the shuttle on a tra[illegible]ry that will terminate at a specified position w.r.t. the workshop ($\underline{r}_{DL}$) at a fixed terminal time ($t_F$). A typical limit-cycle trajectory is shown in Figure 3 for the case where the station-keeping zone is above and in front of the workshop.

The terminal time ($t_F$) is based on the desired limit-cycle trajectory height ($h_{\ell c}$) and desired minimum altitude of shuttle w.r.t. the workshop ($y_{min}$). The basic relat[illegible]is (Ref. 2):

$$t_F = t + \frac{2}{\omega_W}\sqrt{\frac{6\, y_{\ell c}}{9\, y_{min} + 4\, h_{\ell c}}} \qquad (1)$$

where $t$ is the current time, and $\omega_W$ is the workshop's angular velocity.

The required correction ($\delta \underline{v}_L$) that must be made to the current shuttle velocity ($\underline{v}_L$) in order for the vehicle to arrive at the position ($\underline{r}_{DL}$) at the terminal time $t_F$ is computed in a straight-forward manner (Refs. 1 and 2). The basic relatic is

$$\delta \underline{v}_L = \Phi_{RV}^{-1}(t, t_F)[\underline{r}_{DL} - \Phi_{RR}(t, t_F)\,\underline{r}_L] - \underline{v}_L \qquad (2)$$

where $\underline{r}_L$ and $\underline{v}_L$ represent the position and velocity of the shuttle w.r.t. the workshop, expressed in local-vertical coordinates.

The matrices $\Phi_{RV}$ and $\Phi_{RR}$ are submatrices of the matrix $\Phi$, which is used to extrapolate the shuttle state w.r.t. the workshop forward in time, using local-vertical coordinates. The relation is

$$\begin{bmatrix} \underline{r}_L(t_n) \\ \underline{v}_L(t_n) \end{bmatrix} = \left[\begin{array}{c|c} \Phi_{RR}(\tau) & \Phi_{RV}(\tau) \\ \Phi_{VR}(\tau) & \Phi_{VV}(\tau) \end{array}\right] \begin{bmatrix} \underline{r}_L(t_{n-1}) \\ \underline{v}_L(t_{n-1}) \end{bmatrix} \qquad (3)$$

where $t_{n-1}$ and $t_n$ are arbitrary times ($t_n > t_{n-1}$). The detailed relations for $\Phi_{RR}$, $\Phi_{RV}$, $\Phi_{VR}$ and $\Phi_{VV}$ are given in Refs. (1) and (2) as a function of workshop angular velocity ($\omega_W$) and the time interval from $t_{n-1}$ to $t_n$ (referred to as $\tau$).

In the detailed flow diagram for the guidance routine (Figure 4) the required elements of $\Phi_{RV}^{-1}$ and $\Phi_{RV}^{-1}\ \Phi_{RR}$ are represented by the matrices A, B, C, and the dummy variable d.

Two out-of-plane guidance modes are provided (Ref. 2). If the desired station-keeping zone is centered in the workshop orbital plane, then Eqs. (2) and (3) can be used to compute the required velocity correction ( $\delta v_{ZL}$). The basic equation in this case is simply:

$$\delta v_{ZL} = -\omega_W r_{L,2} \cot\theta - v_{L,2} \tag{4}$$

where $r_{L,2}$ and $v_{L,2}$ are the out-of-plane components of shuttle position and velocity w.r.t. the workshop. The quantity $\omega_W$ is the workshop's angular velocity w.r.t. the earth. The dummy variable $\theta$ is given by:

$$\theta = \omega_W (t_F - t) \tag{5}$$

where $t_F$ is the desired arrival time at the terminal or target point.

If, on the other hand, it is desired that the station-keeping zone be displaced from the workshop orbital plane, then the required velocity correction (Ref. 2) is given by

$$\delta v_{ZL} = \omega_W \sqrt{z_{max}^2 - r_{L,2}^2}\,\omega_W \operatorname{sign}(z_{min}) - v_{L,2} \tag{6}$$

The parameters $z_{max}$ and $z_{min}$ specify the desired maximum and minimum displacements of the shuttle w.r.t. the workshop in the out-of-plane direction. A velocity correction is applied only if $|r_{L,2}|$ is less than $z_{min}$ and the relative velocity is such as decreases $|r_{L,2}|$ still further (i.e. $v_{L,2}\ r_{L,2}$ is negative).

The boundary-avoidance guidance scheme assumes an inverted truncated cone as the desired station-keeping zone. The apex of the cone is at the workshop, and the cone's axis ($\underline{i}_{YWL}$) is assumed fixed w.r.t. the workshop. The lower boundary of the zone is specified by the parameter $r_{min}$ which is its minimum distance from the workshop. The size of the station-keeping zone is specified by the cone half angle $\theta_Z$.

Two boundary-avoidance tests are made. First, if the shuttle is too close to the workshop ($r_{W,1} < r_{min}$) and its velocity is taking it towards the shuttle, then a correction is required. The shuttle in this case is given a preselected velocity ($v_{DN}$) away from the workshop. This is accomplished by a velocity correction ($\delta \underline{v}_L$) of

$$\delta \underline{v}_L = (v_{DN} - v_{W,1}) \underline{i}_{YWL} \tag{7}$$

where $\underline{i}_{YWL}$ is a unit vector along the workshop-frame Y-axis (station-keeping zone cone axis), and $r_{W,1}$ and $v_{W,1}$ are the components of relative position and velocity along this axis.

Next, a test is made to see if the shuttle is inside the desired zone. The test quantity ($q$) is computed from:

$$q = i_{RW,1} - \cos \theta_Z \tag{8}$$

A second test is now made to see if the shuttle's velocity is directed away from the zone's center line, i.e. the angle between $\underline{r}_W$ and the cone's axis is increasing. The test quantity $\dot{q}$ is given by:

$$\dot{q} = [\, v_{W,1} - (\underline{v}_W \cdot \underline{i}_{RW})\, i_{RW,1} \,] \tag{9}$$

If both $q$ and $\dot{q}$ are negative, then the shuttle's component of velocity (w.r.t. the workshop) in the direction normal to the station-keeping cone boundary ($\underline{i}_{NW}$) is given a prespecified value of $v_{DN}$, directed in towards the cone axis. The required velocity correction to accomplish this is (Ref. 1).

$$\delta \underline{v}_W = (v_{DN} - \underline{v}_W \cdot \underline{i}_{NW})\, \underline{i}_{NW} \tag{10}$$

where the required velocity correction $\delta \underline{v}_W$ is in workshop-fixed coordinates as is the relative velocity ($\underline{v}_W$).

## 5. DETAILED FLOW DIAGRAMS

A detailed flow diagram is shown for the Station-Keeping Guidance Routine in Figure 4. To operate this routine, navigation information is required from the Station-Keeping Navigation Routine. The mode selection and routine-call times for both the Station-Keeping Guidance and Navigation Routines are controlled by the Station-Keeping Executive Routine.

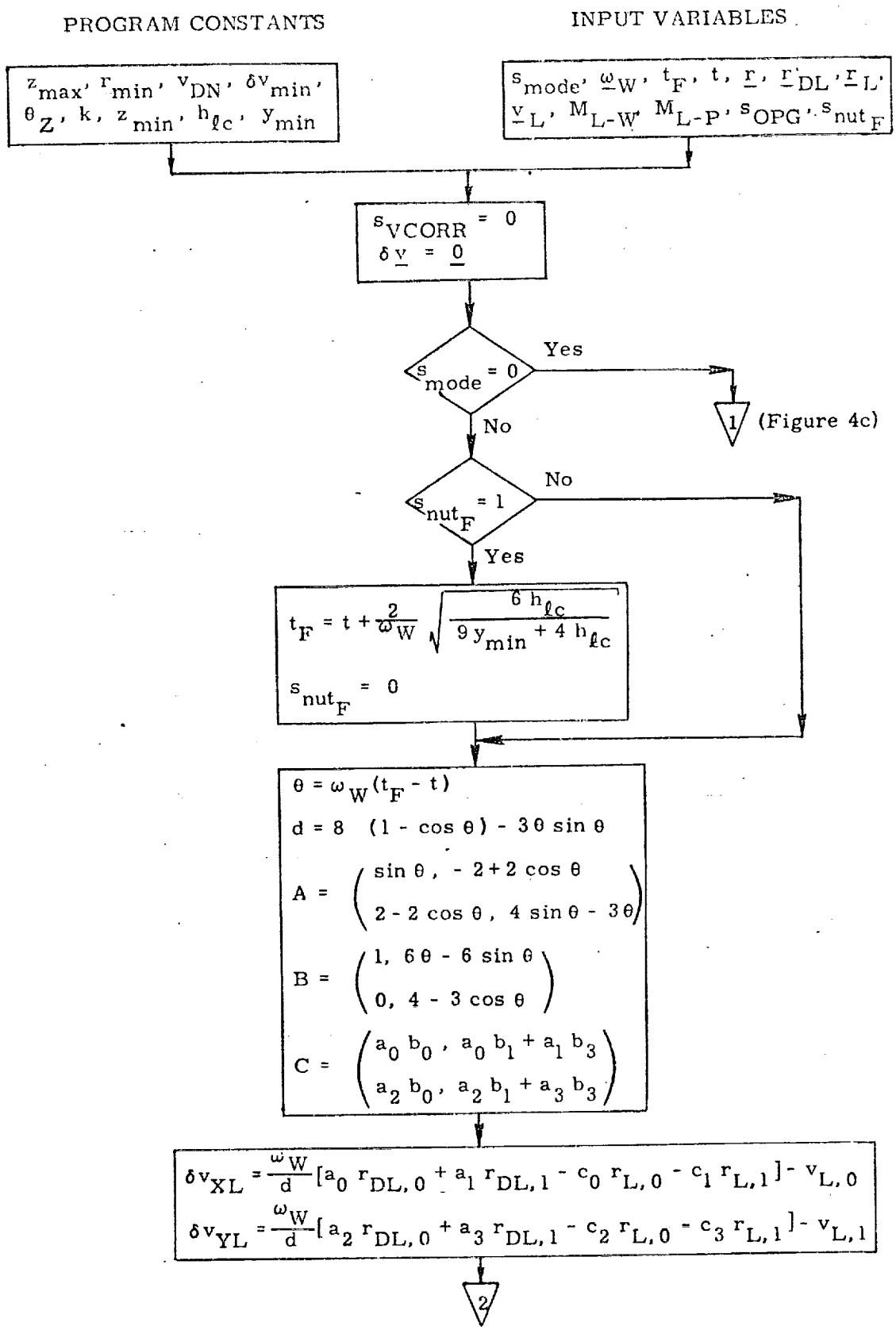


Figure 4a. Station-Keeping Guidance, Detailed Flow Diagram

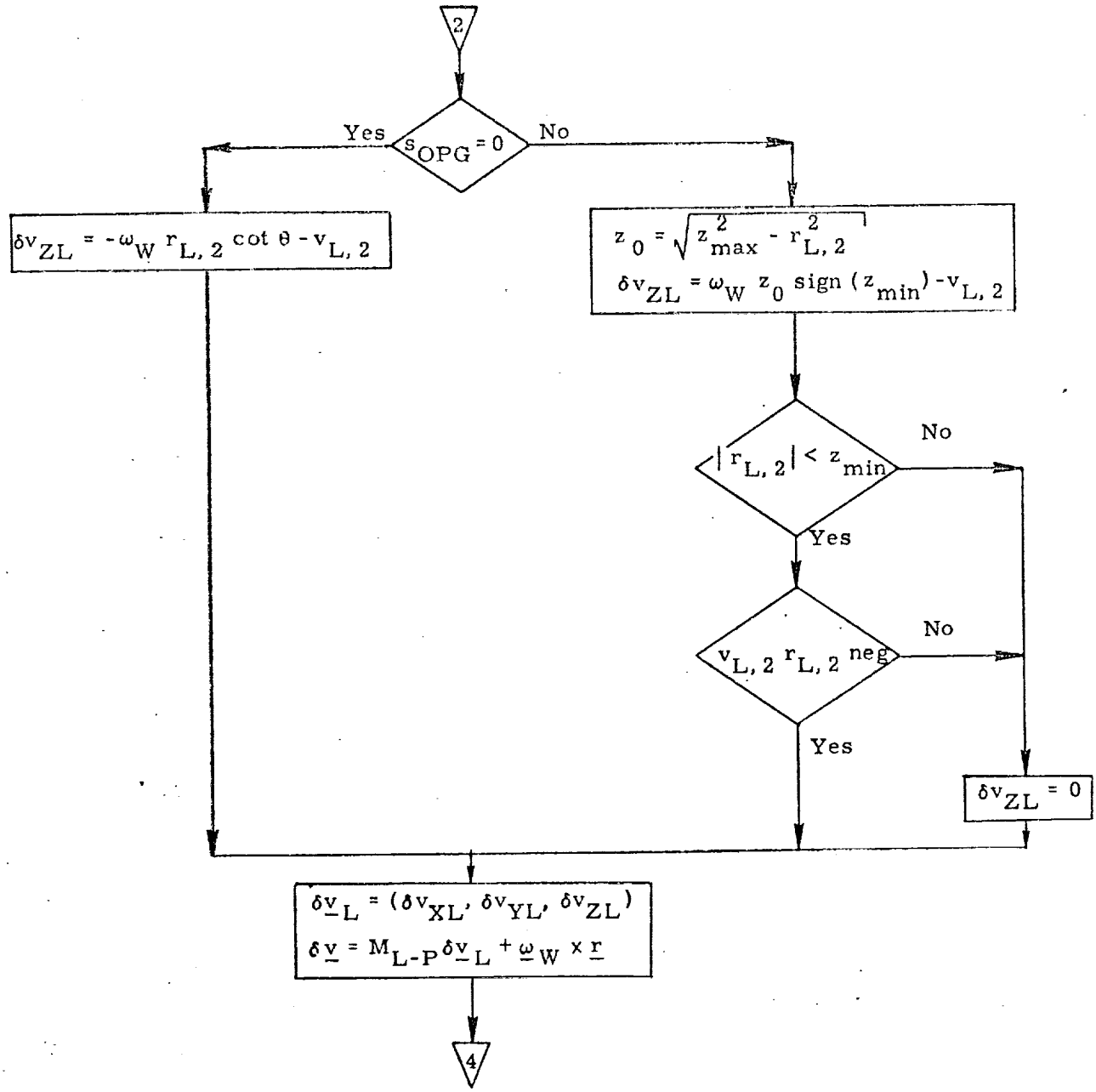


(Figure 4e)

Figure 4b. Station-Keeping Guidance, Detailed Flow Diagram

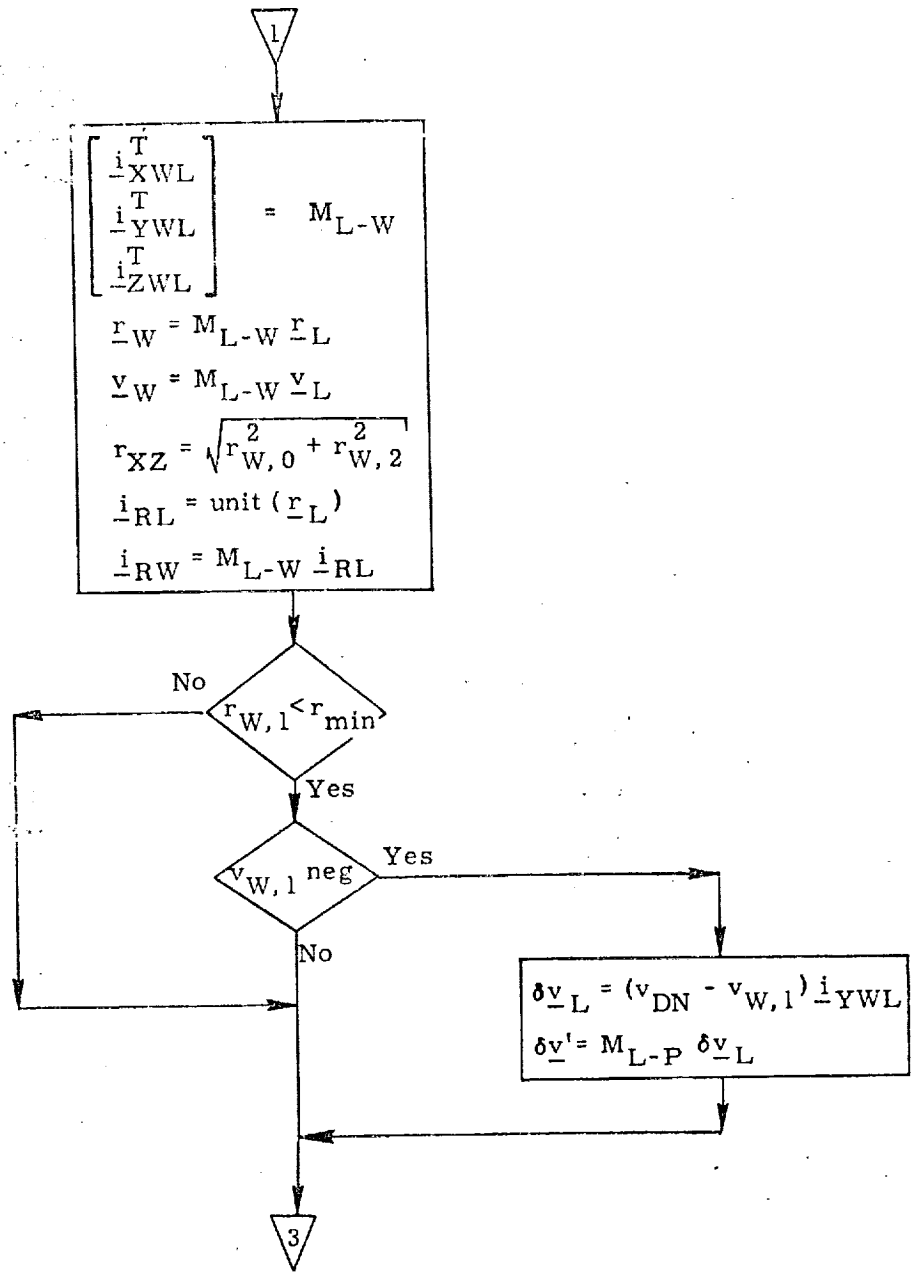


Figure 4c. Station-Keeping Guidance, Detailed Flow Diagram

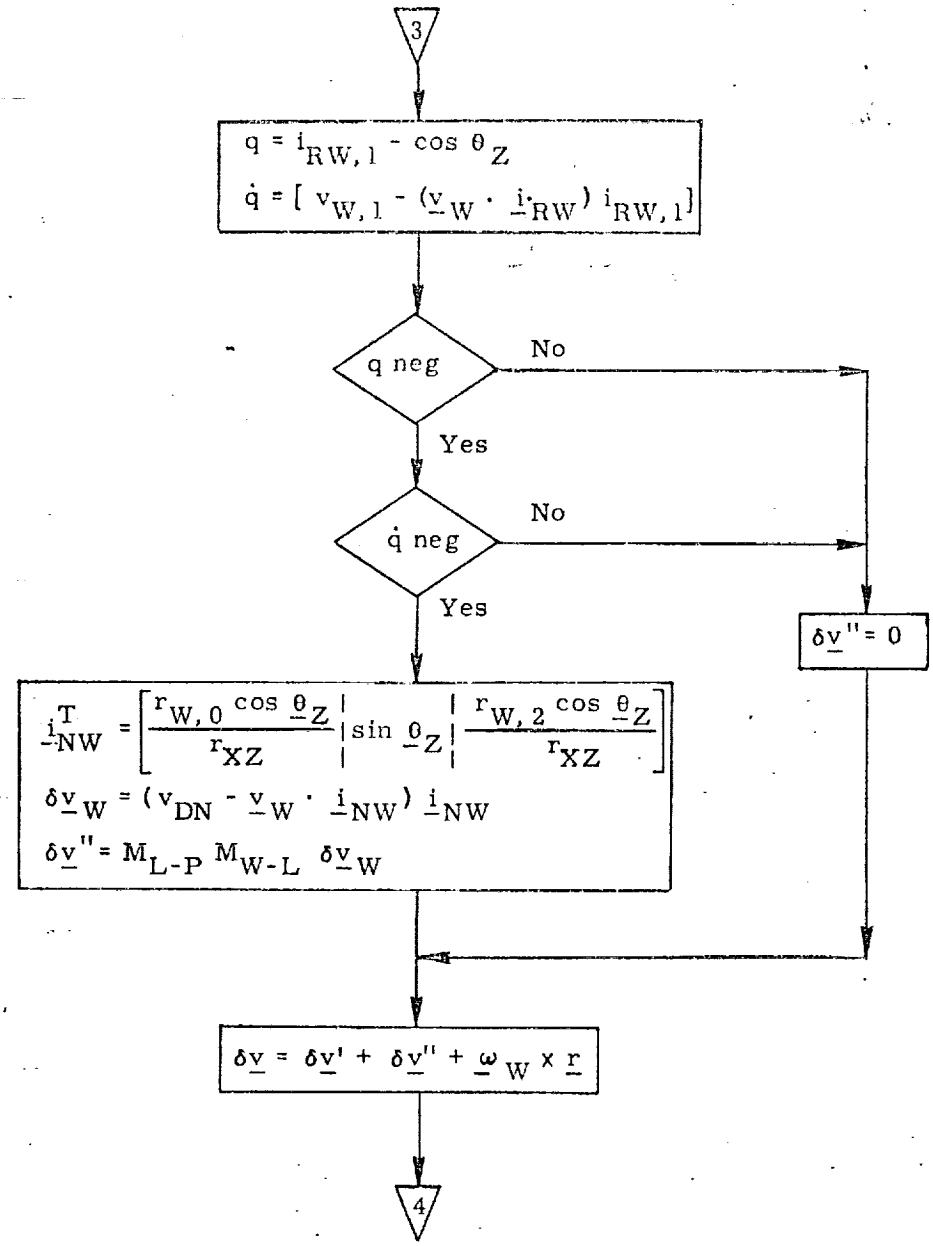


Figure 4d. Station-Keeping Guidance, Detailed Flow Diagram

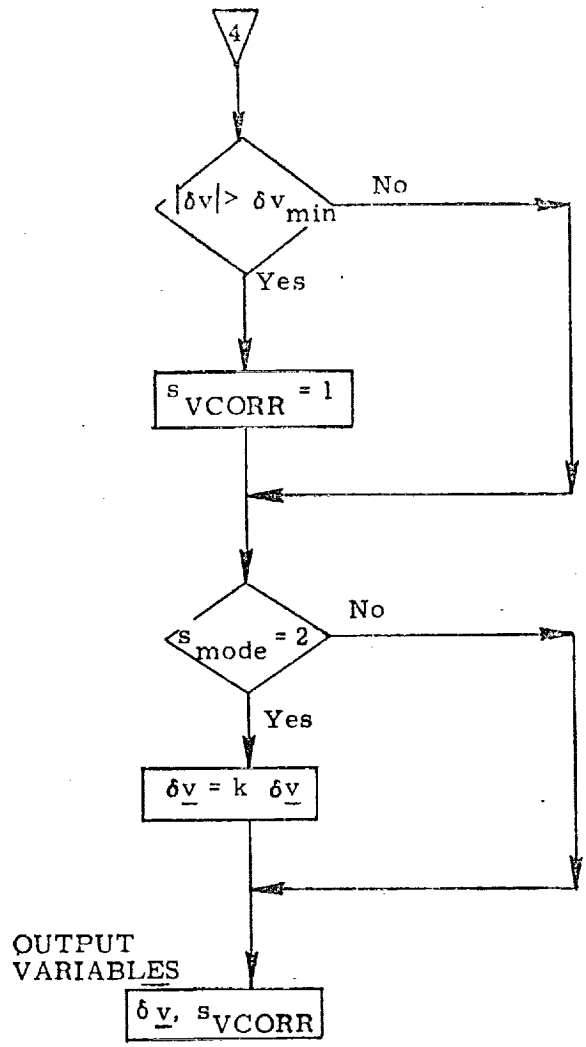


Figure 4e. Station-Keeping Guidance, Detailed Flow Diagram

Submittal 28: Deorbit Targeting

## 1. INTRODUCTION

The large entry crossrange capability of the shuttle permits deorbit to a specified landing site to be accomplished with a single maneuver. Since the required velocity change is smallest when no plane change is made, the equations presented here are designed to target the Powered Flight Guidance Routines (Reference 3) for an in-plane maneuver. The ignition time for this maneuver is selected to satisfy entry interface and landing site constraints with minimum fuel expenditure.

If the shuttle had no crossrange capability, then an in-plane deorbit maneuver to a specified landing site could only occur when that landing site, which rotates with the earth, intersects the orbital plane of the vehicle. Assuming the landing site latitude is less than the orbital inclination angle, and neglecting the effects of precession, the landing site will intersect the orbital plane twice every twenty-four hours. However, the time difference between these two intersections is in general not twelve hours. In the case when the landing site latitude is equal to the orbital inclination there will be only one intersection every twenty-four hours.

Since the shuttle has a high crossrange capability, deorbit does not require intersection of the landing site vector and the orbital plane. It is possible whenever the angle between the landing site vector and the orbital plane is less than approximately 20 deg. In general, there will be two sets of opportunities every twenty-four hours. Within each set, there may be several deorbit opportunities occurring on consecutive orbits with varying crossrange requirements. When the latitude of the landing site approaches the inclination of the orbit, these two sets merge to become one. It should be noted, in addition, that if the landing site latitude is greater than the orbital inclination, the landing site may still fall within the crossrange capability of the vehicle. With these facts in mind, this routine has been designed to continue stepping through successive solutions, allowing the crew to select a particular deorbit opportunity based upon entry crossrange, time-to-ignition, required velocity change, landing site lighting conditions, urgency of the return, etc.

The desired entry range and flight path angle will be considered inputs to this routine, since available data relating to footprint size and shape, entry heating at various ranges, and optimal entry flight path angle are only preliminary. In future revisions, consideration should be given to computing the optimum values of these quantities for the particular situation.

## 2. FUNCTIONAL FLOW DIAGRAM

A functional flow diagram presenting the basic approach to the deorbit targeting problem can be found in Figure 3. In addition to the state vector, the primary inputs to the routine are the landing site location (latitude and longitude), the entry downrange distance, the entry angle (at 400,000 ft) and the earliest desired time of landing. Since the high crossrange capability may make deorbit possible on two or more consecutive orbits, after each solution the crew has the option to recycle the program to determine the next possible deorbit opportunity. To give the crew the flexibility to evaluate solutions in the future without stepping through all earlier opportunities, the earliest desired time-of-landing is included as an input. However, the vehicle is assumed to be in coasting flight until the deorbit maneuver, and therefore the effects of any maneuvers prior to deorbit are not accounted for.

After the vehicle state vector is extrapolated forward to the earliest desired time-of-landing, the solution process is initiated. This consists of three major steps. During the first step the vehicle state is further advanced until the landing site, which rotates with the earth, lies sufficiently near the orbital plane so that it is within the crossrange (or out-of-plane) capability of the entry phase. During the next step an iterative process is used to select the ignition time for this deorbit opportunity which requires the smallest velocity change, thus minimizing the fuel expenditure. Since the first two steps involve several conic approximations to minimize the computer time used, the third step fine tunes the solution by generating a precision trajectory which satisfies the constraint on the desired entry angle while accounting for gravitational perturbations and the non-impulsive nature of the deorbit maneuver. After completion of this step the results are displayed to the crew. They may then elect to accept the solution, recycle the routine to solve for the next deorbit opportunity, or exit. If they accept the solution, a few minor computations are required to initialize the Powered Flight Guidance Routines for a modified Lambert aimpoint maneuver.

To aid the reader in understanding the functional flow diagram, each of the three major steps in the solution process is discussed in more detail below.

### 2.1 Determination of the Next Deorbit Opportunity (Step 1)

To determine the next possible deorbit opportunity, it is necessary to calculate the inertial location of the landing site (which rotates with the earth) at the time-of-landing. Then the angle between the orbital plane and the landing site can be used to estimate the crossrange required during entry. To accomplish this, an estimate of the time-of-flight difference $\Delta t_{DE}$ between (1) the interval from deorbit through entry to landing, and (2) the time spent in orbit over the same total

central angle is used. Analysis has shown that a constant is probably adequate to represent this difference since more precise calculations in the following step will compensate for any error.

Upon completion of the initialization process, the state vector is extrapolated forward to the earliest desired time-of-landing. Then the inertial location of the landing site at the present state vector time, biased by the time difference $\Delta t_{DE}$, is computed. This landing site vector is projected into the orbital plane, allowing the in-plane central angle $\theta_{IP}$ between the vehicle position and the projection of the landing site to be determined.

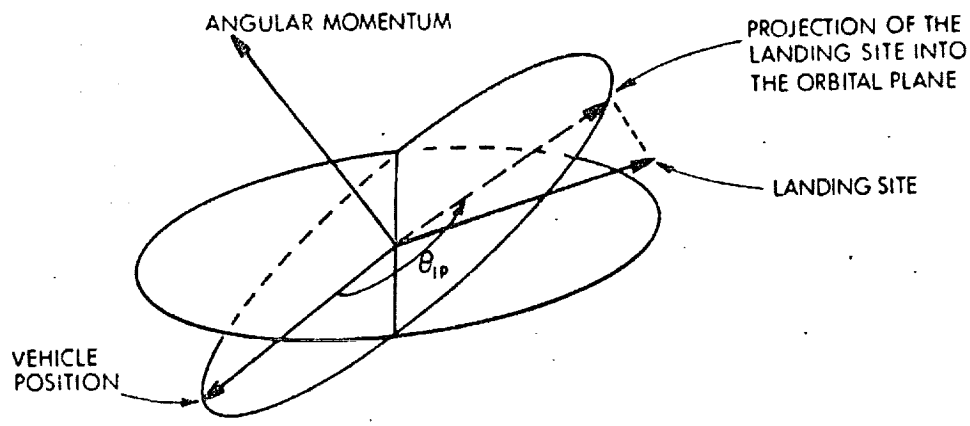


Figure 1. Out-of-plane Geometry

The conic routines can now be used to determine the time-of-flight $\Delta t_{IP}$ required to coast in orbit through the central angle $\theta_{IP}$. If the state was then propagated through this central angle, its position vector would be aligned with the previously determined projection of the landing site vector. Unfortunately, the landing site will move slightly due to earth rotation while the vehicle transfers through the central angle. Therefore, the inertial location of the landing site must be recomputed, accounting for the time difference $\Delta t_{DE}$ explained previously. Thus, an iterative process is required to precisely determine the location of the landing site at the expected time-of-landing. During the first pass through the deorbit targeting routine, the previously described steps are repeated once to insure convergence. However, on subsequent passes no iteration is required, since the initial guess achieved by extrapolating the state vector one orbit beyond the previous solution guarantees a small value for the time-of-flight correction $\Delta t_{IP}$.

Assuming the deorbit maneuver is in-plane, the angle between the orbital plane and the landing site location at the estimated time-of-landing can be used to measure the crossrange required during the entry phase. If the crossrange is within the capability of the vehicle, the solution process continues on to the next

step. If not, the vehicle state is extrapolated forward one revolution to the next potential deorbit opportunity and the process of estimating the crossrange is repeated.

It should be noted that the process used to determine the crossrange requirement is only approximate, and therefore a small increment is added to the tolerance used in the crossrange check to allow for this. A small number of cases which pass this check will actually lie outside the vehicle crossrange capability, however, a more precise check later will screen these out.

## 2.2 Ignition Time Selection (Step 2)

During this step in the solution process, an ignition time is selected which minimizes the impulsive velocity change required. For these computations the projection of the landing site into the orbital plane is assumed to be the real landing site. Then, based upon the desired entry downrange distance, a target position at entry interface which also lies in the orbital plane can be defined. This target position is set 400,000 ft above the Fischer ellipsoid.

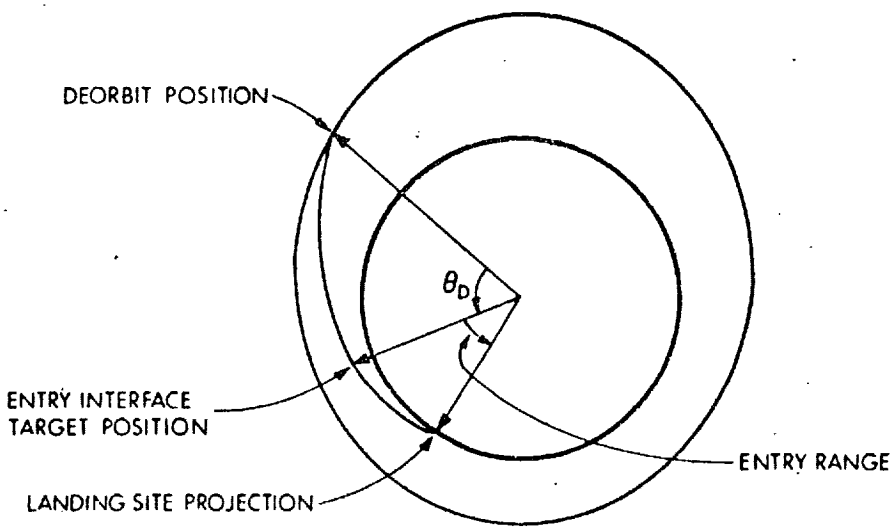


Figure 2. In-plane Geometry

Using this entry interface target, and the desired entry flight path angle, a search is made on the central angle $\theta_D$ traversed between the deorbit maneuver and entry interface to locate the position and time of the minimum $\Delta v$ maneuver.

Then the time-of-flight required for the deorbit and entry phases can be accurately determined. Using this time-of-flight, an accurate calculation of the inertial location of the landing site at the time-of-landing can be made, and the entry interface target can also be updated. To preserve the central angle of the deorbit phase, the impulsive maneuver time is adjusted. Then the ignition time is biased from the impulsive time by half the expected length of the maneuver and the state vector is extrapolated to this time.

Since the location of the landing site at the time-of-landing is now known accurately, the angle between the orbital plane and the landing site is recomputed to precisely measure the entry crossrange required. Then a precision check is made, and any solution exceeding the crossrange capability is rejected, thus returning the routine to step one to search for the next opportunity.

## 2.3 Precision Solution (Step 3)

During this step a precision integrated trajectory from deorbit to entry interface is generated which accounts for both the finite length of the thrusting maneuver and the effects of gravitational perturbations. Since the time-of-flight from deorbit to entry interface is known, the Precision Required Velocity Determination Routine can be used to generate this trajectory. However, the effects of conic approximations in the previous steps and the finite length of the maneuver can cause significant error in the reentry angle. Therefore, the resulting entry angle is checked and if it is in error, a slight modification is made in the time-of-flight from the deorbit maneuver to entry interface to adjust the entry angle. Then the precision trajectory is recomputed. After satisfying the flight path angle constraint, pertinent data relating to the maneuver can be displayed to the crew or transferred to the Mission Planning Module.

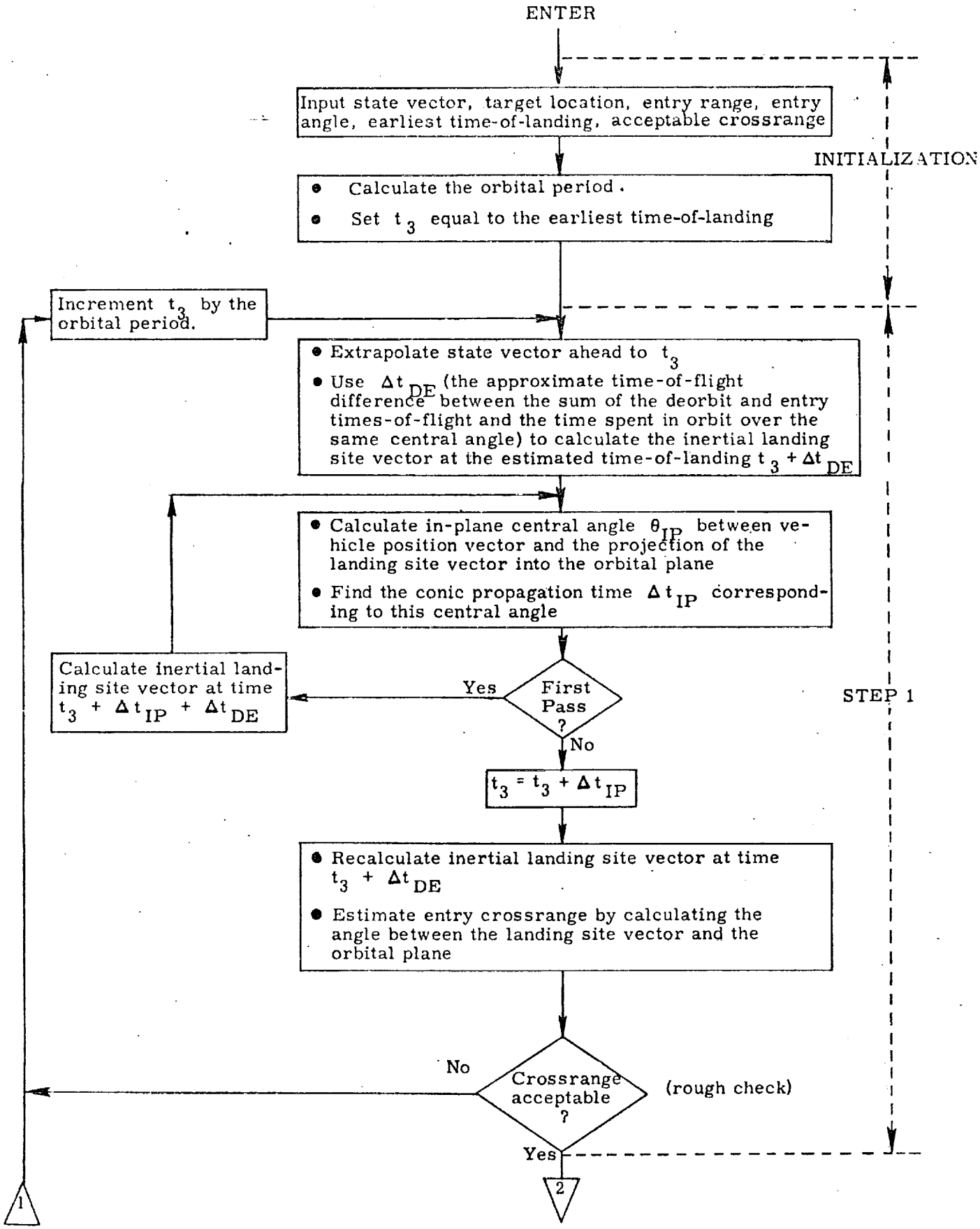


Figure 3a. Functional Flow Diagram

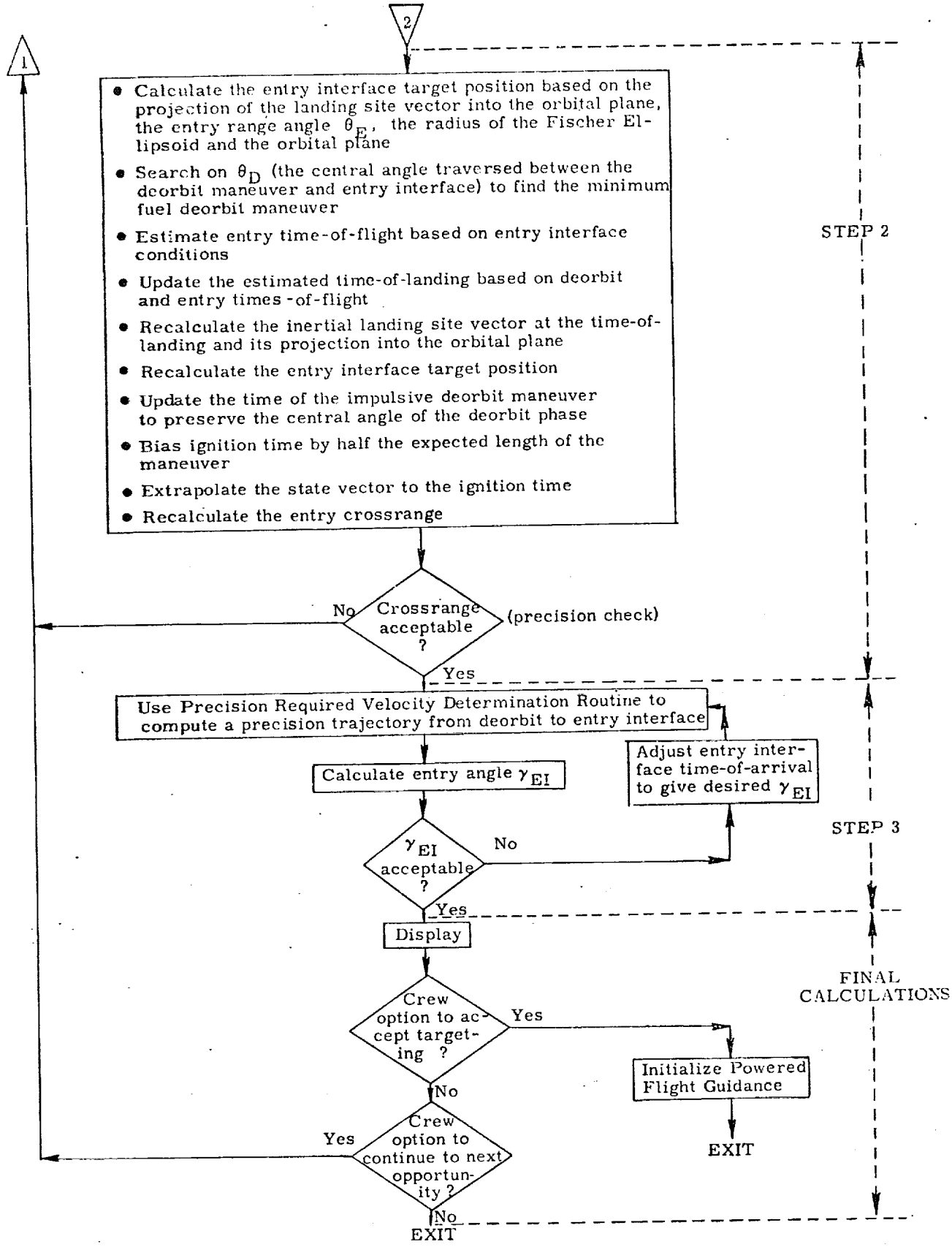


Figure 3b. Functional Flow Diagram

## NOMENCLATURE

| | |
|---|---|
| $a$ | Semimajor axis |
| $a_1$ | Alarm code—failure in $\Delta v$ minimization loop |
| $a_2$ | Alarm code—failure in Precision Required Velocity Determination Routine |
| $a_F$ | Semimajor axis of Fischer Ellipsoid |
| $a_T$ | Estimated magnitude of the thrust acceleration |
| $b_F$ | Semiminor axis of Fischer Ellipsoid |
| $d$ | Number of columns of navigation filter weighting matrix (set to 0 in this routine since the matrix is not required) |
| $d_{ACR}$ | Maximum acceptable crossrange distance of Orbiter |
| $d_{CR}$ | Estimated entry crossrange distance |
| $d_{DR}$ | Entry downrange distance |
| $f$ | Magnitude of the engine thrust |
| $f_{ACS}$ | Magnitude of the attitude control system translational thrust |
| $f_{OMS}$ | Magnitude of the orbital maneuvering system engine thrust |
| $h_{EI}$ | Entry interface altitude (400,000 ft) |

| | |
|---|---|
| $\underline{i}$ | Unit vector formed by the cross product of the angular momentum and the landing site vectors |
| $\underline{i}_{EI}$ | Unit vector in the direction of $\underline{r}_{EI}$ |
| $\underline{i}'_{EI}$ | First estimate of $\underline{i}_{EI}$ |
| $i'_{EI,z}$ | Z-component of the unit vector $\underline{i}'_{EI}$ (z-axis assumed North) |
| $\underline{i}_h$ | Unit vector in the direction of the angular momentum |
| $\underline{i}_{LSP}$ | Unit vector in the direction of the landing site projection into the orbital plane |
| $\underline{i}_N$ | Unit normal to the trajectory plane (in the direction of the angular momentum at ignition) |
| $k_\gamma$ | Sensitivity coefficient used to compute adjustment to time-of-arrival at entry interface |
| $m$ | Estimated vehicle mass |
| $n$ | Iteration counter |
| $n_{max}$ | Iteration limit |
| $n_{rev}$ | Integral number of complete revolutions to be made in the transfer (set to zero in this routine) |
| $p_D$ | Semilatus rectum of deorbit trajectory |
| $p_\gamma$ | Secant squared of the desired entry flight path angle |
| $p_{PF\gamma}$ | Secant squared of the offset entry angle used by the Powered Flight Guidance Routine |
| $\underline{r}_0$ | Precision position vector |

| | |
|---|---|
| $\underline{r}''_2$ | Entry interface position from Precision Required Velocity Determination Routine |
| $\underline{r}_D$ | Position of the impulsive deorbit maneuver |
| $\underline{r}_{EI}$ | Entry interface position |
| $\underline{r}_{ig}$ | Position vector at ignition |
| $\underline{r}_{LS}$ | Estimated landing site position at the time of landing |
| $\underline{r}_{PFT}$ | Powered flight offset target vector |
| $s_{eng}$ | Engine select switch |
| $s_{fail}$ | Switch set to indicate non-convergence of Precision Required Velocity Determination Routine |
| $s_{FP}$ | Switch set equal to one after the first pass through step one |
| $s_{pert}$ | Switch indicating which perturbations are to be included in the Precision State and Filter Weighting Matrix Extrapolation Routine (See Reference 5) |
| $s_{proj}$ | Switch set when the target vector must be projected into the plane defined by $\underline{i}_N$ |
| $t_0$ | Precision state vector time |
| $t_1$ | Time of impulsive deorbit maneuver |
| $t_2$ | Time-of-arrival at entry interface |
| $t_3$ | Estimated time at which in-orbit position vector is coincident with the landing site projection into the orbital plane |

| | |
|---|---|
| $t_{ETL}$ | D[illegible] earliest time-of-landing |
| $t$ [illegible] | [illegible]e |
| [illegible] | [illegible] time-of-landing |
| $t_{LTL}$ | Desired latest time-of-landing |
| $\underline{v}_0$ | [illegible] velocity vector |
| $\underline{v}''_2$ | Entry interface velocity from Precision Required [illegible] Determination Routine |
| $\underline{v}_D$ | Pre-impulse velocity |
| $\underline{v}_{EI}$ | Entry interface velocity |
| $\underline{v}_{ig}$ | Ignition velocity vector |
| $\underline{v}_{PFT}$ | [illegible] associated with the powered flight [illegible] et vector |
| $v_{RD}$ | Post-impulse radial component of velocity |
| $\underline{v}_{req}$ | Required velocity |
| $\underline{v}'_{req}$ | Required velocity on the coasting trajectory |
| $v_{HD}$ | Post-impulse horizontal component of [illegible] |
| $\delta t_{01}$ | Adjustment to $\Delta t_{01}$ |
| $\Delta d_{ACR}$ | Increment added to the acceptable crossrange, [illegible]ed in rough crossrange check |
| $\Delta p_\gamma$ | Difference between the predicted and desired $p_\gamma$ |

| | |
|---|---|
| $\Delta r_{proj}$ | Out-of-plane target miss due to the projection of the target vector |
| $\Delta t_{01}$ | Transfer time $(t_1 - t_0)$ |
| $\Delta t_{12}$ | Transfer time $(t_2 - t_1)$ |
| $\Delta t_{23}$ | Transfer time $(t_3 - t_2)$ |
| $\Delta t_B$ | Estimated duration of the powered maneuver |
| $\Delta t_{DE}$ | Time-of-flight difference between (1) the interval from deorbit through entry to landing, and (2) the time spent in orbit over the same total central angle |
| $\Delta t_{IP}$ | Time-of-flight required to transfer through the central angle $\theta_{IP}$ |
| $\Delta \underline{v}$ | Required velocity change |
| $\Delta v_P$ | Previous value of $\lvert \Delta \underline{v} \rvert$ |
| $\Delta\theta$ | Increment in in-plane angle $\theta_D$ |
| $\Delta\theta_0$ | Initial increment in in-plane angle $\theta_D$ |
| $\epsilon_{p\gamma}$ | Convergence criterion on $\Delta p_\gamma$ |
| $\epsilon_\theta$ | Convergence criterion on angle $\Delta\theta$ |
| $\gamma_1$ | Post-impulse flight path angle |
| $\gamma_{EI}$ | Desired entry flight path angle measured from the horizontal |
| $\lambda_{LS}$ | Landing site longitude |
| $\theta$ | In-plane angle between precision state vector and entry interface |

| | |
|---|---|
| $\theta_{01}$ | In-plane angle between precision state vector and deorbit position |
| $\theta_D$ | In-plane angle over which search is made to find minimum deorbit $\Delta v$ |
| $\theta_E$ | In-plane central angle traversed during entry |
| $\theta_{IP}$ | Angle between precision state vector and the projection of the landing site into the orbital plane |
| $\theta_P$ | Previous value of $\theta_D$ |
| $\mu$ | Gravitational parameter of the earth (product of the earth's mass and universal gravitation constant) |
| $\phi_{LS}$ | Landing site latitude |
| $\tau$ | Orbital period |

## 4. DESCRIPTION OF EQUATIONS

To minimize the size of the Deorbit Targeting Routine, extensive use is made of other routines. Therefore, this routine consists primarily of simple equations, logical operations, and calls to other routines. Since most of the complicated equations requiring detailed explanation are contained in the description of the other routines, this section will be limited to a list of items not covered in the text describing the functional flow diagram. These items will be listed in their order of occurence, and are intended to supplement the detailed flow diagram in subsection 5.

### 4.1 Selection of Perturbing Acceleration during Precision State Extrapolation

During the first step in the solution process, which may require long term state vector extrapolation, it is desirable to maximize accuracy by including all significant perturbing accelerations in the extrapolation process. Therefore, the switch $s_{pert}$, which controls the selection of perturbing accelerations in the Precision State Extrapolation Routine, is set to 2. During the later portion of the routine, referred to as step three, the switch is reset to 1, thus limiting the disturbing acceleration to the $J_2$ term, the second harmonic of the earth's gravitational potential function. Since extrapolation during step three is limited to the interval from the deorbit maneuver to entry interface, the effects of smaller perturbing accelerations are not significant. In addition, extrapolation over this interval lies within an iterative loop, and thus may be repeated several times. The simplified model can therefore significantly reduce the running time of this step.

### 4.2 Selection of $\theta_{IP}$ Quadrant

During the discussion of the functional flow diagram, it was mentioned that successive solutions to the deorbit problem (when successive solutions exist) are about one revolution apart. To find succeeding solutions to the problem, the state vector is extrapolated forward one revolution and then the in-plane central angle $\theta_{IP}$ between the state vector and the projection of the landing site into the orbital plane is computed. Analysis has shown that for some selections of orbital inclination and landing site, the correction to the assumption of one revolution may be as large as $29^{\circ}$. A lower limit on $\theta_{IP}$ of $-30^{\circ}$ was chosen, thus allowing a small margin from the empirically determined limit of $-29^{\circ}$. The upper limit on $\theta_{IP}$ is $+330^{\circ}$. Large positive values for $\theta_{IP}$ only occur in situations where no solution existed on the previous revolution.

To determine $\theta_{IP}$, the following equation is used,

$$\theta_{IP} = \cos^{-1}\left[\text{unit}\,(\underline{r}_0)\cdot \underline{i}'_{LSP}\right] \text{ sign}\left[(\underline{r}_0 \times \underline{i}'_{LSP})\cdot \underline{i}_h\right]$$

where

$\underline{r}_0$ = vehicle position vector

$\underline{i}'_{LSP}$ = unit vector in the direction of the landing site projection

$\underline{i}_h$ = unit angular momentum vector

This places $\theta_{IP}$ between $-180^\circ$ and $+180^\circ$ and therefore an additional test, shown in Figure 4b, is made to force $\theta_{IP}$ between $-30^\circ$ and $+330^\circ$.

In order to make the first entry into step one compatible with subsequent entries, the state vector is initially extrapolated forward beyond the earliest desired time-of-landing $t_{ETL}$ by one-twelfth of the orbital period, to the time $t_3$, where

$$t_3 = t_{ETL} + \tau/12$$

One-twelfth of the period is nearly equivalent to a central angle of $30^\circ$ for typical (near circular) orbits, and hence makes the first entry into step one compatible with later entries.

## 4.3 Effect of Approximate Entry and Deorbit Times-of-Flight on Entry Crossrange Calculation

During the first step in the solution process, an estimate of the time of landing is necessary to compute the inertial location of the landing site and the associated entry crossrange. Since the parameters of the deorbit trajectory have not been computed, the deorbit and entry times-of-flight are not known. To estimate the landing time, a constant $\Delta t_{DE}$ is used to approximately represent the difference between the sum of the deorbit and entry times-of-flight and the time spent in orbit over the same total central angle. Preliminary analysis has shown that if an average value is selected for this time difference, the maximum error will be about 6 minutes. This analysis, described in Reference 7, did not include variations in entry time-of-flight for the particular entry range, but further analysis is expected to show this effect is small.

During the first step in the solution, this error will affect the calculation of the inertial landing site vector and subsequent entry crossrange computation. This effect on the crossrange estimate will be largest for deorbit from a polar orbit, and result in a maximum error of less than 90 n.mi. To insure that potentially acceptable solutions are not rejected due to errors in the initial crossrange estimate, the rough check on crossrange during the first step uses a test criterion 90 n.mi. larger than the acceptable crossrange input to the routine. In step two, after the time-of-landing has been refined, the crossrange is recomputed and a precision check is made. Thus a few cases which pass the first test will be rejected later.

## 4.4 Velocity Change Minimization Method

Step two of the routine includes an iterative search to determine the location of the impulsive maneuver which minimizes the velocity change $\Delta v$. As shown in Figure 4d, this iteration uses $\theta_D$, the central angle traversed between the impulsive maneuver and entry interface, as the independent variable. A very simple halving step iterator is used to search for the minimum. Although this does not converge quickly, it is safe and reliable. The more efficient technique of using a slope iteration was not selected because analysis has shown that inflection points exist in the relationship of $\Delta v$ and $\theta_D$. These inflection points would greatly complicate any iteration designed to determine the minimum by driving the slope to zero.

## 4.5 Required Velocity Equations

The equations used in the previously described iterative loop to determine the required velocity can be found in Reference 2. These equations, shown in Figure 4d of the detailed flow diagram, use the initial vehicle position $\underline{r}_D$, the entry interface position $\underline{r}_{EI}$, and the desired entry angle $\gamma_{EI}$ as follows. First the tangent of the initial (post-impulse) flight path angle $\gamma_1$ is computed by

$$\tan \gamma_1 = (1 - r_D/r_{EI}) \cot(\theta_D/2) - r_D/r_{EI} \tan(\gamma_{EI})$$

where $\theta_D$ is the central angle between $\underline{r}_D$ and $\underline{r}_{EI}$ and also the independent variable in the search. The semilatus rectum $p_D$ of the deorbit trajectory can then be determined from

$$p_D = \frac{2 r_D (r_D/r_{EI} - 1)}{(r_D/r_{EI})^2 p_\gamma - (1 + \tan \gamma_1^2)}$$

The parameter $p_\gamma$, the secant squared of the desired entry angle, is computed once during initialization of the routine.

The horizontal and radial components of the required velocity are then obtained from

$$v_{HD} = \sqrt{\mu p_D}/r_D$$
$$v_{RD} = v_{HD} \tan \gamma_1$$

The required velocity is then formed and differenced with the premaneuver velocity to obtain the impulsive $\Delta v$.

$$\underline{v}_{req} = \underline{v}_{RD} \text{ unit } (\underline{r}_D) + v_{HD} \text{ unit } \left[ (\underline{r}_D \times \underline{v}_D) \times \underline{r}_D \right]$$
$$\Delta \underline{v} = \underline{v}_{req} - \underline{v}_D$$

## 4.6 Entry Time-of-Flight Computation (TBD)

In Figure 4e of the detailed flow diagram, the time-of-flight $\Delta t_{23}$ from entry interface to landing is shown as a function of entry velocity, flight path angle, and range. Functionalization of this time-of-flight will be included later when entry guidance analysis is complete.

## 4.7 In-Plane Effect of Approximate Deorbit and Entry Times-of-Flight

As discussed in subsection 4.3, the first estimate of the inertial location of the landing site is dependent upon an estimate of the time-of-landing. A constant time difference $\Delta t_{DE}$, used to estimate the landing time, may be in error by as much as 6 minutes. This led to a significant error in the crossrange estimate for a high inclination orbit. For orbits of lower inclination, where the movement of the landing site can be nearly parallel to the orbital plane, this same error can affect the definition of the entry interface location used in the $\Delta v$ minimization iteration.

The entry interface location, computed early in step two, is based upon the projection of the landing site vector into the orbital plane and the desired entry range. After the minimization process is complete, the deorbit and entry times-of-flight can be accurately calculated. As shown in Figure 4e, another calculation of the inertial landing site position is made, thus removing the error due to the $\Delta t_{DE}$ approximation. To maintain the desired entry range input to the routine, the entry interface position is recalculated. This new position will be, at most, $1.5^{\circ}$ (equivalent to 6 minutes of earth rotation) from the entry interface used in the $\Delta v$ minimization. To maintain the geometry of the deorbit phase, the time of the deorbit maneuver is adjusted accordingly so that the central angle from deorbit to entry interface is preserved. This adjustment in deorbit time $\delta t_{01}$ is computed from the following equation

$$\delta t_{01} = \left[\left(\underline{i}'_{EI} \times \underline{i}_{EI}\right) \cdot \underline{i}_h\right] \frac{\tau}{2\pi}$$

where $\underline{i}'_{EI}$ is a unit vector in the direction of the entry interface position used during minimization, $\underline{i}_{EI}$ is the new value, $\underline{i}_h$ is a unit angular momentum vector, and $\tau/2\pi$ is the inverse of the mean orbital rate. The cross product of the unit vectors is nearly equivalent to the angle between them, and the dot product gives the proper sign. The mean orbital rate is used to calculate the deorbit time adjustment from the angular adjustment. Following this adjustment to the impulsive deorbit time, the ignition time for the maneuver is biased from the impulsive time by one-half the expected length of the maneuver, thus centering the finite thrust maneuver about the impulsive maneuver.

## 4.8 Compensation for Oblateness and Finite Maneuver Length

Step three of the solution process contains calculations which account for the finite length of the thrusting maneuver on the required velocity change, and compensate for the effects of the $J_2$ gravitational perturbation on the deorbit trajectory. The Precision Required Velocity Determination Routine is used to accomplish these objectives, and the reader should refer to Reference 1 for a description of the technique. That routine, however, is designed to maintain the terminal (entry interface) time-of-arrival, and this can cause changes in the entry angle. Preliminary analysis, described in Reference 7, has shown that the nominal entry flight path angle error resulting from the oblateness and finite maneuver length is about $0.2^{\circ}$, but can be as large as $0.6^{\circ}$ in extreme cases. Therefore, to preserve the desired entry angle, the time-of-arrival at entry interface is adjusted slightly. Delaying the time-of-arrival tends to loft the trajectory and thus increase the entry angle. An earlier time-of-arrival will depress the trajectory and result in a shallower flight path angle.

To determine the time-of-arrival adjustment, the approximate sensitivity of changes in time-of-flight to changes in entry angle is used. Analysis has shown that this sensitivity varies by a factor of about 13, depending on the characteristics of the pre-maneuver trajectory. However, the sensitivity divided by the deorbit time-of-flight varies by a factor of less than 3. This variation is sufficiently small such that a constant can be used as the sensitivity coefficient for all cases.

To reduce the computations required to constrain entry angle, both here and in the Powered Flight Guidance Routines*, the secant squared of the entry angle $p_\gamma$ is used rather than the actual angle. In particular, no inverse trigonometric function evaluations are required.

The sequence of calculations designed to reduce the entry angle error are shown in Figures 4f and 4g. First the error $\Delta p_\gamma$ in the secant squared of the entry flight path angle is computed from the following equation:

$$\Delta p_\gamma = \frac{1}{1 - \left[\text{unit}\,(\underline{r}_2'') \cdot \text{unit}\,(\underline{v}_2'')\right]^2} - p_\gamma$$

where $\underline{r}_2''$ and $\underline{v}_2''$ are the terminal position and velocity determined by the Precision Required Velocity Determination Routine and $p_\gamma$ is the desired value. If the error is too large, the entry interface time-of-arrival $t_2$ is adjusted as follows:

$$t_2 = t_2 - k_\gamma \, \Delta t_{12} \, \Delta p_\gamma$$

*The Powered Flight Guidance Routines, described in Reference 3, use the same basic technique described here to maintain entry angle in the event of off-nominal thrusting conditions.

where $k_\gamma$ is the sensitivity coefficient described earlier and $\Delta t_{12}$ is the time-of-flight from deorbit to entry interface. After adjusting the time-of-arrival, the Precision Required Velocity Determination Routine is recalled with the adjusted time-of-arrival and the results are checked.

## 4.9 Offset Entry Angle

In the process of computing a required velocity, the Precision Required Velocity Determination Routine computes an offset target for use during the powered flight. For the deorbit maneuver, the powered flight guidance also requires an offset entry angle. This offset entry angle, actually the secant squared of the angle, is computed from the following equation

$$p_{PF\gamma} = \frac{1}{1 - \left[ \text{unit}(\underline{r}_{PFT}) \cdot \text{unit}(\underline{v}_{PFT}) \right]^2}$$

where $\underline{r}_{PFT}$ is the offset target for the powered flight guidance and $\underline{v}_{PFT}$ is the associated velocity.

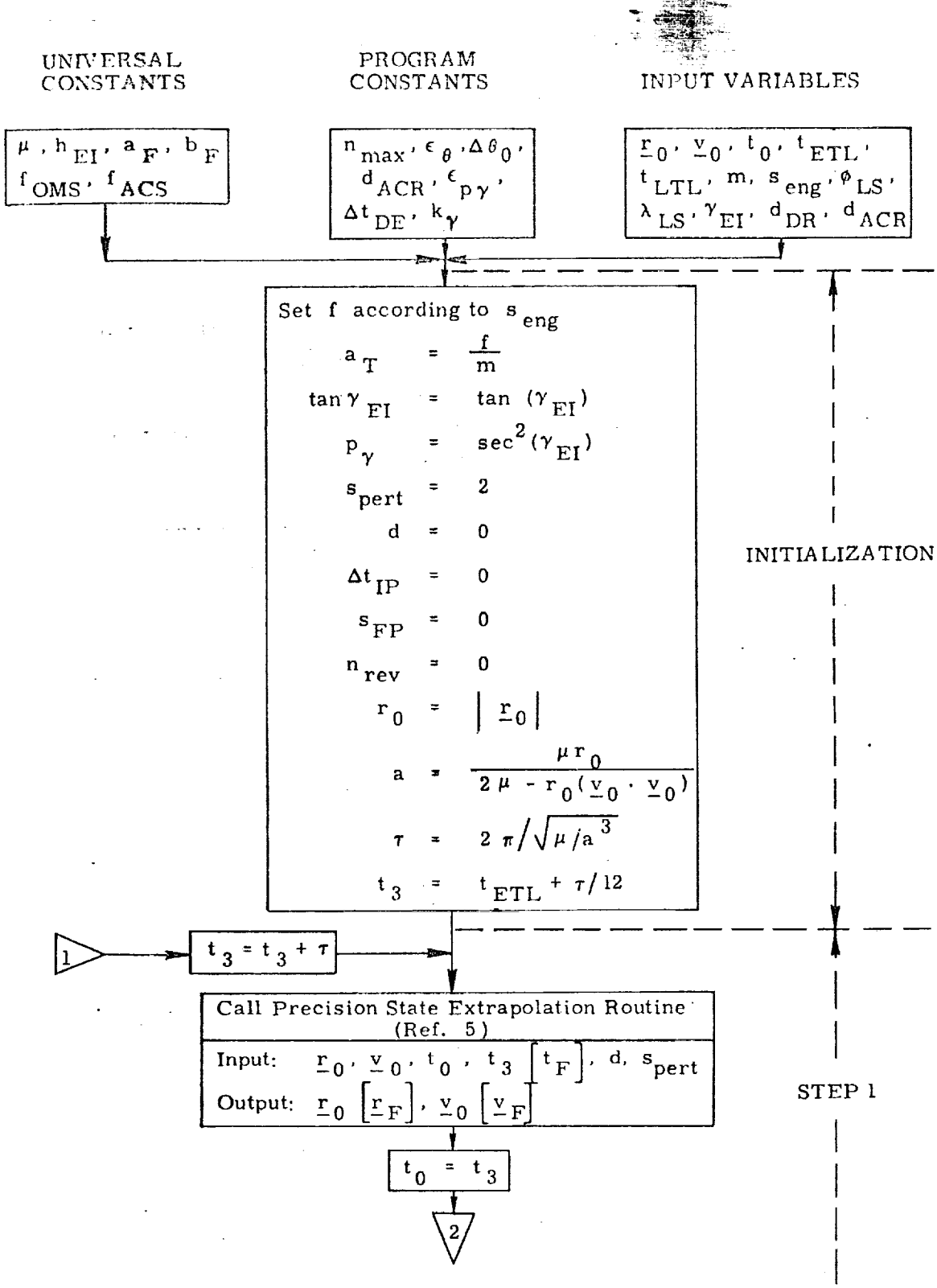


Figure 4a. Detailed Flow Diagram

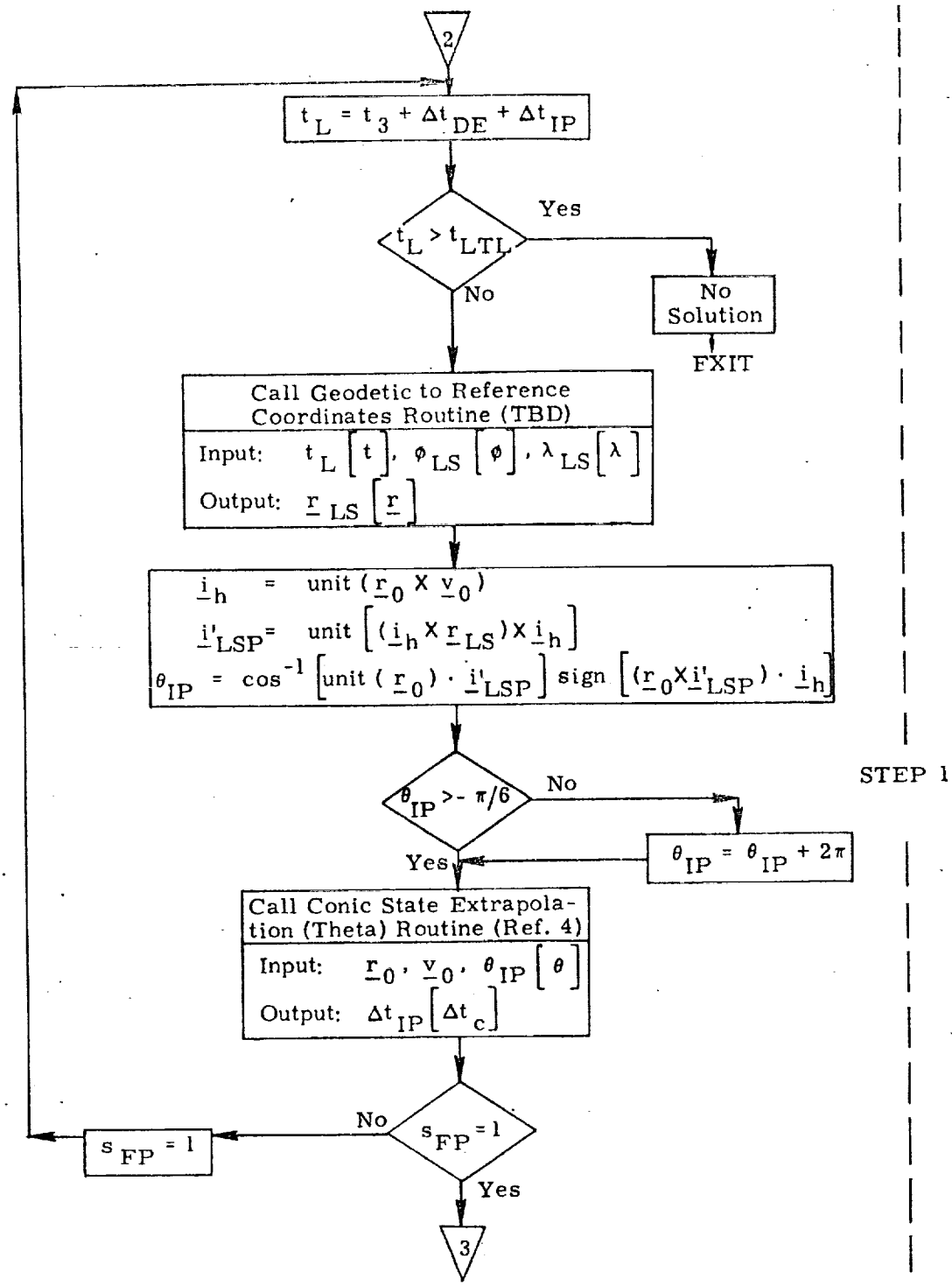


Figure 4b. Detailed Flow Diagram

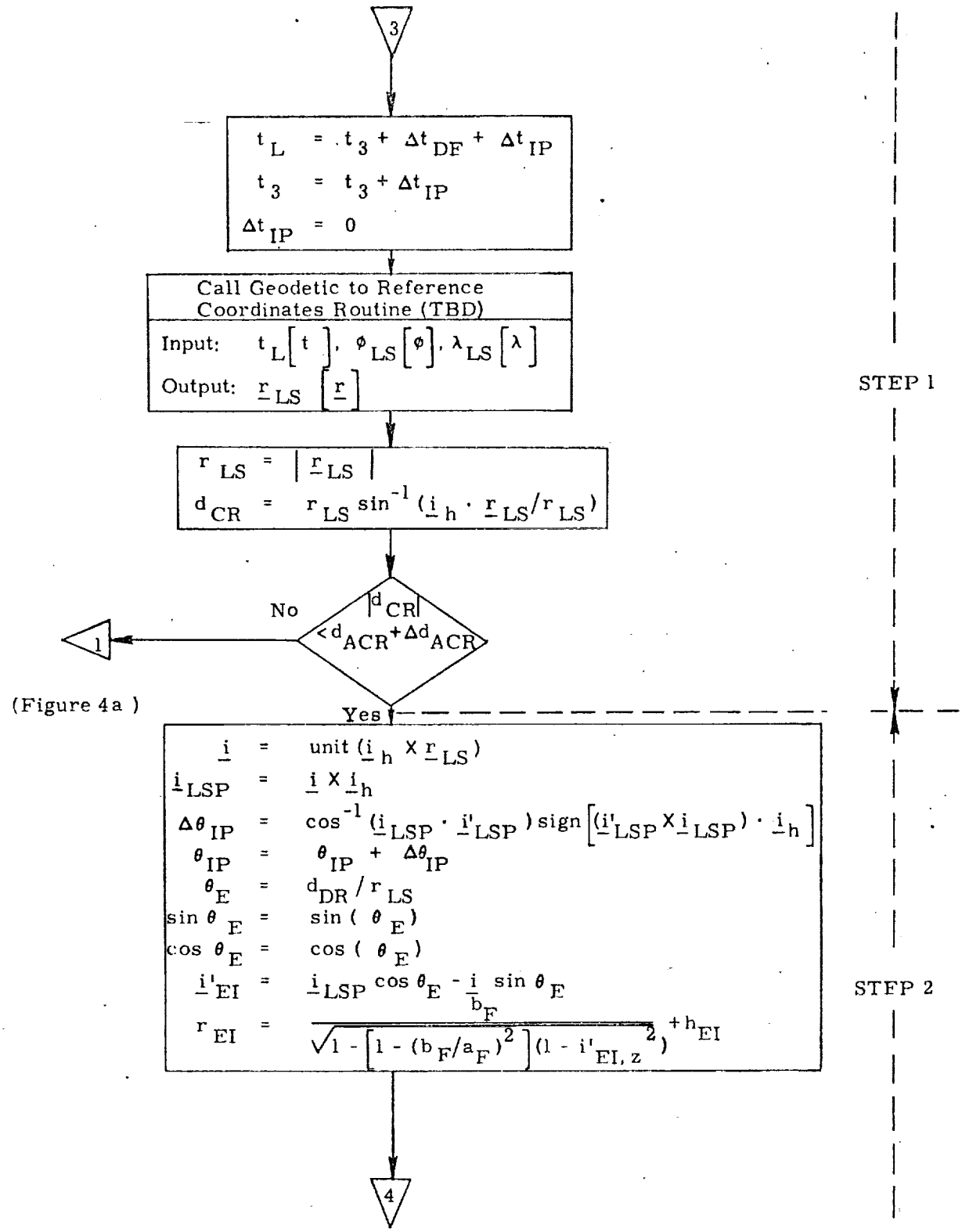


Figure 4c. Detailed Flow Diagram

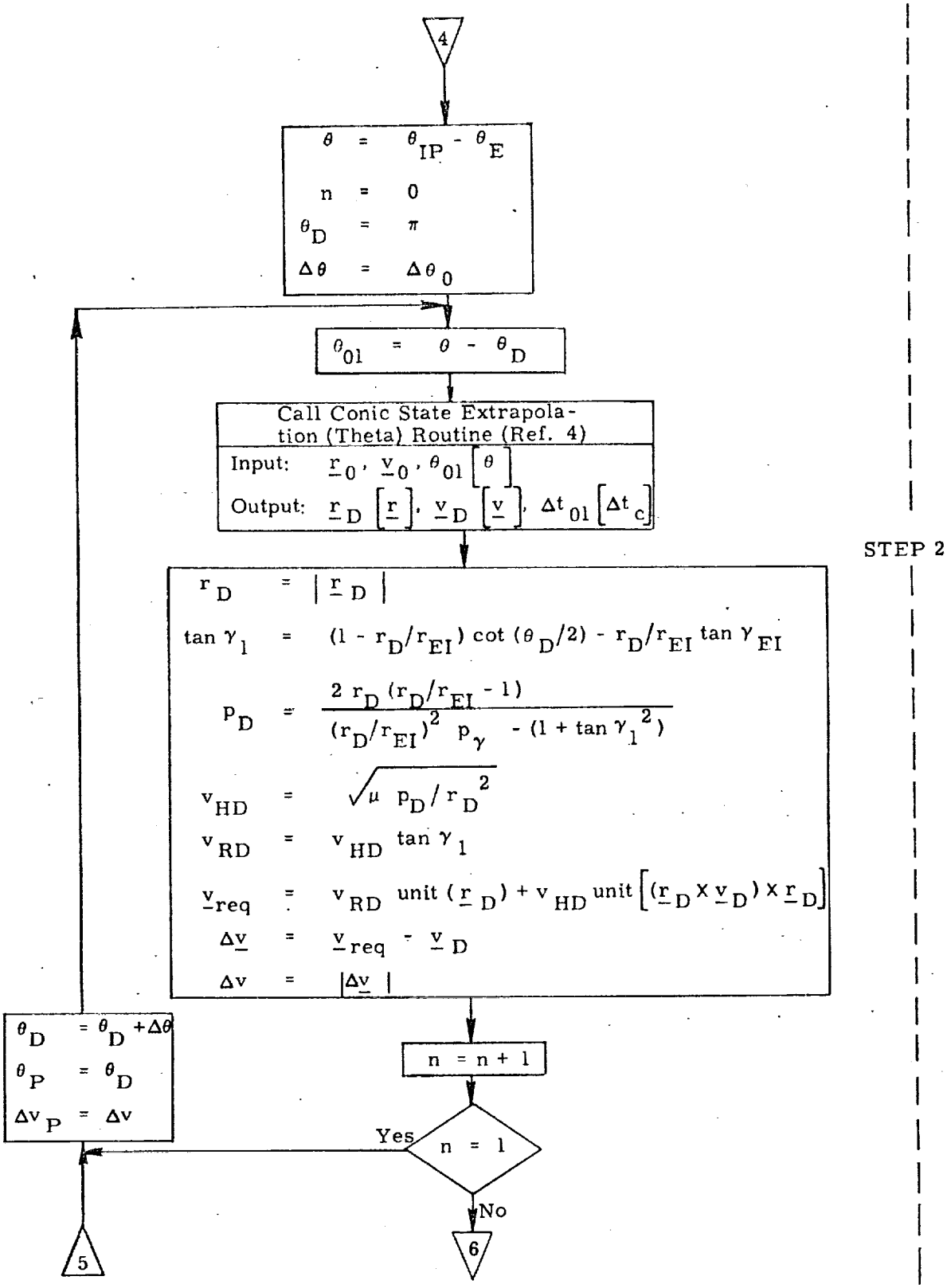


Figure 4d. Detailed Flow Diagram

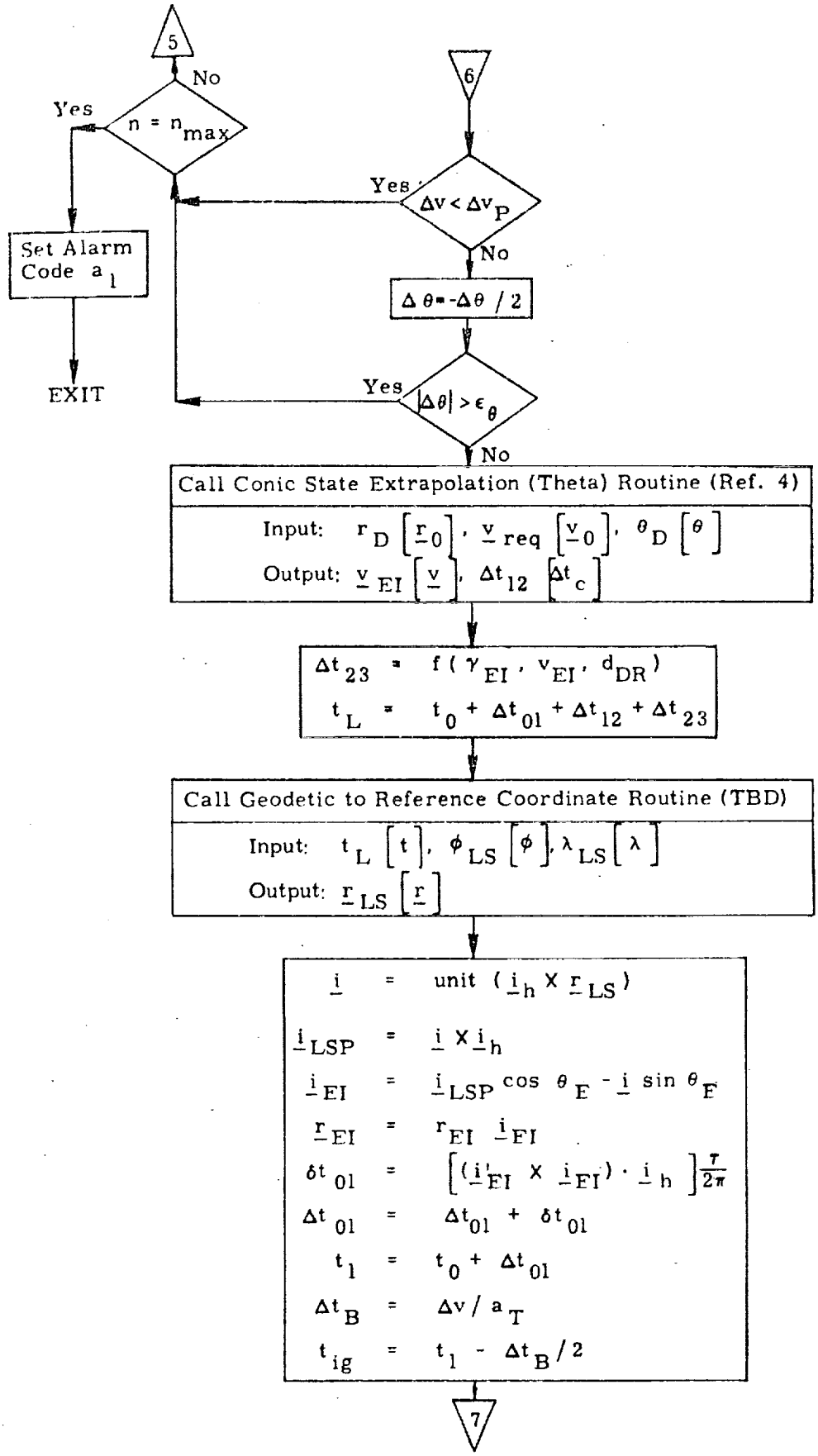


STEP 2

Figure 4e. Detailed Flow Diagram

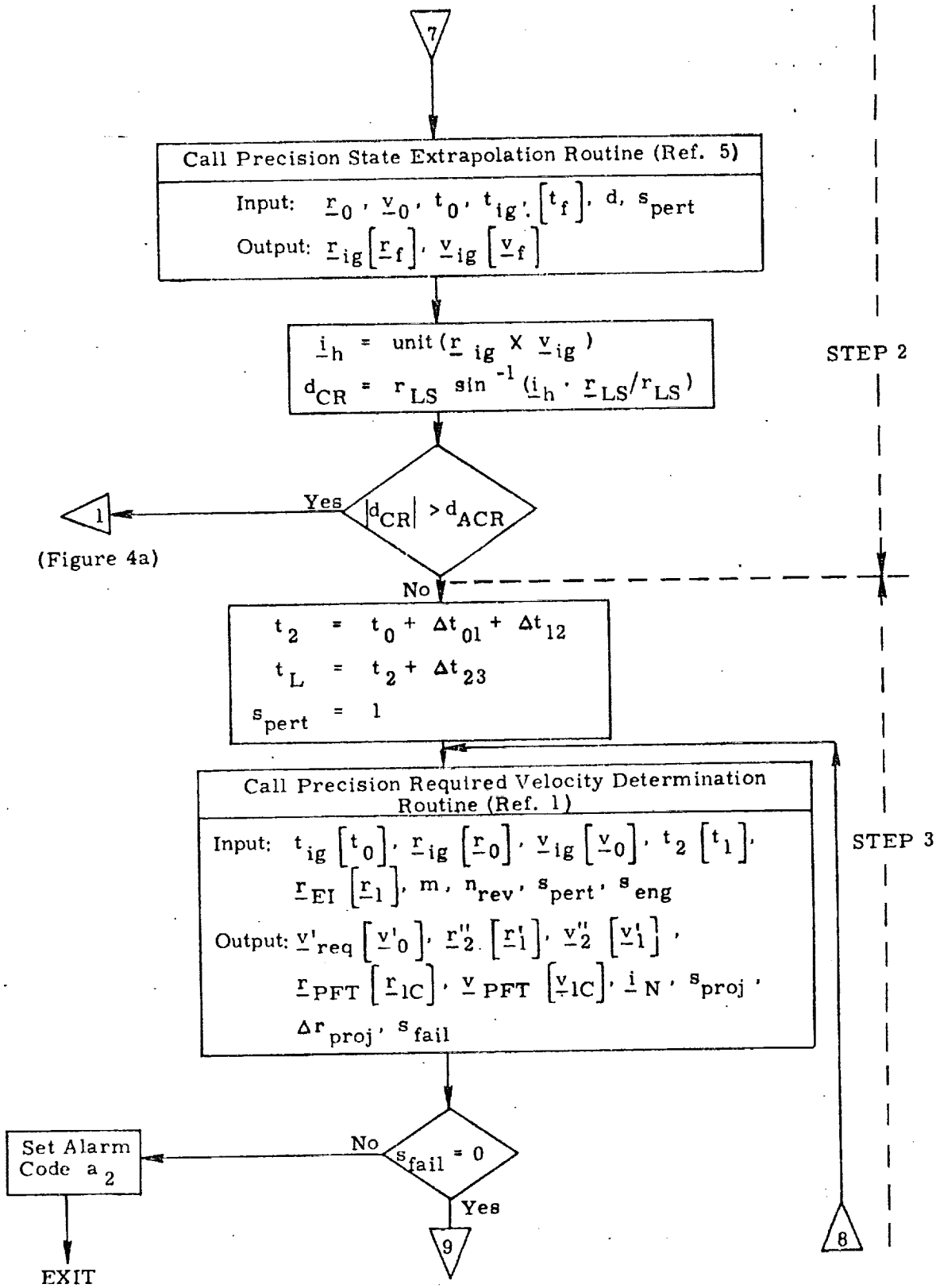


Figure 4f. Detailed Flow Diagram

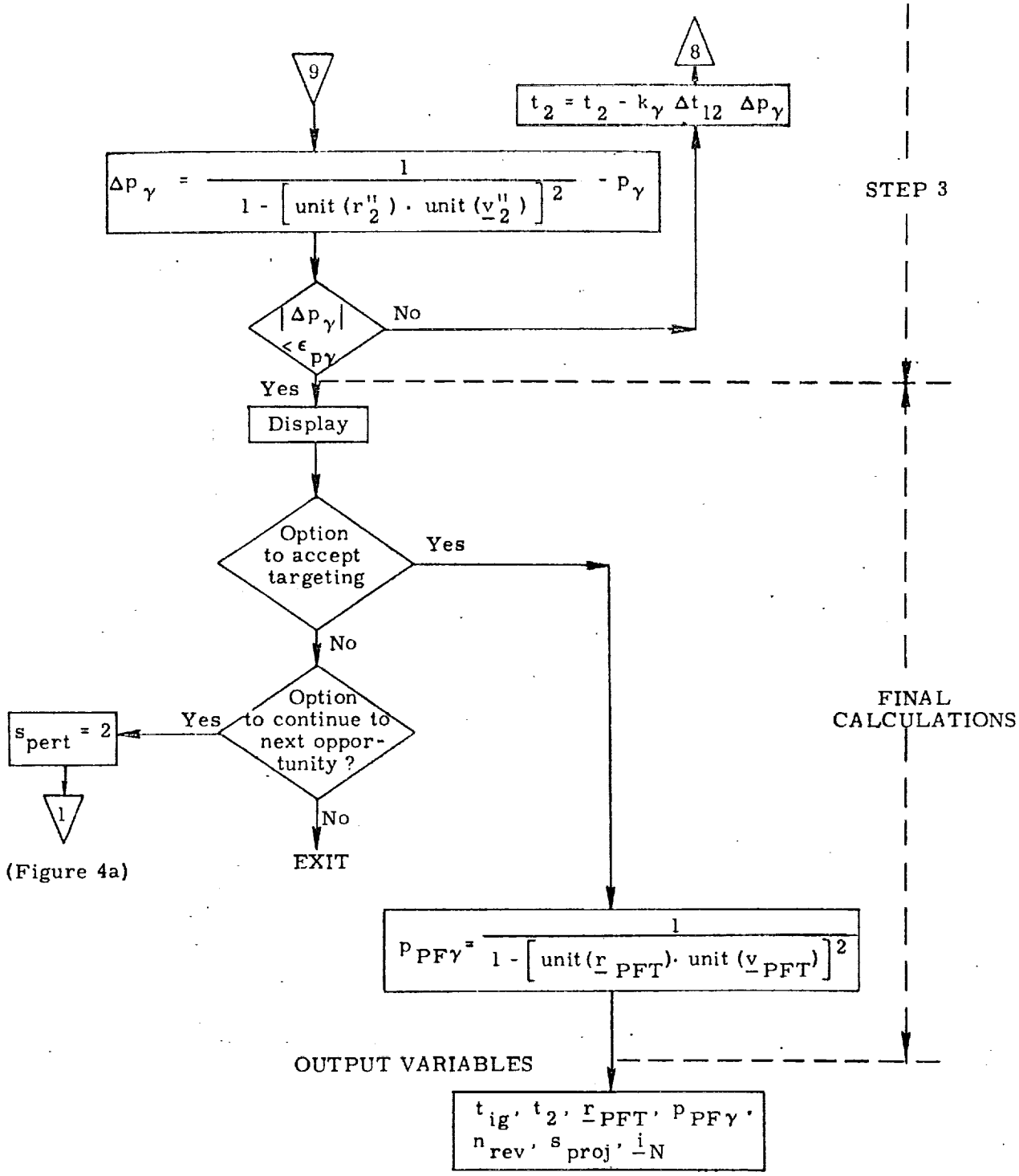


Figure 4g. Detailed Flow Diagram

## 1. INTRODUCTION

The objective of the Powered Flight Guidance Routines is to issue the proper steering and engine cutoff commands such that the desired terminal conditions of the maneuver are satisfied. The basic powered flight guidance law used in the orbiter is a velocity-to-be-gained concept with cross-product steering.

The two principle modes of the Powered Flight Guidance Routines are:

1. Delta-V Maneuver Guidance Mode
2. Real-Time Required Velocity Updating Guidance Mode.

The Delta-V Maneuver Guidance Mode is essentially equivalent to the External Delta-V Maneuver Guidance Mode used in APOLLO. The input desired velocity change is modified to compensate for the estimated central angle to be traversed during the maneuver. Then the object of the powered phase is simply to steer the vehicle to achieve this velocity change.

The Real-Time Required Velocity Updating Mode is a generalized version of the Lambert Aim Point Maneuver Mode used in APOLLO. The object of these maneuvers is to place the vehicle on a coasting trajectory which will intercept a specified target at a specified time. Two new concepts which greatly improve the accuracy of these maneuvers are introduced. First, guidance during the maneuver is based on a state vector navigated from ignition in a spherical (Keplerian) gravity field. Second, the required velocity is not determined using the present vehicle position but rather an offset position which accounts for the finite length of the maneuver. Since this is primarily an equations document, these new concepts are treated only briefly in the text. A detailed description and derivation can be found in Reference 5.

Because the calculation of required velocity can be a lengthy process, the ability to update the required velocity every major cycle is dependent upon the speed of the computer. The APOLLO Guidance Computer required portions of several major cycles to complete the solution. The guidance equations described here will assume that the orbiter computer will also need portions of several major cycles to complete the solution for required velocity. A faster computer would not alter the basic concepts presented here, but would simplify the mechanization somewhat.

The Real-Time Required Velocity Updating Mode may select a specific required velocity routine to accomplish one of the following maneuvers:

1. Lambert Aim Point Maneuver
2. Deorbit Maneuver
3. Other maneuvers such as a maneuver to an orbit with certain specified constraints (TBD).

The required velocity routines will be subjects of separate documents. Since this report is mainly concerned with the documentation of guidance equations, logic or computations concerned with monitoring or controlling system operation will not be presented.

## 2. FUNCTIONAL FLOW DIAGRAM

Powered Flight Guidance involves both the prethrust and thrusting phases of [illegible] prethrust computations, shown in Figure 1, are a single step process performed several minutes prior to the maneuver to prepare the vehicle for thrusting [illegible] required to process targeting parameters to determine the desired vehicle attitude at ignition. In addition, the state vector is advanced to a specified time prior to ignition. At this time, an integral number of major cycles prior to ignition, the thrusting phase computations, including Powered Flight Navigation, are initiated. Of course, the attitude maneuver necessary to align the vehicle to the desired attitude at ignition should be completed before entering the thrusting phase computations.

The sequence of functions performed during the main branch of the powered flight phase is illustrated in Figure 2. The guidance computer program known as the Servicer Routine, which controls the various subroutines to create a powered flight sequence, is not included in this document. The Servicer Routine will call the main branch every guidance cycle until engine shutdown has occurred.

Each guidance cycle begins with the reading of the accelerometers and is followed by the updating of the state vector in the Powered Flight Navigation Routine. Then the velocity-to-be-gained is updated in the Cross-Product Steering Routine. If steering is [illegible] the latter also computes the time-to-go and the steering command beginning [illegible] time after ignition.

The targeting calculations used to predict and compensate for gravitational perturbations establish an offset target which assumes that the vehicle is under the influence of only a spherical gravity field after the expected ignition time. Therefore, in the Real-Time Required Velocity Updating Mode, it is necessary to maintain an additional state vector navigated in a spherical gravity field. This dual navigation should begin at the ignition time assumed in the targeting program if it differs from the actual.

In the Real-Time Required Velocity Mode, another branch of the Powered Flight Guidance Routine involving the calculation of required velocity is operated independent of the main guidance branch. This separate branch, called the Velocity-to-be-Gained Routine, is initiated and controlled by the Servicer Routine and may require portions of several major guidance cycles to complete its solution. Of course, simple velocity-to-be-gained updates computed by decrementing the previous value by the [illegible] velocity change continue in the Cross-Product Steering Routine every major cycle. Normally, the Velocity-to-be-Gained Routine operates on a lower priority than the main guidance loop so that the new velocity-to-be-gained vector is not used by the Cross-Product Steering Routine until the next guidance cycle.

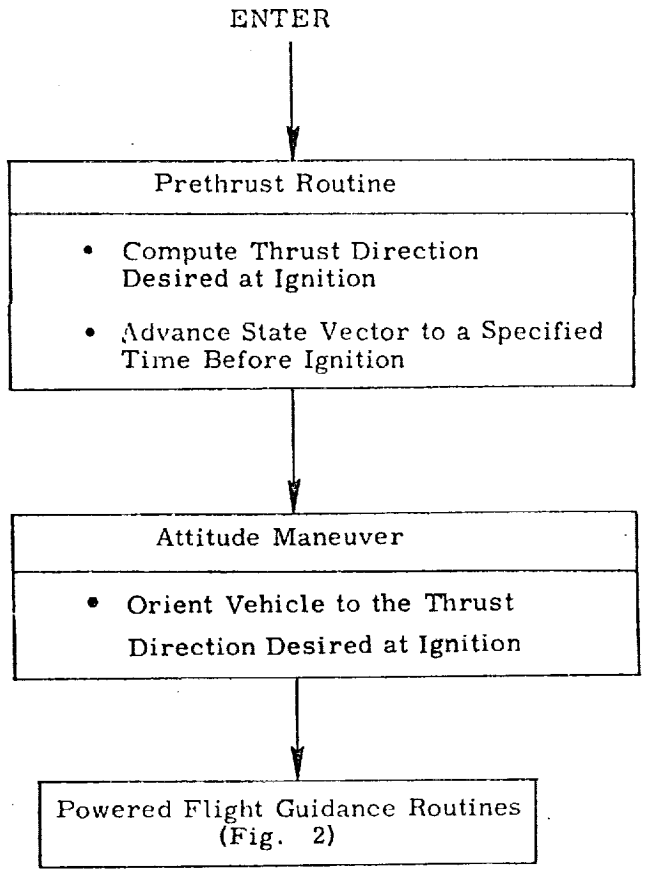


Figure 1. Powered Flight Program

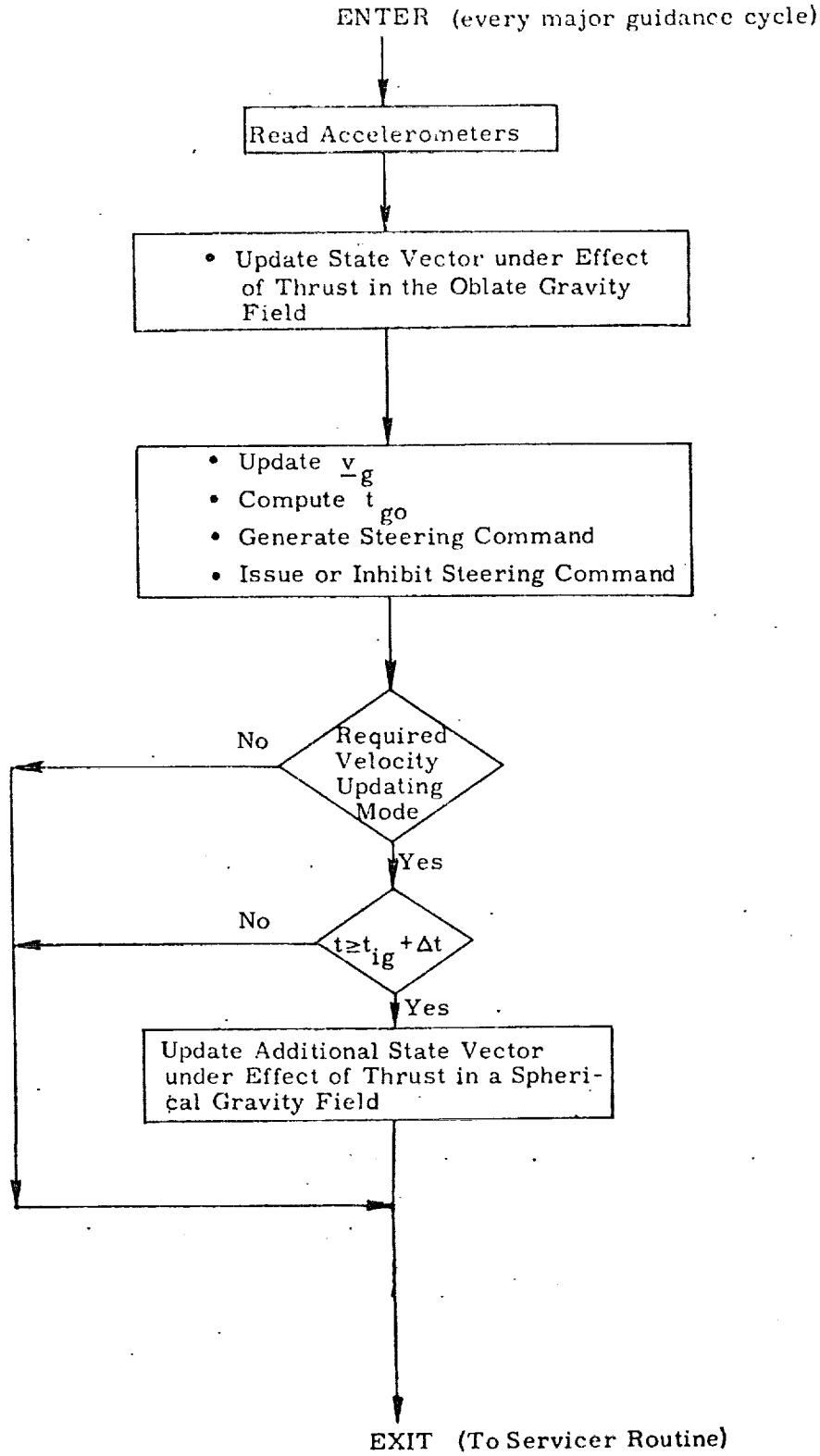


Figure 2. Powered Flight Guidance Routines

The characteristic of the transfer in the Real-Time Required Velocity Updating Mode in relation to the singularity cone of the Lambert problem is determined by the targeting program before the powered phase is initiated. This information is passed on to this guidance program through the $s_{proj}$ switch and is used by the Conic Required Velocity Determination Routine to define the transfer plane. (See Ref. 3 for a detailed explanation of the singularity cone and Ref. 6 for the targeting procedure).

If the $s_{proj}$ switch has been set, the transfer will take place in the plane defined by the unit vector $\underline{i}_N$ in the direction of the angular momentum vector at ignition. If this switch has not been set, there are two possibilities. Under normal circumstances the transfer will take place in the plane defined by the vehicle and target position vectors. However, unexpected degradation in engine performance during flight may prolong the powered maneuver to such an extent that the input position vector to the Conic Required Velocity Determination Routine is inside the singularity cone. The procedure to cope with this situation is presented below.

If the $s_{proj}$ switch has not been set by the targeting program, the $s_{cone}$ switch, which is an output of the Conic Required Velocity Determination Routine, is checked at each guidance cycle. If it is found that this switch has been set, indicating that the input position vector is inside the singularity cone, the Servicer Routine is directed to bypass the Velocity-to-be-gained Routine for the remainder of the powered maneuver. In other words, the remaining powered maneuver will be completed simply by decrementing the previous value of the velocity-to-be-gained by the sensed velocity change as is done in the Delta-V Mode.

When the time-to-go becomes less than some predetermined value, active steering is suspended and an engine cut-off command is set to be issued at the proper time.

## NOMENCLATURE

| | |
|---|---|
| $a_T$ | Estimated magnitude of thrust acceleration |
| C | Matrix to rotate the target vector to compensate for earth rotation due to change in time of flight during deorbit maneuver |
| d | Dimension of navigation filter weighting matrix (d = 0 in this routine since the matrix is not used) |
| f | Thrust |
| $f_{OMS}$ | Magnitude of orbital maneuvering system engine thrust |
| $f_{ACS}$ | Magnitude of attitude control system engine translational thrust |
| $\underline{g}$ | Gravity vector in the oblate gravity field |
| $\underline{g}_s$ | Gravity vector in the spherical gravity field |
| $\underline{i}_N$ | Unit vector in the direction of the angular momentum vector normal to the transfer plane |
| $\underline{i}_x, \underline{i}_y, \underline{i}_z$ | Unit vectors of local vertical coordinates |
| $\underline{i}_{TD}$ | Unit vector of desired thrust direction |
| k | Iteration counter in acceleration computation |
| $k_\gamma$ | Sensitivity used in computing the desired change in flight time to control entry angle during deorbit |
| $k_{steer}$ | Steering gain |
| $k_{tgo}$ | Intermediate variable in $t_{go}$ computation |
| m | Current estimated vehicle mass |
| $n_{min}$ | Number of guidance cycles used in thrust acceleration magnitude filter |

| | |
|---|---|
| $n_{rev}$ | Integer number of $360^{\circ}$ revolutions used in Conic Required Velocity Determination Routine |
| $p_N$ | Normalized semi-latus rectum of conic transfer orbit |
| $p_\gamma$ | Parameter defining the desired terminal flight path angle |
| $p_\gamma'$ | Parameter defining the projected terminal flight path angle |
| $\underline{r}$ | Position vector navigated in the oblate gravity field |
| $\underline{r}'$ | Position vector on the coasting trajectory |
| $\underline{r}_s$ | Position vector navigated in the spherical gravity field |
| $\underline{r}(t_2)$ | Offset target vector at $t_2$ |
| $\Delta\underline{r}$ | Initial position offset |
| $s_{accel}$ | Switch indicating whether the acceleration is computed from sensed $\Delta v$'s $\left(\begin{array}{ll} = 0 & \text{prethrust estimate} \\ = 1 & \text{sensed } \Delta v\text{'s} \end{array}\right)$ |
| $s_{cone}$ | Switch in the Conic Required Velocity Determination Routine to indicate if the transfer is near $180^{\circ}$ (see Ref. 3 for details) |
| $s_{eng}$ | Engine select switch |
| $s_{guess}$ | Switch to indicate whether estimate of independent variable $\Gamma$ will be input to the Conic Required Velocity Determination Routine (see Ref. 3 for details) |
| $s_{pert}$ | Switch indicating the perturbing accelerations to be included in Precision State and Filter Weighting Matrix Extrapolation Routine (see Ref. 2 for details) |
| $s_{proj}$ | Switch indicating whether the initial and target position vectors are to be projected into the plane defined by $\underline{i}_N$ (see Ref. 6 for details) |

| | |
|---|---|
| $s_{soln}$ | Switch indicating which of two possible solutions is [illegible] the multi-revolution case (see Ref. 3 for [illegible]) |
| $s_{steer}$ | Steering enable switch $\left( \begin{array}{l} = 0 \text{ inhibit} \\ = 1 \text{ enable} \end{array} \right)$ |
| $s_{tgo}$ | Switch indicating whether initial $t_{go}$ computation has [illegible] $\left( \begin{array}{l} = 0 \ t_{go} \text{ not yet computed} \\ = 1 \ t_{go} \text{ computed} \end{array} \right)$ |
| $t$ | Current state vector time (during thrusting phase, this is the time at which the accelerometers are read) |
| $\Delta t$ | Guidance cycle time step |
| $\Delta t'$ | Dummy transfer time set to 0 |
| $\Delta t_{cut\text{-}off}$ | Value [illegible] used to define time to issue engine cut-off command and terminate active steering |
| $\Delta t_{enable}$ | Value of $t_{go}$ which distinguishes between long or short maneuver |
| $\Delta t_{t0}$ | Time interval before $t_{ig}$ to start thrusting phase computations |
| $\Delta t_{t1}$ | Time interval prior to $t_{ig}$ when initial $t_{go}$ prediction is made |
| $\Delta t_{t2}$ | Time interval after $t_{ig}$ when steering is permitted |
| $\Delta t_{tail\text{-}off}$ | Time interval representing the duration of a burn at maximum thrust equivalent to the tail-off impulse after the engine-off signal is issued |
| $\Delta t_{tail\text{-}off,\ OMS}$ | $\Delta t_{tail\text{-}off}$ of orbital maneuvering system engine |

| | |
|---|---|
| $\Delta t_{\text{tail-off, ACS}}$ | $\Delta t_{\text{tail-off}}$ of attitude control system engine for translational maneuver |
| $\delta t_2$ | Change in time of arrival required to satisfy terminal flight path angle in a deorbit maneuver |
| $t_2$ | Time of arrival at $\underline{r}(t_2)$ |
| $t_{go}$ | Time-to-go before engine cut-off |
| $t_{ig}$ | Nominal engine ignition time |
| $\underline{v}$ | Velocity vector navigated in the oblate gravity field |
| $\underline{v}_s$ | Velocity vector navigated in the spherical gravity field |
| $\underline{v}_g$ | Velocity-to-be-gained vector |
| $v_g$ | Magnitude of $\underline{v}_g$ |
| $\underline{v}'_{req}$ | Required velocity vector at the offset initial position (defines the coasting trajectory) |
| $\underline{v}_{req}$ | Required velocity at current position (no initial position offset) |
| $\Delta\underline{v}$ | Measured velocity increment vector due to thrust in one guidance cycle |
| $\Delta v$ | Magnitude of $\Delta\underline{v}$ |
| $\Delta v_k$ | kth value of sensed $\Delta v$ saved for acceleration computation |
| $\Delta\underline{v}_{LV}$ | Desired velocity change vector input to Delta-V Guidance Mode |
| $\Delta v_{min}$ | Minimum sensed $\Delta v$ which will allow acceleration filter computations to be made |
| $\Delta v_N$ | $\sum \Delta v_k$ for $n_{min}$ cycles |

| | |
|---|---|
| $\Delta \underline{v}_{xz}$ | In-plane components of $\Delta \underline{v}_{LV}$ |
| $\Delta \underline{v}_c$ | Compensated in-plane components of $\Delta \underline{v}_{LV}$ |
| $\Delta v_x$, $\Delta v_y$, $\Delta v_z$ | Components of $\Delta \underline{v}_{LV}$ |
| $v_{exh}$ | Exhaust velocity |
| $v_{exh,OMS}$ | Exhaust velocity of the orbital maneuvering system engine |
| $v_{exh,ACS}$ | Exhaust velocity of the attitude control system engine for translational maneuver |
| $\alpha_N$ | Reciprocal of normalized semi-major axis of conic transfer orbit |
| $\epsilon_{\theta G}$ | Tolerance criterion establishing a cone around the negative target position direction inside of which the Conic Required Velocity Determination Routine will define the transfer plane by $\underline{i}_N$ |
| $\gamma_{t2}$ | Projected terminal flight path angle with respect to local horizontal (negative downward) |
| $\Gamma$ | Converged value of iteration variable used in Conic Required Velocity Determination Routine |
| $\Gamma_P$ | Previous value of $\Gamma$ |
| $\Gamma_{guess}$ | Estimated value of $\Gamma$ |
| $\dot{\Gamma}$ | Time rate of change of $\Gamma$ |
| $\kappa$ | Ratio of $\lvert \underline{r}(t_2) \rvert$ to $\lvert \underline{r}'(t) \rvert$ |
| $\theta_T$ | Estimated central angle traversed during thrusting maneuver in Delta-V Guidance Mode |
| $\mu$ | Earth's gravitational constant |

| | |
|---|---|
| $\tau$ | Time associated with current required velocity |
| $\tau_P$ | Previous value of $\tau$ |
| $\underline{\omega}_c$ | Angular velocity command |
| $\omega_{earth}$ | Magnitude of the earth's angular velocity |

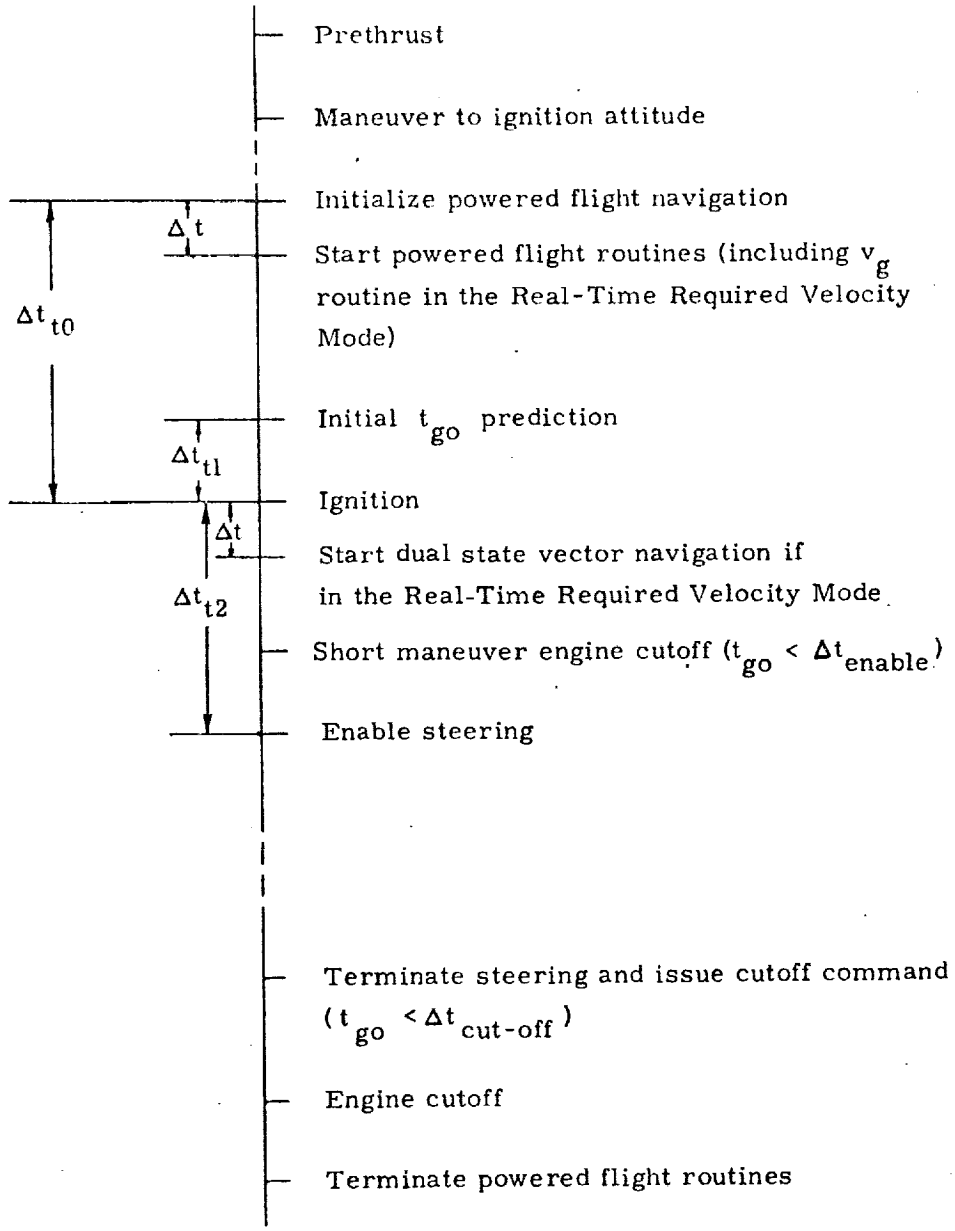


Figure 5. Sequence of Events

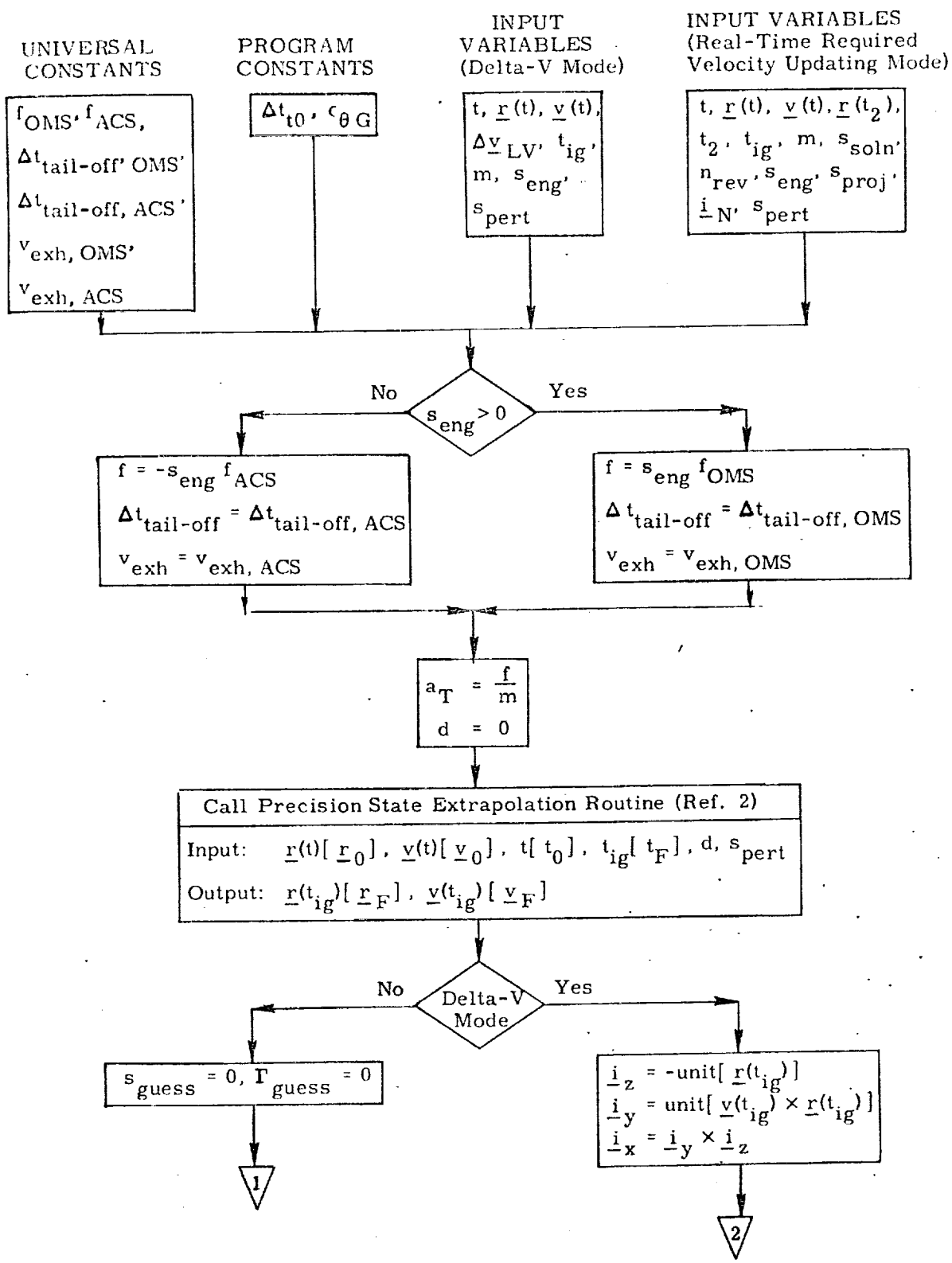


Figure 6a. Prethrust Phase, Detailed Flow Diagram

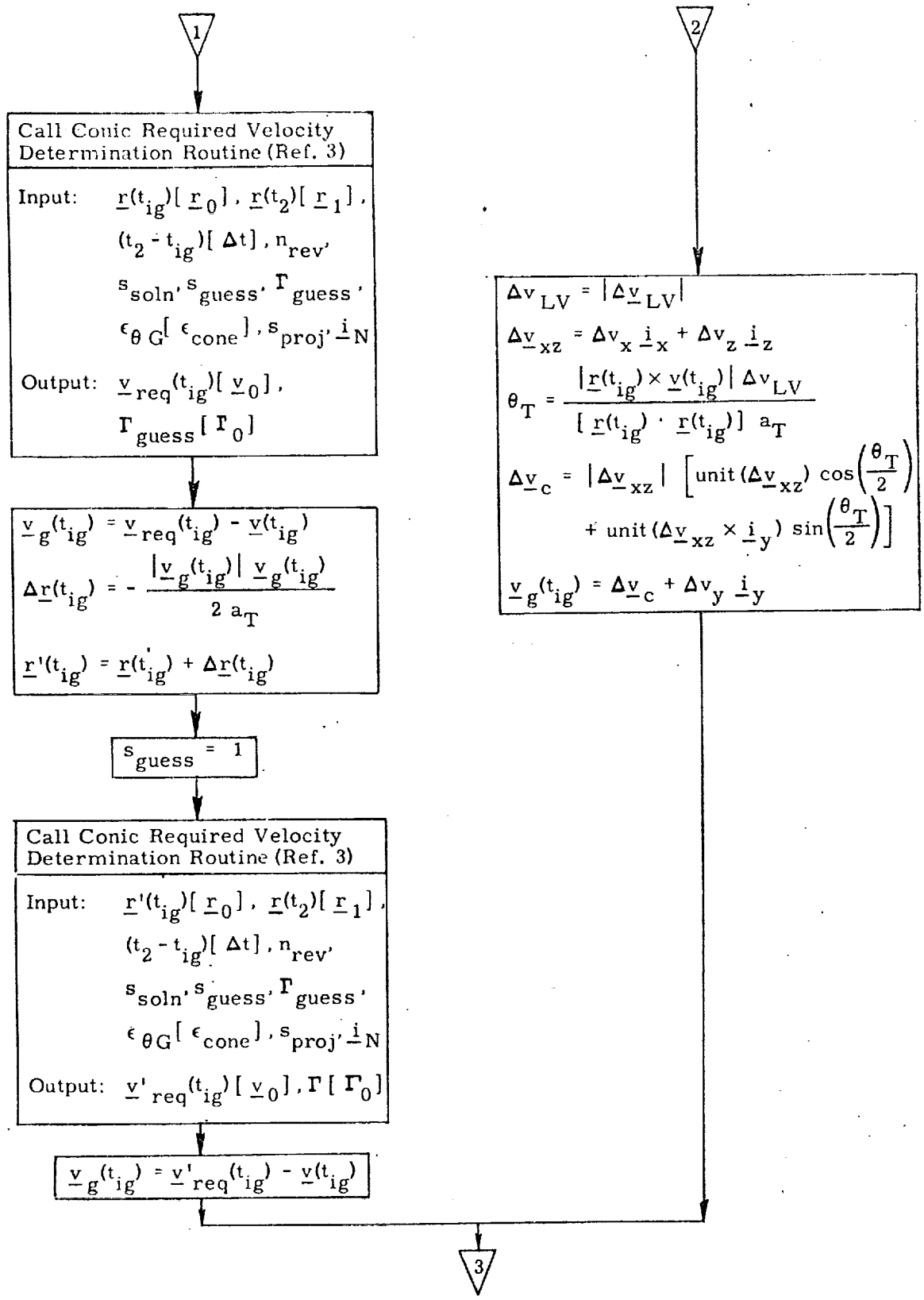


Figure 6b. Prethrust Phase, Detailed Flow Diagram

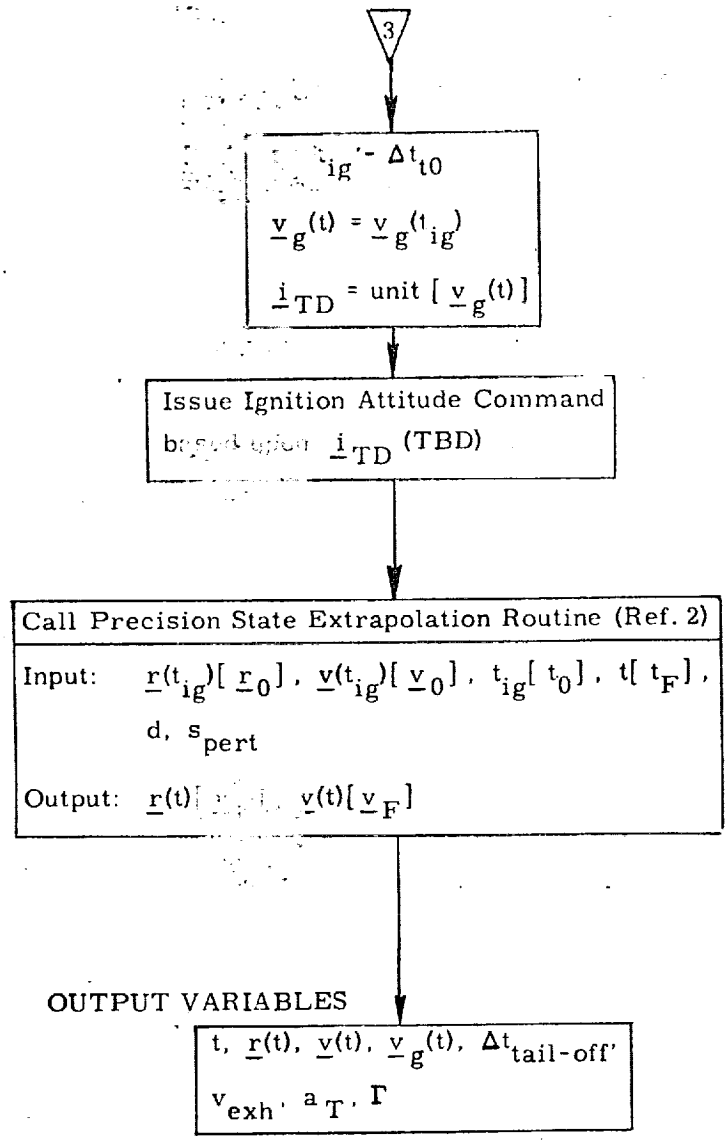


Figure 6c. Prethrust Phase, Detailed Flow Diagram

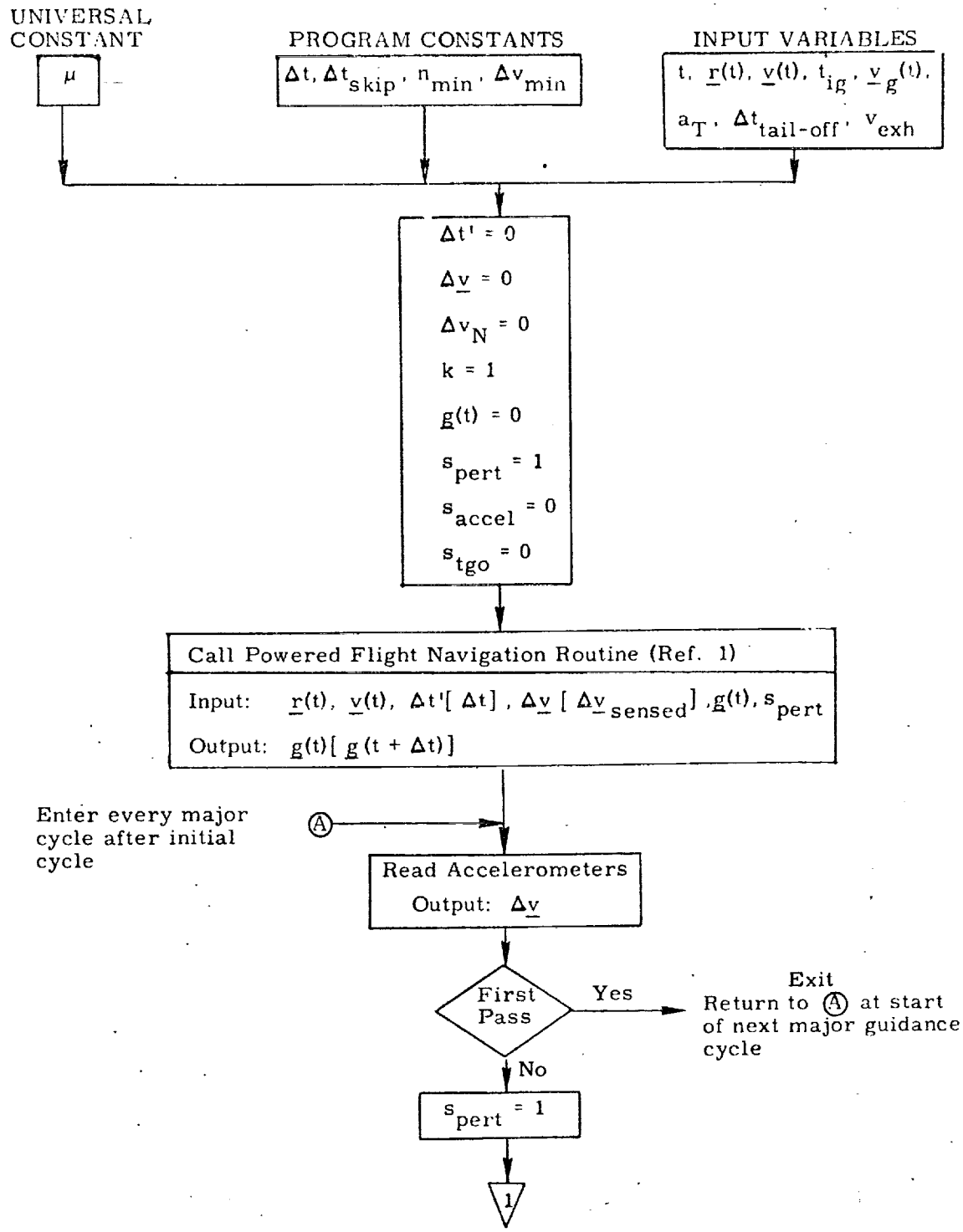


Figure 7a. Powered Flight Routines, Detailed Flow Diagram

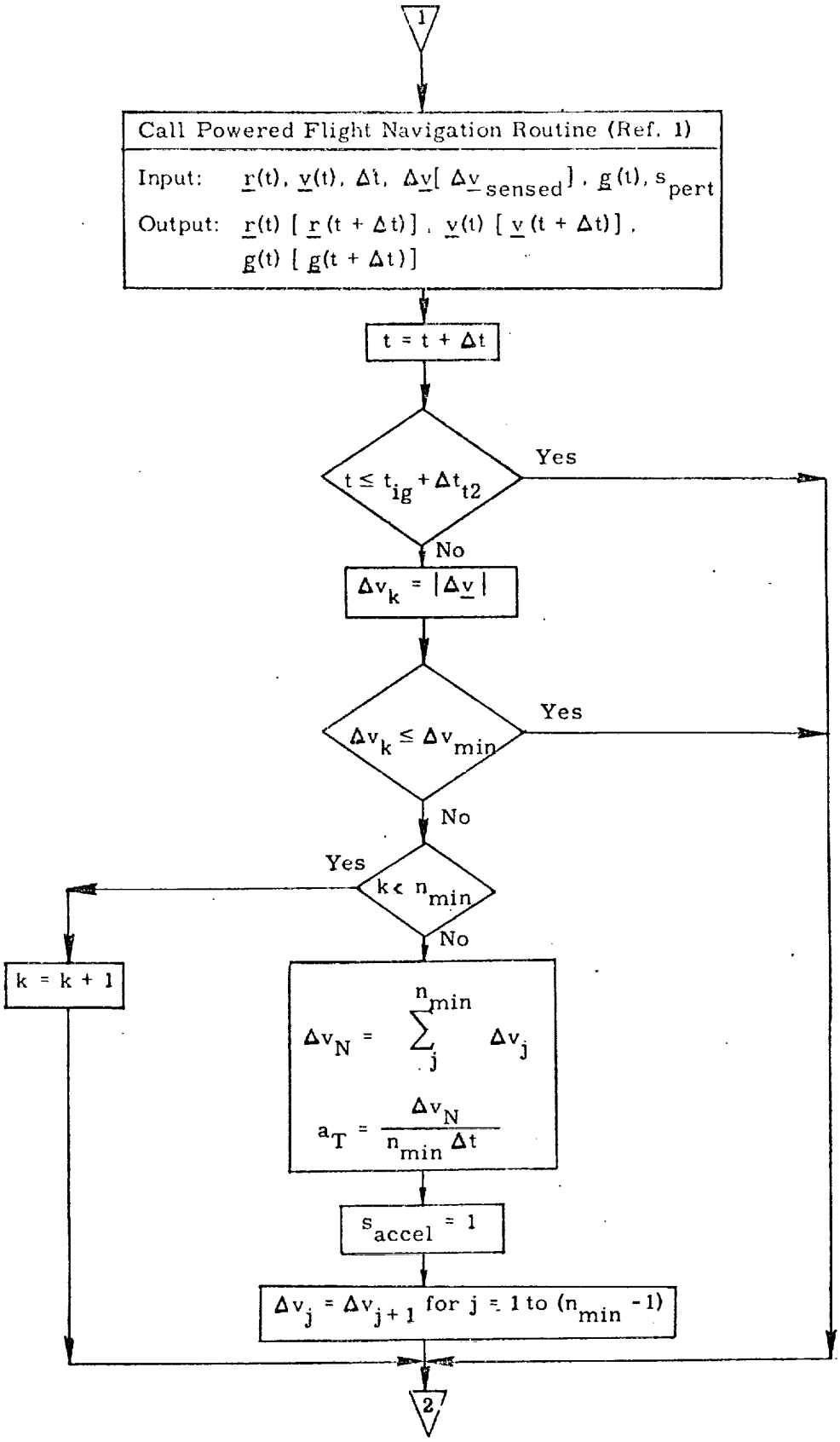


Figure 7b. Powered Flight Routines, Detailed Flow Diagram

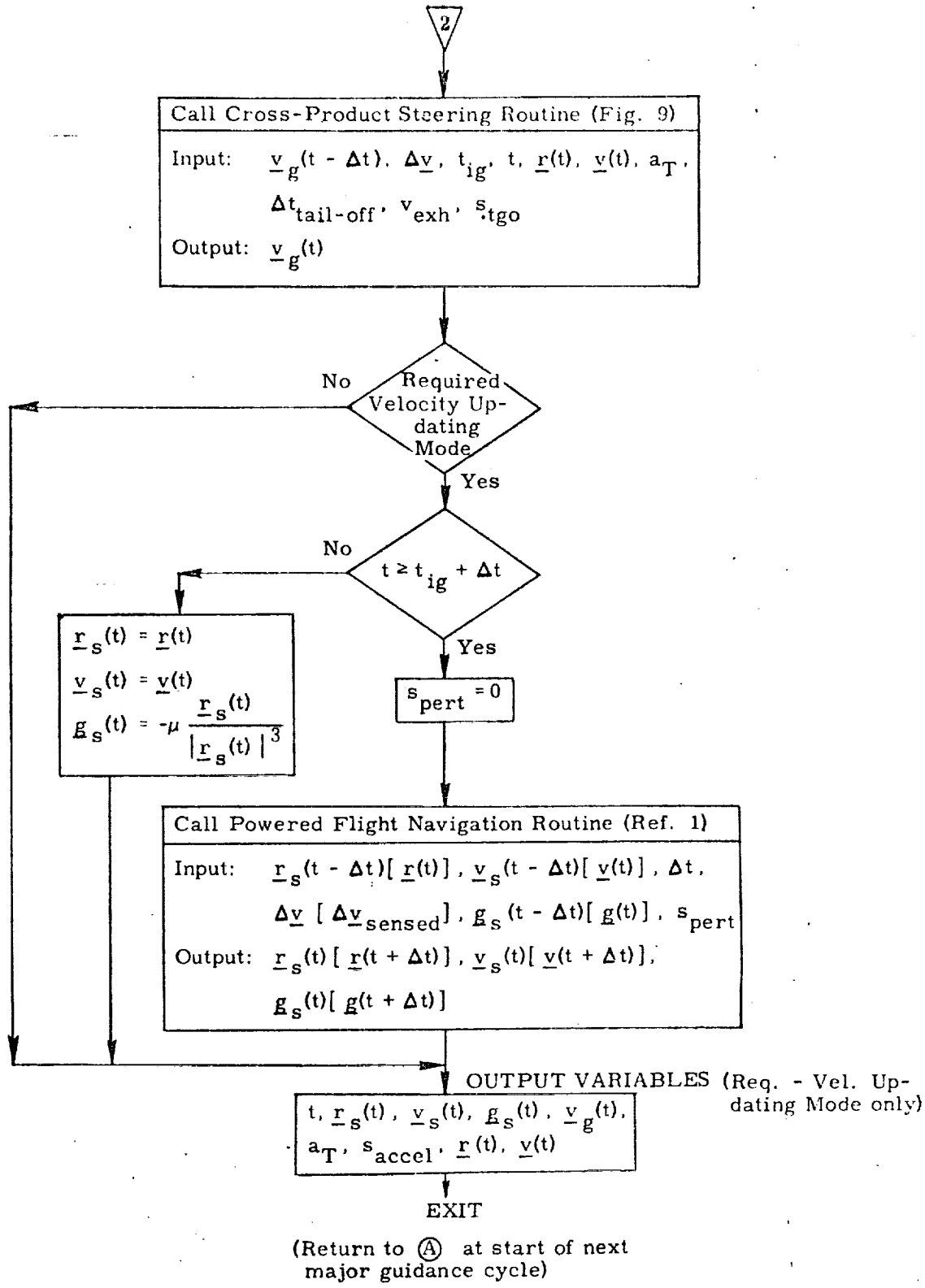


Figure 7c. Powered Flight Routines, Detailed Flow Diagram

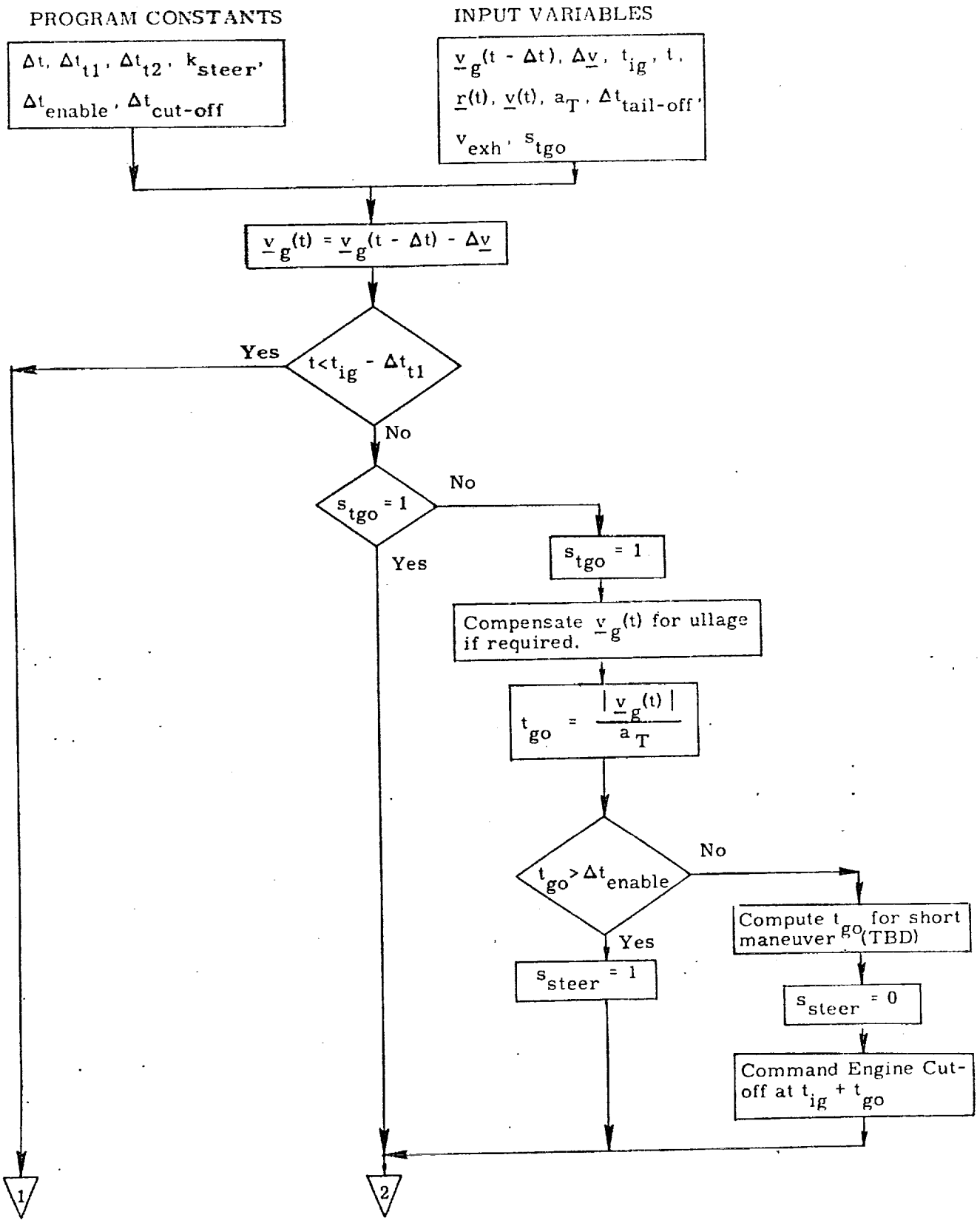


**Figure 8a.** Cross-Product Steering Routine, Detailed Flow Diagram

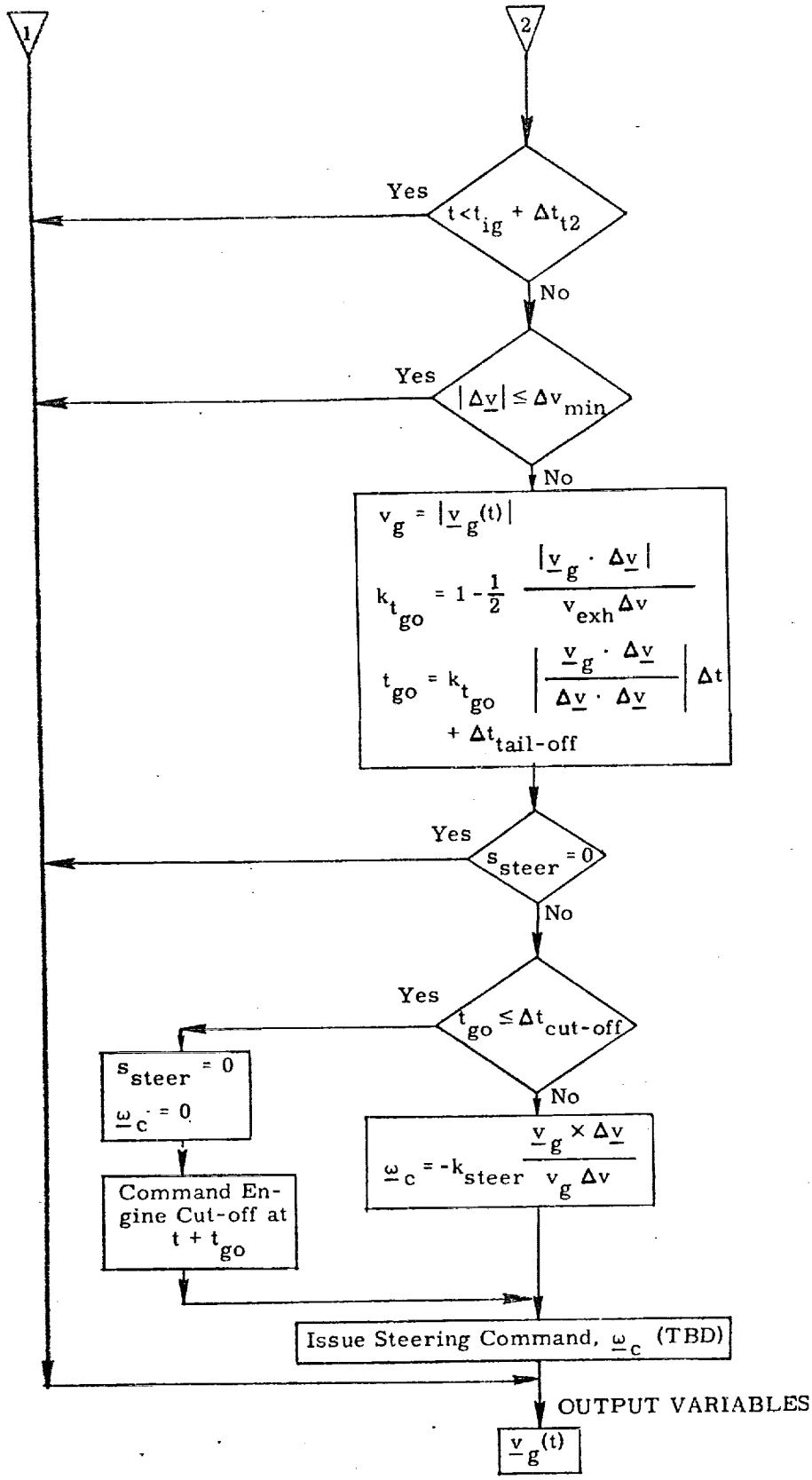


Figure 8b. Cross-Product Steering Routine, Detailed Flow Diagram

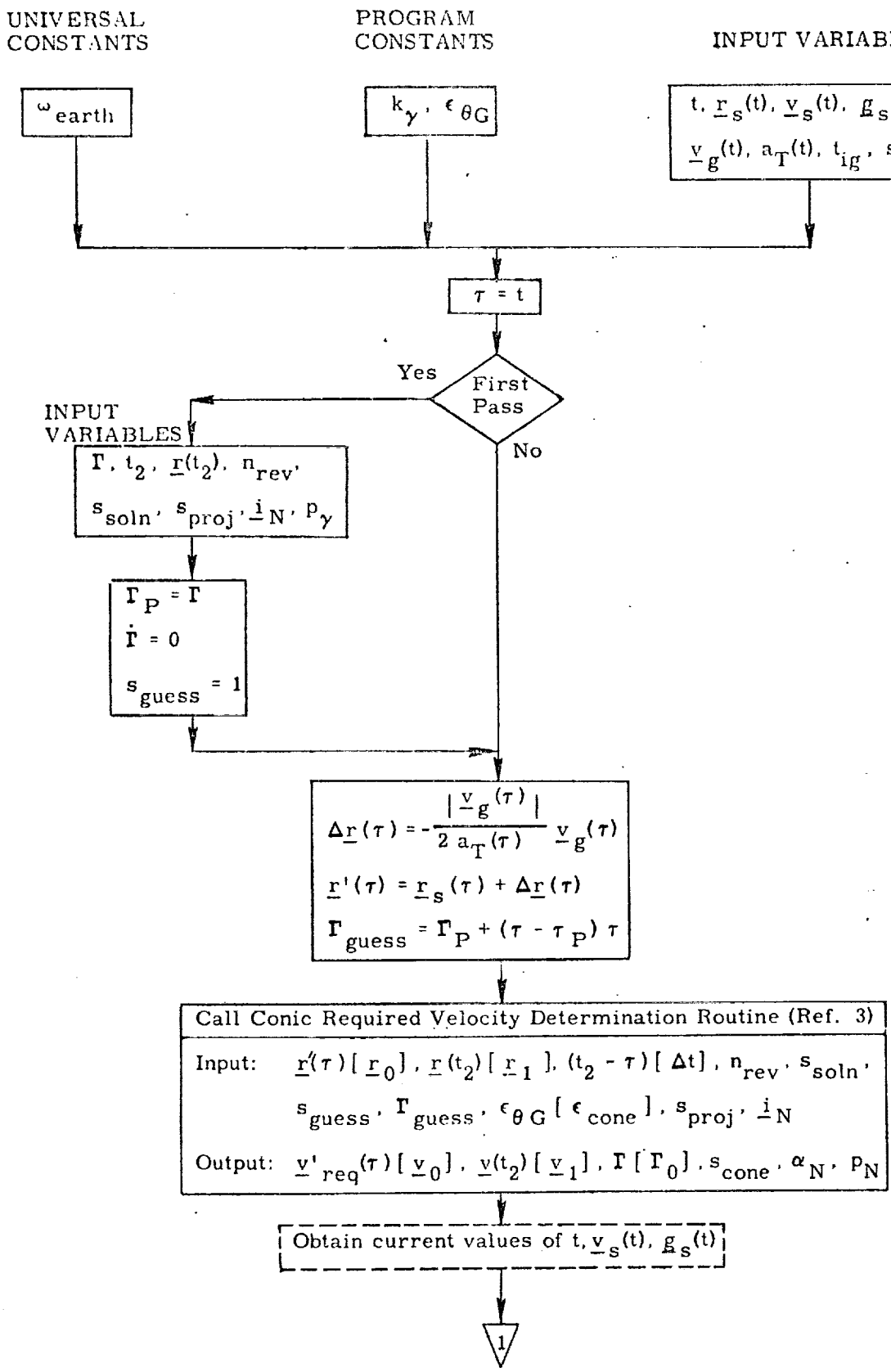


Figure 9a. Velocity-to-be-Gained Routine, Detailed Flow Diagram

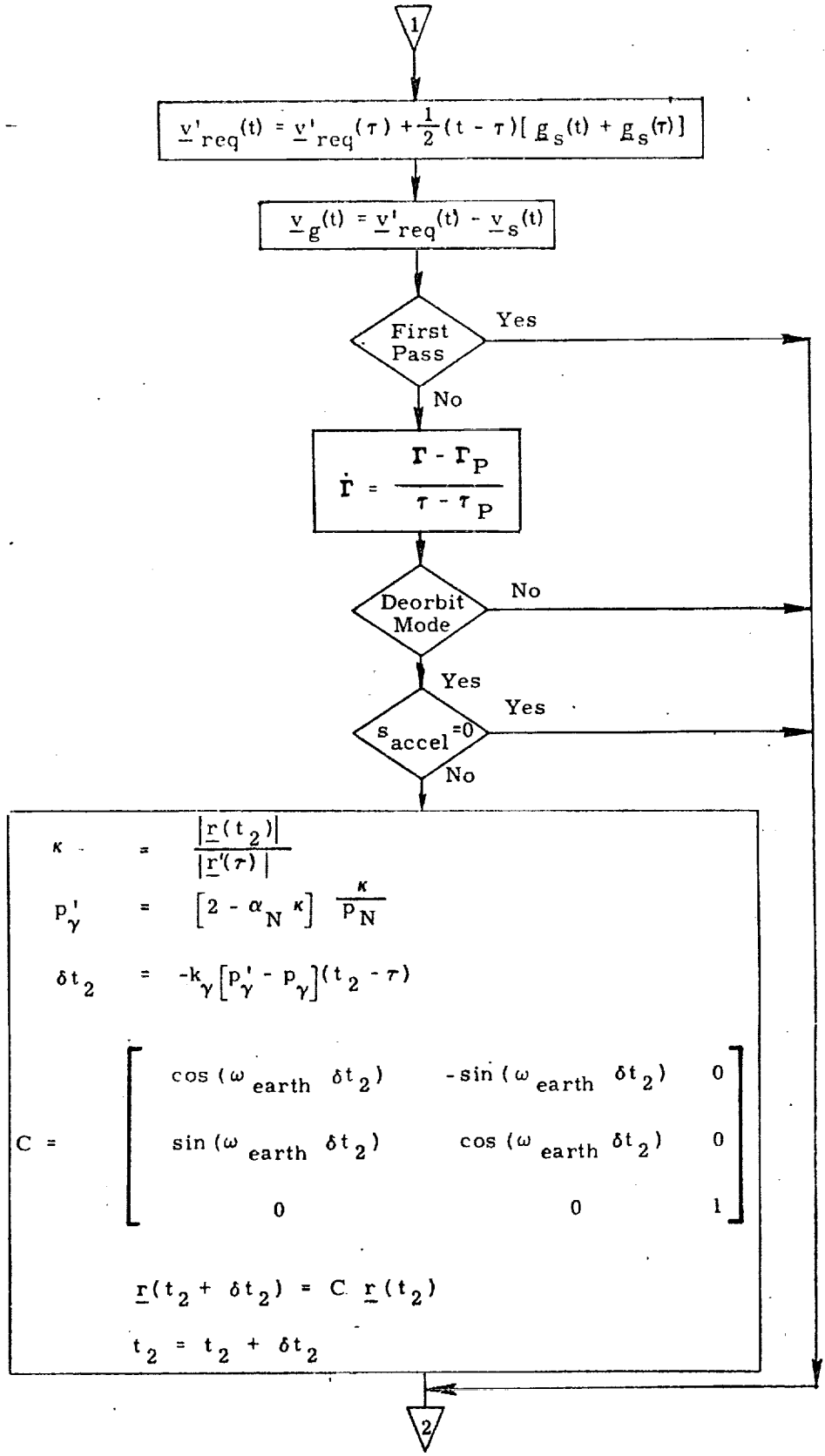


Figure 9b. Velocity-to-be-Gained Routine, Detailed Flow Diagram

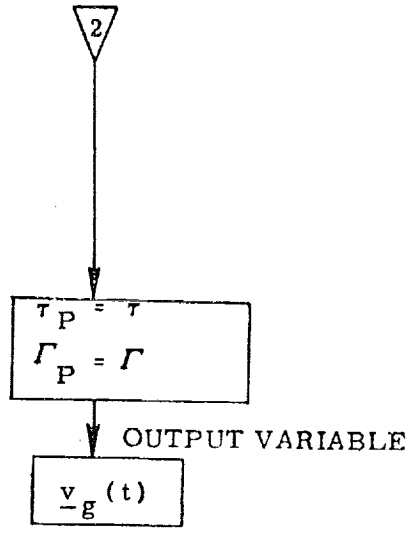


Figure 9c. Velocity-to-be-Gained Routine, Detailed Flow Diagram

## Submittal 4/ [illegible]ry Guidance

### 1. INTRO[illegible]

The Entry-Guidance Routine presented here is designed to take the orbiter vehicle from en[illegible] ($h \approx 400,000$ ft) through the critical heating phase of entry down to the start of the approach phase ($h \approx 100,000$ ft). The basic ideas are outlined in Re[illegible]). Simulation results demonstrating the feasibility of the concept are given in Ref. (2).

There are three basic guidance modes:

(1.) [illegible] programmed-maneuver mode in which the vehicle is oriented with a zero roll angle (wings up), and an angle-of-attack corresponding to maximum [illegible] the point of pullup.

(2.) A constant heating-rate mode during which the stagnation-point heating rate is held constant at a preselected value, chosen essentially to minimize heat loads on the vehicle without violating maximum temperature constraints.

(3.) A reference trajectory mode during which the vehicle follows a prestored stored trajectory designed to get [illegible]le to the terminal point with a minimum re-[illegible] RPS weight, and without violating operational constraints on the vehicle.

Thermal control is provided by varying the magnitude of the roll angle so as to follow a density-vs.-speed profile. Density information is derived from IMU measurements of the aerodynamic specific force acting on the vehicle. A-priori knowledge of the vehicle's mass, effective aerodynamic area, and drag coefficient ($c_D$) are required in the process.

Range control is provided by changing the angle-of-attack of the vehicle. Upper and lower limits on angle-of-attack are required in order not to violate operational con[illegible]s on the vehicle. Lateral trajectory control is obtained by reversing the d[illegible]ection of the roll angle.

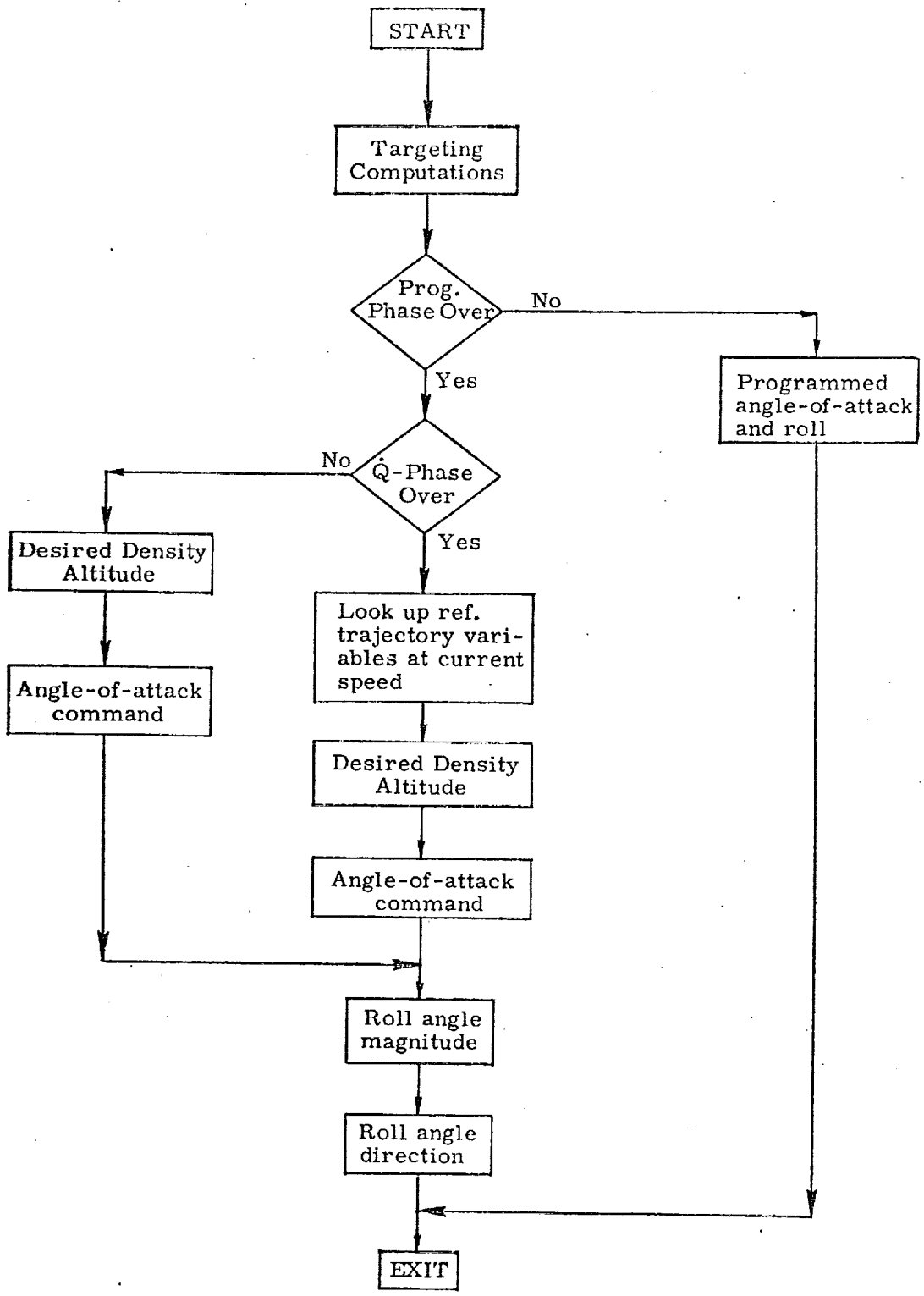
START
Targeting Computations
Prog. Phase Over
No
Yes
Programmed angle-of-attack and roll
No
Q̇-Phase Over
Yes
Desired Density Altitude
Angle-of-attack command
Look up ref. trajectory variables at current speed
Desired Density Altitude
Angle-of-attack command
Roll angle magnitude
Roll angle direction
EXIT

## NOMENCLATURE

Notational Conventions

Upper-case letters represent matrices

Lower-case and Greek letters reserve for scalars and vectors

Vector quantities are underlined, e.g. $\underline{x}$

Vectors are assumed to be column vectors unless explicitly noted

Symbols

| | |
|---|---|
| $a$ | Effective aerodynamic area for vehicle |
| $c_0, c_1$ | Coefficients used to compute $\alpha_C$ from $c_D$ |
| $c_D$ | Aerodynamic drag coefficient for vehicle |
| $c_\rho$ | Coefficient in desired-density relation for constant heating-rate mode |
| $c_{\dot{q}}$ | Coefficient used in relation for desired $c_D$ |
| $c_{D_{\dot{q}}}$ | Desired value of $c_D$ for constant heating-rate mode |
| $c_{D_{MIN}}$ | Lowest permissible value of $c_D$ for constant heating-rate mode |
| $c_{D_{MAX}}$ | Highest permissible value of $c_D$ for constant heating-rate mode |
| $d$ | Drag force per unit mass |
| $f$ | Aerodynamic force per unit mass on vehicle |
| $\underline{h}_N$ | Stored array of reference trajectory altitudes |
| $h$ | Vehicle altitude above Fischer ellipsoid |
| $h_\rho$ | Density altitude |

| | |
|---|---|
| $h_{F_{prog}}$ | Vertical velocity at which programmed mode is terminated |
| $h_I, \dot{h}_I$ | Inertial altitude and derivative w.r.t. time |
| $h_I, \dot{h}_I$ | Inertial vertical velocity and derivatives w.r.t. time |
| $h_s$ | Scale height for exponential density-variation model |
| $h_F$ | Filtered vertical velocity |
| $h_\rho, \dot{h}_\rho$ | Altitude at which $\rho$ would occur and its derivative w.r.t. time |
| $\underline{i}_{RE}$ | Unit vector along $\underline{r}_E$ (earth-fixed coordinates) |
| $\underline{i}_{pole}$ | Unit vector along North pole (earth-fixed coordinates) |
| $\underline{i}_{EE}$ | Unit vector directed towards local East (earth-fixed coordinates) |
| $\underline{i}_{SE}$ | Unit vector directed towards local South (earth-fixed coordinates) |
| $\underline{i}_{GCE}$ | Unit vector along desired great-circle heading direction (earth-fixed coordinates) |
| $\underline{i}_{RDE}$ | Unit vector along desired terminal position (earth-fixed coordinates) |
| $\underline{i}_{VR}$ | Unit vector along $\underline{v}_R$ (stable-member coordinates) |
| $\underline{i}_{XA}$ | Unit vector along vehicle longitudinal axis (stable member coordinates) |
| $\underline{i}_{YA}$ | Unit vector along vehicle lateral axis (stable-member coordinates) |
| $\underline{i}_{HOR}$ | Unit vector normal to plane of vehicle's position and relative velocity vectors |
| k | Index variable used for reference-trajectory lookup |

| | |
|---|---|
| $k_\alpha$ | Sensitivity factor in angle-of-attack relation |
| $k_{\alpha TC}$ | Value used for $k_\alpha$ in thermal control portion of ref. traj. mode |
| $k_{\alpha PC}$ | Value used for $k_\alpha$ in final position control portion of ref. traj. mode |
| $k_{\phi 0}, k_{\phi 1}$ $k_{\phi 2}, k_{\phi 3}$ | Coefficients used in roll-command relation |
| $k_\eta$ | Fraction of $\eta$ at which roll angle should be reversed |
| $\ell_{AD}$ | Desired latitude at the end of entry |
| $\ell_{OD}$ | Desired longitude at the end of entry |
| $M_{SM-E}$ | Transformation matrix from stable member to earth-fixed coordinates |
| m | Mass of vehicle |
| n | Index for computation-cycle time |
| $n_{mach}$ | Mach number |
| $\underline{r}$ | Vehicle position (stable-member coordinates) |
| $\underline{r}_{DE}$ | Target-point position vector (earth-fixed coordinates) |
| $r_e$ | Earth radius (nominal) |
| $\underline{r}_E$ | Vehicle position (earth-fixed coordinates) |
| $r_G$ | Range to go to target point |
| $r_{GD}$ | Desired value of $r_G$ at current $v_R$ (from stored trajectory) |
| $r_{G_{\dot{q}}}$ | Desired range to be covered in the constant heating-rate mode |

| | |
|---|---|
| $r_{G_{REF}}$ | Nominal range to be covered in the reference trajectory mode |
| $r_{G_{APP}}$ | Nominal range to be covered in approach phase |
| $r_{G_{MIN}}$ | Lower limit for $r_{G_{\dot{q}}}$ in angle-of-attack computation |
| $r_G^*$ | Range-to-go used in reference-trajectory mode guidance computations |
| $\underline{r}_{GN}$ | Stored array of reference-trajectory range-to-go |
| $s_\phi$ | Dummy variable used in roll-reversal logic |
| $s_{\dot{q}}$ | Switch used to start constant heating rate mode |
| $s_{REF}$ | Switch used to start reference-trajectory mode |
| $s_v$ | Vertical component of specific force on vehicle |
| $s_{\dot{v}_D}$ | Desired vertical component of specific force |
| $t$ | Current time |
| $\underline{v}$ | Vehicle velocity (absolute in stable-member coordinates) |
| $v_\alpha$ | Speed factor used in angle-of-attack command relation |
| $v_{F_{\dot{q}}}$ | Relative velocity at which constant heating-rate mode is terminated |
| $\underline{v}_N$ | Reference-trajectory array of vehicle speed w.r.t. air mass (22 elements) |
| $v_H$ | Horizontal component of vehicle's velocity (absolute) |

| | |
|---|---|
| $\underline{v}_R$ | Vehicle velocity w.r.t. air mass (stable-member coordinates) |
| $\underline{v}_{RE}$ | Vehicle velocity w.r.t. air mass (earth-fixed coordinates) |
| $\underline{v}_{RHE}$ | Horizontal component of $\underline{v}_{RE}$ |
| $v_{RLO}$ | Lower limit on $v_\alpha$ |
| $\alpha_C$ | Angle-of-attack command |
| $\alpha_{c_{L_{MAX}}}$ | Angle-of-attack corresponding to maximum $c_L$ |
| $\alpha_{CMAX}$ | Maximum permissible value of $\alpha_C$ |
| $\alpha_{CMIN}$ | Minimum permissible value of $\alpha_C$ |
| $\alpha_D$ | Desired value of $\alpha$ at current $v_R$ (from stored trajectory) |
| $\alpha_{MAX_{\dot{q}}}$ | Maximum permissible angle-of-attack in constant heating-rate mode |
| $\alpha_{MIN_{\dot{q}}}$ | Smallest permissible angle of attack in constant heating-rate mode |
| $\underline{\alpha}_N$ | Stored array of reference-trajectory angle of attack |
| $\phi_C$ | Roll angle command |
| $\phi_T$ | Computed vehicle roll angle |
| $\Delta\psi$ | Different between current and desired heading of vehicle w.r.t. air mass |
| $\Delta\psi_0$ | Value of $\Delta\psi$ on first pass |
| $\Delta\underline{v}$ | Accelerometer-measured velocity change from previous to present computation-cycle time |
| $\Delta t$ | Time interval from previous to present computation-cycle time |
| $\psi$ | Local heading (w.r.t. South) |

| | |
|---|---|
| $\psi_D$ | Desired heading (w.r.t. South) |
| $\omega_f$ | Parameter in vertical velocity filter |
| $\phi^*_{MAX}$, $\phi^*_{MIN}$ | Levels used in $\phi_C$ computations |
| $\phi_{MAX}$, $\phi_{MIN}$ | Levels used in $\phi_C$ computations |
| $\phi^*$ | Dummy variable used in roll-angle computations |
| $\phi_{OLD}$ | Previous value of $\phi_C$ |
| $\theta$ | Great-circle angle from the current position to the desired target point |
| $\theta_{CT}$ | Cross track component of $\theta$ |
| $\theta_{DR}$ | Down range component of $\theta$ |
| $\eta$ | Ratio of $\theta_{CT}$ to $\theta_{DR}$ |
| $\eta_D$ | Desired value of $\eta$ at current $v_R$ (from stored trajectory) |
| $\underline{\eta}_N$ | Stored array of reference-trajectory $\eta$ |
| $\rho_0$ | Sea-level value of earth's density |
| $\rho$ | Estimated density from specific force measurements |
| $\rho_{\dot{q}}$ | Desired density for constant heating-rate mode |
| $\mu$ | Earth's gravitational constant |
| $\zeta$ | Dummy variable used in reference trajectory lookup |

Special Notation

| | |
|---|---|
| $(\ )'$ | A-priori estimated value prior to measurement incorporation |
| $\overline{(\ )}$ | Ensemble average of ( ) |
| $\lvert(\ )\rvert$ | Magnitude of ( ) |
| $(\ )^T$ | Transpose of ( ) |
| unit (__) | Unit vector for ( __ ) |
| sign ( ) | Algebraic sign associated with ( ). Value is +1 or -1, with sign (0) $\triangleq$ +1 |

## 3. INPUT AND OUTPUT VARIABLES

### Input Variables

| | |
|---|---|
| $\underline{i}_{XA}$ | Unit vector along vehicle longitudinal axis |
| $\underline{i}_{YA}$ | Unit vector along vehicle lateral axis |
| $M_{SM-E}$ | Transformation matrix from stable-member to earth-fixed coordinates |
| $\underline{r}$ | Vehicle position (stable-member coordinates) |
| $\underline{v}_R$ | Vehicle velocity w. r. t. air mass (stable-member coordinates) |
| $\underline{v}$ | Vehicle velocity (stable-member coords.) |
| $\Delta \underline{v}$ | IMU-measurement velocity change |
| $\Delta t$ | Time interval over which $\Delta \underline{v}$ is taken |

### Output Variables

| | |
|---|---|
| $\alpha_C$ | Angle-of-attack command |
| $\phi_C$ | Roll angle command |

## 4. DETAILED FLOW DIAGRAMS

This section contains detailed flow diagrams of the Entry Guidance Routine.

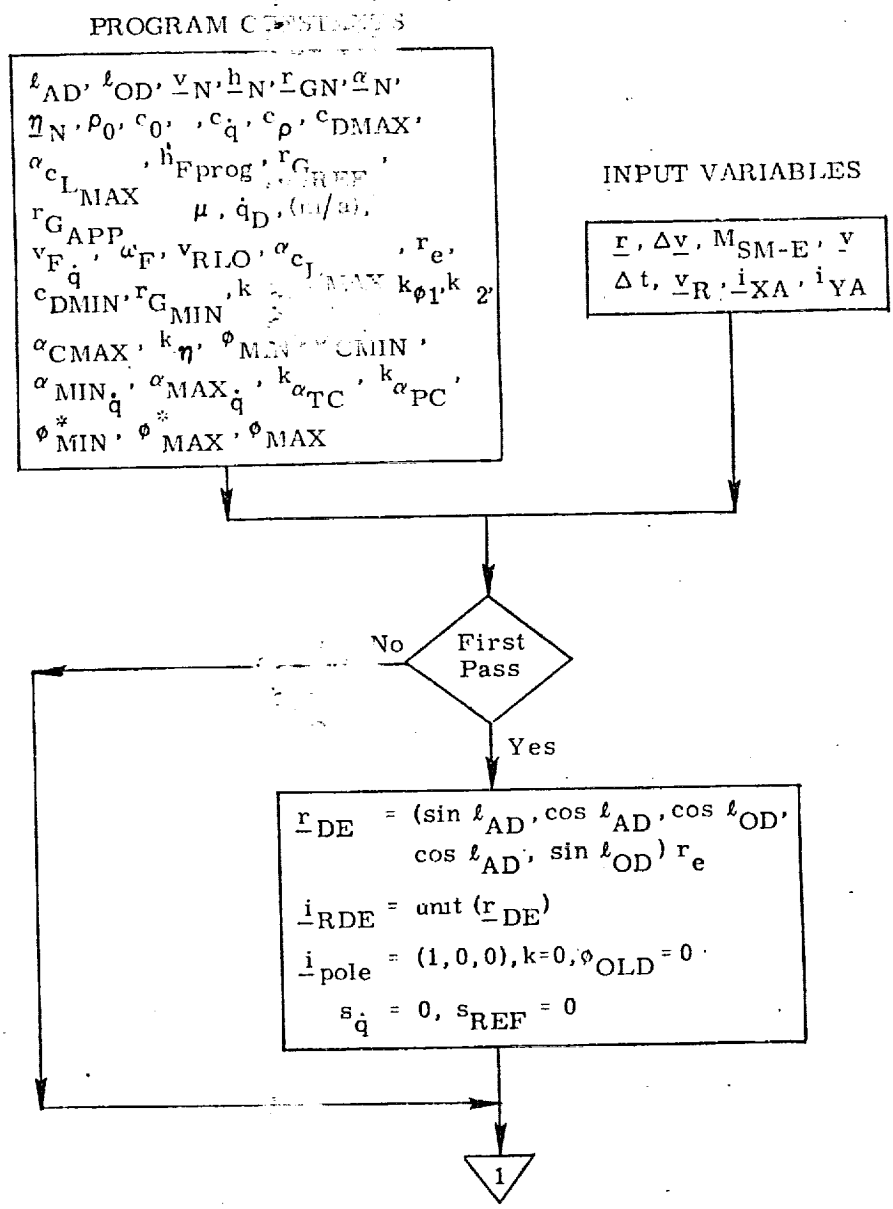


Figure 2a. Entry Guidance Routine, Detailed Flow Diagram

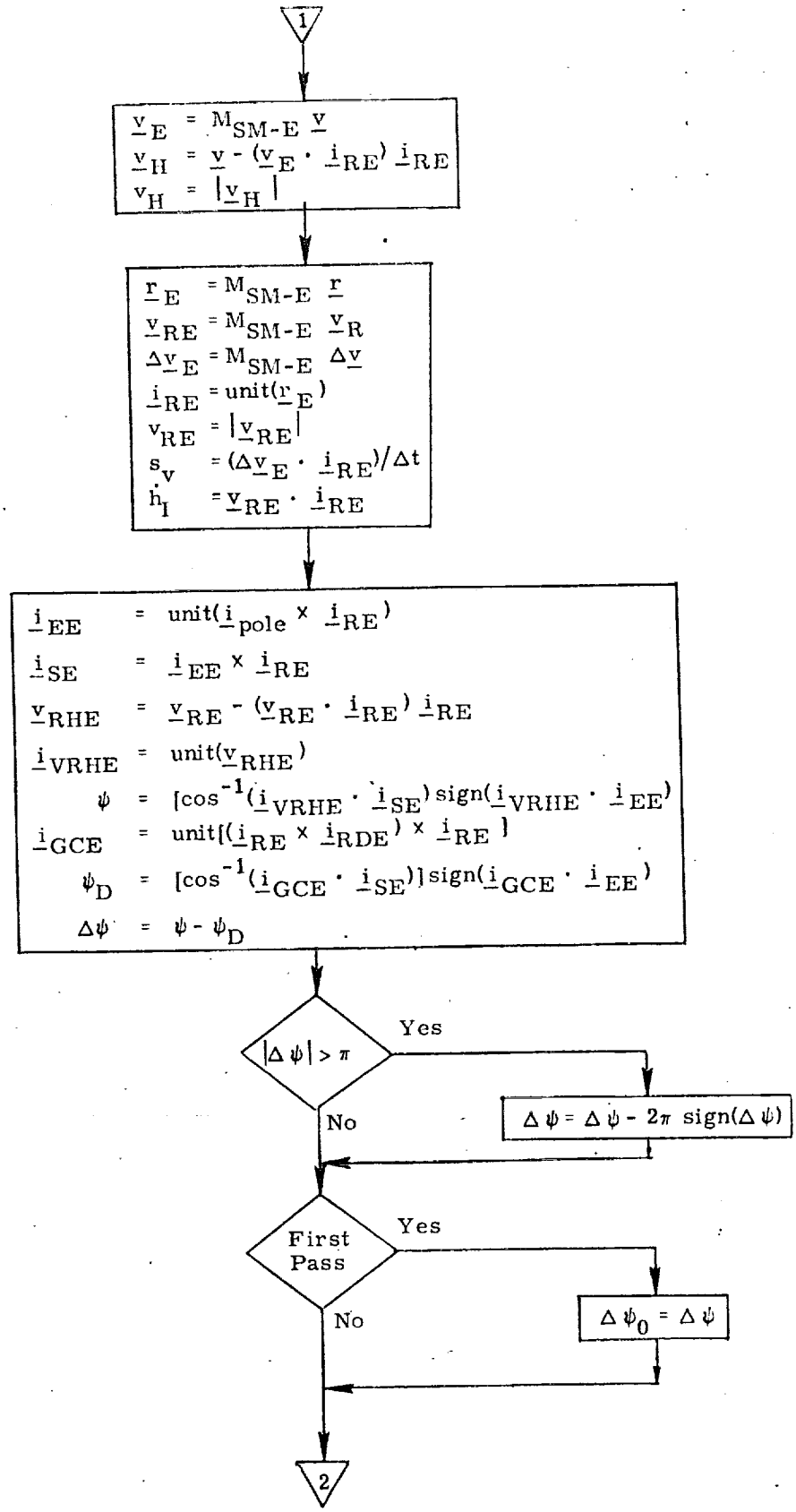


Figure 2b. Entry Guidance Routine, Detailed Flow Diagram

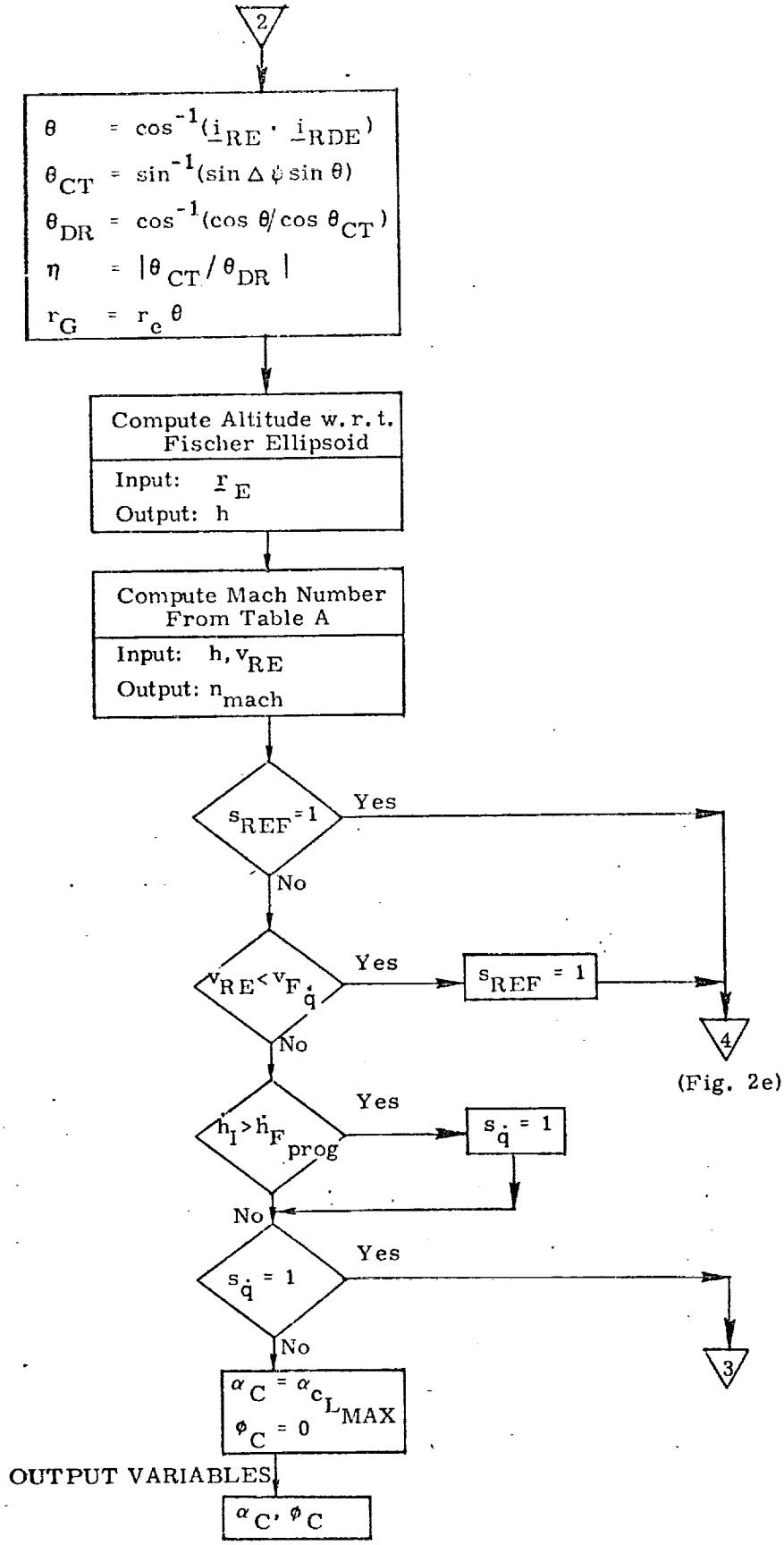


Figure 2c. Entry Guidance Routine, Detailed Flow Diagram

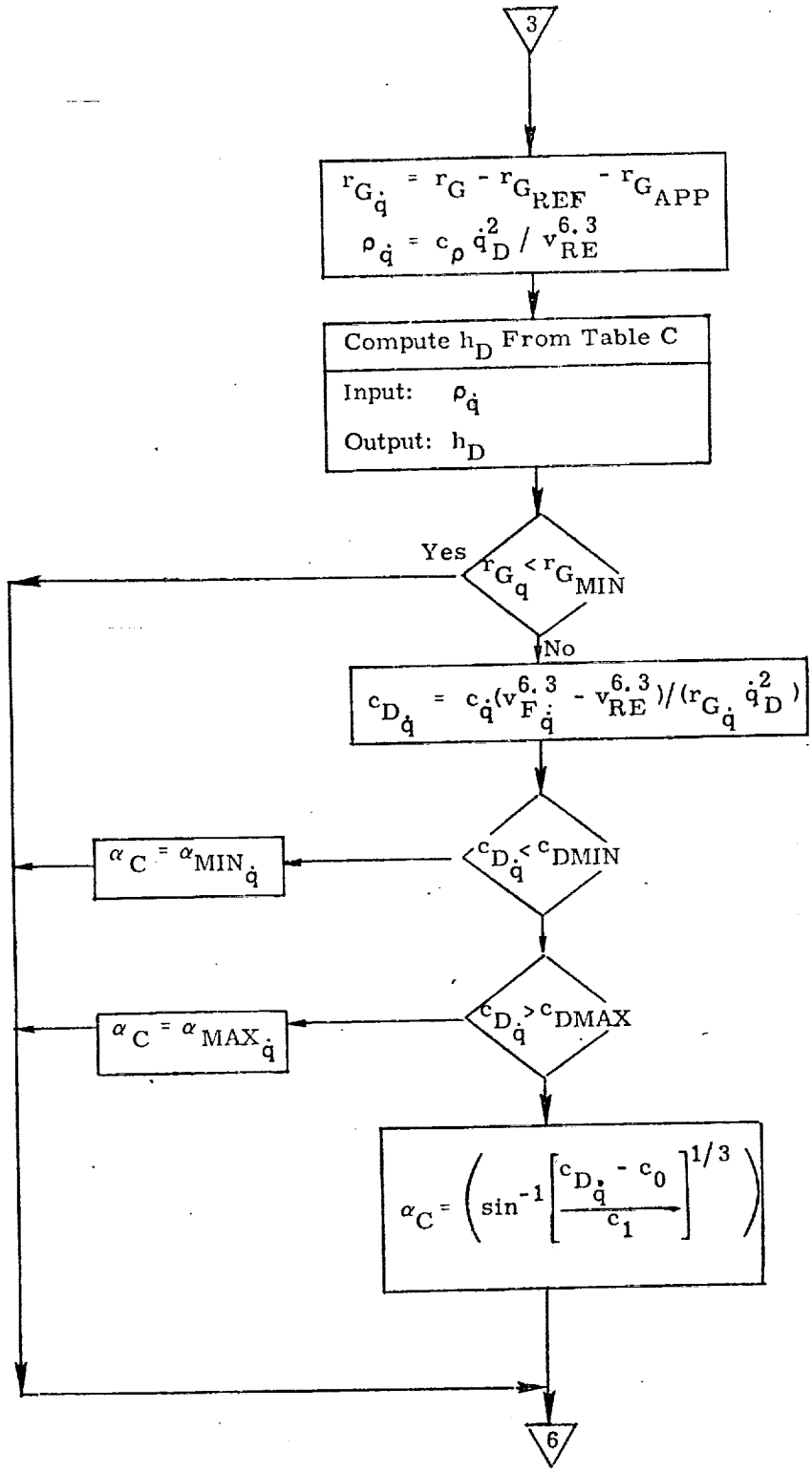


(Fig. 2g)

Figure 2d. Entry Guidance Routine, Detailed Flow Diagram

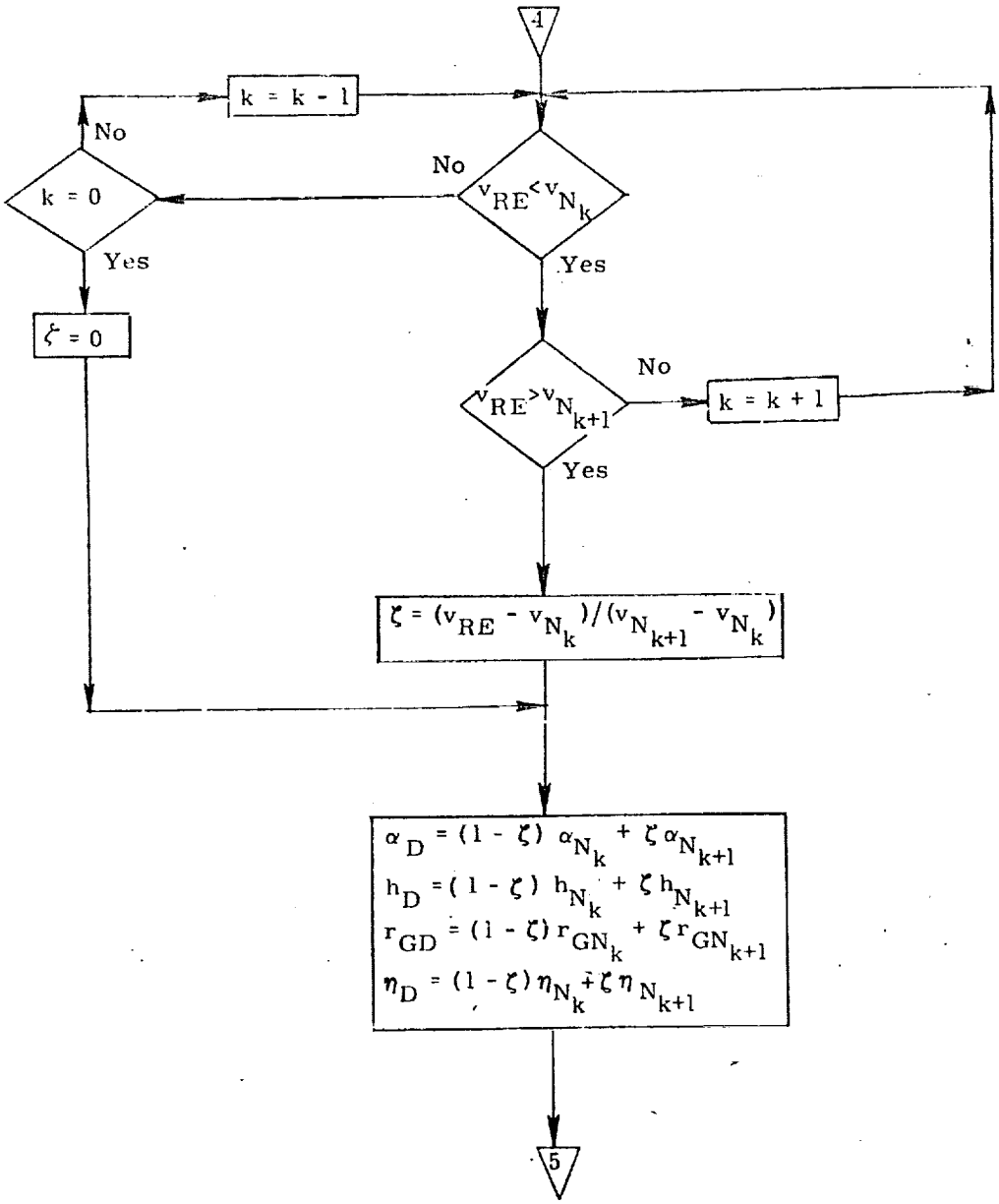


**Figure 2e.** Entry Guidance Routine, Detailed Flow Diagram

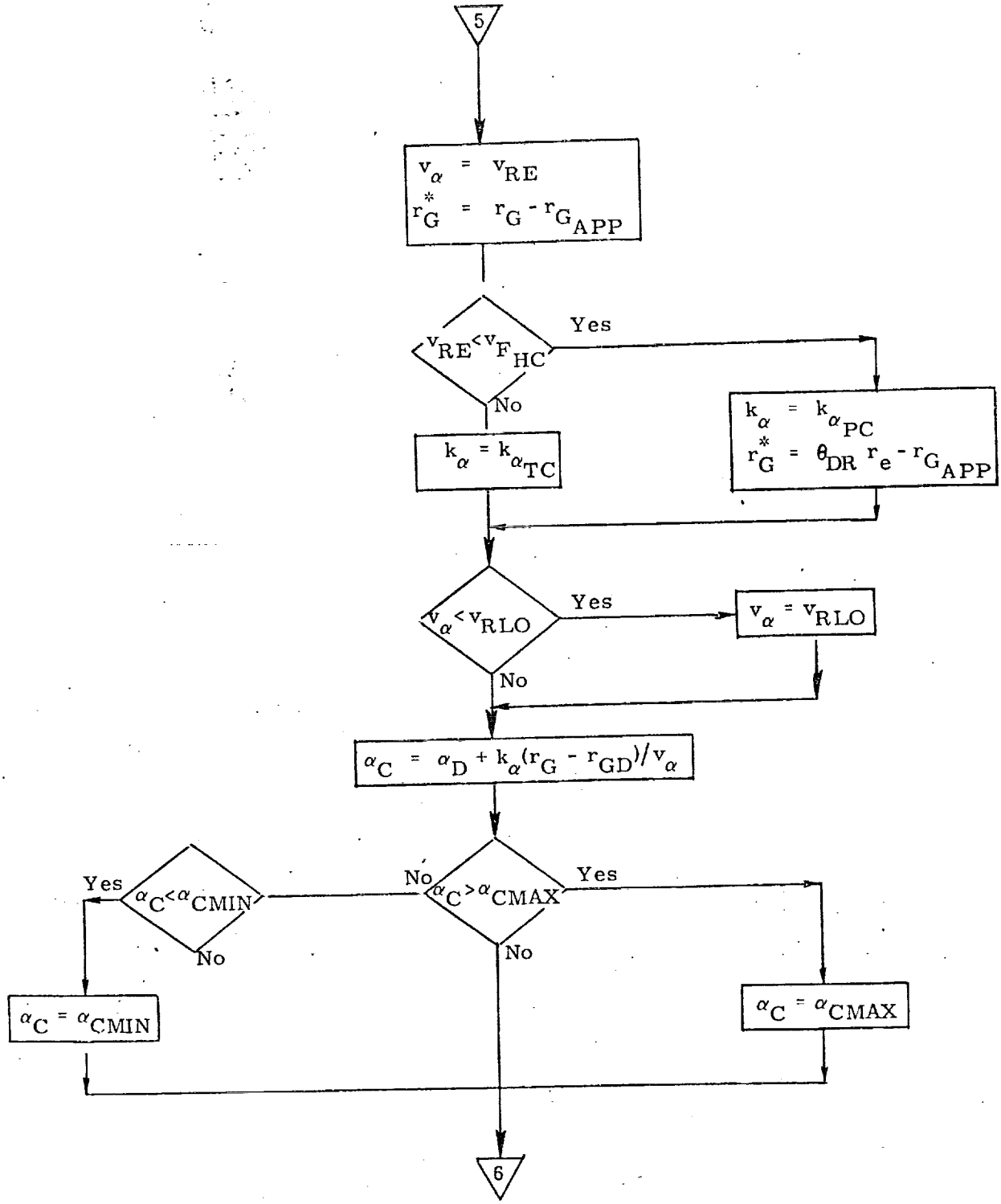


Figure 2f. Entry Guidance Routine, Detailed Flow Diagram

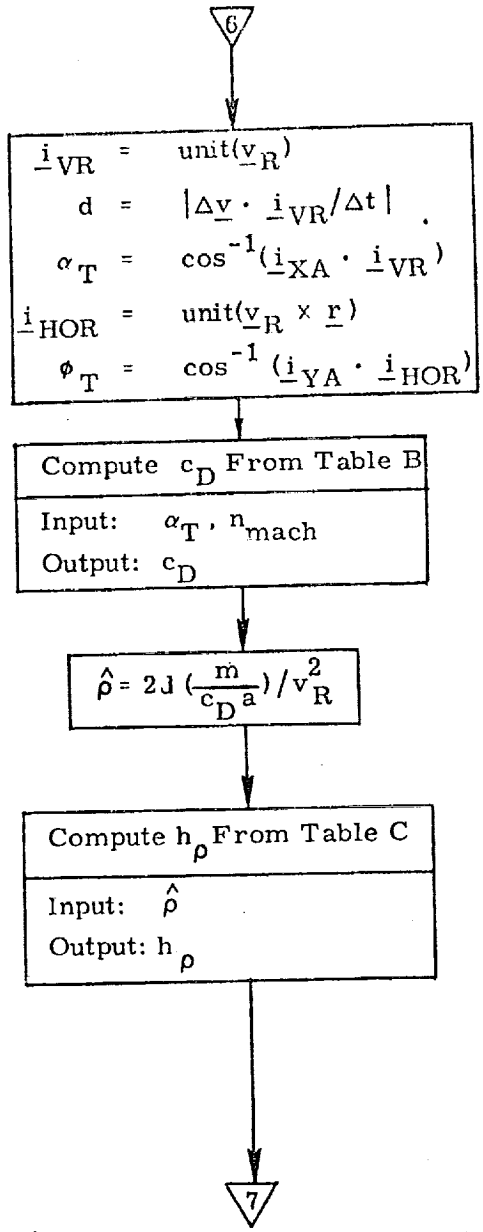


Figure 2g. Entry Guidance Routine, Detailed Flow Diagram

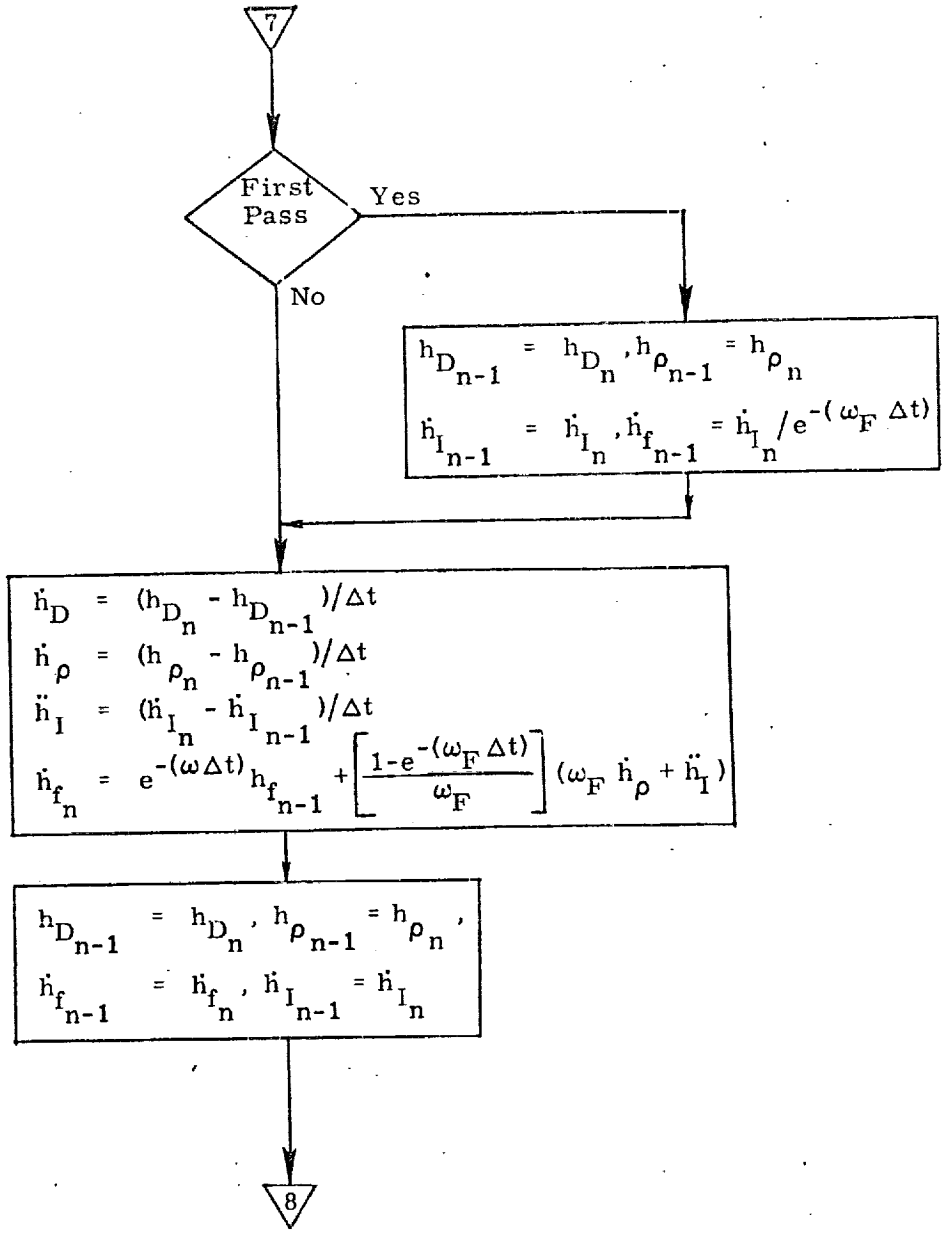


Figure 2h. Entry Guidance Routine, Detailed Flow Diagram

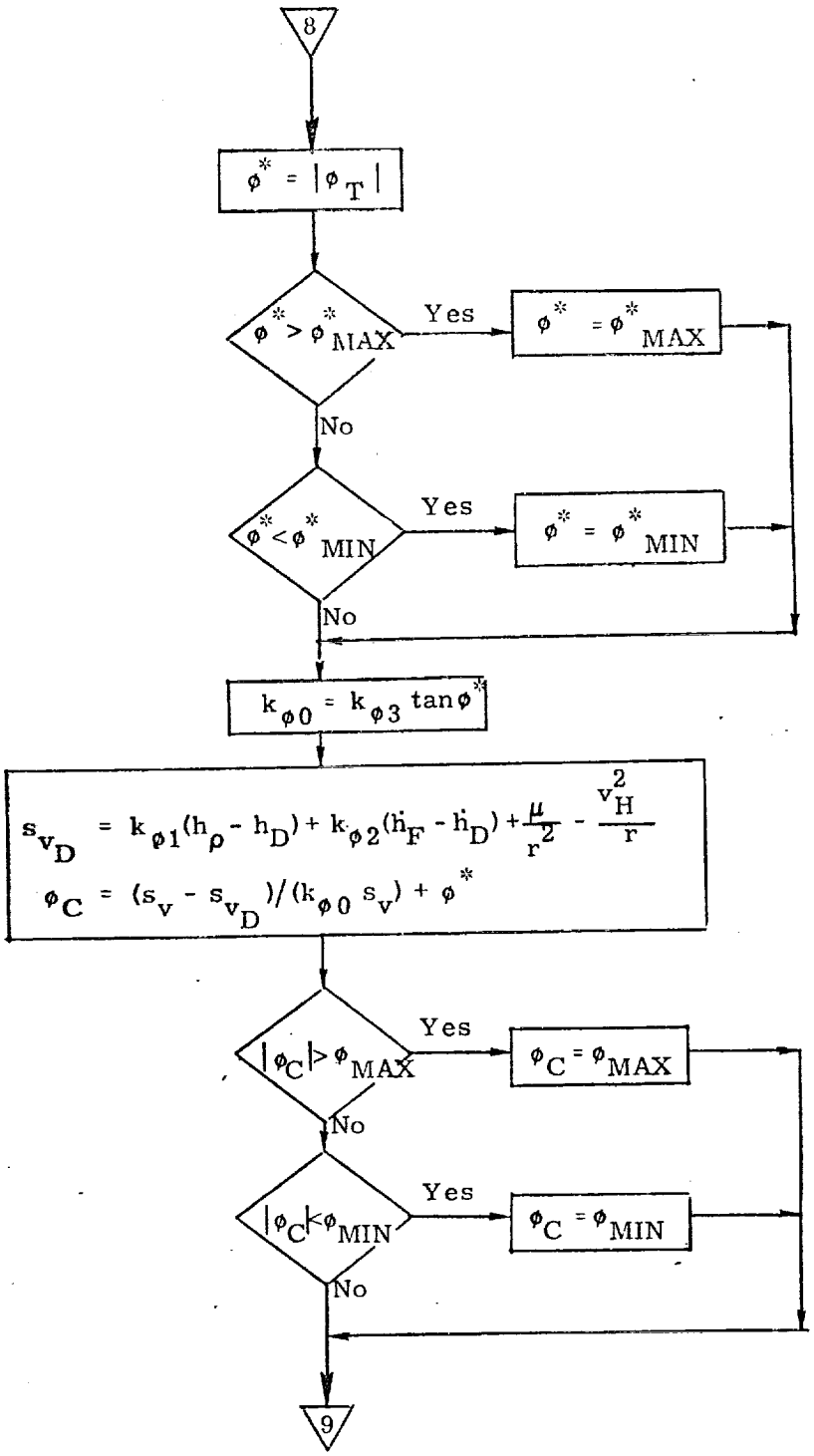


Figure 2i. Entry Guidance Routine, Detailed Flow Diagram

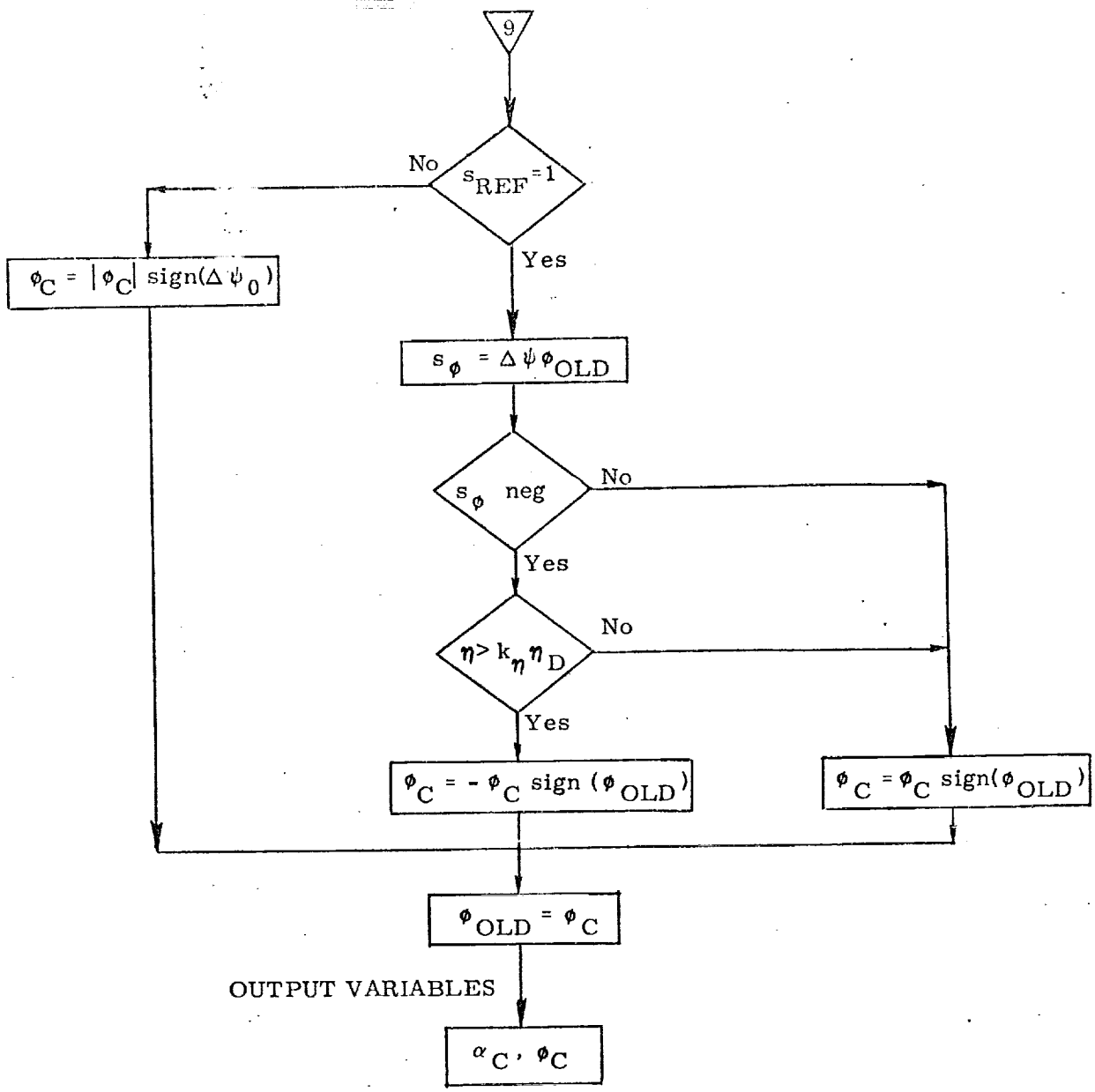


Figure 2j. Entry Guidance Routine, Detailed Flow Diagram

## REFERENCES


1. Marcus, F., "A Heat-Control Phase Guidance Law for Entry Based on a Density-vs. Speed Profile", MIT Draper Lab 23A STS Memo No. 16-72, March 17, 1972.

2. Kriegsman, B., "Entry Guidance System for Shuttle Orbiter", MIT Draper Lab 23A STS Memo No. 54-72, October 24, 1972.

3. Marcus, F., "A Simple Entry Guidance System for the Heat-Control Phase of Entry", MIT Draper Lab 23A STS Memo No. 7-72, January 28, 1972.

4. Kriegsman, B., "Shuttle Entry-Guidance System--- Design Rationale", MIT Draper Lab 23A STS Memo No. 56-72, November 7, 1972.

Submittal 59

# CLOSED FORM ENTRY GUIDANCE LOGIC FOR THE HIGH CROSS-RANGE ORBITER

## 1.0 SUMMARY

Entry guidance logic has been developed for the space shuttle which controls the entry trajectory by roll modulation while using a preselected angle of attack profile, which is a function of velocity. Range predictions are based upon an analytic solution to the equation of motion for equilibrium glide and constant load factor profiles. Inplane range errors are nulled by changing the magnitude of the roll angle and cross-range errors are nulled by roll reversals.

The basic guidance concept consists of three phases: a constant temperature phase, an equilibrium glide phase, and a constant load factor phase. The constant temperature phase is entered first and is designed to control the trajectory to a constant temperature profile until an inertial velocity of 25 000 fps is reached. At this point in the trajectory, the initial descent rate has been controlled and near equilibrium flight conditions exist. At this point, the equilibrium glide phase is entered and entry range predictions are intiated. These range predictions are based on an equilibrium glide trajectory until a load factor of 1.5g is reached, followed by a constant load factor trajectory of 1.5g until transition.

The roll angle during the equilibrium glide phase is selected to null the inplane range errors. When the resultant equilibrium glide trajectory intersects the constant g trajectory required to reach the target, control is transferred from the equilibrium glide phase to the constant g phase. At Mach 6, the entry guidance is terminated and control is transferred to the transition guidance.

## 2.0 INTRODUCTION

Analysis of entry trajectory shaping studies of the high cross-range orbiter has resulted in an understanding of the relationship between trajectory shaping and entry constraints and objectives (such as temperature limits, minimum TPS weight requirements, and load factor constraints). This analysis indicated that all know orbiter constraints and objectives could be met through proper entry targeting, and therefore, direct control of the trajectory to minimize constraint parameters is not necessary. This analysis also indicated that ranging could be accomplished early in the entry with negligible effect on the trajectory shape. In fact, indications are that delaying ranging until after the major aerodynamic heating has been passed could cause an impact on other constraints, such as load factor, later in the entry.

The analysis further indicated that several simple control modes can be used to satisfactorily control the orbiter trajectory. Analysis of these modes indicated that a combination equilibrium glide and constant g mode will not only produce a satisfactory trajectory but can also be used as a basis for closed-form guidance logic. This document presents an analytical guidance technique based on this concept. Roll angle is used to control inplane ranging and roll reversals are used to control cross range. The angle of attack profiles are predefined functions of velocity. Section 4 discusses the guidance concept and subsequent sections present a description of the guidance logic. Equation derivations, guidance flow charts, and a detailed description of the guidance logic are presented in the appendixes.

## 3.0 SYMBOLS

| | |
|---|---|
| $\bar{A}$ | vector pointing at target |
| $\bar{A}_T$ | $\bar{A}$ projected into EFT |
| $A_{TX}$, $A_{TY}$, $A_{TZ}$ | components of $\bar{A}_T$ |

| | |
|---|---|
| ALMN* | desired load factor for constant g range prediction |
| C1 | controller gain on drag term. |
| C2 | controller gain on $\dot{R}$ term |
| $C_D$* | drag coefficient |
| $C^{EFT}_{E}$ | transformation matrix from EFF to EFT frame |
| $C_{FNM}$* | conversion from feet to n. mi. |
| $C_{rnm}$* | conversion from radians to n. mi. |
| CTH | cos sine θ |
| D* | drag |
| $D_{cg}$ | desired drag level for constant g range prediction |
| $D_o$ | drag [illegible] required to reach target |
| $D_{ref}$* | drag reference |
| g* | gravity acceleration of earth |
| G2* | drag limit |
| H | altitude |
| $\dot{H}$ | altitude rate |
| HS* | atmospheric density altitude constant |
| $H_{up}$* | lift vector orientation flag ro preentry |

*These symbols appear in the guidance flow charts in appendix D

| | |
|---|---|
| IFT* | flar for first pass through range prediction |
| IG* | flag to transfer to constant g phase |
| ISTP* | flag to determine sequence in range prediction |
| K1O* | constant in $D_{ref}$ equation in constant heat rate |
| K2ROL* | roll direction indicator |
| L | lift force magnitude in the vertical plane |
| L/D | lift to drag ratio of the orbiter |
| $\frac{L}{D_V}$command | commanded L/D in the vertical plane |
| $\frac{L}{D_V}$ref | reference L/D in the vertical plane |
| LATSW* | flag to inhibit roll reversals through $180^\circ$ |
| LMN* | L/D command for $5^\circ$ deviation from lift vector up for cross-range control |
| LOD* | vehicle L/D |
| LOD1* | desired inplane L/D |
| m | vehicle mass |
| N | total load factor |
| $\dot{Q}$ | stagnation point heat rate |
| $\dot{Q}_c$* | commanded $\dot{Q}$ |
| R* | radius vector |

*These symbols appear in the guidance flow charts in appendix D

| | |
|---|---|
| $\dot{R}$* | altitude rate |
| $R_{CG}$* | predicted constant g range |
| REQ* | predicted equilibrium glide range |
| RPT* | predicted transition range |
| RT* | total range to target |
| RTD* | conversion from radians to degrees |
| RTG | total range to transition point |
| $\dot{R}_{ref}$* | reference $\dot{R}$ |
| Select* | flag to determine guidance phase |
| TPS | thermal protection system |
| $\overline{UR}$ | unit position vector |
| $\overline{UT}$ | unit target vector |
| V | velocity |
| $\dot{V}$ | time derivative of velocity |
| $V_{CG}$* | inertial velocity to enter constant g phase |
| $V_E$* | relative velocity |
| $V_{EI}$ | inertial velocity at entry interface |
| $V_I$* | inertial velocity |
| $V_Q$* | relative velocity to start transition |
| $V_{Q2}$* | inertial velocity to start transition |

*These symbols appear in the guidance flow charts in appendix D



C3

| | |
|---|---|
| $V_S$* | local satellite velocity |
| $V_{sat}$ | local satellite velocity |
| VSW* | velocity to start range prediction |
| $V_{XX}$* | velocity to start transition $\alpha$ modulation |
| $X_E$, $Y_E$, $Z_E$ | earth fixed frame (EFF) |
| $X_T$, $Y_T$, $Z_T$ | earth fixed topocentric frame (EFT) |
| $w_e$* | earth rotation rate |
| WT* | vehicle weight |
| Y* | lateral deadband switch point |
| $\alpha$ | angle of attack |
| $\alpha_c$* | angle of attack command |
| $\gamma$ | flight-path angle |
| $\dot{\gamma}$ | time derivative of $\gamma$ |
| $\gamma_{EI}$ | inertial flight-path angle at entry interface |
| $\theta$ | central angle to target |

*These symbols appear in the guidance flow charts in appendix D

| | |
|---|---|
| $\pi$* | pi |
| $\rho$ | density |
| $\rho_o$* | density at sea level |
| $\rho_s$ | density at sea level |
| $\phi$ | roll angle |
| $\phi_c$* | roll angle command |
| $\psi$* | relative azimuth |
| $\psi_T$* | relative azimuth to target |
| O5GSW* | flag to begin guidance |

*These symbols appear in the guidance flow charts in appendix D

## 4.0 GUIDANCE CONCEPT

The entry guidance must keep peak acceleration levels, maximum temperatures, and heat loads within limits while maintaining ranging capability. The guidance must operate over a wide range of initial conditions and vehicle lift to drag ratios with a minimum of changes to the guidance software. The guidance must also be insensitive to navigation system errors. One means of accomplishing this is to develop a set of analytic trajectory prediction equations based on a flight profile that satisfies the objectives previously mentioned. Trajectory shaping studies showed that two control modes can be combined to satisfy the trajectory limits and objectives, and would also be amenable to analytic solutions of trajectory parameters for constant and near optimum angle of attack profiles. These modes are equilibrium glide and constant g. This document presents the guidance logic for both a constant and a near optimum variable angle of attack profile. A detailed description of the guidance logic can be found in section 5.0, however, a brief overview of the guidance concept follows.

From 0.05g to an inertial velocity of 25 000 fps, the guidance controls the trajectory to a constant temperature profile. This profile controls the initial descent rate and stabilizes the trajectory prior to initiating ranging at an inertial velocity of 25 000 fps. Between an inertial velocity of 25 000 fps and a load factor of 1.5g, the entry trajectory is controlled to an equilibrium glide flight mode. During this phase the roll angle for equilibrium flight is analytically computed to satisfy the entry ranging requirements. The resultant equilibrium glide trajectory is maintained from the point in the trajectory where the equilibrium glide drag level is greater than the constant heat rate drag level (point 1 in fig. 1) to the point in the trajectory where the constant drag level required to reach the target is equal to the drag level resulting from the equilibrium glide trajectory (point 2 in fig. 1). From this point until transition, the guidance commands the roll angle required to maintain the constant g level required to reach the target. At Mach 6, the guidance transfers to the transition guidance mode.

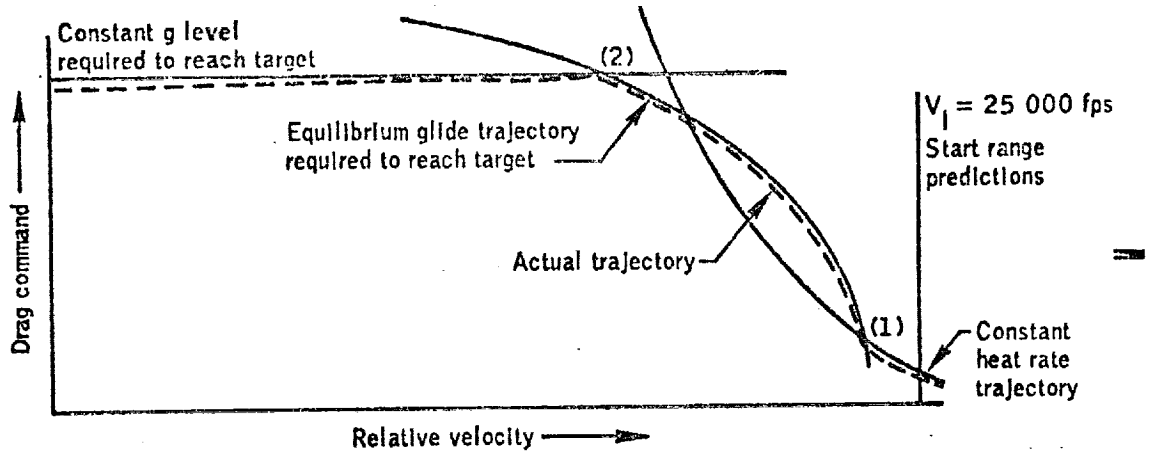


**Figure 1.- Guidance concept for the high cross-range orbiter.**

## 5.0 GUIDANCE LOGIC DESCRIPTION

The basic guidance logic must perform three primary functions, these are trajectory parameter prediction, targeting, and attitude command generation. The guidance first performs trajectory and range predictions and then the controller converts these data into attitude commands which are provided to the autopilot for execution. An analytic reference trajectory is recomputed each computer cycle to correct for range errors. Based on this recomputed reference trajectory, a reference lift to drag ratio (L/D), drag level, and altitude rate are analytically computed and provided to the controller.

The total guidance logic can be divided into four major phases as depicted in figure 2. These phases are preentry, constant heat rate, equilibrium glide ranging, and constant g ranging. Several service routines are used during each phase such as targeting, lateral logic, roll command, and controller. The major phases are described in sections 5.1 through 5.4, and the service routines are described in section 5.5. A complete derivation of the range prediction equations and math flow is presented in the appendixes.

## 5.1 Preentry Phase

The primary activity of the preentry phase is the computation of the attitude hold commands prior to the atmospheric entry and the beginning of the computation of the entry targeting data. This computation defines a total range to target (RT) and the current heading to target $\psi_T$. The equations used for targeting are discussed in section 5.5.2. Until 0.05g, the spacecraft will be in a three axis attitude hold mode. At 0.05g, rate damping will be initiated and the guidance will transfer to the constant heat rate phase.

## 5.2 Constant Heat Rate Phase

During the constant heat rate phase a stable trajectory is established at an acceptable temperature prior to the initiation of ranging. A roll command is generated which will control the spacecraft along a desired constant temperature profile through pullout ($\dot{\gamma} = 0$). This phase is required to stabilize the trajectory prior to entering the equilibrium glide phase. The equilibrium glide ranging phase is entered after pullout at an inertial velocity of 25 000 fps. Appendix A presents the derivation of the guidance equations for the constant heat rate phase.

## 5.3 Equilibrium Glide Ranging Phase

At an inertial velocity of 25 000 fps, the guidance enters the equilibrium glide ranging phase. During this phase entry range predictions and reference trajectory parameters are computed which are required by the trajectory controller to eliminate range errors. However, trajectory control is not transferred to the equilibrium glide mode until the drag command from the reference equilibrium glide profile is greater than the drag command from the constant heat rate phase. This control mode transfer prevents a discontinuity in the total drag reference trajectory, thus eliminating an undesirable transient in the trajectory.

Closed form solutions of the equations of motion are used to predict the entry range and the reference trajectory parameters. These parameters are based upon an equilibrium glide flight at constant bank angle. If the equilibrium glide profile is flown at low speeds, higher than desired load factors may result; therefore, the trajectory profile is based upon a constant load factor starting when the load factor reaches 1.5g. The range prediction is accomplished by analytically

predicting the inertial velocity at which the equilibrium glide trajectory will reach a total load factor of 1.5g ($V_{CG}$), and then analytically predicting the range from the current orbiter velocity to $V_{CG}$ based upon an equilibrium glide trajectory, and analytically predicting the range from $V_{CG}$ to transition by assuming a constant 1.5g trajectory. The equilibrium glide roll angle is selected to make the resultant range prediction equal to the current range to the target.

Once the desired equilibrium glide roll angle has been determined, a reference trajectory is analytically computed and a reference vertical L/D, a drag reference, and an altitude rate reference is computed and sent to the controller. The controller then computes a vertical L/D command based upon the difference between the reference drag and altitude rate commands and the actual trajectory drag and altitude rate. This vertical L/D command is converted into a roll command in the ROLL COMMAND service routine (section 5.5.4).

A new equilibrium glide roll angle is computed each pass through the guidance logic until the constant g ranging phase is entered. In addition to the equilibrium glide and constant g reference trajectory, a constant g reference profile is analytically computed based on the constant g level required to reach the target from the current spacecraft velocity. This constant g level is compared to the g reference level from the equilibrium glide trajectory. When the equilibrium glide drag reference is greater than the constant g reference profile required to reach the target, the equilibrium glide phase is terminated and control is transferred to the constant g ranging phase. Appendixes B and C present the derivation of the equations used in the equilibrium glide ranging phase.

## 5.4 Constant g Ranging Phase

The constant g phase predicts the constant g level required to reach the target and then computes the reference parameters required by the controller to fly the desired constant g profile. The range prediction is based on an analytic solution of the equations of motion which predicts the range flown from the current velocity to transition (assumed to start at Mach 6). The L/D reference, the desired drag reference, and the altitude rate reference is computed and sent to the controller. The constant g phase is terminated at the velocity for beginning transition. Appendix D presents the derivation of the equations used in this phase.

## 5.5 Service Routines

Four service routines are used by the guidance system: controller, targeting, lateral logic, and roll command.

5.5.1 Controller.- The controller generates an L/D command in the vertical plane based upon the reference L/D, the reference drag level, and the reference altitude rate computed in the guidance phases previously described. The basic controller equation is defined as follows.

$$\frac{L}{D_V}\text{command} = \frac{L}{D_V}\text{ref} + C1(D - D_{ref}) + C2(\dot{R} - \dot{R}_{ref}) \qquad (1)$$

The constants C1 and C2 vary depending on the particular guidance phase.

5.5.2 Targeting.- The targeting program computes the total range to target, the spacecraft heading to target, and the initial roll direction. These computations are made in the earth relative coordinate system. The total range is computed as the great circle range between the present vehicle position and the target position. As shown in appendix E, the current heading to target $\psi_T$ is computed based upon the current position and the target position. Knowing the heading to target, the initial roll direction is chosen to reduce the angle between the present heading and the heading to the target.

5.5.3 Lateral logic.- The lateral logic consists of a lateral deadband about the spacecraft heading. When the magnitude of the difference between the spacecraft heading and the heading to the target exceeds the lateral deadband and the roll direction is such that this difference will increase, the guidance commands a roll reversal. The azimuth deadband method of cross-range control was chosen because a cross-range deadband technique will cause a high L/D vehicle to spiral above Mach 1. Direct control of azimuth eliminates the spiral. For vehicles with a low roll response, it may be necessary to prevent a roll through negative lift at high g levels. This capability has been included in the guidance logic as presented in appendixes E and F.

5.5.4 Roll and alpha command.- The roll and alpha command subroutine generates angle of attack and roll commands for the autopilot. This subroutine also converts the vertical L/D command from the controller into a roll command. The direction of the roll command is determined by the lateral logic.

## 6.0 CONCLUSIONS

An entry guidance logic for preselected angle of attack trajectories has been developed and initial studies using this guidance demonstrate excellent performance. This guidance logic combines control of load factor and temperature with ranging by means of an analytically computed reference trajectory. Analysis of this guidance concept has indicated the following:

a. Closed loop ranging can be provided by an analytical guidance logic while implicitly controlling temperatures and load factor.

b. The guidance system affords at appropriate times close control of all critical constraints (i.e., temperatures, load factor, and heat load).

c. The closed form range predictions afford fast computational capability which is desirable for an onboard guidance system.

d. Preliminary navigation error analysis indicates that this system is sensitive to navigation system errors.

## APPENDIX A - CONSTANT HEAT RATE PHASE

The constant heat rate phase computes a reference trajectory which is used until the ranging solution from the equilibrium glide and constant g phases is valid. The purpose of the constant heat rate phase is to stabilize the trajectory at a constant temperature during the initial entry into the atmosphere prior to the initiation of ranging which begins at an inertial velocity of 25 000 fps. This reference trajectory consists of a vertical L/D reference, a drag level reference, and an altitude rate reference. These reference trajectory parameters are used by the controller during the constant heat rate phase.

Stagnation point heat rate for a 1-foot radius sphere is defined as

$$\dot{Q} = 17\ 600\sqrt{\frac{\rho}{\rho_o}}\left(\frac{V_E}{26\ 000}\right)^{3.15} \tag{A1}$$

Specific aerodynamic drag is along the negative velocity vector with the magnitude computed as follows:

$$D = \frac{\rho V_E C_D S}{2m} \tag{A2}$$

Solving (A1) for $\rho$

$$\rho = \frac{\dot{Q}^2 \rho_o}{(17\ 600)^2 (V_E/26\ 000)^{3.15}} \tag{A3}$$

Substituting (A3) into (A2) gives

$$D = D_{ref} = \frac{26\ 000^{6.3} \rho_o C_D S \dot{Q}^2}{(2 \times 17\ 600^2) m V_E^{4.3}} \tag{A4}$$

Equation (A4) provides an expression for constant heat rate in terms of a reference drag force. The reference drag is used in the controller. The altitude rate reference term used by the controller can be derived as follows:

Assume $\rho = \rho e^{-H/HS}$

$$\dot{\rho} = \frac{\partial \rho}{\partial H}\frac{\partial H}{\partial t} = \left(-\frac{1}{HS}\right)\rho_S e^{-\frac{H}{HS}}(\dot{H}) = -\frac{\dot{H}}{HS}\rho = -\frac{\dot{R}}{HS}\rho \tag{A5}$$

$$D = \frac{\rho V_E{}^2 C_D S}{2m}$$

$$\rho = \frac{2mD}{V_E{}^2 C_D S}$$

Then taking the derivative assuming that $C_D$ is a constant gives

$$\dot{\rho} = -\frac{4mD\dot{V}}{V_E{}^3 C_D S} + \frac{2m\dot{D}}{V_E{}^2 C_D S} \tag{A6}$$

$$\dot{\rho} = -\frac{2\rho\dot{V}}{V_E} + \frac{\rho\dot{D}}{D}$$

$$\frac{\dot{\rho}}{\rho} = -\frac{2\dot{V}}{V_E} + \frac{\dot{D}}{D}$$

Since $\dot{V} = -D$

$$\frac{\dot{\rho}}{\rho} = \frac{2D}{V_E} + \frac{\dot{D}}{D}$$

Since $\dot{R} = -\frac{\dot{\rho}}{\rho}HS$

$$\dot{R} = -HS\left(\frac{2D}{V_E} + \frac{\dot{D}}{D}\right) \tag{A7}$$

$$\dot{R}_{ref} = -HS\left(\frac{2D_{ref}}{V_E} + \frac{\dot{D}_{ref}}{D_{ref}}\right) \tag{A8}$$

Equation (A4) gave

$$D_{ref} = \frac{26\ 000^{4.3}\rho_o C_D S\dot{Q}^2}{(2 \times 17\ 600^2)mV_E^{4.3}} = K10V_E^{-4.3} \tag{A9}$$

where

$$K10 = \frac{26\ 000^{6.3}\rho_o C_D S\dot{Q}^2}{(2 \times 17\ 600^2)m} \tag{A10}$$

$$\dot{D}_{ref} = \frac{\partial D_{ref}}{\partial V}\frac{\partial V}{\partial t}$$

$$\dot{D}_{ref} = -4.3K10V_E^{-5.3}\dot{V}$$

$$\dot{D}_{ref} = 4.3K10V_E^{-5.3}D_{ref} = \frac{4.3D_{ref}^2}{V_E} \tag{A11}$$

Substituting (A4) and (A11) into (A8) gives

$$\dot{R}_{ref} = -HS\left(\frac{2D_{ref}}{V_E} + \frac{\dot{D}_{ref}}{D_{ref}}\right)$$

$$= -HS\left(\frac{2D_{ref}}{V_E} + \frac{4.3D_{ref}}{V_E}\right)$$

$$\dot{R}_{ref} = -6.3HS\frac{D_{ref}}{V_E} \tag{A12}$$

The nominal L/D required to fly the desired profile, $\frac{L}{D}_{reference}$, is derived in the following manner:

$$V\dot{\gamma} = \frac{V_I^2 \cos\gamma}{R} + L - g\cos\gamma$$

or

$$V\dot{\gamma} = \frac{V_I^2 \cos \gamma}{R} + \left(\frac{L}{D_V}\right)D - g \cos \gamma$$

therefore,

$$\frac{L}{D_V} = \left(g \cos \gamma - \frac{V_I^2 \cos \gamma}{R} + V\dot{\gamma}\right)/D \tag{A13}$$

Assume $\cos \gamma = 1$, $Rg = V_{sat}{}^2$

$$\frac{L}{D_V} = \frac{g}{D}\left(1 - \frac{V_I^2}{V_{sat}{}^2}\right) + \frac{V\dot{\gamma}}{D} \tag{A14}$$

Since

$$\dot{h} = V \sin \gamma \approx V\gamma$$

$$\ddot{h} = V\dot{\gamma} + \dot{V}\gamma$$

$$V\dot{\gamma} = \ddot{h} - \dot{V}\gamma \tag{A15}$$

for constant heat rate

$$\dot{h} = -6.3HS\frac{D}{V}$$

$$\ddot{h} = -6.3HS\left(\frac{V\dot{D} - D\dot{V}}{V^2}\right)$$

therefore

$$V\dot{\gamma} = -6.3HS\left(\frac{\dot{D}}{V} - \frac{D\dot{V}}{V^2}\right) - \dot{V}\gamma \tag{A16}$$

Since $\gamma = \frac{\dot{h}}{V}$

$$\dot{V}\gamma = \frac{\dot{h}\dot{V}}{V} = \left(-6.3HS\frac{D}{V}\right)\left(-\frac{D}{V}\right) = 6.3HS\frac{D^2}{V^2} \tag{A17}$$

Combining (A16) and (A17) gives

$$V\dot{\gamma} = -6.3HS\left(\frac{\dot{D}}{V} + 2\frac{D^2}{V^2}\right) \tag{A18}$$

Therefore

$$\frac{L}{D_V} = \frac{g}{D}\left(1 - \frac{V_I^2}{V_{sat^2}}\right) - 6.3\frac{HS}{D}\left(\frac{\dot{D}}{V} + 2\frac{D^2}{V^2}\right) \tag{A19}$$

However, since $\dot{D} = 4.3\frac{D^2}{V}$ for constant heat rate

$$\frac{L}{D_V} = \frac{g}{D}\left(1 - \frac{V_I^2}{V_{sat}{}^2}\right) - 6.3\frac{HS}{D}\left(4.3\frac{D^2}{V^2} + 2\frac{D^2}{V^2}\right) \tag{A20}$$

or

$$\frac{L}{D_V} = \frac{g}{D}\left(1 - \frac{V_I^2}{V_{sat^2}}\right) - 39.69HS\frac{D}{V^2} \tag{A21}$$

Therefore

$$\frac{L}{D_V}{}_{ref} = \frac{g}{D_{ref}}\left(1 - \frac{V_I^2}{V_{sat^2}}\right) - 39.69HS\frac{D_{ref}}{V^2} \tag{A22}$$

Evaluating the second term in the $\frac{L}{D_{ref}}$ equation for the constant angle of attack case produces a maximum change in $\frac{L}{D_V}$ of 0.0097 units and for the variable angle of attack case 0.0216 units. Since this term is negligible

$$\left(\frac{L}{D}\right)_{V_{ref}} = \frac{g}{D_{ref}}\left(1 - \frac{V_I^2}{V_{sat}^2}\right) \tag{A23}$$

Equations (A4), (A12), and (A23) provide the D reference, $\dot{R}$ reference, and L/D reference that are required by the controller to maintain a constant heat rate trajectory. Figure A-1 shows a time history of the commanded and actual heat rate during the constant heat rate phase.

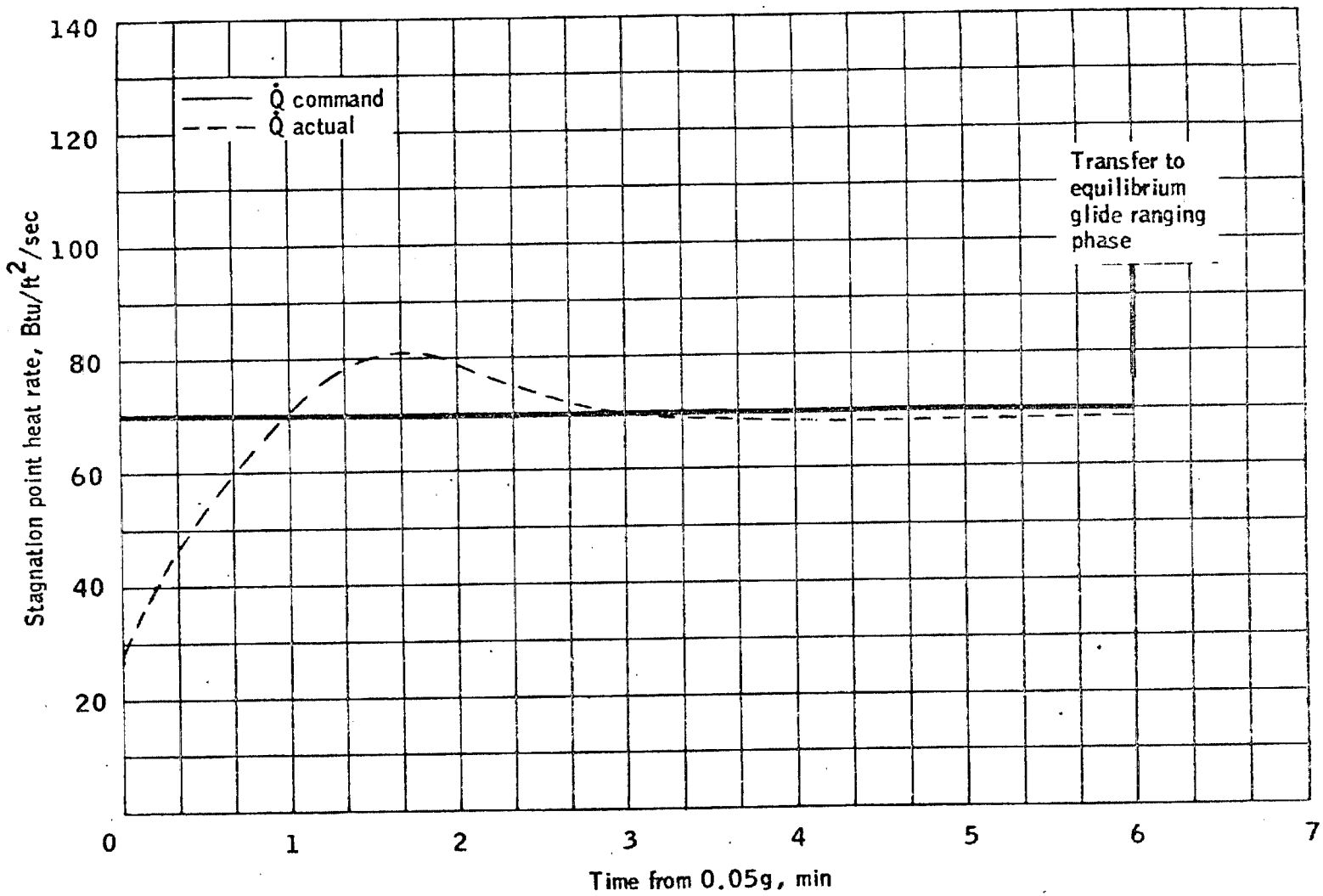


Figure A1.- Comparison of commanded and actual heat rate, $\dot{Q}$.

## APPENDIX B - EQUILIBRIUM GLIDE PHASE FOR A CONSTANT ANGLE OF ATTACK

The purpose of the equilibrium glide phase is to predict the range capability of the spacecraft and to compute a reference trajectory which will terminate at the target point. This is accomplished by predicting analytically the range flown from the current orbiter velocity to the velocity at which a load factor of 1.5g is reached. Then the resultant range for a constant 1.5g trajectory is predicted in the remainder of the entry. The initial range prediction assumes an equilibrium glide trajectory with a roll angle selected to correct for range errors. Once the equilibrium roll angle has been predicted that will satisfy the range requirements, a reference drag trajectory is commanded that will correspond to the desired equilibrium glide trajectory.

The basic equilibrium glide equation is

$$V\dot{\gamma} = \frac{V_I^2 \cos \gamma}{R} + L - g \cos \gamma \tag{B1}$$

For equilibrium glide, $\dot{\gamma} = 0$; therefore

$$0 = \frac{V_I^2 \cos \gamma}{R} + L - g \cos \gamma$$

Assuming $\cos \gamma = 1$, equation (B1) reduces to

$$0 = g\left(\frac{V_I^2}{Rg} - 1\right) + L \tag{B2}$$

Since $Rg = V_{sat}{}^2$, this equation reduces further to

$$0 = g\left(\frac{V_I^2}{V_{sat}{}^2} - 1\right) + \left(\frac{L}{D_V}\right) D \tag{B3}$$

Solving for D gives

$$D = \frac{g}{\frac{L}{D_V}}\left(1 - \frac{V_I^2}{V_{sat}^2}\right) \tag{B4}$$

Since L/D in the vertical plane = L/D × cos $\phi$, equation (B4) becomes

$$D = \frac{g}{\frac{L}{D}\cos\phi}\left(1 - \frac{V_I^2}{V_{sat}^2}\right) \tag{B5}$$

Using equation (B5), it is possible to predict the range that will be flown during the equilibrium glide phase by means of the following equations.

Assume that the equilibrium glide trajectory will be based on a constant roll angle, $\phi$, and will be flown to the inertial velocity at which the predicted trajectory reaches 1.5g ($V_{CG}$). $V_{CG}$ can be predicted by solving for $V_I$ in equation (B5).

$$V_{CG} = \sqrt{V_{sat}^2 - \frac{D_{cg} V_{sat}^2 \frac{L}{D}\cos\phi}{g}} \tag{B6}$$

Where $D_{cg}$ is the drag along the velocity vector equivalent to 1.5g

$$D_{cg} = \frac{1.5g}{\sqrt{1 + (L/D)^2}} \tag{B7}$$

Equation (B6) is valid for all equilibrium glide roll angles that result in trajectories that reach 1.5g. However, trajectories based on small equilibrium glide roll angles do not obtain 1.5g. For this class of trajectories, the guidance can determine this by checking for a negative square root in equation (B6). When this occurs, the guidance must assume that the constant g phase is eliminated and the equilibrium glide trajectory required to reach the target is flown all the way to transition at Mach 6.

The range flown during the equilibrium glide phase can be predicted by the following equations:

$$\frac{\partial R}{\partial V} = \frac{\partial R}{\partial T}\frac{\partial T}{\partial V} = -\frac{V}{D} = -\frac{V_I}{D_{ref}} \tag{B8}$$

Using equation (B8)

$$\frac{\partial R}{\partial V} = \frac{\frac{L}{D}\cos\phi\, V_{sat}^{\,2}}{g}\left(\frac{V_I}{V_I^2 - V_{sat}^{\,2}}\right) \tag{B9}$$

$$R = \frac{(L/D)\cos\phi\, V_{sat}^{\,2}}{g}\int_{V_I}^{V_{CG}} \frac{V_I}{V_I^2 - V_{sat}^{\,2}}\, dV \tag{B10}$$

Integrating equation (B10)

$$R = \frac{(L/D)\cos\phi\, V_{sat}^{\,2}}{2g}\, LN\left(\frac{V_{CG}^{\,2} - V_{sat}^{\,2}}{V_I^2 - V_{sat}^{\,2}}\right) = R_{EQ} \tag{B11}$$

The range from $V_{CG}$ to transition can be analytically predicted by the equations

$$\frac{\partial R}{\partial V} = \frac{\partial R}{\partial T}\frac{\partial T}{\partial V} = -\frac{V}{D} = -\frac{V_I}{D_{cg}} \tag{B12}$$

$$R = -\frac{1}{D_{cg}}\int_{V_{CG}}^{V_{TRAN}} V\, dV = \frac{V_{CG}^{\,2} - V_{TRAN}^{\,2}}{2D_{cg}} \tag{B13}$$

Therefore equations (B11) and (B13) represent the total predicted range for the entry from the current orbiter velocity to transition.

$$R_P = R_{EQ} + R_{CG} \quad . \tag{B14}$$

A comparison between $R_P$ and the actual range to the target (assumed to be the transition point) will produce a range error which can be nulled by changing $\phi$, the equilibrium glide roll angle. Figure B-1 presents the range correction capability as a function of the equilibrium glide roll angle. This figure shows that for an equilibrium glide roll angle below 43.5°, the equilibrium glide trajectory will not intersect 1.5g. Thus for targets that require these roll angles, an equilibrium glide trajectory will be flown throughout entry. This figure also shows that for large equilibrium glide roll angles (to the right of the line marked $V_{CG}$ greater than $V_I$ in fig. B-1), the desired equilibrium glide roll angle will intersect 1.5g prior to the current velocity. So for these cases, the guidance will immediately transfer into the constant g ranging phase whenever $V_{CG}$ is computed to be greater than $V_I$.

Once the equilibrium glide roll angle has been determined, the controller reference parameters must be computed in order to fly the desired equilibrium glide trajectory. The controller requires a L/D reference, a drag reference, and an altitude rate reference. The drag reference term is simply equation (B5).

$$D_{ref} = \frac{g}{\frac{L}{D}\cos\phi}\left(1 - \frac{V_I^2}{V_{sat}^2}\right)$$

The L/D reference term is simply

$$\frac{L}{D_V}\text{ref} = \frac{L}{D}\cos\phi \tag{B15}$$

where $\frac{L}{D}\cos\phi$ is the inplane $\frac{L}{D}$ required to reach the target.

The altitude rate reference can be derived as follows:

From equation (A8)

$$\dot{R}_{ref} = -HS\left(\frac{2D_{ref}}{V_E} + \frac{\dot{D}_{ref}}{D_{ref}}\right)$$

$$D_{ref} = \frac{R}{\frac{L}{D} \cos \phi} \left(1 - \frac{V_I^2}{V_{sat}^2}\right)$$

Taking the derivative of $D_{ref}$

$$\dot{D}_{ref} = \frac{2g\, D_{ref} V_I}{\frac{L}{D} \cos \phi\, V_{sat}^2} \tag{B16}$$

Combining equation (A8) with equations (B5) and (B16) gives

$$\dot{R}_{ref} = - \frac{2gHS}{\frac{L}{D} \cos \phi} \left[ \frac{\left(1 - \frac{V_I^2}{V_{sat}^2}\right)}{V_E} + \frac{V_I}{V_{sat}^2} \right] \tag{B17}$$

Equations (B5), (B15) and (B17) are sufficient to establish an equilibrium glide trajectory.

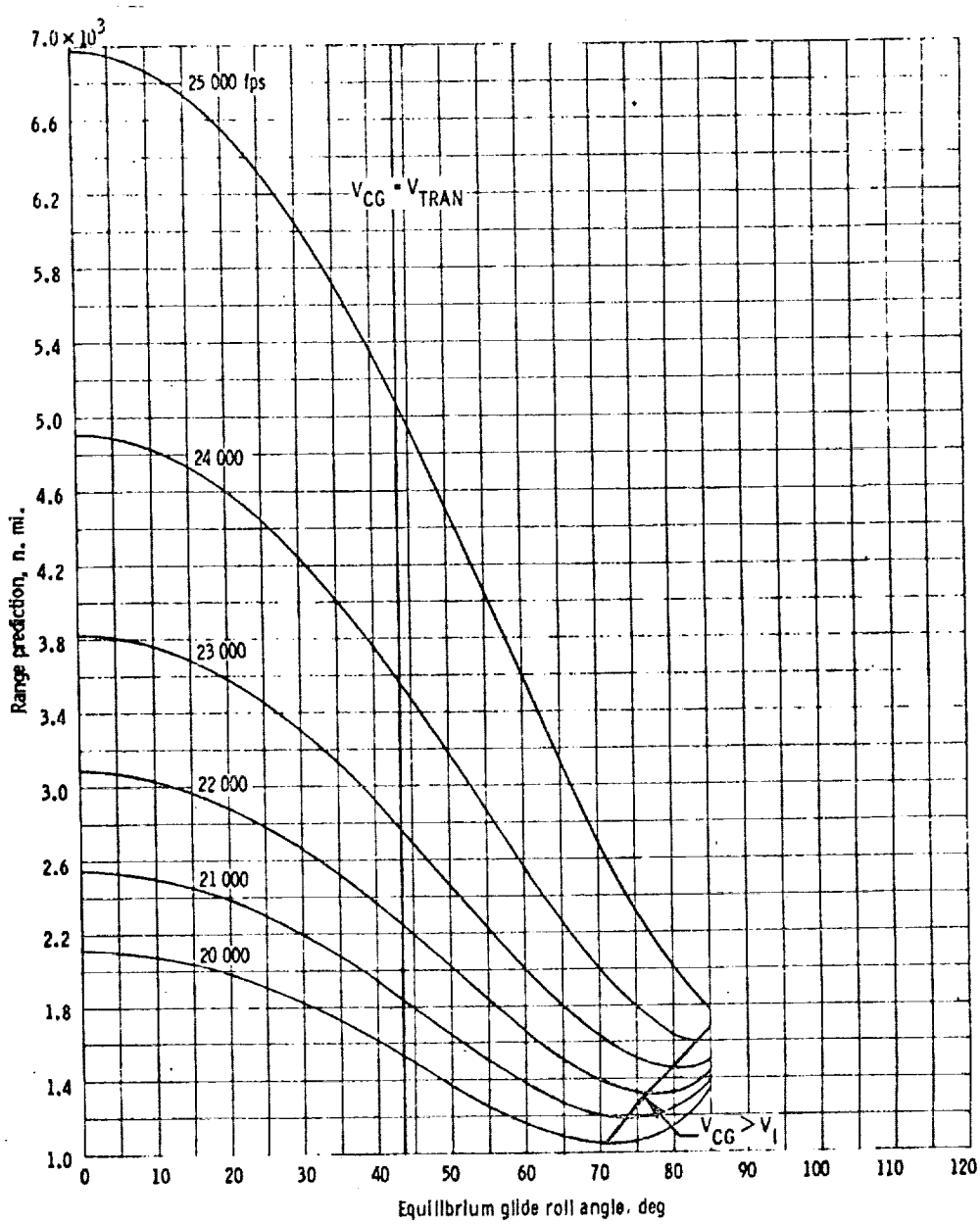


(a) $V_I$ = 20 000 fps to 25 000 fps.

Figure B1. - Equilibrium glide range predictions.

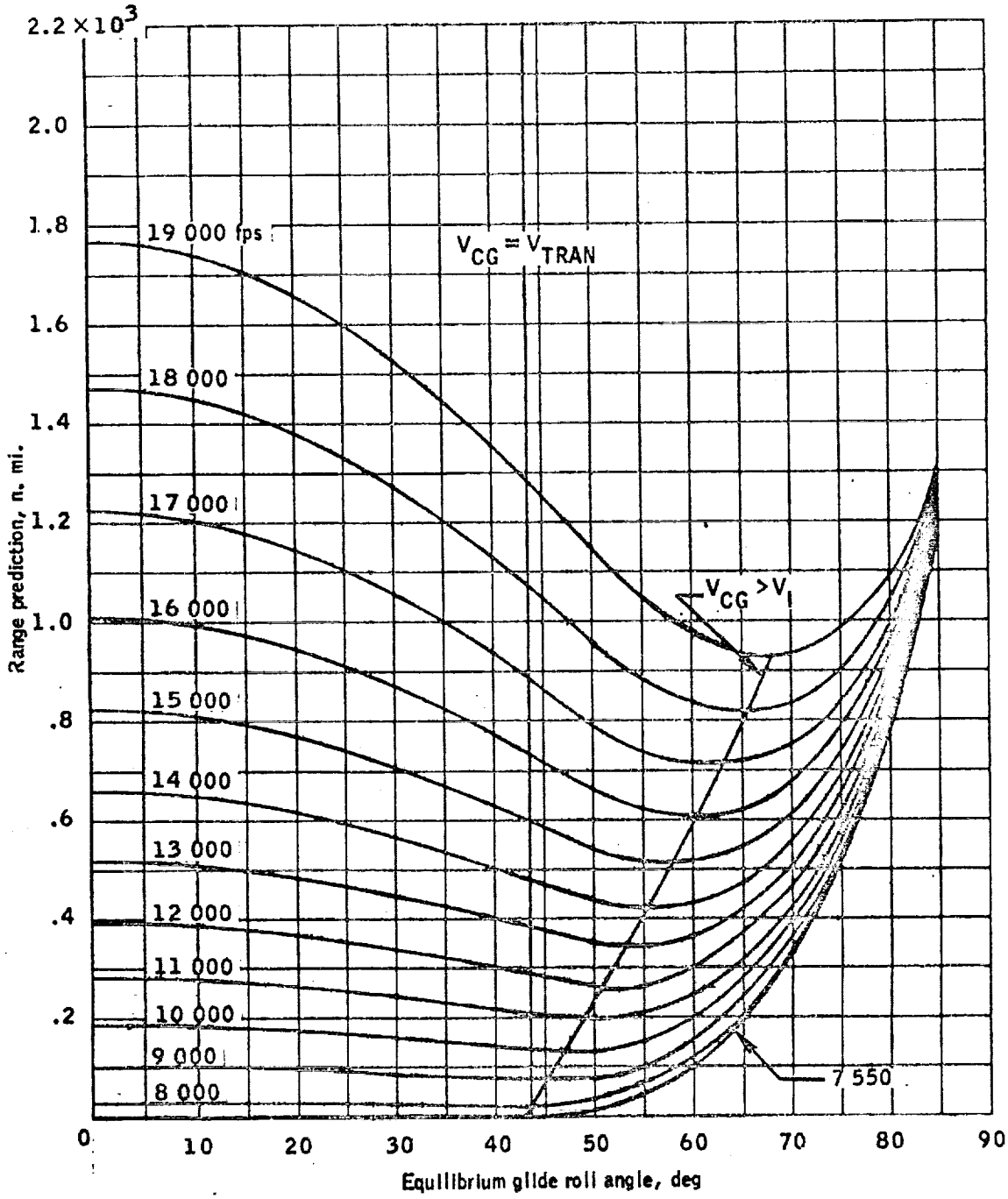


(b) $V_I$ = 7 550 fps to 19 000 fps.

Figure B1.- Concluded.

## APPENDIX C - CONSTANT g PHASE

The purpose of the constant g phase is to predict the constant g level required to reach the target and to generate a $D_{ref}$, $\dot{R}_{ref}$, and a $\frac{L}{D_{ref}}$ for the controller.

Equation (B13) presents the equation that analytically predicts the range that will be flown if a constant g profile ($D_{cg}$) is flown between $V_{CG}$ and transition. This equation is as follows:

$$R_{CG} = \frac{V_{CG}^2 - V_{TRAN}^2}{2D_{cg}}$$

The range to the transition point is obtained from the targeting logic and is equal to the total range to target minus the desired range to the target at transition

$$R_{TG} = R_T - R_{PT}$$

The constant g level to reach the target becomes

$$D_o = \frac{V_{CG}^2 - V_{TRAN}^2}{2R_{TG}} \tag{C1}$$

The constant g trajectory is controlled by means of the drag controller where

$$D_{ref} = D_o$$

$$\dot{R}_{ref} = -HS\left(\frac{2D_{ref}}{V_E} + \frac{\dot{D}_{ref}}{D_{ref}}\right)$$

For constant g $\dot{D}_{ref} = 0$, therefore

$$\dot{R}_{ref} = -2HS\frac{D_{ref}}{V_E} \tag{C2}$$

As was the case for constant heat rate, a L/D reference term can be derived from the equation of motion

$$V\dot{\gamma} = \frac{V^2 \cos \gamma}{R} + L - g \cos \gamma$$

or

$$\frac{L}{D_V} = \frac{g}{D}\left(1 - \frac{V^2}{V_{sat}{}^2}\right) + \frac{V\dot{\gamma}}{D} \qquad \text{(A14)}$$

and from equation (A15)

$$V\dot{\gamma} = \ddot{H} - \dot{V}\gamma$$

For constant g

$$\dot{H} = -2HS\,\frac{D}{V}$$

$$\ddot{H} = -2HS\left(\frac{\dot{D}}{V} - \frac{D\dot{V}}{V^2}\right) = -2HS\,\frac{D^2}{V^2} \qquad \text{(C3)}$$

$$V\dot{\gamma} = -2HS\,\frac{D^2}{V^2} - \dot{V}\gamma \qquad \text{(C4)}$$

$$\dot{V}\gamma = \frac{\dot{H}\dot{V}}{V} = \left(-2HS\,\frac{D}{V}\right)\left(-\frac{D}{V}\right) = \frac{2HSD^2}{V^2} \qquad \text{(C5)}$$

$$V\dot{\gamma} = -4HS\,\frac{D^2}{V^2} \qquad \text{(C6)}$$

Therefore,

$$\frac{L}{D_V} = \frac{g}{D}\left(1 - \frac{V^2}{V_{sat}{}^2}\right) - 4\frac{HSD}{V^2} \qquad \text{(C7)}$$

so

$$\frac{L}{D_V}_{ref} = \frac{g}{D_{ref}}\left(1 - \frac{V_E^2}{V_{sat}{}^2}\right) - 4HS\frac{D_{ref}}{V_E^2} \qquad \text{(C8)}$$

Relative velocity was assumed for the constant g phase because of the requirement to switch from inertial velocity to relative velocity late in the entry when velocity is approximately equal to $V_{sat}/2$.

## APPENDIX D - MATH FLOW LOGIC FOR THE CONSTANT ANGLE OF ATTACK GUIDANCE

All necessary equations have been developed in the main text and in appendixes A through C. The final step is to connect these equations with decision logic to convert trajectory data from the navigation into a commanded roll angle and a commanded angle of attack for the autopilot. This appendix presents the guidance flow logic and all necessary equations and constants for the constant angle of attack case. Table D-I presents the constants and initial variable values for the guidance. Flow charts 1 through 13 presents the math flow logic for the guidance.

TABLE E-I.- CONSTANTS AND INITIAL VARIABLE VALUES

| | | |
|---|---|---|
| ALMN | 1.5 | g |
| $C_D$ | 0.336 | n.d. |
| $C_{FNM}$ | 0.000164578836 | n. mi./ft |
| $C_{RNM}$ | 3437.7468 | n. mi./rad |
| g | 32.2 | $ft/sec^2$ |
| G2 | 2.5 | g |
| HS | 28 500. | fps |
| $H_{up}$ | 1 | n.d. |
| IFT | 0 | n.d. |
| IG | 0 | n.d. |
| ISTP | 1 | n.d. |
| LATSW | 0 | n.d. |
| LOD | 1.497 | n.d. |
| $\dot{Q}_C$ | 80. | $Btu/ft^2/sec$ |
| R | 21 041 776. | ft |
| RPT | 182.4 | n. mi. |
| RTD | 57.29577951 | rad/deg |
| SELECT | 1 | n.d. |
| VQ | 6443. | fps |
| VS | 25 766.1976 | fps |
| VSW | 25 000. | fps |
| Vxx | 6443. | fps |
| WE | .72921149 E-4 | rad/sec |
| WT | 140 000. | lb |
| Y | 20./RTD | rad |
| $\pi$ | 3.14159265 | n.d. |
| $\rho_o$ | 0.076474 | $lb/ft^2$ |
| 05GSW | 0 | n.d. |

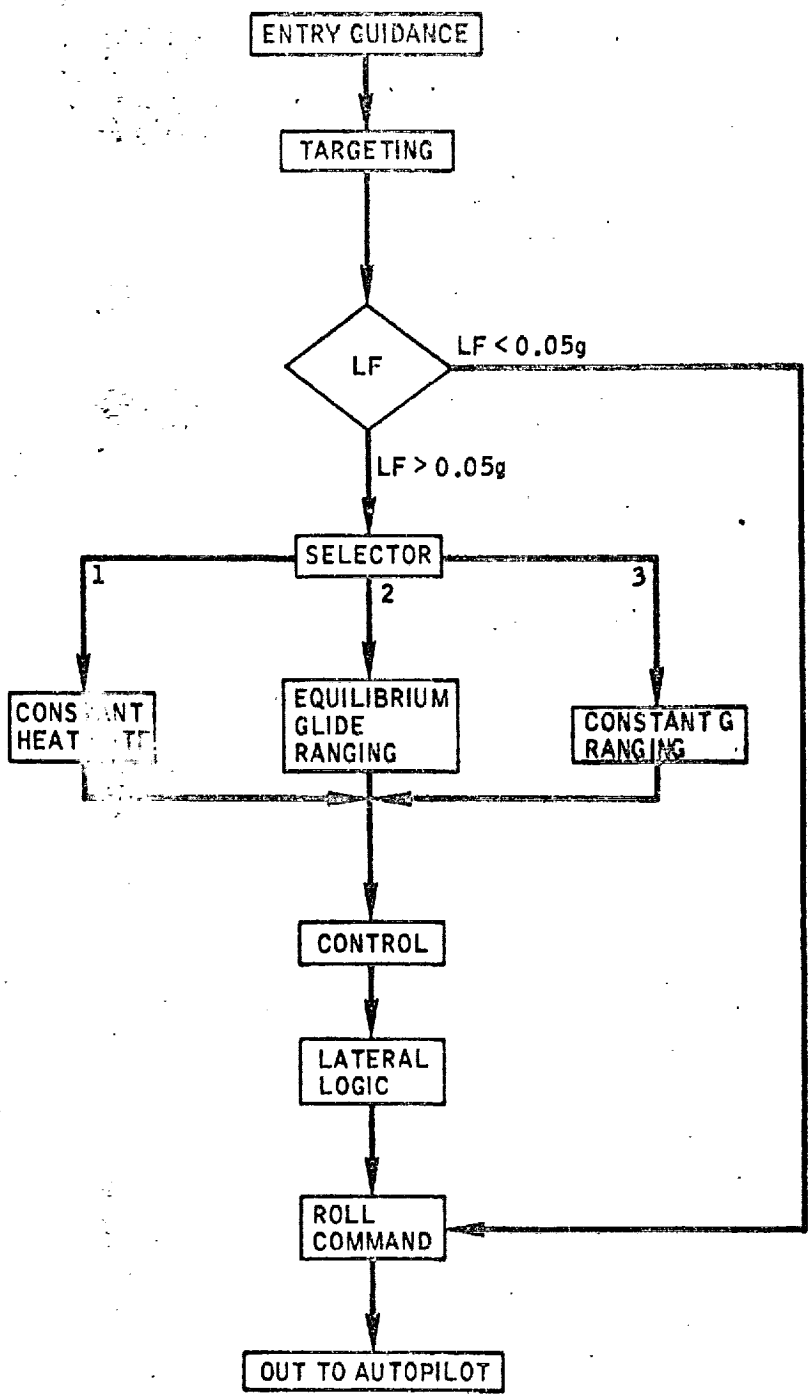


Flow chart D1.- Overall flow logic.

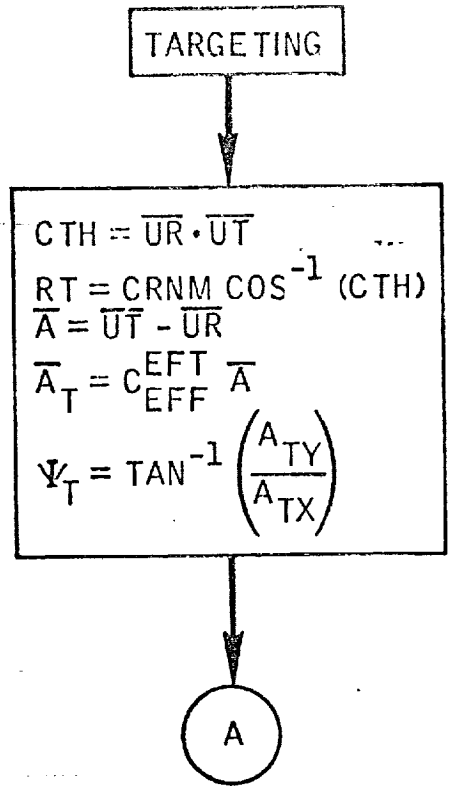


Flow Chart D2. - Targeting

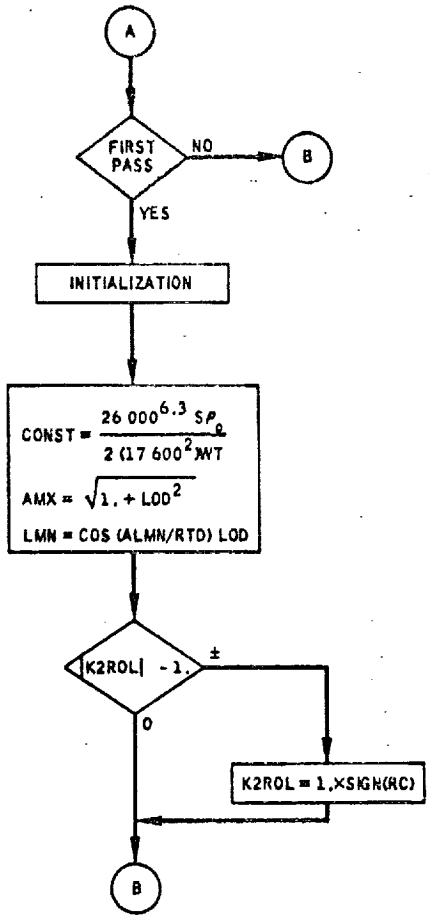


Flow chart B2. - Targeting - Continued.

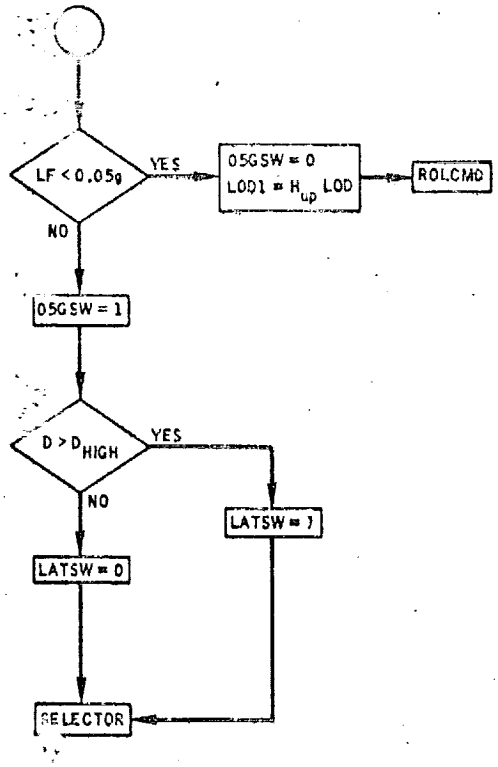


Flow chart D2.- Targeting - Concluded.

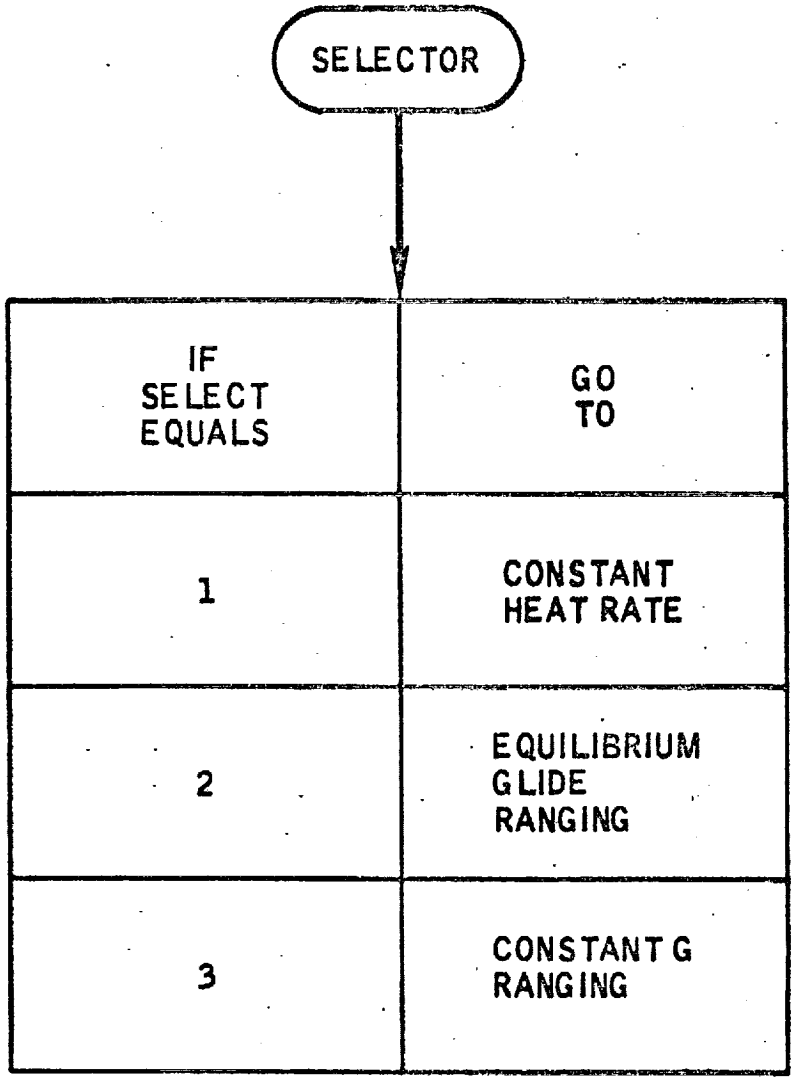


Flow chart D3.- Selector.

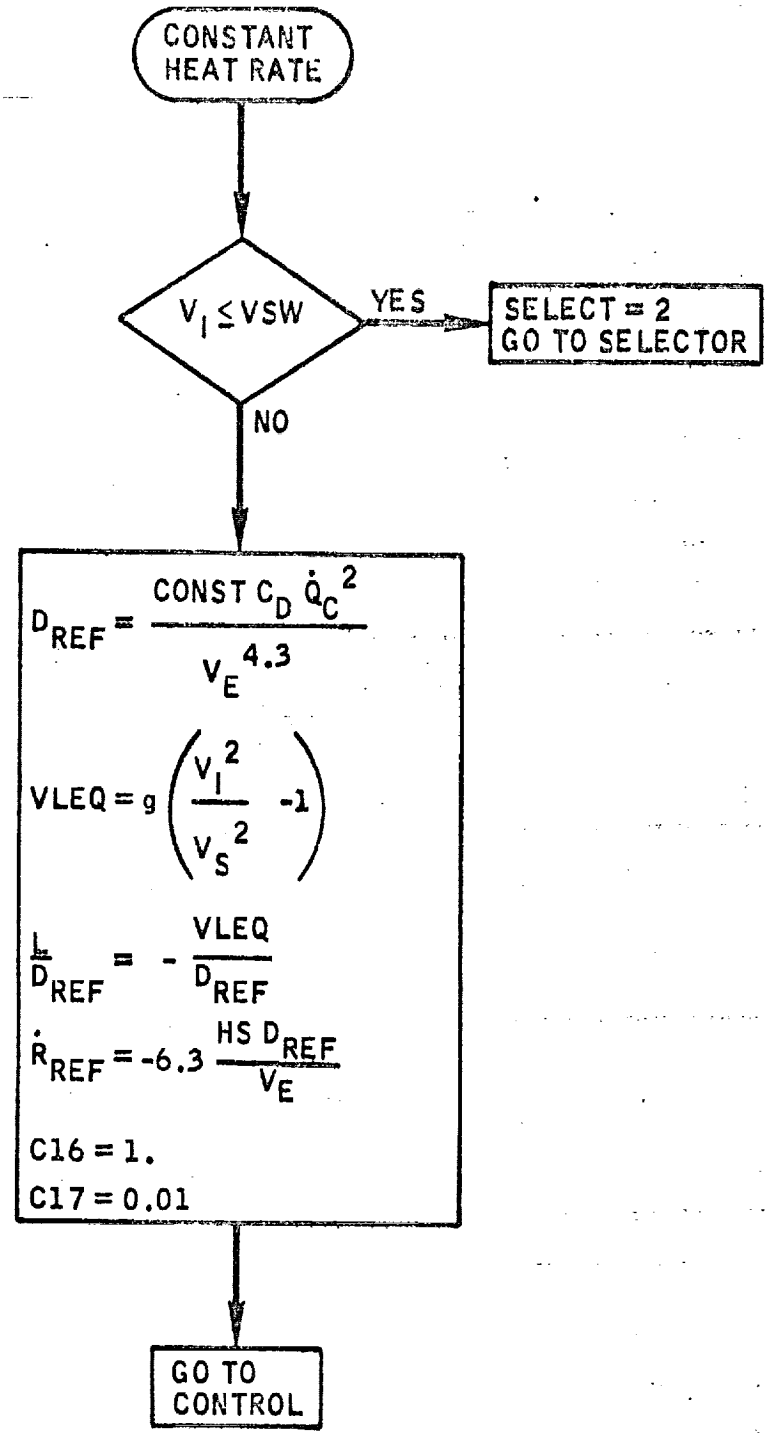


Flow chart D 4.- Constant heat rate.

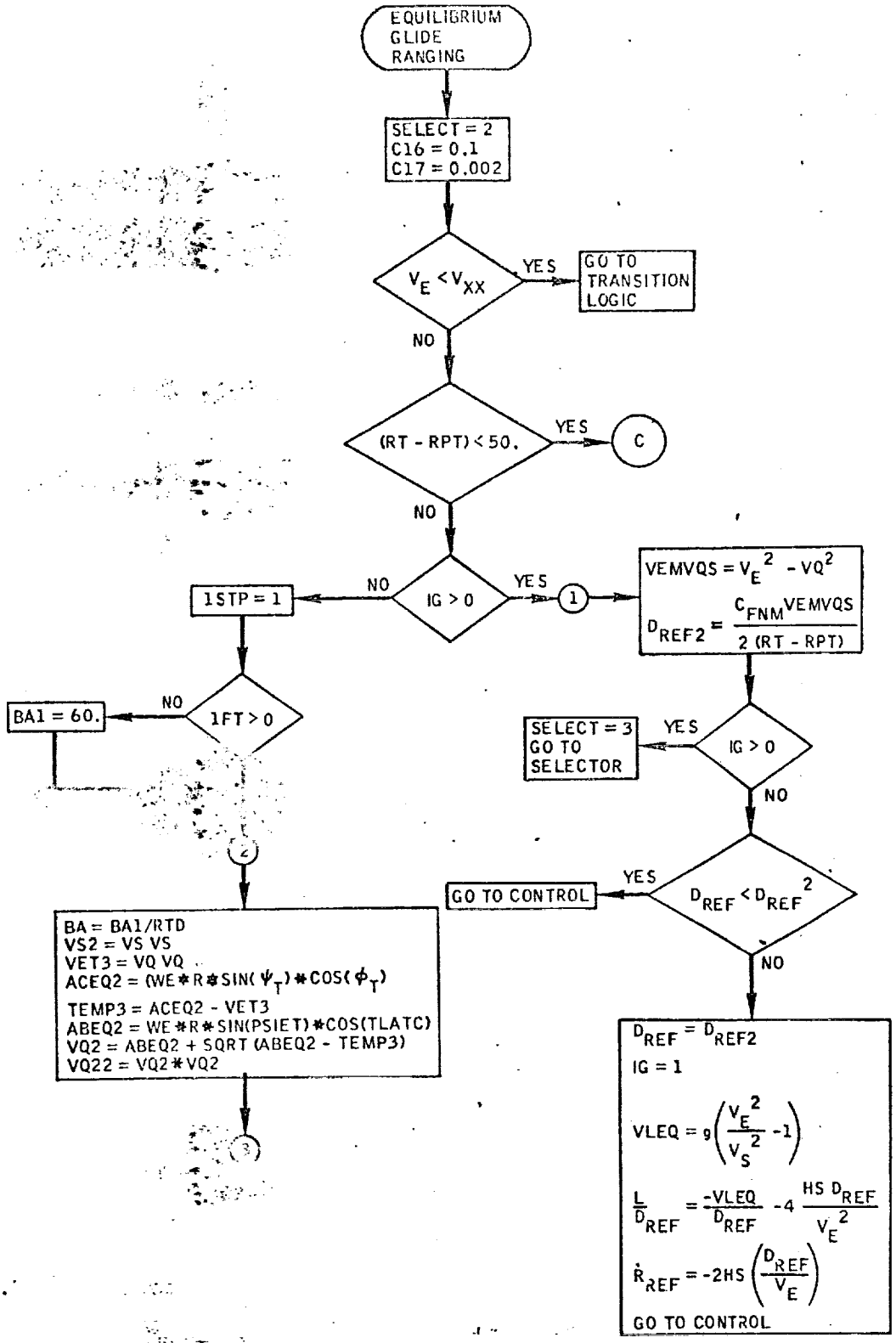


Flow chart D5. - Equilibrium glide ranging.

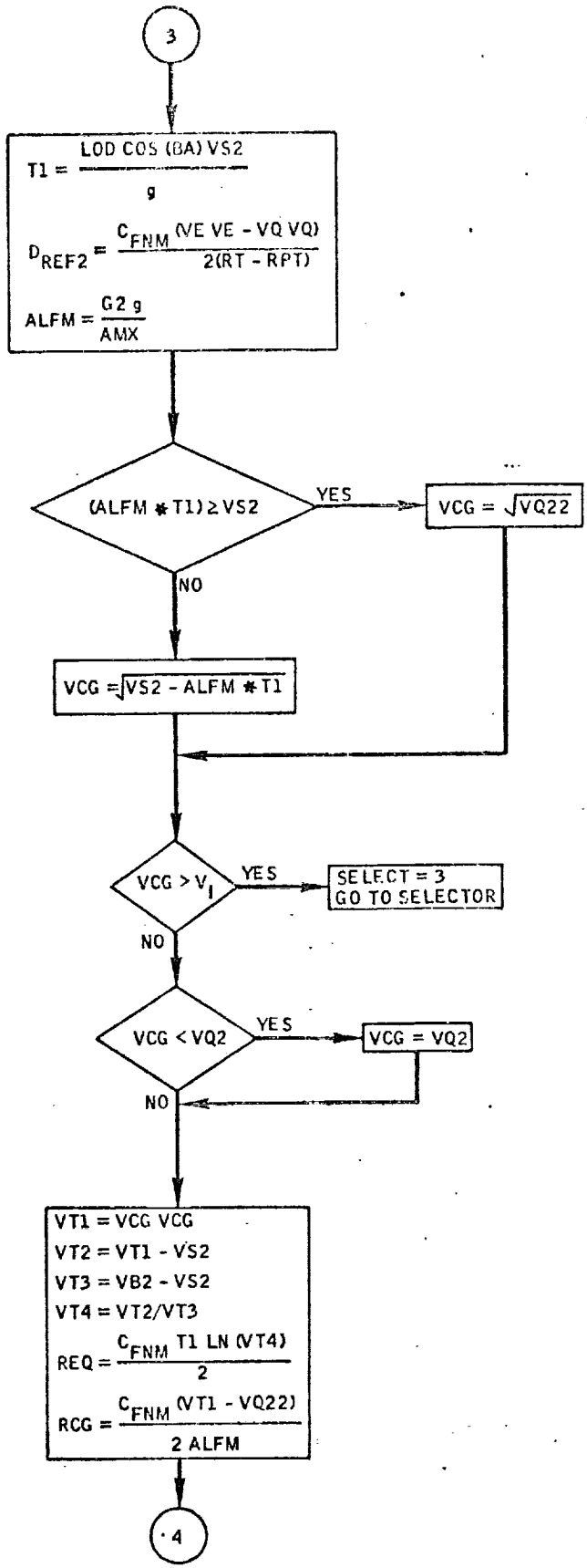


Flow chart D4.- Equilibrium glide ranging - Continued.

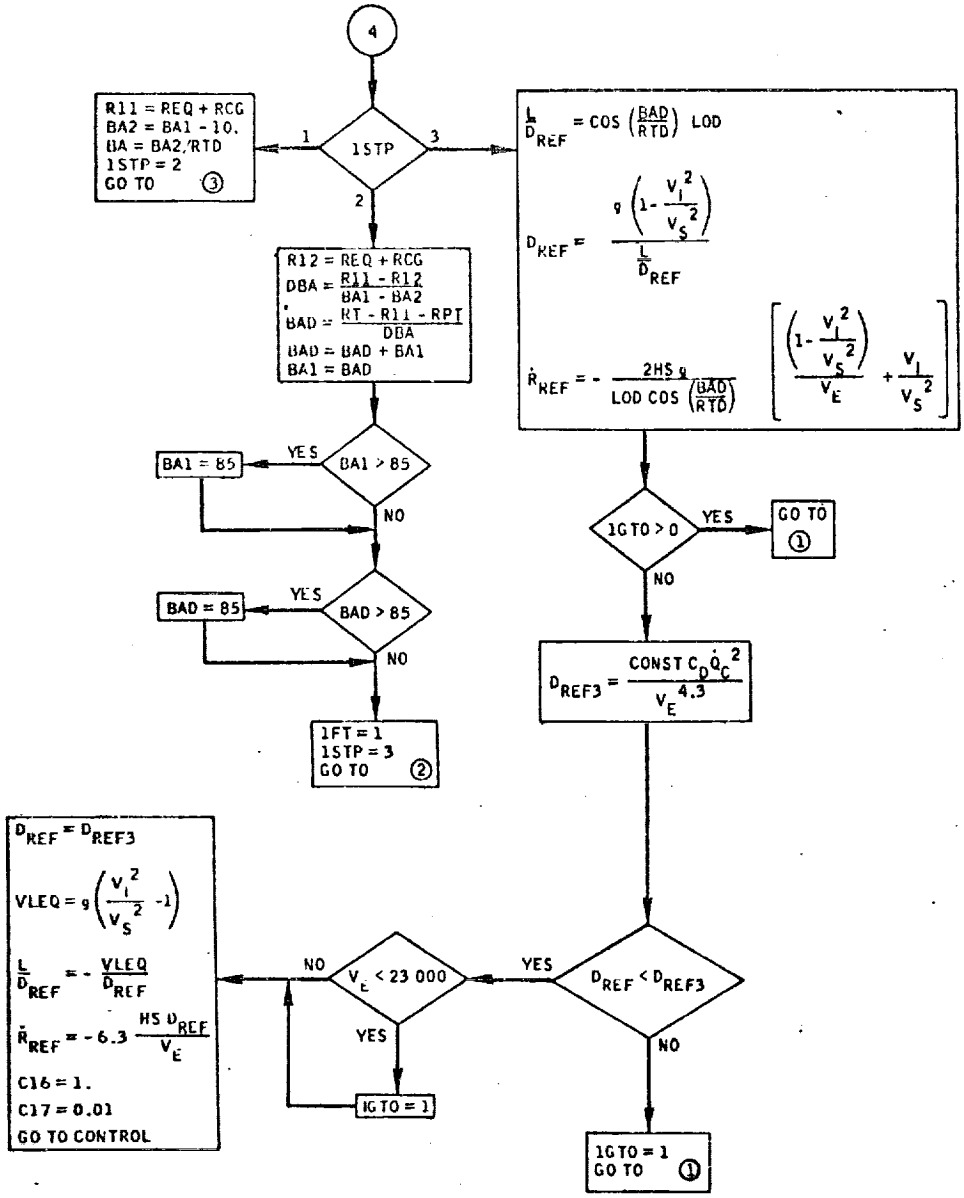


Flow chart B5. - Equilibrium glide ranging - Continued.

C

$$\frac{L}{D}_{REF} = \cos\left(\frac{BAD}{RTD}\right) LOD$$

$$\dot{\theta}_{REF} = \frac{g\left(1 - \frac{V_I^2}{V_S^2}\right)}{\frac{L}{D}_{REF}}$$

$$\dot{R}_{REF} = -\frac{2g\,HS}{\frac{L}{D}\cos\left(\frac{BAD}{RTD}\right)}\left[\frac{\left(1 - \frac{V_I^2}{V_S^2}\right)}{V_E} + \frac{V_I}{V_S^2}\right]$$

GO TO CONTROL

Flow chart 85. - Equilibrium glide ranging - Concluded.

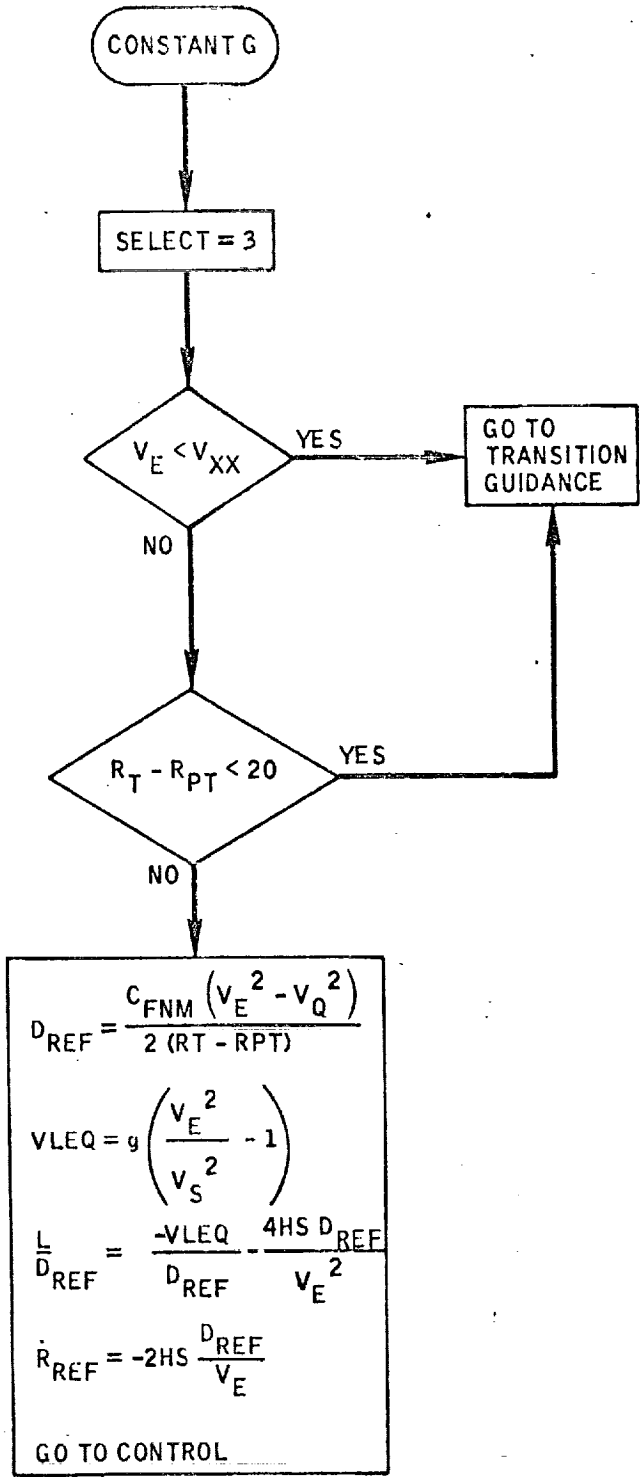


Flow chart D6 Constant g phase.

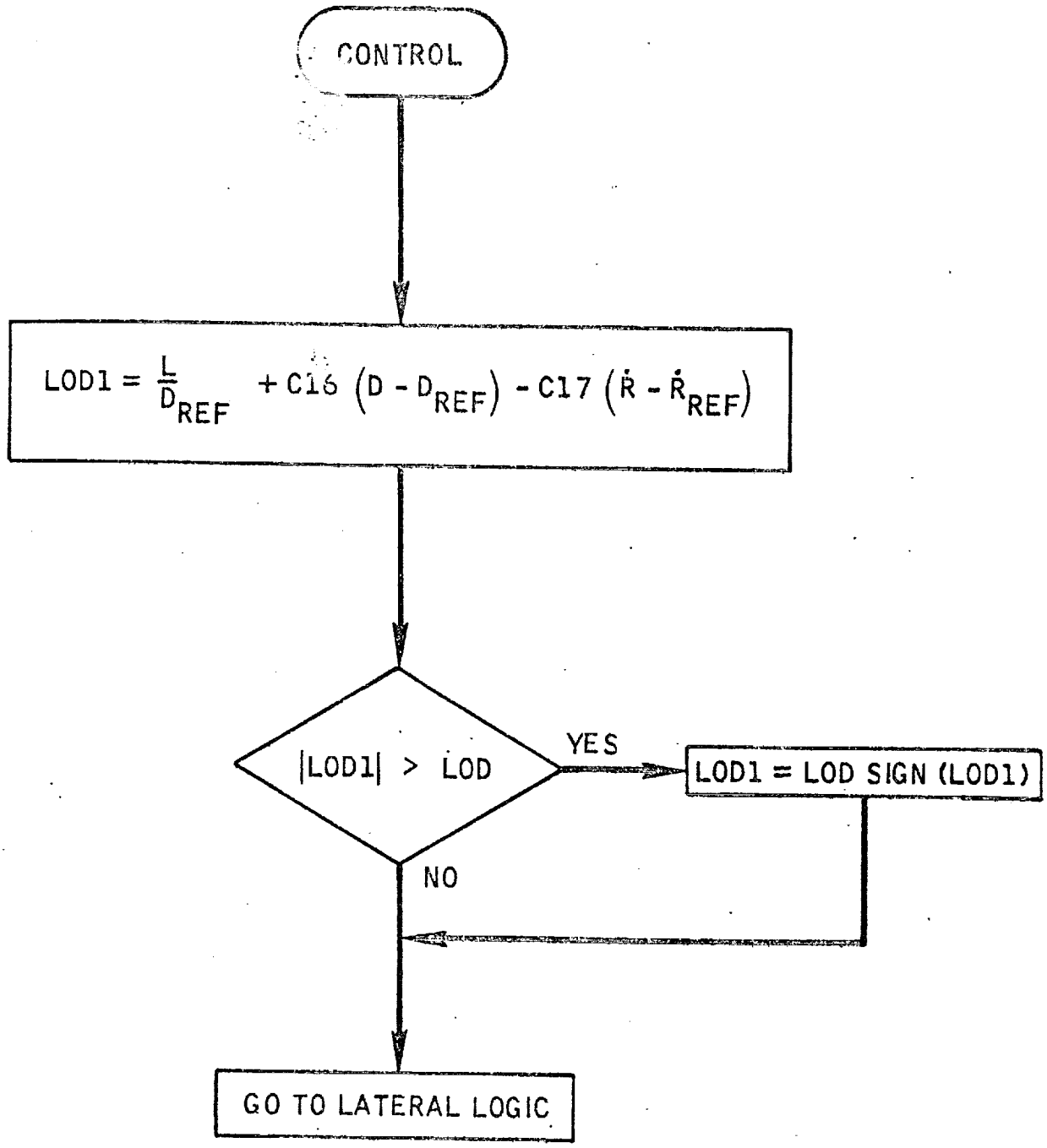


Flow chart D 7.- Controller.

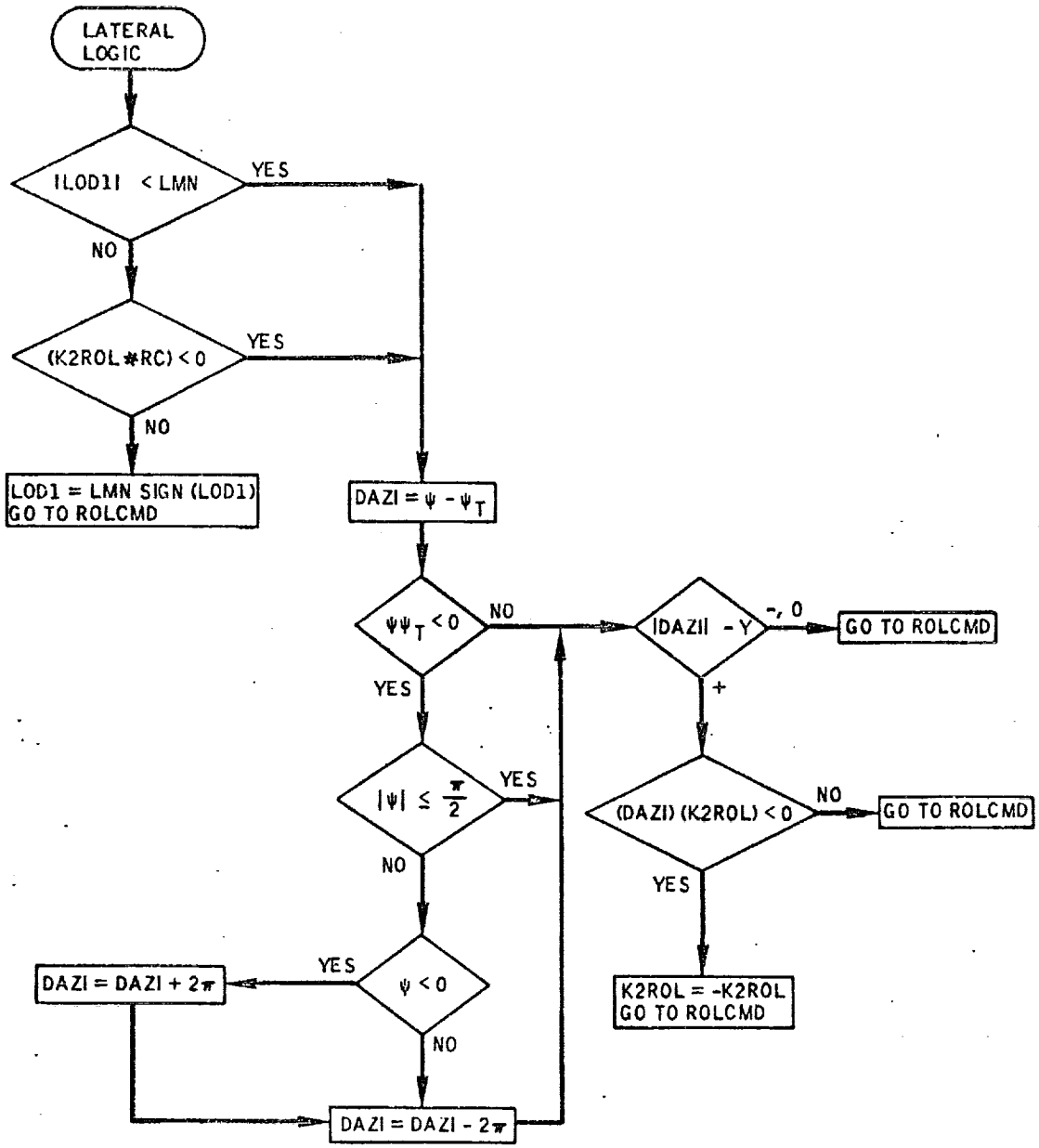


Flow chart D8. - Lateral logic.

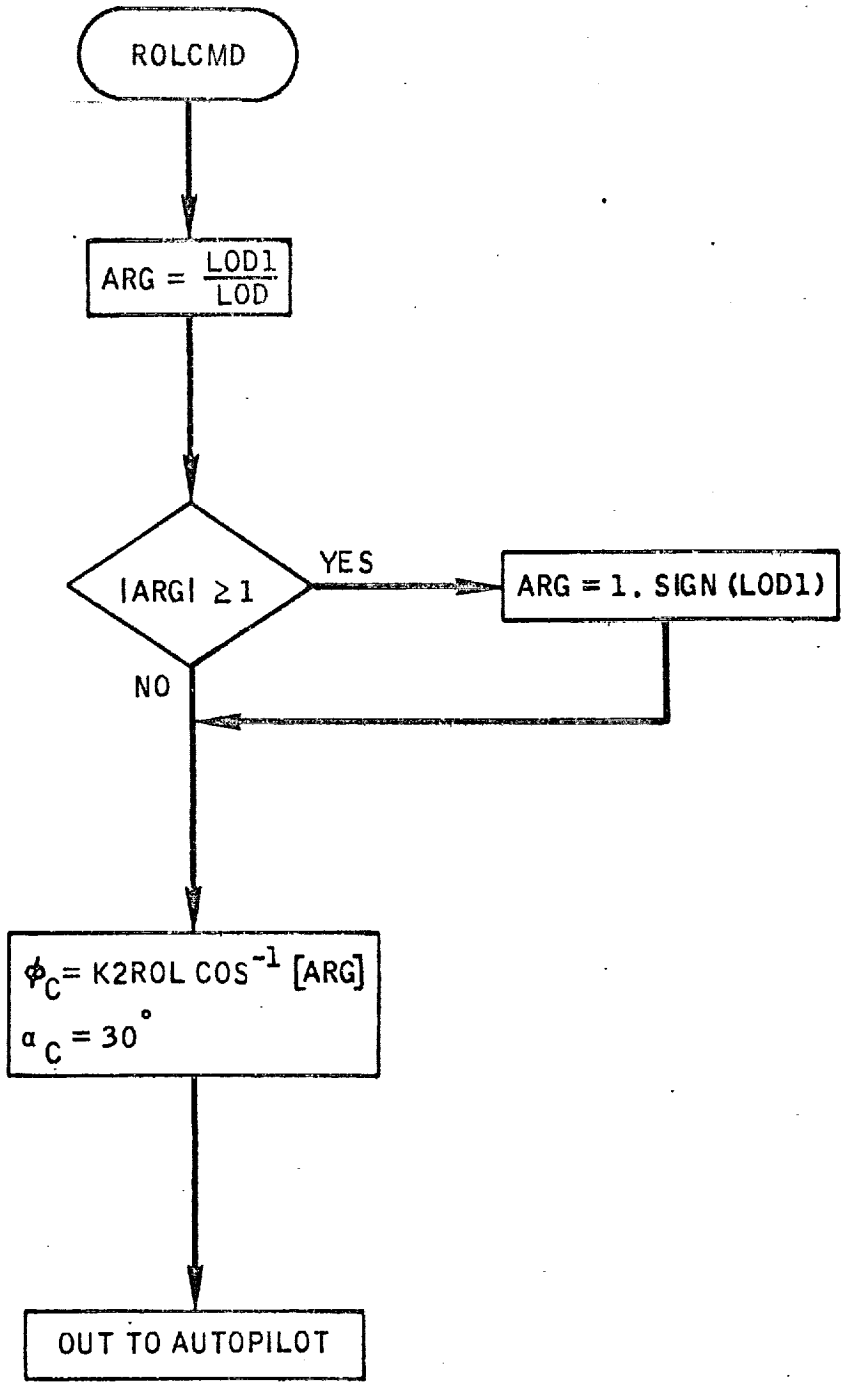


Flow chart D9 .- Roll command.

Submittal 58-Approach Guidance

## 1. INTRODUCTION

The Approach Guidance Routine presented here is designed to take the orbiter vehicle from the end of the entry phase (altitude ≈100,000 ft) down to the start of the terminal guidance phase 5.9 n.mi. from the runway at an altitude of 6900 ft. and a velocity of 480 ft/sec. It is based on the ideas of Refs. (1) and (2).

The guidance routine consists of six modes: Acquisition, Energy Dissipation, Turn-in, Initial Approach, Heading Alignment, and Final Approach. The horizontal geometry is illustrated in Figure 1 in which the circled numbers refer to the various modes. The Acquisition Mode begins at 100,000 ft altitude, contains an angle-of-attack transition maneuver, and ends when the vehicle is within about 15 n.mi. of the runway. Energy dissipation involves flight in the vicinity of the runway around a cylinder of radius 13.5 n.mi. During this mode the vehicle descends from about 50,000 ft altitude to 26,000 ft. This helical flight usually comprises less than one half of a revolution around the cylinder. The next three modes, i.e. Turn-in, Initial Approach, and Heading Alignment, constitute a two-turn maneuver to place the vehicle on the appropriate final approach path. The Final Approach Mode establishes the proper interfaces with the Terminal Guidance Routine for the final maneuvers required to land on the runway.

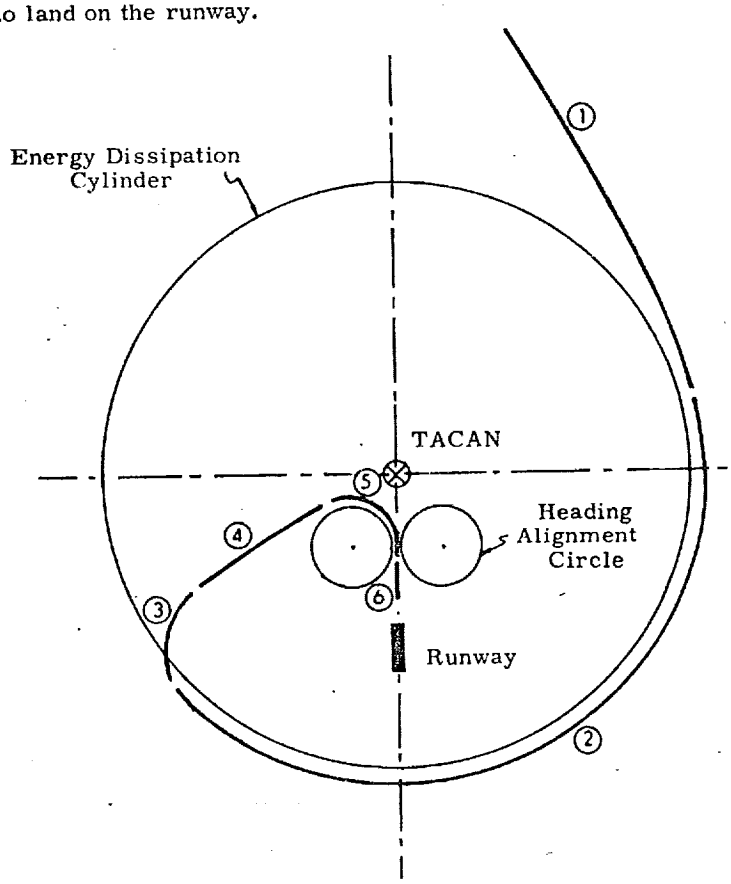


Figure 1. Horizontal Geometry, Approach Guidance

## 2. FUNCTIONAL FLOW DIAGRAM

The basic flow of the Approach Guidance Routine is shown in Figure 2.

After the routine is entered and initialized, targeting computations are made to obtain the current values of position and velocity, and direction parameters of the vehicle relative to the desired touchdown point. Next, the mode is selected based on the current trajectory conditions, and quantities unique to the specific mode are computed.

The angle-of-attack command is used for vertical control and is computed during the first part of Mode 1 so as to accomplish a constant (-0.3 deg/sec) angle-of-attack transition maneuver. During the remainder of Mode 1 and for Modes 2 and 3, an angle-of-attack which will yield a constant ($210 \frac{lb}{ft^2}$) dynamic pressure is commanded. Finally, during the last three modes, the angle-of-attack which will cause the vehicle to fly at a constant flight path angle (-11 deg) is commanded.

The roll-angle command is used for horizontal control and is computed for the various modes as shown in the following table.

Table 1

Geometric Criteria for Roll-Angle Command

| Mode | Geometric Criterion |
|---|---|
| 1 | Tangent to Energy Dissipation Cylinder (EDC) |
| 2 | Fly on EDC |
| 3 | Turn toward center of EDC |
| 4 | Tangent to Heading Alignment Cylinder (HAC) |
| 5 | Fly on HAC |
| 6 | Align into vertical runway plane |

Finally, the rudder flare or speed brake is deployed during the last three modes in order to achieve a speed of 480 f/s at the end of approach guidance.

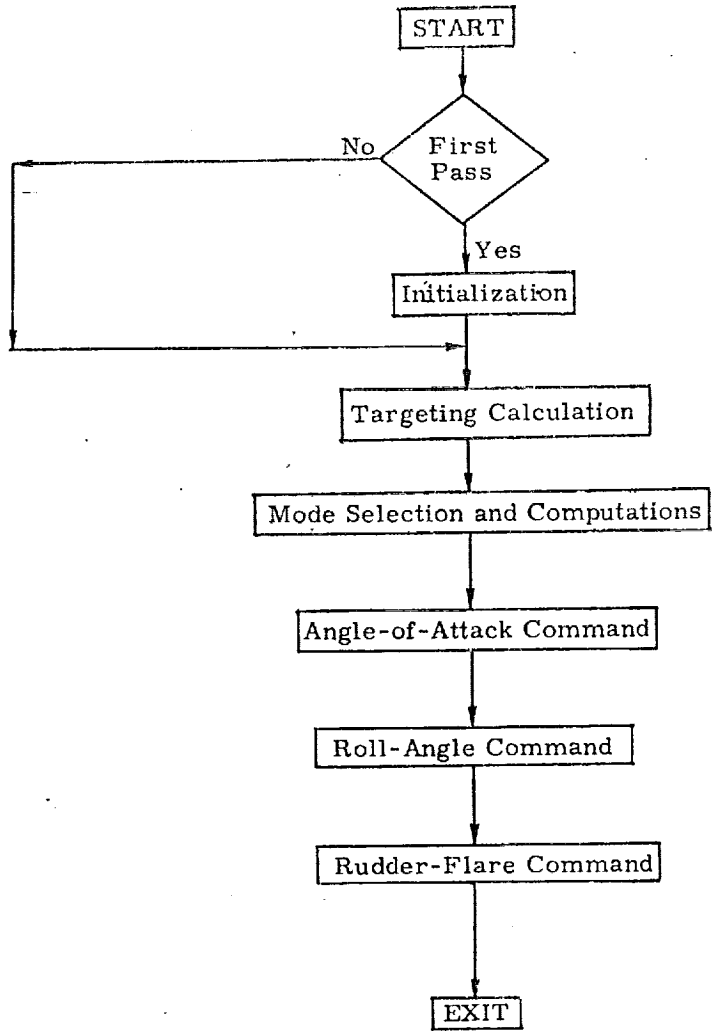


Figure 2. Functional Flow Diagram, Approach Guidance

# NOMENCLATURE

## Notational Conventions

Upper-case letters represent matrices

Lower-case and Greek letters reserved for scalars and vectors

Vector quantities are underlined, e.g. $\underline{x}$

Vectors are assumed to be column vectors unless explicitly noted

## Symbols

| | |
|---|---|
| $a$ | Effective aerodynamic area of vehicle |
| $\underline{a}$ | Acceleration (RW coordinate) |
| $c\ell$ | Coefficient of lift |
| $c\ell_\alpha$ | $\partial(c\ell)/\partial(\alpha)$ |
| $d_c$ | Rudder-flare command |
| $d_{RT}$ | Distance between touchdown point and ED center |
| $f_{turn}$ | Turning factor |
| $g$ | Gravity |
| $h$ | Altitude |
| $\dot{h}$ | $dh/dt$ |
| $\ddot{h}$ | $d\dot{h}/dt$ |
| $h_1$ | Altitude at beginning of Initial Approach |
| $h_R$ | Reference altitude |
| $\dot{h}_R$ | $d(h_R)/dt$ |

| | |
|---|---|
| $k_1$ | Control gain |
| $k_2$ | Control gain |
| $k_{11}$ | Left or right HA selector |
| $\ell_D$ | Desired lift specific force |
| $m$ | Vehicle mass |
| $m_v$ | Mach no. |
| $M_{R\text{-}NED}$ | Run-way to NED Coordinate Transformation Matrix |
| $q$ | Dynamic pressure |
| $q_{old}$ | Dynamic pressure at last guidance call |
| $q_D$ | Desired dynamic pressure |
| $\dot{q}$ | $dq/dt$ |
| $q_v$ | $\partial q/\partial v$ |
| rad | Radians into degree |
| $r_{DME}$ | Distance from vehicle to Tacan |
| $r_{ED}$ | Radius of ED cylinder |
| $\underline{r}_{NED}$ | Horizontal component of vehicle position vector (NED-Tacan Coord.) |
| $\underline{r}_{RT}$ | Horizontal component of position vector (RN-Tacan coord.) |
| $s_{HE}$ | Integration of steady state heading error in Mode 2 |
| $s_m$ | Mode selector |
| $t_c$ | Clock time |

| | |
|---|---|
| $\Delta t$ | Time interval between guidance updates |
| $\underline{u}_1$ | Unit vector (1, 0, 0) |
| $\underline{u}_2$ | Unit vector (0, 1, 0) |
| $\underline{u}_3$ | Unit vector (0, 0, 1) |
| $v$ | Vehicle velocity w.r.t. air mass |
| $\underline{v}_{NED}$ | Horizontal component of vehicle velocity (NED Coord.) |
| $\underline{v}_R$ | Vehicle velocity vector (R.W. Coord.) |
| $\underline{v}_{RT}$ | Horizontal component of vehicle velocity (R.W. - Tacan Coord.) |
| $y$ | Cross range to runway |
| $\dot{y}$ | $dy/dt$ |
| $\alpha$ | Current angle-of-attack |
| $\alpha_c$ | Angle-of-attack command |
| $\phi$ | Roll angle command magnitude |
| $\phi_c$ | Roll angle command |
| $\Delta\alpha_D$ | Desired angle-of-attack change |
| $\Delta\psi_C$ | Desired azimuth change |
| $\psi$ | Azimuth ( $0 \sim 360^\circ$ ) |
| $\psi_c$ | Azimuth command ( $0 \sim 360^\circ$ ) |
| $\psi_{RW}$ | Runway azimuth |
| $\theta_{HA}$ | Azimuth of ($-\underline{\rho}_{HAR}$) vector |

| | |
|---|---|
| $\theta_N$ | Angle to Tacan w.r.t. north (from vehicle) ( 0 - 360$^o$ ) |
| $\theta_T$ | Angle to Tacan w.r.t. velocity (from vehicle) ( 0 - 180$^o$ ) |
| $\rho$ | Air density |
| $\rho_P$ | Predicted range to go to key point |
| $\underline{\rho}_{HAN}$ | Vector from proper HA to vehicle (NED Coord.) |
| $\underline{\rho}_{HAR}$ | Vector from proper HA to vehicle (RW-Tacan Coord.) |
| $\underline{\rho}'_{HAR}$ | Vector from other HA to vehicle (RW-Tacan Coord.) |
| $\underline{\rho}_R$ | Vehicle position vector in (RW Coord.) |
| $\rho_{RD}$ | Distance to touchdown point |
| $\underline{\rho}_{HAT}$ | Vector from Tacan to proper HA center (RW-Tacan Coord.) |

<u>Coordinates:</u>

(RW Coord.)

Runway coordinates, centered at touchdown point

| | |
|---|---|
| z | in runway landing direction, i.e. directed down-range and forward |
| x | up |
| y | x, y, z from right hand orthogonal coordinates |

(RW - Tacan Coord.)

Runway coordinates, centered at Tacan or center of EDC

(NED Coord.)

Local North, East, down coordinates at point of Tacan

Angle Measurements

(0, 360$^o$) or ($0 \leq \theta < 360^o$)

$\theta$ between 0 and 360$^o$, measured clockwise

(0, 180$^o$) or ($-180^o < \theta \leq 180^o$)

$\theta$ between ( 0 180$^o$) if measured (clockwise)
( 0 -180$^o$) if measured (counter clockwise)

## 3. INPUT AND OUTPUT VARIABLES

### Input Variables

| | |
|---|---|
| $\underline{\rho}_R$ | Vehicle position vector (RW Coord.) |
| $\underline{v}_R$ | Vehicle velocity vector (RW Coordinate) |
| $\underline{a}$ | Vehicle acceleration vector (RW Coord.) |
| $\psi_{RW}$ | Runway azimuth ( 0 - 360$^{o}$ ) |
| $\Delta t$ | Time interval between guidance updates |

### Output Variables

| | |
|---|---|
| $\phi_c$ | Command roll angle |
| $\alpha_c$ | Command angle-of-attack |
| $d_c$ | Command rudder flare |

## 5. DETAILED FLOW DIAGRAMS

This section contains detailed flow diagrams of the Approach Guidance Routine.

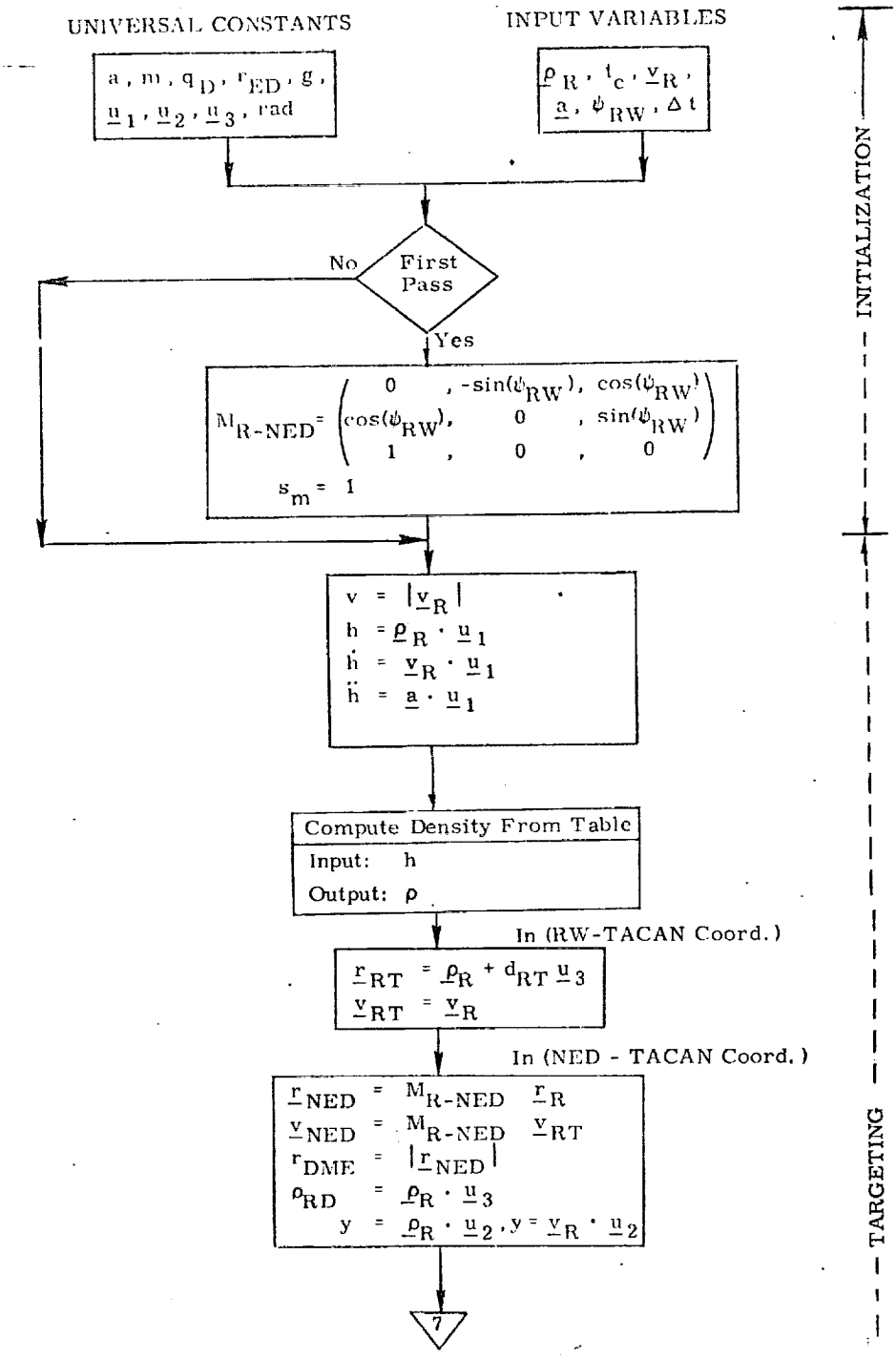


Figure 4a. Detailed Flow Diagram, Approach Guidance Routine

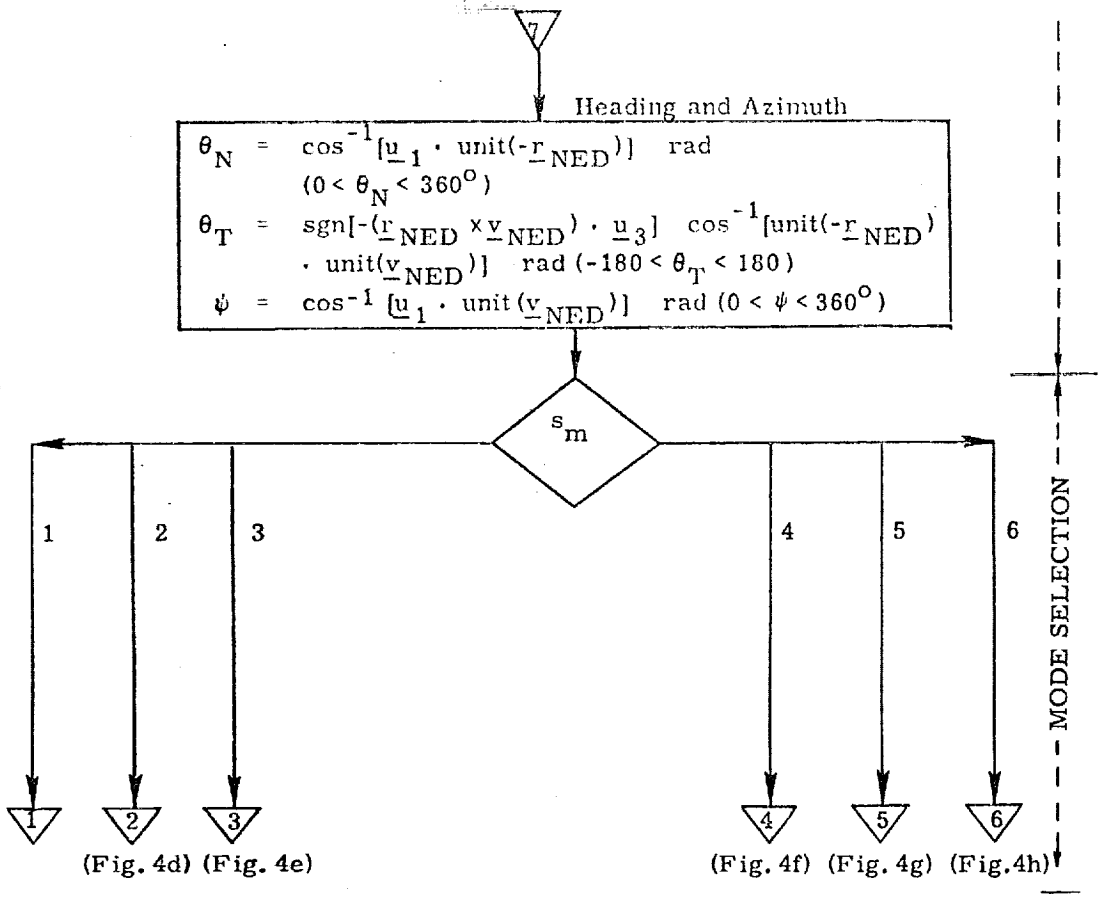


Figure 4b. Detailed Flow Diagram, Approach Guidance Routine

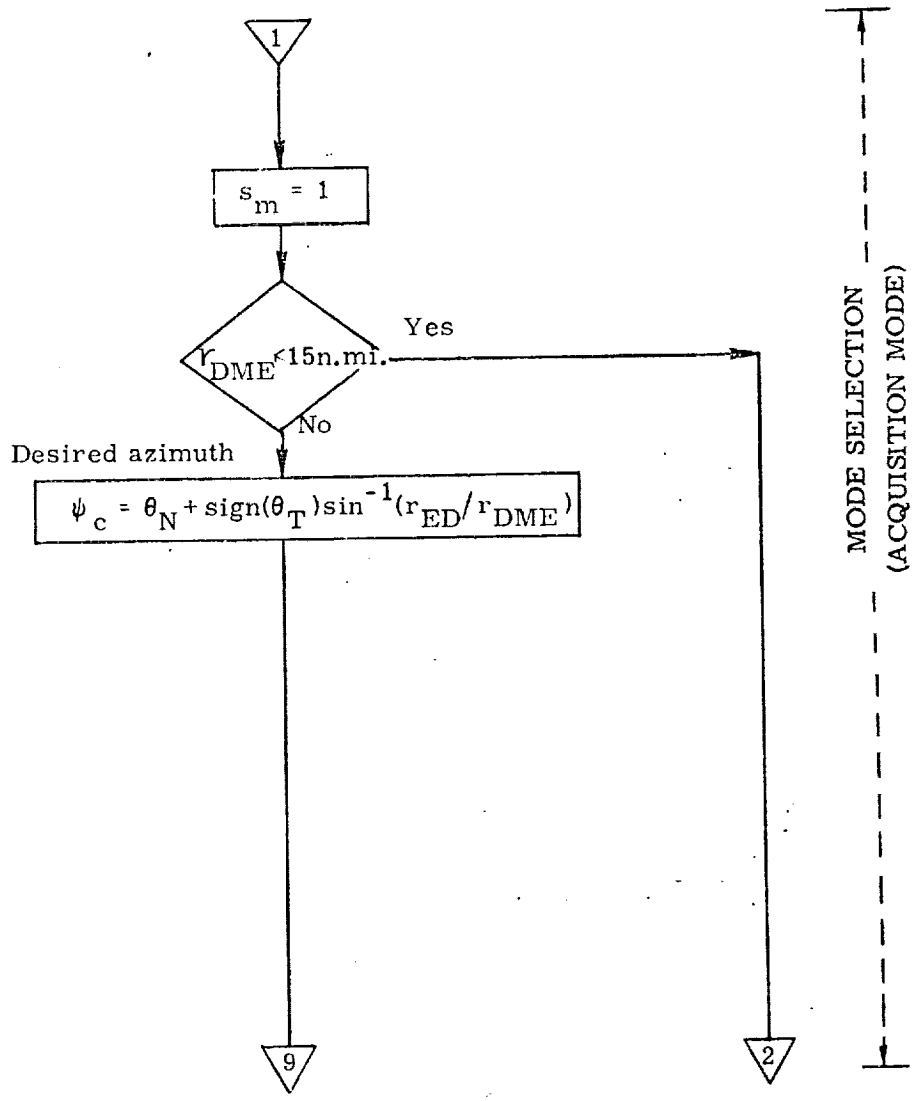


(Figure 4i)

Figure 4c. Detailed Flow Diagram, Approach Guidance Routine

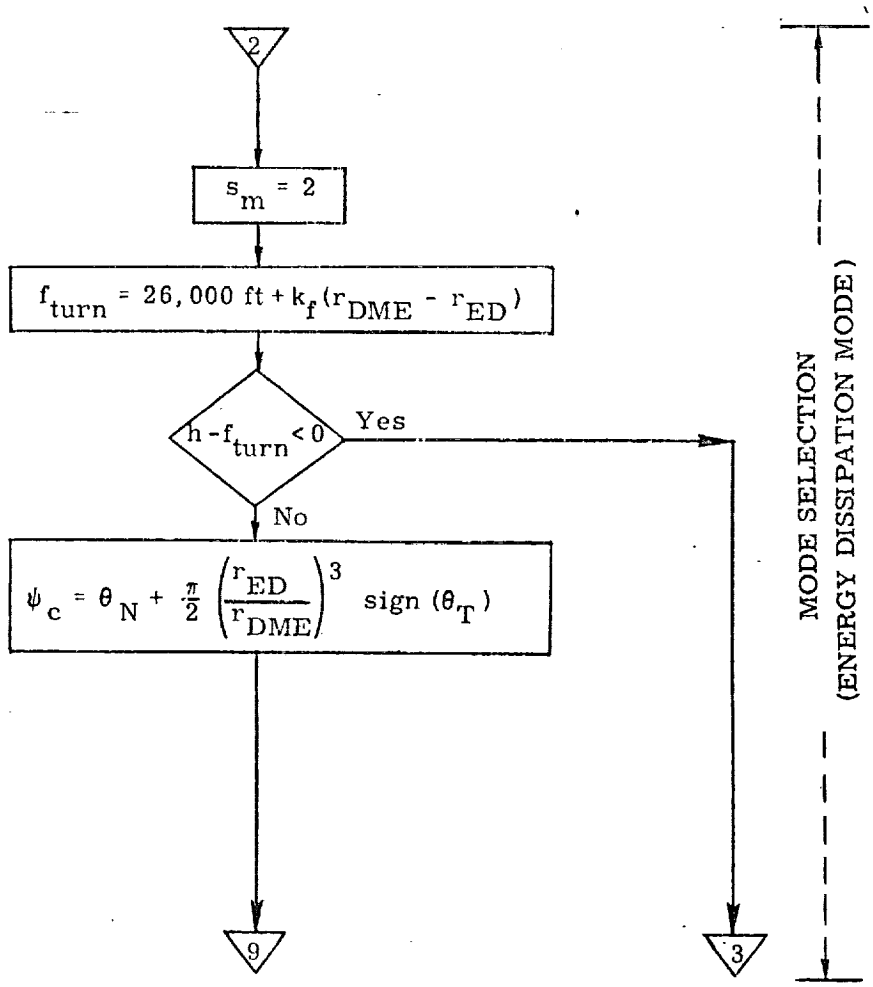


(Figure 4i)

Figure 4d. Detailed Flow Diagram, Approach Guidance Routine

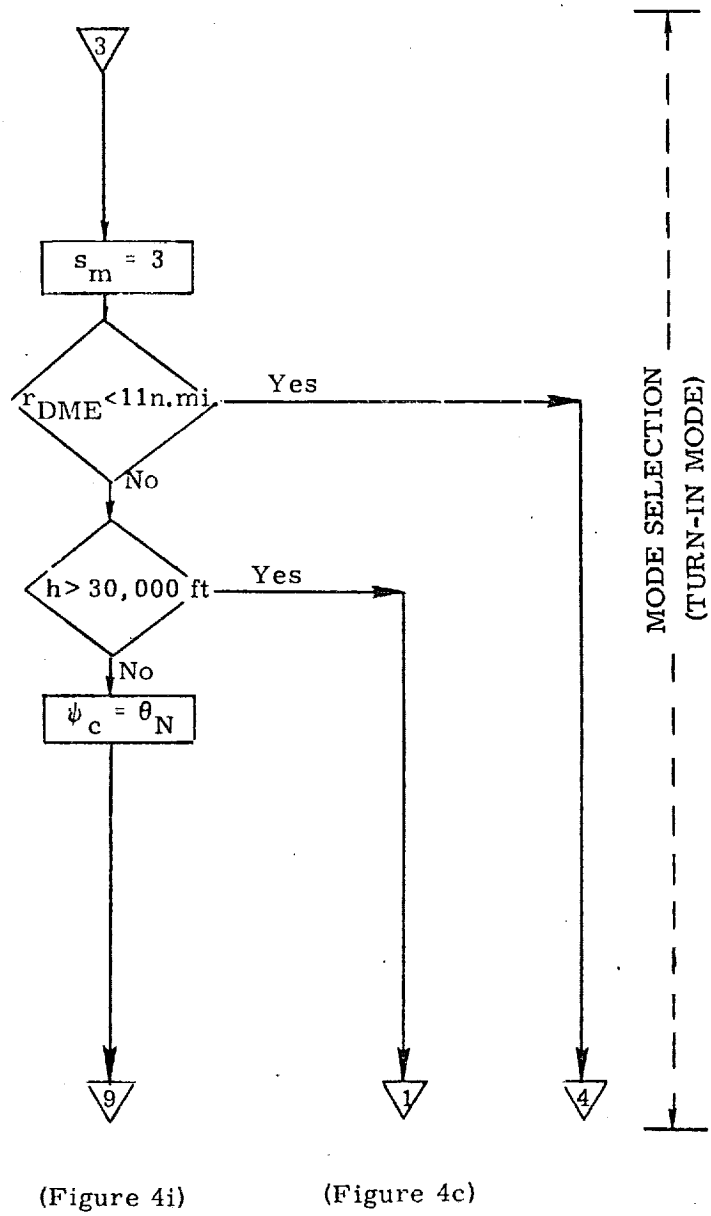


Figure 4e. Detailed Flow Diagram, Approach Guidance Routine

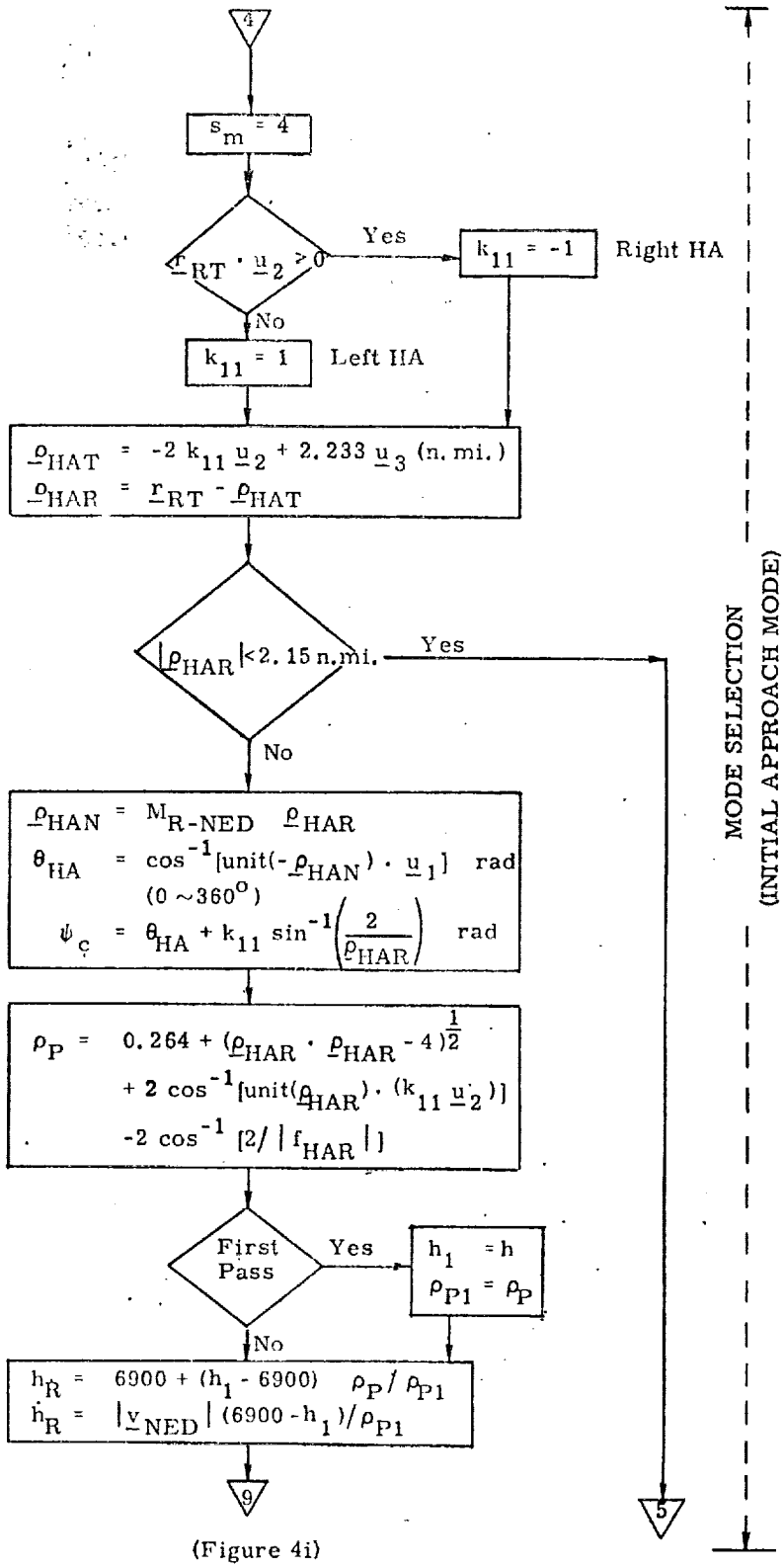


(Figure 4i)

Figure 4f. Detailed Flow Diagram, Approach Guidance Routine

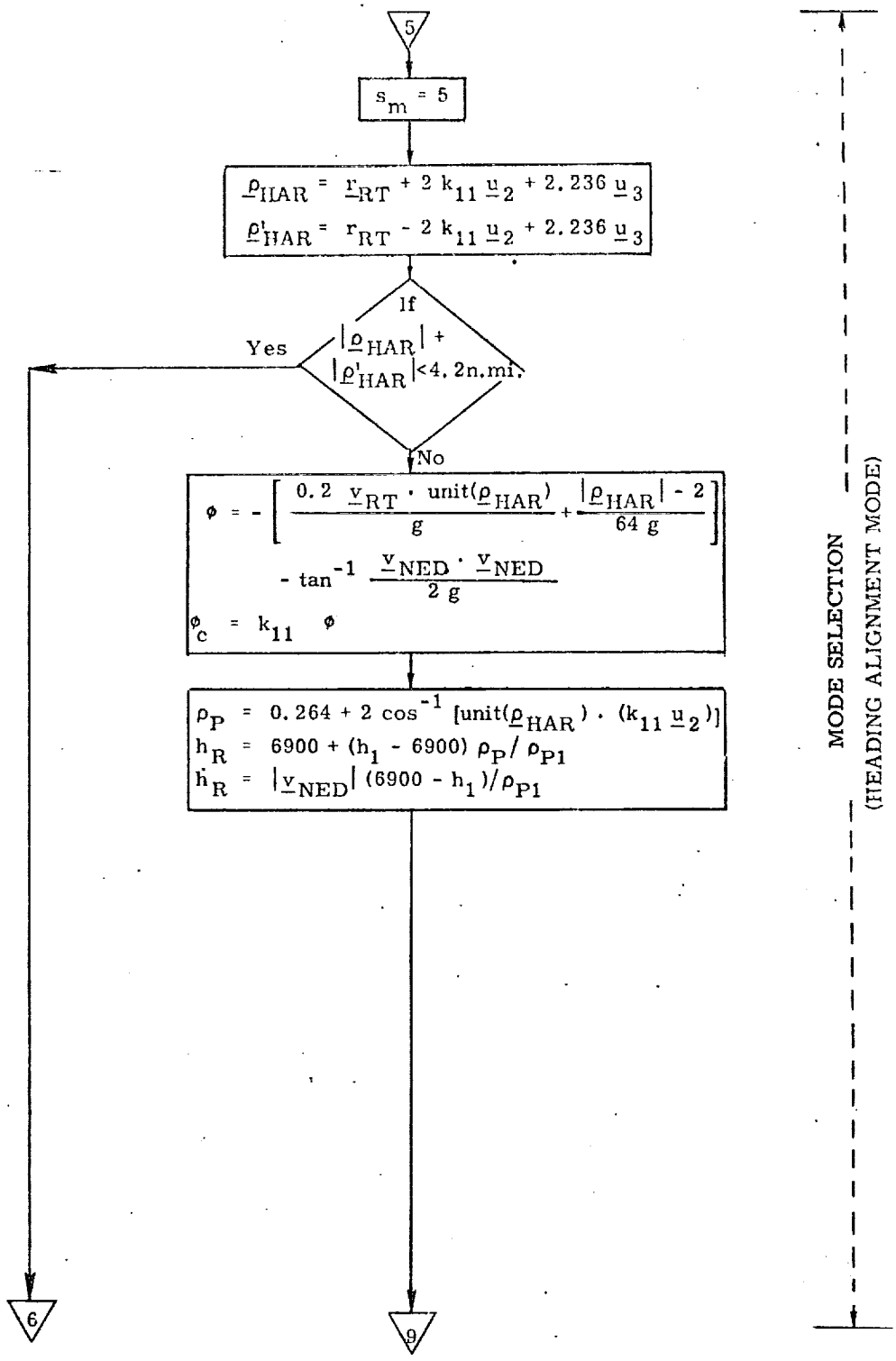


(Figure 4 i)

Figure 4g. Detailed Flow Diagram, Approach Guidance Routine

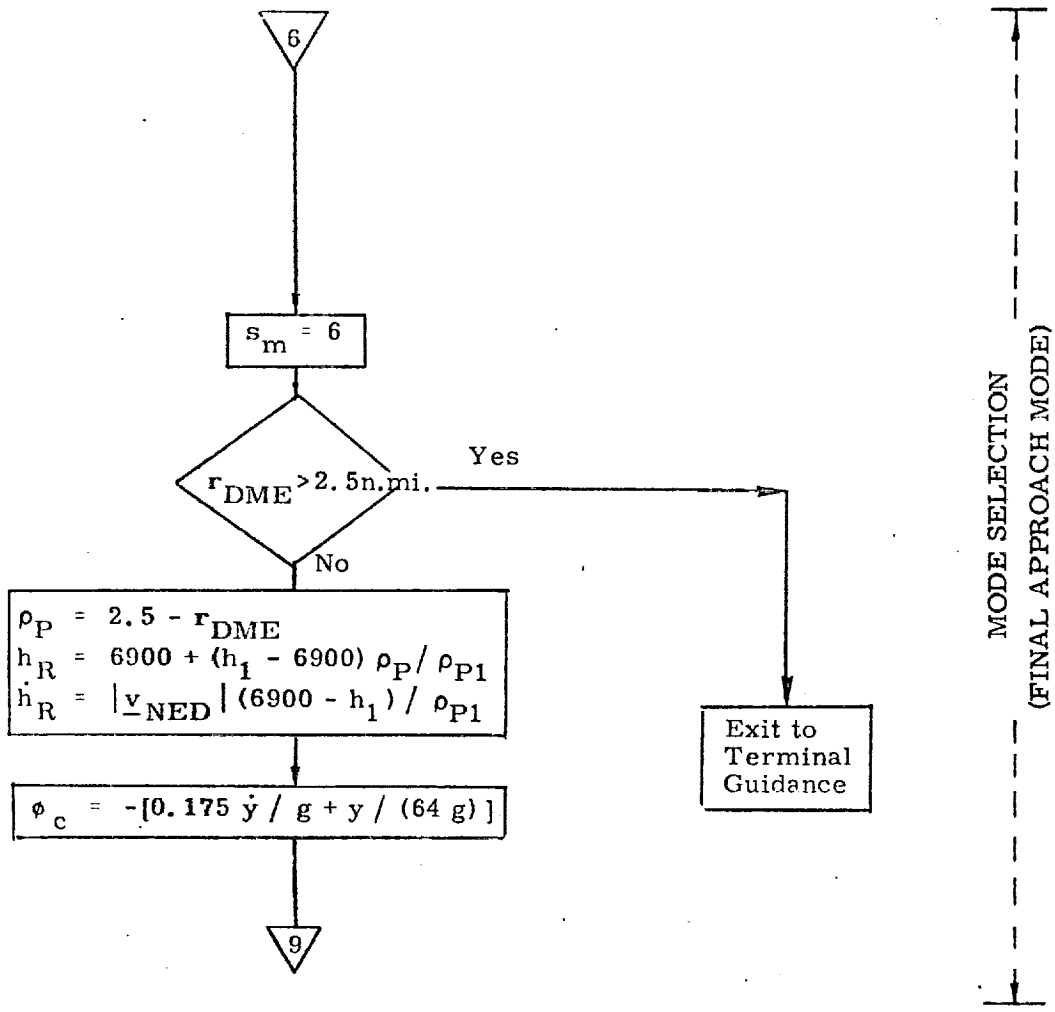


Figure 4h. Detailed Flow Diagram, Approach Guidance Routine

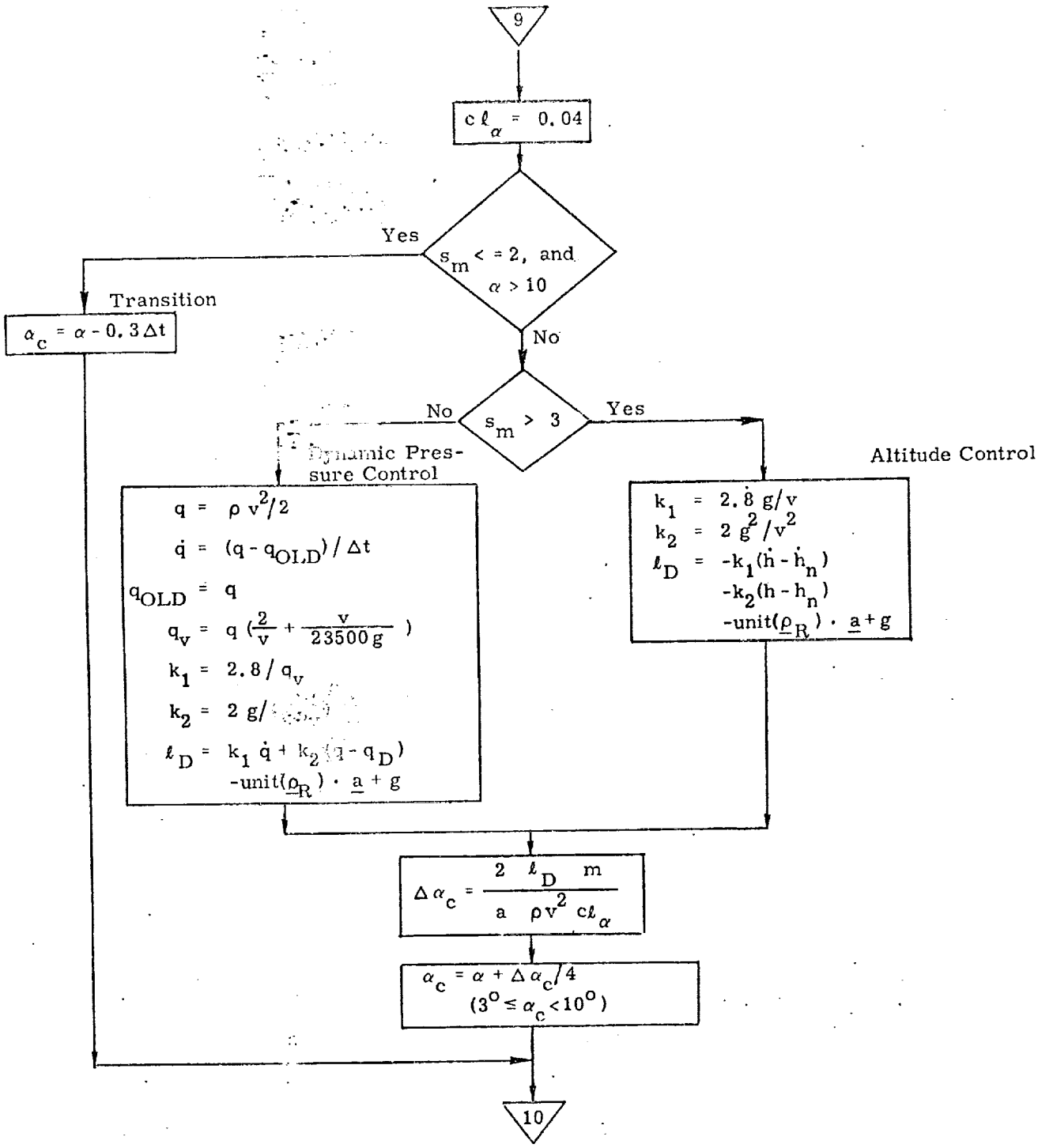


Figure 4i. Detailed Flow Diagram, Approach Guidance Routine

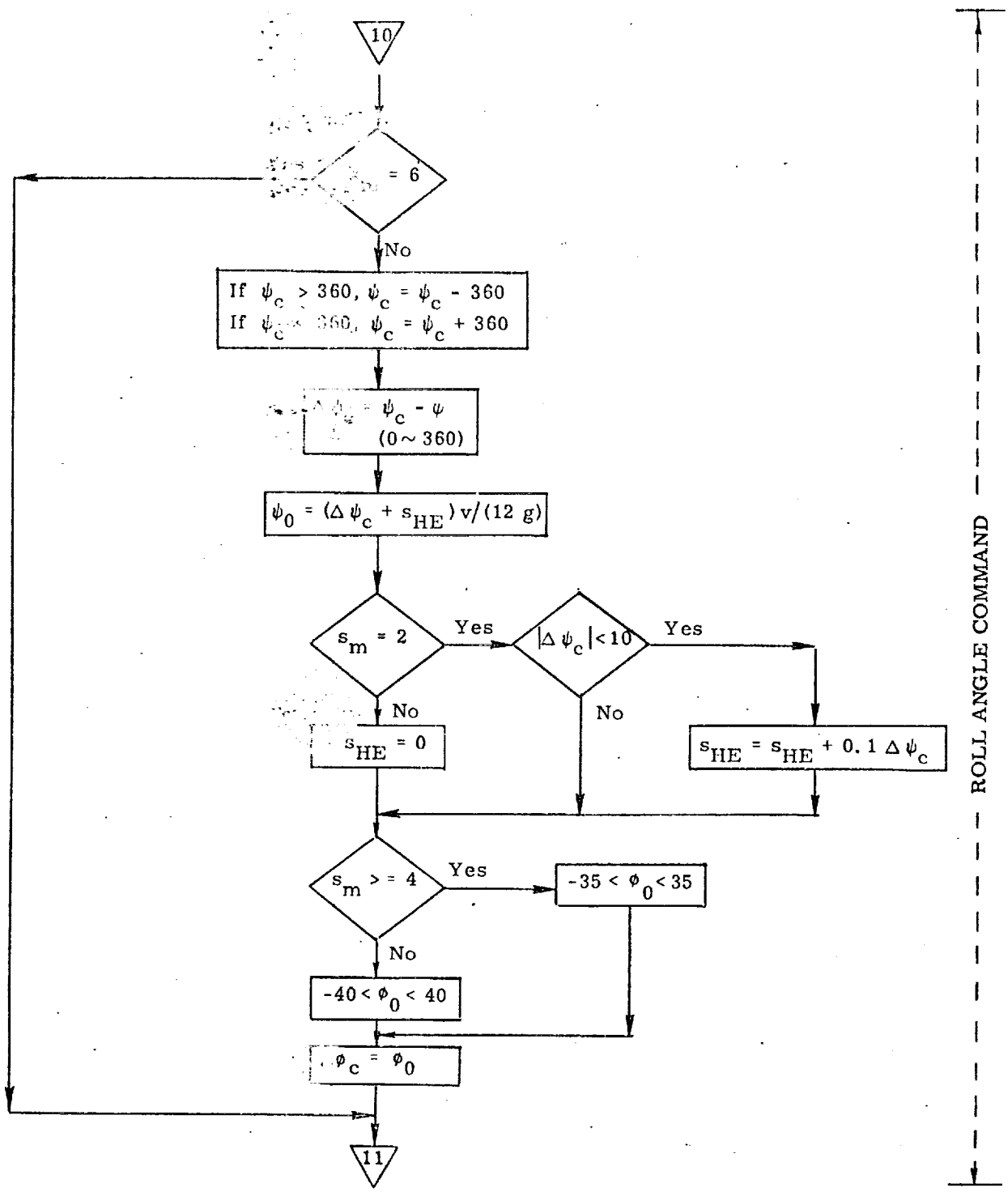


Figure 4j. Detailed Flow Diagram, Approach Guidance Routine

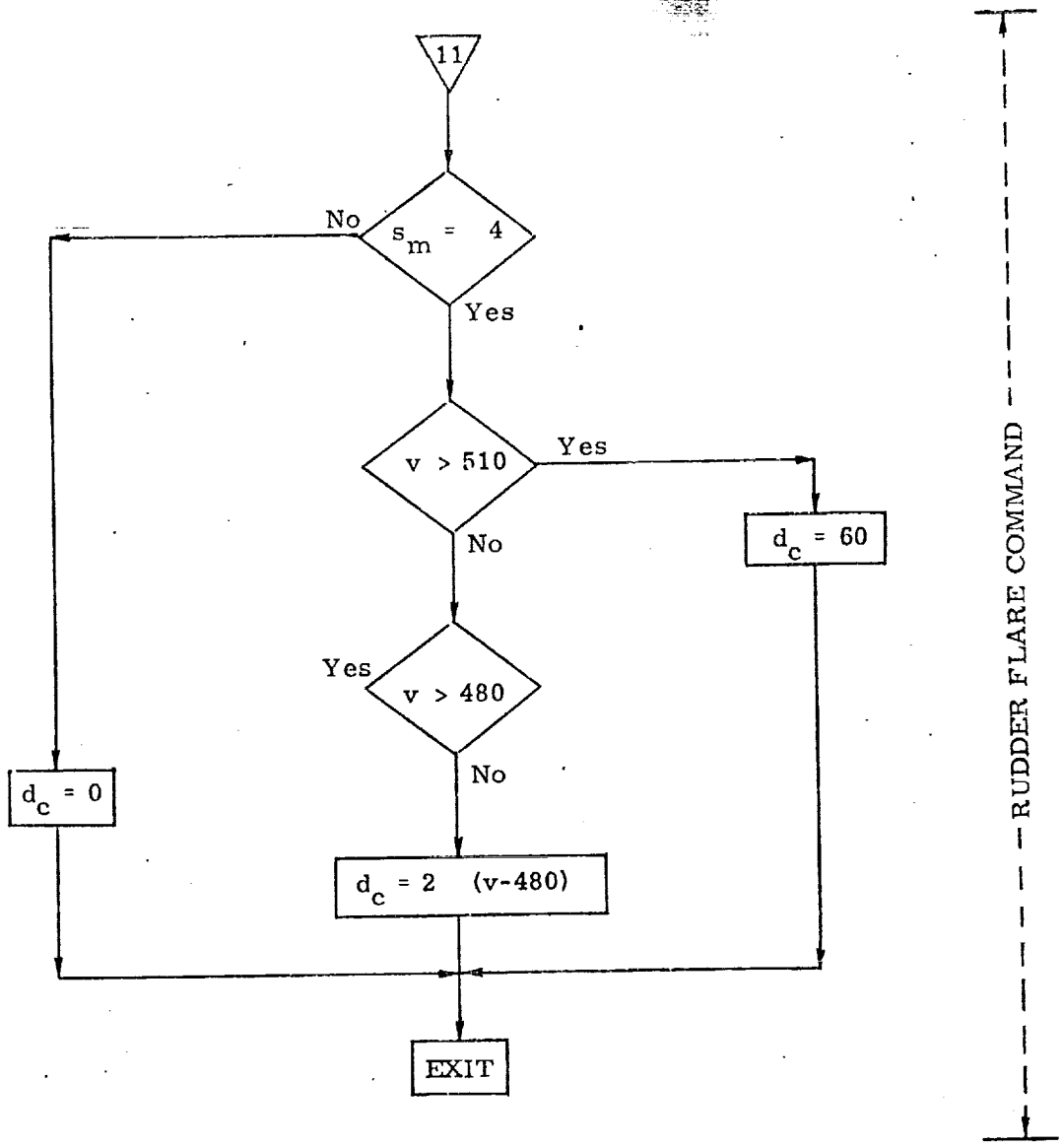


Figure 4k. Detailed Flow Diagram, Approach Guidance Routine

## REFERENCES


1. Deyst, J., Tao, M., "Approach Phase Guidance System", MIT Draper Lab, 23A STS Memo No. 11-A, September 1972.

2. Eterno, J., "Terminal Area Guidance for the Delta-Wing Orbiter", CG43-71M-89.

Submittal 60: Energy Dissipation Rate Guidance for Approach Phase

## 1. INTRODUCTION

The Approach-Guidance Routine presented here is designed to take the orbiter vehicle from the end of the Entry Phase (altitude ≈100,000 ft) to the start of the Final Landing maneuver (altitude ≈7000 ft). A detailed description of the guidance concept along with simulation results demonstrating its feasibility is given in Ref. (1).

The Approach-Guidance system is a closed-feedback-loop scheme. The vehicle energy is managed by controlling the rate at which energy is dissipated during a straight-in approach flight. Energy dissipation rate is controlled by flying at a constant value of dynamic pressure and varying the vehicle's lift to drag ratio with the Rudder Flare and or other available drag-increasing devices (e.g. body flap).

The complete approach flight consists of straight, fixed-length segments from the vehicle's initial position to the airport's main navigational facility (VOR, TACAN) or a suitable artificial checkpoint, then to a point in the final approach plane (intersection point) where the final flight path is intercepted, then straight towards the runway until the Final Landing Guidance System takes over (Outer Marker). Constant-bank turns link the straight flight segments.

The closed-loop energy management policy automatically compensates for any wind component that may affect the energy dissipation rate of the vehicle.

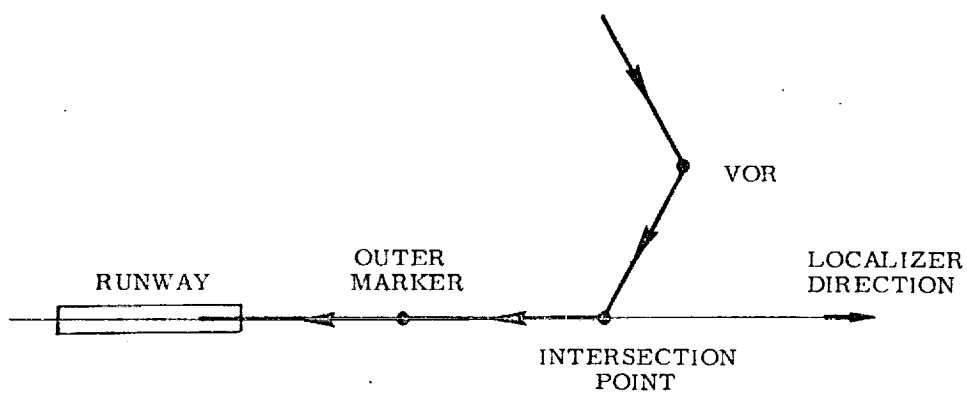

## NOMENCLATURE

Notational Conventions

Lower-case and Greek letters reserved for scalars and vectors

Vector quantities are underlined, e.g. $\underline{x}$

Components of a vector $\underline{x}$ are denoted $x_1, x_2, x_3$

Symbols

| | |
|---|---|
| $a_{TAC}$ | Azimuth of VORTAC |
| $d_{INT}$ | Distance from touchdown point to final approach plane intersection point |
| $d_{OM}$ | Distance from touchdown point to initiation of landing guidance system |
| $d_{TAC}$ | Distance from touchdown point to VORTAC |
| $e$ | Current vehicle energy |
| $e_1, e_2, e_3$ | Desired vehicle energy at target points |
| $e_{OLD}$ | Value of vehicle energy at previous guidance pass |
| $\dot{e}$ | Current vehicle energy dissipation rate |
| $\dot{e}_D$ | Desired value of vehicle energy dissipation rate |
| $\dot{e}_{IN}$ | Value of $\dot{e}_D$ at which flyover mode is entered |
| $\dot{e}_{OUT}$ | Value of $\dot{e}_D$ at which flyover mode is left |

| | |
|---|---|
| $\dot{e}_{MIN}$ | Upper limit of preferred $\dot{e}_D$ region |
| $\dot{e}_{MAX}$ | Lower limit of preferred $\dot{e}_D$ region |
| $g$ | Gravitational constant at sea level |
| $i$ | Current target index variable |
| $\underline{i}_{DH}$ | Unit vector in direction of difference between horizontal components of vehicle and target position vectors |
| $\underline{i}_{VH}$ | Unit vector in direction of horizontal component of velocity w.r.t. touchdown point |
| $k_E$ | Longitudinal channel coefficient |
| $k_L$ | Roll channel coefficient |
| $k_P$ | Vertical (pitch) channel coefficient |
| $\ell_1, \ell_2, \ell_3$ | Horizontal distances from target points at which target switching is to occur |
| $q$ | Current value of dynamic pressure |
| $q_D$ | Desired value of dynamic pressure |
| $\underline{r}_{RT}$ | Vehicle position vector w.r.t. the touchdown point |
| $\underline{r}_1, \underline{r}_2, \underline{r}_3$ | Target points position vectors w.r.t. the touchdown point |
| $\underline{r}_{DH}$ | Vector difference between the horizontal components of vehicle and target position vectors |
| $\underline{r}_{OLD}$ | Vehicle position vector at previous guidance pass |
| $s_{FO}$ | Switch indicating flyover mode is in effect |

| | |
|---|---|
| $s_{FP}$ | Switch indicating this is the first pass |
| $\underline{v}_{RT}$ | Vehicle velocity w. r. t. the touchdown point |
| $\underline{v}_{H}$ | Horizontal projection of velocity vector |
| $\alpha_{CMAX}$ | Maximum permissible angle of attack |
| $\alpha_{CMIN}$ | Minimum permissible angle of attack |
| $\gamma$ | Flight path angle |
| $\dot{\delta}_{RC}$ | Command Rudder Flare deployment angle rate |
| $\dot{\delta}_{RCL}$ | Maximum Rudder Flare deployment angle rate |
| $\Delta\psi$ | Heading error |
| $\theta_{C}$ | Command vehicle pitch angle |
| $\theta_{CMINT}$ | Minimum pitch angle during transition |
| $\theta_{CMC}$ | Current lower limit for command pitch angle |
| $\theta_{CM}$ | Corrected minimum limit for command pitch angle |
| $\theta_{CMAX}$ | Maximum command pitch angle |
| $\phi_{C}$ | Command roll angle |
| $\phi_{CMAX}$ | Maximum command roll angle magnitude |

Special Notation

| | |
|---|---|
| Sign ( ) | Algebraic sign associated with ( ). Value is +1 or -1, with sign (0) = +1 |
| max ( ) | The maximum of all element enclosed in ( ) |

| | |
|---|---|
| min ( ) | The minimum of all elements enclosed in ( ) |
| $\lvert ( \ ) \rvert$ | Magnitude of ( ) |

## 2. FUNCTIONAL FLOW DIAGRAM

The basic information flow for the Approach Guidance Routine is shown in Figure 1. This is based on the guidance concept of Ref. (1).

The guidance task is made up of three independent channels:

1. The pitch angle command is proportional to the difference between the desired and measured dynamic pressure. This command is limited so as to limit the pitch-down during the transition maneuver and the maximum and minimum angles of attack.

2. The desired energy dissipation rate is computed as the ratio of energy-to-be-dissipated to the distance-to-go. The Rudder Flare deployment angle rate is proportional to the difference between the desired and the actual energy dissipation rates. A discrete rate controller is superposed in order to drive the desired dissipation rate to a "preferred" value range.

3. The roll angle command is proportional to the difference between the horizontal velocity direction and the horizontal direction from the vehicle position to the target point.

The three channels guide the vehicle sequentially to three target points. Switchover from one target to the next is made at a predetermined horizontal distance from the current target.

The longitudinal channel (No. 2) is inhibited when the vehicle is initially too close to the first target (desired energy dissipation rate exceeds the maximum available). The guidance is then in "flyover" mode. Target switching is also inhibited in this mode.

---

1. Elias, A., "New Approach Guidance Concept for Shuttle", 23A STS Memo No. 58-72, 4 December 1972, MIT/CSDL.

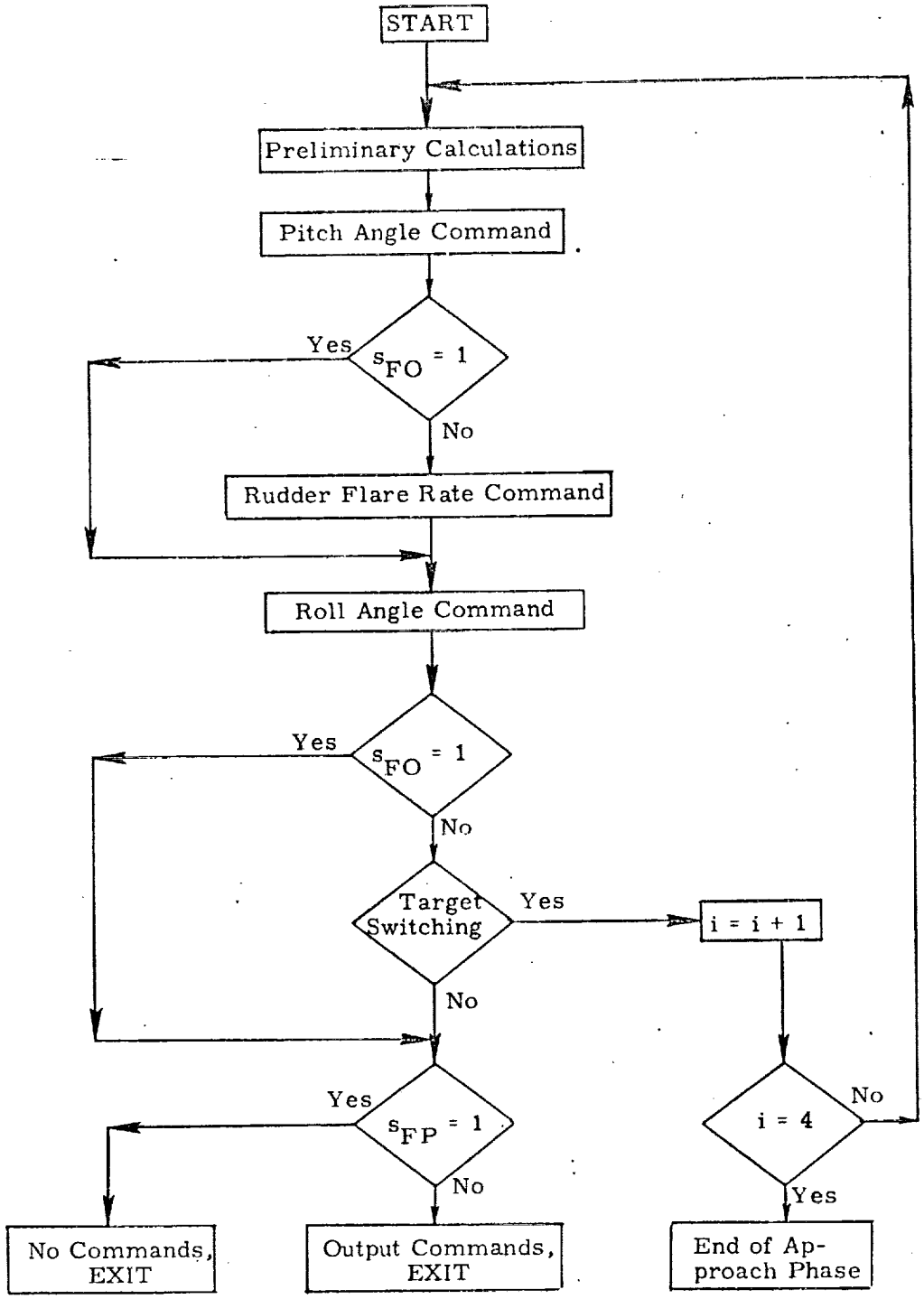


Figure 1. Functional Flow Diagram for Approach Guidance

## 3. INPUT AND OUTPUT VARIABLES

### Input Variables

$\underline{r}_{RT}$ Vehicle position w.r.t. touchdown point (touchdown point coordinates: x-up, z-downrange, y-crosstrack)

$\underline{v}_{RT}$ Vehicle velocity w.r.t. touchdown point (touchdown point coordinates)

$q$ Measured value of Dynamic Pressure

### Output Variables

$\theta_C$ Pitch angle command

$\dot{\delta}_C$ Rudder Flare Deflection angle rate command

$\phi_C$ Roll angle command

## 4. DESCRIPTION OF EQUATIONS

### 4.1 Initial Target Calculations

During the initial pass, the target point horizontal position vectors are constructed from their distances to the touchdown point and the VORTAC azimuth w.r.t. the localizer direction:

VORTAC: $\underline{r}_1 = (0, -d_{TAC} \sin a_{TAC}, -d_{TAC} \cos a_{TAC})$

Intersection: $\underline{r}_2 = (0, 0, -d_{INT})$

Outer Marker: $\underline{r}_3 = (0, 0, -d_{OM})$

Also, the following initialization tasks are performed:

1. Flyover mode switch off — $s_{FO} = 0$,
2. Initial pass switch on — $s_{FP} = 1$,
3. Pitch limit = transition pitch limit (it is assumed that the guidance system is initiated with the vehicle flying on the back side of the L/D curve),
4. The target index $i$ is set to 1 (VORTAC)
5. The "old" values of $e$ and $\underline{r}_{RT}$ are set to zero. This makes the back-difference algorithm of section 4.4 invalid during the first pass, so commands are not issued until the second pass.

### 4.2 Preliminary Calculations

At the beginning of every guidance pass, the flight path angle and horizontal vector from vehicle to target are computed:

$$\gamma = \tan^{-1}\left(v_{RT_1} / \sqrt{v_{RT_2}^2 - v_{RT_3}^2}\right)$$

$$\underline{r}_{DH} = (0, r_{i_2} - r_{RT_2}, r_{i_3} - r_{RT_3})$$

### 4.3 Vertical Channel

The command pitch angle is:

$$\theta_C = k_P(q_D - q)$$

The lower limit for the command pitch angle is the largest of:

1. The current absolute pitch minimum, $\theta_{CMC}$
2. The pitch angle corresponding to the minimum angle of attack, $\gamma + \alpha_{CMIN}$.

The upper limit for the command pitch angle is the pitch angle corresponding to the maximum angle of attack, $\gamma + \alpha_{CMAX}$.

The current absolute pitch minimum is set to $\theta_{CMINT}$ during the transition maneuver, and to an arbitrary low value (e.g. -1 rad.) after the dynamic pressure reaches the desired value for the first time (i.e. at the end of the transition pitch-down).

4.4 Longitudinal Control

The current vehicle energy is computed from the position and velocity:

$$e = r_{RT_1} - (\underline{v}_{RT} \cdot \underline{v}_{RT})/2g$$

The current energy dissipation rate is computed as the back-difference:

$$\dot{e} = \frac{e - e_{OLD}}{\sqrt{(r_{RT_2} - r_{OLD_2})^2 - (r_{RT_3} - r_{OLD_3})^2}}$$

then the values of $e_{OLD}$ and $\underline{r}_{OLD}$ are updated.

The desired value of the energy dissipation rate is then calculated.

$$\dot{e}_D = (e_i - e)/ \left| \underline{r}_{DH} \right|$$

and a Rudder Flare rate is commanded proportional to the difference between desired and actual dissipation rates:

$$\dot{\delta}_{RC} = k_E (\dot{e}_D - \dot{e})$$

this rate is then limited to the $-\dot{\delta}_{RCL}$, $\dot{\delta}_{RCL}$ range. This command is overriden if the value of $e_D$ falls outside of a "preferred" range:

$$\text{if } \dot{e}_D > \dot{e}_{MIN}, \dot{\delta}_{RC} = -\dot{\delta}_{RCL}$$
$$\text{if } \dot{e}_D < \dot{e}_{MAX}, \dot{\delta}_{RC} = \dot{\delta}_{RCL}$$

The "flyover" mode is enabled when $\dot{e}_D$ is lower than $\dot{e}_{IN}$, and is disabled when $\dot{e}_D$ reaches $\dot{e}_{OUT}$. When the "flyover" mode is enabled, the command rudder flare rate is zero.

## 4.5 Lateral Channel

Two unit vectors are computed:

$$\underline{i}_{VH} = \frac{\underline{v}_{RT}}{|\underline{v}_{RT}|} \quad \text{is in the current vehicle heading direction}$$

$$\underline{i}_{DH} = \frac{\underline{r}_{DH}}{|\underline{r}_{DH}|} \quad \text{is in the direction from the vehicle to the target}$$

The dot product of these vectors is the cosine of the angle difference between the desired and the actual headings. In order to resolve the sign indetermination of the $\cos^{-1}$ function, the single component of the cross product

$$\underline{i}_{DH} \times \underline{i}_{VH} = i_{DH_2}\, i_{VH_3} - i_{DH_3}\, i_{VH_2}$$

is computed. This is the sine of the heading difference, and its sign is used to resolve the indetermination.

This command roll angle is then calculated:

$$\phi_C = k_L\, \Delta\psi$$

This command is limited to the $-\phi_{CMAX}$, $\phi_{CMAX}$ range.

## 4.6 Target Switching

The target index variable, is incremented when the horizontal distance to the current target reaches the target's switching value. When the last target's switching distance is reached, (i = 4), the Approach Guidance is terminated. Target switching is inhibited during the "flyover" mode ($s_{FO} = 1$).

Commands are not issued during the first pass.

## 5. DETAILED FLOW DIAGRAMS

This section contains detailed flow diagrams of the Approach Guidance Routine.

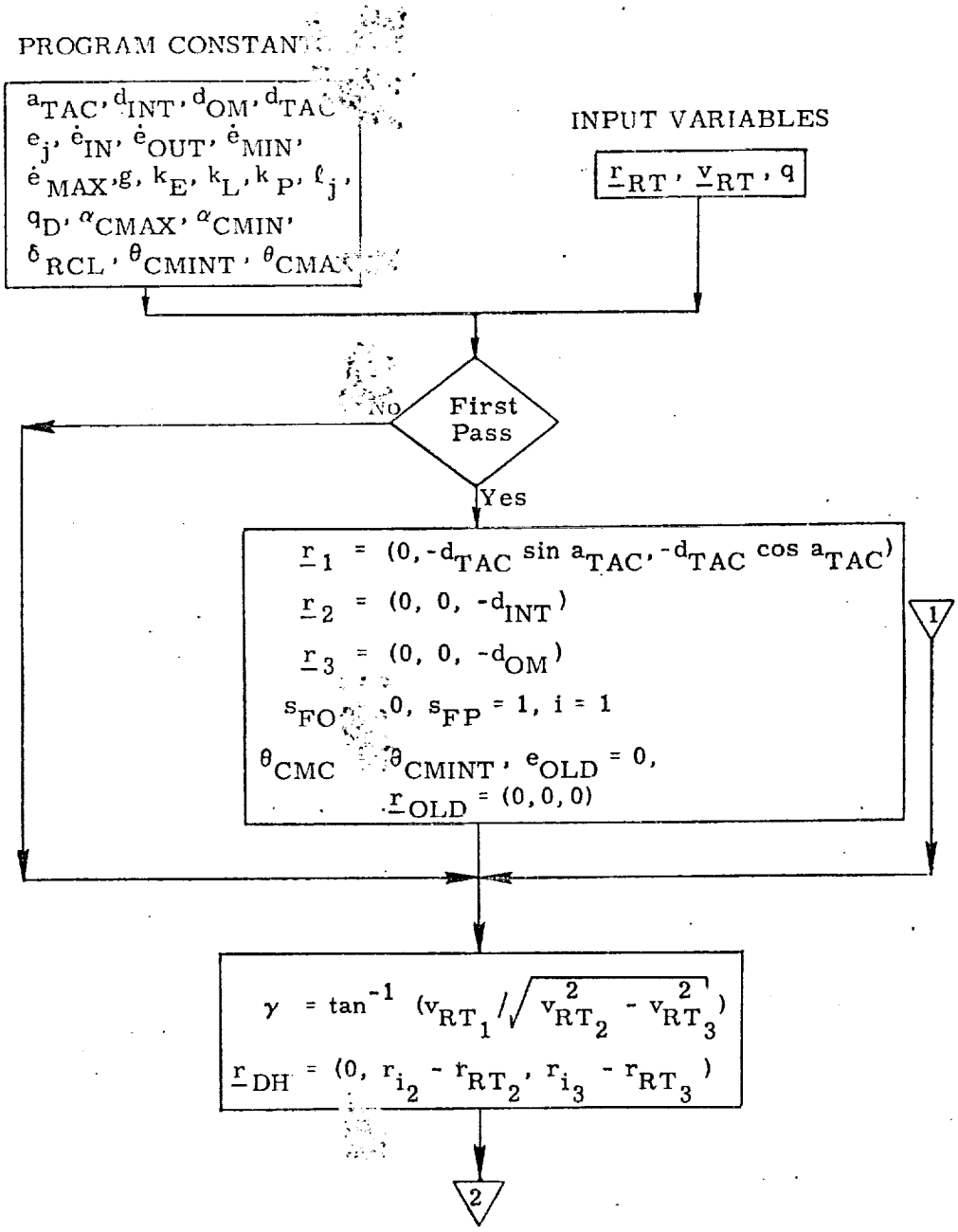


Figure 2a. Approach Guidance Routine, Detailed Flow Diagram

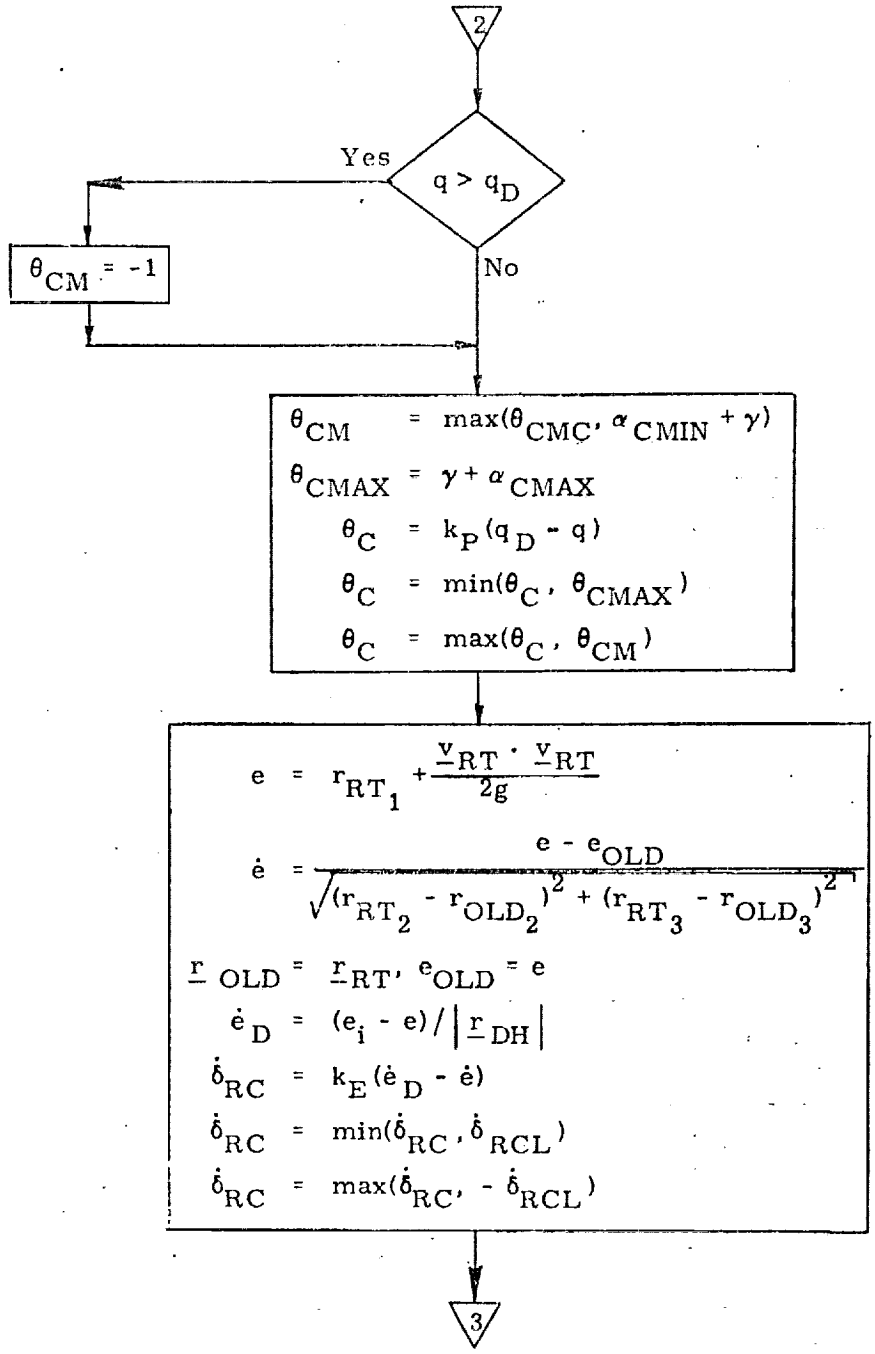


Figure 2b. Approach Guidance Routine, Detailed Flow Diagram

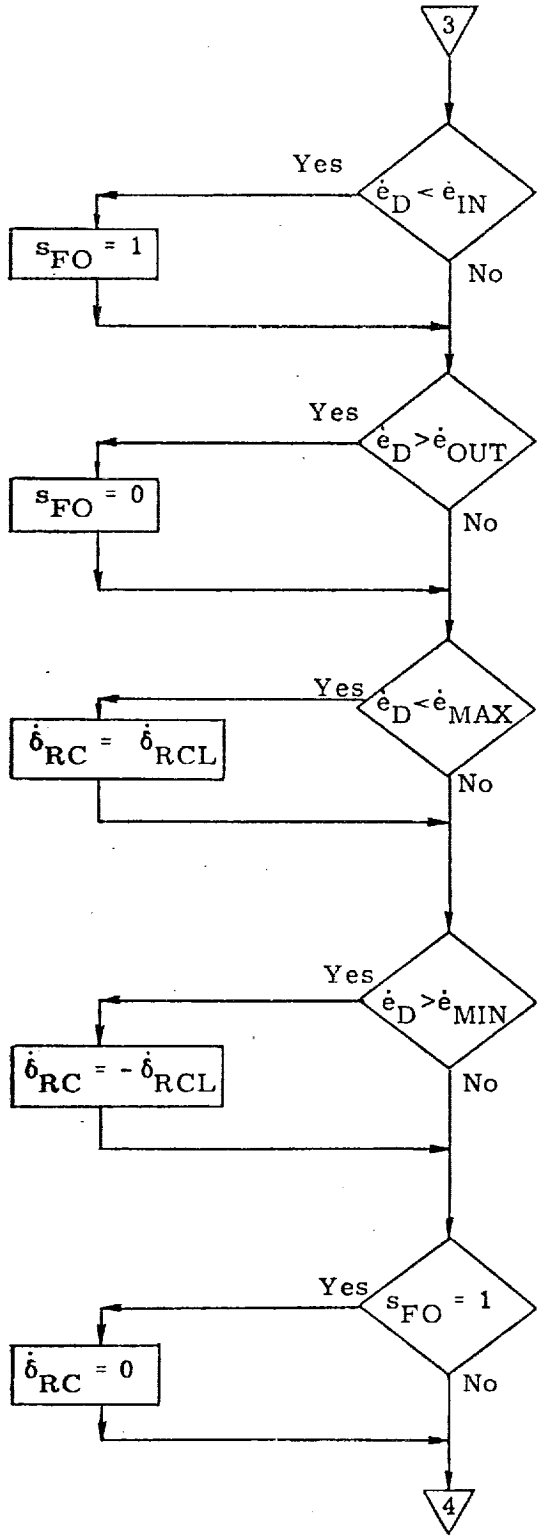


Figure 2c. Approach Guidance Routine, Detailed Flow Diagram

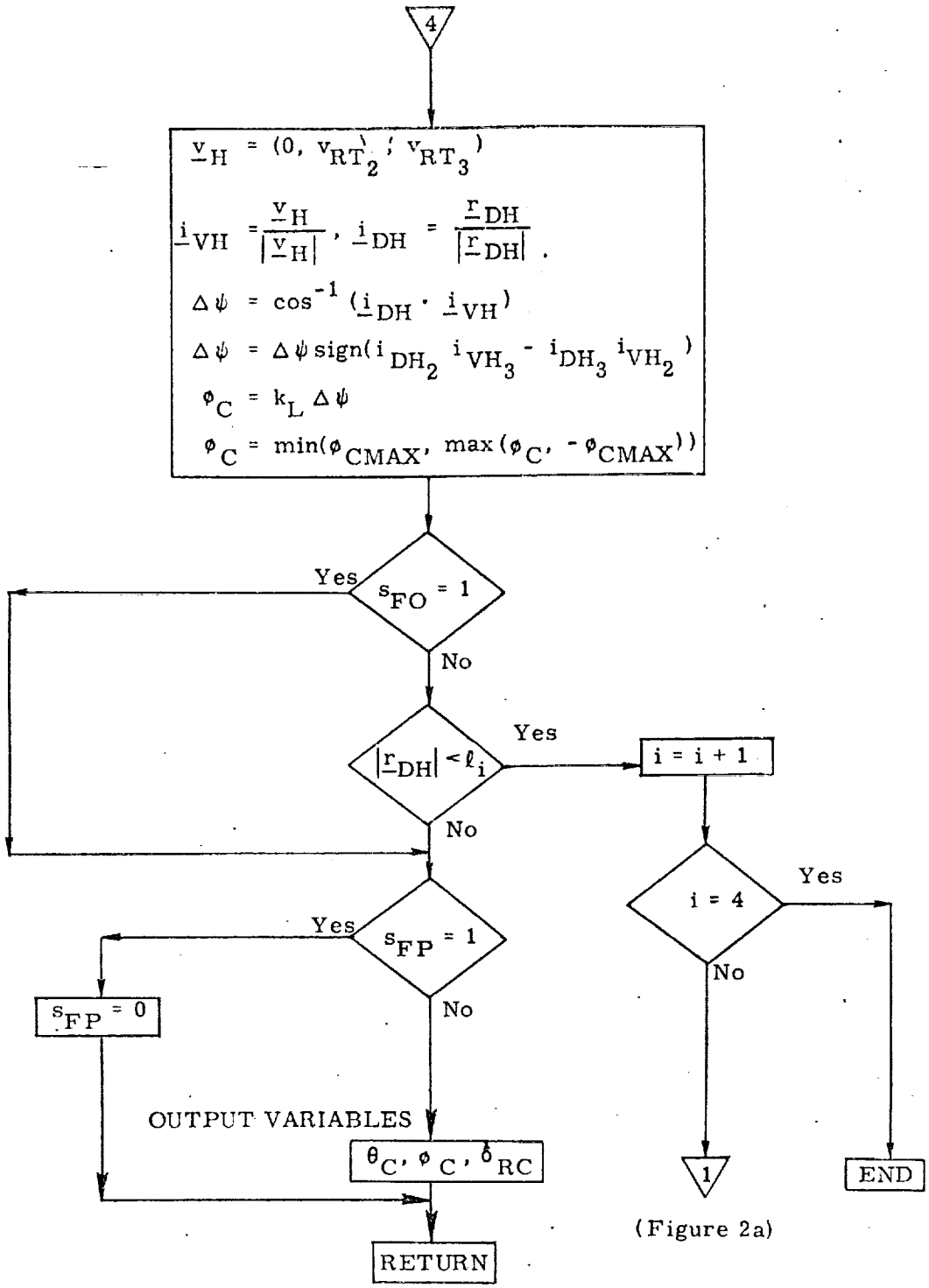


(Figure 2a)

Figure 2d. Approach Guidance Routine, Detailed Flow Diagram

## Submittal 29: Final Approach Guidance

### Introduction

These equations are submitted as candidates to fulfill the unpowered Final Approach Guidance requirements for the space-shuttle Orbiter. They include Autoland lateral and longitudinal guidance equations. The scheme is all inertial; navigations aids are used only to update the navigated vehicle state. Pitch rate and speed-brake commands are computed and issued to control in-plane approach. Lateral position error and its integral plus heading-angle error are used to form the vehicle roll command. (There is no decrab or wings level maneuver; the assumption is made that the gear is designed to accommodate the stress of crabbed landings in design winds).

### Functional Diagram

Figure 1 is a functional diagram. Figure 2 is a block diagram. (For general information, the autopilots being used in simulation runs are included in Figure 2.)

Inputs to the Guidance module are from the Final Approach and Guidance Navigation module; the inputs are the navigated state in the Earth-fixed landing coordinate system. From this are calculated the range to touchdown target, altitude, velocity magnitude, flight-path angle lateral position and heading angle. Outputs are pitch rate command, speed-brake position command and vehicle roll command to the autopilot. The guidance roll command drives a roll-rate aileron-autopilot inner loop with roll attitude outer loop. Roll rate command is interconnected to a rate command rudder autopilot with turn coordination and normal acceleration inputs. The acceleration and heading-angle signals are instrumental in holding the orbiter to the final approach plane in crosswinds.

### Coordinate System

The autoland guidance uses vehicle position and velocity relative to a runway coordinate system, as shown in Figure 3. Figure 3 also indicates longitudinal sign convention for the equations. The "altitude of the IMU" at touchdown is represented in the equations as touchdown altitude.

### Equations and Flow

Figure 4 presents the detailed guidance equations. Autoland guidance is initiated with the vehicle established on the final approach path near the plane of the runway at 3000 to 10000 feet altitude. It is currently entered 8 times per second although little performance degradation is evident at half that frequency.

On the first call, an initialization and targeting section is entered. Targeting variables are used to define the flare, shallow glide, pull up and steep sections of the reference trajectory. A steep reference flight path angle is calculated such that the trajectory passes through the initial vehicle position. If, during the steep phase, navigation updates cause large vehicle altitude errors, the steep portion of the reference trajectory is retargeted to pass through the new vehicle position. A linear desired velocity profile is also computed from the vehicle's current velocity to a target value at the beginning of pull up.

Reference and actual values of h and $\gamma$ are differenced and drive the guidance loops shown in Figure 2. Since altitude is approximately equal to the integral of $V_j$, the velocity term in the denominator of the altitude error gain makes that loop insensitive to velocity variations. The inner loop controls $\dot{\gamma}$ which is proportional to h and provides damping for the outer loop. It is compensated with a second order digital filter which effectively cancels two undesirable pole-zero pairs arising from the autopilot-vehicle dynamics. This allows stable operation of the inner loop at a higher gain level and tighter closed loop control. The accuracy of the autoland maneuver is improved by injecting the open loop pitch rate commands $\dot{\gamma}_r$ and $q_{cop}$. The $q_{cop}$ signal is composed of three parts ($q_{cv}$, $q_{cm}$, $q_{cge}$) all of which are tuned to the specific vehicle being flown. The $q_{cm}$ term is a sinusodial pitch rate term added during pull up and again, with a different amplitude and period, during flare to lead the vehicle through these maneuvers. The $q_{cv}$ term ramps up to a constant value after the pull up maneuver and provides the increasing angle-of-attack necessary to maintain lift as the vehicle decelerates along the shallow slope. The $q_{cge}$ term ramps down to a constant value during the flare maneuver which helps the vehicle drive through the ground effects and minimizes runway float. Typical plots of these terms are sketched in Figure 2.

Lateral Guidance

The lateral guidance is all-inertial. A decrab maneuver was not studied; the assumption being that the gear is stressed for crabbed landings in design winds. The roll gain is halved during flare which levels the wings somewhat in steady-state crosswinds.

The lateral guidance equations are presented in Figure 4. On the initial pass, the roll gain, crossrange integral gain, and the heading gain are stored. On a normal pass the crossrange gain, $K_y$, is calculated as a function of velocity. When altitude becomes less than 50 ft, the roll command gain is decreased from 6 to 3 over a 2-second period. The roll command is the sum of a crossrange,

integral of crossrange, and velocity heading angle term. It is limited and issued to the autopilot.

Velocity Control

The speed brake is commanded to a position proportional to the sine of the velocity error. Zero error is at 30 degrees brake for bi-directional control. At the beginning of pull up the brake is completely retracted to eliminate pitch rates from transients near touchdown.

Constants/Variables Summary

Figure 6 summarizes variables and constants.

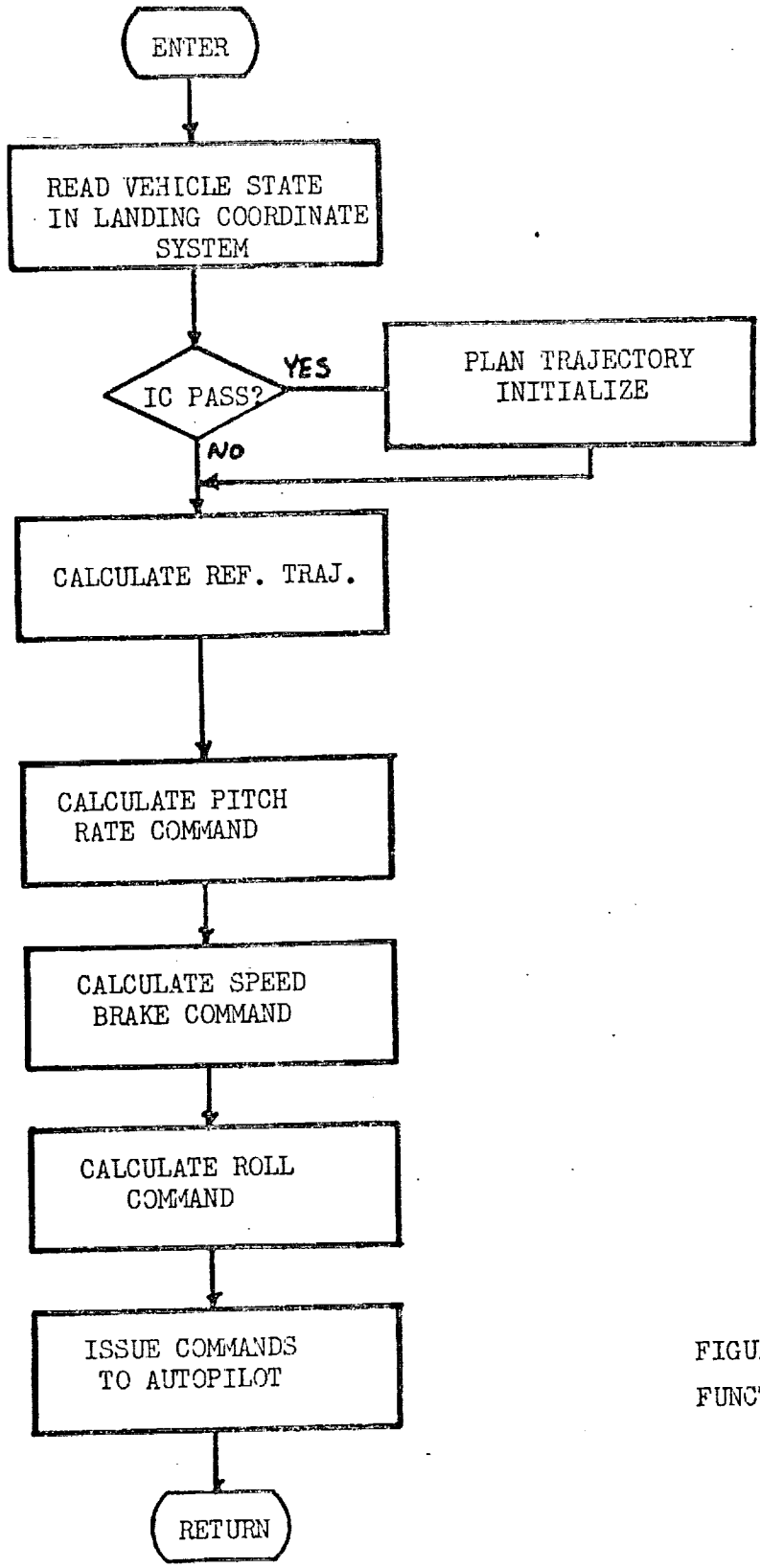


FIGURE I

FUNCTIONAL DIAGRAM

| Prepared | NAME Petrolas | DATE | LOCKHEED ELECTRONICS COMPANY HOUSTON AEROSPACE SYSTEMS DIVISION | Page | TEMP | PERM |
|---|---|---|---|---|---|---|
| Checked | | | TITLE FIGURE 2-1 AUTOLAND BLOCK DIAGRAM | Model | | |
| Approved | | | | Report No. | | |

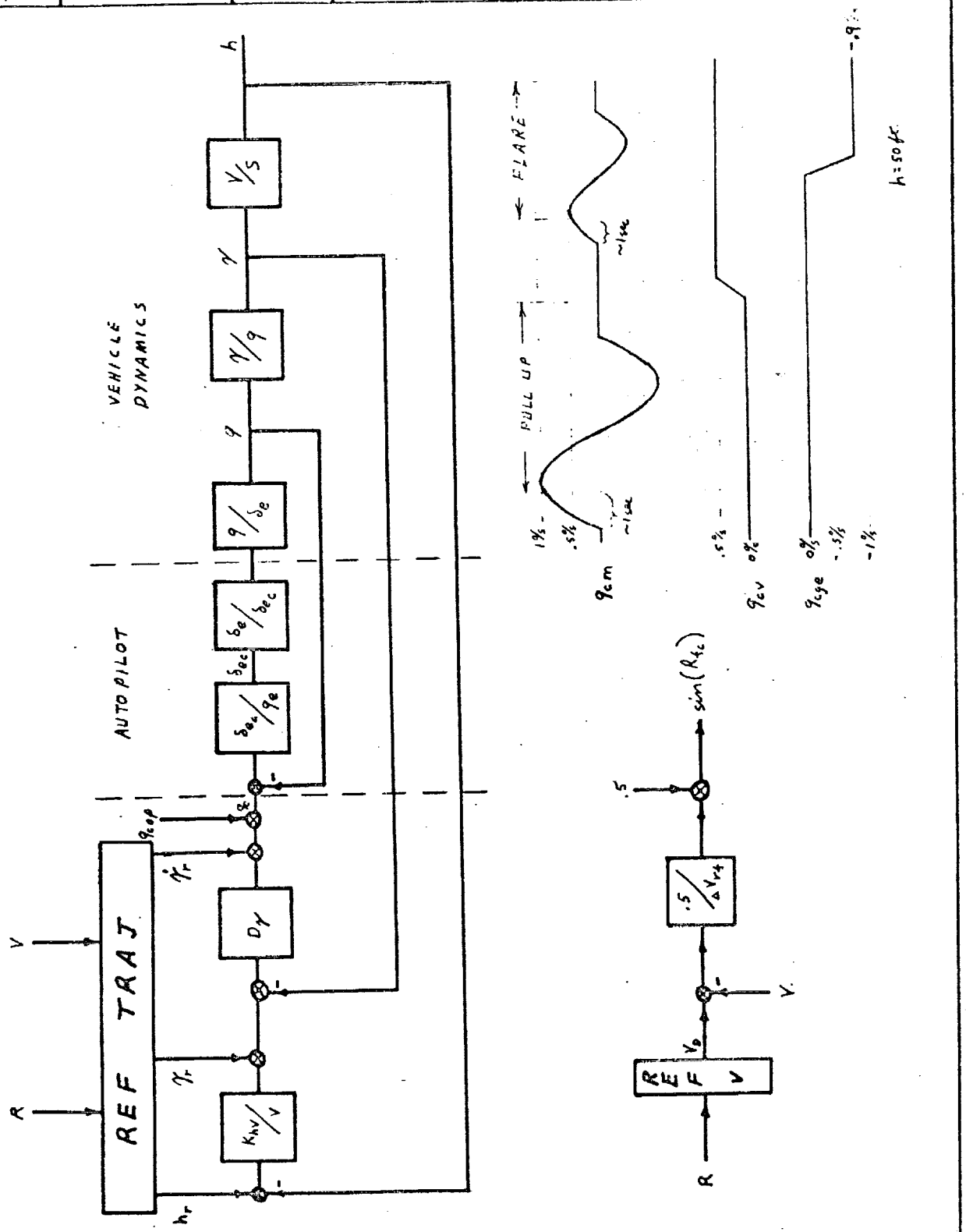




HASD 055

SION 1

$K_{hv} = .4$

$$D_\gamma = \frac{3.(z-.935)(z-.846)}{(z-.883)(z-.745)} \quad \text{for } T = \frac{1}{8} \text{ sec}$$

$$\delta_{ec}/q_e = \frac{1.4\,(z-.93)}{z} \quad \text{DAP } T = 1/8$$

$$\delta_e/\delta_{ec} = \frac{1}{1+.1S} \quad \text{actuator}$$

$$q/\delta_e = \frac{2.695\left(1+\frac{S}{.6188}\right)}{1+2\left(\frac{.5522}{.8586}\right)S+\left(\frac{S}{.8586}\right)^2}$$

$$\gamma/q = \frac{\left(1+\frac{S}{2.361}\right)\left(1-\frac{S}{2.636}\right)}{S\left(1+\frac{S}{.6188}\right)}$$

linearized at $V = 350$ fps used in gain determination only

| Prepared | NAME Petisdoe | DATE | LOCKHEED ELECTRONICS COMPANY HOUSTON AEROSPACE SYSTEMS DIVISION | Page | TEMP | PERM |
|---|---|---|---|---|---|---|
| Checked | | | TITLE FIGURE 2-3 AUTOLAND BLOCK DIAGRAM | Model | | |
| Approved | | | | Report No. | | |

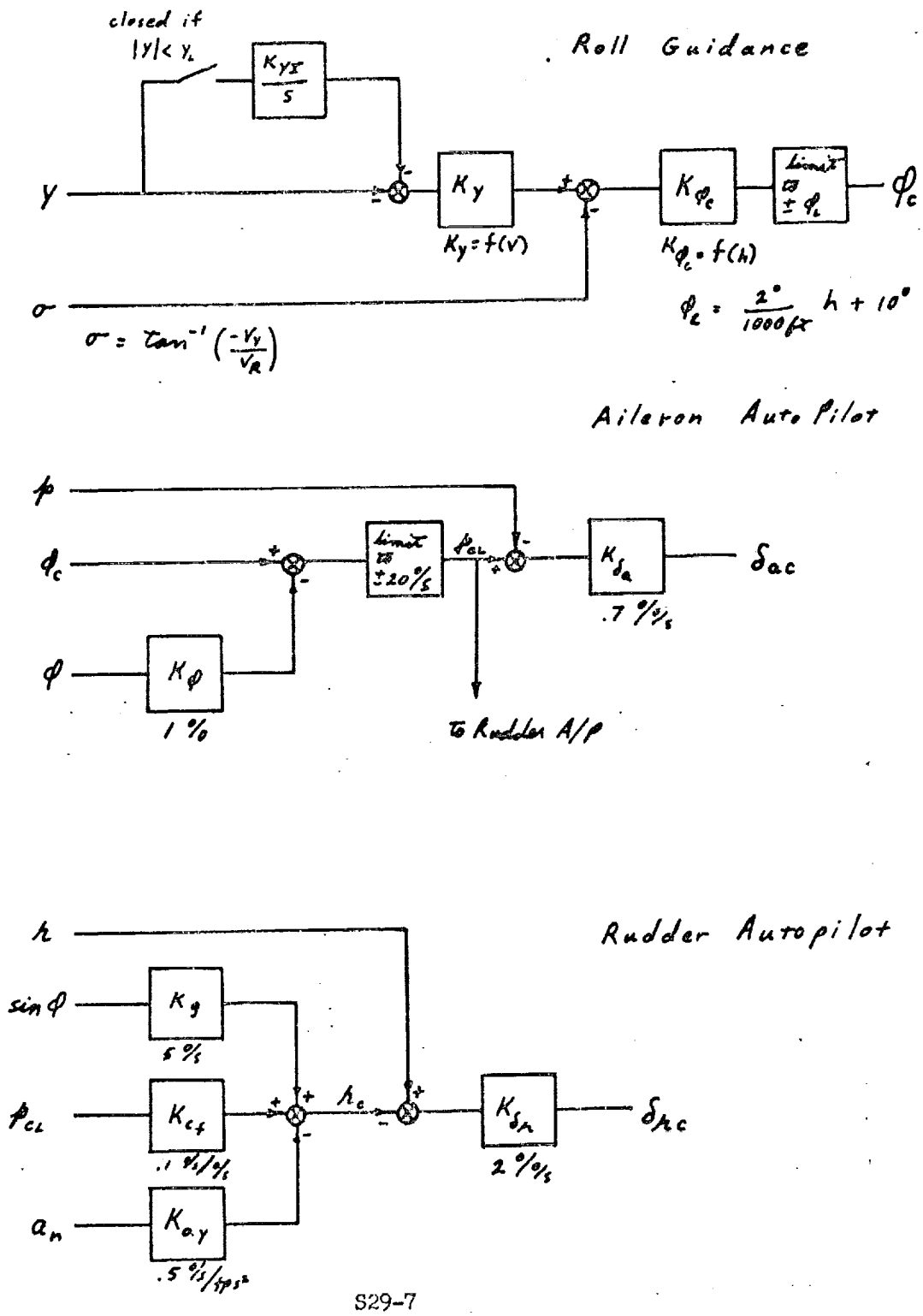




HASD 055

SION 1

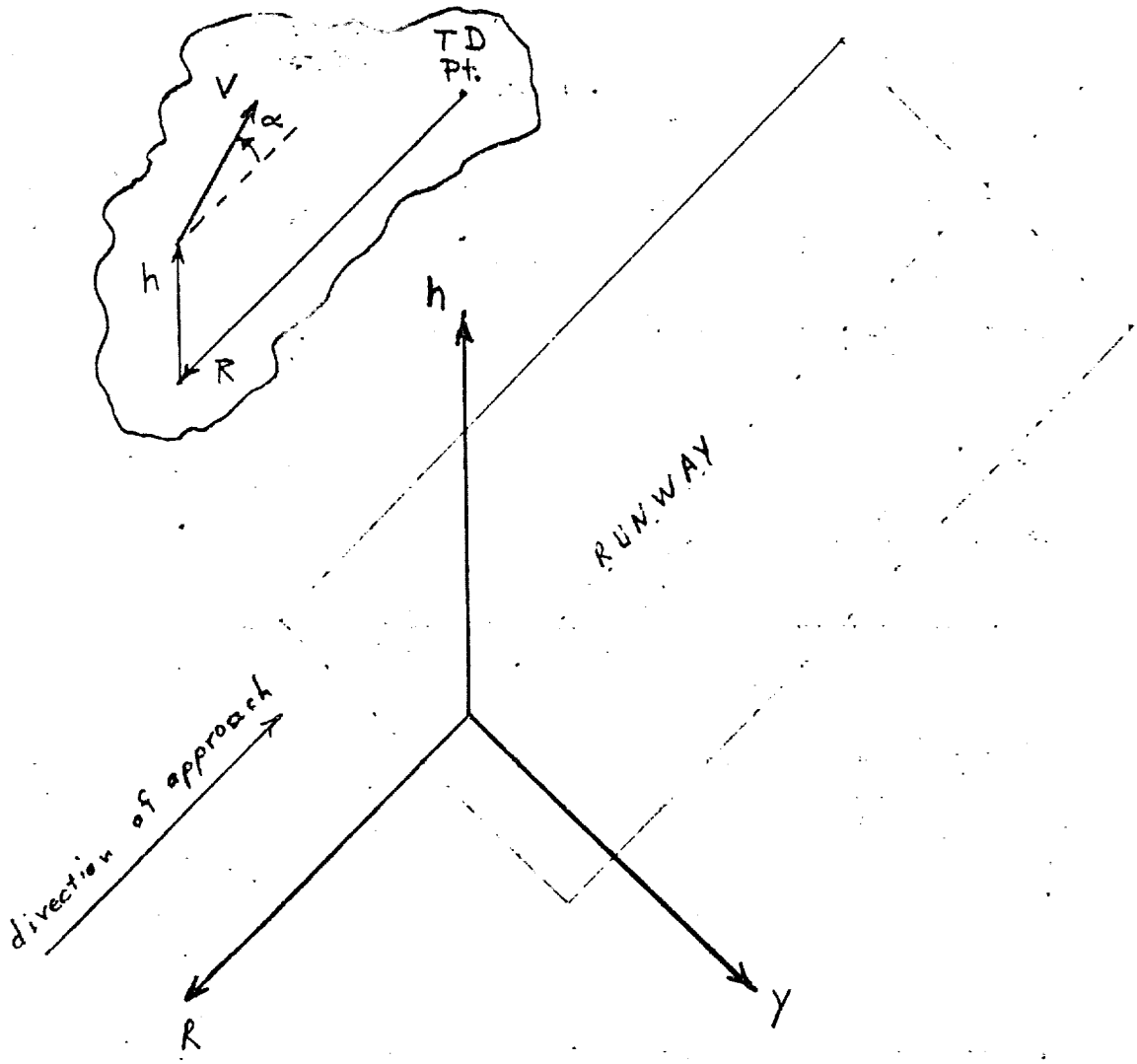


Figure 3. Runway Coordinate System

FIGURE 4-1

AUTOLAND EQUATIONS

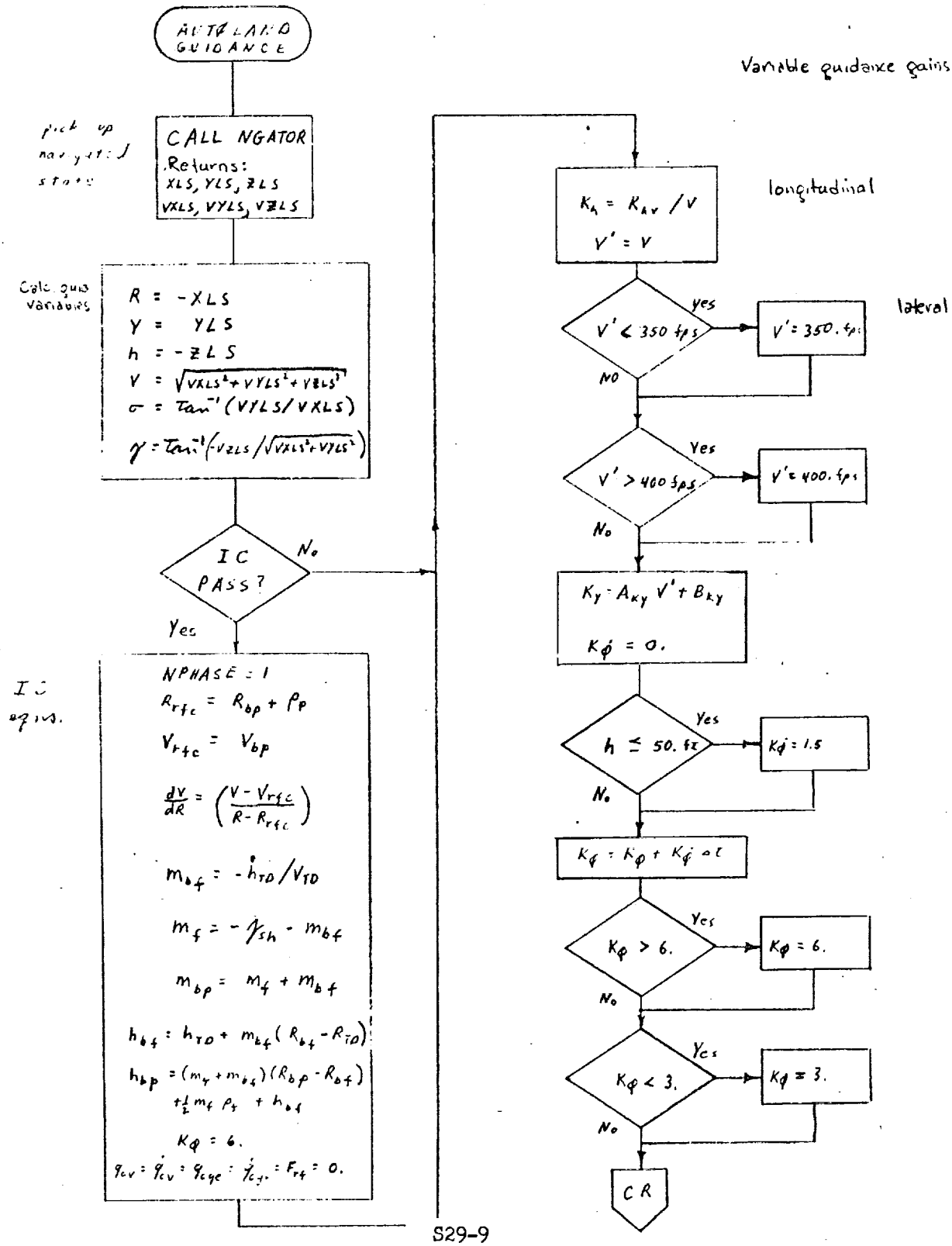

FIGURE 4-2
AUTOLAND EQUATIONS

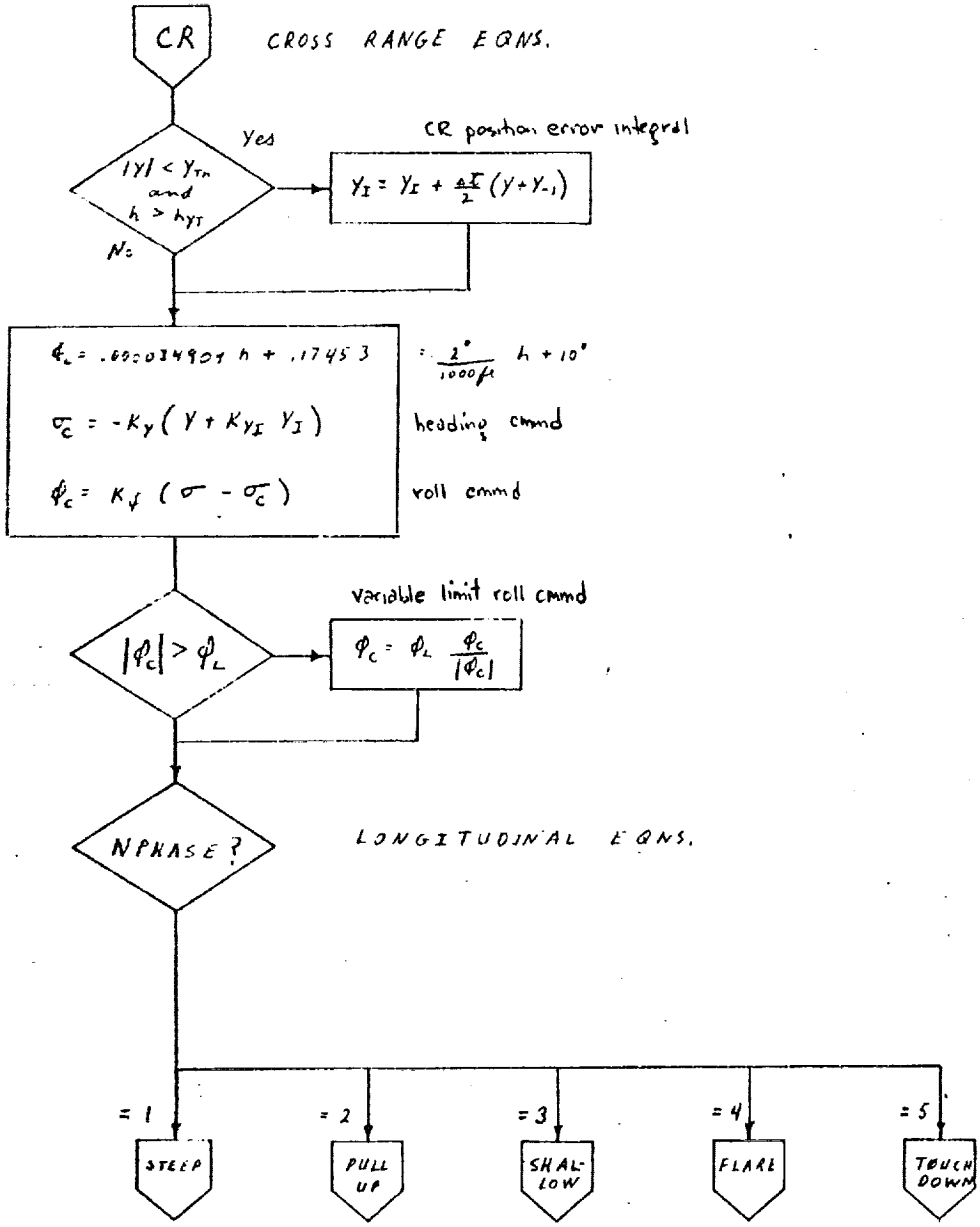

FIGURE 4-3

AUTOLAND EQUATIONS

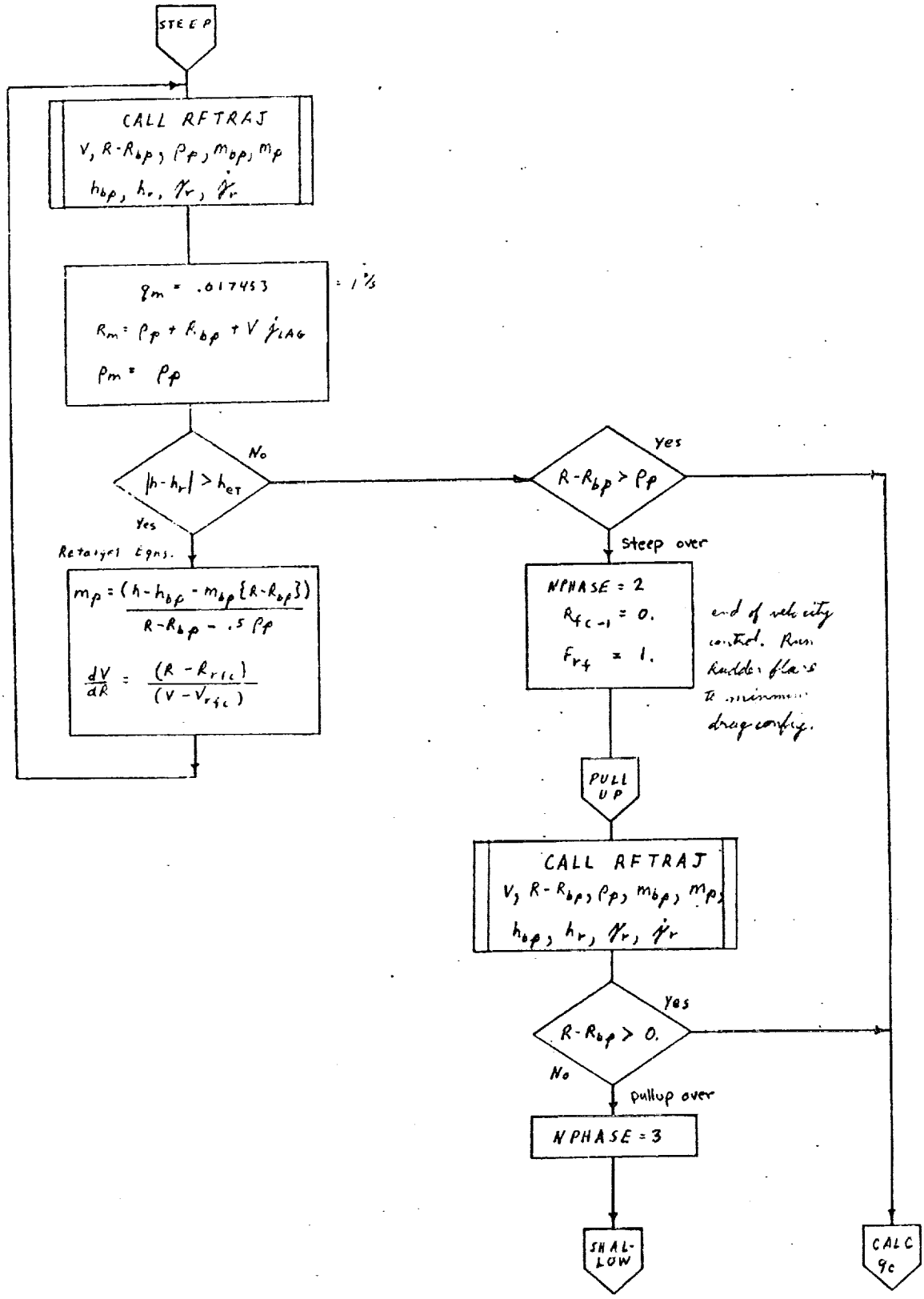

FIGURE 4-4

AUTOLAND EQUATIONS

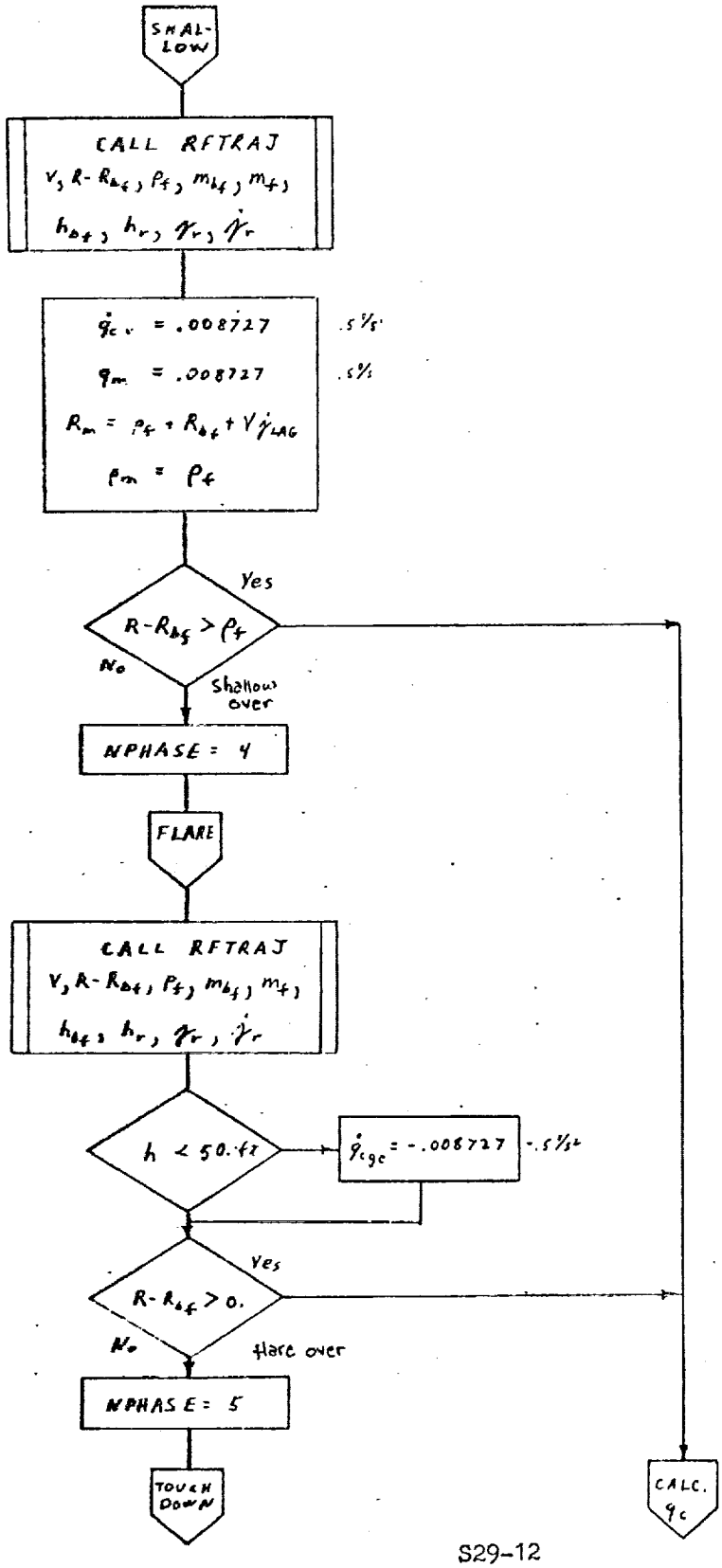

FIGURE 4-5

AUTOLAND EQUATIONS

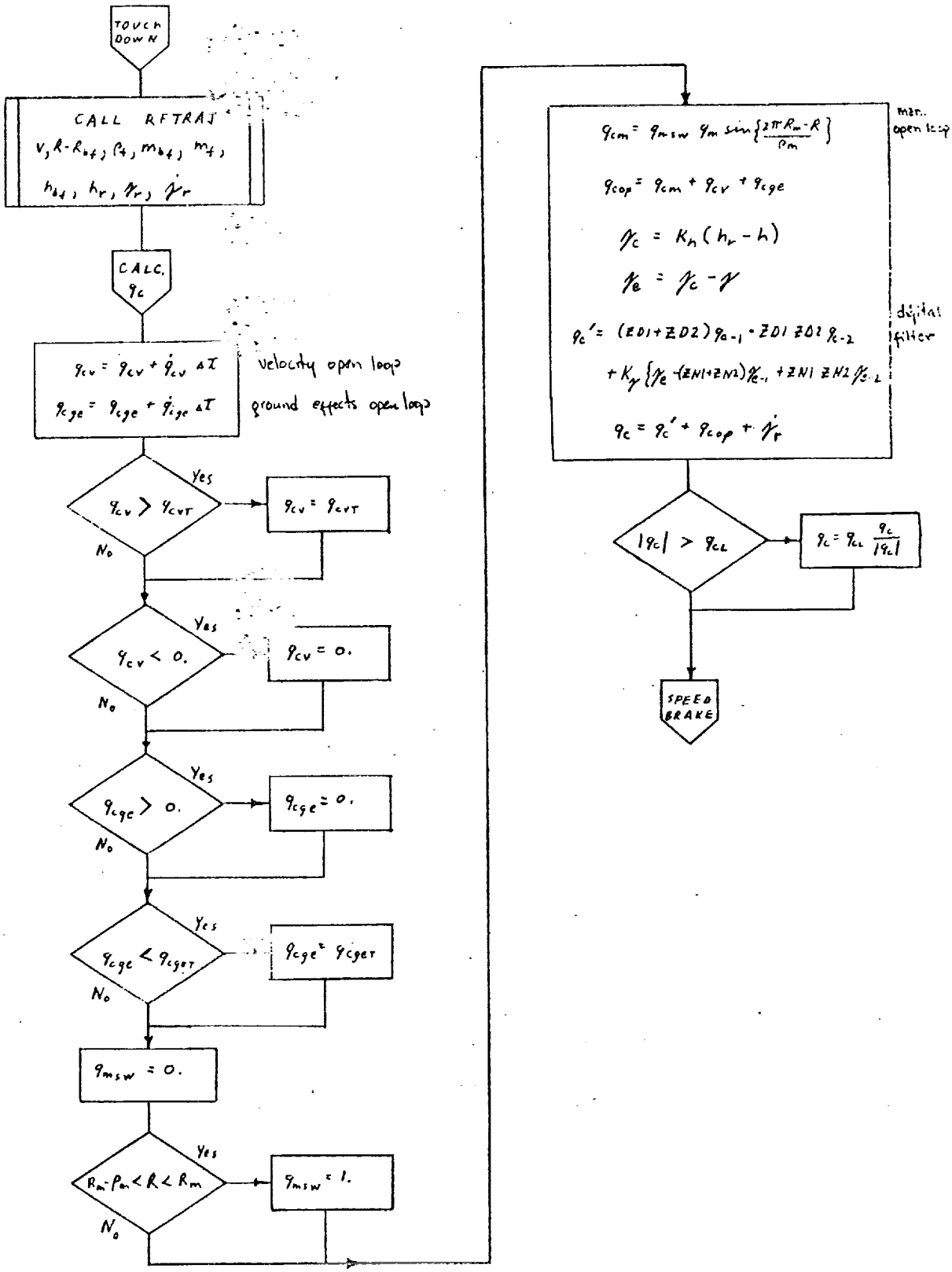

FIGURE 4-6
AUTOLAND EQUATIONS

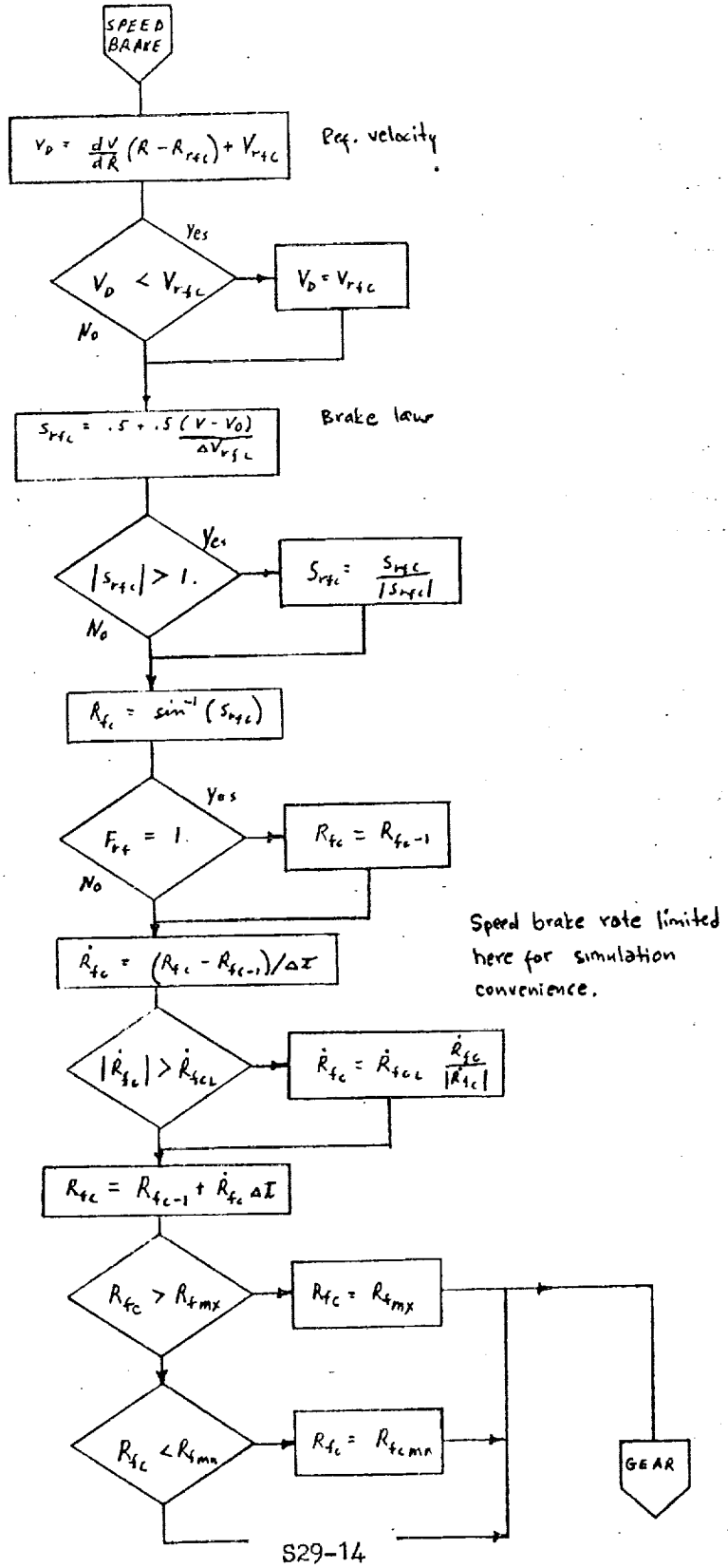

FIGURE 4-7
AUTOLAND EQUATIONS

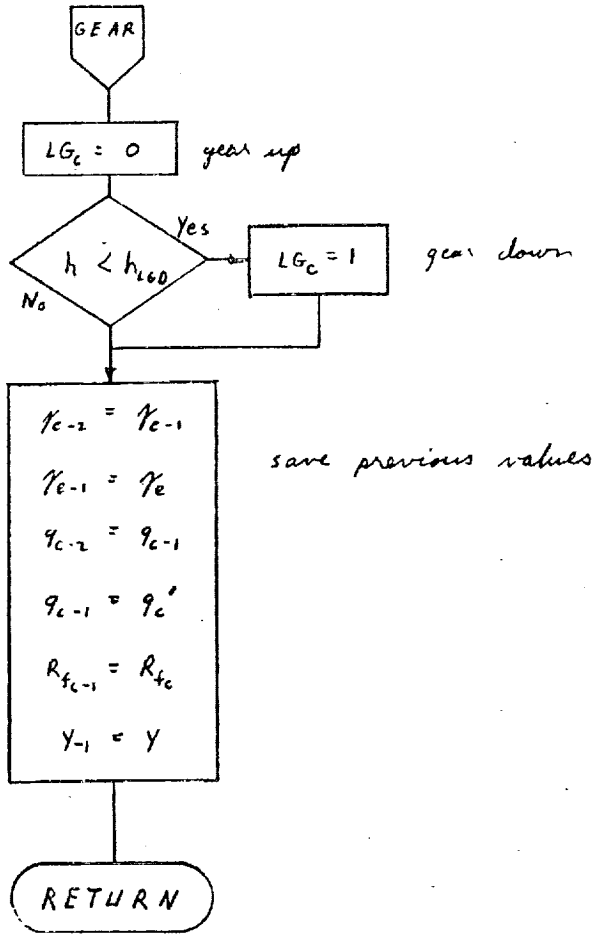

| Prepared | Petricolas | 4/31/72 | LOCKHEED ELECTRONICS COMPANY<br>HOUSTON AEROSPACE SYSTEMS DIVISION | Page | TEMP | PERM |
|---|---|---|---|---|---|---|
| Checked | | | TITLE FIGURE 4-8<br>REFERENCE TRAJECTORY EQUATIONS | Model | | |
| Approved | | | | Report No. | | |

RFTRAJ

calling sequence $\underbrace{V, RR, \rho, m, m_b, h_b}_{\text{inputs}}, \underbrace{h_r, \gamma_r \text{ and } \dot{\gamma}_r}_{\text{outputs}}$

$RR < \rho$

Yes

$$h_r = (m + m_b)\,RR - \frac{m \rho h_b}{2}$$

$$\gamma_r = -(m + m_b)$$

$$\dot{\gamma}_r = 0.$$

No

$$X = \frac{\pi\,(RR + |RR|)}{\rho}$$

$$h_r = m_b\,RR + \frac{m\rho}{4\pi^2}\left\{\frac{X^2}{2} - 1 + \cos X\right\} + h_b$$

$$\gamma_r = -\left\{m_b + \frac{m}{2\pi}(X - \sin X)\right\}$$

$$\dot{\gamma}_r = \frac{mV\cos\gamma_r}{\rho}\{1 - \cos X\}$$

RETURN

$$X = \begin{cases} 0 & \text{if } RR \le 0 \\ \frac{2\pi}{\rho} RR & \text{if } RR > 0 \end{cases}$$

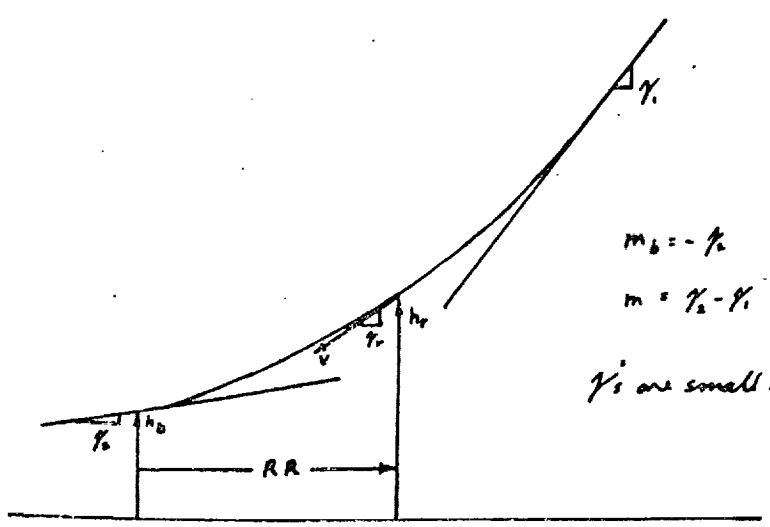


$m_b = -\gamma_2$

$m = \gamma_2 - \gamma_1$

$\gamma$'s are small neg. angles

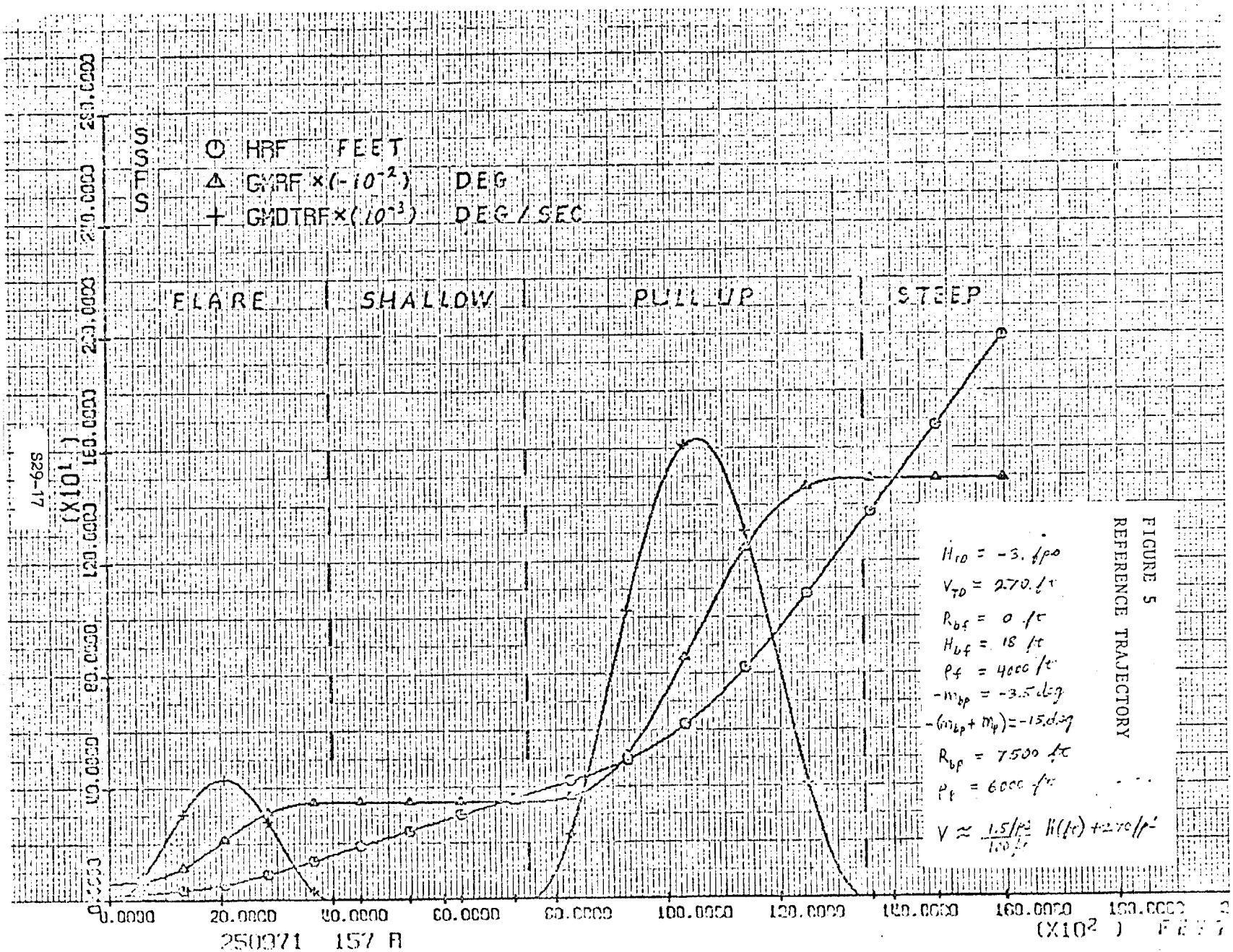


FIGURE 5
REFERENCE TRAJECTORY

S29-17

250971 157 R

FIGURE 6-1
VARIABLE SUMMARY

| | | MNEMONIC | UNITS | DEFINITION | NOMINAL VALUE OR EXPECTED RANGE | PROGRAMMING RANGE, ± NOM OR 0. TO NOM |
|---|---|---|---|---|---|---|
| 3 | $\Delta T$ | DELTAT | SEC | GUIDANCE TIME INTERVAL | .12500 | 2.00000 |
| 233 | $\dot{H}_{DR}$ | DVDR | FT/SEC | DESIRED DERIVATIVE OF VEL. ART RANGE | .00000, .01000 | ±.10000 |
| 212 | $h_{DB}$ | FHB | FT | DESIRED ALT. AT END OF FLARE | 12. | 20. |
| 268 | $m_T$ | FM | NONE - RAD | TARGETING CONSTANT = FMB - FMB | .06000 | ±1.00000 |
| 267 | $m_{DR}$ | FMB | NONE - RAD | DESIRED TOUCHDOWN FLIGHT PATH ANGLE | .01000 | ±1.00000 |
| 204 | $\rho_{DB}$ | FRB | FT | RANGE AT END OF FLARE | 0. | 1000. |
| 209 | $\rho_F$ | FRHD | FT | RANGE COVERED DURING FLARE | 2400. | 10000. |
| 94 | $\gamma$ | GAMA | RAD | FLIGHT PATH ANGLE | -1.00000, 1.00000 | ±2.00000 |
| 401 | $\gamma_C$ | GAMC | RAD | COMMANDED FLIGHT PATH ANGLE | -1.00000, 1.00000 | ±2.00000 |
| 409 | $\dot{\gamma}$ | GAMDT | RAD/SEC | TIME DERIVATIVE OF FLIGHT PATH ANGLE | -.17453, .17453 | ±.17453 |
| 406 | | GAMDTI | RAD/SEC | TIME DERIVATIVE OF FLIGHT PATH ANGLE | -.17453, .17453 | ±.17453 |
| 89 | $\dot{\gamma}_r$ | GAMDTR | RAD/SEC | TIME DERIVATIVE OF REF FLIGHT PATH ANGLE | -.17453, .17453 | ±.17453 |
| 88 | $\gamma_r$ | GAMR | RAD | REFERENCE FLIGHT PATH ANGLE | -.50000, .00000 | ±1.00000 |
| 207 | $\gamma_{SH}$ | GAMSH | RAD | FLIGHT PATH ANGLE FOR SHALLOW PHASE | -.05236 | ±1.00000 |
| 208 | | GAMST | RAD | FLIGHT PATH ANGLE FOR STEEP PHASE | -.22689 | ±1.00000 |
| 93 | $\dot{\gamma}_{LAG}$ | GDTLAG | SEC | TIME LAG FROM Q TO GAMA DOT | 1.00000 | 10.00000 |
| 90 | $\gamma_E$ | GE | RAD | GAMA ERROR | -.34907, .34907 | ±1.00000 |
| 91 | $\gamma_{E-1}$ | GEM1 | RAD | PREVIOUS VALUE OF GE | -.34907, .34907 | ±1.00000 |
| 92 | $\gamma_{E-2}$ | GEM2 | RAD | PREVIOUS VALUE OF GEM1 | -.34907, .34907 | ±1.00000 |
| 23 | $K_\gamma$ | GKG | 1/SEC | GAMA GAIN | 3.00000 | 10.00000 |

FIGURE 6-2
VARIABLE SUMMARY

| | | MNEMONIC | UNITS | DEFINITION | NOMINAL VALUE OR EXPECTED RANGE | PROGRAMMING RANGE, ± NOM OR 0. TO NOM |
|---|---|---|---|---|---|---|
| 24 | | GKGD | RPS/RPS | GAMA DOT GAIN | 1.00000 | 10.00000 |
| 21 | $K_h$ | GKH | 1/FT | ALTITUDE GAIN = GKHAV DIVIDED BY V | .00100, .00200 | .01000 |
| 30 | $K_{hv}$ | GKHAV | 1/SEC | CONSTANT = VELOCITY TIMES ALTITUE GAIN | .40000 | 10.00000 |
| 28 | $K_\phi$ | GKPHIC | RAD/RAD | ROLL ANGLE GAIN | 3.00000, 6.00000 | 10.00000 |
| 25 | $K_y$ | GKY | RAD/FT | CROSS RANGE GAIN | .00020, .00040 | .00100 |
| 26 | $K_{yI}$ | GKYI | 1/SEC | CROSS RANGE INTEGRAL GAIN | .06700 | 1.00000 |
| 226 | $LG_c$ | GRCMND | NONE | LANDING GEAR COMMAND (1=DOWN; 0=UP) | .00000, 1.00000 | 1.00000 |
| 36 | $h$ | H | FT | ALTITUDE | 0., 10000. | 10000. |
| 218 | | HDD | FT/SEC**2 | ALTITUDE ACCELERATION | -10., 10. | ±20. |
| 216 | | HDDI | FT/SEC | ALTITUDE RATE | -30., 0. | ±100. |
| 203 | $\dot{h}_{TD}$ | HDTD | FT/SEC | DESIRED TOUCHDOWN ALTITUDE RATE | -3.00000 | ±10.00000 |
| 293 | $h_e$ | HE | FT | ALTITUDE ERROR HR-H | -10., 10. | 1000. |
| 248 | $\sigma$ | HEDING | RAD | HEADING ANGLE = ATAN(VYLS/VXLS) | -.10000, .10000 | ±2.00000 |
| 412 | $\sigma_c$ | HEDNGC | RAD | COMMANDED HEADING ANGLE | -.10000, .10000 | 2.00000 |
| 405 | $h_{ET}$ | HERTRG | FT | ALT. ERROR TO RETARGET PHASE 1 | 100. | 1000. |
| 227 | $h_{GD}$ | HGERDW | FT | ALTITUDE TO COMMAND LANDING GEAR DOWN | 5000. | 10000. |
| 426 | | HMNPLT | FT | MAXIMUM OF HPLT AND HRPLT | 0. | 10000. |
| 427 | | HMXPLT | FT | MAXIMUM OF HPLT AND HRPLT | 140. | 10000. |
| 422 | | HPLT | FT | ALTITUDE LIMITED FOR PLOTS | 0., 140. | 10000. |
| 67 | $h_r$ | HR | FT | REFERENCE ALTITUDE | 0., 5000. | 1000. |

FIGURE 6-3
VARIABLE SUMMARY

| | | MNEMONIC | UNITS | DEFINITION | NOMINAL VALUE OR EXPECTED RANGE | | PROGRAMMING RANGE, ± NOM OR 0. TO NOM |
|---|---|---|---|---|---|---|---|
| 217 | | HRDOT | FT/SEC | REFERENCE ALTITUDE RATE | -30., | -3. | ±100. |
| 423 | | HRPLT | FT | REF ALTITUDE LIMITED FOR PLOTS | 0., | 140. | 1000. |
| 201 | $h_{TD}$ | HTD | FT | TOUCHDOWN ALTITUDE | 12. | | 100. |
| 279 | | HYTHRS | FT | ALT THRESHOLD FOR CROSS RANGE INTEGRATION | 0. | | 10000. |
| 1 | | INIT | NONE | INITIALIZATION SWITCH | .00000, | 1.00000 | 1.00000 |
| 438 | $F_{\pm}$ | NFRZRF | NONE | FREEZE RUDDER FLARE SWITCH | .00000, | 1.00000 | 1.00000 |
| 414 | | NPHASE | NONE | FLIGHT PHASE SWITCH | 1.00000, | 5.00000 | 5.00000 |
| 77 | | NPTIME | NONE | PRINT SWITCH | 1., | 10000. | 10000. |
| 95 | $\gamma_{-1}$ | OGAM | RAD | PREVIOUS VALUE OF GAMA | -1.00000, | 1.00000 | ±2.00000 |
| 439 | $\dot{\ell}_{c_1}$ | ORFC | RAD | PREVIOUS VALUE OF RFC | .00000, | 1.50000 | 1.50000 |
| 440 | | OT | SEC | PREVIOUS VALUE OF TIME | 0., | 160. | 1000. |
| 441 | $Y_1$ | OY | FT | PREVIOUS VALUE OF CROSS RANGE | 0., | 1000. | 10000. |
| 211 | $h_{bp}$ | PHB | FT | DESIRE ALTITUDE AT END OF ~~FLARE~~ *PULL UP* | 202. | | 1000. |
| 411 | $\phi_c$ | PHIC | RAD | ROLL COMMAND | .17453, | .52360 | ±1.00000 |
| 413 | $\phi_L$ | PHICL | RAD | ROLL COMMAND LIMIT | .17453, | .52360 | 1.00000 |
| 265 | $m_p$ | PM | NONE - RAD | TARGETING CONSTANT = GAMSH - GAMST | .17591 | | 1.00000 |
| 266 | $m_{op}$ | PMB | NONE - RAD | NEG. OF SHALLOW SLOPE FLIGHT ANGLE | .05236 | | 1.00000 |
| 205 | $R_{bp}$ | PRB | FT | RANGE AT END OF PULL UP | 4600. | | 10000. |
| 210 | $\rho_p$ | PRHO | FT | RANGE COVERED DURING PULL UP | 5000. | | 10000. |
| 206 | $V_{bp}$ | PVB | FT/SEC | DESIRED VELOCITY AT START OF PULL UP | 395. | | 1000. |

FIGURE 6-4
VARIABLE SUMMARY

| | | MNEMONIC | UNITS | DEFINITION | NOMINAL VALUE OR EXPECTED RANGE | PROGRAMMING RANGE, ± NUM OR 0. TO NUM |
|---|---|---|---|---|---|---|
| 410 | $q_c$ | QC | RAD/SEC | PITCH RATE COMMAND | -.08727, .08727 | ±.17453 |
| 402 | $q_{cge}$ | QCGE | RAD/SEC | GROUND EFFECT COMPENSATION PITCH RATE CMD | .00000 .01745 | ±.17453 |
| 403 | $\dot{q}_{cge}$ | QCGEDT | RAD/SEC**2 | QCGE RATE | -.00873, .00000 | .00000 |
| 400 | $q_{cL}$ | QCLIM | RAD/SEC | LIMIT FOR PITCH RATE COMMAND | .08725 | ±.17453 |
| 430 | $q_{cm}$ | QCMAN | RAD/SEC | MANUVER PITCH RATE COMMAND | .00000, .01745 | .17453 |
| 407 | $q_{c-1}$ | QCM1 | RAD/SEC | PREVIOUS VALUE OF QC | -.08727, .08727 | ±.17453 |
| 408 | $q_{c-2}$ | QCM2 | RAD/SEC | PREVIOUS VALUE OF QCM1 | -.08727, .08727 | ±.17453 |
| 215 | $q_{cop}$ | QCOPEN | RAD/SEC | OPEN LOOP PITCH RATE CMD = QCV+QCGE+QCMAN | -.08727, .08727 | ±.17453 |
| 433 | $q_c'$ | QCP | RAD/SEC | CLOSED LOOP PITCH RATE COMMAND | -.08727, .08727 | ±.17453 |
| 434 | $q_{cv}$ | QCV | RAD/SEC | PITCH RATE CMD TO COMPENSATE FOR V DOT | .00000, .00698 | .17453 |
| 435 | $\dot{q}_{cv}$ | QCVDOT | RAD/SEC**2 | TIME RATE OF CHANGE OF QCV | .00000, .00873 | .17453 |
| 213 | $q_{cvT}$ | QCVTRG | RAD/SEC | MAXIMUM QCV | .00698 | 1.00000 |
| 431 | $q_{ge,t}$ | QGETRG | RAD/SEC | MINIMUM QCGE | -.01571 | 1.00000 |
| 428 | $q_m$ | QMAN | RAD/SEC | MAXIMUM MANUVER PITCH RATE COMMAND | .00000, .01745 | .17453 |
| 429 | $q_{m,sw}$ | QMANSW | NONE | MANUVER SWITCH | .00000, 1.00000 | 1.00000 |
| 59 | $R$ | R | FT | RANGE | -1000., 30000. | 100000. |
| 283 | $R_{fc}$ | RFC | RAD | RUDDER FLARE COMMAND | .00000, 1.50000 | 2.00000 |
| 256 | $\Delta Y_{v_{fc}}$ | RFCDV | FT/SEC | RUDDER FLARE GAIN | 7. | 50. |
| 284 | $R_{fc_{max}}$ | RFCMAX | RAD | MAXIMUM RFC | 1.50000 | 2.00000 |
| 285 | $R_{fc_{min}}$ | RFCMIN | RAD | MINIMUM RFC | .00000 | ±1.00000 |



C4

FIGURE 6-5
VARIABLE SUMMARY

| | | MNEMONIC | UNITS | DEFINITION | NOMINAL VALUE OR EXPECTED RANGE | PROGRAMMING RANGE, ± NOM OR 0. TO NOM |
|---|---|---|---|---|---|---|
| 299 | | RFCPLT | DEG | RUDDER FLARE COMMAND BIASED BY 300 | 300., 400. | 1000. |
| 286 | $\dot{F}_L$ | RFCRAT | RAD/SEC | MAXIMUM RUDDER FLARE RATE | .34907 | 1.00000 |
| 436 | $\rho_m$ | RHOMAN | FT | RANGE COVERED DURING MANUVER | 2400., 5000. | 10000. |
| 424 | | RMNPLT | FT | MINIMUM OF RPLT | -1000. | ±100000. |
| 425 | | RMXPLT | FT | MAXIMUM OF RPLT | 4000. | ±100000. |
| 200 | $\rho_{TD}$ | RNTD | FT | DESIRED RANGE AT TOUCHDOWN | 0. | ±10000. |
| 437 | $R_m$ | ROMAN | FT | APPROX. RANGE AT START OF MANUVER | 2000., 5000. | 10000. |
| 421 | | RPLT | FT | RANGE LIMITED FOR PLOTS | -1000., 4000. | ±10000. |
| 254 | $R_{FLC}$ | RRFC | FT | RANGE BIAS FOR RUDDER FLARE COMMAND | 0., 9600. | 10000. |
| 2 | | TIME | SEC | TIME | 0., 180. | 100000. |
| 10 | | TPHCHG | SEC | TIME OF THE LAST PHASE CHANGE | 0., 180. | 100000. |
| 40 | V | V | FT/SEC | VEHICLE VELOCITY MAGNITUDE | 250., 450. | 1000. |
| 243 | $V_D$ | VD | FT/SEC | DESIRE VELOCITY | 300., 400. | 1000. |
| 255 | $V_{FLC}$ | VRFC | FT/SEC | VELOCITY BIAS FOR RUDDER FLARE COMMAND | 300., 400. | 1000. |
| 202 | $V_{TD}$ | VTD | FT/SEC | DESIRED TOUCHDOWN VELOCITY | 303. | 500. |
| 7 | | VXLS | FT/SEC | VEHICLE VELOCITY DOWN RUNWAY | 250., 400. | 1000. |
| 8 | | VYLS | FT/SEC | VEHICLE VELOCITY CROSSRANGE | -50., 50. | 1000. |
| 9 | | VZLS | FT/SEC | VEHICLE VELOCITY DOWN | 0., 25. | 1000. |
| 4 | | XLS | FT | X VEH. POS., POSITIVE DOWN RUNWAY | -1000., 30000. | 100000. |
| 249 | Y | Y | FT | CROSS RANGE | -10000., 10000. | ±100000. |

FIGURE 6-6
VARIABLE SUMMARY

| | MNEMONIC | UNITS | DEFINITION | NOMINAL VALUE OR EXPECTED RANGE | PROGRAMMING RANGE, ± NOM OR 0. TO NOM |
|---|---|---|---|---|---|
| 250 | YI | FT | INTEGRAL OF CROSS RANGE | -5000., 5000. | ±10000. |
| 5 | YLS | FT | Y VEH. POS. | -1000., 10000. | ±100000. |
| 251 | YTHRES | FT | Y THRESHOLD FOR CROSS RANGE INTEGRATION | 50. | 1000. |
| 6 | ZLS | FT | Z VEH. POS., POSITIVE DOWN | -500., 0. | ±100000. |
| 17 | ZRD1 | NONE | FIRST DENOMINATOR Z-PLANE ROOT | .88300 | 1.00000 |
| 19 | ZRD2 | NONE | SECOND DENOMINATOR Z-PLANE ROOT | .74500 | 1.00000 |
| 16 | ZRN1 | NONE | FIRST NUMERATOR Z-PLANE ROOT | .93500 | 1.00000 |
| 18 | ZRN2 | NONE | SECOND NUMERATOR Z-PLANE ROOT | .84600 | 1.00000 |

Submittal 6: CONIC STATE EXTRAPOLATION

## 1. INTRODUCTION

The Conic State Extrapolation Routine provides the capability to conically extrapolate any spacecraft inertial state vector either backwards or forwards as a function of time or as a function of transfer angle. It is merely the coded form of two versions of the analytic solution of the two-body differential equations of motion of the spacecraft center of mass. Because of its relatively fast computation speed and moderate accuracy, it serves as a preliminary navigation tool and as a method of obtaining quick solutions for targeting and guidance functions. More accurate (but slower) results are provided by the Precision State Extrapolation Routine.

## NOMENCLATURE

| | |
|---|---|
| $a$ | Semi major axis of conic |
| $c_1$ | First conic parameter $((\underline{r}_0 \cdot \underline{v}_0)/\sqrt{\mu})$ |
| $c_2$ | Second conic parameter $(r_0 v_0^2/\mu - 1)$ |
| $c_3$ | Third conic parameter $(r_0 v_0^2/\mu)$ |
| $C(\xi)$ | Power series in $\xi$ defined in text |
| $E$ | Eccentric anomaly |
| $f$ | True anomaly |
| $H$ | Hyperbolic analog of eccentric anomaly |
| $i$ | Counter |
| $i_{max}$ | Maximum permissible number of iterations |
| $\underline{i}_{r_0}$ | Unit vector in direction of $\underline{r}_0$ |
| $\underline{i}_{v_0}$ | Unit vector in direction of $\underline{v}_0$ |
| $p$ | Semilatus rectum of conic |
| $p_N$ | Normalized semilatus rectum $(p/r_0)$ |
| $P$ | Period of conic orbit |
| $r_0$ | Magnitude of $\underline{r}_0$ |
| $\underline{r}_0$ | Inertial position vector corresponding to initial time $t_0$ |
| $r$ | Magnitude of $\underline{r}(t)$ |
| $\underline{r}(t)$ | Inertial position vector corresponding to time t |
| $s$ | Switch used in Secant Iterator to determine whether secant method or offsetting will be performed |

| | |
|---|---|
| $S(\xi)$ | Power series in $\xi$ defined in text |
| $t$ | Final time (end of time interval through which an extrapolation is made) |
| $t_0$ | Initial time (beginning of time interval through which an extrapolation is to be made) |
| $t_{err}$ | Difference between specified time interval and that calculated by Universal Kepler Equation |
| $v_0$ | Magnitude of $\underline{v}_0$ |
| $\underline{v}_0$ | Inertial velocity vector corresponding to initial time $t_0$ |
| $\underline{v}(t)$ | Inertial velocity vector corresponding to time t |
| $x$ | Universal eccentric anomaly difference (independent variable in Kepler iteration scheme) |
| $x'$ | Previous value of x |
| $x_c$ | Value of x to which the Kepler iteration scheme converged |
| $x'_c$ | Previous value of $x_c$ |
| $x_i$ | The "i-th" value of x |
| $x_{min}$ | Lower bound on x |
| $x_{max}$ | Upper bound on x |
| $\alpha_0$ | Reciprocal of semi-major axis at initial point $\underline{r}_0$ |
| $\alpha_N$ | Normalized semi-major axis reciprocal ($\alpha r_0$) |
| $\gamma_0$ | Angle from $\underline{r}_0$ to $\underline{v}_0$ |

| | |
|---|---|
| $\Delta t$ | Specified transfer time interval $(t - t_0)$ |
| $\Delta t_c$ | Value of the transfer time interval calculated in the Universal Kepler Equation as a function of x and the conic parameters |
| $\Delta t_c'$ | Previous value of $\Delta t_c$ |
| $\Delta t_c^{(i)}$ | The "i-th" value of the transfer time interval calculated in the Universal Kepler Equation as a function of the "i-th" value $x_i$ of x and the conic parameters |
| $\Delta t_{max}$ | Maximum time interval which can be used in computer due to scaling limitations |
| $\Delta x$ | Increment in x |
| $\epsilon_t$ | Primary convergence criterion: relative error in transfer time interval |
| $\epsilon_t'$ | Secondary convergence criterion: minimum permissible difference of two successive calculated transfer time intervals |
| $\epsilon_x$ | Tertiary convergence criterion: minimum permissible size of increment $\Delta x$ of the independent variable |
| $\theta$ | Transfer angle (true anomaly increment) |
| $\mu$ | Gravitational parameter of the earth |
| $\xi$ | Product of $\alpha_0$ and square of x |
| $\chi_0, \chi_1, \chi_2, \chi_3$ | Coefficients of power series inversion of Universal Kepler Equation |

## 2. FUNCTIONAL FLOW DIAGRAM

The Conic State Extrapolation Routine basically consists of two parts - one for extrapolating in time and one for extrapolating in transfer angle. Several portions of the formulation are, however, common to the two parts, and may be arranged as subroutines on a computer.

### 2.1 Conic State Extrapolation as a Function of Time (Kepler Routine)

This routine involves a single loop iterative procedure, and hence is organized in three sections: initialization, iteration, and final computations, as shown in Fig. 1. The variable "x" is the independent variable in the iteration procedure. For a given initial state, the variable "x" measures the amount of transfer along the extrapolated trajectory. The transfer time interval and the extrapolated state vector are very conveniently expressed in terms of "x". In the iteration procedure, "x" is adjusted until the transfer time interval calculated from it agrees with the specified transfer time interval (to within a certain tolerance). Then the extrapolated state vector is calculated from this particular value of "x".

### 2.2 Conic State Extrapolation as a Function of Transfer Angle (Theta Routine)

This routine makes a direct calculation (i.e. does not have an iteration scheme), as shown in Fig. 2. Again, the extrapolated state vector is calculated from the parameter "x". The value of "x" however, is obtained from a direct computation in terms of the conic parameters and the transfer angle $\theta$. It is not necessary to iterate to determine "x", as was the case in the Kepler Routine.

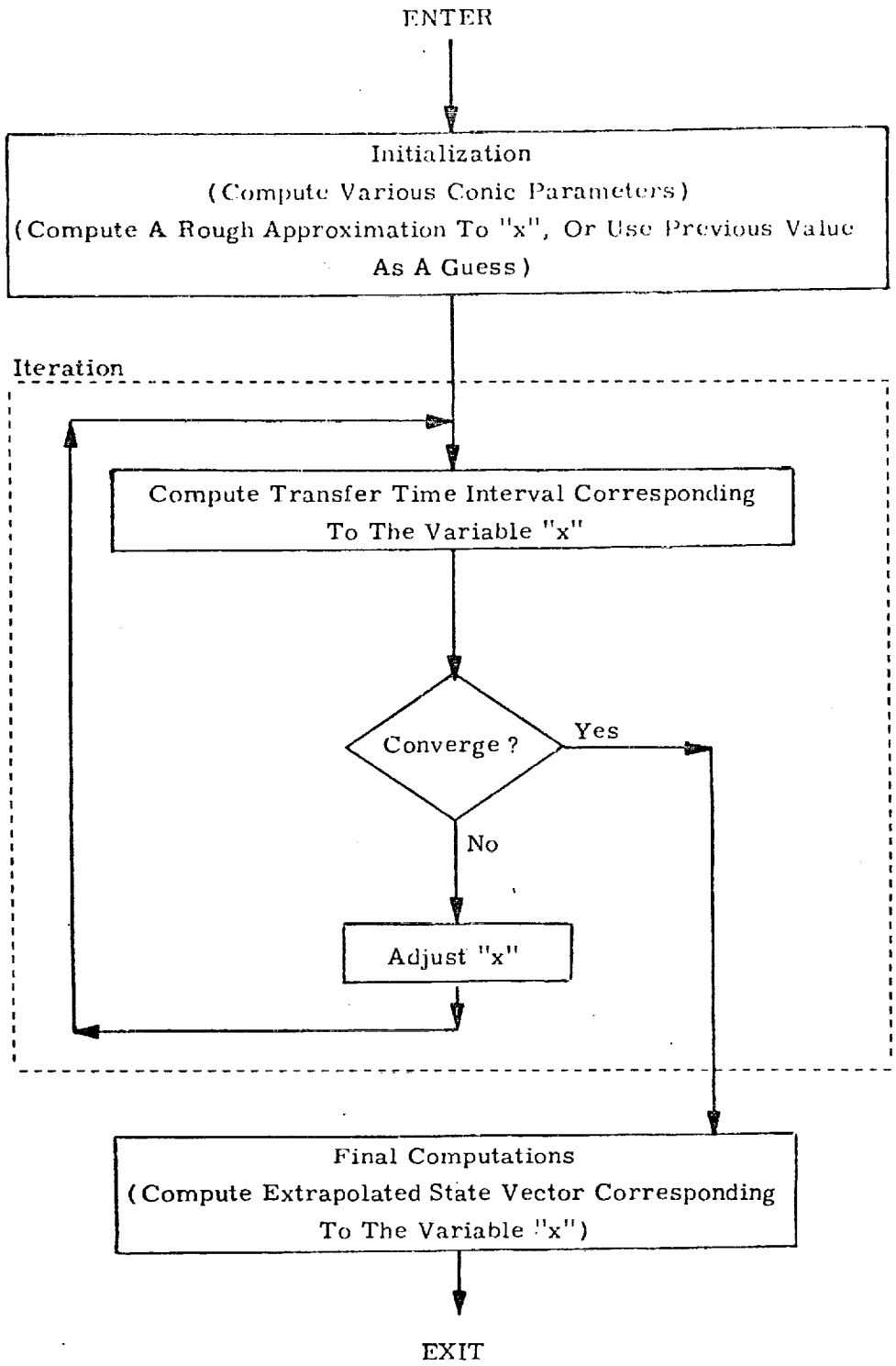


**Figure 1.** Kepler Routine, Functional Flow Diagram

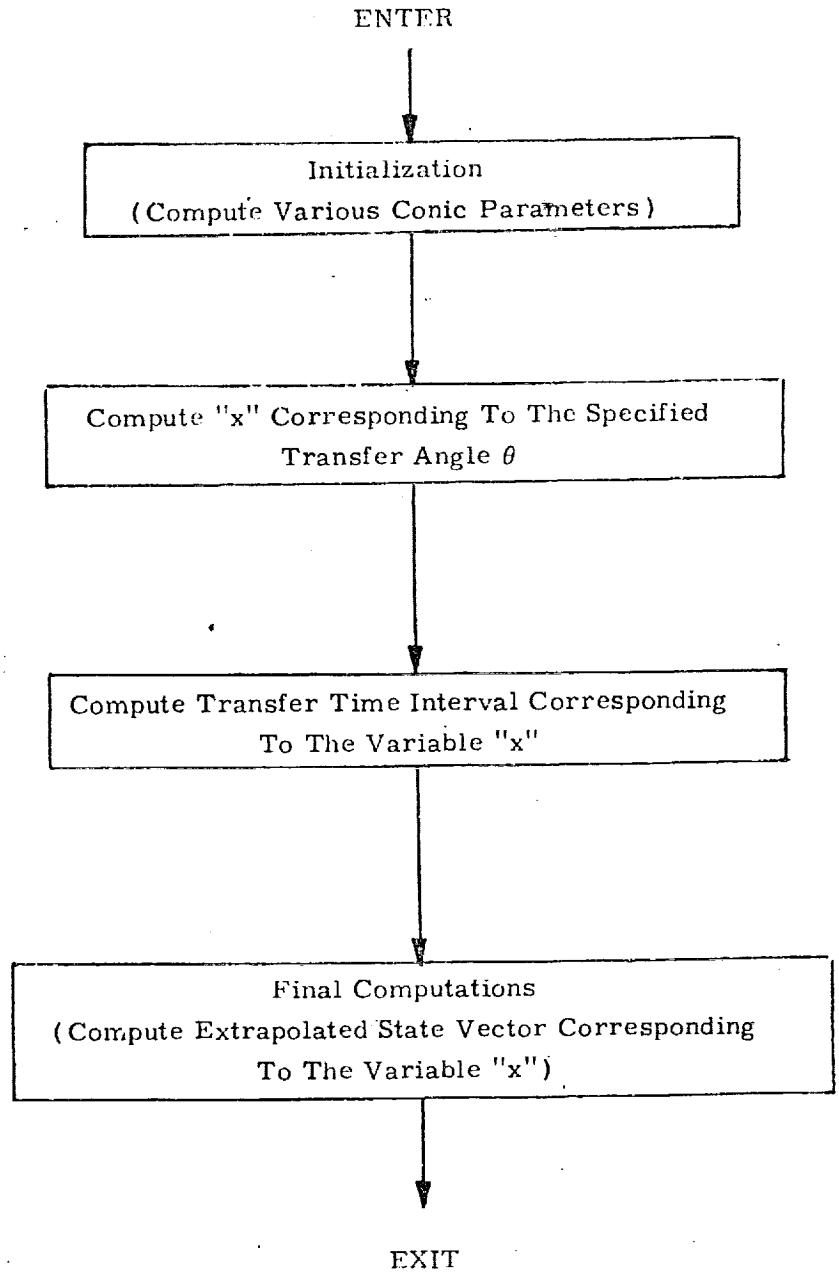


Figure 2. Theta Routine, Functional Flow Diagram

## 3. INPUT AND OUTPUT VARIABLES

The Conic State Extrapolation Routine has only one universal constant: the gravitational parameter of the earth. Its principal input variables are the inertial state vector which is to be extrapolated and the transfer time interval or transfer angle through which the extrapolation is to be made. Several optional input variables may be supplied in the transfer time case in order to speed the computation. The principal output variable of both cases is the extrapolated inertial state vector.

### 3.1 Conic State Extrapolation as a Function of Transfer Time Interval (Kepler Routine)

#### Input Variables

| | |
|---|---|
| $(\underline{r}_0, \underline{v}_0)$ | Inertial state vector which is to be extrapolated (corresponds to time $t_0$). |
| $\Delta t$ | Transfer time interval through which the extrapolation is to be made. |
| $x$ | Guess of independent variable corresponding to solution in Kepler iteration scheme. (Used to speed convergence). [If no guess is available, set $x = 0$, and the routine will generate its own guess]. |
| $\Delta t'_c$ | Value of dependent variable (the transfer time interval) in the Kepler iteration scheme, which was calculated in the last iteration of the previous call to Kepler. |
| $x'_c$ | Value of the independent variable in the Kepler iteration scheme, to which the last iteration of the previous call to Kepler had converged. |

#### Output Variables

| | |
|---|---|
| $(\underline{r}, \underline{v})$ | Extrapolated inertial state vector (corresponds to time $t$). |

$\Delta t_c$ — Value of the dependent variable (the transfer time interval) in the Kepler iteration scheme, which was calculated in the last iteration (should agree closely with $\Delta t$).

$x_c$ — Value of the independent variable in the Kepler iteration scheme to which the last iteration converged.

## 3.2 Conic State Extrapolation as a Function of Transfer Angle (Theta Routine)

### Input Variables

$(\underline{r}_0, \underline{v}_0)$ — Inertial state vector which is to be extrapolated.

$\theta$ — Transfer angle through which the extrapolation is to be made.

### Output Parameters

$(\underline{r}, \underline{v})$ — Extrapolated inertial state vector.

$\Delta t_c$ — Transfer Time Interval corresponding to the conic extrapolation through the transfer angle $\theta$.

## 4. DESCRIPTION OF EQUATIONS

### 4.1 Conic State Extrapolation as a Function of Time (Kepler Routine)

The universal formulation of Stumpff-Herrick-Battin in terms of the universal eccentric anomaly difference is used. This variable, usually denoted by x, is defined by the relations:

$$x = \begin{cases} \sqrt{a}\,(E - E_0) & \text{for ellipse} \\ \sqrt{p}\,(\tan f/2 - \tan f_0/2) & \text{for parabola} \\ \sqrt{-a}\,(H - H_0) & \text{for hyperbola} \end{cases}$$

where a is the semi-major axis, E and H are the eccentric anomaly and its hyperbolic analog, p is the semi-latus rectum and f the true anomaly. The expressions for the transfer time interval $(t - t_0) = \Delta t$, and the extrapolated position and velocity vectors ($\underline{r}$, $\underline{v}$) in terms of the initial position and velocity vectors ($\underline{r}_0$, $\underline{v}_0$) as functions of x are:

(Universal Kepler Equation)

$$\Delta t = \frac{1}{\sqrt{\mu_E}}\left[\frac{\underline{r}_0 \cdot \underline{v}_0}{\sqrt{\mu_E}}\, x^2\, C(\alpha_0 x^2) + (1 - r_0\alpha_0)\, x^3\, S(\alpha_0 x^2) + r_0\, x\right]$$

$$\underline{r}(t) = \left[1 - \frac{x^2}{r_0} C(\alpha_0 x^2)\right]\underline{r}_0 + \left[(t - t_0) - \frac{x^3}{\sqrt{\mu_E}} S(\alpha_0 x^2)\right]\underline{v}_0$$

$$\underline{v}(t) = \frac{\sqrt{\mu_E}}{r\, r_0}\left[\alpha_0 x^3 S(\alpha_0 x^2) - x\right]\underline{r}_0 + \left[1 - \frac{x^2}{r} C(\alpha_0 x^2)\right]\underline{v}_0$$

where

$$\alpha_0 = \frac{1}{a_0} = \frac{2}{r_0} - \frac{v_0^2}{\mu}$$

and

$$S(\xi) = \frac{1}{3!} - \frac{\xi}{5!} + \frac{\xi^2}{7!} - \ldots$$

$$C(\xi) = \frac{1}{2!} - \frac{\xi}{4!} + \frac{\xi^2}{6!} - \ldots$$

Since the transfer time interval $\Delta t$ is given, it is desired to find the x corresponding to it in the Universal Kepler Equation, and then to evaluate the extrapolated state vector ($\underline{r}$, $\underline{v}$) expression using that value of x. Unfortunately, the Universal Kepler Equation expresses $\Delta t$ as a transcendental function of x rather than conversely, and no power series inversion of the equation is known which has good convergence properties for all orbits, so it is necessary to solve the equation iteratively for the variable x.

For this purpose, the secant method (linear inverse interpolation/ extrapolation) is used. It merely finds the increment in the independent variable x which is required in order to adjust the dependent variable $\Delta t_c$ to the desired value $\Delta t$ based on a linear interpolation/ extrapolation of the last two points calculated on the $\Delta t_c$ vs x curve. The method uses the formula

$$(x_{n+1} - x_n) = - \frac{\Delta t_c^{(n)} - \Delta t}{\Delta t_c^{(n)} - \Delta t_c^{(n-1)}} (x_n - x_{n-1})$$

where $\Delta t_c^{(i)}$ denotes the evaluation of the Universal Kepler Equation using the value $x_i$. In order to prevent the scheme from taking an increment back into regions in which it is known from past iterations that the solution does not lie, it has been found convenient to establish upper and lower bounds on the independent variable x which are continually reset during the course of the iteration as more and more values of x are found to be too large or too small. In addition, it has also been found expedient to damp by 10% any increment in the independent variable which would (if applied) take the value of the independent variable past a bound.

To start the iteration scheme, some initial guess $x_0$ of the independent variable is required as well as a previous point ($x_{-1}$, $\Delta t_c^{(-1)}$) on the $\Delta t_c$ vs x curve. If no previous point is available the point (0, 0) may be used as it lies on all $\Delta t_c$ vs x curves. The closer the initial guess $x_0$ is to the value of x corresponding to the solution, the faster the convergence will be. One method of obtaining such a guess $x_0$ is to use a truncation of the infinite series obtained by direct inversion of the Kepler Equation (expressing x as a power series in $\Delta t$). It must be pointed out that this series diverges even for "moderate" transfer time intervals $\Delta t$; hence an iterative solution must be used to solve the Kepler equation for x in the general case. A third order truncation of the inversion of the Universal Kepler Equation is:

$$x = \sum_{n=0}^{3} \chi_n \, \Delta t^{\,n}$$

where

$$\chi_0 = 0, \quad \chi_1 = \sqrt{\mu}/r_0,$$

$$\chi_2 = -\frac{1}{2}\frac{\mu}{r_0^3}\left(\frac{\underline{r}_0 \cdot \underline{v}_0}{\sqrt{\mu}}\right),$$

$$\chi_3 = \frac{1}{6r_0}\left(\frac{\sqrt{\mu}}{r_0}\right)^3\left[\frac{3}{r_0}\left(\frac{\underline{r}_0 \cdot \underline{v}_0}{\sqrt{\mu}}\right)^2 - (1 - r_0\alpha_0)\right],$$

with $\alpha_0 = 2/r_0 - v_0^2/\mu$ .

## 4.2 Conic State Extrapolation as a Function of Transfer Angle (Theta Routine)

As with the Kepler Routine, the universal formulation of Stumpff-Herrick-Battin in terms of the universal eccentric anomaly difference x is used in the Theta Routine. A completely analogous iteration scheme could have been formulated with x again as the independent variable and the transfer angle $\theta$ as the dependent variable using Marscher's universally valid equation:

$$\cot \frac{\theta}{2} = \frac{r_0 \left[ 1 - \alpha_0 x^2 S(\alpha_0 x^2) \right]}{\sqrt{p}\, x\, C(\alpha_0 x^2)} + \cot \gamma_0$$

where

$$p = \left(\frac{r_0 v_0}{\sqrt{\mu}}\right)^2 \sin^2 \gamma_0$$

and

$$\gamma_0 = \text{angle from } \underline{r}_0 \text{ to } \underline{v}_0.$$

However, in contrast to the Kepler equation, it is possible to invert the Marscher equation into a power series which can be made to converge as rapidly as desired, by means of which x may be calculated as a universal function of the transfer angle $\theta$. Knowing x, we can directly calculate the transfer time interval $\Delta t_c$ and subsequently the extrapolated state vectors using the standard formulae.

The sequence of computations in the inversion of the Marscher Equation is as follows:

Let

$$p_N = p/r_0, \quad \alpha_N = \alpha\, r_0$$

and

$$W_1 = \sqrt{p_N}\left(\frac{\sin\theta}{1-\cos\theta} - \cot\gamma_0\right).$$

If

$$|W_1| > 1, \text{ let } V_1 = 1.$$

Let

$$W_{n+1} = +\sqrt{W_n^2 + \alpha_N} + |W_n| \qquad (|W_1| \leq 1)$$

or

$$V_{n+1} = +\sqrt{V_n^2 + \alpha_N (|1/W_1|)^2} + V_n \qquad (|W_1| > 1).$$

Let

$$\omega_n = W_n \qquad (|W_1| \leq 1)$$

or

$$1/\omega_n = (|1/W_1|)/V_n \qquad (|W_1| > 1).$$

Let

$$\Sigma = \frac{2^n}{\omega_n} \sum_{j=0}^{\infty} \frac{(-1)^j}{2j+1} \left(\frac{\alpha_N}{\omega_n^2}\right)^j$$

where n is an integer $\geq 4$. Then

$$x/\sqrt{r_0} = \begin{cases} \Sigma & (W_1 > 0) \\ 2\pi/\sqrt{\alpha_N} - \Sigma & (W_1 < 0) \end{cases}$$

The above equations have been specifically formulated to avoid certain numerical difficulties.

## 5. DETAILED FLOW DIAGRAMS

This section contains detailed flow diagrams of two Conic State Extrapolation Routines (Kepler and Theta) and the subroutines used by them.

Each input and output variable in the routine and subroutine call statements can be followed by a symbol in brackets. This symbol identifies the notation for the corresponding variable in the detailed description and flow diagrams of the called routine. When identical notation is used, the bracket symbol is omitted.

## 5.1 Conic State Extrapolation as a Function of Time (Kepler Routine)

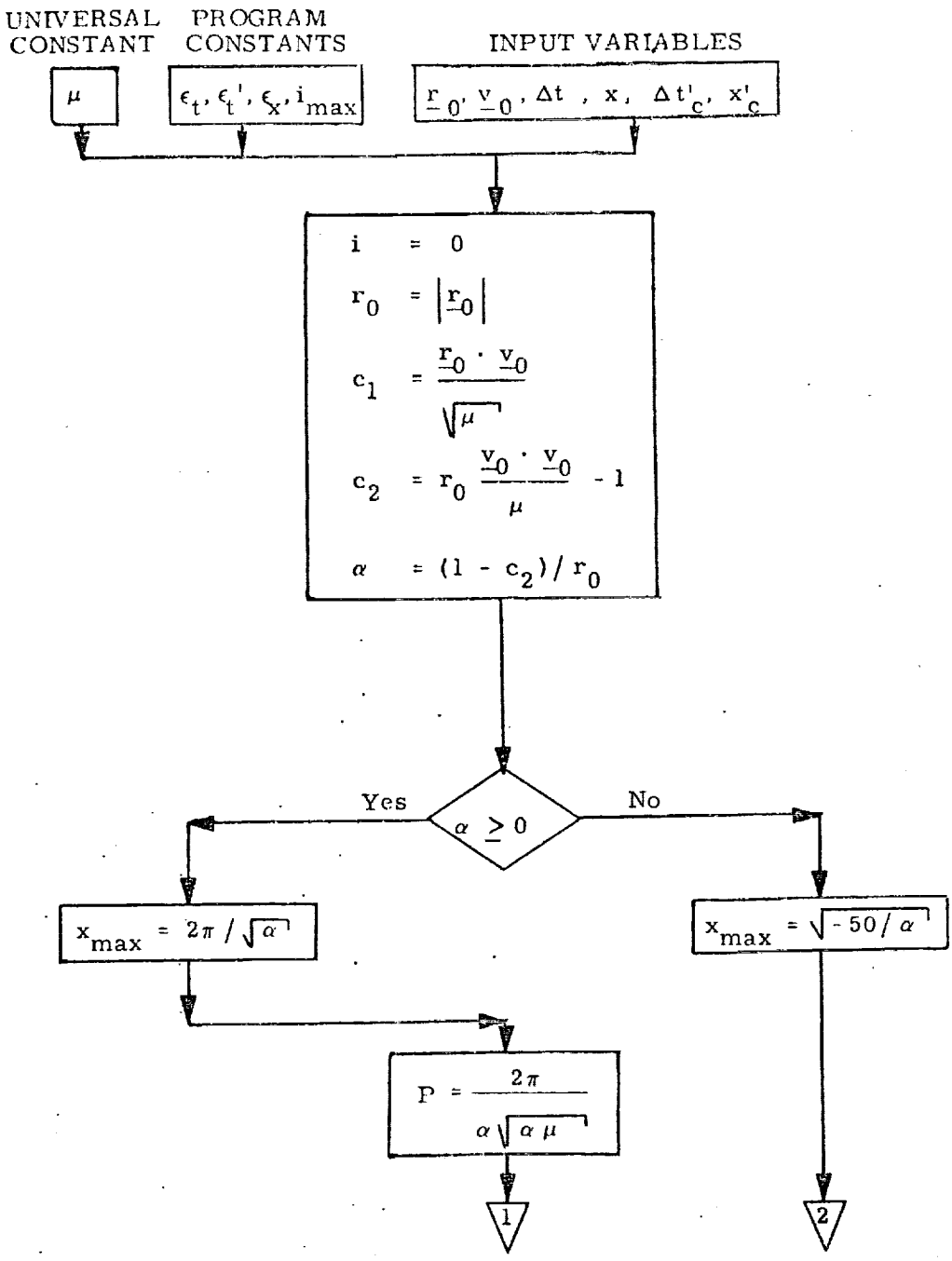


Figure 3a. Kepler Routine, Detailed Flow Diagram

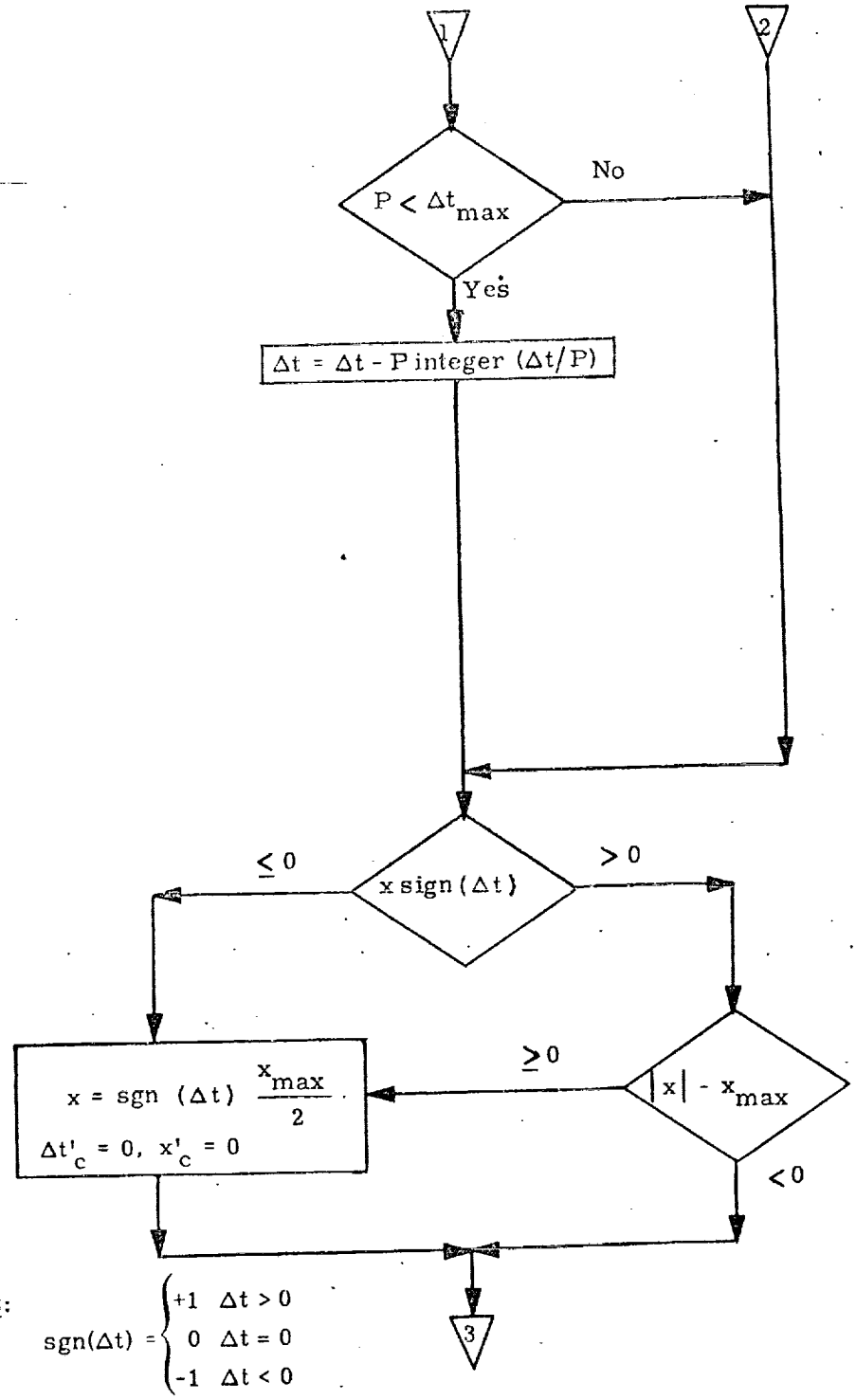


NOTE:

$$\mathrm{sgn}(\Delta t) = \begin{cases} +1 & \Delta t > 0 \\ 0 & \Delta t = 0 \\ -1 & \Delta t < 0 \end{cases}$$

Figure 3b. Kepler Routine, Detailed Flow Diagram

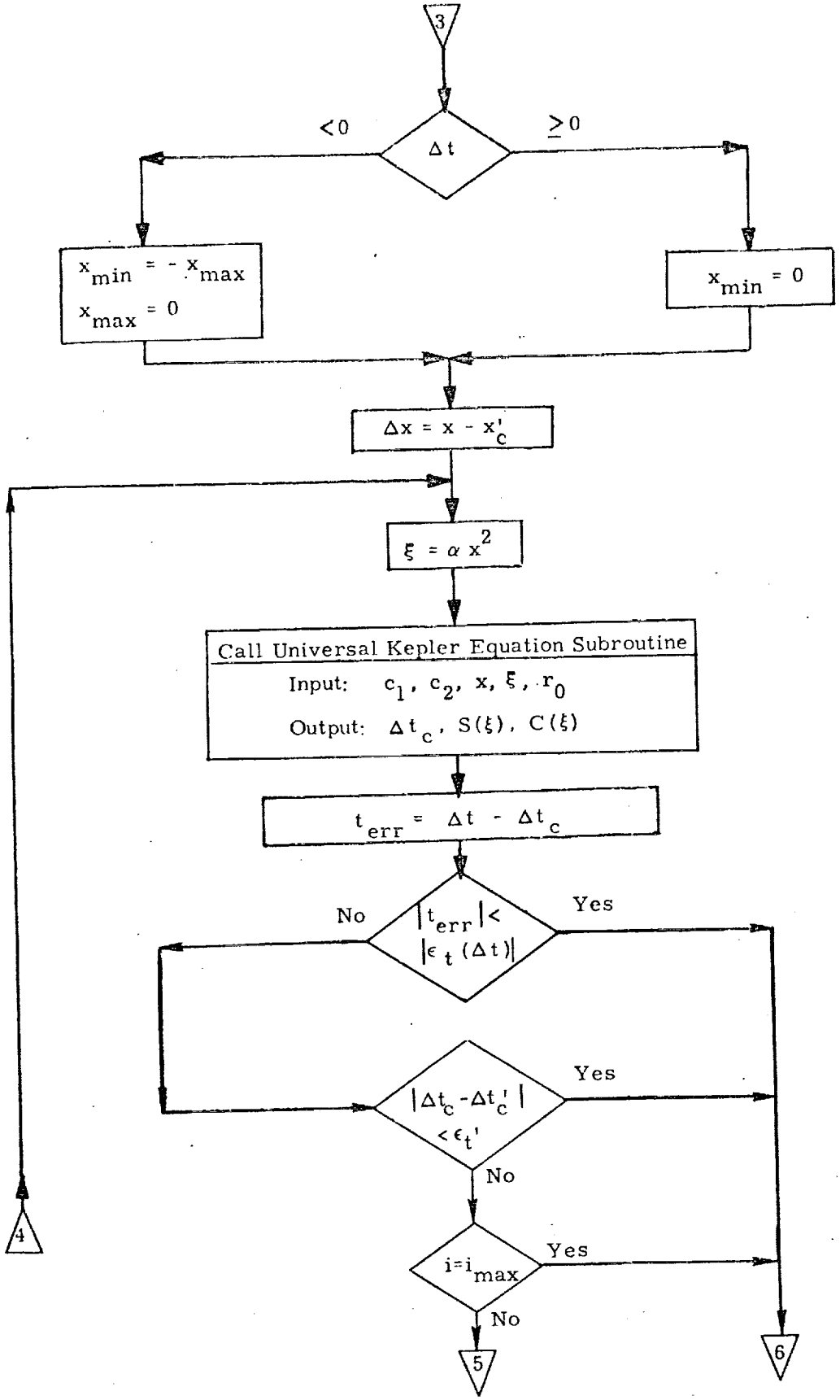


Figure 3c. Kepler Routine, Detailed Flow Diagram

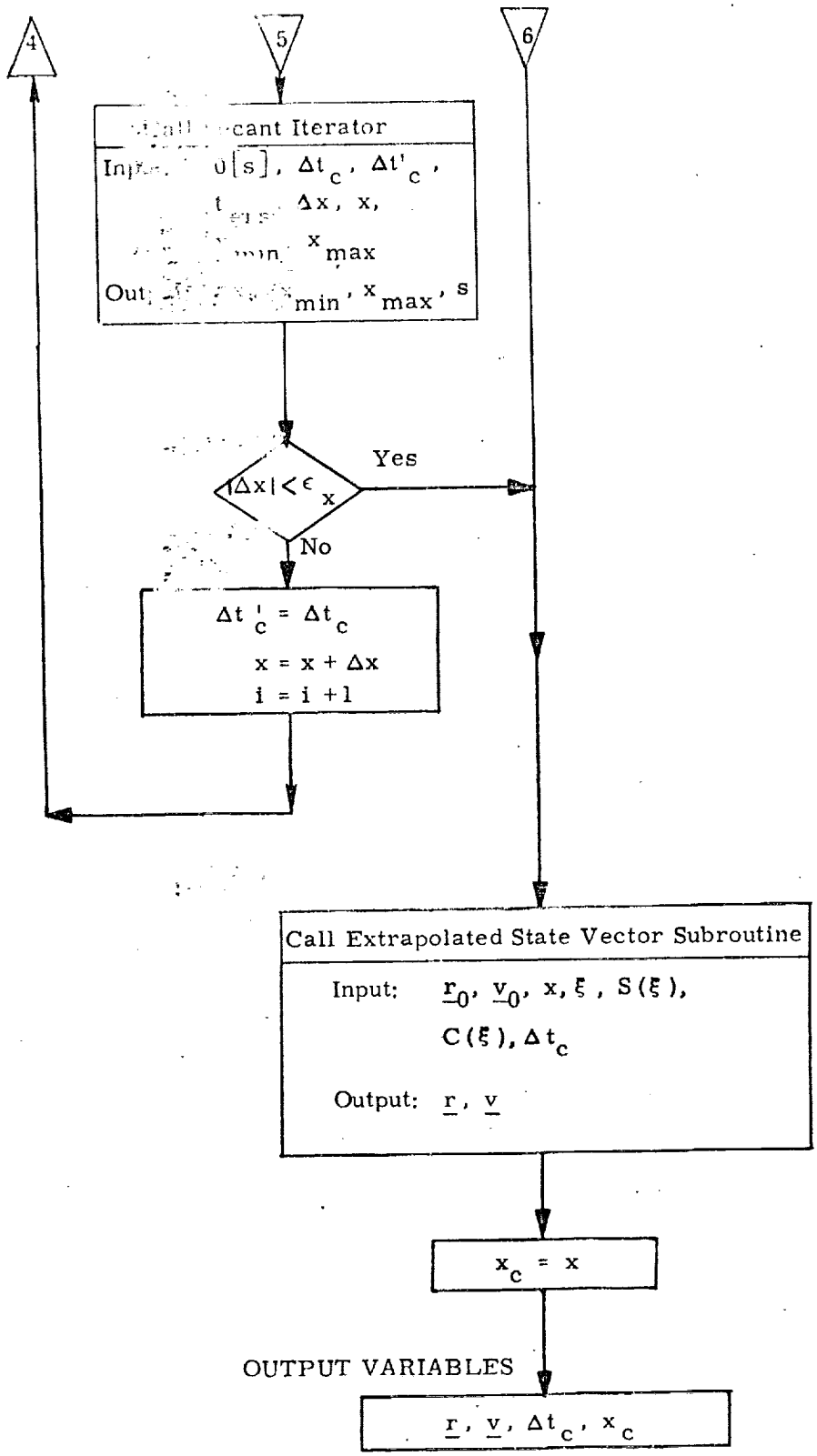


Figure 3d. Kepler Routine, Detailed Flow Diagram

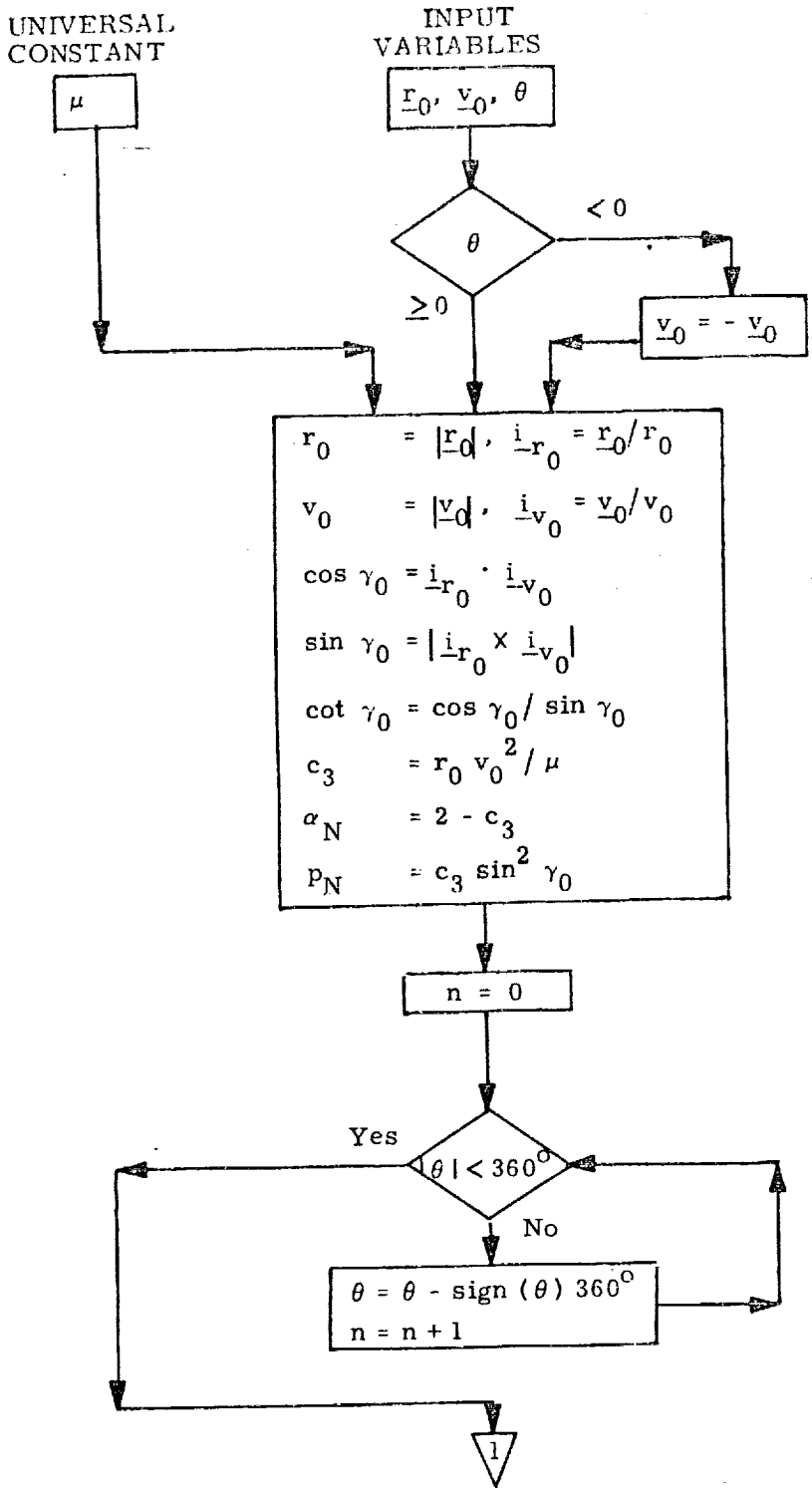


Figure 4a. Theta Routine, Detailed Flow Diagram

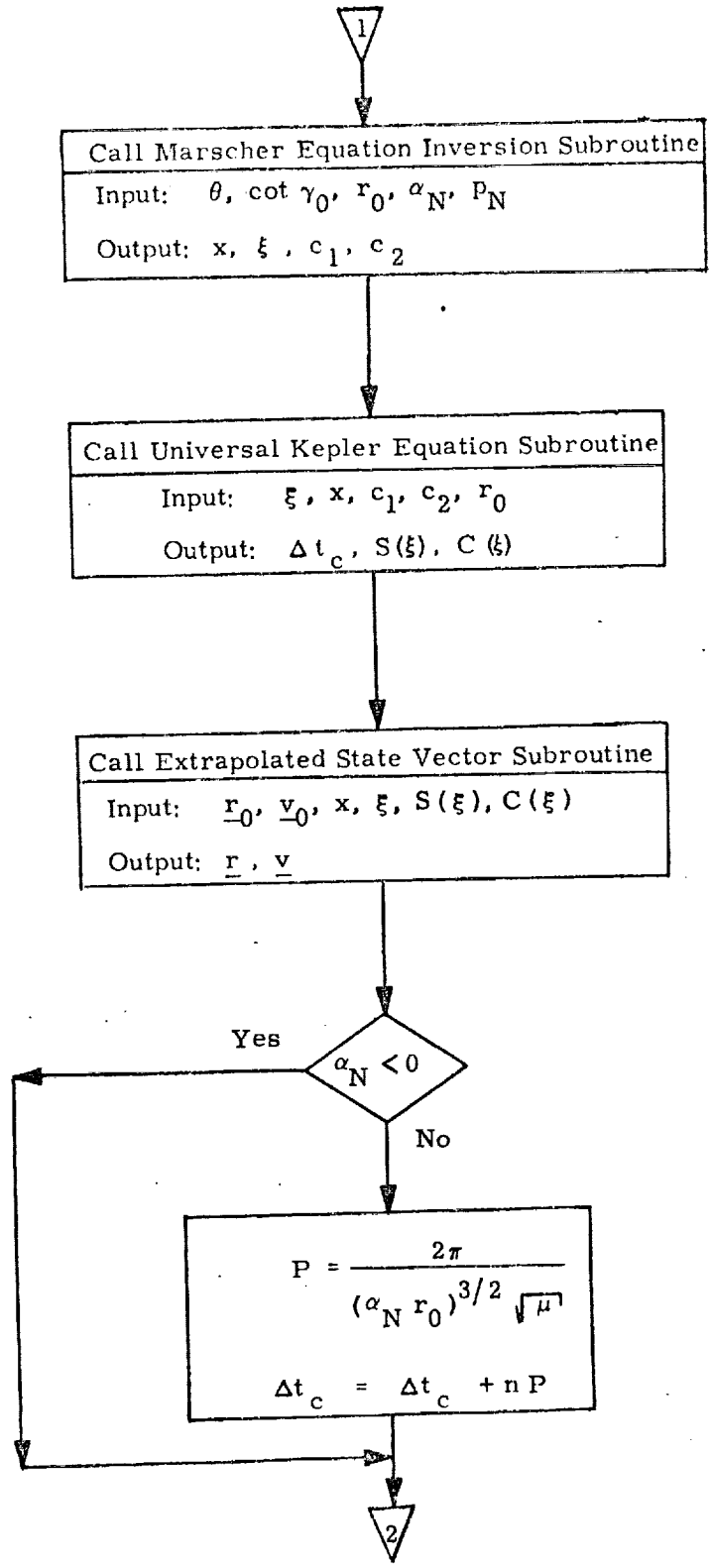


Figure 4b. Theta Routine, Detailed Flow Diagram

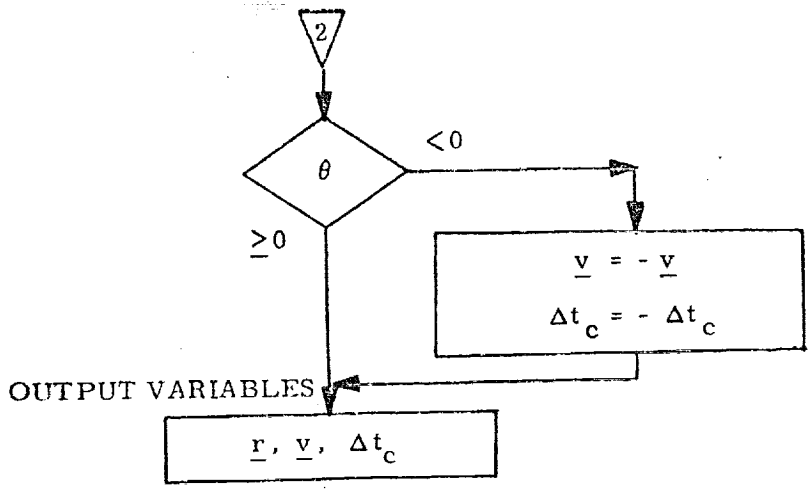


**Figure 4c.** Theta Routine, Detailed Flow Diagram

## 5.3 Subroutines Used By The Transfer Time or Transfer Angle Conic Extrapolation Routines

### 5.3.1 Universal Kepler Equation Subroutine

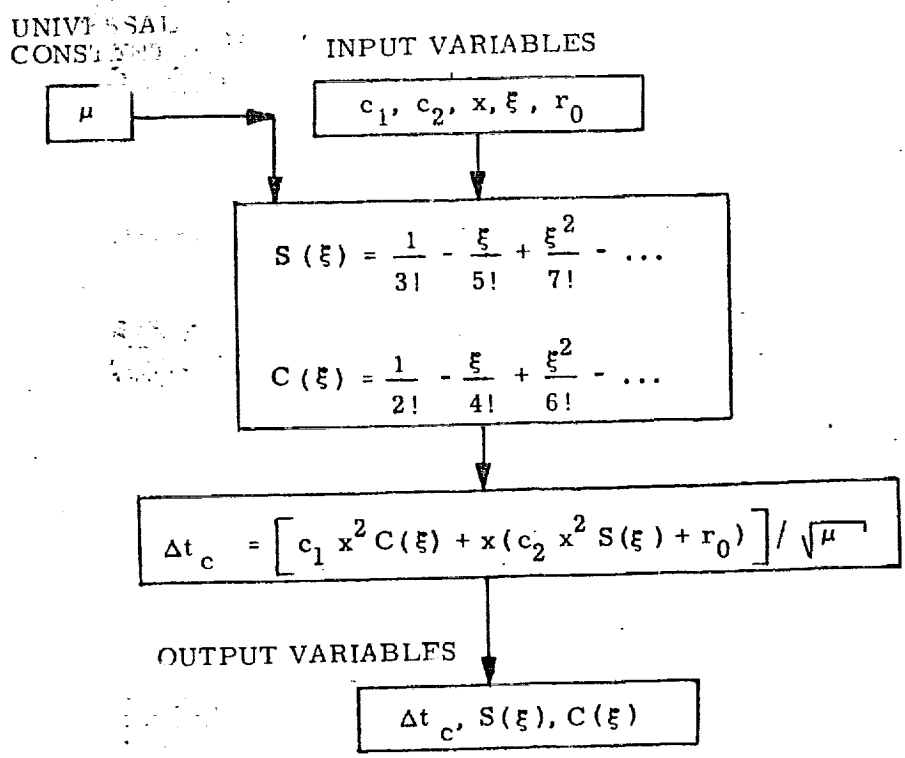


Figure 5. Universal Kepler Equation, Detailed Flow Diagram

### 5.3.2 Extrapolated State Vector Subroutine

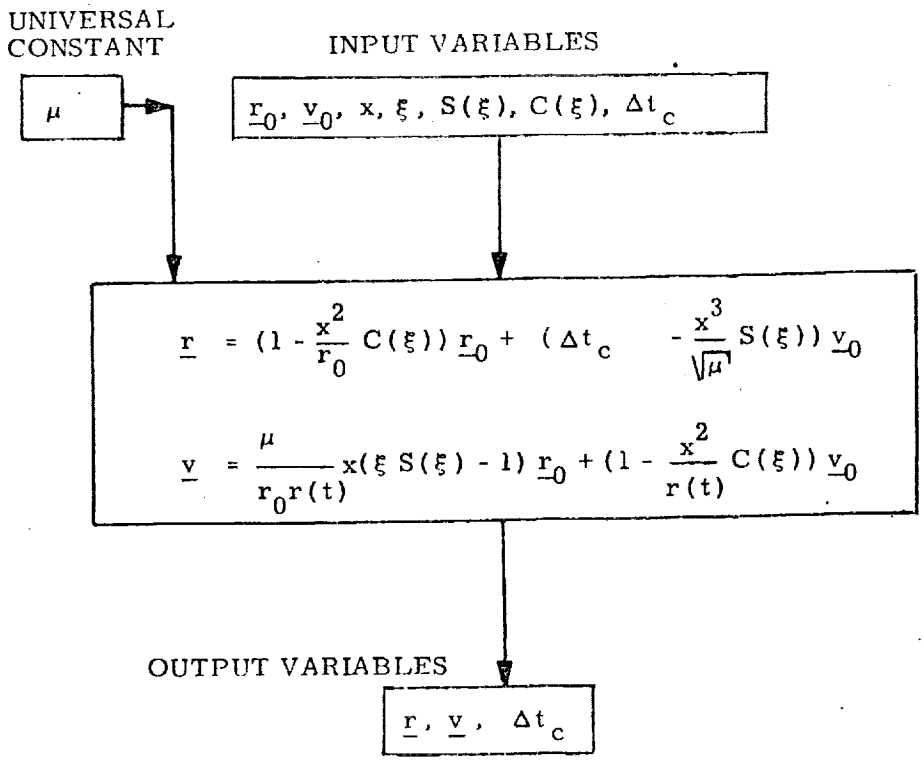


Figure 6. Extrapolated State Vector Equation, Detailed Flow Diagram

5.3.3 Secant Iterator

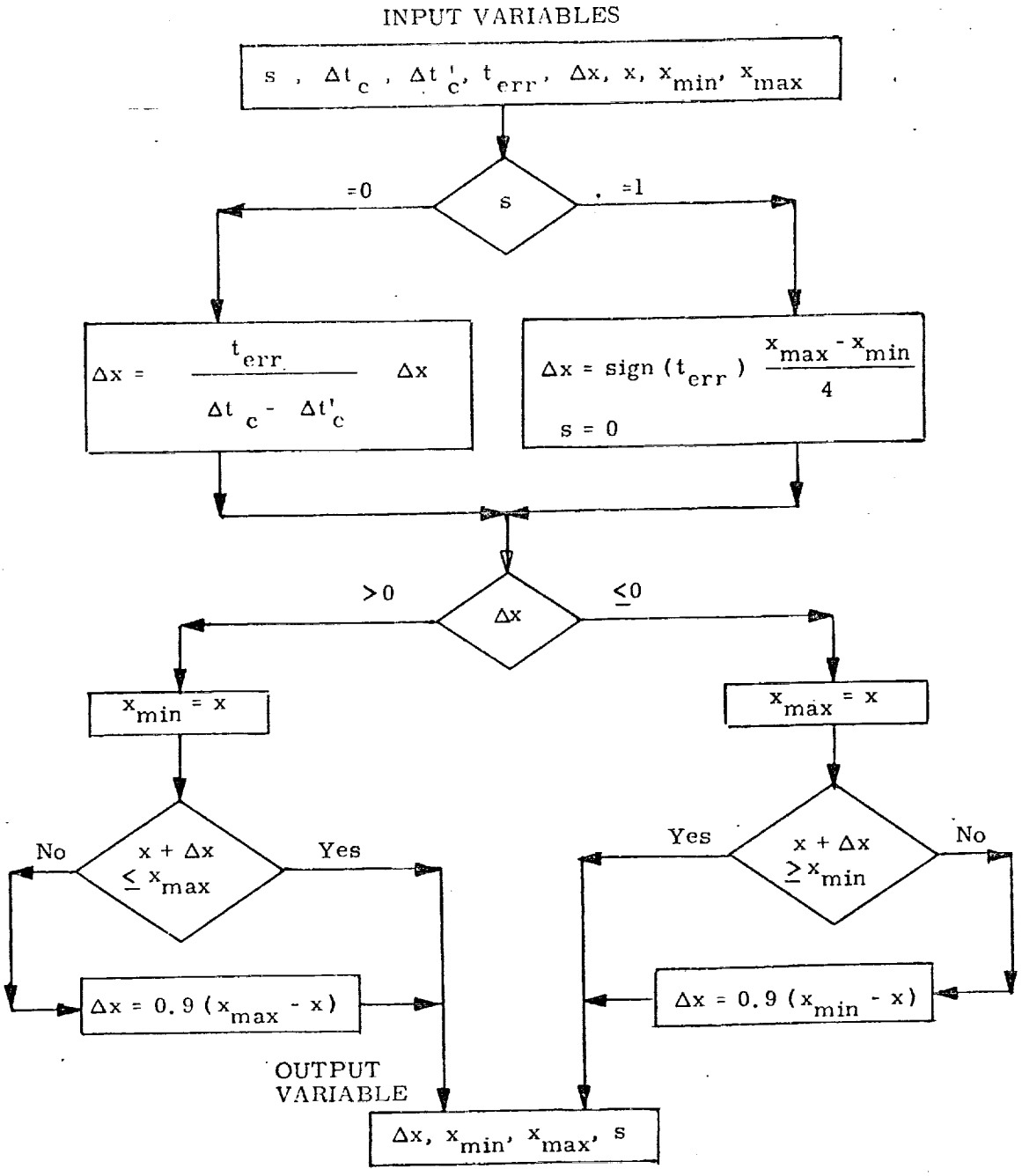


Figure 7. Secant Iterator, Detailed Flow Diagram

5.3.4 Marscher Equation Inversion Subroutine

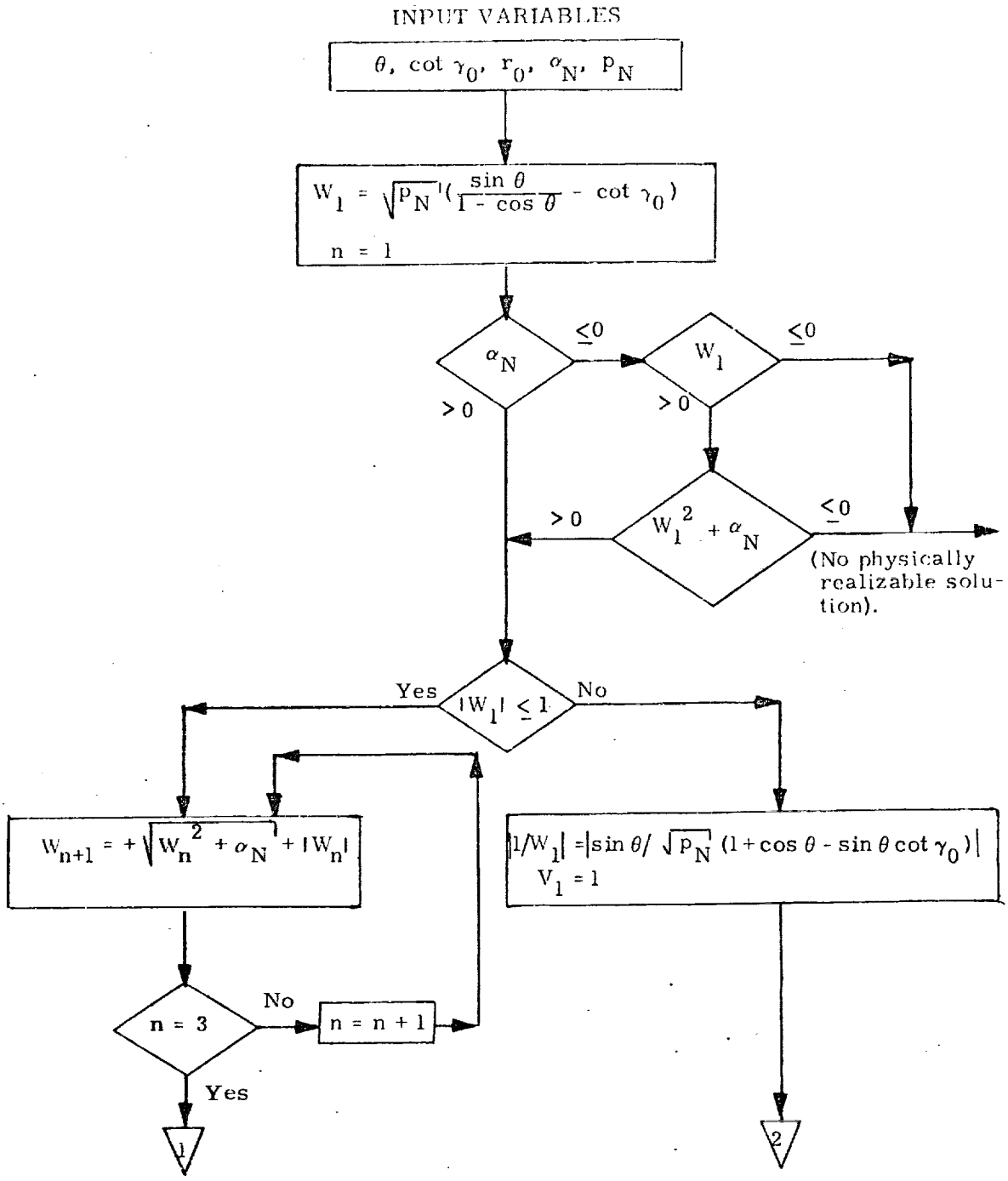


Figure 8a. Marscher Equation Inversion, Detailed Flow Diagram

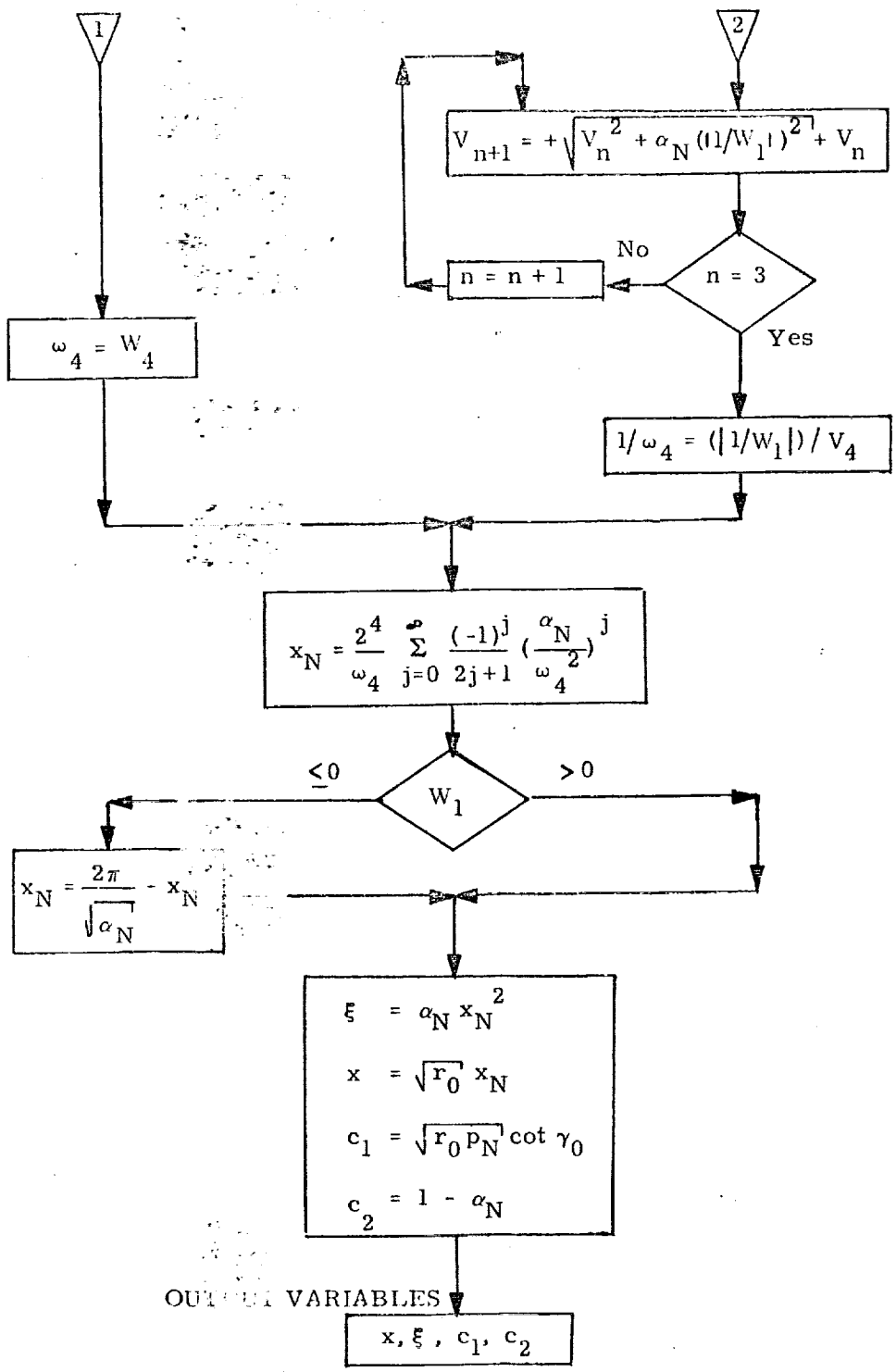


Figure 8b. Marscher Equation Inversion, Detailed Flow Diagram

## 6. SUPPLEMENTARY INFORMATION

The analytic expressions for the Universal Kepler Equation and the extrapolated position and velocity vectors are well known and are given by Battin (1964). Battin also outlines a Newton iteration technique for the solution of the Universal Kepler Equation; this technique converges somewhat faster than the secant technique but requires the evaluation of the derivative. It may be shown that if the derivative evaluation by itself takes more than 44% of the computation time used by the other calculations in one pass through the loop, then it is more efficient timewise to use the secant method.

Marscher's universal equation for cot $\theta/2$ was derived by him in his report (Marscher, 1965), and is the generalization of his "Three-Cotangent" equation:

$$\cot \frac{\theta}{2} = \frac{r_0}{\sqrt{p\,a}} \cot \frac{(E - E_0)}{2} + \cot \gamma_0$$

Marscher has also outlined in the report an iterative method of extrapolating the state based on his universal equation. The inversion of Marscher's universal equation was derived by Robertson (1967a).

Krause organized the details of the computation in both routines.

A derivation of the coefficients in the inversion of the Universal Kepler Equation is given in Robertson (1967 b) and Newman (1967).

## References


1. [illegible] R. H., 1964, Astronautical Guidance, McGraw-Hill.

2. [illegible] W., 1968, A Unified Method of Solving Initial Value and Boundary Value Conic Trajectory Problems, TRW Interoffice Correspondence #3424.9-15 (January 1968).

3. Marscher, W., 1965, A Unified Method of Generating Conic Sections, MIT/IL Report R-479, February 1965.

4. [illegible] C. M., 1967, The Inversion of Kepler's Equation, MIT/IL Space Guidance Analysis Memo #14-67.

5. Robertson, W. M., 1967a, Explicit Universal Series Solutions for the Universal Variable x, MIT/IL Space Guidance Analysis Memo #8-67.

6. Robertson, W. M., 1967b, Time-Series Expansions of the Universal Variable x, MIT/IL Space Guidance Analysis Memo #13-67.

## 1. INTRODUCTION

The Conic Required Velocity Determination Routine provides the capability to solve the following two astrodynamic problems:

"The Multiple Revolution Lambert Required Velocity Determination Problem": compute the velocity vector required at an initial position to transfer through an inverse square central force field from the initial position to a specified target position in a specified transfer time interval by making a specified number of complete revolutions (and some fraction of another one). Also optionally compute the velocity vector at the target position and various parameters of the conic transfer orbit.

"The De-orbit Required Velocity Determination Problem": compute the velocity vector required at an initial position to transfer through an inverse square central force field from the initial position to a specified target radius (which is less than the initial radius) with a specified flight-path angle at that radius in a specified transfer time interval. Also optionally compute the velocity vector at the target position and various parameters of the conic transfer orbit.

The Conic Required Velocity Determination Routine basically consists of two major parts—one for solving the multi-revolution Lambert's problem and one for solving the De-orbit problem—which are quite similar. In fact, certain subsections of the parts are identical as well as being identical to certain subsections of the Conic State Extrapolation Routine (Ref. 7) and these may of course be arranged as subroutines on a computer.

The Conic Lambert and De-orbit Required Velocity Determination Routines each involve a single loop iterative procedure, and hence are organized in three sections: initialization, iteration, and final computations, as shown in Figure 1. The independent variable in the iteration in both routines is the cotangent of the flight-path angle at the initial position measured from local vertical, or equivalently the cotangent of the angle between the initial position vector (extended) and the as yet unknown required velocity vector. The dependent variable is the transfer time interval; it is a function solely of the independent variable and certain other quantities which depend explicitly on the input and which are thus constant in any one problem. In the iterative procedure, the independent variable (denoted by $\Gamma_0$) is adjusted between upper and lower bounds by a secant technique until the

transfer time interval computed from it agrees with the specified transfer time interval (to within a certain tolerance). Then the velocity vector at the initial position (i.e., the required velocity), as well as the velocity vector at the terminal position, is calculated from the last adjusted value of the independent variable.

In the less-than-one-complete revolution case in both routines, the upper and lower bounds on the independent variable are explicitly computed since the dependent and independent variables are monotonically related. However, in the multi-revolution case in the Lambert routine, there are two distinct physically-meaningful transfers which solve the problem, and an iterative procedure (entirely separate from, and not containing nor contained in the previously described iteration scheme) must be used to solve for the value of the independent variable which separates the two regions in each of which exactly one solution lies so that upper and lower bounds may be established corresponding to the unique solution desired. The multi-revolution case for the de-orbit problem is not considered in this document.

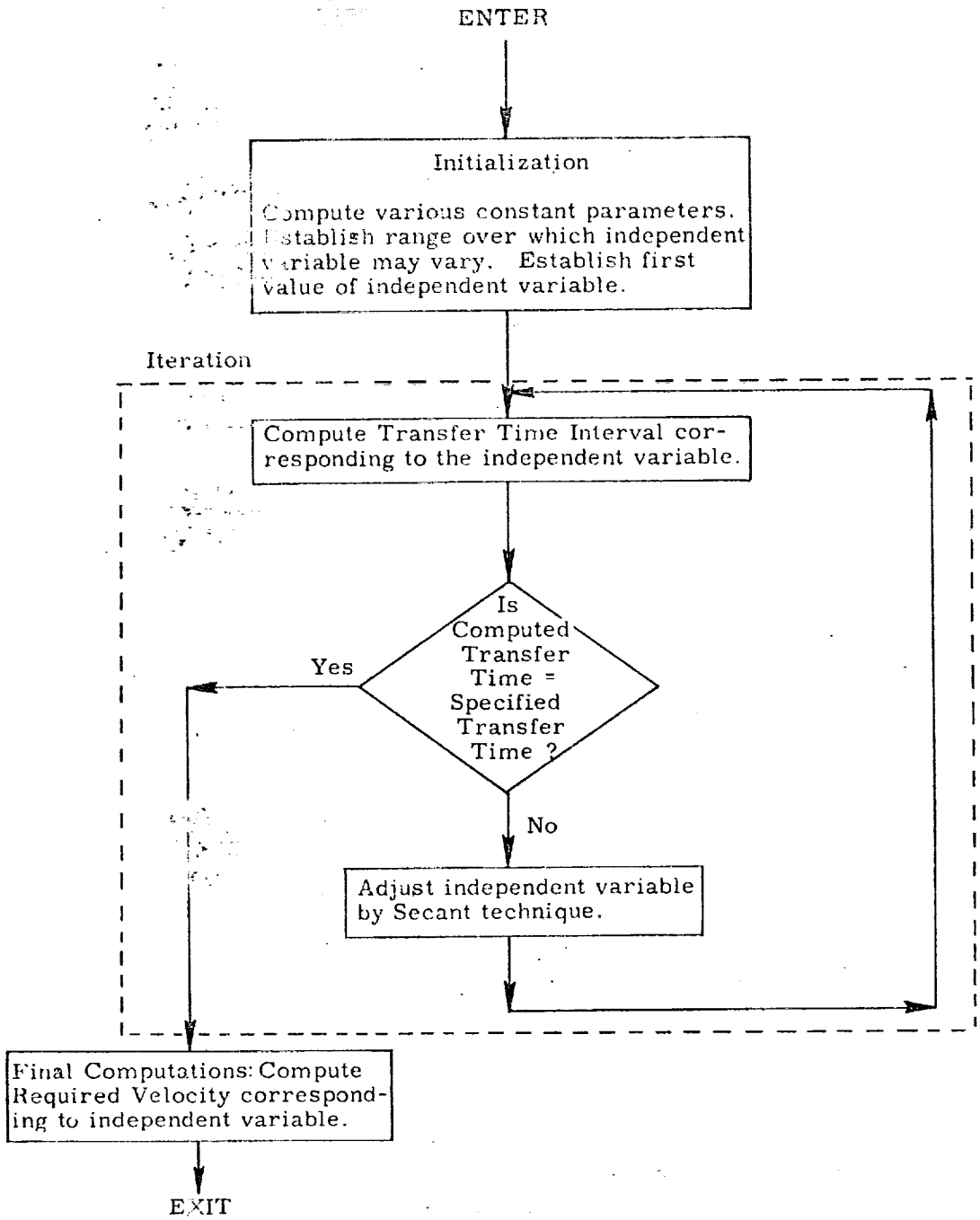


Figure 1. Conic Lambert and De-orbit Required Velocity Determination Routines Functional Flow Diagram

## NOMENCLATURE

| | |
|---|---|
| $a$ | Semi-major axis of conic |
| $c_1$ | First conic parameter [ $c_1 = \sqrt{r_0 p_N}\ \Gamma_0 = (\underline{r}_0 \cdot \underline{v}_0)/\sqrt{\mu_E}$ ] |
| $c_2$ | Second conic parameter [ $c_2 = 1 - \alpha_N = r_0 v_0^2 / \mu_E - 1$ ] |
| C or $C(\xi)$ | Power series in $\xi$ defined in the text |
| $E$ | Eccentric anomaly |
| $f$ | True anomaly |
| $H$ | Hyperbolic analog of eccentric anomaly |
| $i$ | Iteration counter |
| $\underline{i}_{c-}$ | The negative unit chord vector connecting $\underline{r}_0$ and $\underline{r}_1$. [ $\underline{i}_{c-} = -\text{unit}\ (\underline{r}_1 - \underline{r}_0)$ ]. |
| $i_{max}$ | Maximum allowable number of iterations |
| $\underline{i}_N$ | Unit vector in direction of angular momentum vector of the transfer and normal to the transfer plane. In the Lambert Routine the vector $\underline{i}_N$ always determines the direction of the transfer, and will also determine the plane of the transfer when either the switch $s_{proj} = 1$, or the switch $s_{proj} = 0$ but the initial position vector $\underline{r}_0$ is inside one of the cones. In the De-orbit Routine, the vector $\underline{i}_N$ always determines the plane and direction of the transfer. |
| $\underline{i}_{r_0}$ | Unit vector in direction of $\underline{r}_0$ |
| $\underline{i}_{r_1}$ | Unit vector in direction of $\underline{r}_1$ |

| | |
|---|---|
| $k$ | Intermediate variable equal to either $k_{bg}$ or $k_{sm}$ |
| $k_{bg}$ | Constant establishing by what fraction of its permissible range ($\Gamma_{max} - \Gamma_{min}$) the independent variable $\Gamma_0$ will be biased in the first iteration when no guess $\Gamma_{guess}$ is available, in order to establish a second point for the secant iteration |
| $k_{sm}$ | Constant establishing by what fraction of its permissible range ($\Gamma_{max} - \Gamma_{min}$) the independent variable $\Gamma_0$ will be biased in the first iteration when a guess $\Gamma_{guess}$ is available in order to establish a second point for the secant iteration. |
| $m$ | The slope of the line joining two successive points on the transfer time interval vs. independent variable curve. |
| $m'$ | Previous value of m |
| $m_{err}$ | Difference between desired value of the slope m (namely zero) and the value calculated on most recent iteration. |
| $n$ | Loop counter in the Marscher Equation Inversion |
| $n_{rev}$ | Integer number of complete $360^{\circ}$ revolutions to be made in the desired transfer. [Hence the transfer will be between $n_{rev}$ and $n_{rev} + 1$ revolutions]. |
| $\underline{N}$ | Intermediate vector variable normal to transfer plane |
| $p$ | Semi-latus rectum of conic |
| $p_1$ | Intermediate variable in the Lambert problem equal to $1 - \cos\theta$ |
| $p_2$ | Intermediate variable in the Lambert problem equal to $\cos\theta - (r_0 / r_1)$ |
| $p_N$ | Normalized semi-latus rectum of conic transfer orbit ($p_N = p / r_0$). |
| $q$ | Intermediate variable equal to $\lambda/\sin^2 \gamma_1$ |

$\underline{r}_0$ Initial or current inertial position vector (corresponds to time $t_0$).

$\underline{r}_1$ Terminal or target inertial position vector (corresponds to time $t_1$).

$r_1$ Radius at terminal or target position (corresponds to time $t_1$).

$s$ Switch used in Secant Iterator to determine whether secant method or offsetting (biasing) will be performed.

$s_{cone}$ Switch indicating whether the outcome of the cone test involving the tolerance criterion $\epsilon_{cone}$ was that initial position $\underline{r}_0$ lies outside both of the cones around the positive and negative target position vector $\underline{r}_1$ ($s_{cone}$ = 0), or inside one of these cones ($s_{cone}$ = 1). [See Section 4.7.]

$s_{guess}$ Switch indicating whether the routine is to compute its own guess of the independent variable $\Gamma_0$ to start the iterative procedure ($s_{guess}$ = 0), or is to use a guess $\Gamma_{guess}$ supplied by the user ($s_{guess}$ = 1)

$s_{proj}$ Switch indicating whether the initial and target position vectors, $\underline{r}_0$ and $\underline{r}_1$, are to be projected into the plane defined by the unit normal $\underline{i}_N$ before the main Lambert computations are performed. If $s_{proj}$ = 0, no projection will be made unless the initial position $\underline{r}_0$ is found to lie within one of the cones defined by $\epsilon_{cone}$, in which case $s_{cone}$ will be set equal to 1. If $s_{proj}$ = 1, the projections will be carried out immediately, and no cone test will be made.

| | |
|---|---|
| $s_{soln}$ | Switch indicating which of the two physically possible solutions is desired in the multi-revolution case. [ Not used in the less-than-360° transfer case]. In particular, $s_{soln} = -1$ indicates the solution with the smaller initial flight path angle $\gamma_0$ measured from local vertical, and $s_{soln} = +1$ indicates the one with the larger $\gamma_0$. |
| $s_{180}$ | Switch indicating whether the central transfer angle is between 0° and 180° ($s_{180} = +1$), or between 180° and 360° ($s_{180} = -1$). The determination of which one of the above two possibilities is desired is made automatically by the routine on the basis of the direction of the unit normal vector $\underline{i}_N$.<br>[In the multiple-revolution case, the number of complete 360° revolutions is neglected; i.e., $s_{180}$ is the sign of the sine of the transfer angle. ] |
| S or $S(\xi)$ | Power series in $\xi$ defined in the text. |
| $t_{err}$ | Difference between specified time interval and that calculated by Universal Kepler Equation [ $t_{err} = \Delta t - \Delta t_c$ ]. |
| $\underline{v}_0$ | Inertial velocity required at the initial position $\underline{r}_0$ to transfer to the terminal point in exactly the specified time interval $\Delta t$. |
| $\underline{v}_1$ | Inertial velocity at the terminal position $\underline{r}_1$. |
| $V_n$ (n=1, 2..) | Intermediate scalar variables used in Marscher Equation Inversion |
| $W_n$ (n=1, 2..) | Intermediate scalar variables used in Marscher Equation Inversion |

| | |
|---|---|
| $x$ | Universal eccentric anomaly difference corresponding to the transfer from $\underline{r}_0$ to $\underline{r}_1$. |
| $x_N$ | Normalized universal eccentric anomaly difference ($x_N = x / \sqrt{r_0}$) |
| $\alpha_N$ | Reciprocal of normalized semi-major axis of conic transfer orbit ($\alpha_N = r_0 / a$). |
| $\gamma_0$ | Flight path angle at initial position $\underline{r}_0$ measured from local vertical, i.e., angle from $\underline{r}_0$ to $\underline{v}_0$. |
| $\gamma_1$ | Flight-path angle at terminal or target position measured from local vertical (corresponds to time $t_1$). |
| $\Gamma_0$ | Cotangent of flight-path angle $\gamma_0$ at the initial position $\underline{r}_0$ measured from local vertical; i.e., cotangent of the angle between $\underline{r}_0$ and $\underline{v}_0$. [ Independent variable in iterative scheme ]. |
| $\Gamma_0'$ | Previous value of $\Gamma_0$ |
| $\Gamma_0^{(i)}$ | The "i-th" value of $\Gamma_0$ |
| $\Gamma_1$ | Cotangent of flight path angle $\gamma_1$ at the terminal or target position $\underline{r}_1$ measured from local vertical |
| $\Gamma_{guess}$ | Guess of independent variable $\Gamma_0$ corresponding to solution (disregarded when $s_{guess} = 0$). |
| $\Gamma_{parab}$ | Value of $\Gamma_0$ corresponding to the physically realizable parabolic transfer |
| $\Gamma_{max}$ | Upper bound on $\Gamma_0$ |
| $\Gamma_{ME}$ | Value of $\Gamma_0$ corresponding to the minimum energy transfer |

| | |
|---|---|
| $\Gamma_{min}$ | Lower bound on $\Gamma_0$ |
| $\Delta t$ | Specified transfer time interval $(t_1 - t_0)$ between $\underline{r}_0$ and $\underline{r}_1$ |
| $\Delta t_c$ | Value of the transfer time interval calculated in the Universal Kepler Equation from the current value of $\Gamma_0$ and the conic parameters |
| $\Delta t_c'$ | Previous value of $\Delta t_c$ |
| $\Delta t_c^{(i)}$ | The "i-th" value of the transfer time interval calculated in the Universal Kepler Equation as a function of the "i-th" value $\Gamma_0^{(i)}$ of $\Gamma_0$ and the conic parameters |
| $\Delta\Gamma_0$ | Increment in $\Gamma_0$ |
| $\Delta\Lambda$ | Increment in $\Lambda$ |
| $\epsilon_{cone}$ | Tolerance criterion establishing small cones around both the positive and negative target position directions inside of which the Lambert routine will define the plane of the transfer by the unit normal $\underline{i}_N$ rather than the cross product of the initial and target position vectors, $\underline{r}_0$ and $\underline{r}_1$. [ $\epsilon_{cone}$ = sin (the half cone angle) ]. |
| $\epsilon_t$ | Primary convergence criterion: relative error in transfer time interval |
| $\epsilon_t'$ | Secondary convergence criterion: minimum permissible difference of two successive calculated transfer time intervals. |
| $\epsilon_T$ | Convergence criterion in iteration to adjust $\Gamma_{min}$ and $\Gamma_{max}$ in multiple revolution case: absolute precision to which transfer time interval minimum is to be determined |
| $\epsilon_\Gamma$ | Tertiary convergence criterion: minimum permissible size of increment $\Delta\Gamma_0$ of the independent variable |

| | |
|---|---|
| $\epsilon_\Lambda$ | Tolerance criterion in iteration to adjust $\Gamma_{min}$ and $\Gamma_{max}$ in multiple revolution case: absolute difference of two successive values of independent variable to prevent division by zero |
| $\theta$ | Transfer angle (true anomaly increment) |
| $\lambda$ | Ratio of initial position radius to terminal position radius |
| $\Lambda$ | Average of the two most recent values of $\Gamma_0$. [$\Lambda$ is used as the independent variable in the Multi-revolution Bounds Adjustment Coding Sequence Relation]. |
| $\Lambda'$ | Previous value of $\Lambda$ |
| $\mu$ | Gravitational parameter of the earth (product of earth's mass and universal gravitation constant) |
| $\xi$ | The dimensionless variable $\alpha x^2 = x^2 / a = \alpha_N x^2 / r_p$. [Equivalent to square of standard eccentric or hyperbolic anomaly difference]. |

## 5. DETAILED FLOW DIAGRAMS

### 5.1 Multiple-Revolution Lambert Required Velocity Determination Routine

This routine utilizes the following subroutines or coding sequences, which are diagrammed in Section 5.3:

- Lambert Transfer Time Interval Subroutine
  - Marscher Equation Inversion Subroutine
  - Universal Kepler Equation Subroutine
- Secant Iterator
- Multi-revolution Bounds Adjustment Coding Sequence
  - Secant Minimum Iterator

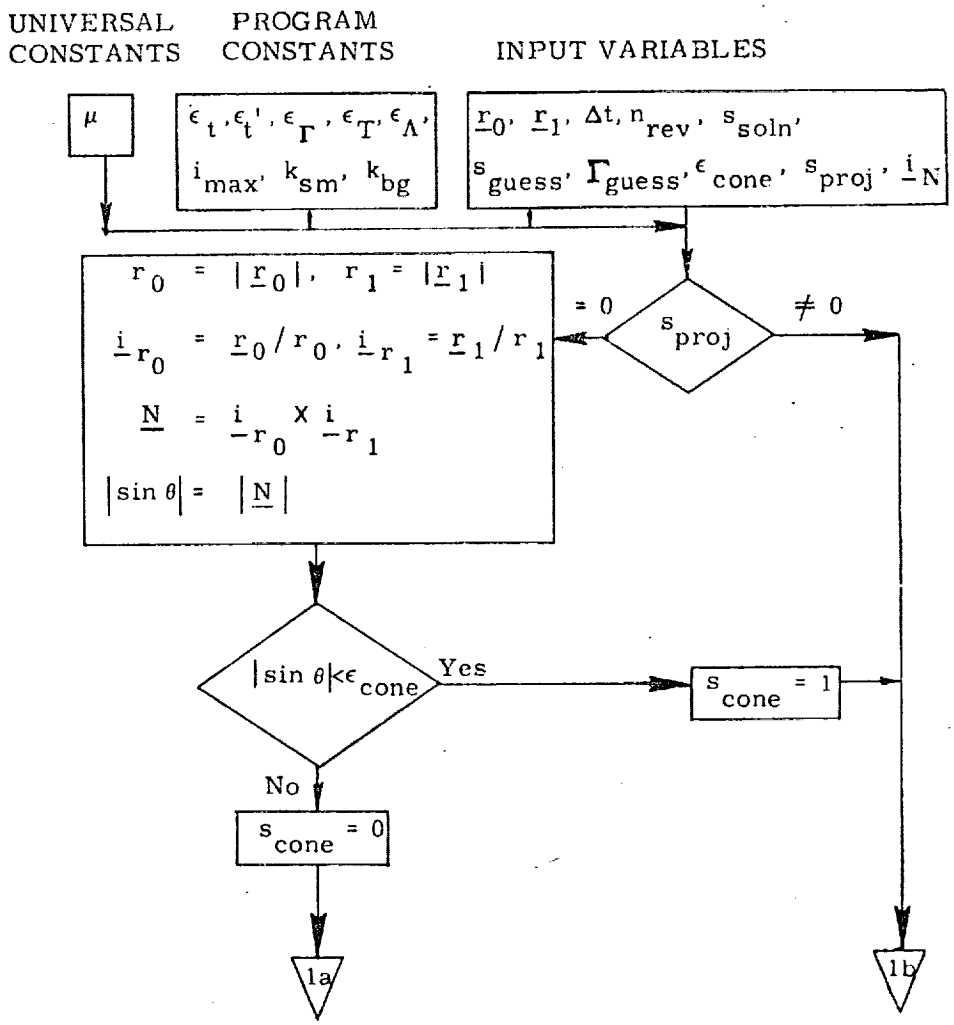


Figure 3a. Multi-Revolution Lambert Routine Detailed Flow Diagram

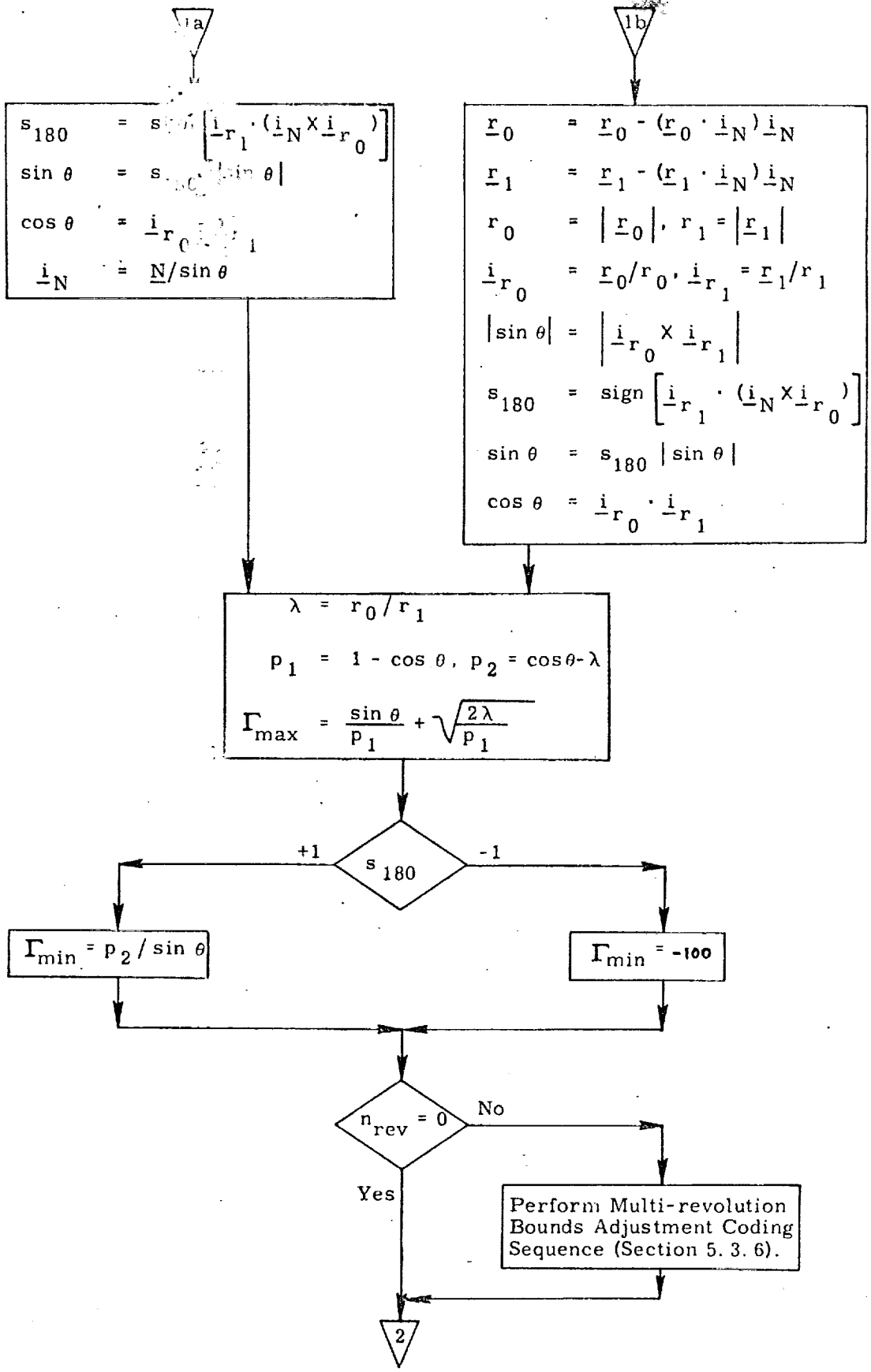


Figure 3b. Multi-Revolution Lambert Routine Detailed Flow Diagram

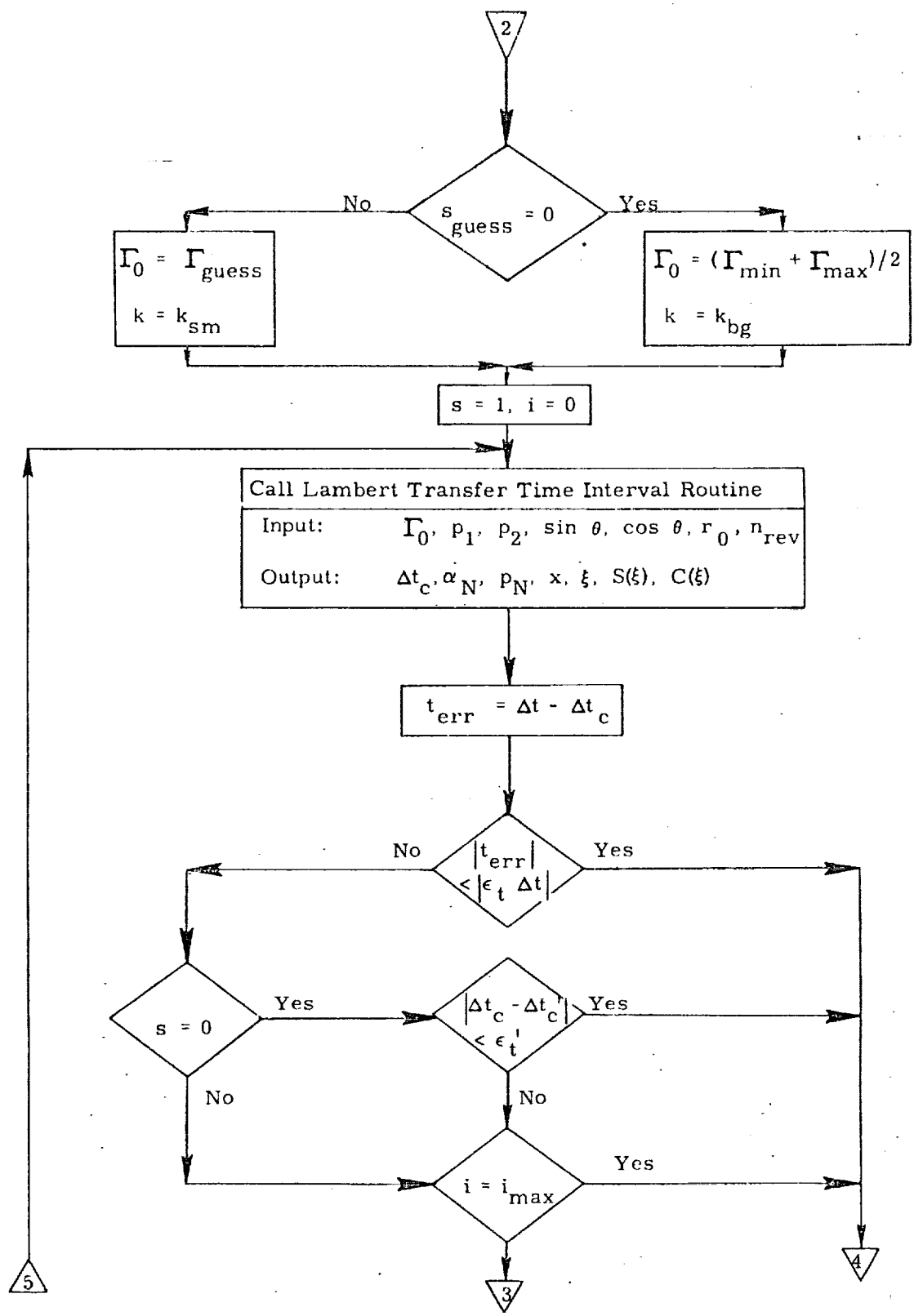


Figure 3c. Multi-Revolution Lambert Routine Detailed Flow Diagram

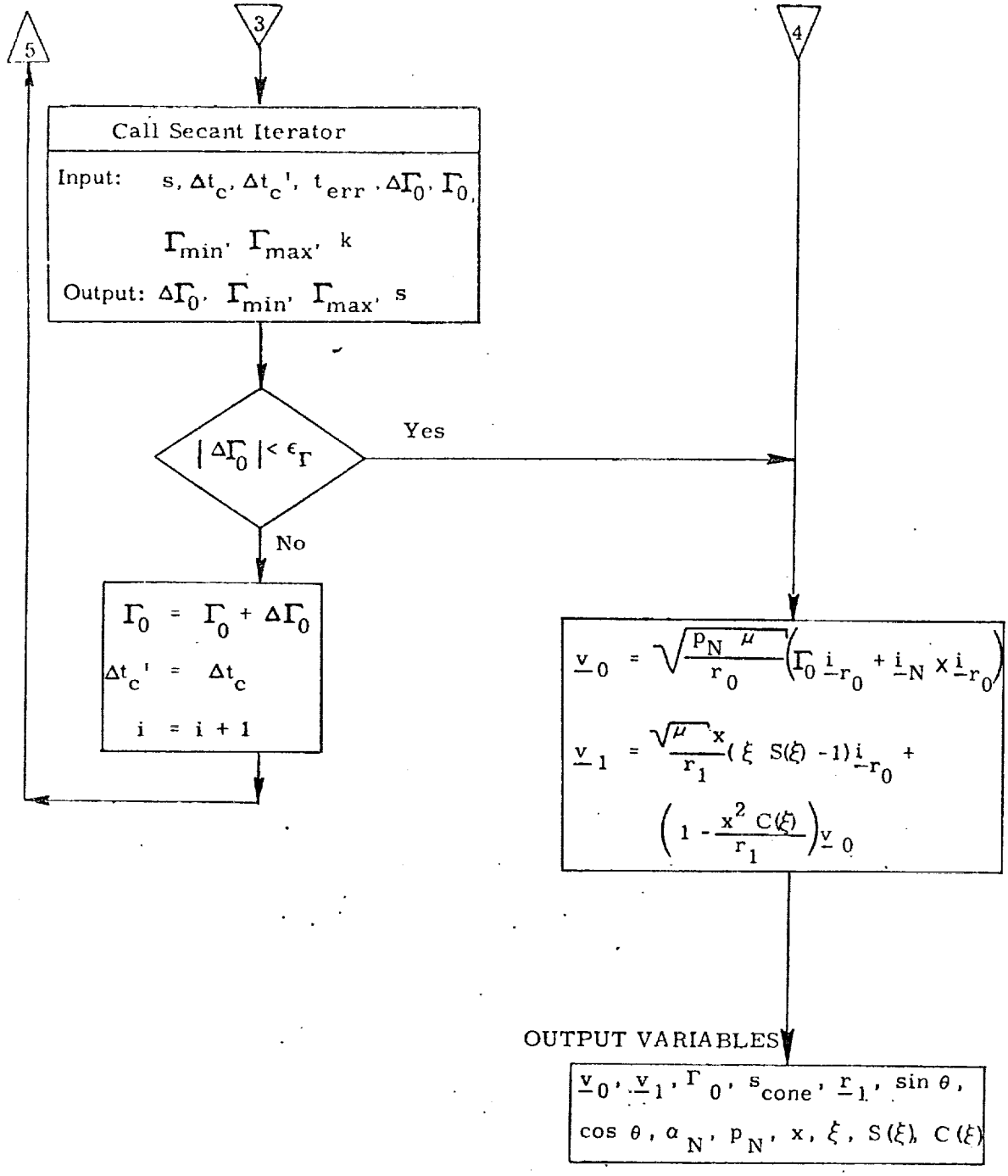


Figure 3d. Multi-Revolution Lambert Routine Detailed Flow Diagram

## 5.2 De-orbit Required Velocity Determination Routine

This routine utilizes the following subroutines which are diagrammed in Section 5.3:

- De-orbit Transfer Time Interval Subroutine
  - Marscher Equation Inversion Subroutine
  - Universal Kepler Equation Subroutine
- Secant Iterator

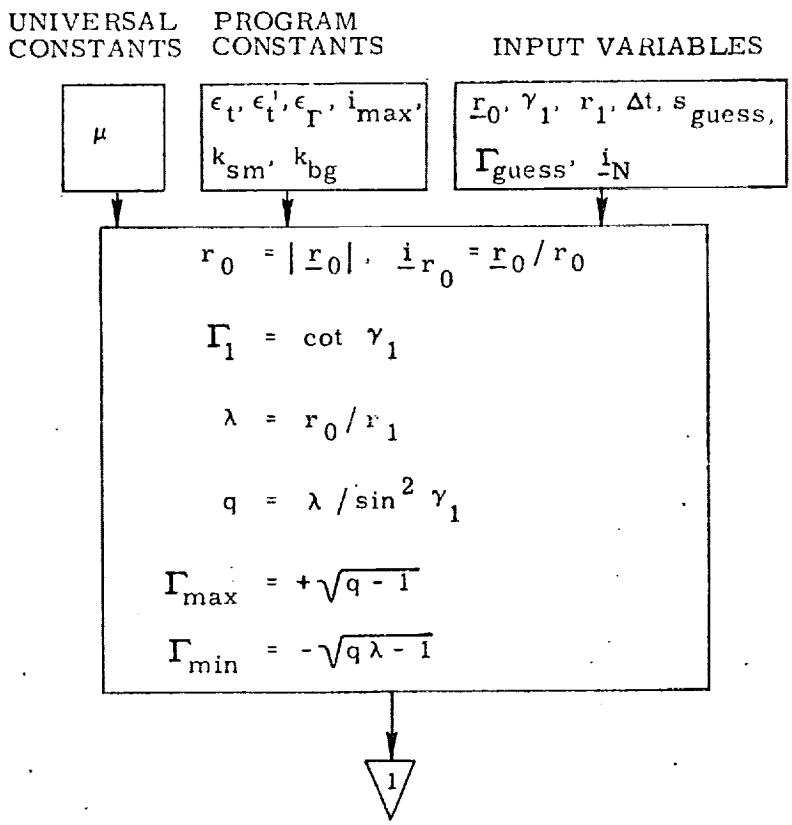


Figure 4a. De-orbit Routine Detailed Flow Diagram

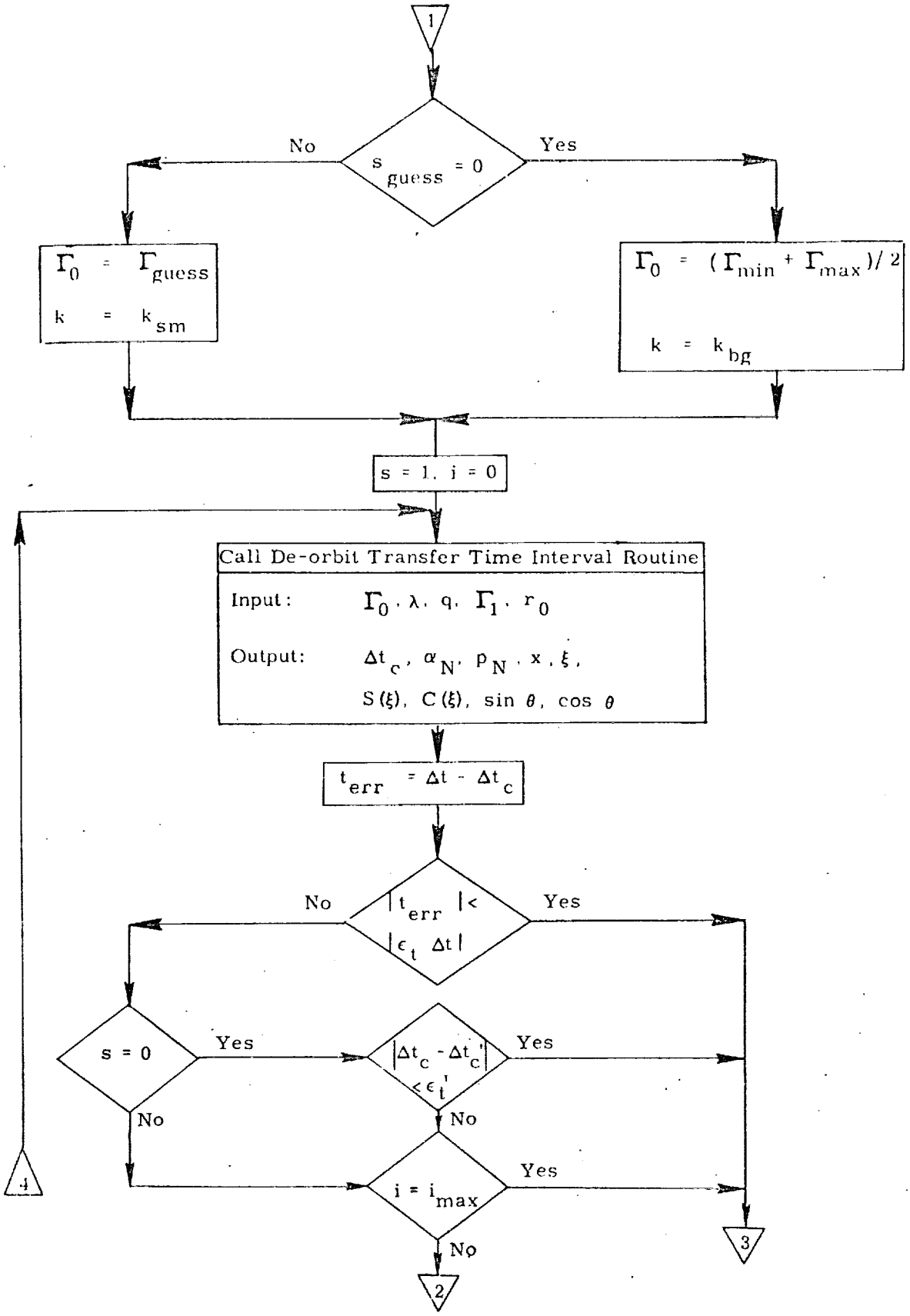


Figure 4b. De-orbit Routine
Detailed Flow Diagram

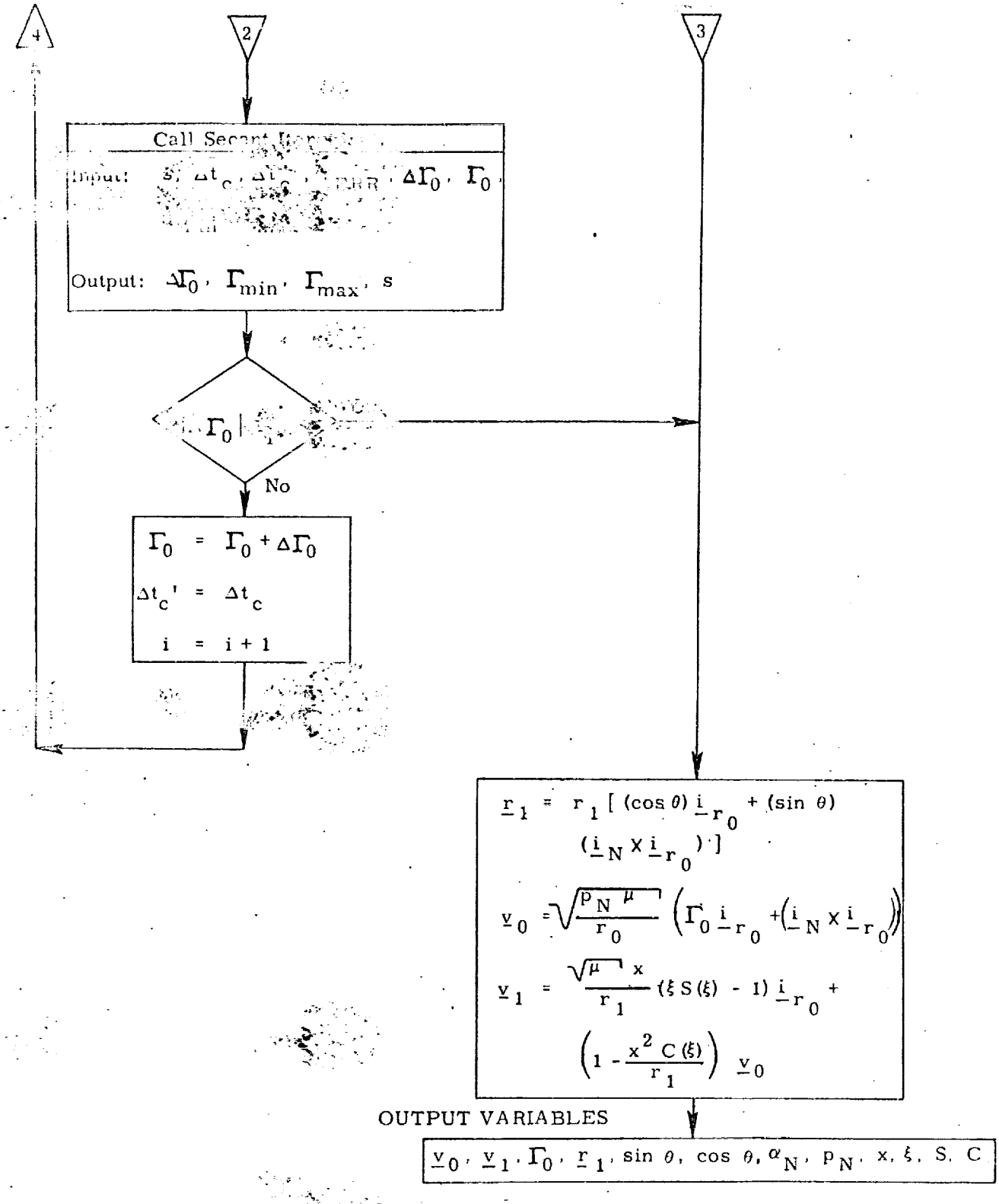


Fig. 4c. De-orbit Routine
Detailed Flow Diagram

## 5.3 Subroutines or Coding Sequences used by the Conic Required Velocity Determination Routines

### 5.3.1 Lambert Transfer Time Interval Subroutine

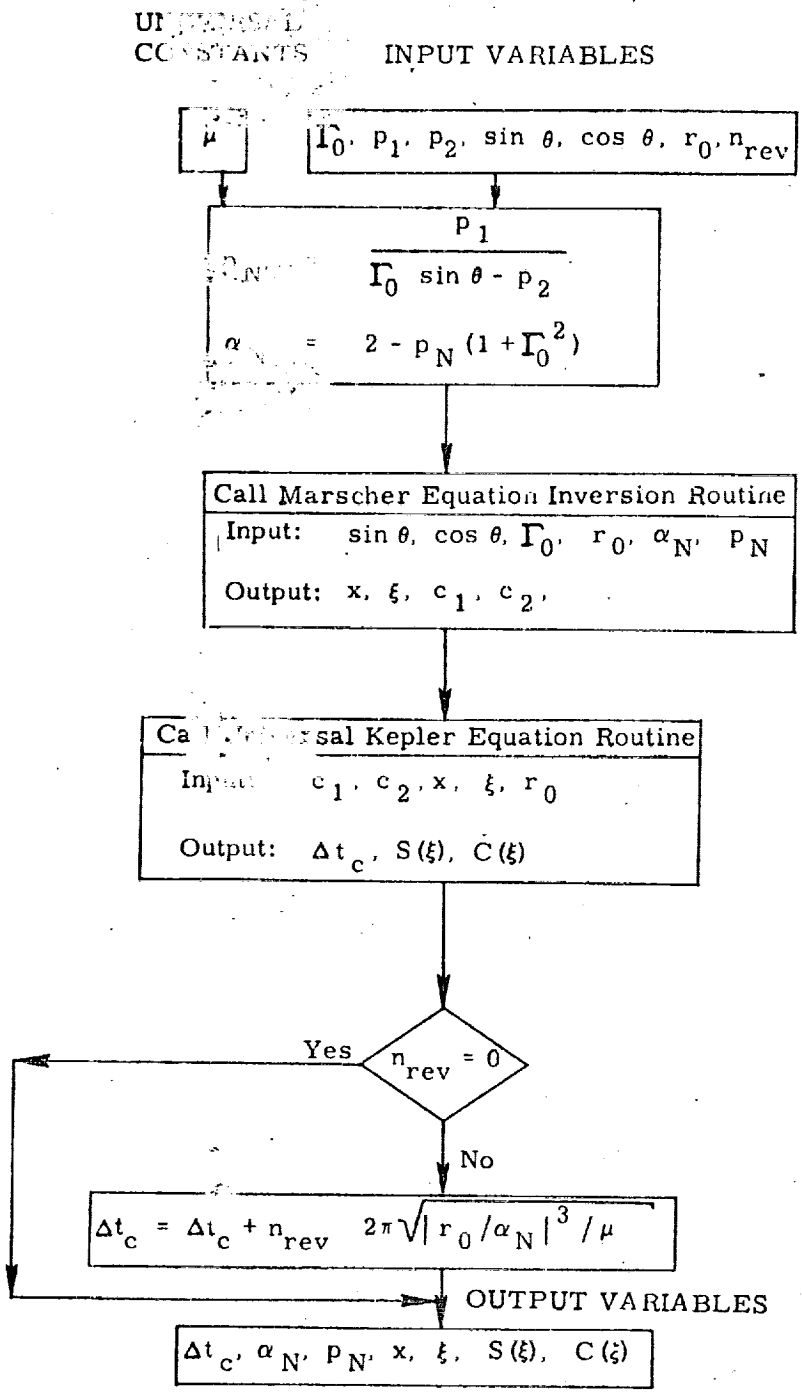


Figure 5. Lambert Transfer Time Interval Subroutine Detailed Flow Diagram

### 5.3.2 De-orbit Transfer Time Interval Subroutine

INPUT VARIABLES

$\Gamma_0,\ \lambda,\ q,\ \Gamma_1,\ r_0$

$$\cot\frac{\theta}{2} = (\Gamma_0 + \lambda\Gamma_1) / (1 - \lambda)$$

$$p_N = \frac{2(\lambda - 1)}{q\lambda - (1 + \Gamma_0^2)}$$

$$\alpha_N = 2 - p_N(1 + \Gamma_0^2)$$

$$\cos\theta = \left\{(\cot\frac{\theta}{2})^2 - 1\right\} / \left\{(\cot\frac{\theta}{2})^2 + 1\right\}$$

$$\sin\theta = (1 - \cos\theta)\ (\cot\frac{\theta}{2})$$

**Call Marscher Equation Inversion Routine**

Input: $\sin\theta,\ \cos\theta,\ \Gamma_0,\ r_0,\ \alpha_N,\ p_N$

Output: $x,\ \xi,\ c_1,\ c_2$

**Call Universal Kepler Equation Routine**

Input: $c_1,\ c_2,\ x,\ \xi,\ r_0$

Output: $\Delta t_c,\ S(\xi),\ C(\xi)$

OUTPUT VARIABLES

$\Delta t_c,\ \alpha_N,\ p_N,\ x,\ \xi,\ S(\xi),\ C(\xi)$

$\sin\theta,\ \cos\theta$

Figure 6. De-orbit Transfer Time Interval Subroutine Detailed Flow Diagram

### 5.3.3 Universal Kepler Equation Subroutine

This subroutine is identical to the one used in the Kepler and Theta problems.

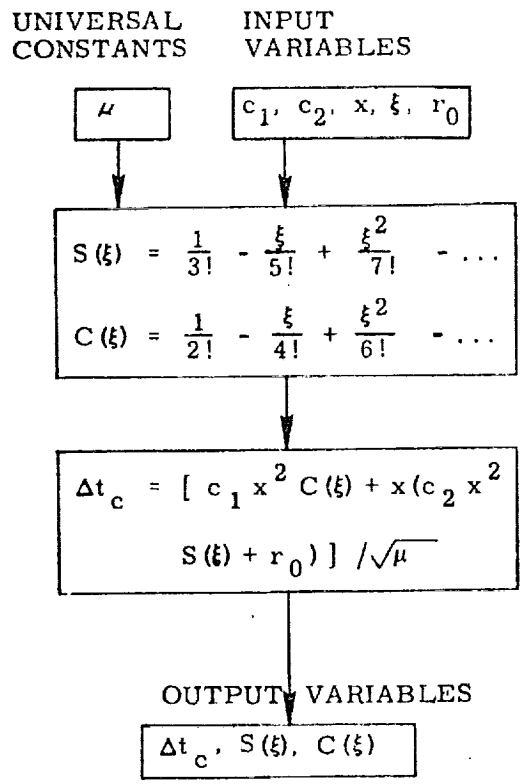


**Figure 7.** Universal Kepler Equation Subroutine Detailed Flow Diagram

5.3.4 Marscher Equation Inversion Subroutine

This subroutine is identical to the one used in the Theta problem.

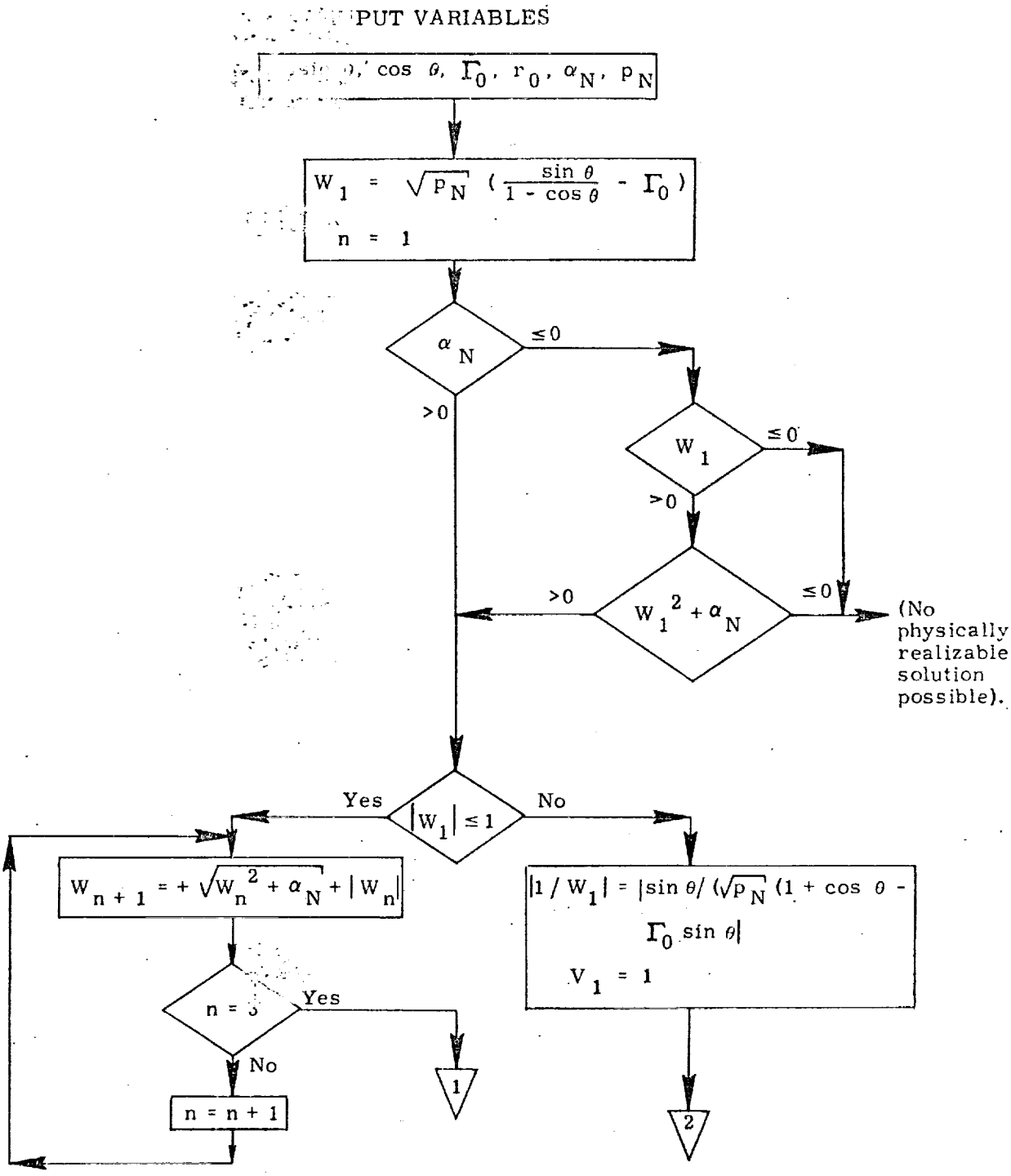


Figure 8a. Marscher Equation Inversion Subroutine Detailed Flow Diagram

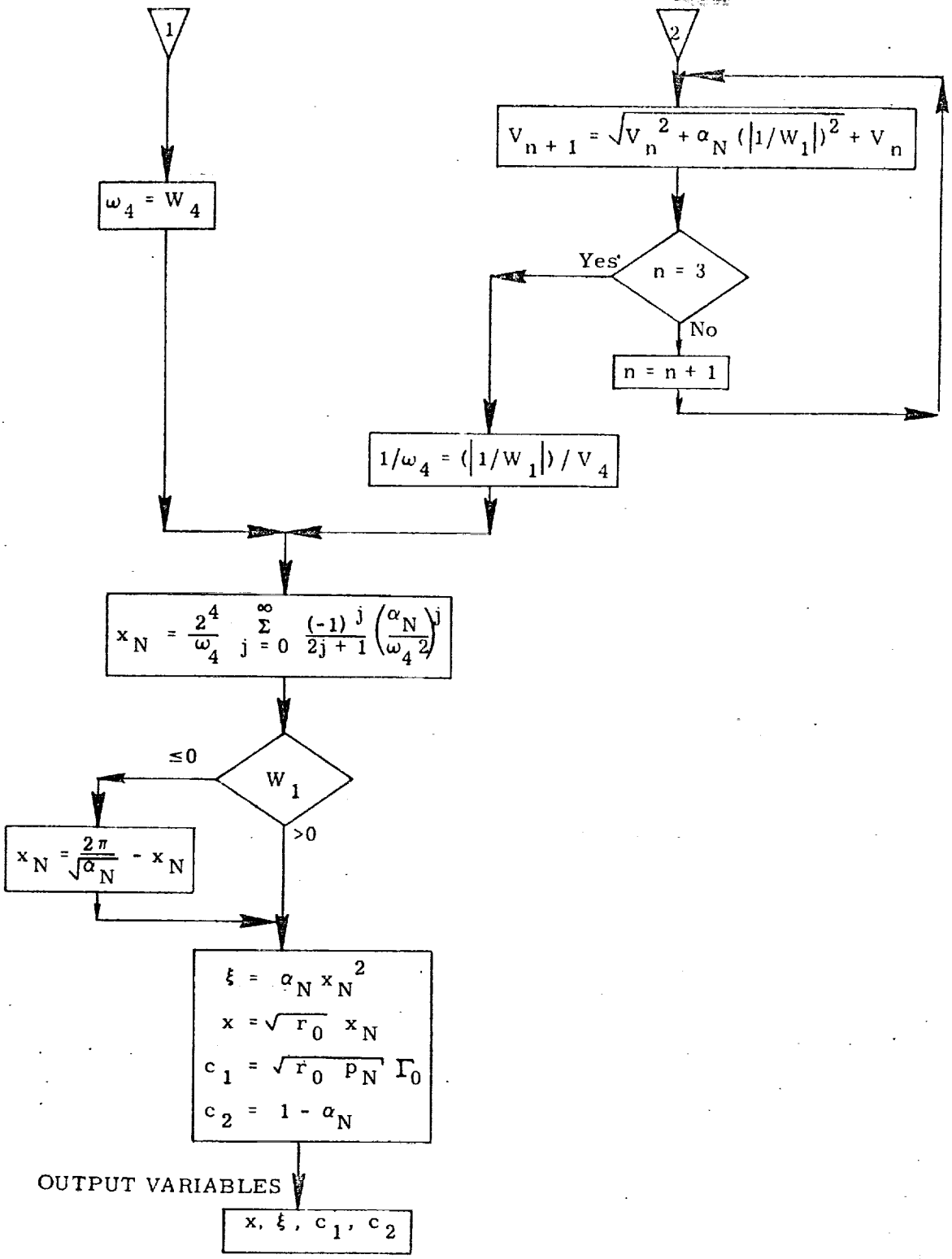


Figure 8b. Marscher Equation Inversion Subroutine Detailed Flow Diagram

5.3.5 Secant Iterator

This subroutine is identical (when k = 1/4) to the one used in the Theta problem.

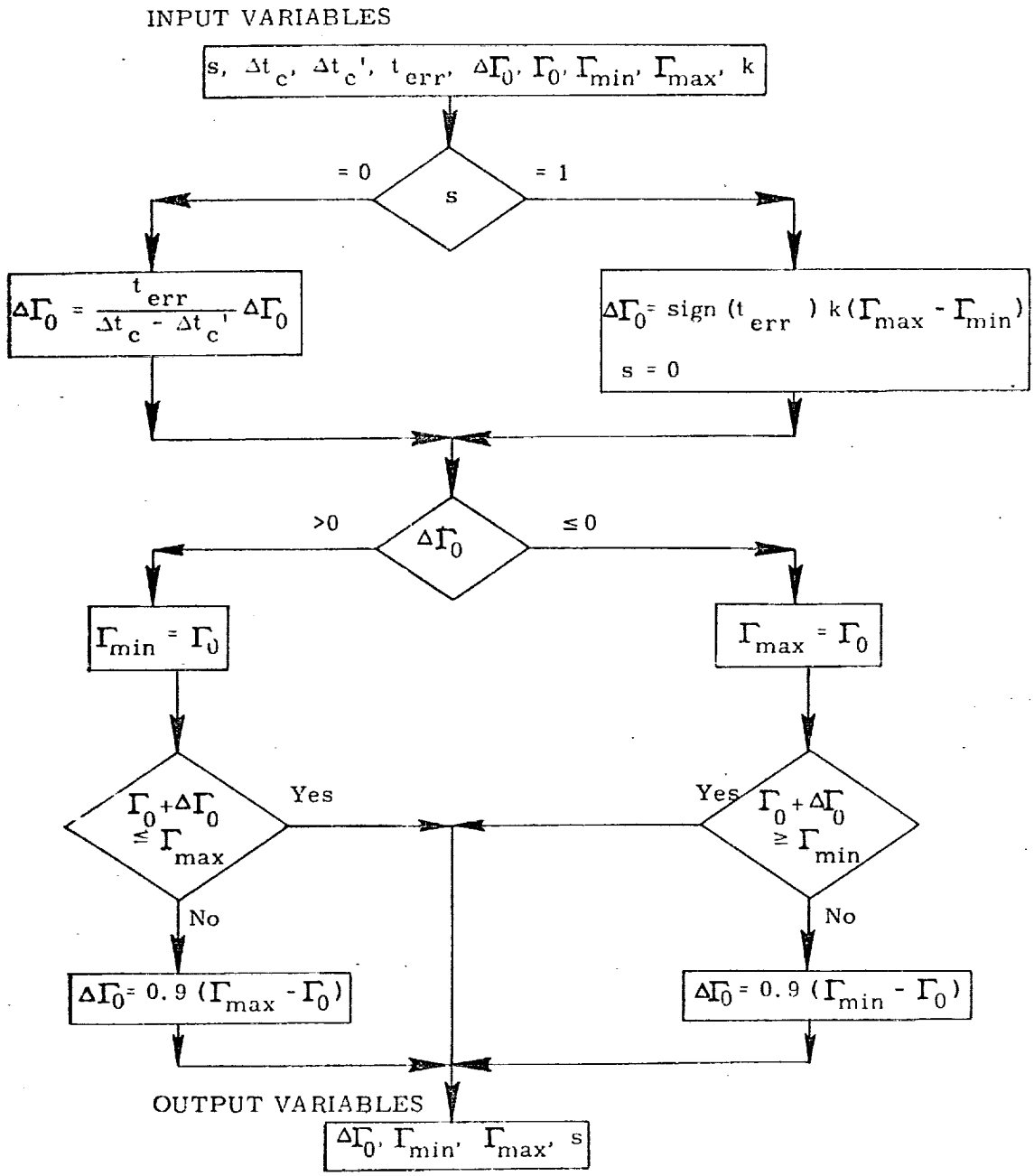


Figure 9. Secant Iterator
Detailed Flow Diagram

5.3.6 Multi-revolution Bounds Adjustment Coding Sequence

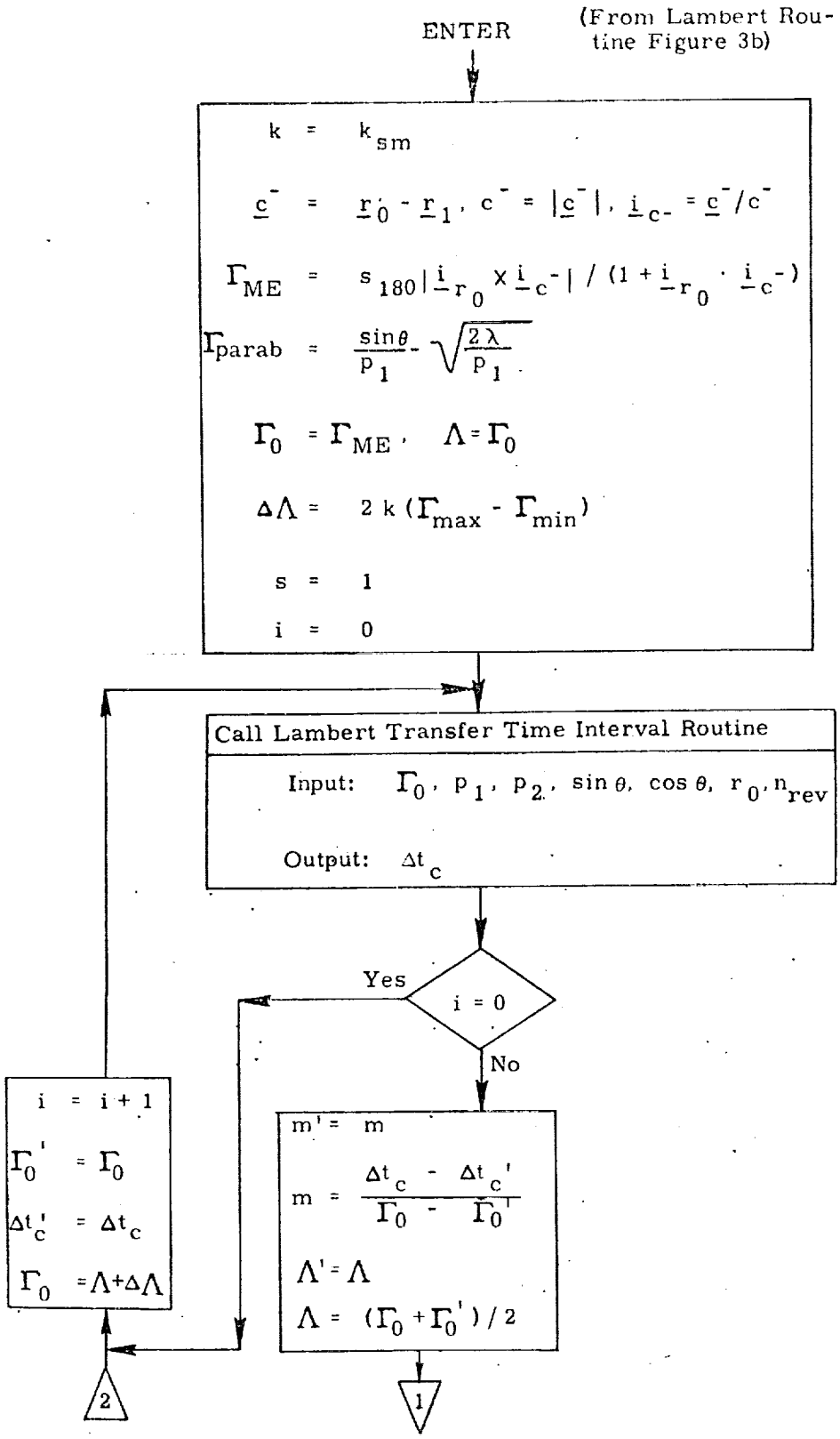


Figure 10a. Multi-Revolution Bounds Adjustment Coding Sequence Detailed Flow Diagram

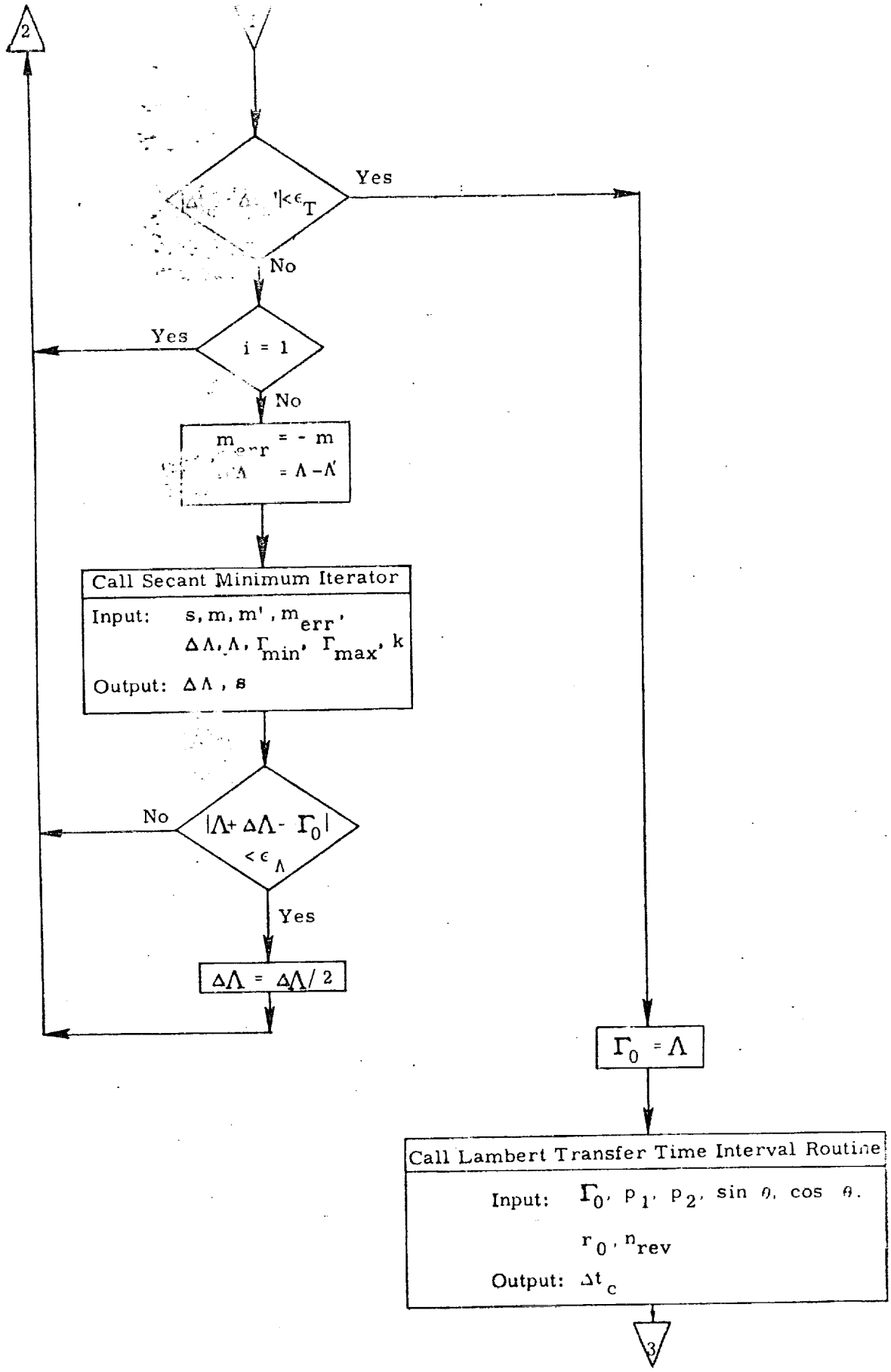


Figure 10b. Multi-Revolution Bounds Adjustment Coding Sequence Detailed Flow Diagram

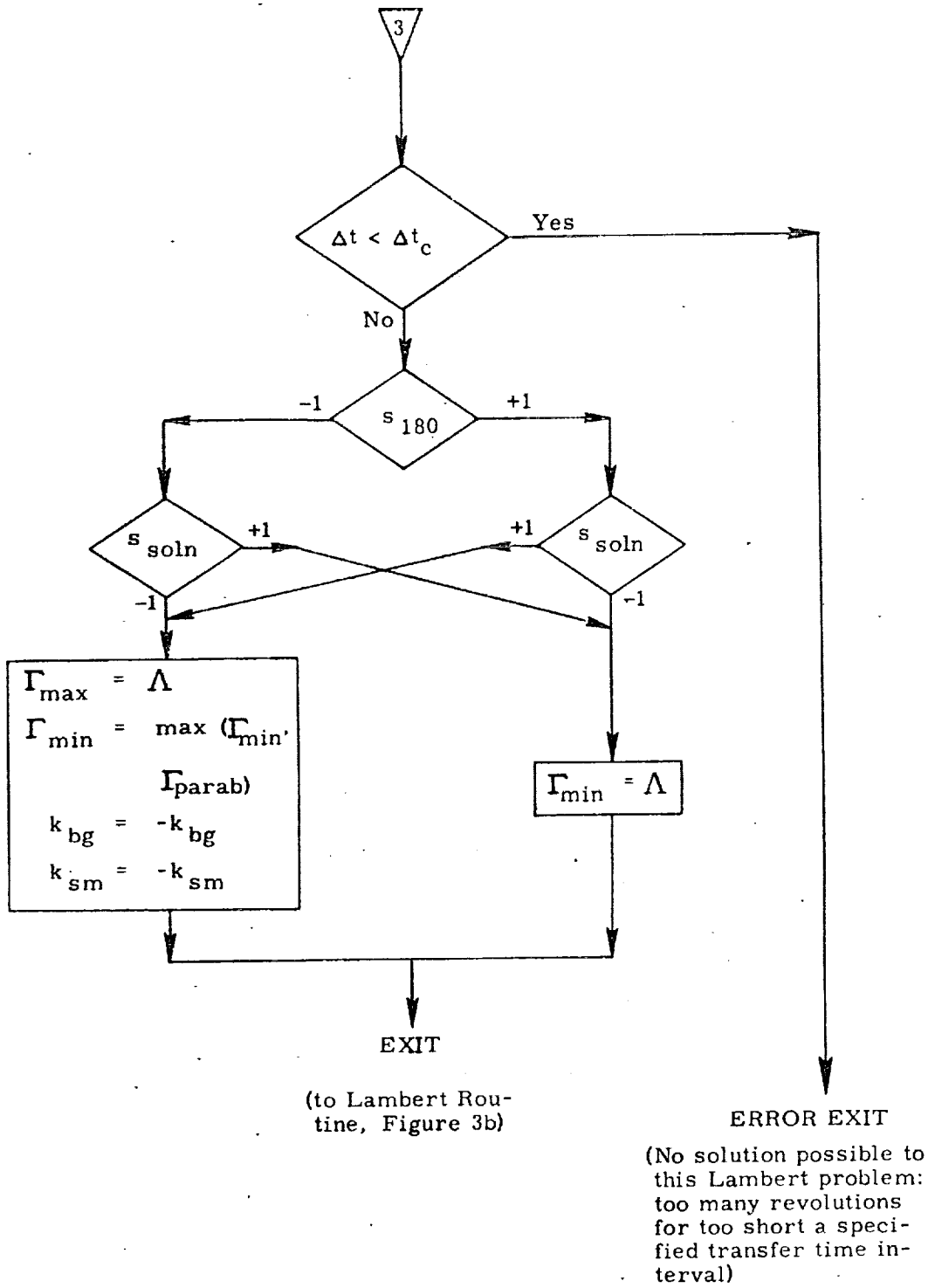


Figure 10c. Multi-Revolution Bounds Adjustment Coding Sequence Detailed Flow Diagram

### 5.3.7 Secant Minimum Iterator

This subroutine is very similar, though not identical, to the Secant Iterator. They can easily be combined into one routine, although they have been diagrammed separately here for purposes of clarity.

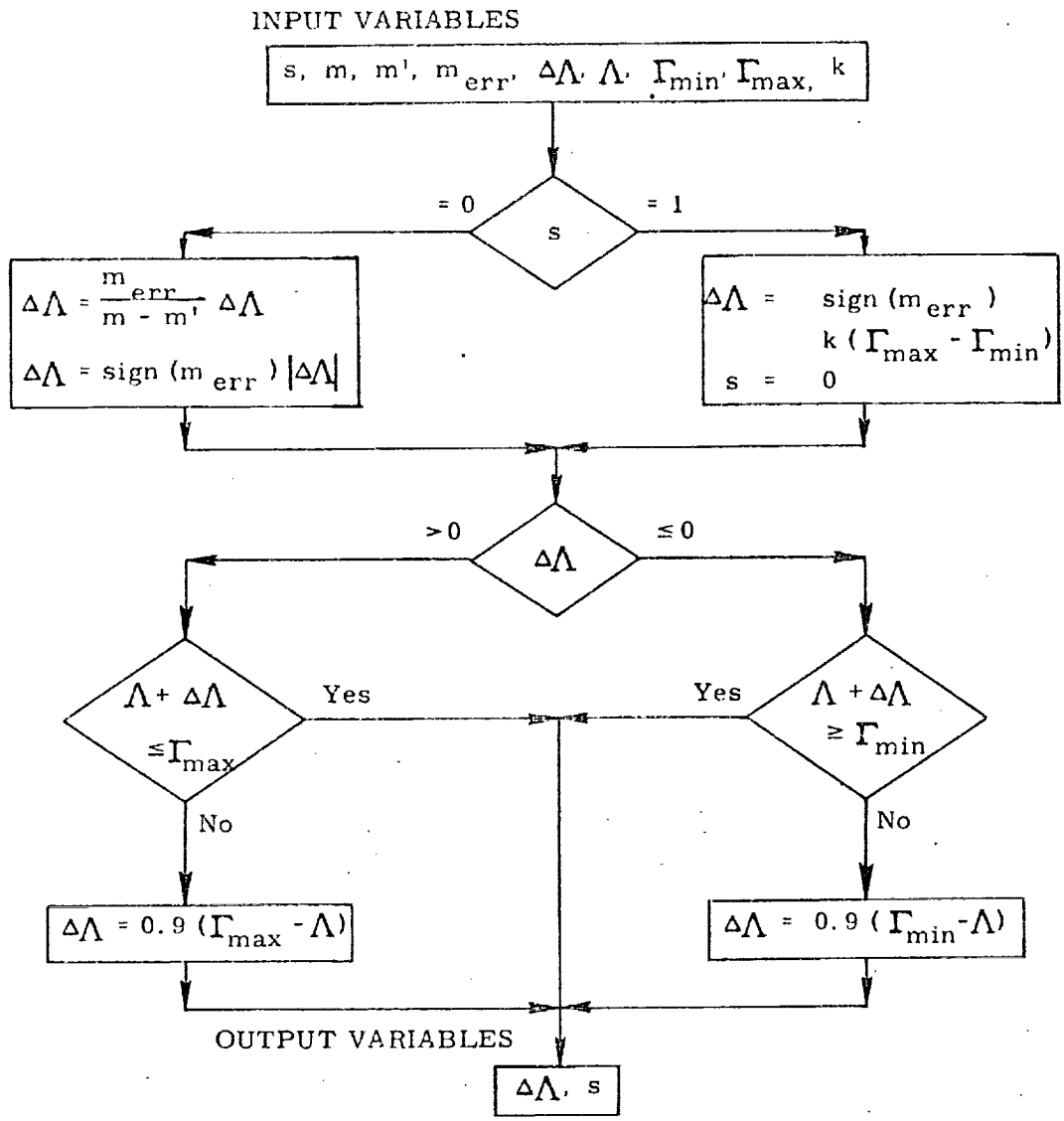


Figure 11. Secant Minimum Iterator Detailed Flow Diagram

## 1. INTRODUCTION

Calculation of the precision required velocity which satisfies terminal position and time-of-flight constraints in a non-Keplerian gravity field is a computation time consuming process, especially in an on-board computer. Therefore, targeting calculations prior to a maneuver are customarily used to predict and compensate for the effects of the perturbations from a conic gravity field, so that during the maneuver only the much simpler conic related computations will have to be performed.

For Lambert aim point maneuvers (described in Reference 2) an adjustment to the terminal (target) position vector will suffice to provide this compensation. This adjusted terminal position, referred to as an offset target, must compensate for gravity perturbations throughout both the maneuver and subsequent coasting flight. Then the required velocity determined by the Lambert routine to intercept the offset target in a conic gravity field is identical to the velocity required to intercept the true target in the non-Keplerian field.

The traditional technique of predicting the effects of gravitational perturbations over the trajectory involves approximating the maneuver by an impulsive velocity change, and hence assuming a coasting trajectory between the initial (ignition) and target positions. However, due to the non-zero length of the maneuver, the actual trajectory will not follow the path predicted by the impulsive approximation, but rather a neighboring path. The difference in the perturbing acceleration between the two paths accumulates over the entire trajectory, resulting in a miss at the target. Since the coasting portion of the trajectory is generally much longer than the thrusting portion, it is important to accurately predict the perturbing effects over this portion of the trajectory. This is accomplished by determining the initial conditions for a coasting trajectory which is coincident with the actual trajectory after thrust termination. A detailed derivation of this technique can be found in Brand (1971) (Reference 1), and a functional description of the procedure follows.

## 2. FUNCTIONAL FLOW DIAGRAM

A functional flow diagram describing the calculations necessary to determine the precision required velocity and offset target is presented in Figure 1. Since this technique compensates for the non-impulsive nature of the maneuver, it requires an estimate of the computed thrust acceleration. Then the initial position can be offset from the actual position such that a coasting trajectory which is coincident with the actual trajectory after thrust termination can be defined. Figure 2 illustrates the concept.

The calculation of the coasting trajectory initial position requires an estimate of the required velocity change, and therefore two passes are made through the Lambert routine before numerically integrating to determine the effects of gravitational perturbations. The first Lambert solution is used to determine the impulsive velocity change required. Based upon this, an estimate of the initial position for the coasting trajectory can be calculated. Then the second Lambert solution determines the velocity required from the adjusted initial position, thus defining the coasting trajectory.

For transfers angles which are odd multiples of $180^{\circ}$, Lambert's problem has a partial physical singularity in that the plane of the transfer becomes indeterminate. A detailed description of this singularity can be found in Reference 4. To prevent possible problems in both targeting and guiding a maneuver whose transfer angle lies near this singularity, logic has been included in this routine to determine whether the transfer angle approaches this singularity at any time during the maneuver. If this is the case, the target vector is projected into the orbital plane defined by the premaneuver position and velocity, thus preventing any plane change.

If only conic calculations are desired, the routine is exited after the two Lambert solutions are completed. If not, subsequent numerical integration determines the target miss resulting from the effects of gravitational perturbations over this path. To compensate for these effects, the target vector for the Lambert routine is offset from the actual target by the negative of the miss vector. Since the adjusted initial position, target offset, and effects of gravitational perturbations are all interdependent, the process is repeated until changes in the offset target position are small enough to indicate convergence. Three passes (two iterations) are normally sufficient to establish the offset within a few feet.

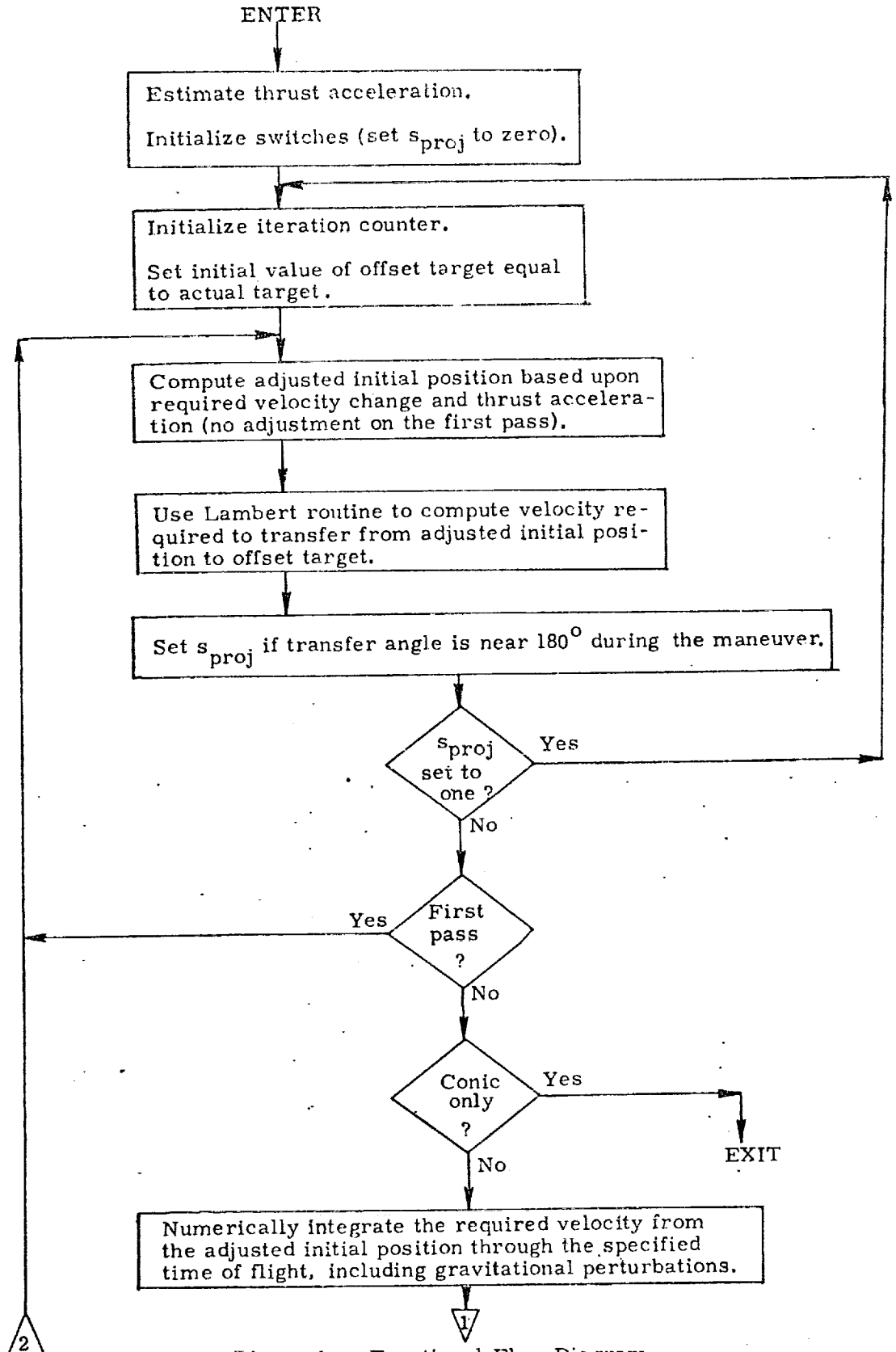


Figure 1a. Functional Flow Diagram

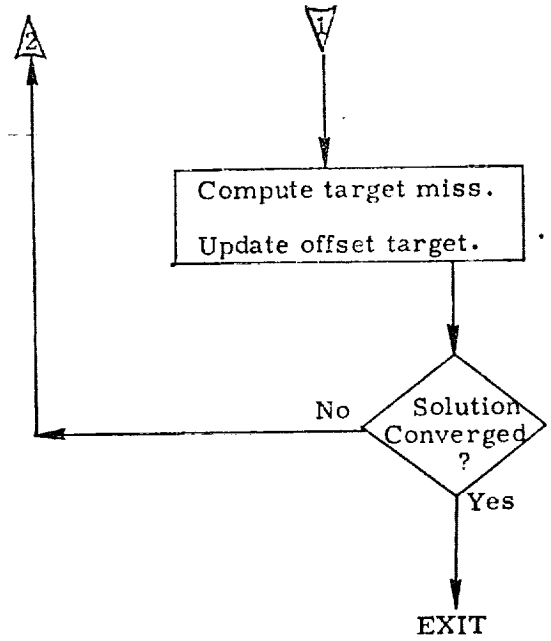


Figure 1b. Functional Flow Diagram

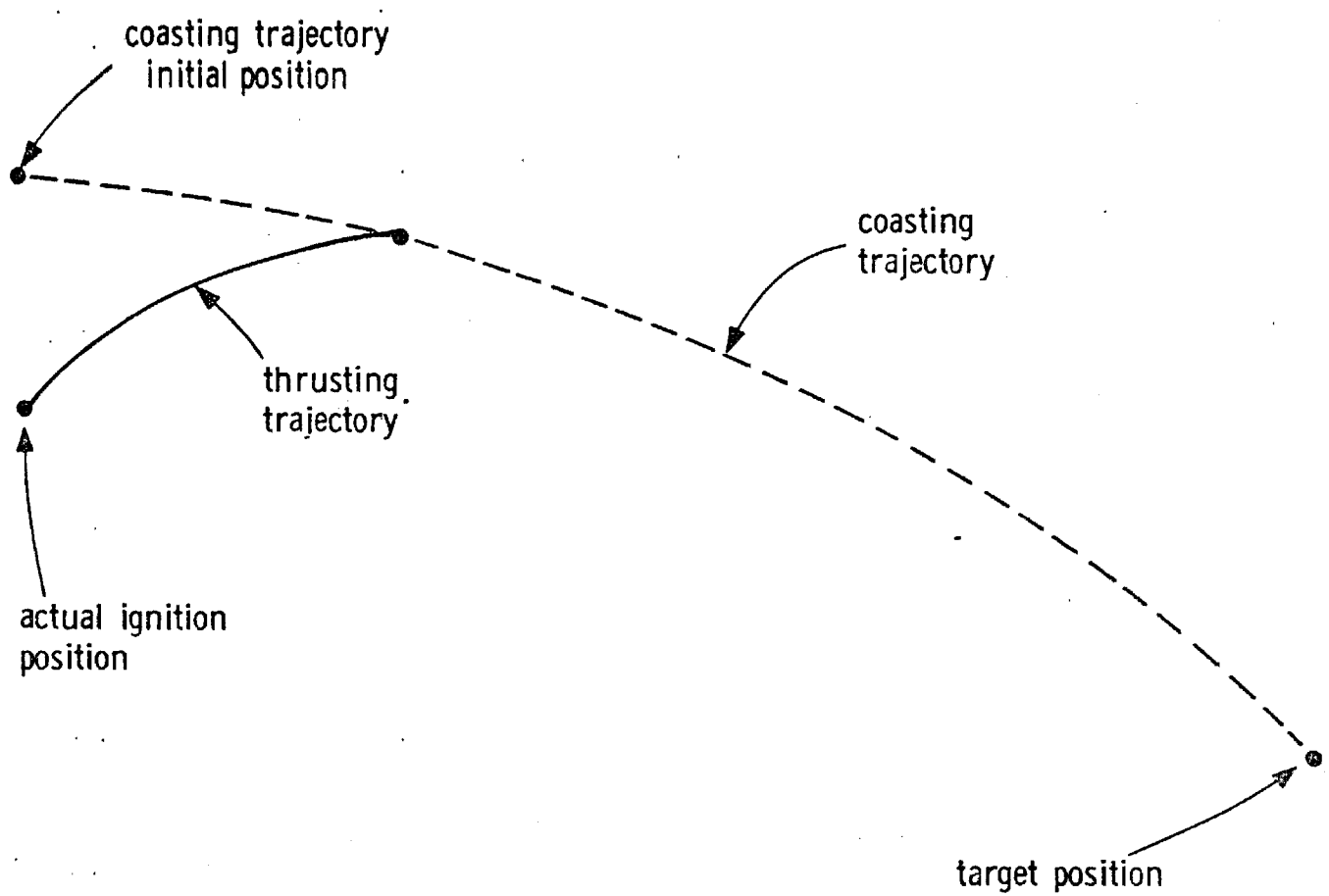


Figure 2. Coasting Trajectory Illustration

## NOMENCLATURE

| | |
|---|---|
| $a_T$ | Estimated m[illegible] the thrust acceleration |
| d | Number of co[illegible] navigation filter weighting matrix (set to 0 in this routine since the matrix is not required) |
| f | Thrust |
| $f_{ACS}$ | Magnitude of the attitude control system translational thrust |
| $f_{OMS}$ | Magnitude of [illegible]nal orbital maneuvering system engine thrust |
| $\underline{i}_N$ | Unit normal to the trajectory plane (in the direction of the angular momentum at ignition) |
| m | Current estimated vehicle mass |
| n | Iteration count |
| $n_{max}$ | Iteration limit |
| $n_{rev}$ | Integral number of complete $360^\circ$ revolutions to be made in the desired transfer |
| $\underline{r}_0$ | Initial (ignition) position |
| $\underline{r}'_0$ | Adjusted initial position used to define coasting trajectory |
| $\underline{r}_1$ | Target position [illegible]put to the routine) |
| $\underline{r}'_1$ | Terminal position (output of the routine) |
| $\underline{r}_{1c}$ | Offset target position |
| $s_{cone}$ | Switch set in the Lambert routine to indicate transfer is near $180^\circ$ (see Reference 4 for complete description) |

| | |
|---|---|
| $s_{eng}$ | Engine select switch |
| $s_{fail}$ | Switch set to indicate non-convergence |
| $s_{guess}$ | Switch set to indicate an estimate of independent variable $\Gamma$ will be input to the Conic Required Velocity Determination Routine |
| $s_{pert}$ | Switch set to indicate which perturbing accelerations should be included in the offset target calculation ($s_{pert} = 0$ indicates only conic calculations; see Reference 3 for complete description of other switch settings) |
| $s_{proj}$ | Switch set when the target vector must be projected into the plane defined by $\underline{i}_N$ |
| $s_{soln}$ | Switch indicating which of two physically possible solutions is desired in the multi-revolution transfer (see Reference 4 for complete description) |
| $t_0$ | Ignition time |
| $t_1$ | Target time of arrival |
| $\underline{v}_0$ | Initial (ignition) velocity |
| $\underline{v}'_0$ | Initial (and required) velocity on the coasting trajectory |
| $\underline{v}_{1c}$ | Terminal velocity of a conic trajectory |
| $\underline{v}'_1$ | Terminal velocity (output of the routine) |
| $\Gamma_{guess}$ | Guess of the independent variable $\Gamma$ used in the Conic Required Velocity Determination Routine |
| $\Delta\underline{r}$ | Target miss resulting from perturbations |
| $\Delta r_{proj}$ | Out-of-plane target miss due to projection of the target vector |

| | |
|---|---|
| $\Delta t$ | Transfer time $(t_1 - t_0)$ |
| $\Delta \underline{v}_0$ | Required velocity change |
| $\Delta v_0$ | Magnitude of the required velocity change |
| $\epsilon_{conv}$ | Convergence criterion: target miss of the numerically integrated trajectory |
| $\epsilon_{\theta T}$ | Tolerance criterion establishing a cone around the minus $\underline{r}_0$ direction inside of which the target vector will be projected into the plane $\underline{i}_N$ $\left[\epsilon_{\theta T} = \sin \text{(half cone angle)}\right]$ |
| $\theta$ | Transfer angle (true anomaly difference) at the start of the thrusting maneuver |
| $\theta_T$ | Approximate central angle traversed during the thrusting maneuver |
| $\theta_1$ | Approximate transfer angle to the target at the termination of the thrusting maneuver $\left[\theta_1 = \theta - \theta_T\right]$ |
| $\omega$ | Approximate orbital rate |

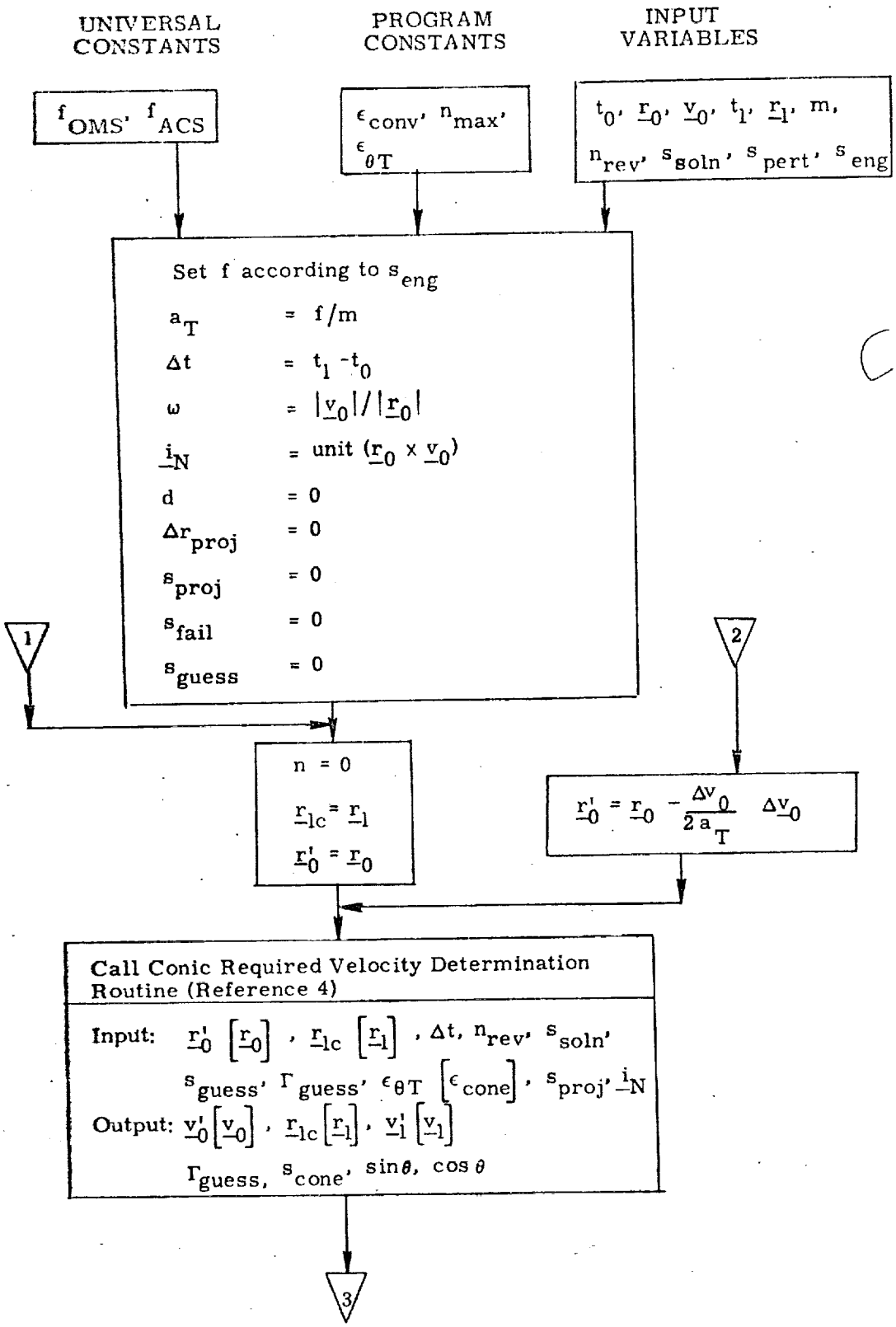


Figure 3a. Detailed Flow Diagram

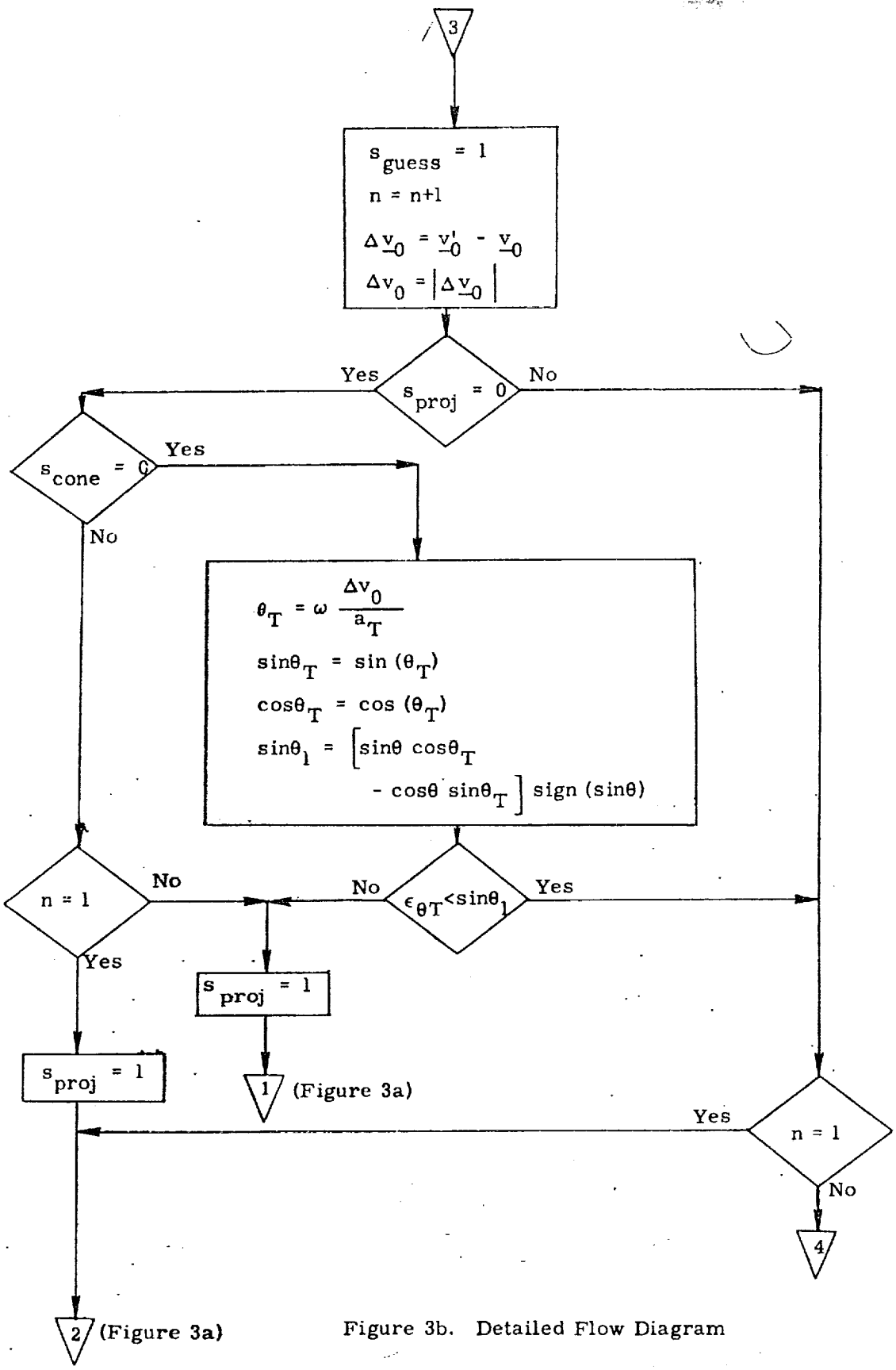


Figure 3b. Detailed Flow Diagram

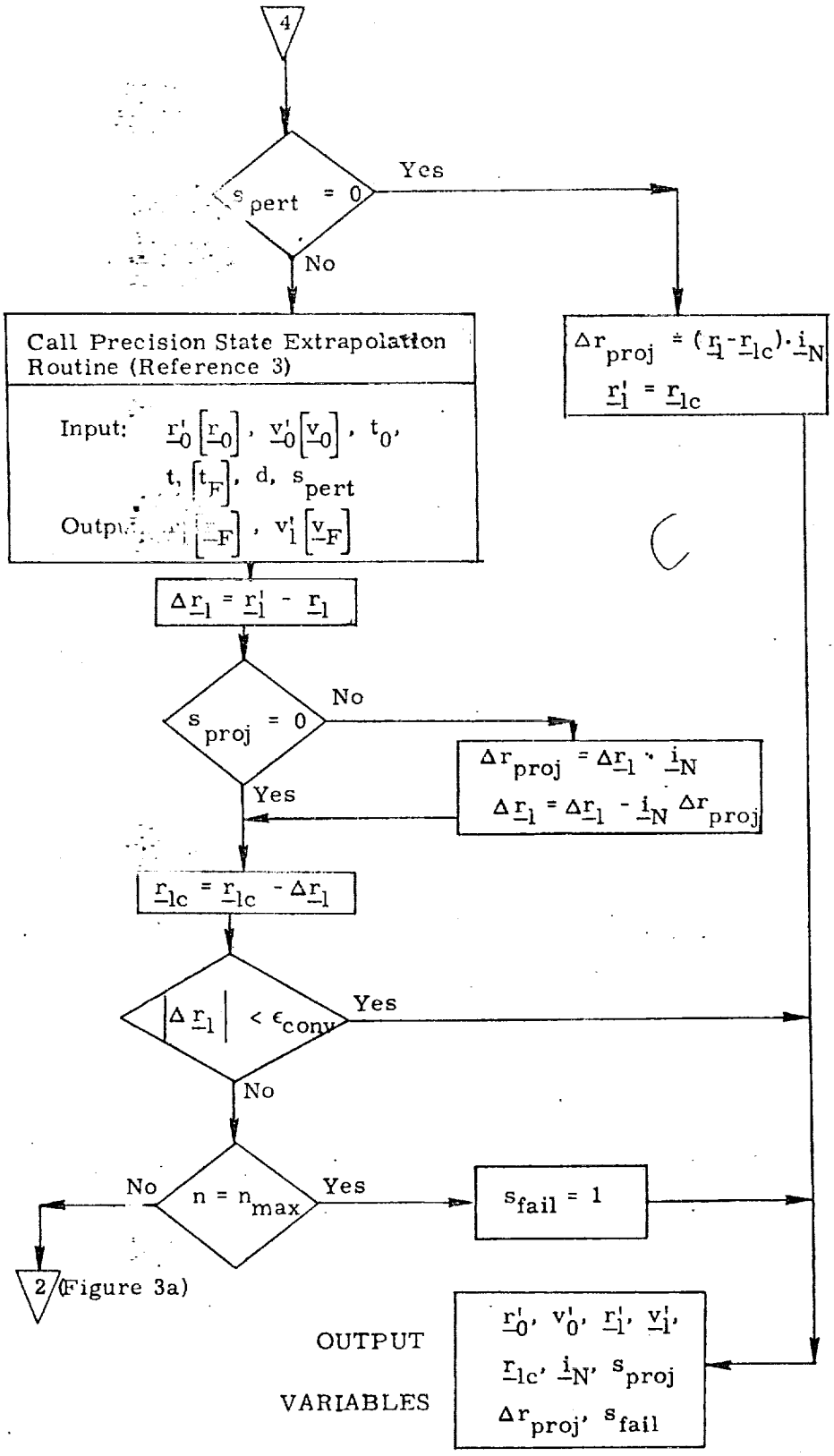


Figure 3c. Detailed Flow Diagram

## Submittal 51: Boost Abort Guidance

Equations and flow diagrams are presented in this Section which fulfill requirements for abort from boost to an entry path which achieves satisfactory landing at the launch site. Constraints and guidelines are presented in Fig. 1. The trajectory and nomenclature are presented in Figs. 2 and 3. A general flow diagram is presented in Figs. 4 and 5.

As shown in Fig. 2, landing is achieved in four phases: An open loop phase of powered flight wherein propellant is expended, powered-flight constraints are observed and conditions are reached where available $\Delta V$ equals $\Delta V$ required to get on the entry trajectory. A closed-loop phase of powered flight achieves entry target conditions with very little fuel. An unpowered flight phase follows where unpowered flight constraints are observed and the trajectory approaches the nominal entry trajectory. The final unpowered phase consists of holding the entry trajectory, i.e., controlling to the trajectory through satisfactory landing. These phases and their Guidance Equations are presented in Figs. 6 thru 11.

Figs. 12 thru 18 are the detailed program flow diagrams. Thereafter follows a definition of terms used in this section.

9.5.1 Aborts (continued)

## BOOST ABORT - CONSTRAINTS/GUIDELINES

- USE NOMINAL MISSION TECHNIQUES
- POWERED PHASE
  - ACHIEVE A SAFE LANDING WEIGHT
  - AVOID LARGE ANGLES-OF-ATTACK/SIDESLIP ANGLES DURING HIGH $\bar{q}$ ENVIRONMENT
  - DO NOT EXCEED 3G TOTAL ACCELERATION
  - SATISFY TANK/ORBITER SEPARATION REQUIREMENTS
  - TANK IMPACT POINT MUST SATISFY RANGE SAFETY REQUIREMENTS
- UNPOWERED PHASE
  - AVOID LARGE NORMAL DECELERATIONS (2.5G) AND DYNAMIC PRESSURES (300 PSF)

Figure 1

9.5.1 Aborts (continued)

RETURN TO LAUNCH SITE FROM ABORT AT STAGING
WITH ONE ORBITER ENGINE OUT(FOUR ENGINE ORBITER)

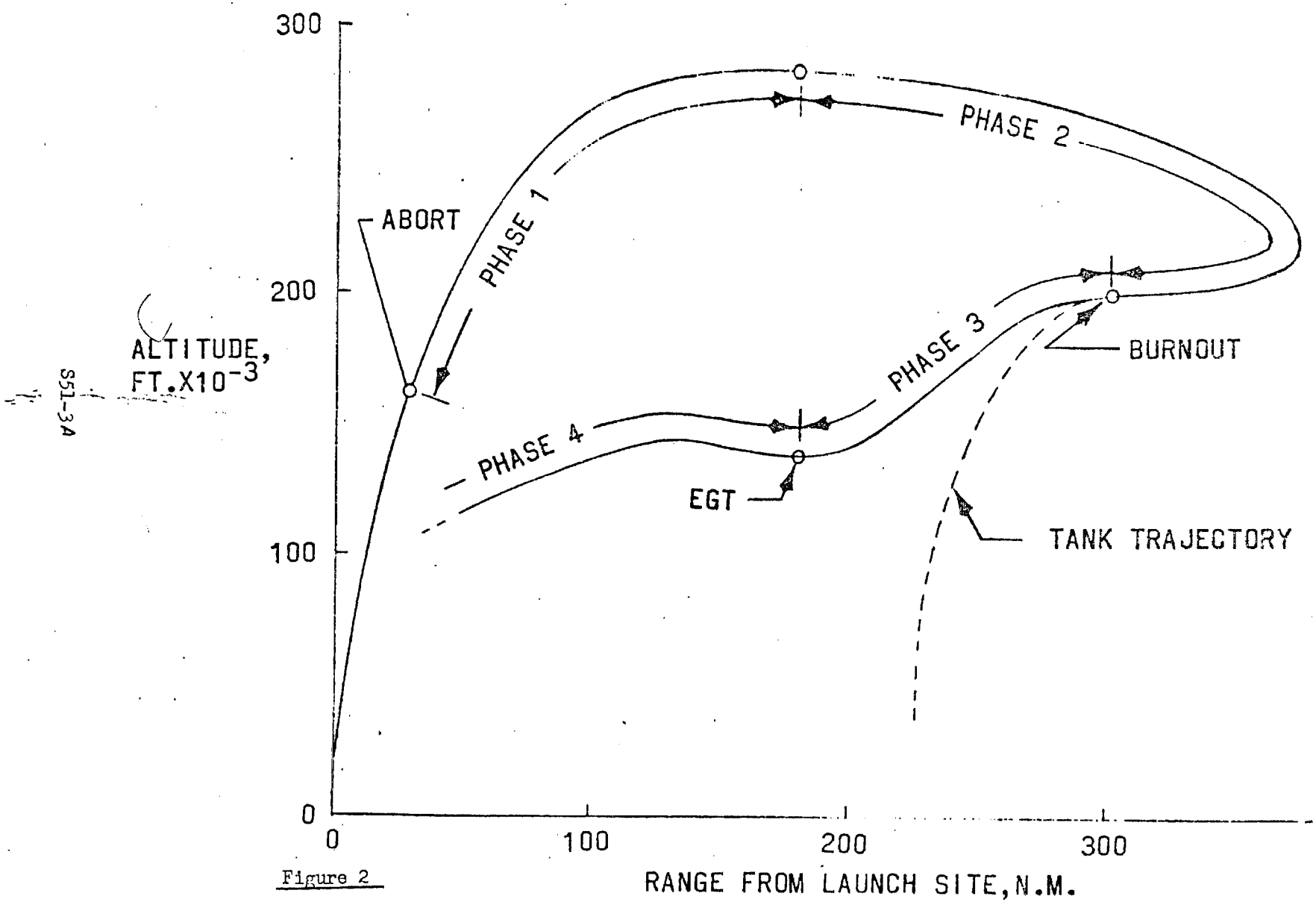


S51-3A

Figure 2

Figure 3

PLANAR REPRESENTATION OF ABORT MANEUVER

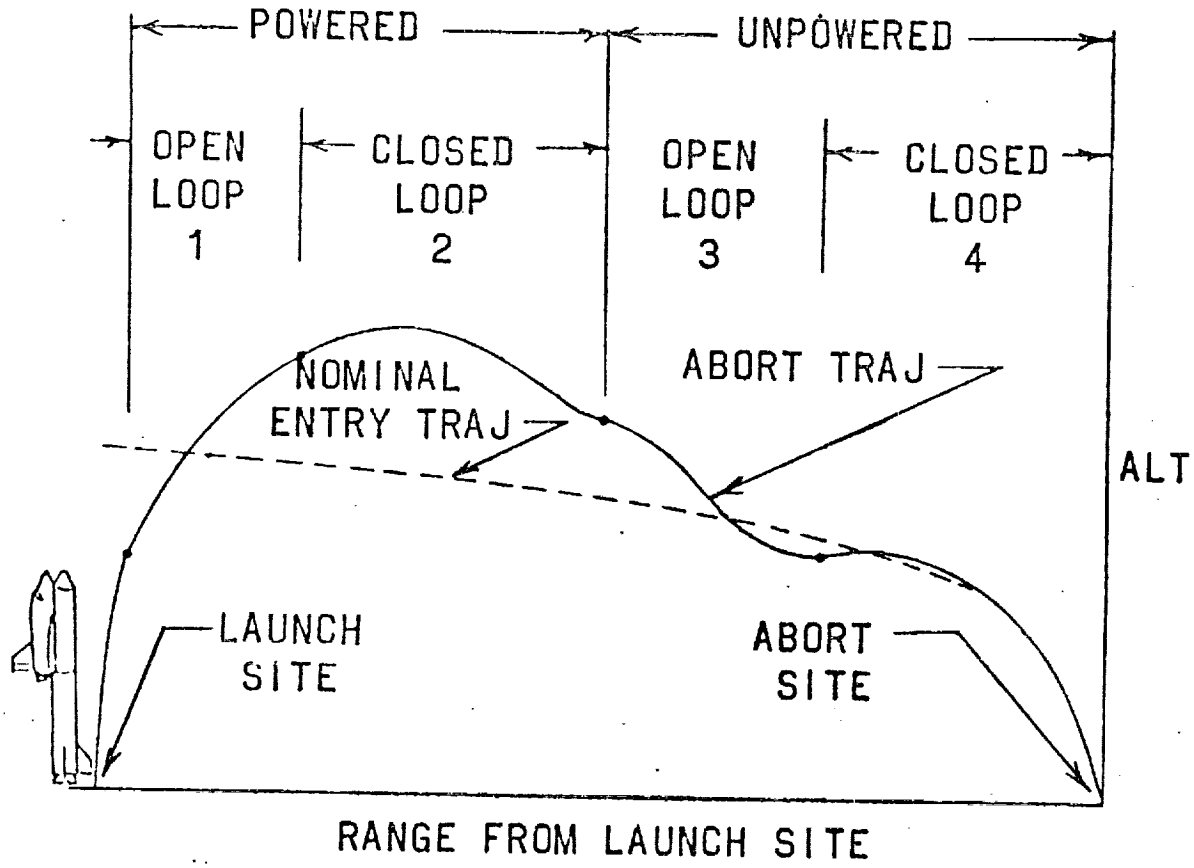

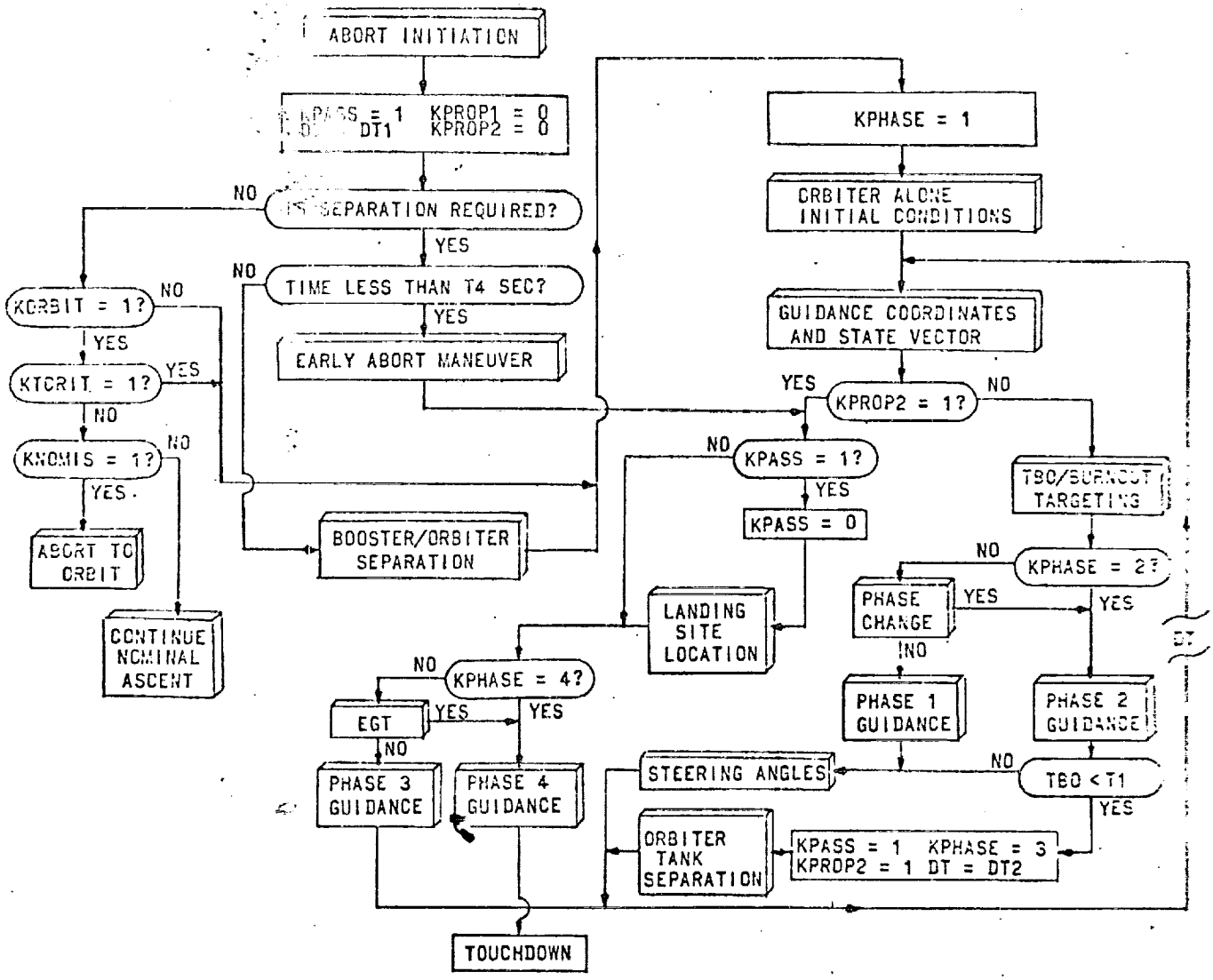
ABORT INITIATION
KPASS = 1 KPROP1 = 0
DT1 KPROP2 = 0
IS SEPARATION REQUIRED?
NO
YES
TIME LESS THAN T4 SEC?
NO
YES
EARLY ABORT MANEUVER
KORBIT = 1?
NO
YES
KTCRIT = 1?
YES
NO
KNOMIS = 1?
NO
YES
ABORT TO ORBIT
CONTINUE NOMINAL ASCENT
BOOSTER/ORBITER SEPARATION
KPHASE = 1
ORBITER ALONE INITIAL CONDITIONS
GUIDANCE COORDINATES AND STATE VECTOR
KPROP2 = 1?
YES
NO
KPASS = 1?
NO
YES
KPASS = 0
TBO/BURNOUT TARGETING
KPHASE = 2?
NO
YES
PHASE CHANGE
YES
NO
PHASE 1 GUIDANCE
PHASE 2 GUIDANCE
LANDING SITE LOCATION
KPHASE = 4?
NO
YES
EGT
YES
NO
PHASE 3 GUIDANCE
PHASE 4 GUIDANCE
STEERING ANGLES
NO
TBO < T1
YES
ORBITER TANK SEPARATION
KPASS = 1 KPHASE = 3
KPROP2 = 1 DT = DT2
TOUCHDOWN

Figure 4

# BURNOUT TARGETING

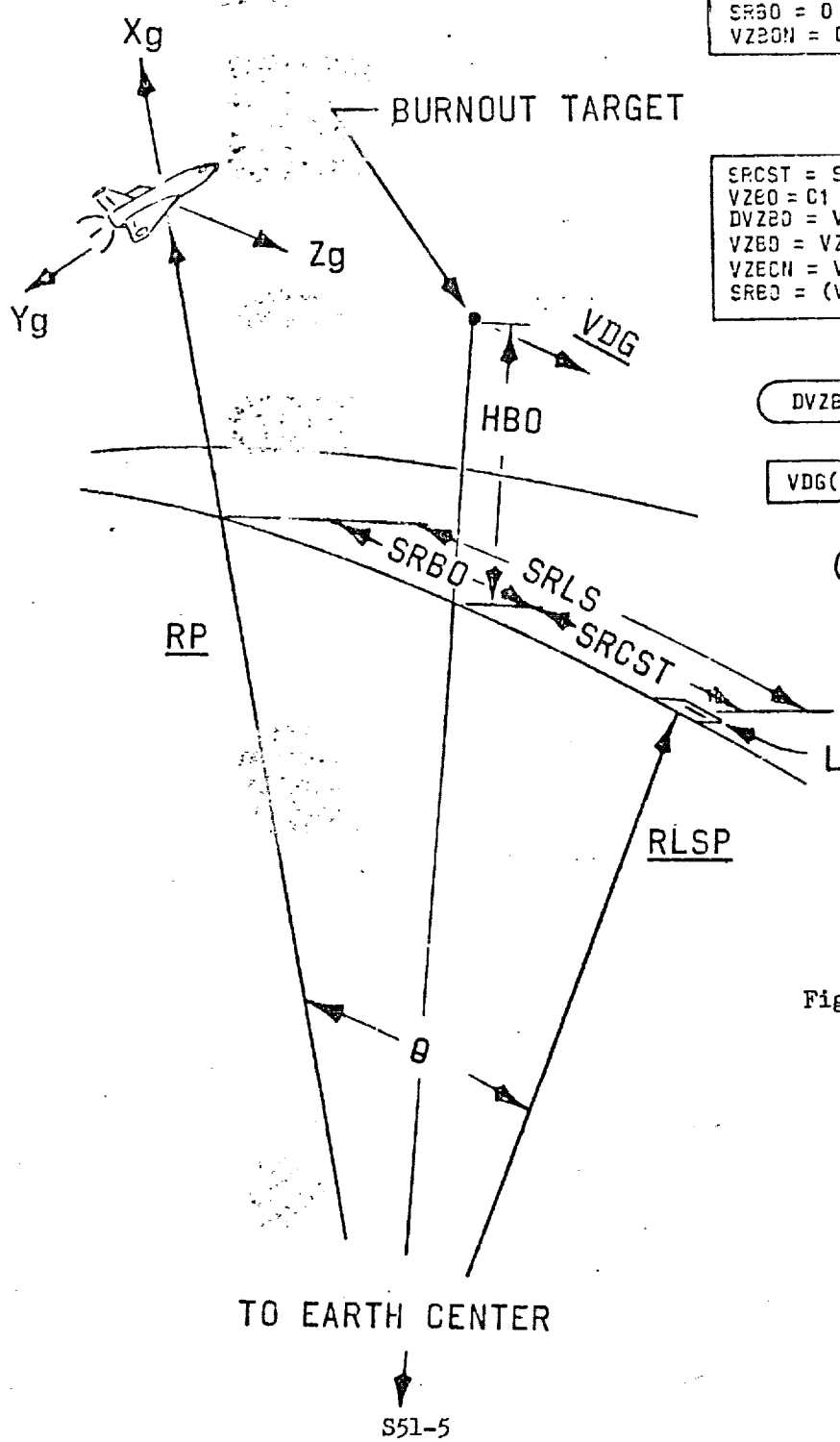


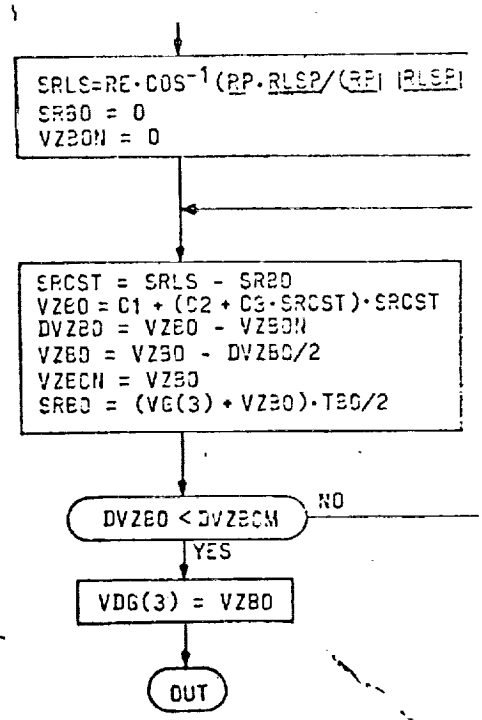


Figure 5

S51-5

## POWERED PHASE OF SUBORBITAL MANEUVER

- ANALOGOUS TO ASCENT PHASE
- COMPOSED OF TWO GUIDANCE PHASES

  PHASE 1

  - AVOID VIOLATION OF POWERED PHASE CONSTRAINTS
  - USE EXCESS PROPELLANT
  - TERMINATE PHASE WHEN $\Delta V_R \approx \Delta V_A$

  PHASE 2

  - DEPLETE PROPELLANT AND ACHIEVE TARGET SIMULTANEOUSLY
  - TERMINATE PHASE WHEN PROPELLANT IS DEPLETED

Figure 6

Figure 7

# PHASE I GUIDANCE EQUATIONS

- RADIAL (PLATFORM X)

  $ATC(1) = K_1(RDG - RG) + K_2(VDG(1) - VG(1)) - G_{EFI}$

- RETURN TO LAUNCH SITE

  $ATC(2) = 0$

  $ATC(3) = AH \qquad AH = (AT^2 - ATC(1)^2)^{\frac{1}{2}}$

- DOWNRANGE $\qquad VDG(3) > VBOZD$

  $AGC(2) = 0$

  $AGC(3) = AH$

- DOWNRANGE $\qquad VDG(3) < VBOZD$

  $AGC(2) = AH \cdot VG(2)/|VG(2)|$

  $AGC(3) = 0$

- TRANSFORMATION

  $ATC(2) = AGC(2)UYGP(2) + AGC(3)UZGP(2)$

  $ATC(2) = AGC(2)UYGP(3) + AGC(3)UZGP(3)$

Figure 8

# PHASE 2 GUIDANCE EQUATIONS

$$AGC(1) = \frac{6}{TBO^2}\,(RDG(1)) - \frac{2}{TBO}\,(VDG(1) + 2VG(1)) - GEFF$$

$$AGC(3) = (VDG(3) - VG(3))/TBO$$

$$AGC(2) = YSIGN(A[illegible] - AGC(1)^2 - AGC(3)^2)^{\frac{1}{2}}$$

$$\underline{ATC} = AGC(1)\ \underline{UXGP} + AGC(2)\ \underline{UYGP} + AGC(3)\ \underline{UZGP}$$

## UNPOWERED PHASE OF SUBORBITAL MANEUVER

- ANALOGOUS TO NOMINAL ENTRY FROM ~600 N.M. UPRANGE OF LANDING SITE
- COMPOSED OF TWO GUIDANCE PHASES

  PHASE 3

  - SEPARATE FROM EMPTY PROPELLANT TANK
  - AVOID VIOLATION OF UNPOWERED PHASE CONSTRAINTS
  - TERMINATE PHASE WHEN CONDITIONS SUITABLE FOR ENTRY GUIDANCE TAKEOVER ARE ACHIEVED

  PHASE 4

  - STEER ORBITER TO ABORT LANDING SITE

Figure 9

Figure 10

# PHASE III GUIDANCE EQUATIONS

$\alpha_c = \theta_D - \gamma$ $\qquad g_n < g_n$ LIMIT

$\alpha_c = \alpha - \dot{\theta}\,\Delta t$ $\qquad g_n > g_n$ LIMIT

BUT

$\alpha_{MIN} \leqslant \alpha_c \leqslant \alpha_{MAX}$

$\phi_{VC} = -15^{\circ} \cdot VG(2)/|VG(2)|$ $\qquad \psi_V > \psi_1$

$\phi_{VC} = -7.5^{\circ} \cdot VG(2)/|VG(2)|$ $\qquad \psi_1 > \psi_V > \psi_2$

$\phi_{VC} = 0$ $\qquad \psi_V < \psi_2$

RATE LIMIT - $.5^{\circ}$/SEC IN PITCH

$\dot{\phi}_V$ IS TBD

# PHASE IV GUIDANCE EQUATIONS

## NOMINAL ENTRY AND TERMINAL AREA GUIDANCE EQUATIONS

Figure 11

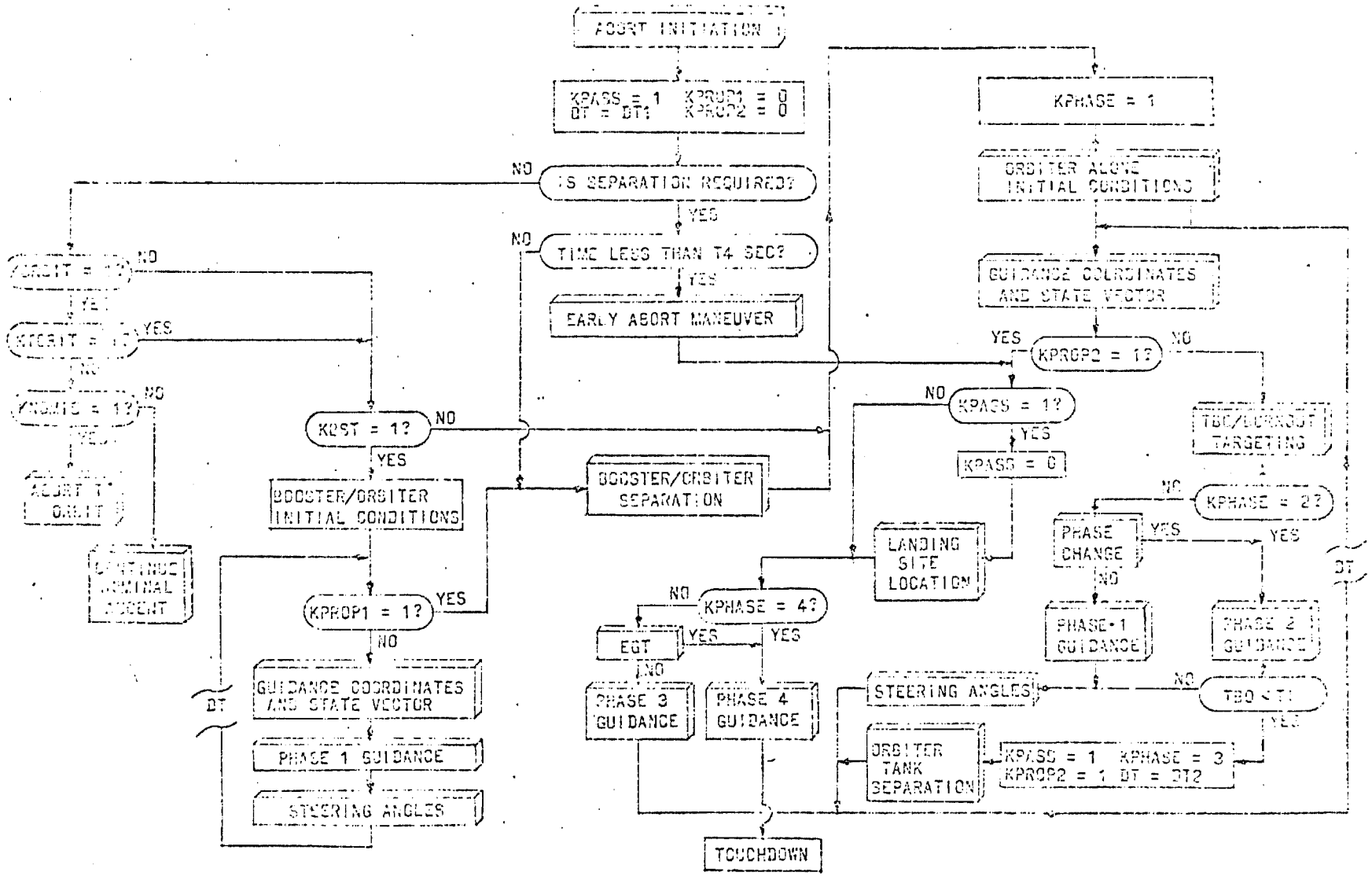
ABORT INITIATION
KPASS = 1 KPROP1 = 0
DT = DT1 KPROP2 = 0
IS SEPARATION REQUIRED?
NO
YES
TIME LESS THAN T4 SEC?
NO
YES
EARLY ABORT MANEUVER
KPHASE = 1
ORBITER ALONE INITIAL CONDITIONS
GUIDANCE COORDINATES AND STATE VECTOR
KPROP2 = 1?
YES
NO
KPASS = 1?
NO
YES
KPASS = 0
TBO/BURNOUT TARGETING
KPHASE = 2?
PHASE CHANGE
PHASE-1 GUIDANCE
PHASE 2 GUIDANCE
TBO < T1
STEERING ANGLES
ORBITER TANK SEPARATION
KPASS = 1 KPHASE = 3
KPROP2 = 1 DT = DT2
LANDING SITE LOCATION
KPHASE = 4?
EGT
PHASE 3 GUIDANCE
PHASE 4 GUIDANCE
TOUCHDOWN
BOOSTER/ORBITER SEPARATION
KRST = 1?
BOOSTER/ORBITER INITIAL CONDITIONS
KPROP1 = 1?
GUIDANCE COORDINATES AND STATE VECTOR
PHASE 1 GUIDANCE
STEERING ANGLES
DT
ABORT TO ORBIT
CONTINUE NOMINAL ASCENT

Figure 12

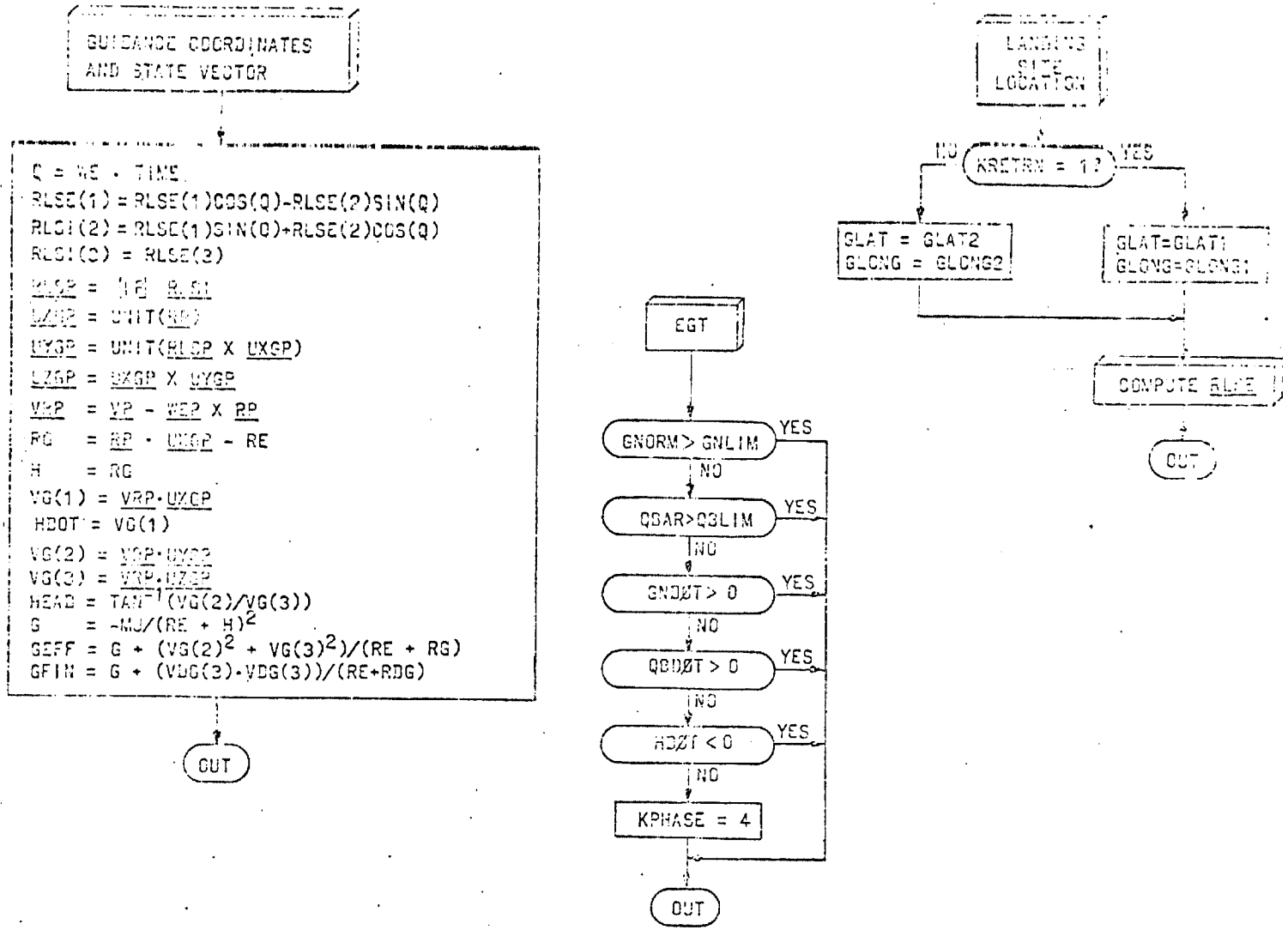
GUIDANCE COORDINATES AND STATE VECTOR
Q = WE · TIME
RLSE(1) = RLSE(1)COS(Q)-RLSE(2)SIN(Q)
RLSE(2) = RLSE(1)SIN(Q)+RLSE(2)COS(Q)
RLSE(3) = RLSE(3)
RLSP = TB RLSE
UXSP = UNIT(RLSP)
UYSP = UNIT(RLSP X UXSP)
UZSP = UXSP X UYSP
VRP = VP - WEP X RP
RG = RP · UXSP - RE
H = RG
VG(1) = VRP·UXSP
HDOT = VG(1)
VG(2) = VRP·UYSP
VG(3) = VRP·UZSP
HEAD = TAN-1(VG(2)/VG(3))
G = -MU/(RE + H)2
GEFF = G + (VG(2)2 + VG(3)2)/(RE + RG)
GFIN = G + (VDG(3)·VDG(3))/(RE+RDG)
OUT
EGT
GNORM > GNLIM
YES
NO
QBAR>QBLIM
YES
NO
GNDØT > 0
YES
NO
QBDØT > 0
YES
NO
HDØT < 0
YES
NO
KPHASE = 4
OUT
LANDING SITE LOCATION
KRETRN = 1?
NO
YES
GLAT = GLAT2
GLONG = GLONG2
GLAT=GLAT1
GLONG=GLONG1
COMPUTE RLSE
OUT

Figure 13

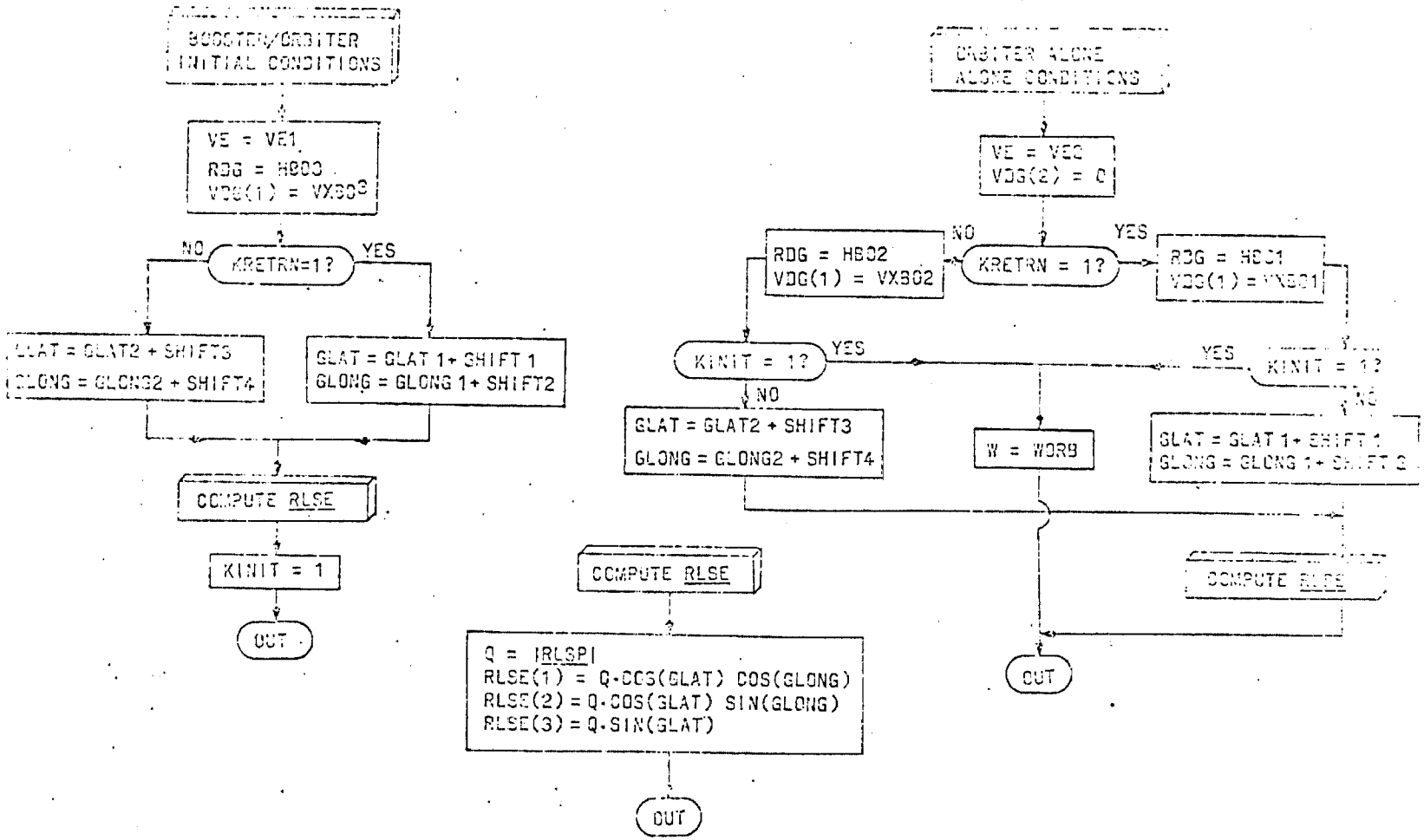
BOOSTER/ORBITER INITIAL CONDITIONS
VE = VE1
RDG = HBOO
VDG(1) = VXBO3
KRETRN=1?
NO
YES
GLAT = GLAT2 + SHIFT3
GLONG = GLONG2 + SHIFT4
GLAT = GLAT 1+ SHIFT 1
GLONG = GLONG 1+ SHIFT2
COMPUTE RLSE
KINIT = 1
OUT
ORBITER ALONE ALONE CONDITIONS
VE = VEO
VDG(2) = 0
RDG = HBO2
VDG(1) = VXBO2
KRETRN = 1?
RDG = HBO1
VDG(1) = VXBO1
KINIT = 1?
GLAT = GLAT2 + SHIFT3
GLONG = GLONG2 + SHIFT4
W = WORB
GLAT = GLAT 1+ SHIFT 1
GLONG = GLONG 1+ SHIFT 2
COMPUTE RLSE
Q = |RLSP|
RLSE(1) = Q·COS(GLAT) COS(GLONG)
RLSE(2) = Q·COS(GLAT) SIN(GLONG)
RLSE(3) = Q·SIN(GLAT)

Figure 14

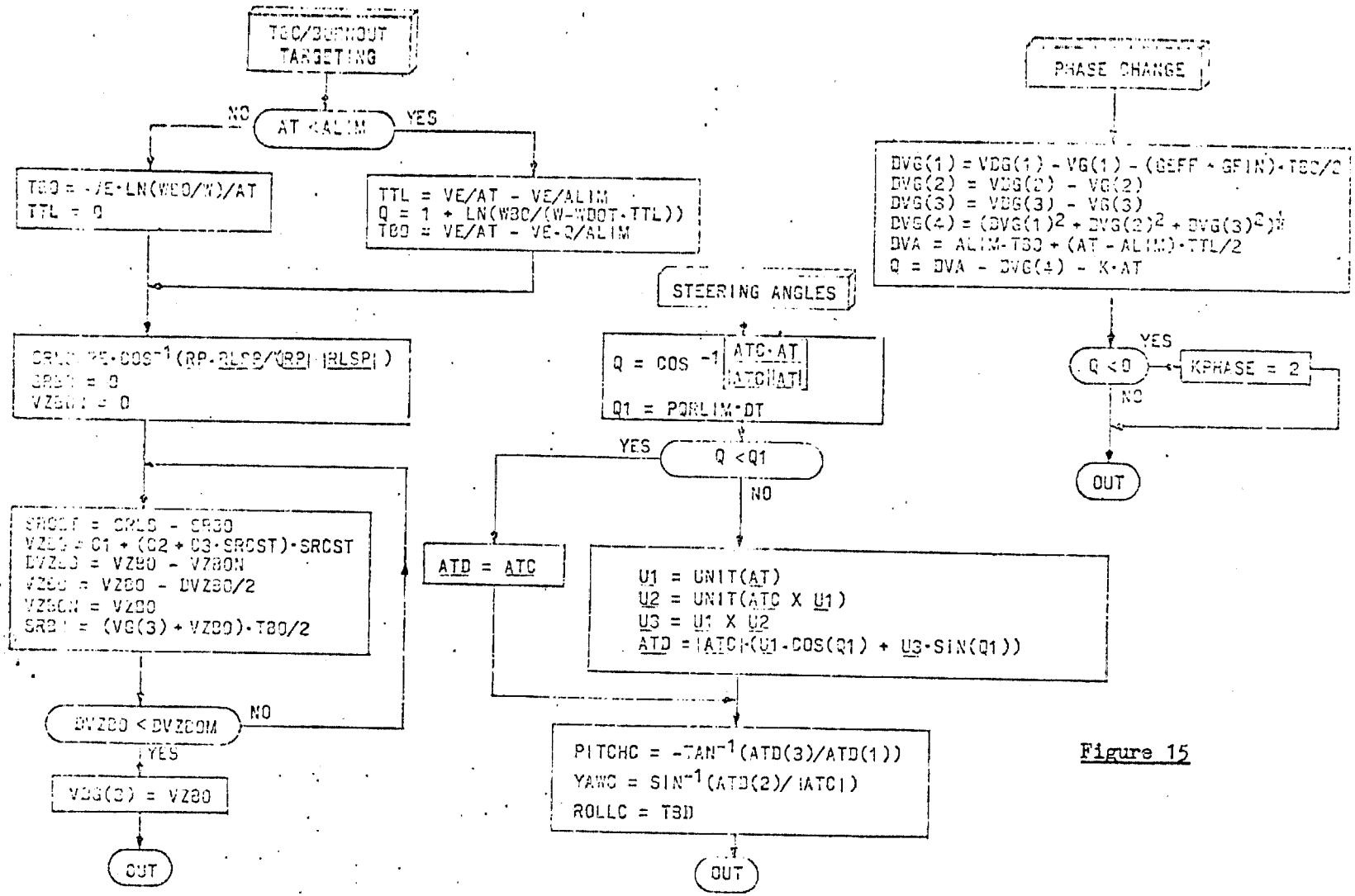
TBO/BURNOUT TARGETING
AT < ALIM
NO
YES
TBO = -VE·LN(WBO/W)/AT
TTL = 0
TTL = VE/AT - VE/ALIM
Q = 1 + LN(WBO/(W-WDOT·TTL))
TBO = VE/AT - VE·Q/ALIM
SRCST = 0
VZBOM = 0
SRCST = SRCS - SRBO
VZBO = C1 + (C2 + C3·SRCST)·SRCST
DVZBO = VZBO - VZBON
VZBO = VZBO - DVZBO/2
VZBON = VZBO
SRBO = (VG(3) + VZBO)·TBO/2
DVZBO < DVZBOM
NO
YES
VDG(3) = VZBO
OUT
STEERING ANGLES
Q = COS -1 ATC·AT / |ATC||AT|
Q1 = PORLIM·DT
Q < Q1
YES
NO
ATD = ATC
U1 = UNIT(AT)
U2 = UNIT(ATC X U1)
U3 = U1 X U2
ATD = |ATC|·(U1·COS(Q1) + U3·SIN(Q1))
PITCHC = -TAN-1(ATD(3)/ATD(1))
YAWC = SIN-1(ATD(2)/|ATC|)
ROLLC = TBD
OUT
PHASE CHANGE
DVG(1) = VDG(1) - VG(1) - (GEFF + GFIN)·TBO/2
DVG(2) = VDG(2) - VG(2)
DVG(3) = VDG(3) - VG(3)
DVG(4) = (DVG(1)2 + DVG(2)2 + DVG(3)2)½
DVA = ALIM-TBO + (AT - ALIM)·TTL/2
Q = DVA - DVG(4) - K·AT
Q < 0
YES
NO
KPHASE = 2
OUT

Figure 15

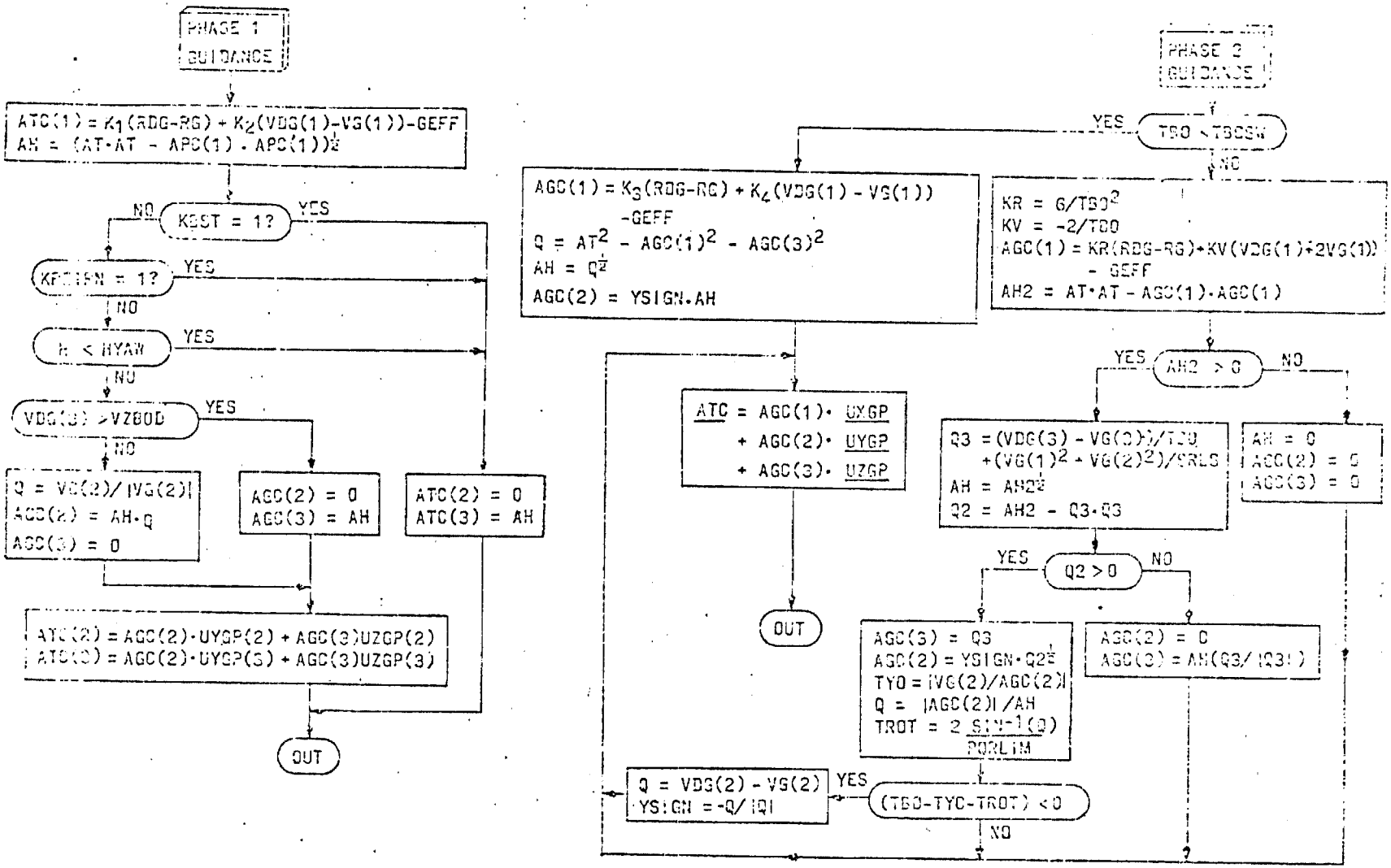
PHASE 1 GUIDANCE
ATC(1) = K1(RDG-RG) + K2(VDG(1)-VG(1))-GEFF
AH = (AT·AT - APC(1) · APC(1))½
KBST = 1?
YES
NO
KPCIGN = 1?
YES
NO
h < HYAW
YES
NO
VDG(3) >VZBOD
YES
NO
Q = VG(2)/|VG(2)|
AGC(2) = AH·Q
AGC(3) = 0
AGC(2) = 0
AGC(3) = AH
ATC(2) = 0
ATC(3) = AH
ATC(2) = AGC(2)·UYGP(2) + AGC(3)UZGP(2)
ATC(3) = AGC(2)·UYGP(3) + AGC(3)UZGP(3)
OUT
PHASE 2 GUIDANCE
TBO <TBOSW
YES
NO
AGC(1) = K3(RDG-RG) + K4(VDG(1) - VG(1)) -GEFF
Q = AT2 - AGC(1)2 - AGC(3)2
AH = Q½
AGC(2) = YSIGN·AH
KR = G/TBO2
KV = -2/TBO
AGC(1) = KR(RDG-RG)+KV(VDG(1)+2VG(1)) - GEFF
AH2 = AT·AT - AGC(1)·AGC(1)
AH2 > 0
YES
NO
ATC = AGC(1)· UXGP + AGC(2)· UYGP + AGC(3)· UZGP
OUT
Q3 = (VDG(3) - VG(3))/TBO +(VG(1)2 + VG(2)2)/SRLS
AH = AH2½
Q2 = AH2 - Q3·Q3
AH = 0
AGC(2) = 0
AGC(3) = 0
Q2 > 0
YES
NO
AGC(3) = Q3
AGC(2) = YSIGN·Q2½
TYO = |VG(2)/AGC(2)|
Q = |AGC(2)|/AH
TROT = 2 SIN-1(Q) / PORLIM
AGC(2) = 0
AGC(3) = AH(Q3/|Q3|)
Q = VDG(2) - VG(2)
YSIGN = -Q/|Q|
YES
(TBO-TYO-TROT) < 0
NO

Figure 16

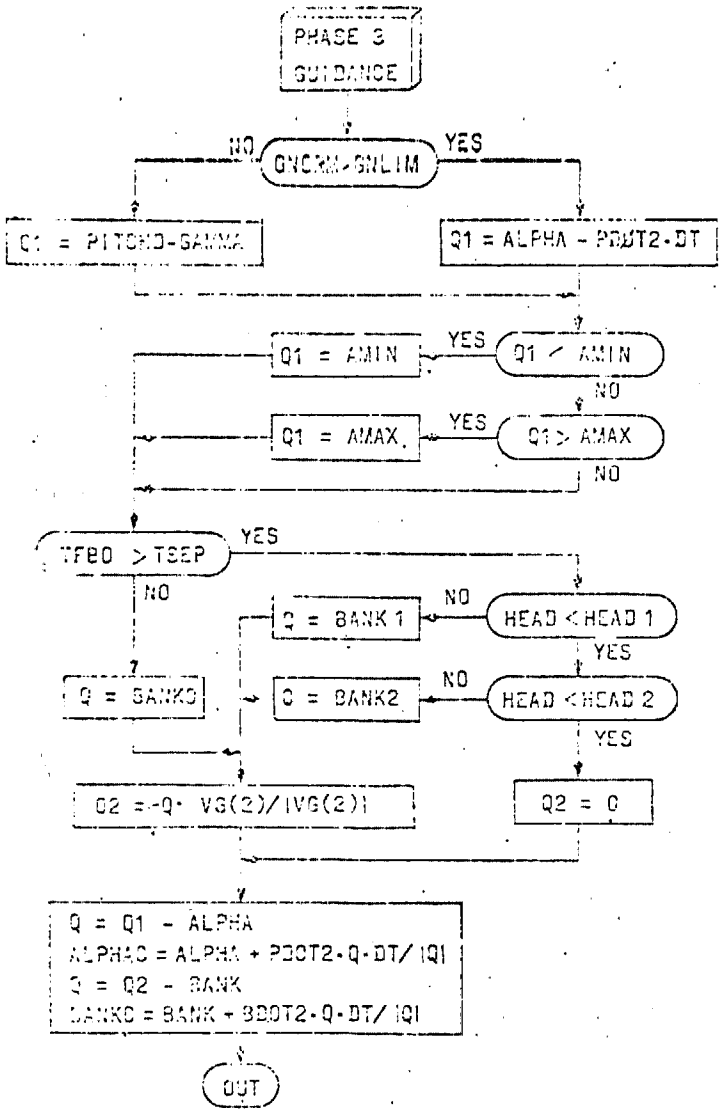
PHASE 3 GUIDANCE
GNORM>GNLIM
NO
YES
Q1 = PITCHD-GAMMA
Q1 = ALPHA - PDOT2·DT
Q1 < AMIN
YES
Q1 = AMIN
NO
Q1 > AMAX
YES
Q1 = AMAX
NO
TFBO > TSEP
YES
NO
HEAD < HEAD 1
NO
Q = BANK 1
YES
HEAD < HEAD 2
NO
Q = BANK2
YES
Q = BANKD
Q2 = -Q· VG(2)/|VG(2)|
Q2 = 0
Q = Q1 - ALPHA
ALPHAD = ALPHA + PDOT2·Q·DT/|Q|
Q = Q2 - BANK
BANKD = BANK + BDOT2·Q·DT/|Q|
OUT

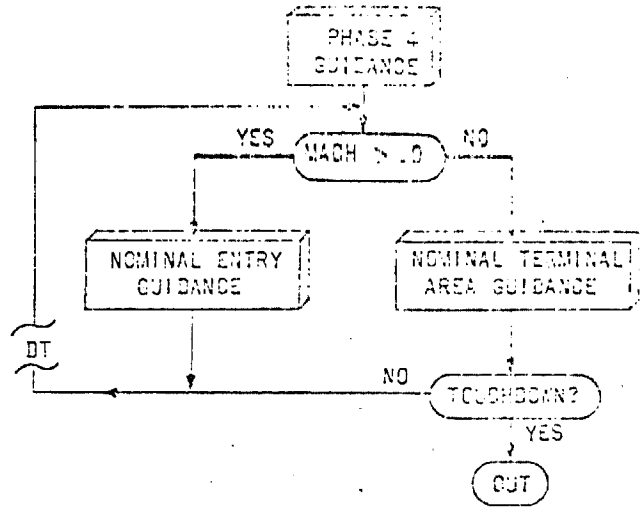
PHASE 4 GUIDANCE
YES
MACH > .0
NO
NOMINAL ENTRY GUIDANCE
NOMINAL TERMINAL AREA GUIDANCE
DT
NO
TOUCHDOWN?
YES
OUT

Figure 17

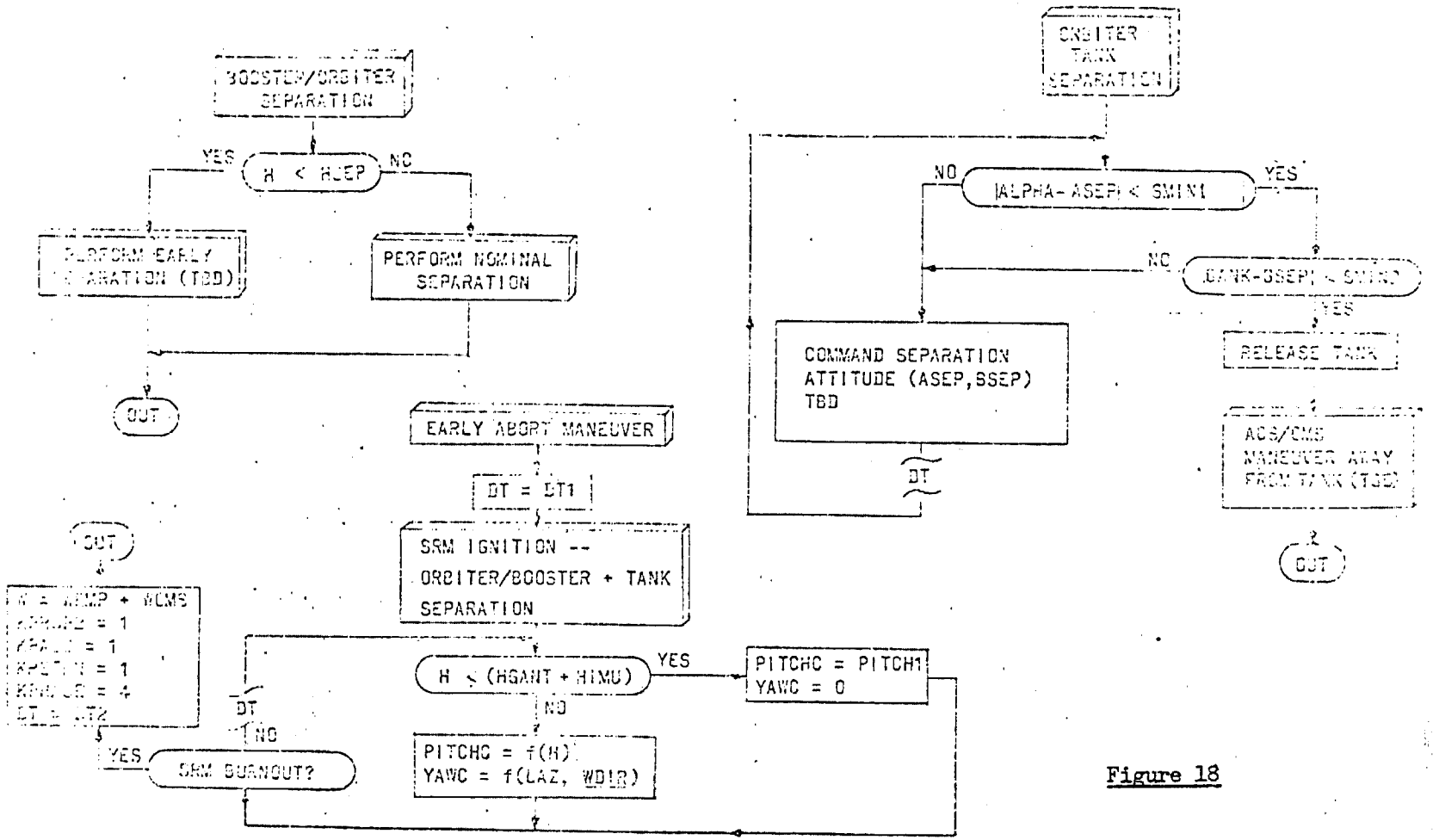
BOOSTER/ORBITER SEPARATION
YES
H < HLEP
NO
PERFORM EARLY SEPARATION (TBD)
PERFORM NOMINAL SEPARATION
OUT
EARLY ABORT MANEUVER
DT = DT1
SRM IGNITION -- ORBITER/BOOSTER + TANK SEPARATION
H ≤ (HGANT + HIMU)
YES
PITCHC = PITCH1
YAWC = 0
NO
PITCHC = f(H)
YAWC = f(LAZ, WDIR)
DT
NO
YES
SRM BURNOUT?
OUT
ORBITER TANK SEPARATION
NO
|ALPHA-ASEP| < SMIN1
YES
NO
|BANK-BSEP| < SMIN2
YES
COMMAND SEPARATION ATTITUDE (ASEP,BSEP) TBD
DT
RELEASE TANK
ACS/OMS MANEUVER AWAY FROM TANK (TBD)
OUT

Figure 18

## DEFINITION OF SYMBOLS

| | |
|---|---|
| ENT | Entry guidance takeover |
| SRM | Solid rocket motor |

### Variables

| | |
|---|---|
| ACC | Thrust acceleration command in guidance coordinates, FPSS |
| AH | Horizontal acceleration, FPSS |
| ALPHA | Angle-of-attack, deg |
| ALPHAC | Commanded angle-of-attack, deg |
| APC | Thrust acceleration command in platform coordinates, FPSS |
| BANK | Bank angle, roll about velocity vector, deg |
| BANKC | Bank angle command, deg |
| DVA | Delta-V available, FPS |
| DVG | Delta-V required, velocity to be gained, FPS |
| DVZBO | Predicted $Z_g$ component of burnout velocity minus previous value |
| G | Acceleration due to gravity, FPSS |
| GAMMA | Relative flight path angle, deg |
| GEFF | Effective gravity acceleration, FPSS |
| GFIN | Predicted effective gravity acceleration at terminus of powered phase, FPSS |
| GLAT | Latitude of abort landing site, degrees |
| GLONG | Longitude of abort landing site, degrees |
| GNDOT | Time rate of change of normal acceleration, FPSS |
| GNORM | Normal acceleration, FPSS |
| H | Altitude, ft |
| HDOT | Altitude rate, FPS |

DEFINITION OF SYMBOLS

Variables (continued)

| | |
|---|---|
| HEAD | Velocity heading angle, degrees |
| LAZ | Launch azimuth, deg |
| MACH | Mach number |
| PITCH | Platform pitch, degrees |
| PITCHC | Platform pitch command, degrees |
| Q | Intermediate variable |
| Q1 | Intermediate variable |
| Q2 | Intermediate variable |
| QBAR | Dynamic pressure, PSF |
| QBDOT | Time rate of change of dynamic pressure, PSFS |
| RG | Altitude used in guidance equation, Ft |
| RLSE | Position vector to abort landing site in geographical coordinates, Ft |
| RLSI | Position vector to abort landing site in inertial (geocentric) coordinates, Ft |
| RLSP | Position vector to abort landing site in platform coordinates, Ft |
| RP | Position vector to vehicle in platform coordinates, Ft |
| SRBO | Surface range to burnout, Ft |
| SRCST | Surface range from burnout to abort landing site, Ft |
| SRLS | Surface range from current vehicle position to abort landing site, ft |
| TBO | Time-to-go until burnout (fuel depletion), Sec |
| TFBO | Time-from-burnout, Sec |
| TIME | Time-from-liftoff, Sec |
| TROT | Time to rotate from current acceleration vector to commanded acceleration |

| | |
|---|---|
| AT | Magnitude of thrust acceleration, FPSS |
| <u>AT</u> | Present thrust acceleration vector, FPSS |
| <u>ATC</u> | Thrust acceleration command in platform coordinates, FPSS |
| K | Coefficient used in determining when to change from phase I to phase II guidance (70) |
| <u>U1</u><br><u>U2</u><br><u>U3</u> | Unit vectors of an orthogonal triad used in steering angle computation when angle between commanded thrust vector and present thrust vector is greater than PQRLIM•DT |

## DEFINITION OF SYMBOLS

### Variable Constants

| | |
|---|---|
| ALIM | Thrust acceleration limit, FPSS |
| AMAX | Maximum angle-of-attack limit, radian |
| AMIN | Minimum angle-of-attack limit, radian |
| ASEP | Desired angle-of-attack for orbiter-tank separation |
| BANK0 | Bank angle commanded during orbiter maneuver away from tank (45 deg) |
| BANK1 | Possible magnitude of bank angle command during phase III guidance (15 deg) |
| BANK2 | Possible magnitude of bank angle command during Phase III guidance |
| BDOT | Bank angle rate limit during orbiter-tank separation |
| BDOT2 | Bank angle rate limit during entry (phase III) |
| BSEP | Desired bank angle for orbiter-tank separation |
| C1<br>C2<br>C3 | Coefficients used in burnout targeting routine |
| DT1 | Powered guidance (phase I and II) cycle time, 1 sec |
| DT2 | Unpowered guidance (phase III) cycle time, .2 sec |
| GLAT1 | Latitude of landing site near launch pad |
| GLAT2 | Latitude of a downrange landing site |
| GLONG1 | Longitude of landing site near launch pad |
| GLONG2 | Longitude of a downrange landing site |
| GNLIM | Normal acceleration limit ( 1.8 G) |
| HBO1 | Burnout altitude for return to the launch site, 200,000 ft |
| HBO2 | Burnout altitude for downrange landing site, 250,000 ft |
| HBO3 | Booster burnout altitude, TBD |

Variable Constants (continued)

| | |
|---|---|
| HEAD1 | If HEAD HEAD1 $3^{o}$, BANK C = BANK1 |
| HEAD2 | If HEAD2 ($1^{o}$) HEAD HEAD1, BANKC = BANK2 |
| HGANT | Height of gantry |
| HIMU | Distance from IMU to tail of orbiter |
| IP | Inertial to platform transformation matrix |
| K1 | Altitude gain used in phase I guidance |
| K2 | Altitude rate gain used in phase I guidance |
| K3 | Altitude gain used in final portion of phase II guidance |
| K4 | Altitude rate gain used in final portion of phase II guidance |
| MU | Earth gravitational constant |
| PDOT | Pitch rate limit during orbiter tank separation |
| PDOT2 | Pitch rate limit during orbiter reentry |
| PITCH1 | Platform pitch required to clear gantry for orbiter pad abort |
| PITCHD | Desired angle between X body axis and local horizontal plane during entry after powered abort maneuver |
| PQRLIM | Attitude rate limit during powered abort |
| QBLIM | Dynamic pressure limit used for guidance purposes only |
| RDG | Desired burnout altitude, ft |
| RE | Radius of the earth, ft |
| SHIFT1 | Shift in latitude, degree |
| SHIFT2 | Shift in longitude, degree |
| SHIFT3 | Shift in latitude, degree |
| SHIFT4 | Shift in longitude, degree |
| SMIN1 | Acceptable angle-of-attack error for orbiter tank separation |
| SMIN2 | Acceptable bank angle error for orbiter tank separation |

## DEFINITION OF SYMBOLS

### Variable Constants (concluded)

| | |
|---|---|
| TBOSW | TBO for [illegible] in guidance equations (10 sec) |
| VE1 | Exhaust [illegible] city for booster |
| VE2 | Exhaust gas velocity for orbiter |
| VXBO1 | Desired altitude rate at burnout for return to the launch site (0) [illegible] |
| VXBO2 | Desired altitude rate at burnout for downrange landing site (0) [illegible] |
| VXBO3 | Desired altitude rate at booster burnout orbiter TBD |
| WBO | Desired orbiter burnout weight weight, TBD |
| WE | Angular rotation rate of earth, deg/sec |
| WEP | Angular velocity of earth in platform coordinates, deg/sec |
| WORB | Orbiter li[illegible]off weight, lb (for para[illegible]urn weight of orbiter after separation from booster; [illegible] variable) |

## Flags

| | |
|---|---|
| KBST | Set to 1 when booster is attached |
| KINIT | Set to 1 if initial conditions for booster-orbiter are used |
| KNOMIS | Set to 1 if nominal mission can not be continued |
| KORBIT | Set to 1 if orbit can be achieved |
| KPASS | Flag used to insure one pass through a loop |
| KTHASE | Flag indicating guidance phase |
| KPROP1 | Set to 1 when booster propellant is depleted |
| KPROP2 | Set to 1 when orbiter propellant is depleted |
| KRETRN | Set to 1 for return to the launch site following an abort |
| KTCRIT | Set to 1 if abort is time-critical |